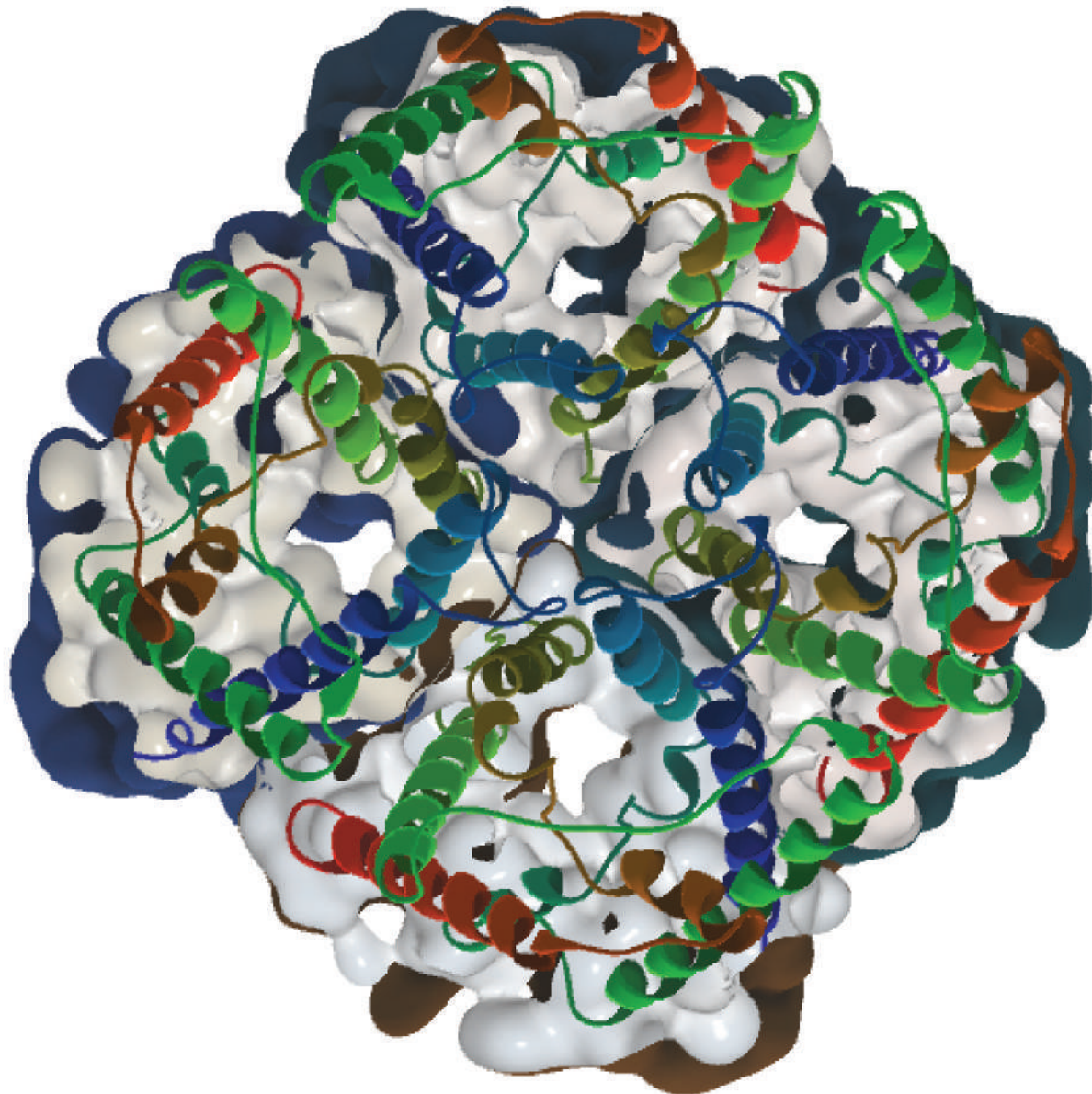
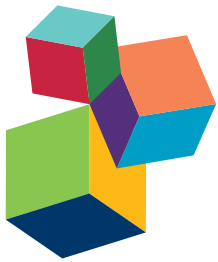


AQUAPORINS: DYNAMIC ROLE AND REGULATION

EDITED BY: Rupesh K. Deshmukh, Henry T. Nguyen and Richard R. Belanger
PUBLISHED IN: Frontiers in Plant Science and Frontiers in Physiology





frontiers

Frontiers Copyright Statement

© Copyright 2007-2017 Frontiers Media SA. All rights reserved.

All content included on this site, such as text, graphics, logos, button icons, images, video/audio clips, downloads, data compilations and software, is the property of or is licensed to Frontiers Media SA ("Frontiers") or its licensees and/or subcontractors. The copyright in the text of individual articles is the property of their respective authors, subject to a license granted to Frontiers.

The compilation of articles constituting this e-book, wherever published, as well as the compilation of all other content on this site, is the exclusive property of Frontiers. For the conditions for downloading and copying of e-books from Frontiers' website, please see the Terms for Website Use. If purchasing Frontiers e-books from other websites or sources, the conditions of the website concerned apply.

Images and graphics not forming part of user-contributed materials may not be downloaded or copied without permission.

Individual articles may be downloaded and reproduced in accordance with the principles of the CC-BY licence subject to any copyright or other notices. They may not be re-sold as an e-book.

As author or other contributor you grant a CC-BY licence to others to reproduce your articles, including any graphics and third-party materials supplied by you, in accordance with the Conditions for Website Use and subject to any copyright notices which you include in connection with your articles and materials.

All copyright, and all rights therein, are protected by national and international copyright laws.

The above represents a summary only. For the full conditions see the Conditions for Authors and the Conditions for Website Use.

ISSN 1664-8714

ISBN 978-2-88945-289-7

DOI 10.3389/978-2-88945-289-7

About Frontiers

Frontiers is more than just an open-access publisher of scholarly articles: it is a pioneering approach to the world of academia, radically improving the way scholarly research is managed. The grand vision of Frontiers is a world where all people have an equal opportunity to seek, share and generate knowledge. Frontiers provides immediate and permanent online open access to all its publications, but this alone is not enough to realize our grand goals.

Frontiers Journal Series

The Frontiers Journal Series is a multi-tier and interdisciplinary set of open-access, online journals, promising a paradigm shift from the current review, selection and dissemination processes in academic publishing. All Frontiers journals are driven by researchers for researchers; therefore, they constitute a service to the scholarly community. At the same time, the Frontiers Journal Series operates on a revolutionary invention, the tiered publishing system, initially addressing specific communities of scholars, and gradually climbing up to broader public understanding, thus serving the interests of the lay society, too.

Dedication to Quality

Each Frontiers article is a landmark of the highest quality, thanks to genuinely collaborative interactions between authors and review editors, who include some of the world's best academicians. Research must be certified by peers before entering a stream of knowledge that may eventually reach the public - and shape society; therefore, Frontiers only applies the most rigorous and unbiased reviews.

Frontiers revolutionizes research publishing by freely delivering the most outstanding research, evaluated with no bias from both the academic and social point of view.

By applying the most advanced information technologies, Frontiers is catapulting scholarly publishing into a new generation.

What are Frontiers Research Topics?

Frontiers Research Topics are very popular trademarks of the Frontiers Journals Series: they are collections of at least ten articles, all centered on a particular subject. With their unique mix of varied contributions from Original Research to Review Articles, Frontiers Research Topics unify the most influential researchers, the latest key findings and historical advances in a hot research area! Find out more on how to host your own Frontiers Research Topic or contribute to one as an author by contacting the Frontiers Editorial Office: researchtopics@frontiersin.org

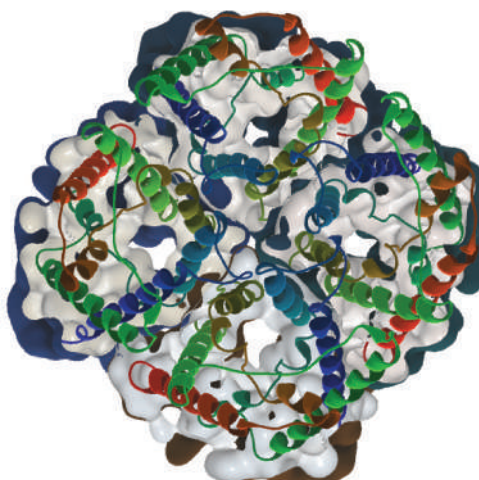
AQUAPORINS: DYNAMIC ROLE AND REGULATION

Topic Editors:

Rupesh K. Deshmukh, Université Laval, Canada

Henry T. Nguyen, University of Missouri, United States

Richard R. Belanger, Université Laval, Canada



Tertiary structure of aquaporin proteins tetramer

Image by Dr. Rupesh K. Deshmukh and Prof. Richard R. Bélanger

influencing pore morphology appears to regulate the permeability of specific solutes such as water, urea, CO_2 , H_2O_2 , boric acid, silicic acid and many more.

The discovery of novel AQPs has been accelerated over the last few years with the increasing availability of genomic and transcriptomic data. The expanding number of well characterised AQPs provides opportunities to understand factors influencing water transport, nutritional uptake, and elemental balance. Homology-based search tools and phylogenetic analyses offer efficient strategies for AQP identification. Subsequent characterization can be based on different approaches involving proteomics, genomics, and transcriptomic tools. The combination of these technological advances make it possible to efficiently study the inter-dependency of AQPs, regulation through phosphorylation and reversible phosphorylation, networking with other transporters, structural features, pH gating systems, trafficking and degradation.

Several studies have supported the role of AQPs in differential phenotypic responses to abiotic and biotic stress in plants. Crop improvement programs aiming for the development of cultivars

Aquaporins (AQPs), a class of integral membrane proteins, form channels facilitating movement of water and many other solutes. In solute transport systems of all living organisms including plants, animals and fungi, AQPs play a vital role. Plants contain a much higher number of AQP genes compared to animals, the likely consequence of genome duplication events and higher ploidy levels. As a result of duplication and subsequent diversification, plant AQPs have evolved several subfamilies with very diverse functions. Plant AQPs are highly selective for specific solutes because of their unique structural features. For instance, ar/R selectivity filters and NPA domains have been found to be key elements in governing solute permeability through the AQP channels. Combination of conserved motifs and specific amino acids

with higher tolerance against stresses like drought, flooding, salinity and many biotic diseases, can explore and exploit the finely tuned AQP-regulated transport system. For instance, a promising approach in crop breeding programs is the utilization of genetic variation in AQPs for the development of stress tolerant cultivars. Similarly, transgenic and mutagenesis approaches provide an opportunity to better understand the AQP transport system with subsequent applications for the development of climate-smart drought-tolerant cultivars.

The contributions to this Frontiers in Plant Science Research Topic have highlighted the evolution and phylogenetic distribution of AQPs in several plant species. Numerous aspects of regulation that seek to explain AQP-mediated transport system have been addressed. These contributions will help to improve our understanding of AQPs and their role in important physiological aspects and will bring AQP research closer to practical applications.

Citation: Deshmukh, R. K., Nguyen, H. T., Belanger, R. R., eds. (2017). *Aquaporins: Dynamic Role and Regulation*. Lausanne: Frontiers Media. doi: 10.3389/978-2-88945-289-7

Table of Contents

06 Editorial: Aquaporins: Dynamic Role and Regulation

Rupesh K. Deshmukh, Henry T. Nguyen and Richard R. Belanger

Section 1 - Solute Specificity, Protein Interactions, and Role of Conserved Features in Aquaporins

09 Soybean TIP Gene Family Analysis and Characterization of GmTIP1;5 and GmTIP2;5 Water Transport Activity

Li Song, Na Nguyen, Rupesh K. Deshmukh, Gunvant B. Patil, Silvas J. Prince, Babu Valliyodan, Raymond Mutava, Sharon M. Pike, Walter Gassmann and Henry T. Nguyen

24 Increased Permeability of the Aquaporin SoPIP2;1 by Mercury and Mutations in Loop A

Andreas Kirscht, Sabeen Survery, Per Kjellbom and Urban Johanson

35 Corrigendum: Increased Permeability of the Aquaporin SoPIP2;1 by Mercury and Mutations in Loop A

Andreas Kirscht, Sabeen Survery, Per Kjellbom and Urban Johanson

36 The Aquaporin Splice Variant NbXIP1;1ao Is Permeable to Boric Acid and Is Phosphorylated in the N-terminal Domain

Henry Ampah-Korsah, Hanna I. Anderberg, Angelica Engfors, Andreas Kirscht, Kristina Norden, Sven Kjellstrom, Per Kjellbom and Urban Johanson

53 Mutual Interactions between Aquaporins and Membrane Components

Maria del Carmen Martínez-Ballesta and Micaela Carvajal

Section 2 - Tools and Approaches for Aquaporin Study

63 Plant Aquaporins: Genome-Wide Identification, Transcriptomics, Proteomics, and Advanced Analytical Tools

Rupesh K. Deshmukh, Humira Sonah and Richard R. Bélanger

Section 3 - Genome-wide Distribution, Evolution and Expression of Aquaporins in Plants

77 Genome-Wide Analysis of the Aquaporin Gene Family in Chickpea (*Cicer arietinum L.*)

Amit A. Deokar and Bunyamin Tar'an

95 Genome-Wide Identification of *Jatropha curcas* Aquaporin Genes and the Comparative Analysis Provides Insights into the Gene Family Expansion and Evolution in *Hevea brasiliensis*

Zhi Zou, Lifu Yang, Jun Gong, Yeyong Mo, Jikun Wang, Jianhua Cao, Feng An and Guishui Xie

- 113 The Eucalyptus Tonoplast Intrinsic Protein (TIP) Gene Subfamily: Genomic Organization, Structural Features, and Expression Profiles**

Marcela . Rodrigues, Agnes A. S. Takeda, Juliana P. Bravo and Ivan G. Maia

Section 4 - Role of AQPs in Stress Tolerance

- 127 Characterization and Regulation of Aquaporin Genes of Sorghum [Sorghum bicolor (L.) Moench] in Response to Waterlogging Stress**

Suhas Kadam, Alejandra Abril, Arun P. Dhanapal, Robert P. Koester, Wilfred Vermerris, Shibu Jose and Felix B. Fritschi

- 141 Root ABA Accumulation Enhances Rice Seedling Drought Tolerance under Ammonium Supply: Interaction with Aquaporins**

Lei Ding, Yingrui Li, Ying Wang, Limin Gao, Min Wang, François Chaumont, Qirong Shen and Shiwei Guo

- 151 Overexpression of a Barley Aquaporin Gene, HvPIP2;5 Confers Salt and Osmotic Stress Tolerance in Yeast and Plants**

Hemasundar Alavilli, Jay Prakash Awasthi, Gyana R. Rout, Lingaraj Sahoo, Byeong-ha Lee and Sanjib Kumar Panda

Section 5 - Role of aquaporins in specific physiological and developmental processes in plants

- 163 Pollen Aquaporins: The Solute Factor**

Juliana A. Pérez Di Giorgio, Gabriela C. Soto, Jorge P. Muschietti and Gabriela Amodeo

- 171 Roles of Aquaporins in Setaria viridis Stem Development and Sugar Storage**

Samantha A. McGaughey, Hannah L. Osborn, Lily Chen, Joseph L. Pegler, Stephen D. Tyerman, Robert T. Furbank, Caitlin S. Byrt and Christopher P. L. Grof



Editorial: Aquaporins: Dynamic Role and Regulation

Rupesh K. Deshmukh^{1*}, Henry T. Nguyen^{2*} and Richard R. Belanger^{1*}

¹ Département de Phytologie—Faculté des Sciences de l’Agriculture et de l’Alimentation, Université Laval, Québec, QC, Canada, ² National Center for Soybean Biotechnology and Division of Plant Sciences, University of Missouri, Columbia, MO, United States

Keywords: water transport, solute specificity, expression profiling, genome wide analysis, protein characterization

Editorial on the Research Topic

Aquaporins: Dynamic Role and Regulation

OPEN ACCESS

Edited by:

Benoit Schoefs,
University of Maine, France

Reviewed by:

Karim Bouhidel,
Université de Bourgogne, France
Caitlin Byrt,
University of Adelaide, Australia

*Correspondence:

Rupesh K. Deshmukh
rupesh.deshmukh@fsaa.ulaval.ca
Henry T. Nguyen
nguyenhenry@missouri.edu
Richard R. Belanger
richard.belanger@fsaa.ulaval.ca

Specialty section:

This article was submitted to
Plant Physiology,
a section of the journal
Frontiers in Plant Science

Received: 19 June 2017

Accepted: 31 July 2017

Published: 15 August 2017

Citation:

Deshmukh RK, Nguyen HT and Belanger RR (2017) Editorial: Aquaporins: Dynamic Role and Regulation. *Front. Plant Sci.* 8:1420. doi: 10.3389/fpls.2017.01420

Aquaporins (AQPs), a class of channel forming integral membrane proteins, play a vital role in the transport of water and many other small solutes in most living organisms. In higher groups, AQPs have evolved in many isoforms with diverse solute specificity, subcellular localization, expression profile, interactions, and regulation mechanisms. Plant AQPs are mainly classified into five subfamilies based on phylogenetic relationships: plasma membrane intrinsic proteins (PIPs), nodulin 26-like intrinsic proteins (NIPs), tonoplast intrinsic proteins (TIPs), small intrinsic proteins (SIPs), and uncharacterized intrinsic proteins (XIPs) (Quigley et al., 2001; Deshmukh et al., 2015). PIPs and TIPs are predominantly involved in water transport, and represent a class of highly expressed AQPs in root and vegetative tissues. For their part, NIPs represents a relatively diverse group of AQPs with very specific expression profiles. They are known to be involved in the transport of metalloids such as silicon (Si), boric acid, germanium, and arsenic. The two remaining subfamilies SIP and XIP consist of only a few members, with the XIPs being present in only a few dicots.

The AQP transport system is highly regulated and complex. Aquaporin channels harbor a precise level of solute specificity and have evolved with a gating mechanism through which the channels can be turned on and off. Aquaporins are known to interact with each other and with other proteins, leading to a regulation of several physiological processes in the plant. For instance, AQPs are involved in root and shoot elongation, source to sink movement of nutrients, seed development, and other specific physiological processes such as stomatal movement, pollen hydration and germination (McGaughey et al.; Pérez Di Giorgio et al.; Song et al.). In recent years, owing to their role in water transport activity and other physiological functions, AQPs have become of great interest for crop improvement programs aimed at developing stress tolerant varieties. As a result, a better understanding of the complex transport system under AQP regulation is required to optimize efficient movement of water and other solutes necessary for healthy plant development, particularly under stress conditions.

SOLUTE SPECIFICITY AND ROLE OF CONSERVED FEATURES IN AQUAPORINS

Solute specificity of AQPs is known to be governed by many conserved features such as NPA motifs and aromatic/arginine (ar/R) selectivity filter (SF). Unlike NPA motifs, which are conserved across all AQPs, the amino acid (AA) sequences at the ar/R SF are more specific to subfamilies, or even groups within a subfamily. In addition, the functional impact of several other conserved AA, or

even the AA distance between conserved features have been highlighted with mutagenesis studies (Deshmukh et al., 2015; Kirscht et al.). The recent study by Kirscht et al. represents a classic case where mutagenesis approaches were used to demonstrate the stabilization of an aquaporin structure with the formation of disulfide bridges involving a conserved cysteine residue. Mutation at the cysteine position was found to increase water permeability as a result of the relaxation at the selectivity filter induced by the mutation.

TOOLS AND APPROACHES FOR AQUAPORIN STUDY

Numerous tools and approaches have been developed over the last decade to study the aquaporin transport system. Notably, tools like the *Xenopus* oocyte system, yeast assays, excised membranes, and proteoliposomes assisted with flow cytometry have been developed to determine solute specificity and transport kinetics (Ampah-Korsah et al.; Deshmukh et al.). As stated previously, protein–protein and lipid–protein interactions play an important role in AQP regulation, and to study these aspects, recent advancements in X-ray crystallography, electron and confocal microscopy, the yeast two-hybrid system, co-precipitation assays, and immunodetection have offered improved opportunities. Review articles by Martínez-Ballesta and Carvajal, and Deshmukh et al. provide detailed examples of the implementation of new approaches for the study of AQPs.

GENOME-WIDE DISTRIBUTION, EVOLUTION AND EXPRESSION OF AQUAPORINS IN PLANTS

Facilitated access to annotated plant genome sequences and large transcriptomic and proteomic data has accelerated the omics scale of AQP research (Deokar and Tar'an; Rodrigues et al.; Zou et al.). Genome-wide identification and characterization of AQPs in many plant species have highlighted several interesting facts about these proteins. For instance, XIPs are missing from the entire monocots as well as from some dicots including the Brassicaceae members (Sonah et al., 2017). Similarly, NIP2s (NIP-III), including the ones recognized as Si transporters, are entirely absent in the Brassicaceae members, a finding that correlates well with the inability of these plants to uptake Si. In primitive plant species, two additional subfamilies, GlpF-like intrinsic protein (GIP) and hybrid intrinsic protein (HIP), have been observed (Deshmukh et al., 2015). The reason behind the loss of HIPs and GIPs in higher plants remains unexplained. Similarly, in spite of numerous recent genome-wide studies of AQPs, their distribution and evolution among plants are still not fully understood.

Expression profiling is a powerful approach to understand the functionality and regulation of AQPs. Recent advancements in sequencing technology have made transcriptome profiling more affordable and efficient, which has led to large amounts of publicly available transcriptomic data (www.ncbi.nlm.nih.gov/sra). Using such resources, Deokar and Tar'an, Zou et al., and

Song et al. have evaluated the expression of AQPs across different tissues and conditions. Using similar approaches, Shivaraj et al. (2017) observed seed specific expression of TIP3 genes in rice, Arabidopsis, soybean, and flax. As more expression studies across a wider range of plant species become available, a more precise understanding of the specific roles of AQPs should emerge.

ROLE OF AQPS IN STRESS TOLERANCE

Aquaporins are prime candidates for deciphering the mechanisms of abiotic stress tolerance in plants. Indeed, hundreds of reports link AQP expression with drought tolerance in plants. Heterologous expression of AQPs has been used to verify their functions under stress conditions. Alavilli et al. overexpressed HvPIP2;5, an AQP from *Hordeum vulgare*, in yeast and Arabidopsis, to investigate its role under high salinity and osmotic stress. In both systems, HvPIP2;5 was found to enhance tolerance to both forms of stress. The increased tolerance induced by HvPIP2;5 is presumably associated with increased expression and activities of reactive oxygen species scavenging enzymes such as catalase, superoxide dismutase, glutathione reductase, and ascorbate peroxidase. Similarly, Ding et al. also observed a correlation between ABA (stress related hormone) biosynthesis and expression of AQPs. Kadam et al. observed differential expression of AQPs among susceptible and tolerant genotypes under waterlogging condition. The expression profiling along with the haplotypic diversity for AQPs reported by Kadam et al. will be helpful for the development of waterlogging stress tolerance cultivars in sorghum.

Unlike abiotic stress, very few studies have addressed the role of AQPs in plants during a biotic stress such as one caused by a pathogen. Along those lines, Deokar and Tar'an performed expression profiling of AQPs during fusarium wilt progression in chickpea. So far, most studies support a role for AQPs under stress conditions, but mechanistic hypotheses are still lacking to explain how their expression influences host-pathogen interactions.

OUTLOOK

Twenty-five years have elapsed since the seminal discovery of AQPs by Peter Agre's team in 1992 (Preston et al., 1992). Over that time period, significant progress was achieved in understanding the AQP transport system in numerous living organisms. Plants in particular have been the topic of intense research leading to major breakthroughs. Nevertheless, the study of AQPs in plants has proven particularly challenging compared to animals because of their higher number of homologs and more complex mechanisms of regulation. To comprehend the complex AQP system in plants, it will be fundamental to acquire a better knowledge of the co-regulation of AQPs, their interactions with other biomolecules and the influence of environmental conditions on their functionality and regulation. Similarly, knowledge of intracellular trafficking is important to understand AQP regulation, especially under adverse conditions. Studies addressing AQP intracellular trafficking have been

greatly facilitated with the development of dynamic imaging techniques (Hachez et al., 2013; Luu and Maurel, 2013; Ueda et al., 2016). Nevertheless, more intense efforts are required to decipher how AQP intracellular trafficking co-ordinates a plant's response. In addition, emphasis should be placed on the structural components and their role on AQP permeability. Apart from water, very little is known about how other solutes are transported through AQP channels. To answer

these questions, bioinformatics, sequence comparisons and high-resolution protein structure analyses are expected to contribute significantly to advance our understanding of plant AQPs.

AUTHOR CONTRIBUTIONS

RD, HN, and RB have co-edited the topic and co-prepared the editorial.

REFERENCES

- Deshmukh, R. K., Vivancos, J., Ramakrishnan, G., Guérin, V., Carpentier, G., Sonah, H., et al. (2015). A precise spacing between the NPA domains of aquaporins is essential for silicon permeability in plants. *Plant J.* 83, 489–500. doi: 10.1111/tpj.12904
- Hachez, C., Besserer, A., Chevalier, A. S., and Chaumont, F. (2013). Insights into plant plasma membrane aquaporin trafficking. *Trends Plant Sci.* 18, 344–352. doi: 10.1016/j.tplants.2012.12.003
- Luu, D. T., and Maurel, C. (2013). Aquaporin trafficking in plant cells: an emerging membrane-protein model. *Traffic* 14, 629–635. doi: 10.1111/tra.12062
- Preston, G. M., Carroll, T. P., Guggino, W. B., and Agre, P. (1992). Appearance of water channels in Xenopus oocytes expressing red cell CHIP28 protein. *Science* 256:385. doi: 10.1126/science.256.5055.385
- Quigley, F., Rosenberg, J. M., Shachar-Hill, Y., and Bohnert, H. J. (2001). From genome to function: the *Arabidopsis* aquaporins. *Genome Biol.* 3:research0001.1. doi: 10.1186/gb-2001-3-1-research0001
- Shivaraj, S. M., Deshmukh, R. K., Rai, R., Bélanger, R., Agrawal, P. K., and Dash, P. K. (2017). Genome-wide identification, characterization, and expression profile of aquaporin gene family in flax (*Linum usitatissimum*). *Sci. Rep.* 7:46137. doi: 10.1038/srep46137
- Sonah, H., Deshmukh, R., Labbé, C., and Belanger, R. (2017). Analysis of aquaporins in Brassicaceae species reveals high-level of conservation and dynamic role against biotic and abiotic stress in canola. *Sci. Rep.* 7:2771. doi: 10.1038/s41598-017-02877-9
- Ueda, M., Tsutsumi, N., and Fujimoto, M. (2016). Salt stress induces internalization of plasma membrane aquaporin into the vacuole in *Arabidopsis thaliana*. *Biochem. Biophys. Res. Commun.* 474, 742–746. doi: 10.1016/j.bbrc.2016.05.028

Conflict of Interest Statement: The authors declare that the research was conducted in the absence of any commercial or financial relationships that could be construed as a potential conflict of interest.

Copyright © 2017 Deshmukh, Nguyen and Belanger. This is an open-access article distributed under the terms of the Creative Commons Attribution License (CC BY). The use, distribution or reproduction in other forums is permitted, provided the original author(s) or licensor are credited and that the original publication in this journal is cited, in accordance with accepted academic practice. No use, distribution or reproduction is permitted which does not comply with these terms.



Soybean TIP Gene Family Analysis and Characterization of GmTIP1;5 and GmTIP2;5 Water Transport Activity

Li Song¹, Na Nguyen¹, Rupesh K. Deshmukh², Gunvant B. Patil¹, Silvas J. Prince¹, Babu Valliyodan¹, Raymond Mutava¹, Sharon M. Pike³, Walter Gassmann³ and Henry T. Nguyen^{1*}

¹ Division of Plant Science, National Center for Soybean Biotechnology, University of Missouri, Columbia, MO, USA,

² Departement de Phytologie, Laval University, Quebec, QC, Canada, ³ Division of Plant Sciences and Interdisciplinary Plant Group, Christopher S. Bond Life Sciences Center, University of Missouri, Columbia, MO, USA

OPEN ACCESS

Edited by:

Janin Riedelsberger,
University of Talca, Chile

Reviewed by:

Martin Hajduch,
Slovak Academy of Sciences,
Slovakia
Andrea Ariani,
University of California, Davis, USA

*Correspondence:

Henry T. Nguyen
nguyenhenry@missouri.edu

Specialty section:

This article was submitted to
Plant Physiology,
a section of the journal
Frontiers in Plant Science

Received: 29 July 2016

Accepted: 04 October 2016

Published: 21 October 2016

Citation:

Song L, Nguyen N, Deshmukh RK,
Patil GB, Prince SJ, Valliyodan B,
Mutava R, Pike SM, Gassmann W
and Nguyen HT (2016) Soybean TIP

Gene Family Analysis and
Characterization of GmTIP1;5 and
GmTIP2;5 Water Transport Activity.

Front. Plant Sci. 7:1564.

doi: 10.3389/fpls.2016.01564

Soybean, one of the most important crops worldwide, is severely affected by abiotic stress. Drought and flooding are the major abiotic stresses impacting soybean yield. In this regard, understanding water uptake by plants, its utilization and transport has great importance. In plants, water transport is mainly governed by channel forming aquaporin proteins (AQPs). Tonoplast intrinsic proteins (TIPs) belong to the plant-specific AQP subfamily and are known to have a role in abiotic stress tolerance. In this study, 23 soybean TIP genes were identified based on the latest soybean genome annotation. TIPs were characterized based on conserved structural features and phylogenetic distribution. Expression analysis of soybean TIP genes in various tissues and under abiotic stress conditions demonstrated tissue/stress-response specific differential expression. The natural variations for TIP genes were analyzed using whole genome re-sequencing data available for a set of 106 diverse soybean genotypes including wild types, landraces and elite lines. Results revealed 81 single-nucleotide polymorphisms (SNPs) and several large insertions/deletions in the coding region of TIPs. Among these, non-synonymous SNPs are most likely to have a greater impact on protein function and are candidates for molecular studies as well as for the development of functional markers to assist breeding. The solute transport function of two TIPs was further validated by expression in *Xenopus laevis* oocytes. GmTIP1;5 was shown to facilitate the rapid movement of water across the oocyte membrane, while GmTIP2;5 facilitated the movement of water and boric acid. The present study provides an initial insight into the possible roles of soybean TIP genes under abiotic stress conditions. Our results will facilitate elucidation of their precise functions during abiotic stress responses and plant development, and will provide potential breeding targets for modifying water movement in soybean.

Keywords: aquaporin, tonoplast intrinsic proteins (TIPs), water transporter, soybean, abiotic stress, expression, SNP

INTRODUCTION

The need for sustainable production of food is a critical issue for human and environmental health due to the continuously growing global population. Soybean, being a source of edible oil and protein rich meal, is considered a promising crop to fulfill the increasing food demand (Krishnamurthy and Shivashankar, 1975). Soybean seed contains over 40% protein and 20%

oil. However, stresses imposed by environmental factors greatly affect soybean yield and quality. Water is one of the important factors causing severe yield losses either with excess availability from flooding or with limitation resulting from drought. Plants combat such stresses by regulating water distribution at different levels, such as the vascular system and the permeability of plasma membranes. Aquaporins (AQPs), a class of channel forming proteins, facilitate transport of water and many other solutes across cellular membranes (Javot and Maurel, 2002; Maurel et al., 2002; Tyerman et al., 2002). AQPs are integral membrane proteins that belong to the major intrinsic protein (MIP) family. In higher plants, MIPs are classified into five subfamilies, including plasma membrane intrinsic proteins (PIPs), tonoplast intrinsic proteins (TIPs), NOD 26-like intrinsic proteins (NIPs), small basic intrinsic proteins (SIPs), and uncategorized intrinsic proteins (XIPs) (Chaumont et al., 2001; Kaldenhoff and Fischer, 2006; Danielson and Johanson, 2008).

It has been shown that the expression of TIP genes varies in different tissue, hormone and abiotic treatments. *ZmTIP2-3* transcripts was detected only in maize root tissues and was induced by salt and water stresses (Lopez et al., 2004). Cotton *GhTIP1:1* transcripts mainly accumulated in roots and hypocotyls under normal conditions, but were dramatically up-regulated in cotyledons and down-regulated in roots within a few hours after cotton seedlings were cold-treated (Li et al., 2009). Several root-specific *RB7-type TIP* genes have been identified from *Arabidopsis thaliana* (Yamamoto et al., 1990), *Solanum tuberosum* (Heinrich et al., 1996), *Petroselinum crispum* (Roussel et al., 1997), *Helianthus annuus* (Sarda et al., 1999), *Mesembryanthemum crystallinum* (Kirch et al., 2000). Recently, one strawberry *RB7-type TIP* gene, *FaRB7* also exhibited a root-specific expression pattern (Vaughan et al., 2006).

Tonoplast intrinsic proteins genes also have been reported to be involved in the elevation of abiotic stress tolerance in several plant species. Notably, the TIP gene *TsTIP1;2* from *Thellungiella salsuginea* provided increased tolerance against drought, salt and oxidative stresses when ectopically expressed in *Arabidopsis* (Wang et al., 2014). Similarly, increased salinity tolerance was achieved with the heterologous expression of tomato *SITIP2;2* in *Arabidopsis* (Xin et al., 2014). In soybean, Zhang et al. (2016) observed that the expression pattern of *GmTIP2;3* was affected by PEG and ABA, and overexpressing *GmTIP2;3* in yeast cells improved osmotic stress tolerance. However, another TIP gene, *GsTIP2;1* cloned from *Glycine soja*, resulted in reduced tolerance to salt and dehydration stress when overexpressed in *Arabidopsis* (Wang et al., 2011). Such contrasting results indicate diverse regulation of TIPs within the subfamily that may be due to tissue-specific expression patterns, since *GmTIP2;3* was found to be highly expressed in roots whereas *GsTIP2;1* showed comparatively higher expression in leaves. Higher water movement by *GmTIP2;3* in roots can be correlated with efficient water uptake, leading to enhanced osmotic stress tolerance. In contrast, water movement regulated by *GsTIP2;1* seems to increase water loss through transpiration. Similar observations have been reported in rice, where unbalanced expression of most aquaporins in leaves compared to root is thought to result in rapid depletion of leaf water and

subsequent inhibition of photosynthesis (Nada and Abogadallah, 2014).

Slow wilting is an important physiological parameter to study water stress tolerance in soybean. Genetic variation observed for the slow wilting trait has proven very useful for improving yield under drought conditions (Sloane et al., 1990). Several genotypes display heritable variation for the slow wilting phenotype. For instance, Sloane et al. (1990) observed delayed wilting in PI 416937 and PI 471938 soybean lines under drought conditions in the field. Recently, two new genotypes, PI 567731 and PI 567690, have been identified for the slow wilting trait under field conditions (Pathan et al., 2014). Interestingly, a study conducted with slow wilting soybean line PI416937 has revealed association between AQPs and hydraulic conductance (Sadok and Sinclair, 2010a,b, 2012). Devi et al. (2015) reported down-regulation of AQPs under high vapor pressure deficit (VPD) conditions in PI 416937, which may be due to the reduced uptake of water, resulting in conservation for later availability. Recently, our study has identified several differentially expressed AQP genes among the slow wilting and fast wilting soybean lines (Prince et al., 2015). These results prompted us to undertake detailed studies of candidate AQPs thought to be involved in soybean abiotic stress tolerance. (Verkman et al., 2014; Madeira et al., 2016).

In the present study, a comprehensive analysis of the soybean TIP gene family was carried out including phylogenetic relationships, chromosomal location, gene duplication status, gene structure, conserved motif, expression profiling under abiotic stress, and natural variation in soybean wild types, landraces and elite lines. The water transport function of two GmTIP proteins was validated through oocyte experiments. *Xenopus laevis* oocytes have very low background activity that helps to achieve a high signal-to-noise ratio as required to study transporters. Therefore, *Xenopus* oocytes have been routinely used for the evaluation of solute permeability by several different transporters (Osawa et al., 2006; Verkman et al., 2014). More particularly, AQPs are frequently analyzed using *X. laevis* oocytes (Maurel et al., 1993; Deshmukh et al., 2015). These data will contribute to future studies to functionally characterize TIP proteins in soybean.

MATERIALS AND METHODS

Identification and Structural Organization of Tonoplast Intrinsic Protein (TIP) Genes

The *Arabidopsis* TIP2;1 amino acid sequence was used as query to perform a database search using BLASTP against predicted proteins in the *G. max* Wm82.a2.v1 genome derived from Phytozome databases. Sequence with at least 50% identity with the query sequence was classified as candidate GmTIPs. BLAST hits with less than a 100 bitscore were removed. Manual curation was then performed to match TIPs identified in the present study with those reported earlier by Deshmukh et al. (2013). The genomic sequences, CDS, and protein sequences

for all GmTIPs were retrieved from Phytozome (V11¹). Novel TIP genes identified with the recent version of the soybean genome annotation were characterized for the aromatic/arginine (Ar/R) selectivity filters (SFs), Froger's residues, Asn-Pro-Ala (NPA) motifs and the spacing between NPAs. The exon/intron organizations of GmTIPs was visualized with the Gene Structure Display Server program (Hu et al., 2015; GSDS²).

Identification of Conserved Protein Motif and Channel Structure Prediction

The protein sequences were analyzed to identify conserved protein motifs (Motif scan) using the 'Multiple EM for Motif Elicitation' (MEME) program (Bailey et al., 2006). Transmembrane domains in newly identified TIPs were predicted using TOPCONS software tools³. Protein structures were modeled based on the structure of *Arabidopsis* TIP2;1⁴. The Pore Walker tool was used to predict the pore feature⁵ (Pellegrini-Celace et al., 2009).

Phylogenetic Tree Analysis

Multiple sequence alignments were conducted with the amino acid sequence of GmTIPs. Subsequently, a phylogenetic tree was constructed using the Maximum-Likelihood method provided in the MEGA 6.0 software tool (Tamura et al., 2013). The reliability of an inferred tree was confirmed with bootstrap analysis performed with 1,000 replications.

Chromosomal Distribution and Gene Duplications in GmTIPs

The chromosomal location of all GmTIP genes was obtained through BLASTN searches against the *G. Max Wm82.a2.v1* genome database in Phytozome. GmTIPs were located on soybean chromosomes based on physical positions. To further analyze gene duplication events, synonymous substitution (Ks) and non-synonymous substitution (Ka) rates were downloaded from the Plant Genome Duplication Database (PGDD) database⁶. The date of duplication events was subsequently estimated according to the equation $T = Ks/2\lambda$, in which the mean synonymous substitution rate (λ) for soybean is 6.1×10^{-9} (Lynch and Conery, 2000).

Expression Profiling Using RNA-seq Datasets

The RNA-seq data generated by Libault et al. (2010) for nine different tissues including flower, leaves, nodules, pod, root, root hair, seed, shoot apical meristem, and stem were used to analyze expression patterns of GmTIPs. Expression profiling of GmTIPs in leaf tissues of PI 567690 (drought tolerant) and Pana (drought susceptible) grown under drought conditions, and PI

408105A (flooding tolerant) and S99-2281 (PI 654356, flooding susceptible) grown under flooding conditions, was extracted from earlier reported data (Mutava et al., 2015; Prince et al., 2015; Syed et al., 2015). Briefly, at the V5 stage (five unfolded trifoliate leaves), drought stress was imposed by withdrawing water for 21 days and flooding stress was imposed by overwatering for 15 days. Similarly, RNA-seq data for Williams 82 plants subjected to very mild stress (VMS), mild stress (MS), and severe stress (SS) conditions, as well as recovery from severe stress after re-watering (SR), was used to study expression of GmTIPs (Song et al., 2016). Hierarchical clustering of expression data was performed using dCHIP software (Li and Wong, 2001).

Analysis of Synonymous and Non-synonymous SNP Variants in 106 Soybean Lines

All single-nucleotide polymorphism (SNP) datasets located in exonic regions were extracted from whole genome re-sequencing (sequencing depth approximately 15X) data (Valliyodan et al., 2016) as described by Patil et al. (2016). Annotation and effect prediction for the SNPs and other variants were performed using SnpEff⁷. SNPs were further classified into synonymous and non-synonymous categories.

Xenopus laevis Oocyte Assay

Full length cDNAs of soybean aquaporins were cloned into the *Xenopus* expression vector pOO2, which contains 5' and 3' UTR regions of the *X. laevis* β -globin gene, including an extended polyA tract for improved mRNA stability and expression (Ludewig et al., 2002). cRNA was synthesized using the SP6 Ambion mMessage mMachine kit with linearized pOO2 constructs as templates. Oocytes were isolated and maintained as described (Pike et al., 2009) and injected with 46 ng of cRNA per oocyte. Water transport was evaluated by perfusing oocytes with hypoosmotic ND96 solution and monitoring swelling over time (Maurel et al., 1993; Durbak et al., 2014). In addition, boron transport was evaluated by replacing the NaCl-containing ND96 with an isoosmotic boron-ND96 solution and monitoring swelling over time (Durbak et al., 2014).

RESULTS

Genome-Wide Identification of Tonoplast Intrinsic Proteins in Soybean

A total of twenty-three TIP genes was identified based on a comprehensive phylogenetic tree analysis within the GmMIP gene family (Deshmukh et al., 2013; Zhang et al., 2013). Here TIP genes were reanalyzed based on a recently released version of the soybean genome annotation (Wm82.a2.v1). The number of TIPs identified in soybean is in good agreement with earlier studies performed with a previous genome annotation (Deshmukh et al., 2013; Zhang et al., 2013). However, the transcript of *GmTIP4;2* (*Glyma04G08830*) reported in earlier studies seems to have

¹<https://phytozome.jgi.doe.gov>

²<http://gsds.cbi.pku.edu.cn/>

³<http://topcons.cbr.su.se/>

⁴<http://swissmodel.expasy.org/interactive>

⁵<http://www.ebi.ac.uk/thornton-srv/software/PoreWalker/>

⁶<http://chibba.agtec.uga.edu/>

⁷<http://snpEff.sourceforge.net>

been based on a mispredicted gene model and was therefore removed from the Wm82.a2.v1 annotation. Another TIP gene, *Glyma12g01490*, earlier reported as a pseudo-gene because of transcript truncation, was determined to generate a full-length transcript (new ID *Glyma.12G012300*) in the new version. Two other TIP pseudogenes reported in earlier studies were not present in the new genome version. Therefore, one gene was removed and one added, resulting in a corrected set of 23 TIPs. The gene names, gene IDs and locations in the genome are listed in Supplementary Table S1. The newly identified TIP gene (*Glyma12G01490*) was named *GmTIP5;2* according to the clustering in the phylogenetic tree.

Phylogenetic Relationship and Gene Structure

To get a better understanding of the evolutionary history, an unrooted phylogenetic tree was constructed using the Maximum-Likelihood (ML) method on the basis of multiple sequence alignment of the 23 soybean TIP proteins (Figure 1A). According to the ML phylogenetic tree, the TIP family is divided into five subgroups designated as Group 1–Group 5. Group 1, the largest clade, contains nine members, representing 39.1% of the total TIP genes. Group 4 constitutes the smallest clade with only one member. To gain further insights into the evolutionary relationships among GmTIP genes, the exon/intron structures of individual GmTIP genes were predicted based on the alignment of CDS sequences with corresponding genomic DNA sequences. As illustrated in Figure 1B, 20 out of 23 GmTIP genes have three exons, while the remaining three only possess two exons. Genes within the same clade demonstrated similar exon/intron distribution patterns in terms of exon/intron length, with the exception of *GmTIP5;2* containing a short second exon.

Chromosomal Location and Duplication of Soybean TIP Genes

The 23 TIP genes were unevenly distributed on 16 of the 20 soybean chromosomes (Figure 2), with three GmTIPs on chromosome 13, and two GmTIPs each on chromosomes 9, 10, 11, 12, and 19. The remaining chromosomes only contained one TIP each.

During evolution, the soybean genome has undergone two rounds of whole genome duplication (Schmutz et al., 2010). In order to examine the duplication patterns of soybean TIP genes, the PGDD was searched to identify segmentally duplicated pairs, and tandem duplication was identified based on the gene loci. No tandem duplication was found in this gene subfamily. To identify duplicated pairs, synonymous (K_s) and non-synonymous substitution (K_a) distance values were calculated and the K_a/K_s ratios were used to evaluate the duplication time. The K_a/K_s ratio for each segmentally duplicated gene pair varied from 0.06 to 0.28 (Supplementary Table S2). This analysis suggests that all mutations in paralogous GmTIP genes are neutral or disadvantageous, as their K_a/K_s ratios were less than 1. We found that the five closest branches of soybean TIP genes experienced duplication during the soybean whole genome

duplication period, while the others were duplicated 67 Mya or earlier. The duplicated GmTIPs exist in the form of sister pairs in the phylogenetic tree (Figure 1) and are shown linked by dotted lines in Figure 2.

Sequence and Conserved Domain Analysis in GmTIP Gene Family

The protein size of TIP members varied from 238 to 256 amino acids with 78–99% identity in each subgroup. All soybean GmTIP proteins contain two NPA motifs, and the amino acids representing the Ar/R selectivity filter (SF) and Froger's residues are highly conserved. The Ar/R SF in the newly identified *GmTIP5;2* consists of the amino acid sequence S-V-G-C, and the spacing between the NPA domains is 110 amino acids, which is consistent with other members of the GmTIP5 subfamily (Supplementary Table S3). Similarly, the sequence A-A-Y-W is a common feature for both *GmTIP5;1* and *GmTIP5;2*.

Tertiary protein structure predicted for TIPs showed six conserved transmembrane domains. However, the three dimensional geometry of the pore structure obtained with PoreWalker software (Pellegrini-Calace et al., 2009) showed substantial variation in pore size and constrictions in the pore. The tertiary structure and pore morphology for *GmTIP1;5* and *GmTIP2;5* are shown in Figure 3.

The characterization of these aquaporins as TIP genes was based on predicted amino acid similarities with known TIPs from other plant species, with location in the tonoplast of the corresponding proteins needing experimental verification. However, the predicted localization of members of the GmTIP subfamily was very diverse, including cytosol, plasma membrane, endoplasmic reticulum, vacuole, mitochondria, and chloroplast (Zhang et al., 2013). We further searched for conserved motifs in GmTIP proteins with the MEME program to gain additional insights into their diversity. As shown in Figure 4, 10 conserved motifs designated as motif 1 to motif 10 were found. All GmTIPs possess motifs 1, 2, and 5. Most of the GmTIPs contain motifs 1 to 8, whereas motif 9 and motif 10 were exclusively present in the GmTIP5 subgroup. Motif 3 was not present in *GmTIP1;1*, *GmTIP4;1*, and *GmTIP5;2*. Motif 4 was not present in *GmTIP1;4*, *GmTIP5;1*, and *GmTIP5;2*.

Differential Expression of Soybean TIPs in Soybean Tissues and Under Abiotic Stress Conditions

Very diverse expression patterns for GmTIPs were observed in the transcriptome data representing nine different tissues, namely flower, leaf, nodule, pod, root, root hair, seed, shoot apical meristem, and stem tissue (Libault et al., 2010). Most of the GmTIPs showed tissue specific expression (Figure 5). For example, *GmTIP1;1*, *1;2*, *1;3*, *1;4*, *2;6*, *2;7*, and *4;1* were highly expressed in root, but have relatively lower expression levels in other tissues. Similarly, *GmTIP1;5*, *1;6*, *2;4*, and *2;5* were highly expressed in stem, but have a relatively lower expression level in other tissues. No gene showed higher expression levels in leaves and root hairs, while most phylogenetically paired genes showed similar

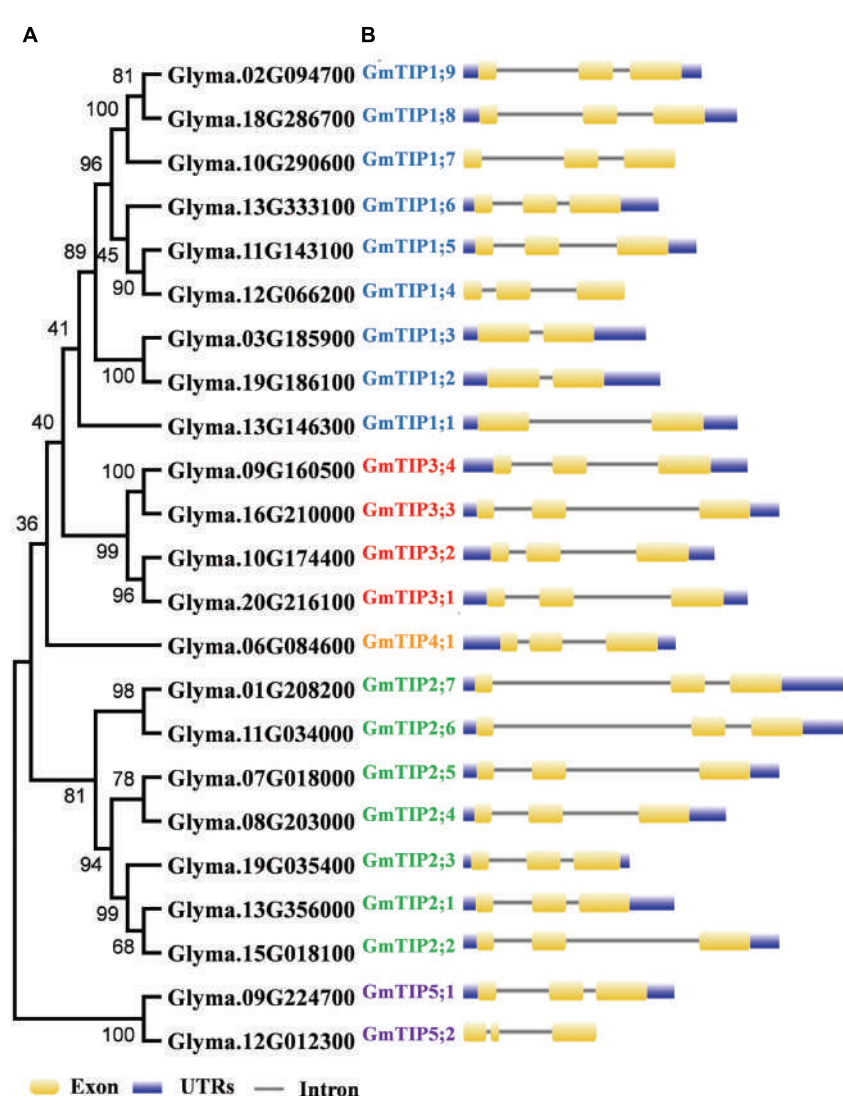


FIGURE 1 | Phylogenetic relationship and exon-intron structure of soybean Tonoplast intrinsic proteins (TIPs). (A) The unrooted tree was constructed via alignment of full-length amino acid sequences from soybean using MEGA6 software by the neighbor-joining method. (B) Lengths of the exons and introns of each TIP gene are displayed proportionally. Exons and introns are indicated by yellow rectangles and thin lines, respectively. The untranslated regions (UTRs) are indicated by blue rectangles.

expression patterns. The GmTIP3 subgroup was only expressed in seed tissue, although this pattern broadened under stress conditions (see below). Interestingly, two phylogenetic gene pairs displayed different expression patterns (*GmTIP2;1/GmTIP2;2*, *GmTIP1;8/GmTIP1;9*), indicating neofunctionalization.

The tissue specific expression pattern of GmTIPs was investigated in the Williams 82 genotype under varying water-deficit conditions (Figure 6A). *GmTIP3;2, 3;3, and 3;4* were up-regulated in shoots under serious drought condition, even after water-recovery, and down-regulated in all other tissues and conditions. Interestingly, the whole GmTIP2 subfamily was down-regulated under very mild drought stress in leaf tissue and up-regulated after severe drought stress and water-recovery,

except one (*GmTIP2;2*). These results indicated that a gene subfamily may share similar regulatory elements, and also have similar physiological functions. Most of the root-specific expressed genes were induced under varying water-deficit conditions.

To further investigate the expression profiles of TIP genes under drought and flooding conditions, the expression patterns of TIP gene families were extracted from two RNA-seq datasets (Prince et al., 2015 and unpublished data) (Figure 6B). PI 567690 is a slow wilting soybean line, and Pana is a fast wilting line under drought conditions (Pathan et al., 2014; Mutava et al., 2015). *GmTIP2;1, 2;2, 2;3, 2;4, 2;5, 3;2, and 5;1* mRNA levels were induced in leaves of Pana, but decreased in leaves of PI

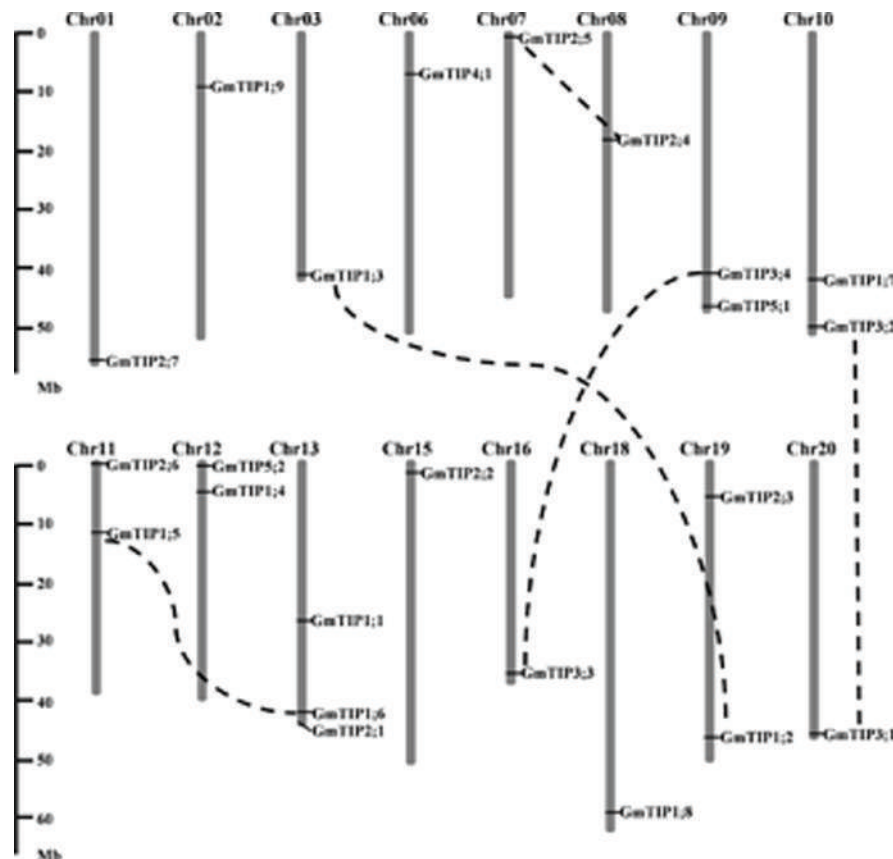


FIGURE 2 | Chromosomal locations and gene duplication events of soybean TIP gene family members. The segmentally duplicated gene pairs are linked by black dotted lines. The left scale represents physical distance along the chromosomes in megabases (Mb). Chromosome numbers are shown at the top of each vertical gray bar.

567690 after drought stress. PI 408105A is a flooding tolerant line, and S99-2281 is a flooding sensitive line (Mutava et al., 2015). *GmTIP1;2, 1;3, 1;4, 1;5, 1;6, 1;9, 2;6, and 4;1* mRNA levels were induced in leaves of S99-2281, but decreased or were not induced in leaves of PI 408105A after flooding stress. Conversely, *GmTIP1;8* and *2;7* were induced in PI 408105A and decreased in S99-2281. These results indicated that GmTIP genes could play a role under drought or flooding stress.

The expression pattern of the newly identified *GmTIP5;2* could not be determined because all reads from the above RNA-seq datasets were aligned to the previous version of the *G. max* reference genome, Gmax1.1, and Phytozome v9.0. *GmTIP3;1* was not induced or decreased in any tissues (Williams 82) or PI lines under abiotic stress conditions (Figures 6A,B). Also *GmTIP3;1, GmTIP3;4, GmTIP3;3*, and *GmTIP1;7*, did not show any response to abiotic stress in the PI or cultivar lines (Figure 6B).

Analysis of SNP Variation of the GmTIP Gene Family in 106 Soybean Lines

Single-nucleotide polymorphisms located in the coding regions of GmTIPs were identified to investigate the genetic variation within this gene family in diverse soybean lines (Supplementary

Table S4). A total of 81 SNPs were observed in the 23 GmTIP genes. These SNPs exhibited an uneven distribution: the GmTIP5 subfamily contains the highest number of SNPs compared to other subfamilies, whereas no SNPs were found in GmTIP2;1 and GmTIP2;3. Out of 81 SNPs, one SNP located in GmTIP5;1 generates a premature stop codon. Thirty-six SNPs were non-synonymous and were distributed in the coding regions of 14 GmTIPs. Some deletions were found in non-synonymous SNP locations, which cause protein-coding changes. Not a single non-synonymous SNP was identified within the remaining seven genes (*GmTIP1;2, GmTIP1;5, GmTIP1;9, GmTIP2;4, GmTIP2;5, GmTIP2;6, and GmTIP4;1*). SNPs unique to *G. soja* lines (PI# highlighted red) are summarized in Supplementary Table S4. Only 18 unique SNPs were identified in seven *G. soja* lines, and eight out of these 18 SNPs were non-synonymous. The pattern of SNP distributions correlates well with the phylogenetic distribution of TIPs (Figure 1; Supplementary Table S2). This sequence information enabled us to identify novel GmTIP alleles from soybean lines that will serve as valuable breeding resources.

Genetic variations were further investigated in four soybean slow wilting lines (PI 471938, PI 416937, PI 567690, and PI 567731) to establish associations between SNPs and the slow

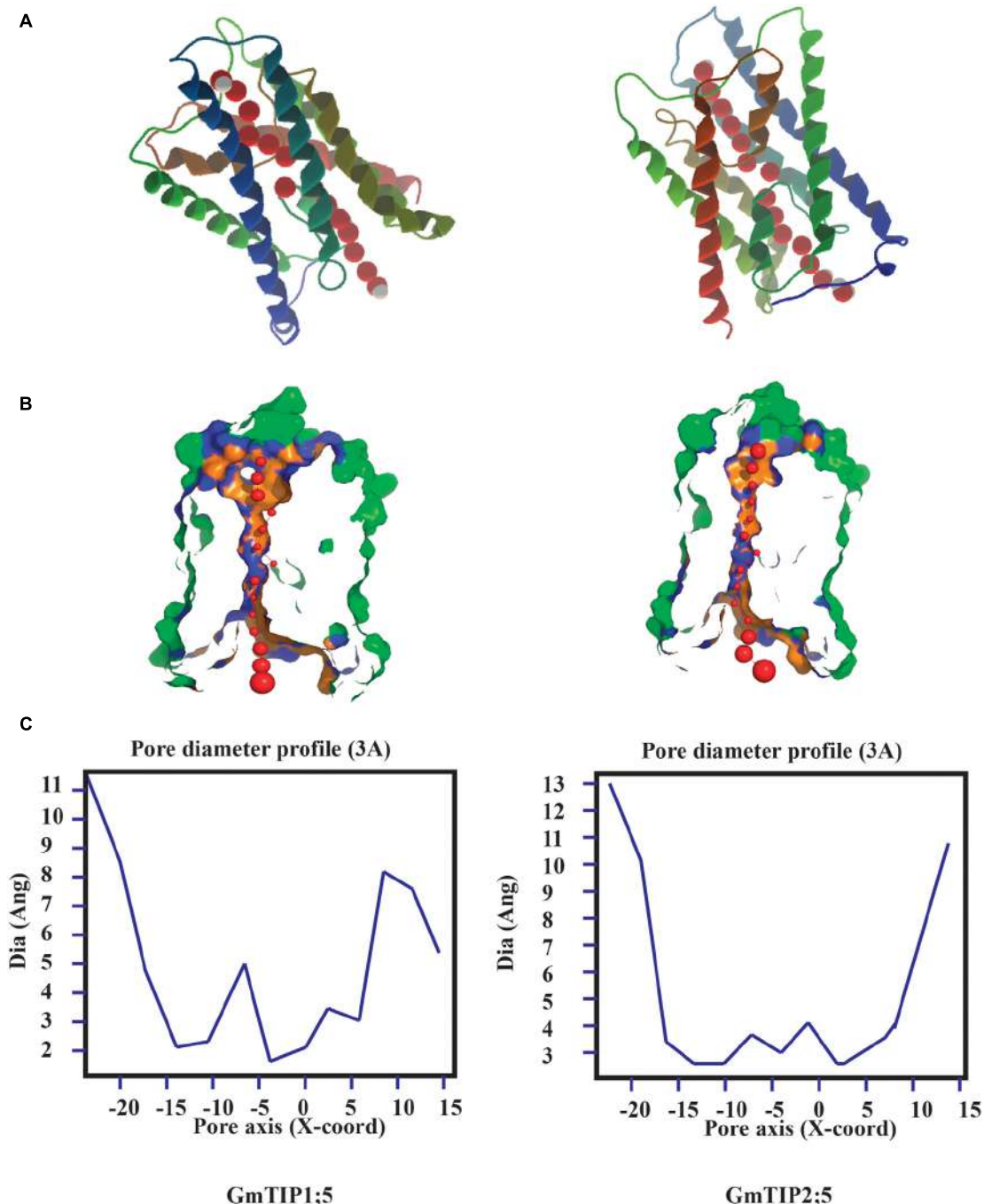


FIGURE 3 | Protein tertiary structure showing pore morphology of GmTIP1;5 and GmTIP2;5. (A) Tertiary structures comprised of six transmembrane domains and water molecules (red) passing through the pores of GmTIP1;5 (left) and GmTIP2;5 (right) visualized with CLC genomic workbench. **(B)** Cross sections of the proteins showing pore. **(C)** Pore diameter profile of GmTIP1;5 (left) and GmTIP2;5 (right) at 3 Å steps corresponding to the pore shape in **(B)**. Pore axis (X-Coord): the position along the pore axis is shown as x-coordinate in Å. Dia (Ang): pore diameter value in Å.

wilting trait. However, no unique SNPs were identified within coding sequences in these four slow wilting lines as compared with other non-slow wilting lines. The effects of non-synonymous SNP on the pore shape were further analyzed in GmTIP5;1 and GmTIP5;2, which have more non-synonymous SNPs in

the protein coding region than other GmTIPs. Interestingly, we find that two non-synonymous SNPs (Gm09_41743311 and Gm09_41743354) in GmTIP5;1 do not influence the channel 3D shape. However, three non-synonymous SNPs (Gm12_895269, Gm12_895302, and Gm12_895476) in GmTIP5;2 have an effect

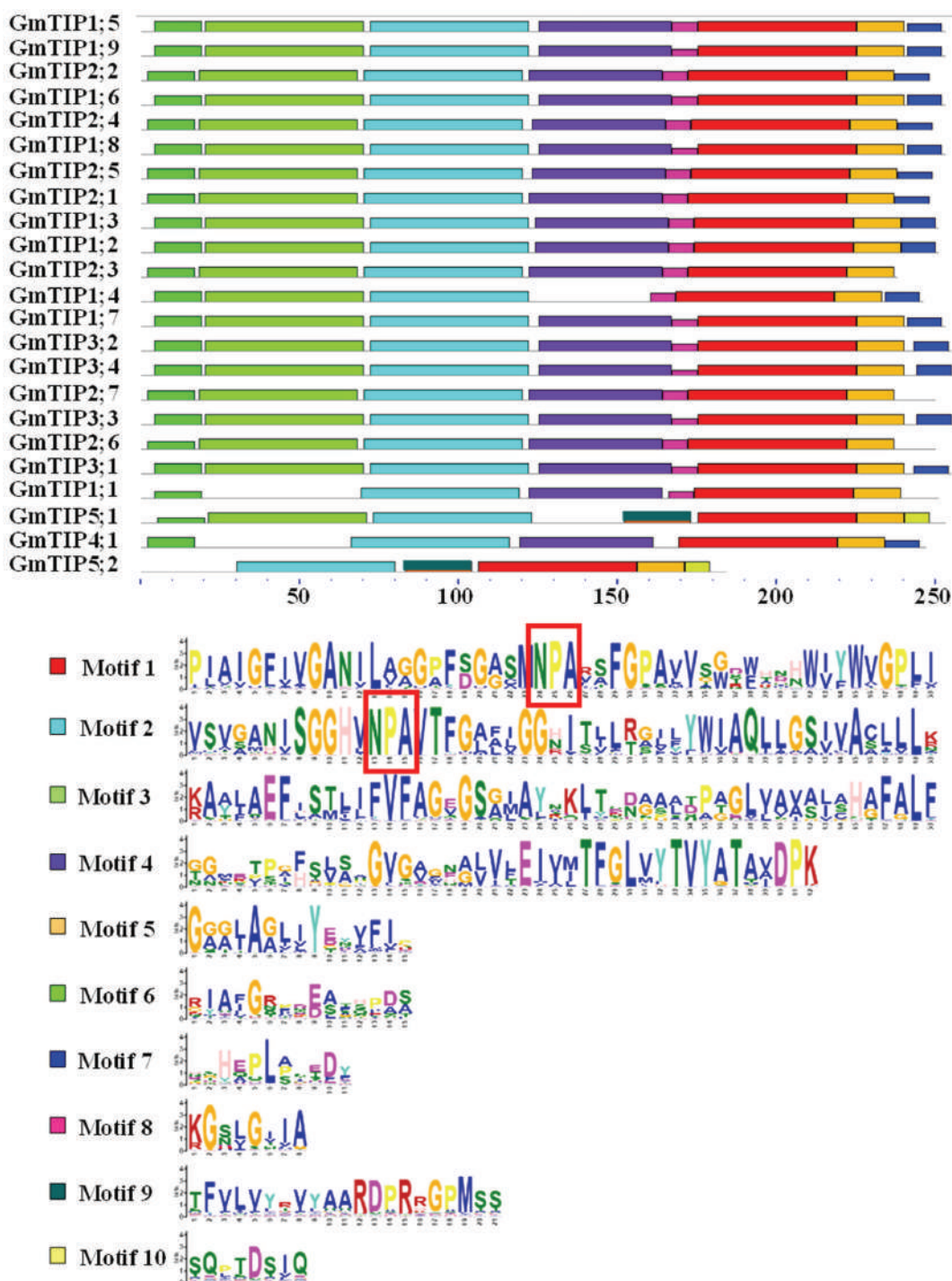


FIGURE 4 | Identification and distribution of conserved motifs in soybean TIP protein sequences. Distribution of conserved motifs in soybean TIP members. All motifs were identified by Multiple EM for Motif Elicitation (MEME) using the complete amino acid sequences of GmTIP proteins. Different motifs are indicated by different colored boxes numbered 1–10. The annotation of each motif is listed at the bottom. Motif 1 and motif 2 contain the NPA domain.

on the pore shape. Different pore diameter profiles were obtained between Williams 82 genotype and some of the other sequenced genotypes (Figure 7). For example, the structure of GmTIP5;2 in PI 567690 was different than that in Williams 82. These

results indicate that the slow wilting trait in these lines may be governed by different molecular mechanisms, such as GmTIP expression level differences or is due to their different 3D structures.

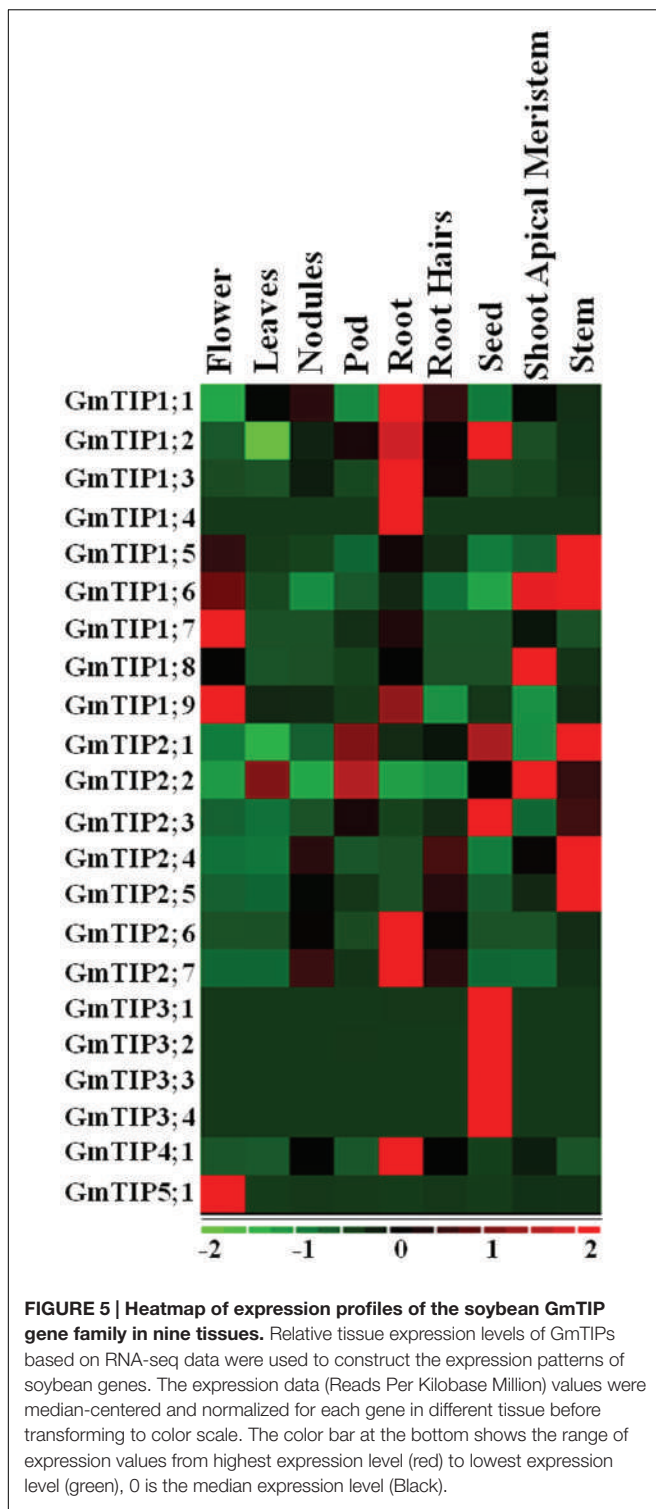


FIGURE 5 | Heatmap of expression profiles of the soybean GmTIP gene family in nine tissues. Relative tissue expression levels of GmTIPs based on RNA-seq data were used to construct the expression patterns of soybean genes. The expression data (Reads Per Kilobase Million) values were median-centered and normalized for each gene in different tissue before transforming to color scale. The color bar at the bottom shows the range of expression values from highest expression level (red) to lowest expression level (green), 0 is the median expression level (Black).

Cloning and Functional Characterization of *GmTIP1;5* and *GmTIP2;5* in *Xenopus* Oocytes

No non-synonymous SNP was found in *GmTIP1;5* and *GmTIP2;5* in 106 soybean germplasm; however, they were shown to

be differentially expressed in response to drought (*GmTIP1;5* and *GmTIP2;5*) and flooding (*GmTIP1;5*) in different varieties of soybeans with contrasting phenotypes and were mainly expressed in stem where they could be highly important in water transport during abiotic stress. Further in-depth analysis of *GmTIP1;5* and *GmTIP2;5* using *X. laevis* oocytes was performed to establish a link between differential expression patterns and trait development. *GmTIP2;5* and *GmTIP1;5*-expressing oocytes showed a rapid rate of swelling for the first 5 min after being subjected to a hypoosmotic solution (Figures 8A–C). After 5 min, the rate of swelling in *GmTIP2;5* expressing oocytes declined as they began to burst. In contrast, *GmTIP1;5* expressing oocytes continued to increase in diameter at a rate greater than the controls for 20 min. *GmTIP2;5*-expressing oocytes swelled more rapidly than *GmTIP1;5*-expressing oocytes during the first 5 min. Mock-injected oocytes displayed a slower rate of swelling, probably due to diffusion of water across the plasma membrane. It was concluded from these results that *GmTIP2;5* and *GmTIP1;5* facilitate the transport of water and are aquaporins.

Some aquaporins transport boron and other solutes in addition to water (Durbak et al., 2014). To test if these GmTIPs can transport boron, we applied an isoosmotic solution containing 200 mM boric acid in place of 96 mM NaCl. The *GmTIP2;5*-expressing oocytes showed significantly increased swelling with boric acid compared to the control (Figure 8D). In contrast, control and *GmTIP1;5*-expressing oocytes did not swell. These results indicated that *GmTIP2;5* can transport water as well as boric acid.

DISCUSSION

GmTIPs Play Important Roles in Abiotic Stress

Here, 23 full-length aquaporin-coding sequences belonging to the TIP subfamily were identified in the soybean genome. The number of TIPs in the soybean genome is much higher than those identified in species like *Arabidopsis*, maize, rice, and sorghum (Regon et al., 2014). Several studies have shown differential expression of plant aquaporins in response to environmental stresses in several different species (Alexandersson et al., 2005; Zhu et al., 2005; Ligaba et al., 2011; Cohen et al., 2013; Li et al., 2014). Therefore, it is important to investigate the interaction between the expression of GmTIPs and abiotic stress. This study explored the expression patterns of GmTIP genes in soybean PI 567690 and Pana lines. The soybean genotype PI 567690 exhibits significantly lower wilting and less yield loss under drought condition than the elite cultivar Pana (Pathan et al., 2014). The difference in gene expression between PI 567690 and Pana had been investigated by RNA-seq (Prince et al., 2015), and our preliminary data indicated that the PI 567690 genotype has a limited transpiration response when exposed to a high vapor pressure deficit (unpublished data). In the present analysis, we found that the expression level of seven TIP genes was reduced in slow-wilting soybean lines but increased in the fast-wilting soybean lines after drought stress (Figure 6B). At the same time, the expression level of

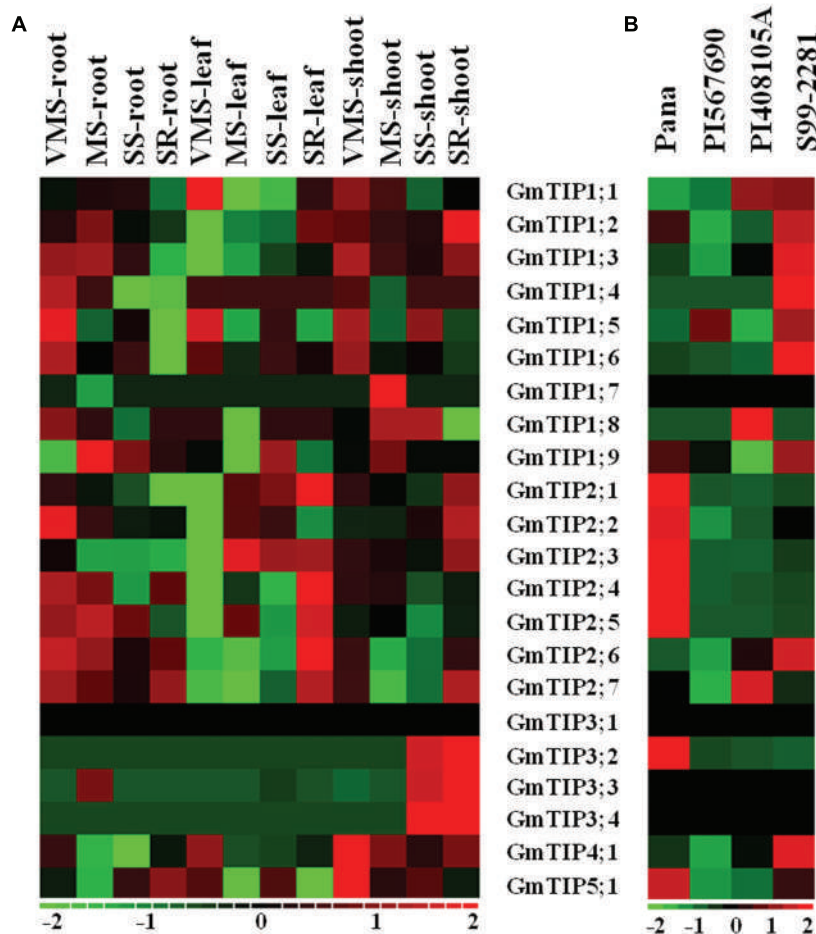
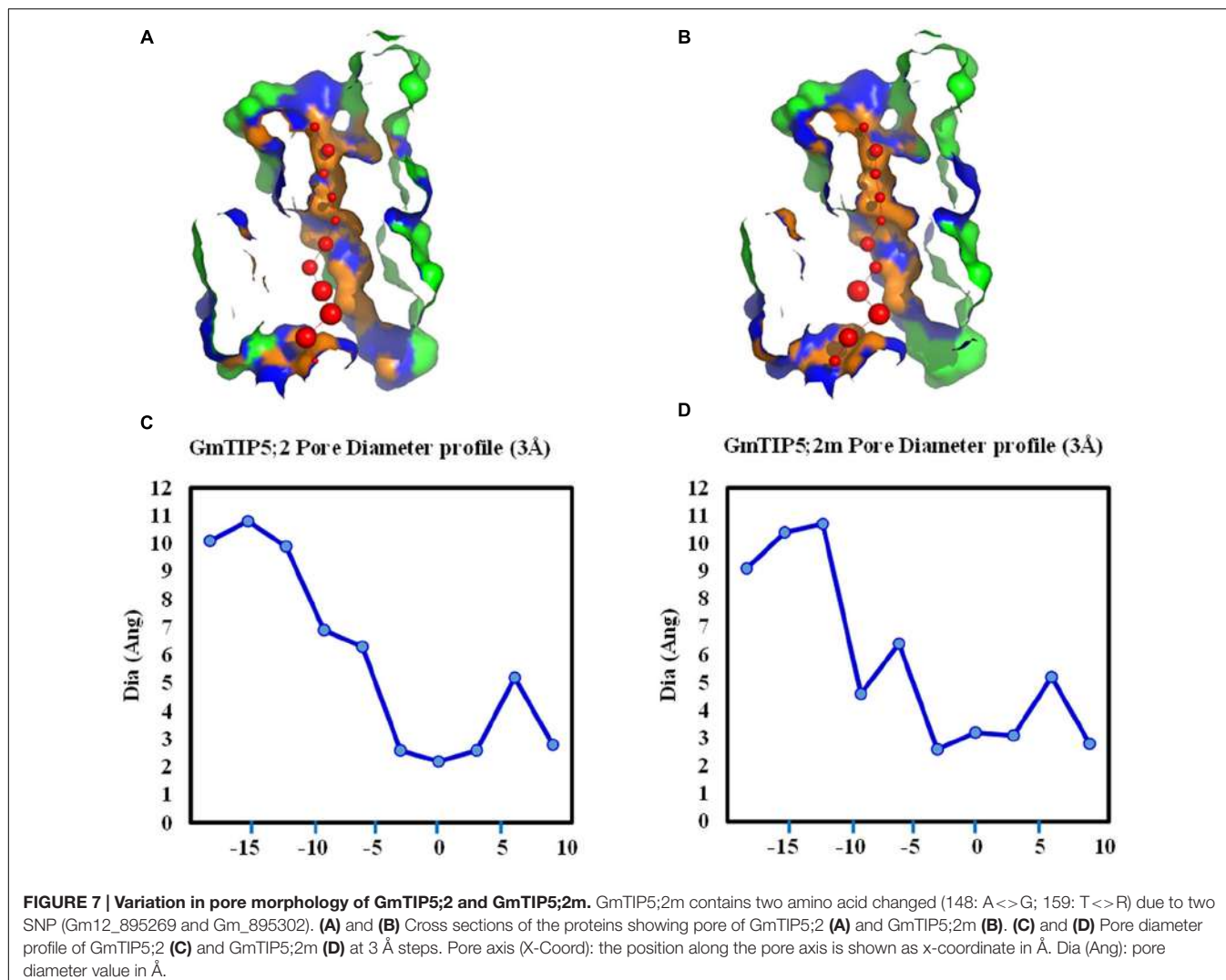


FIGURE 6 | Expression profiles of soybean TIP genes under different abiotic stress conditions or in different germplasms. (A) Heatmap representation of expression patterns of soybean TIP genes across the root, leaf, and shoot tissue in Williams 82 under varying water-deficit stress conditions (VMS: very mild stress; MS: mild stress; SS: severe stress; SR: water recovery after severe stress). **(B)** Expression profiles of the soybean TIP genes in leaves of Pana (fast wilting, drought vs. control), PI 567690 (slow wilting, drought vs. control), PI 408105A (flooding tolerant, flooding vs. control), S99-2281(flooding sensitive, flooding vs. control). The expression data values were median-centered and normalized for each gene before transforming to the color scale (log2-transformed ratios). The color bar at the bottom shows the range of expression values from increased expression (red) to decreased expression (green), 0 means no gene expression pattern changed (Black).

eight different TIP genes was down-regulated or unchanged in the waterlogging tolerant varieties, but upregulated in the waterlogging susceptible varieties. Only one gene was found to be up-regulated in slow-wilting lines under drought conditions, and only three genes were found to be up-regulated in the water-logging tolerant lines. These results are consistent with the hypothesis that due to lessened water transport in soybean leaves, the genotype PI 567690 exhibited more resistance to drought stress. We therefore conclude that GmTIPs may play an important role in soybean both in drought and flooding tolerance. However, the gene regulation patterns in root tissue of water-logging resistant lines should be further explored.

The expression patterns of GmTIPs under a given condition varied among different tissues and was complex (Figures 6A,B).

GmTIP1;5 and *GmTIP2;5* showed a higher expression in stem, but lower expression in other tissues. Interestingly, *GmTIP2;5* transcript was up-regulated under varying water-deficit stress in root, but down-regulated after water-recovery. This is the TIP that showed a very rapid water uptake in *Xenopus* oocytes. *GmTIP1;5*, which showed a slower, but steady uptake in *Xenopus* oocytes, was mainly induced under the VMS condition in root, leaf and shoot, not in other water-deficit conditions. Furthermore, *GmTIP1;5* is the only one that showed upregulation in slow wilting lines under drought condition among all TIP genes. In addition, only one synonymous SNP was located in the coding sequences of *GmTIP1;5* and two synonymous SNPs were located in the coding sequence of *GmTIP2;5*. Therefore, observed variations in gene expression seem to have prominent roles in functional variation. Further investigation of the water



transport function of these two genes in soybean would help to establish a link between differential expression patterns and trait development.

To gain further insight into the possible physiological functions of the members of this large family and aid the development of genetic engineering in soybean, the *TIP* that directs tissue-specific expression pattern and functions in water transport would be highly desirable. Overall, a more comprehensive mechanism will emerge as multiple aquaporin transport functions and integration of the different stress signals are determined at the whole plant level. Further characterization of the GmTIP genes involved in abiotic stress resistance genotypes may aid in developing tolerant germplasm and cultivars.

Water Permeability of GmTIPs

All *G. max* TIP aquaporins showed the canonical double NPA motif and a group ar/R SF that are conserved across different species. These results indicate that GmTIPs may play similar roles in regulating water absorption. As such, it is important to

validate representative candidate genes for water transport by using other methods such as heterologous expression in *Xenopus* oocytes. Basic GmTIP gene family information and phylogenetic sequence analysis in the present study provide a list of candidate genes that may play important roles in soybean drought and flooding tolerance. The function of two of these GmTIP genes has been demonstrated to be involved in water transport. However, AQPs are not only water transporters but also solute transporters (Maurel et al., 2008). Most AQPs can transport glycerol, urea, boric acid or arsenic as we showed with boron and GmTIP2;5. Yet even though a protein has been predicted to be an aquaporin, it may not transport water. Thus GmTIP candidate genes must be functionally characterized.

Aquaporins can be further functionally characterized with transport inhibitors. One such inhibitor, AgNO₃ or silver sulfadiazine, has been reported to inhibit aquaporin water transport by binding to cysteine or histidine residues, resulting in blockage of the pore (Daniels et al., 1996; Ishibashi et al., 1997; Niemietz and Tyerman, 2002). Interestingly, the transpiration rate of the slow-wilting cultivar PI416937 is insensitive to silver

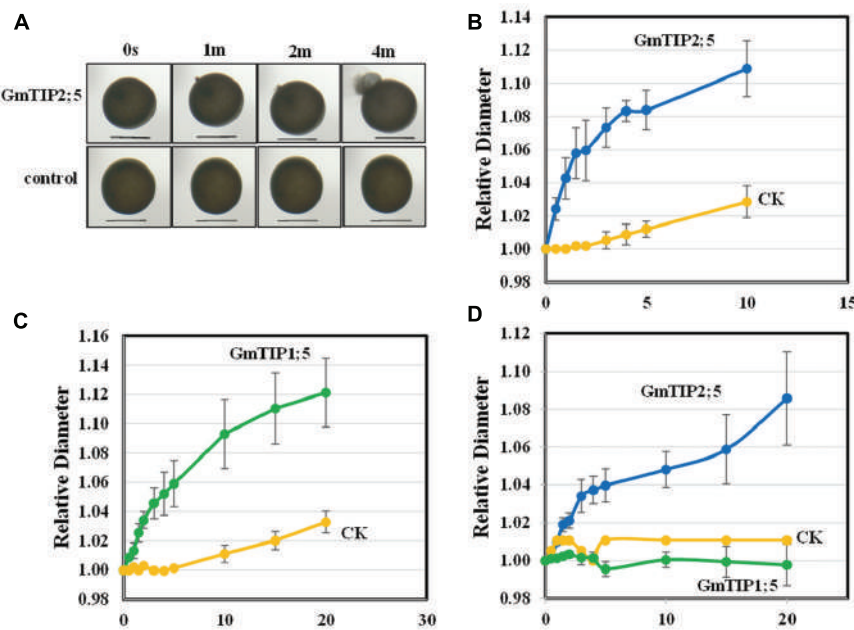


FIGURE 8 | Oocyte Swelling Assays with GmTIP1;5 and GmTIP2;5. The relative diameter of GmTIP-expressing oocytes following exposure to hypoosmotic or boron-containing isosmotic solutions was measured to characterize the osmotic permeability of GmTIP1;5 and GmTIP2;5-containing membranes. **(A)** Water transport assay with *Xenopus laevis* oocytes in hypoosmotic solution showed that GmTIP2;5-mediated water uptake leads to rapid swelling and bursting (top) compared to the control (bottom). Scale bars = 1 mm. **(B)** Rate of oocyte swelling in hypoosmotic solution in mock-injected controls (yellow line) vs. GmTIP2;5-expressing oocytes (blue line). Oocytes were observed to burst after 10 min. **(C)** Rate of oocyte swelling in hypoosmotic solution in mock injected controls (yellow line) vs. GmTIP1;5-expressing oocytes (green line). Results are reported as means \pm SEM ($N = 5$ oocytes). **(D)** Rate of oocyte swelling in isosmotic boric acid solution in mock injected controls (yellow line) vs. GmTIP2;5-expressing oocytes (blue line) and GmTIP1;5 (green line). The volume of each oocyte was measured for 20 min or until it burst.

treatment, and only a small change in AQP abundance following silver treatment was found in this line as compared to sensitive genotypes (Sadok and Sinclair, 2010b). All these results suggest that low AQP abundance may underlie the low leaf hydraulic conductivity of PI 416937 and its limited transpiration rates under high vapor pressure deficit (Sadok and Sinclair, 2010a, 2012; Devi et al., 2015, 2016). The effects of silver ions on water transport in *Xenopus* oocytes expressing GmTIP1;5, GmTIP2;5, or other AQPs could help us to identify key candidate genes linked with the soybean slow-wilting trait. For example, we hypothesize that *GmTIP5;1* would be a good target gene for engineering reduced gene expression for improved water stress tolerance, since under severe water-deficit conditions *GmTIP5;1* was induced in shoot and leaf tissues but showed decreased expression in the slow wilting line and flooding tolerant lines under stress conditions.

Utilization of Natural Variation of GmTIPs

Analysis of whole genome resequencing data provides an immense opportunity to mine natural variants in diverse germplasm (Patil et al., 2016; Valliyodan et al., 2016). The soybean germplasm, both wild and cultivated species, provides a wide range of abiotic stress tolerance. This study initiated characterization of GmTIPs by summarizing and analyzing all available SNP information, including whether SNPs lead to

synonymous or non-synonymous substitutions, in 106 soybean lines (Valliyodan et al., 2016). These 106 soybean lines represent diverse lines (wild types, landraces and elite lines), including four slow wilting soybean lines (PI 416937, PI 471938, PI 567690, and PI 567731). Aside from the expression level, genetic variation (natural or induced) also may impact the functionality of aquaporin genes and cause a variation in phenotypes. To our knowledge, this is the first report of natural variation in soybean for TIP genes. With this information, the correlation between the SNP haplotype and the phenotype (slow wilting score) for these 106 lines can be calculated to further characterize the association between the GmTIP genetic background and the slow-wilting trait. Furthermore, the association analysis can be extended to the whole MIP gene family and the gene promoter region to better understand the mechanism of slow wilting at the genomic level.

It has been reported that plant plasma membrane aquaporins are deactivated by dephosphorylation under conditions of drought stress, or by protonation of a conserved histidine residue following a drop in cytoplasmic pH due to anoxia during flooding (Tournaire-Roux et al., 2003; Törnroth-Horsefield et al., 2006). Analyzing the detailed effects of all non-synonymous SNPs on the existing crystal structure of plant AQPs (for examples: AtTIP2;1, SoPIP2;1) (Törnroth-Horsefield et al., 2006) in some interesting soybean lines may enable us to better understand the structure changes and mechanisms of water transport regulation.

CONCLUSION

In this study, the soybean TIP gene family was identified based on the new soybean genome annotation. Twenty-three TIP members were assigned to five subfamilies based on sequence similarity and phylogenetic relationship. The modulation of expression profiles of these 23 GmTIP genes was examined with deep transcriptome sequencing under drought or flooding conditions and during plant development. The potential roles of these genes in transport of substrates were also discussed. The identified natural variations in this gene family from 106 soybean germplasms will benefit future gene functional analysis and utilization. We also demonstrated that GmTIP1;5 and GmTIP2;5 can function as water transporters in oocytes. All results presented here represent an important resource for designing experiments for functional validation of candidate genes in plant development and abiotic stress responses, and for developing soybean germplasm with improved abiotic stress tolerance.

AUTHOR CONTRIBUTIONS

LS and RD designed the experiments, analyzed data, and prepared the manuscript. NN, SMP, LS and WG worked on the oocytes experiments. GP, RD, and BV analyzed the natural

variation SNP data. RD and LS worked on defining pore-lining residues and solute prediction. SJP and RM were involved in the gene expression pattern analysis. HN conceived and supervised the project. All authors have read, revised, and approved the manuscript.

FUNDING

This project was funded by the Missouri Soybean Merchandising Council and United Soybean Board.

ACKNOWLEDGMENTS

The authors would like to thank Dr. Amanda Durbak and Dr. Paula McStein, University of Missouri, for help with oocyte swelling assays. We thank Theresa Musket and Kevin Ngo for proof-reading and editing the manuscript.

SUPPLEMENTARY MATERIAL

The Supplementary Material for this article can be found online at: <http://journal.frontiersin.org/article/10.3389/fpls.2016.01564>

REFERENCES

- Alexandersson, E., Fraysse, L., Sjövall-Larsen, S., Gustavsson, S., Fellert, M., Karlsson, M., et al. (2005). Whole gene family expression and drought stress regulation of aquaporins. *Plant Mol. Biol.* 59, 469–484. doi: 10.1007/s11103-005-0352-1
- Bailey, T. L., Williams, N., Misleh, C., and Li, W. W. (2006). MEME: discovering and analyzing DNA and protein sequence motifs. *Nucleic Acids Res.* 34, W369–W373. doi: 10.1093/nar/gkl198
- Chaumont, F., Barrieu, F., Wojcik, E., Chrispeels, M. J., and Jung, R. (2001). Aquaporins constitute a large and highly divergent protein family in maize. *Plant Physiol.* 125, 1206–1215. doi: 10.1104/pp.125.3.1206
- Cohen, D., Bogaert-Triboulot, M. B., Vialat-Chabrand, S., Merret, R., Courty, P. E., Moretti, S., et al. (2013). Developmental and environmental regulation of aquaporin gene expression across *Populus* species: divergence or redundancy? *PLoS ONE* 8:e55506. doi: 10.1371/journal.pone.0055506
- Daniels, M. J., Chaumont, F., Mirkov, T. E., and Chrispeels, M. J. (1996). Characterization of a new vacuolar membrane aquaporin sensitive to mercury at a unique site. *Plant Cell* 8, 587–599. doi: 10.1105/tpc.8.4.587
- Danielson, J. A., and Johanson, U. (2008). Unexpected complexity of the aquaporin gene family in the moss *Physcomitrella patens*. *BMC Plant Biol.* 8:45. doi: 10.1186/1471-2229-8-45
- Deshmukh, R. K., Vivancos, J., Guérin, V., Sonah, H., Labbé, C., Belzile, F., et al. (2013). Identification and functional characterization of silicon transporters in soybean using comparative genomics of major intrinsic proteins in *Arabidopsis* and rice. *Plant Mol. Biol.* 83, 303–315. doi: 10.1007/s11103-013-0087-3
- Deshmukh, R. K., Vivancos, J., Ramakrishnan, G., Guérin, V., Carpenter, G., Sonah, H., et al. (2015). A precise spacing between the NPA domains of aquaporins is essential for silicon permeability in plants. *Plant J.* 83, 489–500. doi: 10.1111/tpj.12904
- Devi, M. J., Sinclair, T. R., and Taliercio, E. (2015). Comparisons of the effects of elevated vapor pressure deficit on gene expression in leaves among two fast-wilting and a slow-wilting soybean. *PLoS ONE* 10:e0139134. doi: 10.1371/journal.pone.0139134
- Devi, M. J., Sinclair, T. R., and Taliercio, E. (2016). Silver and zinc inhibitors influence transpiration rate and aquaporin transcript abundance in intact soybean plants. *Environ. Exp. Bot.* 122, 168–175. doi: 10.1016/j.envexpbot.2015.10.006
- Durbak, A. R., Phillips, K. A., Pike, S., O'Neill, M. A., Mares, J., Gallavotti, A., et al. (2014). Transport of boron by the tassel-less1 aquaporin is critical for vegetative and reproductive development in maize. *Plant Cell* 26, 2978–2995. doi: 10.1105/tpc.114.125898
- Heinrich, T., Potter, R., and Jones, M. G. K. (1996). PotRB7: a gene equivalent to TobRB7 from potato. *Plant Physiol.* 112, 862–862.
- Hu, B., Jin, J., Guo, A. Y., Zhang, H., Luo, J., and Gao, G. (2015). GSDS 2.0: an upgraded gene feature visualization server. *Bioinformatics* 3, 1296–1297. doi: 10.1093/bioinformatics/btu817
- Ishibashi, K., Kuwahara, M., Kageyama, Y., Tohsaka, A., Marumo, F., and Sasaki, S. (1997). Cloning and functional expression of a second new aquaporin abundantly expressed in testis. *Biochem. Biophys. Res. Commun.* 237, 714–718. doi: 10.1006/bbrc.1997.7219
- Javot, H., and Maurel, C. (2002). The role of aquaporins in root water uptake. *Ann. Bot.* 90, 301–313. doi: 10.1093/aob/mcf199
- Kaldenhoff, R., and Fischer, M. (2006). Functional aquaporin diversity in plants. *Biochim. Biophys. Acta* 1758, 1134–1141. doi: 10.1016/j.bbamem.2006.03.012
- Kirch, H. H., Vera-Estrella, R., Golldack, D., Quigley, F., Michalowski, C. B., Barkla, B. J., et al. (2000). Expression of water channel proteins in *Mesembryanthemum crystallinum*. *Plant Physiol.* 123, 111–124. doi: 10.1104/pp.123.1.111
- Krishnamurthy, K., and Shivashankar, K. (1975). *Soybean production in Karnataka*. UAS Technical Series. Bangalore: University of Agricultural Science.
- Li, C., and Wong, W. H. (2001). Model-based analysis of oligonucleotide arrays: expression index computation and outlier detection. *Proc. Natl. Acad. Sci. U.S.A.* 98, 31–36. doi: 10.1073/pnas.011404098
- Li, D. D., Tai, F. J., Zhan, Z. T., Li, Y., Zheng, Y., Wu, Y. F., et al. (2009). A cotton gene encodes a tonoplast aquaporin that is involved in cell tolerance to cold stress. *Gene* 438, 26–32. doi: 10.1016/j.gene.2009.02.023
- Li, G., Santoni, V., and Maurel, C. (2014). Plant aquaporins: role in plant physiology. *Biochim. Biophys. Acta* 1840, 1574–1582. doi: 10.1016/j.bbagen.2013.11.004

- Libault, M., Farmer, A., Joshi, T., Takahashi, K., Langley, R. J., Franklin, L. D., et al. (2010). An integrated transcriptome atlas of the crop model *Glycine max* and its use in comparative analyses in plants. *Plant J.* 63, 86–99. doi: 10.1111/j.1365-313X.2010.04222.x
- Ligaba, A., Katsuhara, M., Shibasaki, M., and Djira, G. (2011). Abiotic stresses modulate expression of major intrinsic proteins in barley (*Hordeum vulgare*). *C. R. Biol.* 334, 127–139. doi: 10.1016/j.crvi.2010.11.005
- Lopez, F., Bousser, A., Sissoëff, I., Hoarau, J., and Mahé, A. (2004). Characterization in maize of ZmTIP2-3, a root-specific tonoplast intrinsic protein exhibiting aquaporin activity. *J. Exp. Bot.* 55, 539–541. doi: 10.1093/jxb/052
- Ludewig, U., von Wirein, N., and Frommer, W. B. (2002). Uniport of NH₄⁺ by the root hair plasma membrane ammonium transporter LeAMT1;1. *J. Biol. Chem.* 277, 13548–13555. doi: 10.1074/jbc.M200739200
- Lynch, M., and Conery, J. S. (2000). The evolutionary fate and consequences of duplicate genes. *Science* 290, 1151–1155. doi: 10.1126/science.290.5494.1151
- Madeira, A., Moura, T. F., and Soveral, G. (2016). Detecting aquaporin function and regulation. *Front. Chem.* 4:3. doi: 10.3389/fchem.2016.00003
- Maurel, C., Javot, H., Lauvergeat, V., Gerbeau, P., Tournaire, C., Santoni, V., et al. (2002). Molecular physiology of aquaporins in plants. *Int. Rev. Cytol.* 215, 105–148. doi: 10.1016/S0074-7696(02)15007-8
- Maurel, C., Reizer, J., Schroeder, J. I., and Chrispeels, M. J. (1993). The vacuolar membrane protein γ-TIP creates water specific channels in *Xenopus* oocytes. *EMBO J.* 12, 2241–2247.
- Maurel, C., Verdoueq, L., Luu, D., and Santoni, V. (2008). Plant aquaporins: membrane channels with multiple integrated functions. *Annu. Rev. Plant Biol.* 59, 595–624. doi: 10.1146/annurev.arplant.59.032607.092734
- Mutava, R. N., Prince, S. J., Syed, N. H., Song, L., Valliyodan, B., Chen, W., et al. (2015). Understanding abiotic stress tolerance mechanisms in soybean: a comparative evaluation of soybean response to drought and flooding stress. *Plant Physiol. Biochem.* 86, 109–120. doi: 10.1016/j.plaphy.2014.11.010
- Nada, R. M., and Abogadallah, G. M. (2014). Aquaporins are major determinants of water use efficiency of rice plants in the field. *Plant Sci.* 227, 165–180. doi: 10.1016/j.plantsci.2014.08.006
- Niemietz, C. M., and Tyerman, S. D. (2002). New potent inhibitors of aquaporins: silver and gold compounds inhibit aquaporins of plant and human origin. *FEBS Lett.* 531, 443–447. doi: 10.1016/S0014-5793(02)03581-0
- Osawa, H., Stacey, G., and Gassmann, W. (2006). ScOPT1 and AtOPT4 function as proton-coupled oligopeptide transporters with broad but distinct substrate specificities. *Biochem. J.* 393, 267–275. doi: 10.1042/BJ20050920
- Pathan, S. M., Lee, J. D., Sleper, D. A., Fritsch, F. B., Sharp, R. E., Carter, T. E. Jr., et al. (2014). Two soybean plant introductions display slow leaf wilting and reduced yield loss under drought. *J. Agron. Crop Sci.* 200, 231–236. doi: 10.1111/jac.12053
- Patil, G., Do, T., Vuong, T. D., Valliyodan, B., Lee, J. D., Chaudhary, J., et al. (2016). Genomic-assisted haplotype analysis and the development of high-throughput SNP markers for salinity tolerance in soybean. *Sci. Rep.* 6:19199. doi: 10.1038/srep19199
- Pellegrini-Calace, M., Maiwald, T., and Thornton, J. M. (2009). PoreWalker: a novel tool for the identification and characterization of channels in transmembrane proteins from their three-dimensional structure. *PLoS Comput. Biol.* 5:e1000440. doi: 10.1371/journal.pcbi.1000440
- Pike, S., Patel, A., Stacey, G., and Gassmann, W. (2009). *Arabidopsis* OPT6 is an oligopeptide transporter with exceptionally broad substrate specificity. *Plant Cell Physiol.* 50, 1923–1932. doi: 10.1093/pcp/pcp136
- Prince, S. J., Joshi, T., Mutava, R. N., Syed, N., Joao Vitor Mdos, S., Patil, G., et al. (2015). Comparative analysis of the drought-responsive transcriptome in soybean lines contrasting for canopy wilting. *Plant Sci.* 240, 65–78. doi: 10.1016/j.plantsci.2015.08.017
- Regon, P., Panda, P., Kshetrimayum, E., and Panda, S. K. (2014). Genome-wide comparative analysis of tonoplast intrinsic protein (TIP) genes in plants. *Funct. Integr. Genomics* 14, 617–629. doi: 10.1007/s10142-014-0389-9
- Roussel, H., Bruns, S., Gianinazzi-Pearson, V., Hahlbrock, K., and Franken, P. (1997). Induction of a membrane intrinsic protein-encoding mRNA in arbuscular mycorrhiza and elicitor-stimulated cell suspension cultures of parsley. *Plant Sci.* 126, 203–210. doi: 10.1016/S0168-9452(97)00106-4
- Sadok, W., and Sinclair, T. R. (2010a). Genetic variability of transpiration response of soybean [(L.) Merr.] Shoots to Leaf Hydraulic Conductance Inhibitor AgNO₃. *Crop Sci.* 50, 1423–1430. doi: 10.2135/cropsci2009.10.0575
- Sadok, W., and Sinclair, T. R. (2010b). Transpiration response of 'slow-wilting' and commercial soybean (*Glycine max* (L.) Merr.) genotypes to three aquaporin inhibitors. *J. Exp. Bot.* 61, 821–829. doi: 10.1093/jxb/erp350
- Sadok, W., and Sinclair, T. R. (2012). Zinc treatment results in transpiration rate decreases that vary among soybean genotypes. *J. Plant Nutr.* 35, 1866–1877. doi: 10.1080/01904167.2012.706683
- Sarda, X., Tousch, D., Ferrare, K., Cellier, F., Alcon, C., Dupuis, J. M., et al. (1999). Characterization of closely related delta-TIP genes encoding aquaporins which are differentially expressed in sunflower roots upon water deprivation through exposure to air. *Plant Mol. Biol.* 40, 179–191. doi: 10.1023/A:1026488 605778
- Schmutz, J., Cannon, S. B., Schlueter, J., Ma, J., Mitros, T., Nelson, W., et al. (2010). Genome sequence of the paleopolyploid soybean. *Nature* 463, 178–183. doi: 10.1038/nature08670
- Sloane, R. J., Patterson, R. P., and Carter, T. E. (1990). Field drought tolerance of a soybean plant introduction. *Crop Sci.* 30, 118–123. doi: 10.2135/cropsci1990.0011183X003000010027x
- Song, L., Prince, S., Valliyodan, B., Joshi, T., Maldonado dos Santos, J. V., Wang, J., et al. (2016). Genome-wide transcriptome analysis of soybean primary root under varying water-deficit conditions. *BMC Genomics* 17:57. doi: 10.1186/s12864-016-2378-y
- Syed, N. H., Prince, S. J., Mutava, R. N., Patil, G., Li, S., Chen, W., et al. (2015). Core clock, SUB1, and ABAR genes mediate flooding and drought responses via alternative splicing in soybean. *J. Exp. Bot.* 66, 7129–7149. doi: 10.1093/jxb/erv407
- Tamura, K., Stecher, G., Peterson, D., Filipski, A., and Kumar, S. (2013). MEGA6: molecular evolutionary genetics analysis version 6.0. *Mol. Biol. Evol.* 30, 2725–2729. doi: 10.1093/molbev/mst197
- Törnroth-Horsefield, S., Wang, Y., Hedfalk, K., Johanson, U., Karlsson, M., Tajkhorshid, E., et al. (2006). Structural mechanism of plant aquaporin gating. *Nature* 439, 688–694. doi: 10.1038/nature04316
- Tournaire-Roux, C., Sutka, M., Javot, H., Gout, E., Gerbeau, P., Luu, D. T., et al. (2003). Cytosolic pH regulates root water transport during anoxic stress through gating of aquaporins. *Nature* 425, 393–397. doi: 10.1038/nature01853
- Tyerman, S. D., Niemietz, C. M., and Bramley, H. (2002). Plant aquaporins: multifunctional water and solute channels with expanding roles. *Plant Cell Environ.* 25, 173–194. doi: 10.1046/j.0016-8025.2001.00791.x
- Valliyodan, B., Dan, Q., Patil, G., Zeng, P., Huang, J., Dai, L., et al. (2016). Landscape of genomic diversity and trait discovery in soybean. *Sci. Rep.* 6:23598. doi: 10.1038/srep23598
- Vaughan, S. P., James, D. J., Lindsey, K., and Massiah, A. J. (2006). Characterization of FaRB7, a near root-specific gene from strawberry (*Fragaria × ananassa* Duch.) and promoter activity analysis in homologous and heterologous hosts. *J. Exp. Bot.* 57, 3901–3910. doi: 10.1093/jxb/erl185
- Verkman, A. S., Anderson, M. O., and Papadopoulos, M. C. (2014). Aquaporins: important but elusive drug targets. *Nat. Rev. Drug Discov.* 13, 259–277. doi: 10.1038/nrd4226
- Wang, L. L., Chen, A. P., Zhong, N. Q., Liu, N., Wu, X. M., Wang, F., et al. (2014). The *Thellungiella salsuginea* tonoplast aquaporin TsTIP1;2 functions in protection against multiple abiotic stresses. *Plant Cell Physiol.* 55, 148–161. doi: 10.1093/pcp/pct166
- Wang, X., Li, Y., Ji, W., Bai, X., Cai, H., Zhu, D., et al. (2011). A novel *Glycine soja* tonoplast intrinsic protein gene responds to abiotic stress and depresses salt and dehydration tolerance in transgenic *Arabidopsis thaliana*. *J. Plant Physiol.* 168, 1241–1248. doi: 10.1016/j.jplph.2011.01.016
- Xin, S., Yu, G., Sun, L., Qiang, X., Xu, N., and Cheng, X. (2014). Expression of tomato SiTIP2;2 enhances the tolerance to salt stress in the transgenic *Arabidopsis* and interacts with target proteins. *J. Plant Res.* 127, 695–708. doi: 10.1007/s10265-014-0658-7
- Yamamoto, Y. T., Cheng, C. L., and Conkling, M. A. (1990). Root-specific genes from tobacco and *Arabidopsis* homologous to an evolutionarily conserved gene family of membrane channel proteins. *Nucleic Acids Res.* 18, 7449–7449. doi: 10.1093/nar/18.24.7449

- Zhang, D., Tong, J., He, X., Xu, Z., Xu, L., Wei, P., et al. (2016). A novel soybean intrinsic protein gene, GmTIP2;3, involved in responding to osmotic stress. *Front. Plant Sci.* 6:1237. doi: 10.3389/fpls.2015.01237
- Zhang, D. Y., Ali, Z., Wang, C. B., Xu, L., Yi, J. X., Xu, Z. L., et al. (2013). Genome-wide sequence characterization and expression analysis of major intrinsic proteins in soybean (*Glycine max* L.). *PLoS ONE* 8:e56312. doi: 10.1371/journal.pone.0056312
- Zhu, C., Schraut, D., Hartung, W., and Schaffner, A. R. (2005). Differential responses of maize MIP genes to salt stress and ABA. *J. Exp. Bot.* 5, 2971–2981. doi: 10.1093/jxb/eri294

Conflict of Interest Statement: The authors declare that the research was conducted in the absence of any commercial or financial relationships that could be construed as a potential conflict of interest.

Copyright © 2016 Song, Nguyen, Deshmukh, Patil, Prince, Valliyodan, Mutava, Pike, Gassmann and Nguyen. This is an open-access article distributed under the terms of the Creative Commons Attribution License (CC BY). The use, distribution or reproduction in other forums is permitted, provided the original author(s) or licensor are credited and that the original publication in this journal is cited, in accordance with accepted academic practice. No use, distribution or reproduction is permitted which does not comply with these terms.



Increased Permeability of the Aquaporin SoPIP2;1 by Mercury and Mutations in Loop A

Andreas Kirscht^t, Sabeen Survery^t, Per Kjellbom and Urban Johanson*

Department of Biochemistry and Structural Biology, Center for Molecular Protein Science, Lund University, Lund, Sweden

OPEN ACCESS

Edited by:

Rupesh Kailasrao Deshmukh,
Laval University, Canada

Reviewed by:

Gurvant Baliram Patil,
University of Missouri, USA

Dirk Schneider,
University of Mainz, Germany

Micaela Carvajal,
Spanish National Research Council,
Spain

*Correspondence:

Urban Johanson
urban.johanson@biochemistry.lu.se

^tThese authors shared first authorship, names in alphabetical order.

Specialty section:

This article was submitted to
Plant Physiology,
a section of the journal
Frontiers in Plant Science

Received: 29 May 2016

Accepted: 08 August 2016

Published: 30 August 2016

Citation:

Kirscht A, Survery S, Kjellbom P and Johanson U (2016) Increased Permeability of the Aquaporin SoPIP2;1 by Mercury and Mutations in Loop A. *Front. Plant Sci.* 7:1249.
doi: 10.3389/fpls.2016.01249

Aquaporins (AQPs) also referred to as Major intrinsic proteins, regulate permeability of biological membranes for water and other uncharged small polar molecules. Plants encode more AQPs than other organisms and just one of the four AQP subfamilies in *Arabidopsis thaliana*, the water specific plasma membrane intrinsic proteins (PIPs), has 13 isoforms, the same number as the total AQPs encoded by the entire human genome. The PIPs are more conserved than other plant AQPs and here we demonstrate that a cysteine residue, in loop A of SoPIP2;1 from *Spinacia oleracea*, is forming disulfide bridges. This is in agreement with studies on maize PIPs, but in contrast we also show an increased permeability of mutants with a substitution at this position. In accordance with earlier findings, we confirm that mercury increases water permeability of both wild type and mutant proteins. We report on the slow kinetics and reversibility of the activation, and on quenching of intrinsic tryptophan fluorescence as a potential reporter of conformational changes associated with activation. Hence, previous studies in plants based on the assumption of mercury as a general AQP blocker have to be reevaluated, whereas mercury and fluorescence studies of isolated PIPs provide new means to follow structural changes dynamically.

Keywords: aquaporin, water channel, major intrinsic protein, *Spinacia oleracea*, tryptophan fluorescence

INTRODUCTION

Aquaporins (AQPs) are common in all domains of life and facilitate permeation of a wide range of small polar molecules through biological membranes (Abascal et al., 2014). AQPs are generally found as homotetramers, where each monomer constitutes a separate pore formed by six transmembrane helices and two short helices that are connected in the middle of the lipid bilayer at their N-termini (Fu et al., 2000; Sui et al., 2001; Törnroth-Horsefield et al., 2006; Horsefield et al., 2008; Kirscht et al., 2016). Members belonging to the plant subfamily of plasma membrane intrinsic proteins (PIPs) are specifically permeable to water and show a more strict amino acid sequence conservation than AQPs in other subfamilies (Danielson and Johanson, 2010). Function and abundance of these proteins is tightly regulated and the high number of isoforms suggests a highly redundant system for water homeostasis (Johanson et al., 2001; Alexandersson et al., 2005, 2010). Structure and regulation of one particular member of the PIP subfamily from spinach (*Spinacia oleracea*), SoPIP2;1, which constitutes a dominating integral protein of the plasma membrane has been thoroughly studied (Johansson et al., 1996, 1998; Kukulski et al., 2005; Törnroth-Horsefield et al., 2006; Nyblom et al., 2009; Frick et al., 2013).

The structure of SoPIP2;1 was solved in different conformations, which elucidated a general molecular gating mechanism for the regulation of PIPs, including some specific elements only relevant for members of the PIP2 subgroup (Törnroth-Horsefield et al., 2006). The gating of the pore is the result of conformational changes on the cytoplasmic side of the membrane and is controlled in several different ways, including, pH changes, binding of calcium and a PIP2 specific phosphorylation. The second cytosolic loop, Loop D, undergoes a major conformational change and its stabilization in certain positions is increasing the probability of an either open or closed conformation. In the closed conformation, unphosphorylated serine 274, situated close to the C-terminus, occupies a place near the tetrameric center of the protein while the preceding region resides in a groove between the monomers. When this positioning is impossible, e.g., by phosphorylation of serine 274, the C-terminus becomes unordered and the place earlier occupied by this residue is instead taken by the carbonyl oxygen of leucine 197 from the neighboring monomer, resulting in the unblocking of the pore in this monomer.

Already in early protein preparations, it became clear that interactions between monomers are strong in SoPIP2;1 tetramers (Johansson et al., 1996). Even during separation by a standard SDS-PAGE, which denatures most proteins, a large fraction of the protein is found to stay as dimers and tetramers (Karlsson et al., 2003). PIPs differ from all other plant AQPs by a highly conserved cysteine in the first extracellular loop (loop A). The conserved cysteines (C69 in SoPIP2;1) from all four monomers are located at the tetrameric center (Törnroth-Horsefield et al., 2006). Based on low resolution structures, it had been suggested that the reason for the conservation stems from the necessity to stabilize the PIP tetramers by fostering hydrogen bonds or complexing a metal ion (Kukulski et al., 2005).

To analyze the nature of possible interactions of the conserved cysteine (C69) in the tetramer, we probed possible disulfide

bridges by addition of reducing agents. For further analysis, we created mutants and purified the heterologously expressed proteins. In this study, we measured stability changes for cysteine 69 mutants and compared these to their kinetic properties to elucidate the structural and functional basis for the strong evolutionary conservation of this amino acid residue. In addition we show that mercury – generally regarded as a blocker of AQPs – is activating SoPIP2;1 and concentration-response experiments suggest that quenching of tryptophan fluorescence reports on conformational changes associated with the activation. Our findings of disulfide bridges and mercury activation are largely consistent with results recently published by other groups (Bienert et al., 2012; Frick et al., 2013).

RESULTS

A Conserved Cysteine Forms Disulfide Bridges between Monomers

To discern inter-monomeric interactions of SoPIP2;1 further, we decided to study structural and functional properties of isolated wild type (WT) and mutant protein. Therefore, we overexpressed SoPIP2;1 in *Pichia pastoris* and performed different stability tests of solubilized and purified protein. The isolated WT protein was incubated for various length of time with different reducing agents prior to analysis by SDS-PAGE, in order to monitor any effect of potentially disrupted disulfide bridges on the migration pattern in acrylamide gels (Figure 1). The relative amount of SDS resistant dimer in the gel could be decreased by DTT and β -mercaptoethanol. The latter was more effective, but none of the reducing agents could increase the monomer-to-dimer ratio further after the first hour of incubation. Surprisingly, the split of the dimer was not increased above 100 mM DTT and the final ratio of monomer to dimer was less than 1/10, while β -mercaptoethanol decreased the dimers by 50% at most (not

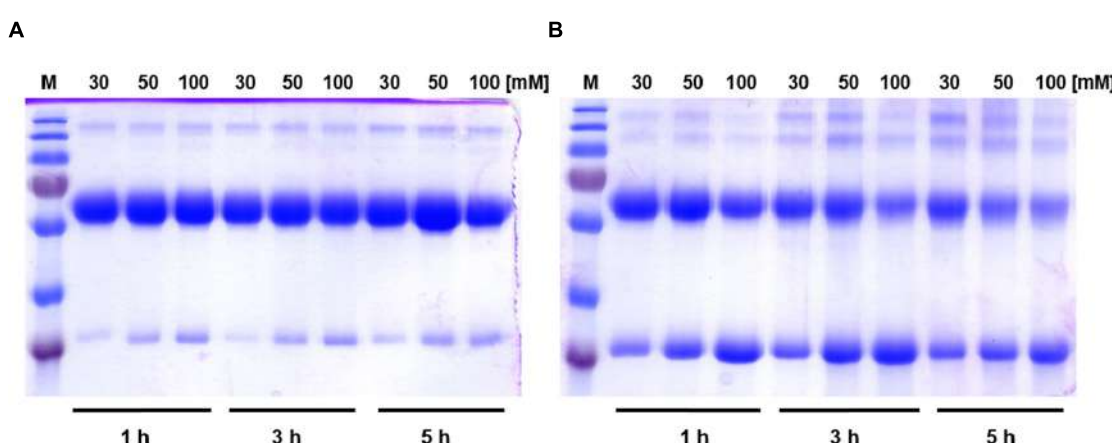


FIGURE 1 | The effect of reducing agents on relative amounts of dimers and monomers of SoPIP2;1. **(A)** Incubation of SoPIP2;1 with DTT. The concentration of DTT and the incubation time are shown at the top and at the bottom of the gel, respectively. It is evident from the gel that DTT is unable to completely reduce dimers into monomers, even after 5 h incubation with 100 mM DTT. **(B)** Effect of incubation of SoPIP2;1 with β -mercaptoethanol. The concentration of β -mercaptoethanol and the incubation time are shown on top and bottom of the gel, respectively. The results show that β -mercaptoethanol is more effective than DTT, but it still fails to reduce the dimers into monomers completely. M = molecular weight marker (from top 250, 130, 100, 70, 55, 35, and 25 kDa).

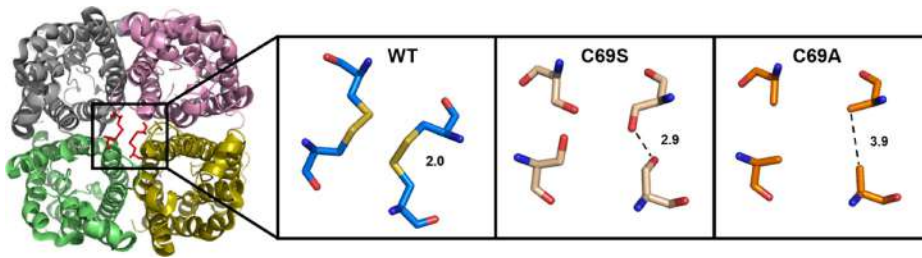


FIGURE 2 | Extracellular view of the SoPIP2;1 wild type (WT) tetramer with the expected disulfide bridges at the center (Left). Close up on C69 with distances between cysteines (PDB ID: 2B5F) or modeled residues in mutant proteins with this cysteine replaced by serine (Middle) or alanine (Right).

shown). Either this reflects the equilibrium between monomeric and dimeric fraction when all disulfide bonds are reduced, mainly stabilized by hydrophobic interactions (Törnroth-Horsefield et al., 2006), or some of the SDS solubilized dimers have disulfide bonds that are inaccessible so that they cannot be reduced under these conditions. The latter is supported by the apparent higher efficiency of β -mercaptoethanol which has about half the molecular weight compared to DTT. Adding urea to the reduction step increased the monomeric fraction (not shown). However, not even incubation for 1 h with 8 M urea and 300 mM DTT and resolving the samples on an 8 M denaturing urea gel was sufficient to completely remove the multimeric bands (Supplementary Figure 1). From a physical and evolutionary point of view it is of interest if the stability of the protein is changed upon removal of the cysteine. Two mutants, substituted at cysteine 69 with serine (C69S) or alanine (C69A) (Figure 2), were expressed and purified and their oligomeric patterns (as shown by standard SDS-PAGE) were compared to the WT protein (Figure 3A). Although dimeric bands were still visible in both mutants, they were significantly weaker as compared to the WT protein, which was expected from the destabilizing effect of reducing agents on dimers of the WT protein. In order to compare the thermodynamic stability of WT SoPIP2;1 and the two cysteine 69 mutants, we performed thermal denaturation circular dichroism (CD) spectroscopic measurements. A thermal denaturation curve was constructed based on the normalized mean residual ellipticity (MRE) at 222 nm (Figure 3B). The midpoint of transition in WT (56.9°C) was slightly higher in comparison with the mutants (54.6°C for C69S and 53.4°C for C69A), suggesting that the interactions at this position do not contribute much toward the thermodynamic stability, which is expected since the contribution of disulfide bonds to protein stability is kinetic rather than thermodynamic (Clarke and Fersht, 1993). Considering the high stability of SoPIP2;1 in lipid bilayers (Plasencia et al., 2011), it is not clear if the relatively small additional thermal stabilization due to the disulfide bonds is sufficient to explain the strict conservation of this cysteine.

Water Permeability Is Increased by Mutations in Loop A

To investigate if the disulfide bonds have an effect on function all three proteins were reconstituted in proteoliposomes to examine

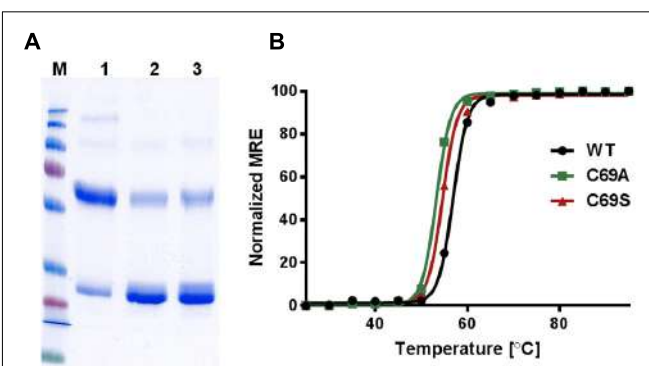
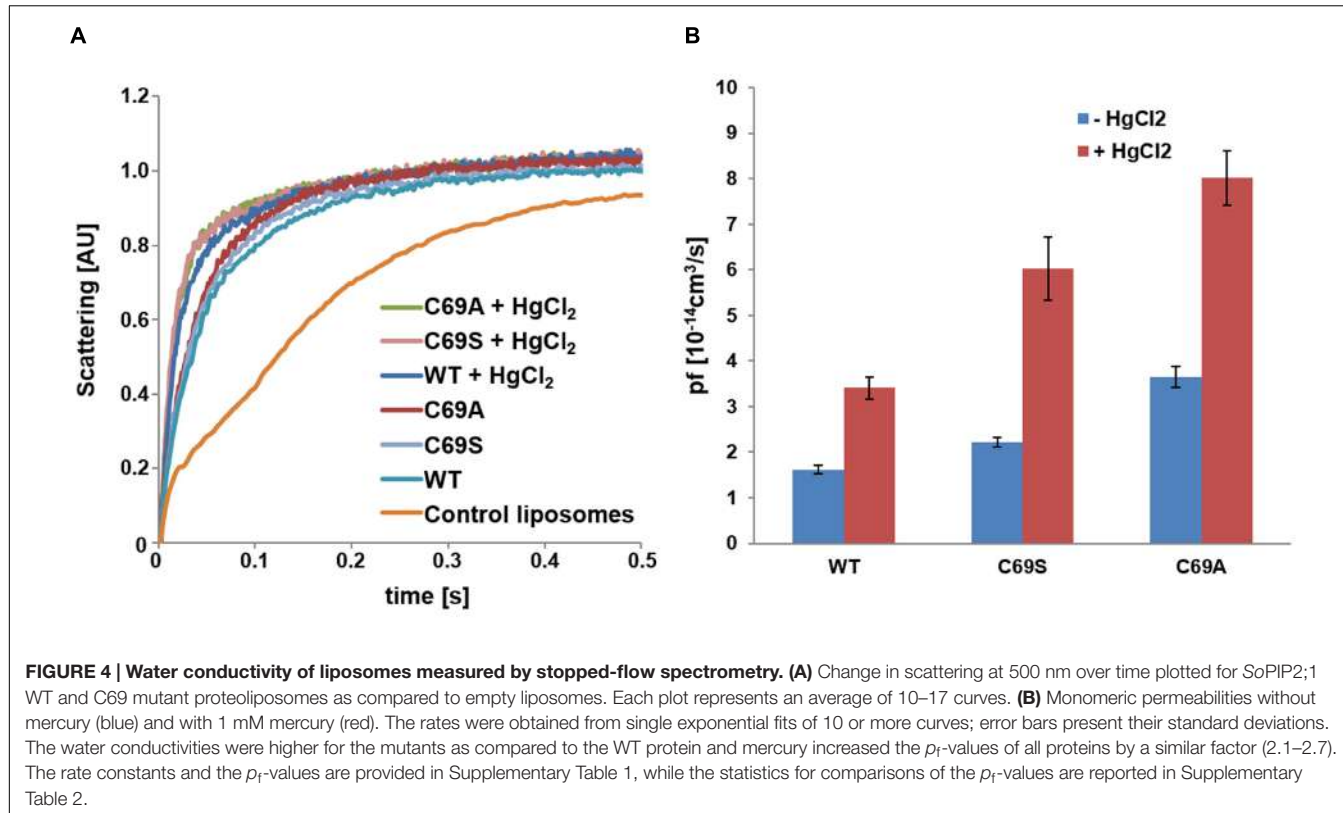


FIGURE 3 | Stability of WT SoPIP2;1 and the mutants C69A and C69S. (A) The integrity and purity of WT and mutant protein after Ni-NTA affinity chromatography were assessed by SDS-PAGE. 1 = WT SoPIP2;1, 2 = C69A, 3 = C69S. The purified WT SoPIP2;1 exists as tetramers under native conditions. Under standard denaturing conditions (SDS-PAGE), the WT SoPIP2;1 mainly runs as a dimer. In case of cysteine mutants, the monomeric form is predominant. This indicates that the cysteine residue in loop A is involved in disulfide bond formation between two PIP monomers. M = molecular weight marker (from top 250, 130, 100, 70, 55, 35, 25, 15, and 10 kDa). (B) Thermal denaturation of SoPIP2;1 recorded by CD spectrometry. The midpoint of the two-state unfolding transition is slightly higher for the WT (56.9°C) compared to the mutants (C69S 54.6°C ; C69A 53.4°C). The midpoints are based on one experiment. The normalized mean residual ellipticity (MRE) at 222 nm is plotted as a function of temperature.

their kinetic properties. Since the activity assays confirmed functional proteins (Figure 4A), we assessed their permeabilities. The protein content in the liposomes was estimated by quantitative western blots and the monomeric permeabilities, the p_f -values, were calculated. Surprisingly, the mutant C69S shows increased water permeability ($P < 0.001$) and this is even more pronounced in the C69A mutant ($P < 0.0001$; Figure 4B). The location of this residue immediately raises the question about water transport through the central pore. This scenario would be consistent with the observed larger enhancement of water permeability when cysteine is exchanged with an amino acid residue smaller than serine. Alternatively the increase is purely caused by destabilization of the dimer, where the alanine mutant would not be able to form hydrogen bonds like the serine mutant, which may partially compensate for the missing disulfide bridges.



Mercury Increases Water Permeability and Quench Intrinsic Tryptophan Fluorescence

If some water permeation is independent of the pore in the monomer, it could be measured by eliminating the conductivity of the monomeric pore. Beside reported pH and Ca^{2+} dependent gating, mercury is a well-known inhibitor of AQPs (Preston et al., 1993; Hukin et al., 2002). To our surprise, mercury instead increased the permeability of SoPIP2;1 proteoliposomes ($P < 0.0001$; Figure 4). If this effect is a result of conformational changes, there is a chance to observe mercury binding by CD measurements or by monitoring the intrinsic tryptophan fluorescence of SoPIP2;1. The CD spectrum of SoPIP2;1 in detergent micelles did not change significantly upon the addition of mercury (data not shown). However, the tryptophan fluorescence was altered and quenched by a factor of three after an incubation with 200 μM mercury chloride (Figure 5). Moreover, the quenching could be reversed by chelating mercury with β -mercaptoethanol, supporting that it is caused by reversible conformational changes rather than denaturation of SoPIP2;1. This is in accordance with the kinetic experiments, where mercury activation can be reversed by addition of β -mercaptoethanol (Figure 6A). It should be noted that the concentrations of reducing agent used for the reversal of quenching and activation, 1 and 2 mM, respectively, are much lower than the levels required to partially reduce the disulfide bridge of the dimers. Thus given the modest increase in activity of the C69S mutant completely lacking

the disulfide bridge, any increase due to reduction of cysteine 69 is expected to be small. This is consistent with the more or less identical rates of untreated proteoliposomes and the activated and reversed ditto. To investigate the concentration dependency of the activation stopped-flow experiments were done and the EC_{50} for mercury was calculated to be around 4 μM (Figure 6B). Interestingly, a concentration-response curve of the quenching of tryptophan fluorescence gives an EC_{50} value of 1.6 μM (Figure 7). Thus the quenching in micelles may be caused by conformational changes associated with activation in proteoliposomes.

Activation by Mercury and by Loop A Mutations Are Additive

Cysteine 69 mutants present an increased water transport compared to the WT, which might be explained by opening of a tetrameric central pore or by indirect effects on the structure of the monomeric pore. WT SoPIP2;1 can be activated by mercury, but are the cysteine mutants also affected by mercury? Analysis of stopped-flow data, showed that the activation by mercury and the increase of permeability by mutations were not overlapping, but additive (Figure 4B). While the p_f of the WT permeability changes from 1.6 ± 0.1 to 3.4 ± 0.2 [$10^{-14} \text{ cm}^3/\text{s}$], the p_f of alanine and serine mutants are amplified by about the same factor, rising from 3.6 ± 0.2 to 8.0 ± 0.6 and 2.2 ± 0.1 to 6.0 ± 0.7 [$10^{-14} \text{ cm}^3/\text{s}$], respectively. This suggest that the mercury activation is independent of the increase in water permeability caused by the mutations in loop A.

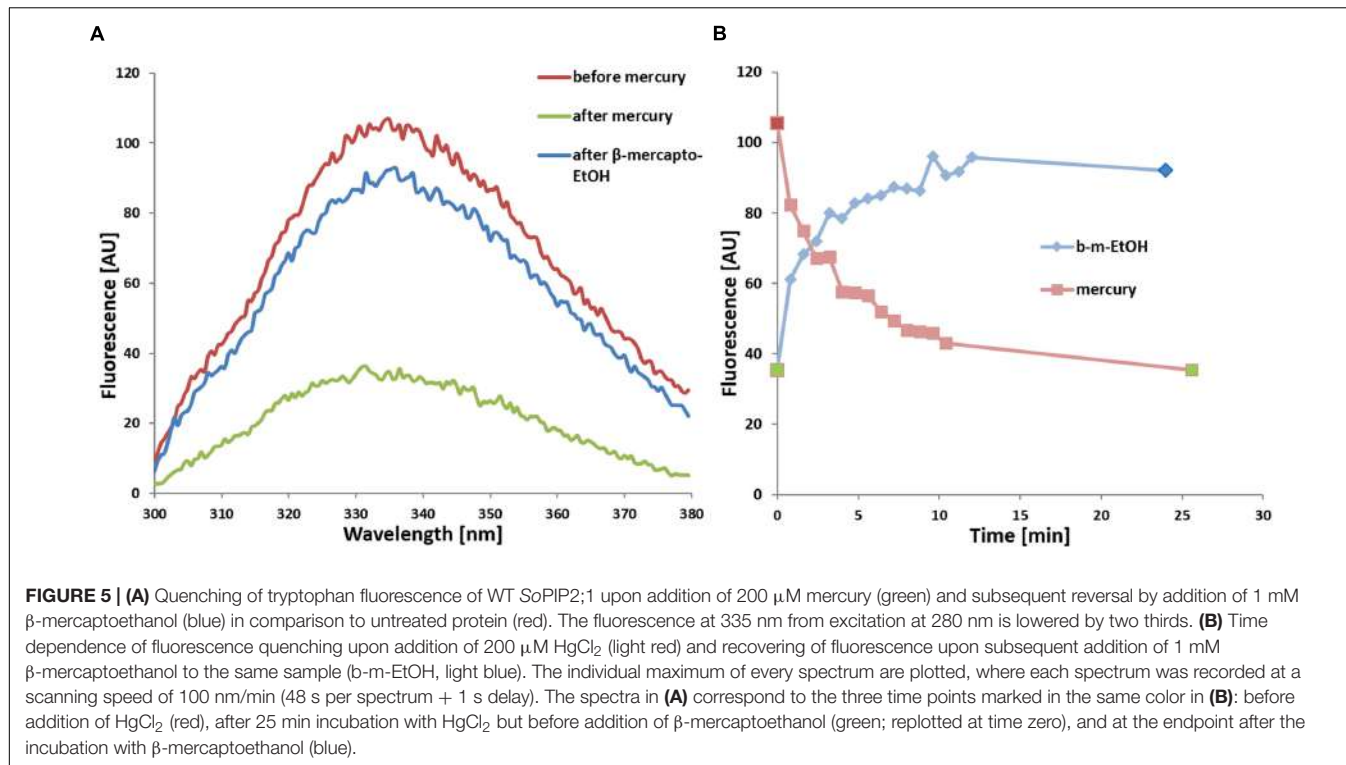


FIGURE 5 | (A) Quenching of tryptophan fluorescence of WT SoPIP2;1 upon addition of 200 μ M mercury (green) and subsequent reversal by addition of 1 mM β -mercaptoethanol (blue) in comparison to untreated protein (red). The fluorescence at 335 nm from excitation at 280 nm is lowered by two thirds. **(B)** Time dependence of fluorescence quenching upon addition of 200 μ M $HgCl_2$ (light red) and recovering of fluorescence upon subsequent addition of 1 mM β -mercaptoethanol to the same sample (b-m-EtOH, light blue). The individual maximum of every spectrum are plotted, where each spectrum was recorded at a scanning speed of 100 nm/min (48 s per spectrum + 1 s delay). The spectra in **(A)** correspond to the three time points marked in the same color in **(B)**: before addition of $HgCl_2$ (red), after 25 min incubation with $HgCl_2$ but before addition of β -mercaptoethanol (green; replotted at time zero), and at the endpoint after the incubation with β -mercaptoethanol (blue).

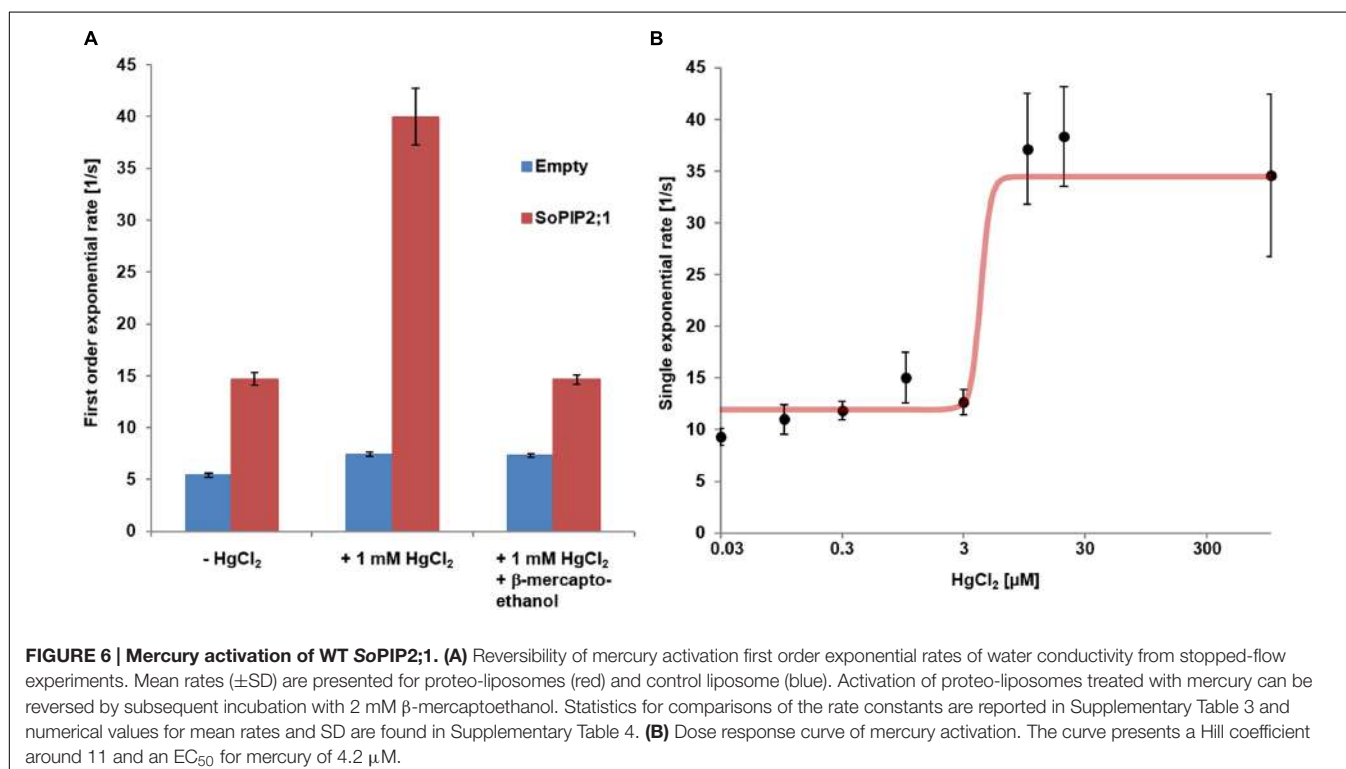
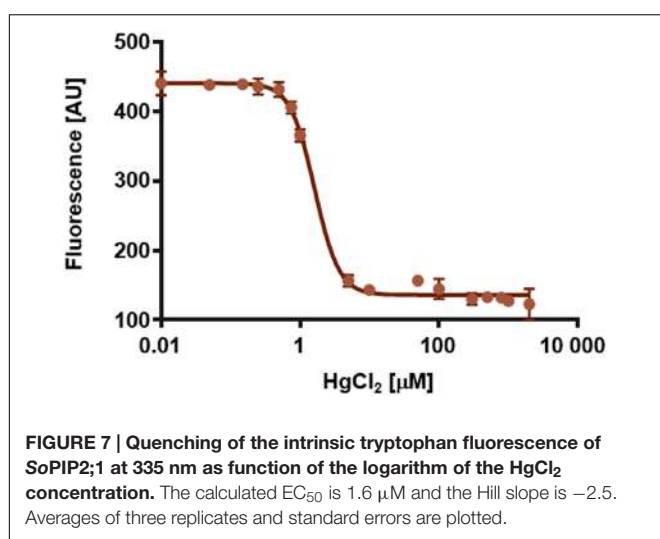


FIGURE 6 | Mercury activation of WT SoPIP2;1. (A) Reversibility of mercury activation first order exponential rates of water conductivity from stopped-flow experiments. Mean rates (\pm SD) are presented for proteo-liposomes (red) and control liposome (blue). Activation of proteo-liposomes treated with mercury can be reversed by subsequent incubation with 2 mM β -mercaptoethanol. Statistics for comparisons of the rate constants are reported in Supplementary Table 3 and numerical values for mean rates and SD are found in Supplementary Table 4. **(B)** Dose response curve of mercury activation. The curve presents a Hill coefficient around 11 and an EC_{50} for mercury of 4.2 μ M.

DISCUSSION

This work was originally initiated to describe intermonomeric interactions and their effects. The effect of reducing agents

on the oligomeric pattern in SDS-PAGE indicated the existence of disulfide bonds that stabilize protein dimers. This was also concluded in studies mutating corresponding cysteines in the tetrameric center of various PIP2s from



maize (Bienert et al., 2012). Additional to the more detailed analysis of disulfide bridges in the tetrameric center, we discovered that our preparation of SoPIP2;1 was not maximally permeable under our standard conditions. It should be noted that the obtained p_f -values here (1.6–8.0 [$10^{-14}\text{cm}^3\text{s}^{-1}$]) are in the same range as has been estimated for other AQPs using *Xenopus* oocytes (0.2–24 [$10^{-14}\text{cm}^3\text{s}^{-1}$]; Yang and Verkman, 1997) and correspond to a passage of more than 10^{11} water molecules per second through each monomer of SoPIP2;1. Although activation of a water specific channel by mercury is unlikely to have a physiological role, the molecular details of its binding and conformational changes may still be relevant for our understanding of physiological gating mechanisms.

Increased Permeability in Mutants and by Mercury

Our results suggest that the mechanism for activation by mercury is independent of the enhancement of water permeability caused by the mutations in the A loop. A simple mechanistic explanation of this would be that permeation through the monomeric pore is increased in the mutants and this is amplified by mercury by stabilization of the gate in an open conformation. However, looking at the structure it is not obvious how a mutation of cysteine 69 could achieve this, but it cannot be excluded that the release of loop A is resulting in a relaxation at the selectivity filter and thereby a higher permeability. If instead also the central pore of the mutant proteins permeates water, how would that be enhanced by mercury binding? Possibly in the same way mercury may support the open conformation of loop D at the monomeric pore; the C-terminal end is removed from its position in the inter-monomeric space. If the highest energy barrier for water permeation through the central pore is caused by interactions between the four C-termini, a destabilization of the C-terminal regions would increase the water leakage through this hypothetical pore. One should keep in mind that these

C-terminal interactions are not structurally supported as the last modeled amino acid residues in the closed structures are still too far from the center. Thus a possible contribution of the central pore to the increased permeability remains speculative.

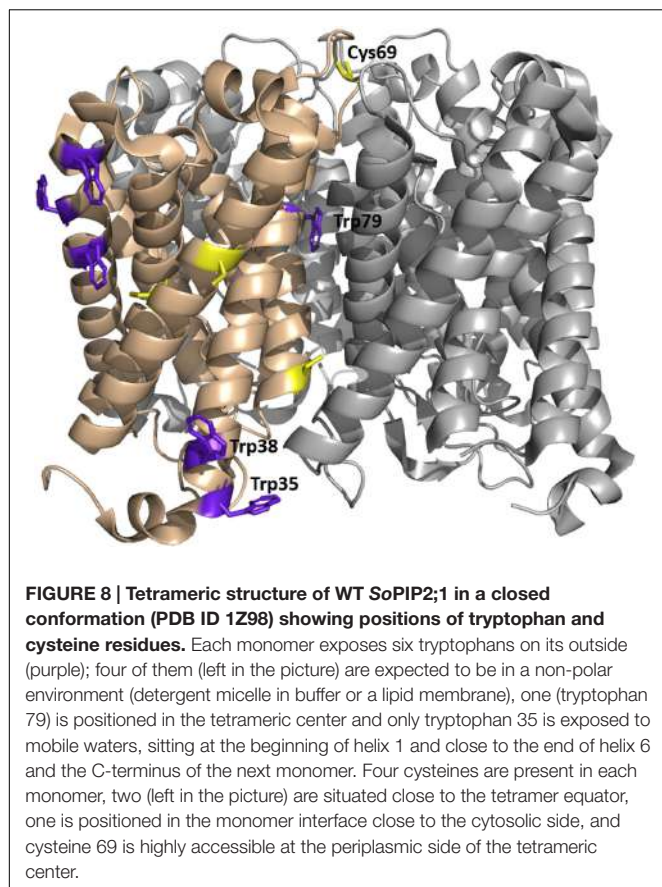
Tryptophan Fluorescence

The observation that both activation and quenching of tryptophan fluorescence can be triggered by the same ligand, mercury, may suggest that these two effects are not independent but caused by structural rearrangements initiated from the same binding site. So where is the mercury binding and which conformational changes lead to a fluorescence drop of 2/3? If all six tryptophans of the monomer have the same quantum yield, at least four of them must be quenched. That involves a huge structural change of the protein or putatively a rearrangement of the micelle. Restructuring the micelle of a membrane protein is thought to denature the protein, which is unlikely here, as quenching (Figure 5) and increase in activity (Figure 6A) are both reversible, and no denaturation was indicated in CD measurements or by precipitating protein (data not shown). Fluorescence intensity of tryptophans can vary greatly depending on their environment (Lakowicz, 2006). Therefore, it appears more likely that one or two tryptophans with high quantum yields, located in a hydrophobic/hydrophilic interface, are responsible for the observed quenching of fluorescence by mercury. According to analyses of structural parameters tryptophans can be classified into five spectral-structural classes (Shen et al., 2008). The observed emission maximum at 335 nm would suggest that Class I and possibly Class II tryptophans dominate the fluorescence spectrum of SoPIP2;1. This automatic analysis of PDB-files is most likely not applicable for tryptophans that are expected to interact with detergents in a micelle, since the micelle is not included in the structure file. However, it should be relevant for buried residues, like tryptophan 79 situated at the center of the tetramer (Figure 8). Based on the closed tetrameric structure (4JC6, omitting detergents or metal atoms) this residue belongs to Class S with an expected emission maximum range between 321 and 325 nm, and is therefore not likely to contribute much to the intensity at 335 nm.

As speculated above the mercury activation may be achieved by stabilizing an open conformation and interestingly the positions of tryptophans 35 and 38 differ in the open and closed structure (Törnroth-Horsefield et al., 2006). In the closed structure tryptophan 35 is potentially in a hydrophobic-polar interface and close to the C-terminus of the next monomer. In the open structure of SoPIP2;1 tryptophan 35 is repositioned and in addition this conformation is expected to have released the C-terminus, which could have an effect on the environment of tryptophan 35 and therefore quench its fluorescence.

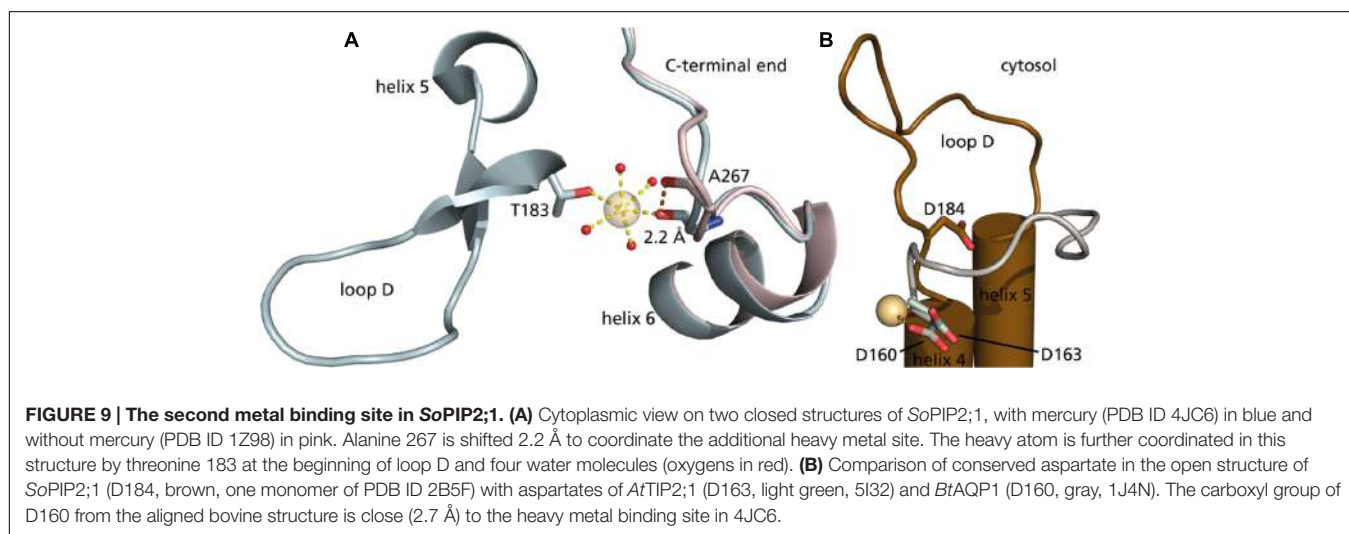
Mercury Binding Site

In a mutational study of SoPIP2;1 by Frick et al. (2013) it was found that mercury activation is independent of the presence



of cysteines. They were able to determine a structure at 2.15 Å with bound mercury and cadmium, in a closed conformation. Additional to the expected binding to cysteines and the known Ca²⁺ site, a new metal binding site was reported. It is described as a second binding site for cadmium, but given the comparable size of the cations and similar preference for hexagonal coordination, one could imagine that also mercury has a potential to bind.

The metal seen at this site interacts with a carbonyl (A267) from the C-terminal region (**Figure 9A**). The carbonyl of A267 is actually occupying the same space as the carbonyl of A266 in the first closed structure of SoPIP2;1 (Törnroth-Horsefield et al., 2006), and consequently there is a different position and orientation of preceding residues up to the end of helix 6. This distinctive change in the structure does not change the averaged static view on the C-terminal regions, which overall are located at the interfaces of the monomers in a closed conformation. Still, the binding strength might be reduced and thereby lower the probability to find this conformation in solution. The conformation of the protein when incubated in β-mercaptoethanol after binding mercury does not change within seconds (**Figure 5B**). We expect that mercury binding or chelating is much faster. Thus, the observed time dependence could be a result of the restructuring of the C-terminal end. If the activation is caused by destabilization of the C-terminal stretch, the effect could be reduced in situations where it is already destabilized for other reasons. This is observed, when comparing the permeability of an untagged SoPIP2;1 WT and the permeability of the same isoform that ends with a c-myc epitope followed by a hexa-his-tag. The basal (i.e., not fully activated) permeability is higher for the tagged protein, seemingly because the closed conformation of the unphosphorylated C-terminal end is less stabilized (data not shown). It should not go unnoticed that similar conclusions were drawn before (Nyblom, 2008, Ph.D. thesis, paper III, page 5). When incubated with mercury the specific water permeability, of both the tagged and untagged protein, levels out at approximately the same permeability values. Conclusively, destabilization by binding of mercury overlaps the destabilization caused by the tag, suggesting that the gate is close to its maximum opening probability in the mercury activated state. Frick et al. (2013) suggested an indirect activation of SoPIP2;1 via a mercury induced change in membrane properties. This possibility cannot be ruled out, but the relatively low EC₅₀ of about 4 μM, which is about 10-fold lower than the IC₅₀ for HsAQP5 in proteoliposomes with the same lipid composition (Horsefield et al., 2008), and the correlation with the quenching



of fluorescence in micelles, would argue for a direct binding to and activation of SoPIP2;1.

Here, we describe the activation by mercury as a result of moving serine 274 away to leave space for leucine 197 in an open position, to promote the conformation. However, could mercury further stabilize the open conformation? As mercury is positively charged, we looked for a negatively charged residue in the vicinity. There is an aspartate in loop D, which is conserved among water-specific AQPs from both plants and animals. This residue approaches the binding site in the open conformation (**Figure 9B**), but the distance is still too far. Comparison to other water-specific AQPs suggests that the aspartate could come close enough to bind mercury and thereby stabilize the D-loop in an open position. Although the aspartate corresponding to aspartate 184 in SoPIP2;1 is well conserved not only among PIPs, there is considerable sequence variation at the position aligned to alanine 267 of SoPIP2;1 even within the PIP2 group, making it difficult discern if the proposed activation mechanism is valid for other PIPs. However, the fact that it is the back bone carbonyl of this residue that contributes to the metal binding site, and the general observation that structure is more conserved than sequence, argues that the binding site and the suggested mechanism may be relevant also for other PIP2s of terrestrial plants. It should be noted that the plant plasma membrane has a different lipid composition and is much more complex than the liposomes of *E. coli* lipids used here. Hence, the relevance of the demonstrated mercury activation remains to be shown in a physiological context where indirect effects by mercury via interacting lipids or proteins may override a direct activation.

Is There a Central Pore?

The functionality of the protein is determined by stabilization of certain conformational states and thereby dependent on the availability of certain interacting residues, not only within a monomer, but also with neighboring monomers. This has already been described for many proteins and underlines that proteins evolve based on their final oligomeric structure. This brings us back to cysteine 69, which is found to be strongly conserved among PIPs and covalently links the monomers but does not add much thermodynamic stability. Interaction studies with PIPs in maize demonstrated that expression rate and localization is also independent of disulfide bond formation (Bienert et al., 2012). Taking only our own results into account, one could suggest the prevention of water leakage through the tetrameric center, but this is inconclusive with the mutational study of maize PIPs measured in oocytes. As the utilized maize PIP2 is very similar to SoPIP2;1, the most prominent difference between these studies is the protein environment. As several AQP structures, including SoPIP2;1, have presented a detergent or a lipid molecule in the tetrameric center (Jiang et al., 2006; Horsefield et al., 2008; Frick et al., 2013), one could assume the presence of a lipid molecule at these sites in the native environment to avoid water or even proton leakage. In this study, the protein was heterologously expressed and extracted from the hydrophobic environment by a detergent. These detergent molecules are capable of removing most or all of the lipid molecules bound to the protein. Additionally, the protein–lipid

mixture was thoroughly dialyzed to reconstitute this protein in liposomes, potentially removing all detergent molecules. Thus cysteine 69 mutants could leak water through a central pore. As other AQP isoforms without this cysteine have also evolved to be proton tight, there is probably a different reason for the high degree of conservation. We therefore agree with Bienert et al. (2012) that disulfide bonds between monomers result in a higher kinetic stability and thereby stabilize the oligomeric state of the protein, which may comprise certain functions *in planta*.

CONCLUSION

In agreement with studies on maize PIPs we show that disulfide bridges stabilize the oligomeric state of SoPIP2;1, but contrary to results on maize PIPs we find that mutations preventing the disulfide bridge increase the permeability. Furthermore, the permeability of both WT and mutant protein can be enhanced by mercury and based on quenching of the intrinsic tryptophan fluorescence by mercury we speculate on a binding site, possibly responsible for both effects of this heavy metal. Mercury has been regarded as general inhibitor for AQPs and therefore used to classify observed *in vivo* phenomena as being “AQP dependent.” The sole possibility that some AQPs under certain circumstances can be activated by mercury puts these conclusions into a new perspective. Mercury is not a physiological relevant ligand to regulate protein function, but presents a tool to study functional properties of the gating mechanism of PIPs and thereby potentially revealing new opportunities to modulate water homeostasis in plants.

MATERIALS AND METHODS

Overexpression and Purification of Cysteine Mutants of SoPIP2;1

Cysteine mutants of SoPIP2;1 were generated by using Quickchange site directed mutagenesis kit (Stratagene), using the plasmid pPICZB-SoPIP2;1 (WT) with C-terminal His-tag as a template (Karlsson et al., 2003). Mutations were confirmed by DNA sequencing (Eurofins MWG operon). Mutants were overexpressed in methylotropic yeast *Pichia pastoris* as previously described (Karlsson et al., 2003) for WT SoPIP2;1 purification. Similar procedure was followed for membrane preparation and purification of mutated proteins as described previously (Karlsson et al., 2003) with a minor change; the detergent used in the present study is *n*-Octyl- β -D-Glucopyranoside (OG; Affymetrix, O311).

Electrophoresis

The purified SoPIP2;1 (WT) was incubated at room temperature for varying time periods, with different concentration of dithiothreitol (DTT) or β -mercaptoethanol to reduce the dimeric form into monomers. After incubation with reducing agent the sample loading buffer (125 mM Tris-HCl, pH 6.8, 20% glycerol, 4% SDS) was mixed with protein sample and further

incubated for 10 min at room temperature. To monitored the effect of reducing agent concentration and incubation time, the oligomeric forms of the protein were resolved by SDS-PAGE (12%) and visualized by staining with coomassie brilliant blue R250 (Laemmli, 1970).

In order to compare the SDS-PAGE profile of the WT and mutant proteins (**Figure 3**), the protein was directly mixed with sample loading buffer (as mentioned above) supplemented with 10% β -mercaptoethanol and incubated for 10 min at room temperature, before resolving on SDS-PAGE (12%).

Circular Dichroism (CD) Spectroscopy

Far-UV CD spectra were measured for the WT SoPIP2;1 and the mutants using a Jasco J-720 spectrometer (Jasco, Tokyo, Japan). Spectra were recorded at 25–95°C (with 5°C interval) between 250 nm and 190 nm at 20 nm/min as an average of three scans with a response time 8 s and a data pitch of 0.1 nm. Baselines were collected in the same manner on the buffer solution, and spectra were baseline corrected (Galka et al., 2008; Plasencia et al., 2011).

Mean residue ellipticity (MRE, $[\theta]_M \times 10^{-3}$ deg cm² dmol⁻¹) was calculated by using Eq. (1).

$$[\theta]_M = M \times \theta / (10 \times l \times c \times n) \quad (1)$$

where M is the molecular weight of protein (e.g., 32512 g/mol), θ is the measured ellipticity in millidegrees, l is the cell path length, c is the concentration in [g/l], and n is the number of residues (303).

The MRE at 222 nm was plotted over temperature. For curve fitting, following Boltzmann sigmoidal equation was used:

$$Y_{\text{obs}} = Y_{\text{native}} - \frac{Y_{\text{denatured}} - Y_{\text{native}}}{1 + e^{T_{1/2} - \frac{T}{m}}} \quad (2)$$

Where Y_{obs} is the MRE, $T_{1/2}$ is the temperature at which MRE is halfway between native and denatured state, m is the slope of the curve. Data was analyzed using Prism (Graphpad software, Inc.).

Reconstitution into Liposomes

E. coli POLAR lipids (Avanti) provided in chloroform were dried with N₂ for 4 h and kept at –20°C until use. For reconstitution the lipids were solubilized with 10% OG in dialyze buffer (20 mM Tris pH 8, 100 mM NaCl, 0.003% NaN₃, 2 mM DTT) for concentration of 4 mg/mL and aliquoted. Proteins were added and solution was mixed thoroughly. Lipid–protein mix was diluted with dialyze buffer to 2 mg/mL lipids and 66 μ g/mL proteins (LPR30) and dialyzed using a membrane with 6–8 kDa cut-off (Spectrum Laboratories) against dialyze buffer for 7 days at room temperature.

Water Conductivity

Liposomes were extruded 11 times with a pore size of 200 nm (Avestin) and their resulting average radius was determined by dynamic light scattering DLS (Malvern Zetasizer). Samples were diluted with dialyze buffer (with or without mercury) to

0.2 mg/mL lipids. To show that activation of the protein is reversible, a sample incubated for 30 min with 1 mM HgCl₂, 2 mM β -mercaptoethanol was added and incubated at least 30 min further prior to the activity assay. Water transport activity was measured by stopped-flow with a hyper-osmolar gradient of 100 mM sorbitol using Hi-Tech stopped-flow device at a volume of 150 μ L per shot. Rise in scattering upon shape change due to water transport out of the vesicles was observed at 90° angle at a wavelength of 500 nm. Unless mentioned otherwise, single exponential functions were fitted to 10 to 17 individual curves by the software Kinetic Studio (TgK Scientific Limited 2010). Total water permeability P_f is used to calculate individual p_f -values by multiplying relative P_f [P_f (proteoliposome) – P_f (control liposomes)] with the surface area of the liposome and dividing with the number of monomers per vesicle.

$$P_f = k \cdot \frac{V_0}{A \cdot V_w \cdot c_{\text{out}}} \quad (3)$$

$$p_f = \frac{(P_f - P_{f, \text{control}}) \cdot A}{\# \text{monomers}} \quad (4)$$

Protein concentration was analyzed by Western-blot using tetra-His antibody, and vesicle concentration was calculated assuming no lipid loss during dialysis and an area of 0.52 nm² per lipid molecule (for a monolayer). To construct a dose response curve of mercury activation, single exponential rates from 10 to 16 stopped-flow measurements were averaged per samples exposed to different mercury concentration; each average is presented with their standard deviations. Curve fitting was done employing a Hill-function.

Statistical Analyses

The significance was analyzed in Prism (Graphpad software, Inc.), using the unpaired *t*-test with Welch's correction and two-tailed *P*-values.

Tryptophan Fluorescence

Fluorescence was measured with His-tag purified and desalted protein in Buffer A supported by 0.8% OG. Monochromatic light at a wavelength of 280 nm was used for excitation while scans were done from 300 to 380 nm at a speed of 100 nm/min and a data pitch of 0.5 nm. Fifteen scans were accumulated to reduce noise. For kinetic experiments, mercury chloride to a final concentration of 200 μ M was added and briefly mixed before starting scans. First, single records were done with a delay of 1 s, resulting in one plot every 49 s. The averages of five data points were used to determine height of the curve maximum. After incubating for 25 min, another accumulated spectrum was recorded. Sequentially, β -mercaptoethanol to a final concentration of 1 mM was added to reverse the binding, followed by the same measurement procedure as before.

For dose-response experiments, the sample was pre-incubated with mercury chloride at room temperature for 15 min before

recording the fluorescence between 310 and 400 nm. Three scans were accumulated to reduce the noise and the measurement was repeated three times. The emission data at 335 nm were fitted with four parameters to sigmoidal dose response equation using Prism version 6.00 (GraphPad Software, La Jolla, CA, USA) to estimate the EC₅₀ value.

AUTHOR CONTRIBUTIONS

AK and SS contributed equally to this work, did all the technical work, and analyzed the data. PK and UJ conceived the project. AK drafted the manuscript and all authors contributed to writing of the final article.

REFERENCES

- Abascal, F., Irisarri, I., and Zardoya, R. (2014). Diversity and evolution of membrane intrinsic proteins. *Biochim. Biophys. Acta* 1840, 1468–1481. doi: 10.1016/j.bbagen.2013.12.001
- Alexandersson, E., Danielson, J. A., Råde, J., Moparthi, V. K., Fontes, M., Kjellbom, P., et al. (2010). Transcriptional regulation of aquaporins in accessions of *Arabidopsis* in response to drought stress. *Plant J.* 61, 650–660. doi: 10.1111/j.1365-313X.2009.04087.x
- Alexandersson, E., Fraysse, L., Sjövall-Larsen, S., Gustavsson, S., Fellert, M., Karlsson, M., et al. (2005). Whole gene family expression and drought stress regulation of aquaporins. *Plant Mol. Biol.* 59, 469–484. doi: 10.1007/s11103-005-0352-1
- Bienert, G. P., Cavez, D., Besserer, A., Berny, M. C., Gilis, D., Rooman, M., et al. (2012). A conserved cysteine residue is involved in disulfide bond formation between plant plasma membrane aquaporin monomers. *Biochem. J.* 445, 101–111. doi: 10.1042/bj20111704
- Clarke, J., and Fersht, A. R. (1993). Engineered disulfide bonds as probes of the folding pathway of barnase: increasing the stability of proteins against the rate of denaturation. *Biochemistry* 32, 4322–4329. doi: 10.1021/bi00067a022
- Danielson, J. A. H., and Johanson, U. (2010). “Phylogeny of Major Intrinsic Proteins,” in *Mips and Their Role in the Exchange of Metalloids*, eds T. P. Jahn and G. P. Bienert (New York, NY: Springer), 19–32.
- Frick, A., Järvinen, M., Ekwall, M., Uzdavinys, P., Nyblom, M., and Törnroth-Horsefield, S. (2013). Mercury increases water permeability of a plant aquaporin through a non-cysteine-related mechanism. *Biochem. J.* 454, 491–499. doi: 10.1042/BJ20130377
- Fu, D., Libson, A., Miercke, L. J., Weitzman, C., Nollert, P., Krucinski, J., et al. (2000). Structure of a glycerol-conducting channel and the basis for its selectivity. *Science* 290, 481–486. doi: 10.1126/science.290.5491.481
- Galka, J. J., Baturin, S. J., Manley, D. M., Kehler, A. J., and O’neil, J. D. (2008). Stability of the glycerol facilitator in detergent solutions. *Biochemistry* 47, 3513–3524. doi: 10.1021/bi7021409
- Horsefield, R., Nordén, K., Fellert, M., Backmark, A., Törnroth-Horsefield, S., Terwisscha van Scheltinga, A. C., et al. (2008). High-resolution x-ray structure of human aquaporin 5. *Proc. Natl. Acad. Sci. U.S.A.* 105, 13327–13332. doi: 10.1073/pnas.0801466105
- Hukin, D., Doering-Saad, C., Thomas, C. R., and Pritchard, J. (2002). Sensitivity of cell hydraulic conductivity to mercury is coincident with symplasmic isolation and expression of plasmalemma aquaporin genes in growing maize roots. *Planta* 215, 1047–1056. doi: 10.1007/s00425-002-0841-2
- Jiang, J., Daniels, B. V., and Fu, D. (2006). Crystal structure of AqpZ tetramer reveals two distinct Arg-189 conformations associated with water permeation through the narrowest constriction of the water-conducting channel. *J. Biol. Chem.* 281, 454–460. doi: 10.1074/jbc.M508926200
- Johanson, U., Karlsson, M., Johansson, I., Gustavsson, S., Sjövall, S., Fraysse, L., et al. (2001). The complete set of genes encoding major intrinsic proteins in *Arabidopsis* provides a framework for a new nomenclature for major intrinsic proteins in plants. *Plant Physiol.* 126, 1358–1369. doi: 10.1104/pp.126.4.1358
- Johansson, I., Karlsson, M., Shukla, V. K., Chrispeels, M. J., Larsson, C., and Kjellbom, P. (1998). Water transport activity of the plasma membrane aquaporin PM28A is regulated by phosphorylation. *Plant Cell* 10, 451–459. doi: 10.1105/tpc.10.3.451
- Johansson, I., Larsson, C., Ek, B., and Kjellbom, P. (1996). The major integral proteins of spinach leaf plasma membranes are putative aquaporins and are phosphorylated in response to Ca²⁺ and apoplastic water potential. *Plant Cell* 8, 1181–1191. doi: 10.1105/tpc.8.7.1181
- Karlsson, M., Fotiadis, D., Sjövall, S., Johansson, I., Hedfalk, K., Engel, A., et al. (2003). Reconstitution of water channel function of an aquaporin overexpressed and purified from *Pichia pastoris*. *FEBS Lett.* 537, 68–72. doi: 10.1016/S0014-5793(03)00082-6
- Kirsch, A., Kaptan, S. S., Bienert, G. P., Chaumont, F., Nissen, P., de Groot, B. L., et al. (2016). Crystal structure of an ammonia-permeable aquaporin. *PLoS Biol.* 14:e1002411. doi: 10.1371/journal.pbio.1002411
- Kukulski, W., Schenk, A. D., Johanson, U., Braun, T., de Groot, B. L., Fotiadis, D., et al. (2005). The 5A structure of heterologously expressed plant aquaporin SoPIP2;1. *J. Mol. Biol.* 350, 611–616. doi: 10.1016/j.jmb.2005.05.001
- Laemmli, U. K. (1970). Cleavage of structural proteins during the assembly of the head of bacteriophage T4. *Nature* 227, 680–685. doi: 10.1038/227680a0
- Lakowicz, J. R. (ed.) (2006). *Principles of Fluorescence Spectroscopy*. Berlin: Springer.
- Nyblom, M. (2008). *Water Transport Regulation: Biochemical and Structural Analyses of Eukaryotic Aquaporins*. Ph.D. thesis, Chalmers University of Technology, Gothenburg.
- Nyblom, M., Frick, A., Wang, Y., Ekwall, M., Hallgren, K., Hedfalk, K., et al. (2009). Structural and functional analysis of SoPIP2;1 mutants adds insight into plant aquaporin gating. *J. Mol. Biol.* 387, 653–668. doi: 10.1016/j.jmb.2009.01.065
- Plasencia, I., Survery, S., Ibragimova, S., Hansen, J. S., Kjellbom, P., Helix-Nielsen, C., et al. (2011). Structure and stability of the spinach aquaporin SoPIP2;1 in detergent micelles and lipid membranes. *PLoS ONE* 6:e14674. doi: 10.1371/journal.pone.0014674
- Preston, G. M., Jung, J. S., Guggino, W. B., and Agre, P. (1993). The mercury-sensitive residue at cysteine 189 in the CHIP28 water channel. *J. Biol. Chem.* 268, 17–20.
- Shen, C., Menon, R., Das, D., Bansal, N., Nahar, N., Guduru, N., et al. (2008). The protein fluorescence and structural toolkit: database and programs for the analysis of protein fluorescence and structural data. *Proteins* 71, 1744–1754. doi: 10.1002/prot.21857

FUNDING

This work was supported by the Swedish Research Council.

ACKNOWLEDGMENT

We thank Adine Karlsson for technical assistance and Dr S. Raza Haq for help with statistical analyses.

SUPPLEMENTARY MATERIAL

The Supplementary Material for this article can be found online at: <http://journal.frontiersin.org/article/10.3389/fpls.2016.01249>

- Sui, H., Han, B. G., Lee, J. K., Walian, P., and Jap, B. K. (2001). Structural basis of water-specific transport through the AQP1 water channel. *Nature* 414, 872–878. doi: 10.1038/414872a
- Törnroth-Horsefield, S., Wang, Y., Hedfalk, K., Johanson, U., Karlsson, M., Tajkhorshid, E., et al. (2006). Structural mechanism of plant aquaporin gating. *Nature* 439, 688–694. doi: 10.1038/nature04316
- Yang, B., and Verkman, A. S. (1997). Water and glycerol permeabilities of aquaporins 1–5 and MIP determined quantitatively by expression of epitope-tagged constructs in *Xenopus* oocytes. *J. Biol. Chem.* 272, 16140–16146. doi: 10.1074/jbc.272.26.16140

Conflict of Interest Statement: The authors declare that the research was conducted in the absence of any commercial or financial relationships that could be construed as a potential conflict of interest.

Copyright © 2016 Kirscht, Survery, Kjellbom and Johanson. This is an open-access article distributed under the terms of the Creative Commons Attribution License (CC BY). The use, distribution or reproduction in other forums is permitted, provided the original author(s) or licensor are credited and that the original publication in this journal is cited, in accordance with accepted academic practice. No use, distribution or reproduction is permitted which does not comply with these terms.



Corrigendum: Increased Permeability of the Aquaporin SoPIP2;1 by Mercury and Mutations in Loop A

Andreas Kirscht [†], Sabeen Survery [†], Per Kjellbom and Urban Johanson ^{*}

Department of Biochemistry and Structural Biology, Center for Molecular Protein Science, Lund University, Lund, Sweden

Keywords: aquaporin, water channel, major intrinsic protein, *Spinacia oleracea*, tryptophan fluorescence

A corrigendum on

OPEN ACCESS

Edited and reviewed by:

Rupesh Kailasrao Deshmukh,
Laval University, Canada

*Correspondence:
Urban Johanson
urban.johanson@biochemistry.lu.se

[†]Shared first authors.

Specialty section:

This article was submitted to
Plant Physiology,
a section of the journal
Frontiers in Plant Science

Received: 21 November 2016

Accepted: 30 November 2016

Published: 19 December 2016

Citation:

Kirscht A, Survery S, Kjellbom P and Johanson U (2016) Corrigendum: Increased Permeability of the Aquaporin SoPIP2;1 by Mercury and Mutations in Loop A. *Front. Plant Sci.* 7:1888. doi: 10.3389/fpls.2016.01888

Increased Permeability of the Aquaporin SoPIP2;1 by Mercury and Mutations in Loop A
by Kirscht A., Survery S., Kjellbom P., and Johanson U. (2016) *Front. Plant Sci.* 7:1249. doi: 10.3389/fpls.2016.01249

In our Original Research article it was incorrectly stated that cadmium and mercury have a similar preference for hexagonal coordination. Although both cadmium and mercury can bind at octahedral (not hexagonal) coordination sites their coordination preferences are not similar (Rulisek and Vondrasek, 1998). Hence, the fourth sentence under the subheading “Mercury Binding Site” in the Discussion should read: “It is described as a second binding site for cadmium, but given the comparable size of the cations and that both are capable of forming an octahedral coordination geometry (Rulisek and Vondrasek, 1998), one could imagine that also mercury has a potential to bind.” The authors apologize for the mistake. This error does not change the scientific conclusions of the article in any way.

REFERENCES

Rulisek, L., and Vondrasek, J. (1998) Coordination geometries of selected transition metal ions (Co^{2+} , Ni^{2+} , Cu^{2+} , Zn^{2+} , Cd^{2+} , and Hg^{2+}) in metalloproteins. *J. Inorg. Biochem.* 71, 115–127.

Conflict of Interest Statement: The authors declare that the research was conducted in the absence of any commercial or financial relationships that could be construed as a potential conflict of interest.

Copyright © 2016 Kirscht, Survery, Kjellbom and Johanson. This is an open-access article distributed under the terms of the Creative Commons Attribution License (CC BY). The use, distribution or reproduction in other forums is permitted, provided the original author(s) or licensor are credited and that the original publication in this journal is cited, in accordance with accepted academic practice. No use, distribution or reproduction is permitted which does not comply with these terms.



The Aquaporin Splice Variant *NbXIP1;1α* Is Permeable to Boric Acid and Is Phosphorylated in the N-terminal Domain

Henry Ampah-Korsah, Hanna I. Anderberg, Angelica Engfors, Andreas Kirscht, Kristina Nordén, Sven Kjellström, Per Kjellbom and Urban Johanson*

Center for Molecular Protein Science, Department of Biochemistry and Structural Biology, Lund University, Lund, Sweden

OPEN ACCESS

Edited by:

Rupesh Kailasrao Deshmukh,
Laval University, Canada

Reviewed by:

Christophe Maurel,
Institut National de la Recherche
Agronomique, France

Zhi Zou,
Chinese Academy of Tropical
Agricultural Sciences, China

*Correspondence:

Urban Johanson
urban.johanson@biochemistry.lu.se

Specialty section:

This article was submitted to
Plant Physiology,
a section of the journal
Frontiers in Plant Science

Received: 26 April 2016

Accepted: 01 June 2016

Published: 16 June 2016

Citation:

Ampah-Korsah H, Anderberg HI, Engfors A, Kirscht A, Nordén K, Kjellström S, Kjellbom P and Johanson U (2016) The Aquaporin Splice Variant *NbXIP1;1α* Is Permeable to Boric Acid and Is Phosphorylated in the N-terminal Domain. *Front. Plant Sci.* 7:862.
doi: 10.3389/fpls.2016.00862

Aquaporins (AQPs) are membrane channel proteins that transport water and uncharged solutes across different membranes in organisms in all kingdoms of life. In plants, the AQPs can be divided into seven different subfamilies and five of these are present in higher plants. The most recently characterized of these subfamilies is the XIP subfamily, which is found in most dicots but not in monocots. In this article, we present data on two different splice variants (α and β) of *NbXIP1;1* from *Nicotiana benthamiana*. We describe the heterologous expression of *NbXIP1;1 α* and β in the yeast *Pichia pastoris*, the subcellular localization of the protein in this system and the purification of the *NbXIP1;1 α* protein. Furthermore, we investigated the functionality and the substrate specificity of the protein by stopped-flow spectrometry in *P. pastoris* spheroplasts and with the protein reconstituted in proteoliposomes. The phosphorylation status of the protein and localization of the phosphorylated amino acids were verified by mass spectrometry. Our results show that *NbXIP1;1 α* is located in the plasma membrane when expressed in *P. pastoris*, that it is not permeable to water but to boric acid and that the protein is phosphorylated at several amino acids in the N-terminal cytoplasmic domain of the protein. A growth assay showed that the yeast cells expressing the N-terminally His-tagged *NbXIP1;1 α* were more sensitive to boric acid as compared to the cells expressing the C-terminally His-tagged isoform. This might suggest that the N-terminal His-tag functionally mimics the phosphorylation of the N-terminal domain and that the N-terminal domain is involved in gating of the channel.

Keywords: XIP, AQP, NIP, *Nicotiana benthamiana*, boric acid, phosphorylation, *Pichia pastoris*

INTRODUCTION

Aquaporins (AQPs), also referred to as Major Intrinsic Proteins, facilitate the transport of water and/or other small uncharged molecules across membranes in all kingdoms of life (Gomes et al., 2009). AQPs primarily exist as homotetramers in which each monomer has six transmembrane helices and five loops with both the N and the C terminus located in the cytoplasm. Two of the loops form half-helices that contain the highly conserved AQP asparagine-proline-alanine (NPA) motif at their N termini. The two short α -helices dip into the membrane from opposite sides and the N

termini, with the NPA boxes, meet in the middle of the pore creating a seventh transmembrane structural unit, in addition to the six membrane spanning α -helices.

In mammals, 13 AQP isoforms have been identified, which are involved in various physiological functions (Agre and Kozono, 2003). In plants, however, more than 13 AQP isoforms have been identified; for instance, 35 in *Arabidopsis*, 36 in maize, 33 in rice, 55 in poplar, and 71 in cotton (Chaumont et al., 2001; Johanson et al., 2001; Sakurai et al., 2005; Gupta and Sankararamakrishnan, 2009; Park et al., 2010). Based on sequence similarity, AQPs of higher plants are divided into five subfamilies namely: the Plasma Membrane Intrinsic Proteins (PIPs), the Tonoplast Intrinsic Proteins (TIPs), the Nodulin-26 like Intrinsic Proteins (NIPs), the Small basic Intrinsic Proteins (SIPs), and the X Intrinsic Proteins (XIPs; Johanson et al., 2001; Danielson and Johanson, 2008; Bienert et al., 2011). Interestingly, XIPs which were first discovered in the moss *Physcomitrella patens* (Danielson and Johanson, 2008) have not only been identified in plants such as grapevine (*Vitis vinifera*; Danielson and Johanson, 2008), poplar (*Populus trichocarpa*; Gupta and Sankararamakrishnan, 2009), tomato (*Solanum lycopersicum*; Sade et al., 2009; Reuscher et al., 2013), cotton (*Gossypium hirsutum*; Park et al., 2010), tobacco (*Nicotiana tabacum*; Bienert et al., 2011), and bean (*Phaseolus vulgaris*; Ariani and Gepts, 2015) but also in fungi (Gupta and Sankararamakrishnan, 2009) and protozoa (Danielson and Johanson, 2008). Based on phylogenetic analysis, XIPs of higher plants have been grouped into two distinct clusters termed XIP-A and XIP-B, where XIP-A includes only a XIP1 subgroup and XIP-B is divided into four subgroups, i.e., XIP2, XIP3, XIP4, and XIP5 (Lopez et al., 2012). According to this classification *Solanaceae* XIPs including the XIPs from *N. tabacum*, *N. benthamiana*, *Ipomoea nil*, and *S. lycopersicum* were assigned to subgroup XIP4 (Lopez et al., 2012), while XIPs in rubber tree (*Hevea brasiliensis*), castor bean (*Ricinus communis*), physic nut (*Jatropha curcas*) and poplar (*P. trichocarpa*) have been assigned to subgroups XIP1, XIP2, and XIP3 (Zou et al., 2015a,b, 2016). In a more recent phylogenetic classification of XIPs of land plants only four groups (XIP I-IV) are proposed (Venkatesh et al., 2015). In this classification, subgroup XIP IV is corresponding to group XIP4. For simplicity the original naming of the *Solanaceae* XIPs as XIP1s has been retained as it is also used in the work of Venkatesh et al. (2015). In *Solanaceae* the pre-mRNAs of some *XIP1* genes undergo alternative splicing resulting in two variants of the transcript and thus in two slightly different proteins (Bienert et al., 2011). *XIP1;1* mRNAs were found to be expressed in all organs of the tobacco plant and the proteins were localized in the plasma membrane of plant cells (Bienert et al., 2011). Transiently expressed *Solanaceae* XIP1;1s facilitated the transport of glycerol but not water in *Xenopus oocytes* and when expressed in *Saccharomyces cerevisiae* mutants increased the sensitivity of the cells to boric acid, urea, and hydrogen peroxide (Bienert et al., 2011), which suggests that XIP1;1s are not primarily water transporters (Bienert et al., 2011; Lopez et al., 2012). However, the physiological function and the *in vivo* substrate of XIPs are yet to be discerned. It is therefore necessary to characterize XIPs further with regard to selectivity, structure, and regulation.

The opening and closing of the pore of AQPs, often referred to as AQP gating, have been observed for mammalian, plant, and yeast AQPs (Törnroth-Horsefield et al., 2006; Fischer et al., 2009). Divalent cations, pH and phosphorylation have been reported to regulate AQP gating and water permeability (Maurel et al., 1995; Johansson et al., 2000; Guenther et al., 2003; Daniels and Yeager, 2005; Temmei et al., 2005; Törnroth-Horsefield et al., 2006; Azad et al., 2008). Phosphorylation increased the water channel activity of *PvTIP3;1* (Maurel et al., 1995), *SoPIP2;1* (PM28A; Johansson et al., 1998), soybean nodulin 26 (Guenther et al., 2003), and *TgPIP2;2* (Azad et al., 2008). The *SoPIP2;1* in *Spinacia oleracea* was shown to be regulated by phosphorylation at Ser 115 and Ser 274 (Johansson et al., 1998; Törnroth-Horsefield et al., 2006). Likewise, the soybean nodulin 26 was reported to be phosphorylated at Ser 262 (Lee et al., 1995; Guenther et al., 2003).

For crystallization and structural determination, not only large amounts of proteins are required but also homogenous samples are essential for successful crystallization. *Pichia pastoris* as expression system has been shown to generate high yields of functional AQPs (Karlsson et al., 2003; Horsefield et al., 2008; Nordén et al., 2011) and *P. pastoris* has the machinery to phosphorylate heterologously expressed eukaryotic proteins (Hori et al., 2010). Phosphorylation of plant AQPs in *P. pastoris* has been shown (Daniels and Yeager, 2005) and this correlates with results from mutant studies and from studies involving chemical inhibition of kinases and phosphatases (Azad et al., 2008).

In this study, we present results concerning the expression, purification and characterization of *N. benthamiana* XIP1;1 splice variants in *P. pastoris* and demonstrate phosphorylation of NbXIP1;1 α in its N-terminal region.

MATERIALS AND METHODS

Cloning and Generation of Multi-copy *P. pastoris* Transformants

The cDNA encoding NbXIP1;1 α and NbXIP1;1 β (Nb_Ea0003A8 and Nb_Ea0006N9, Arizona Genomics Institute) were amplified by PCR, generating either N- or C- terminally His-tagged constructs with the following primer pairs: For N-terminally His-tagged constructs, TEVEcoRI-XIPfw (5'-TTGAATTCCGACCGAAAACCTGTATTTCAGGGCATGTC TGCTTCCAATACTAGTCA-3') and TEVNotI-XIPPrev (5'-T TGCAGGCCGCTCATACATGCAACCCAAATGAAG-3'); and for C-terminally His-tagged constructs, EcoRI-XIPfw (5'-CGGAATTCAAATGTCTGCTTCCAATACTAGTCA-3') and NotI-XIPPrev (5'-TTGCGGCCGCTACATGCAACCCAAATGA-3') where EcoRI and NotI restriction sites are indicated in bold and *P. pastoris* consensus start sequence are underscored. The PCR products were cloned into a modified pPICZB vector (Invitrogen) conferring the addition of a His₁₀-tag and a TEV protease cleavage site to the N-terminus or the unmodified plasmid adding a myc antibody epitope and a His₆-tag to the C-terminus of the amino acid sequence. The resulting plasmids were sequenced and transformed into wild type X-33 or protease deficient SMD1168H *P. pastoris* cells by electroporation

according to the EasySelect™ *Pichia* Expression Kit manual (Invitrogen, 2005). To obtain clones with potentially high copy numbers of the *NbXIP1;1α* or *NbXIP1;1β* splice forms, a zeocin selection was performed as described previously (Nordén et al., 2011). Briefly, transformed *P. pastoris* cells were plated onto YPDS [1% (w/v) yeast extract, 1% (w/v) peptone, 2% (w/v) dextrose, 1 M sorbitol] agar plates containing 100 µg/mL zeocin. The resulting colonies were then resuspended and the transformants were spread on plates containing higher zeocin concentrations. The plates were incubated at 28°C for 3 days and colonies were restreaked to obtain *P. pastoris* clones derived from single cells.

Small-scale Expression Screen

A small scale expression screen was performed in order to analyze *NbXIP1;1α* and *NbXIP1;1β* expression capacity of X-33 and SMD1168H clones selected at the different antibiotic levels. Clones were cultured in 5 mL BMGY [1% (w/v) yeast extract, 2% (w/v) peptone, 100 mM potassium phosphate pH 6.0, 1.34% (w/v) yeast nitrogen base, 4 × 10⁻⁵% (w/v) biotin, 1% (v/v) glycerol] over night to generate biomass. Cells were harvested and resuspended in 5 mL BMMY [1% (w/v) yeast extract, 2% (w/v) peptone, 100 mM potassium phosphate pH 6.0, 1.34% (w/v) yeast nitrogen base, 4 × 10⁻⁵% (w/v) biotin, 0.5% (v/v) methanol] to an optical density at 600 nm (OD₆₀₀) of 1. To sustain induction, methanol was added to a final concentration of 0.5% (v/v) every 24 h. Cell cultures were incubated with continuous agitation at 245 rpm for 72 h at 28°C. Cells corresponding to 20 OD₆₀₀ units were harvested and disrupted, by vigorous vortexing with glass beads, in cold breaking buffer [50 mM NaPO₄ pH 7.4, 1 mM EDTA, 5% (v/v) glycerol, 1 mM PMSF]. The lysate was cleared by centrifugation and the supernatant, containing the crude cell extracts was analyzed for *NbXIP1;1* content by western blot as described below. Since recombinant expression was more efficient in wild type cells, X-33 *P. pastoris* clones were used in further trials.

Western Blot Analysis

To the crude cell extracts, 3.33 × SDS loading buffer [250 mM Tris-HCl pH 6.8, 40% (v/v) glycerol, 8% (w/v) SDS, 2.4 M β-mercaptoethanol, 0.1% (w/v) bromophenol blue] was added. Samples were solubilized at ambient temperature for 30 min. Proteins were separated on 12% SDS-PAGE gels and transferred onto polyvinylidene difluoride (PVDF) membranes (Millipore). His-tagged *NbXIP1;1* protein was visualized by probing with primary antibody mouse anti-(His)₄ (Qiagen) and secondary antibody horseradish peroxidase-conjugated polyclonal goat anti-mouse IgG. Blots were developed by enhanced chemiluminescence.

Yeast Growth Assay

To verify the functionality of the heterologously expressed *NbXIP1;1* protein, a yeast growth assay was performed. The X-33-XIP_αHis₆ clone, the X-33-His₁₀XIP_α clone, the X-33-His₁₀NIP5;1 clone and a X-33 clone transformed with an empty pPICZB vector were cultured in small scale, as described above,

and methanol induced protein expression was sustained for 26 h. The cell density was subsequently measured and the cultures were diluted to OD₆₀₀ of 1. The induced *P. pastoris* cells were spotted onto YPD agar plates without boric acid and plates with 10 mM boric acid in a 1:10 dilution series. The plates were incubated at 28°C and after 5 days differences in growth were recorded.

Stopped-Flow Spectrometric Assay of *P. pastoris* Spheroplasts

To test for water or glycerol permeability in the transformed cells, *P. pastoris* spheroplasts were prepared as published previously (Fischer et al., 2009) with slight modifications. In brief, *NbXIP1;1α* or *AtNIP5;1* protein production was induced in transformed *P. pastoris* cells in BMMY with a starting OD₆₀₀ of 1, as described above. After 26 h of induction, the cells were harvested, resuspended and incubated in TE-buffer (100 mM Tris-HCl pH 8.0, 1 mM EDTA) and 0.5% β-mercaptoethanol for 1.5 h to destabilize the cell wall. The cells were then washed and equilibrated in 20 mM MES pH 6.5, 1.2 M sorbitol with a final OD₆₀₀ of 5 for 2 h. For water transport, equilibrated spheroplasts were subjected to a hyperosmolar solution (20 mM MES pH 6.5, with 1.8 M sorbitol) and the shrinkage upon mixture was observed by light scattering at 90° angle in a stopped-flow apparatus (SF-61 DX2 Double Mixing Stopped-flow System, Hi-Tech Scientific) at 500 nm. For glycerol transport, the equilibrated spheroplasts in 20 mM MES pH 6.5, 1.2 M sorbitol were mixed with equal volume of a hyperosmolar solution containing 20 mM MES pH 6.5 and 1.8 M glycerol and the initial shrinkage and subsequent swelling upon mixture were observed by light scattering at 90° angle in a stopped-flow apparatus at 500 nm. Kinetic Studio version 2.28 (TgK Scientific Limited) was used to calculate the rate constants and the standard error of estimate (SEE) of the traces.

Isolation of *P. pastoris* Plasma Membrane

Plasma membranes were isolated from *P. pastoris* clones as previously described (Grillitsch et al., 2014) with slight modifications. Briefly, 20 g cell wet weight of *P. pastoris* cells were lysed by 8 × 30 s runs with 30 s intervening cooling sessions in a breaking buffer (25 mM Tris-HCl pH 8.5, 1 mM EDTA, 1 mM PMSF) by means of a BeadBeater apparatus (BioSpec Products). The cell lysate was centrifuged (1,000 × g, 10 min, 4°C) to sediment unbroken cells. Bulk membranes were pelleted by centrifugation (35,000 × g, 30 min, 4°C) from the supernatant. The pelleted bulk membranes were homogenized with 10 strokes using a hand homogenizer in TEDG-buffer [20% (v/v) glycerol in 10 mM Tris-HCl pH 7.5, 0.2 mM EDTA, 0.2 mM DTT] and the membrane suspension subsequently loaded onto a discontinuous sucrose density gradient consisting of 1:1 volume ratio of 43 and 53% (w/v) sucrose in TED-buffer (10 mM Tris-HCl pH 7.5, 0.2 mM EDTA, 0.2 mM DTT). Crude plasma membranes were collected from the gradient at the 43/53% sucrose interface after centrifugation in a swing-out rotor (SW 28, Beckman coulter) at 100,000 × g, 4°C for 4 h. The crude plasma membranes were diluted threefold in ice-cold water and

spun at $45,000 \times g$, 4°C for 20 min in a JA-25.50 Beckman coulter rotor. The resulting pellet was homogenized with 10 strokes in MES-buffer (5 mM MES pH 6.0, 0.2 mM EDTA). Subsequently, the crude plasma membranes were loaded onto a second discontinuous sucrose density gradient consisting of 53, 43, and 38% (w/v) sucrose in 1:1:1 volume ratio in MES-buffer and centrifuged for 2.5 h at $100,000 \times g$, 4°C . After centrifugation, the purified plasma membranes were collected at the 43/53% sucrose interface, diluted in Tris buffer (10 mM Tris-HCl pH 7.4) and pelleted as earlier described. Finally, the sedimented plasma membranes were homogenized in the Tris buffer and analyzed on a western blot for the presence of the His-tagged *NbXIP1;1* protein. The remainder of the plasma membranes were stored at -80°C .

Large Scale Expression for Purification

Two clones of *NbXIP1;1 α* (designated X-33-XIP α His₆ and X-33His₁₀XIP α ;1 α) and one of *NbXIP1;1 β* (designated X-33-XIP β His₆) with the highest protein expression levels, were used for purification trials. The X-33His₁₀XIP α ;1 α clone gave the highest yield of purified *NbXIP1;1 α* protein and therefore was chosen for further purification and downstream application. Due to the benefits the controlled growth in bioreactors confer (Nyblom et al., 2007), the X-33His₁₀XIP α ;1 α clone was eventually cultured in large scale using a 3 L bench top fermenter (Belach Bioteknik). A 100 mL X-33His₁₀XIP α ;1 α *P. pastoris* pre-culture in BMGY was incubated at 30°C and 250 rpm over night to OD₆₀₀ \sim 10. The BMGY culture was, together with 6.5 mL PTM₁ salts (Bushell et al., 2003), added to 1.5 L basal salt medium (Stratton et al., 1998), pre-tempered to 30°C in the fermenter. When the initial glycerol was consumed after approximately 24 h, a feed with 50% (v/v) glycerol was initiated to increase biomass. After 6 h, 200 mL of glycerol had been consumed and the culture had reached an OD₆₀₀ of 210. To induce expression of *NbXIP1;1 α* , 100% methanol with 1.2% (w/v) PTM₁ salts was added to the *P. pastoris* culture at a steady feed rate. Induction was sustained for 50 h after which 390 mL methanol had been consumed and the culture had reached an OD₆₀₀ of 300. Cells were harvested by centrifugation and stored at -80°C until further use.

Membrane Preparation

Cells corresponding to a wet weight of 40 g were thawed and resuspended in 150 mL ice-cold breaking buffer supplemented with complete Ultra protease inhibitor cocktail tablets (Roche). The cell suspension was, together with 200 mL cold glass beads, transferred to a BeadBeater (BioSpec Products) container. The cells were mechanically resuspended by 12 \times 30 s runs with intervening 30 s cooling sessions. Unbroken cells and cell debris were removed by centrifugation at $1,400 \times g$ at 4°C for 30 min. Crude membrane fraction was subsequently collected by ultracentrifugation of the $1,400 \times g$ supernatant at $186,000 \times g$ at 4°C for 2 h and the resulting membranes were homogenized in cold buffer A [20 mM HEPES-NaOH pH 8.0, 50 mM NaCl, 10% (v/v) glycerol, 2 mM β -mercaptoethanol]. In order to remove peripherally bound membrane proteins and render the membranes more easily solubilized, a urea/alkali membrane wash

procedure (Kistler et al., 1994; Fotiadis et al., 2001) was evaluated. However, since the 20 mM NaOH solution discharged part of the *NbXIP1;1* protein from the membrane, only the urea wash was subsequently applied. Briefly, 100 mL cold urea solution (4 M urea, 5 mM Tris-HCl pH 9.5, 2 mM EDTA, 2 mM EGTA) was added to crude membranes with a total membrane protein content of approximately 200 mg, and the mixture was incubated on ice for 30 min. The stripped membranes were sedimented by centrifugation at $186,000 \times g$ for 1.5 h at 4°C . Sedimented stripped membranes were resuspended and diluted ten-fold in cold buffer A. Finally, washed stripped membranes were collected by ultracentrifugation and homogenized in buffer A. The membranes were kept at -80°C until further use.

Protein Solubilization and Ni-NTA Affinity Chromatography

Stripped membranes were solubilized by a dropwise addition of 280 mM of *N*-nonyl- β -D-glucopyranoside (NG; Anatrace) in buffer A. After overnight incubation at 4°C with gentle agitation, unsolubilized material was sedimented at 40,000 rpm for 30 min at 4°C . To reduce unspecific binding, 20 mM imidazole was added to the solubilized protein and mixed with 1 mL of Ni-NTA agarose slurry (Qiagen) preequilibrated with 20 mM imidazole in buffer B (20 mM HEPES-NaOH pH 8, 500 mM NaCl, 10% Glycerol, 2 mM β -mercaptoethanol and 12 mM NG) and incubated for 16 h with continuous tumbling at 4°C . The resin/protein suspension was loaded onto a poly-prep chromatographic column (Bio-Rad) at 4°C and the flow through containing non-bound protein was removed by gravity flow. The column was washed with buffer B + 70 mM imidazole. The protein was eluted with buffer B + 500 mM imidazole. Since *NbXIP1;1 α* was not stable in the elution buffer after 24 h at 4°C , the eluted protein fraction was desalting and the buffer exchanged for buffer C (20 mM Bis Tris Propane-HCl pH 8.6, 100 mM NaCl, 10% Glycerol, 2 mM β -mercaptoethanol and 12 mM NG) on a PD-10 desalting column (GE Healthcare). The purity of the eluted protein was evaluated by colloidal coomassie staining of SDS-PAGE gels (Neuhoff et al., 1988) and *NbXIP1;1 α* content analyzed by western blot.

Circular Dichroism (CD) Spectrum

Circular Dichroism spectrum for *NbXIP1;1 α* was acquired as previously published (Plasencia et al., 2011). In brief, the purified *NbXIP1;1 α* or buffer without protein was transferred into a quartz cuvette with a path length of 0.1 cm and the spectra collected at 50 nm/min between 260 and 190 nm with a response time of 8 s and a data pitch of 1 nm in a Jasco Spectrophotometer (Jasco, UK) with a built-in Peltier device for sample temperature regulation. Spectrum of the buffer without protein was used for baseline correction.

Stopped-Flow Spectrometric Assay of Proteoliposomes

To test for boric acid permeability, purified *NbXIP1;1 α* was reconstituted into proteoliposomes by mixing with *Escherichia*

coli polar lipid extracts (Avanti Polar lipids) and 20% cholesterol (Sigma) solubilized in 2.5% (w/v) NG in reconstitution buffer (20 mM Tris-HCl pH 8.0, 100 mM NaCl) at a lipid to protein ratio (LPR) of 50 and a final lipid concentration of 2 mg lipids/mL. Approximately 1 g of bio-beads (SM2, Bio-Rad) was added to the lipid/protein solution to remove the detergent. Reconstitution occurred spontaneously as observed by the increase in turbidity of the solution. After 30 min of reconstitution, the supernatant containing the lipid vesicles was collected. The vesicles were extruded nine times through a polycarbonate filter (200 nm pore size) and subjected to an inwardly directed boric acid gradient of 100 mM through rapid mixing in a stopped-flow apparatus. The shrinkage of the vesicles depicting water efflux and the subsequent swelling of the vesicles depicting boric acid and water influx was observed by light scattering at 90° angle in a stopped flow apparatus at 500 nm. Control vesicles without protein were subjected to the same steps. One independent reconstitution was performed for each protein and control liposomes were done in parallel. The traces (mean of 8 and 29 traces for the phosphorylated and dephosphorylated protein, respectively) were fitted to double exponential equations. The traces for the control liposomes (mean of 8 and 15 traces for the control liposomes used in the phosphorylated and dephosphorylated reconstitution experiments, respectively) were also fitted to double exponential equations. Kinetic Studio version 2.28 (TgK Scientific Limited) was used to calculate the rate constants and the standard error of estimate (SEE) of the traces.

Identification of Phosphorylation in NbXIP1;1 α with Phos-tagTM BTL-111

To probe for phosphorylation in the purified NbXIP1;1 α , a phosphate binding tag (Phos-tagTM BTL-111, Wako Pure Chemical Industries, Ltd) was utilized as described previously (Kinoshita et al., 2012) with slight modifications. In brief, a complex of Phos-tagTM BTL-111 with Horse Radish Peroxidase conjugated Streptavidin (HRP-SA) was prepared as follows; 5 μ L of 10 mM aqueous solution of Phos-tagTM BTL-111, 20 μ L of 10 mM aqueous solution of Zn(NO₃)₂, 1 μ L of HRP-SA (GE Healthcare Biosciences) and 469 μ L of TBS-T (10 mM Tris-HCl pH 7.5, 100 mM NaCl, 0.1% Tween 20) were mixed together and incubated in the dark at ambient temperature. After 1 h of incubation, the mixture was transferred into a 30 K Nanosep filtration column (Pall Corporation) and spun for 10 min at 14,000 \times g to remove excess Phos-tagTM BTL-111. The remaining solution in the reservoir was diluted with 25 mL of TBS-T solution containing 1% (w/v) Bovine Serum Albumin (BSA) and 1 M sodium acetate and used as a probing reagent (Zn²⁺-Phos-tagTM BTL-111-bound HRP-SA solution). Equal amounts of purified NbXIP1;1 α untreated and treated with alkaline phosphatase for 20 h at 30°C in 5 mM Tris-HCl (pH 7.9), 10 mM NaCl, 1 mM MgCl₂, and 0.1 mM DTT, were subjected to SDS-PAGE. The proteins were then transferred onto a PVDF membrane. For probing with the Zn²⁺-Phos-tagTM BTL-111-bound HRP-SA, the membrane was blocked with 10% (w/v) BSA in TBS-T solution for 6 h followed by overnight incubation at 4°C with the Zn²⁺-Phos-tag BTL-111-bound HRP-SA solution.

The membrane was washed twice for 5 min with TBS-T solution containing 1% (w/v) BSA and 1 M sodium acetate. The blot was developed by enhanced chemiluminescence. Probing with mouse anti-(His)₄ was done as described above.

Identification of Phosphorylation Sites in NbXIP1;1 α by Mass Spectrometry

To identify phosphorylation sites in the purified NbXIP1;1 α , a protein band corresponding to NbXIP1;1 monomeric band was excised from a coomassie-stained SDS-PAGE gel and in-gel digested overnight at 37°C with trypsin (Promega) as published previously (Shevchenko et al., 2006). The trypsin digestion was stopped by the addition of 10% trifluoroacetic acid. The digested peptides were analyzed with an EasyLC nanoflow HPLC interfaced with a nanoEasy spray ion source (Proxeon Biosystems) connected to an LTQ-Orbitrap Velos Pro mass spectrometer (Thermo Fisher Scientific) as described previously (Don-Doncow et al., 2014). The raw data was processed by Mascot distiller search through an in-house Mascot database consisting of amino acid sequences of *N. benthamiana* XIP1;1s, *Arabidopsis thaliana* NIP5;1, and NIP1;1. The parameter settings used in the database search are as follows: fixed modifications: carbidomethyl (C); variable modifications: phospho (ST); enzyme: no enzyme cleavage specificity; maximum missed cleavage sites: one; peptide tolerance: \pm 6 ppm; MS/MS tolerance: \pm 0.15 Da. Phosphopeptides identified once and/or with ion score of less than 25 were discarded.

Phylogenetic Analysis

To construct the alignment, XIP amino acid sequences from *N. tabacum*, *N. benthamiana*, *S. tuberosum*, *S. lycopersicum*, *I. nil*, *P. patens*, and *Selaginella moellendorffii* were manually added to a structural alignment of *BtAQP1* (1J4N, Sui et al., 2001), *EcGLPF* (1LDA, Fu et al., 2000), *EcAQPZ* (1RC2, Savage et al., 2003), *SoPIP2;1* (1Z98, Törnroth-Horsefield et al., 2006), *RnAQP4* (2D57, Hiroaki et al., 2006) *MmAQP* (2F2B, Lee et al., 2005) *PfAQP* (3C02, Newby et al., 2008), *HsAQP5* (3D9S, Horsefield et al., 2008), and *BtAQP0* (2B6P, Gonen et al., 2005) made in DeepView/Swiss-PdbViewer v4.0.1 using MEGA6 (Tamura et al., 2013). The N- and C-termini were aligned with the built-in Muscle algorithm under the default settings (Edgar, 2004).

The phylogenetic tree was inferred using the Maximum Likelihood method based on the Le_Gascuel_2008 model (LG) with discrete Gamma distributions (+G, 5 categories with the parameter 4.8049) and 2.9126% evolutionary invariant sites (+I). All positions with site coverage less than 95% were removed and an initial tree was obtained using the Neighbor-Joining method under a JTT model. The robustness of the nodes was tested by 1000 bootstrap replications.

RESULTS

Three XIP Genes in *N. benthamiana*

Isoforms belonging to the XIP subfamily of AQPs are present in mosses and in most dicotyledonous plants, while

monocotyledonous plants have lost the genes coding for XIP isoforms and so have the dicotyledonous model plant *Arabidopsis thaliana* (Danielson and Johanson, 2008). An examination of the *N. benthamiana* genome revealed three genes coding for full length XIPs, two of which are alternatively spliced. In a phylogenetic analysis the resulting five *N. benthamiana* proteins cluster and form a monophyletic clade together with XIP proteins of other Solanaceae species such as *N. tabacum*, *S. tuberosum*, and *S. lycopersicum* (**Figure 1**). This clade also encompass a XIP protein from *I. nil* (Morning glory), whereas XIPs from the moss *P. patens* and the spike moss *S. moellendorffii*, are basal (Danielson and Johanson, 2008; Bienert et al., 2011; Anderberg et al., 2012). Our finding and naming of the *N. benthamiana* XIPs is consistent with what was reported in the course of our work (Venkatesh et al., 2015). In the current study we heterologously expressed the two splice variants α and β of the AQP XIP1;1 from *N. benthamiana*, and subsequently, purified and characterized the α splice-variant.

Expression of NbXIP1;1 in *Pichia pastoris*

Both splice variants ($NbXIP1;1\alpha$ and $NbXIP1;1\beta$) of $NbXIP1;1$ were successfully expressed in wild type X-33 (**Figure 2**) and in a protease deficient strain SMD1168H of *P. pastoris* with a slightly higher expression level in the X-33 strain (**Supplementary Figure 1**). There was no significant difference in the expression levels of the two splice variants. The migration pattern of $NbXIP1;1\alpha$ is typical for AQPs separated by SDS-PAGE (**Figure 3A**; Nordén et al., 2011) with the monomeric and dimeric protein bands running below the expected bands at 37 and 74 kDa, respectively. The selection of multi-copy insertions of the XIP genes were also successful as the clones selected on higher concentrations of zeocin generally had higher protein expression than the clones selected on low concentrations of zeocin (**Figure 2**). The protease deficient SMD1168H clones had a significant reduction in protein degradation (**Supplementary Figure 1**), however, due to the lower protein expression and yield in the SMD1168H clones as compared to the wild type, the wild-type X-33 *P. pastoris* clones were chosen for further studies. To

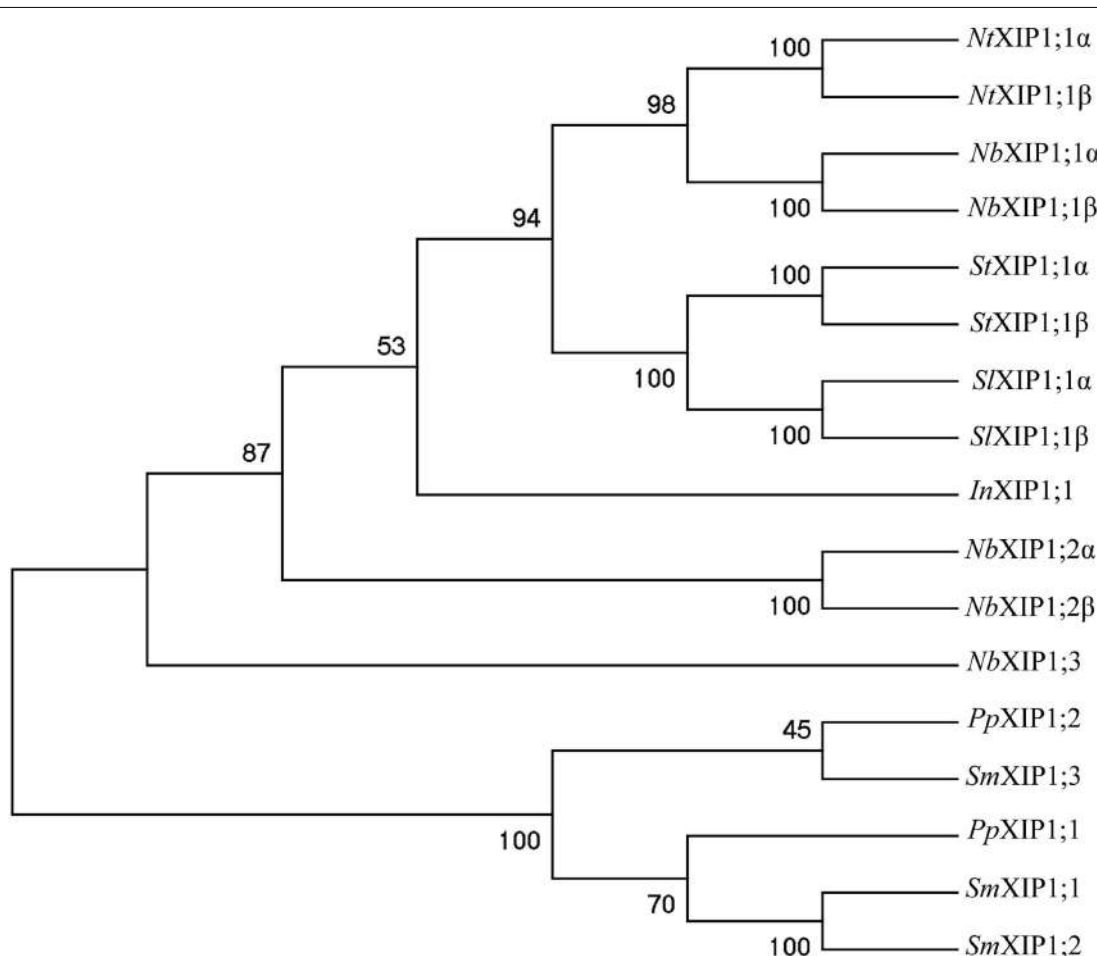


FIGURE 1 | Phylogenetic tree of XIPs. The tree shows the phylogenetic relationship between XIPs in *Nicotiana benthamiana*, and selected XIPs of *N. tabacum*, *S. tuberosum*, *S. lycopersicum*, and *I. nil*, when XIP sequences from *P. patens* and *S. moellendorffii* are used to root the tree. The numbers at the nodes represents the bootstrap support in %. The XIPs of *N. benthamiana*, *N. tabacum*, *S. tuberosum*, *S. lycopersicum*, and *I. nil* represent a subset the XIP IV group of clade B, while *P. patens* and *S. moellendorffii* sequences belong to the basal XIP I group (Venkatesh et al., 2015).

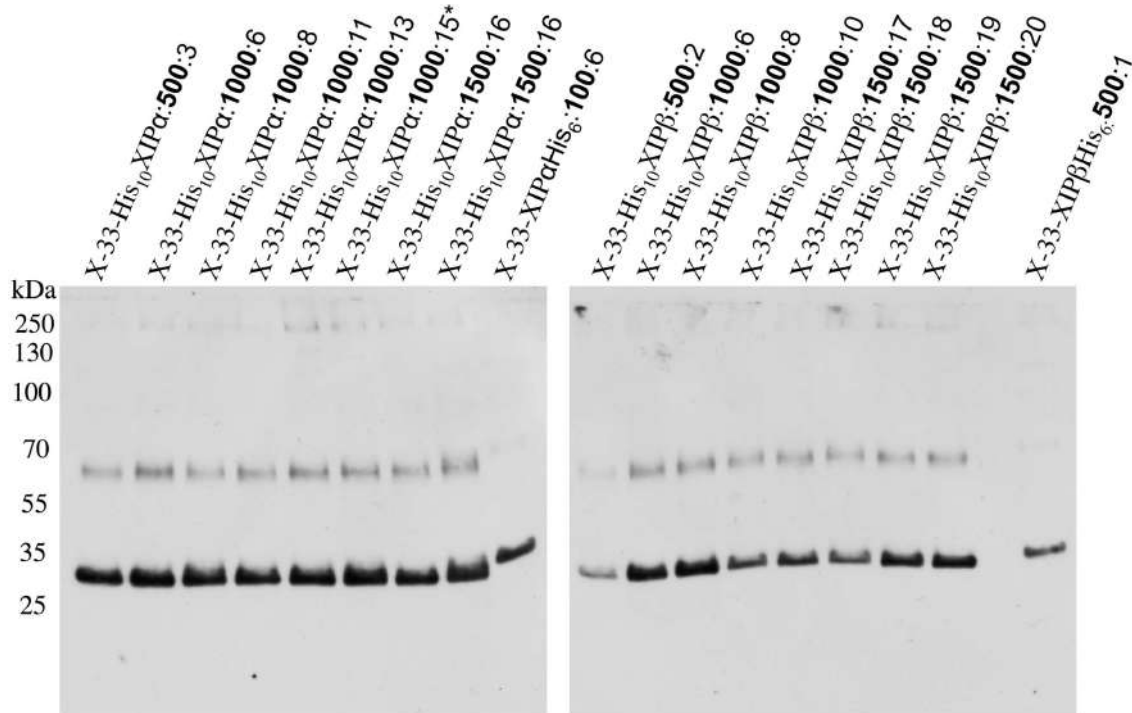


FIGURE 2 | Recombinant N-terminally His-tagged *NbXIP1;1* expression in *P. pastoris* clones selected at different zeocin levels. Western blot showing the recombinant expression levels in crude cell extracts of representative X-33 N-terminally His-tagged *NbXIP1;1* proteins in clones selected at 500 µg/mL, 1000 µg/mL or 1500 µg/mL (µg/mL zeocin resistance levels in bold). C-terminally His-tagged *NbXIP1;1* clones were used as reference. The X-33His₁₀XIP1;1α:1000:15* clone was used for large scale purification.

our knowledge, this is the first time that XIP AQP isoforms have been shown to be successfully expressed in *P. pastoris*.

P. pastoris Cells Expressing NbXIP1;1α Are Sensitive to Boric Acid

Saccharomyces cerevisiae yeast mutant ($\Delta fsp1$) cells expressing a XIP isoform from *N. tabacum* (*NtXIP1;1*) have previously been shown to possess a growth impeded phenotype when exposed to boric acid (Bienert et al., 2011). Due to the high sequence similarity among the *Nicotiana* XIPs and the relatively close relationship between *S. cerevisiae* and *P. pastoris*, we expected that a boric acid growth assay could be applied to verify the functionality of the heterologously expressed *NbXIP1;1α* protein. *P. pastoris* cells harboring *NbXIP1;1α*, *AtNIP5;1* or the empty pPICZB grew to the same extent on the control plates (YPD without boric acid). *AtNIP5;1* was used as a positive control as it has been shown to be a transporter of boric acid (Takano et al., 2006). A *P. pastoris* X-33 clone transformed with empty pPICZB was used as a negative control. The result (Figure 4) showed a general reduction in growth of all the cells plated on 10 mM boric acid. However, expression of *NbXIP1;1α* or *AtNIP5;1* rendered the yeast cells more sensitive to boric acid as there was appreciable inhibition of growth in these clones. This indicated that *NbXIP1;1α* just like *AtNIP5;1* facilitates the transport of boric acid into the *P. pastoris* cells. As shown in Figure 4, switching the His-tag from the C-terminus to the

N-terminus of the amino acid sequence appears to increase the sensitivity of the cells to boric acid to a similar level as the positive control *AtNIP5;1*.

NbXIP1;1α Does Not Facilitate Water Transport in *P. pastoris* Spheroplasts

The ability of *NbXIP1;1α* to facilitate the transport of water was tested by subjecting *P. pastoris* spheroplasts heterologously expressing *NbXIP1;1α* to a stopped-flow spectrometric analysis. After fitting the data to a single exponential function, the rate constants \pm standard error of estimate (SEE) for water permeation through the control transformed with the empty pPICZB plasmid, *NbXIP1;1α* and *AtNIP5;1* spheroplasts were calculated as: $2.77 \pm 0.04 \text{ s}^{-1}$; $3.20 \pm 0.03 \text{ s}^{-1}$; and $4.90 \pm 0.04 \text{ s}^{-1}$, respectively. This suggested that there was, if any, little or no difference in water permeability between the *NbXIP1;1α* and control spheroplasts as shown in Figure 5A. However, the *AtNIP5;1* spheroplasts had an approximately twofold increase in water permeation as compared to the control spheroplasts.

NbXIP1;1α Does Not Facilitate Glycerol Transport in *P. pastoris* Spheroplasts

In previous studies, *NtXIP1;1* was shown to facilitate the transport of glycerol in *Xenopus oocytes* (Bienert et al., 2011). In the light of that, glycerol transport by the recombinant

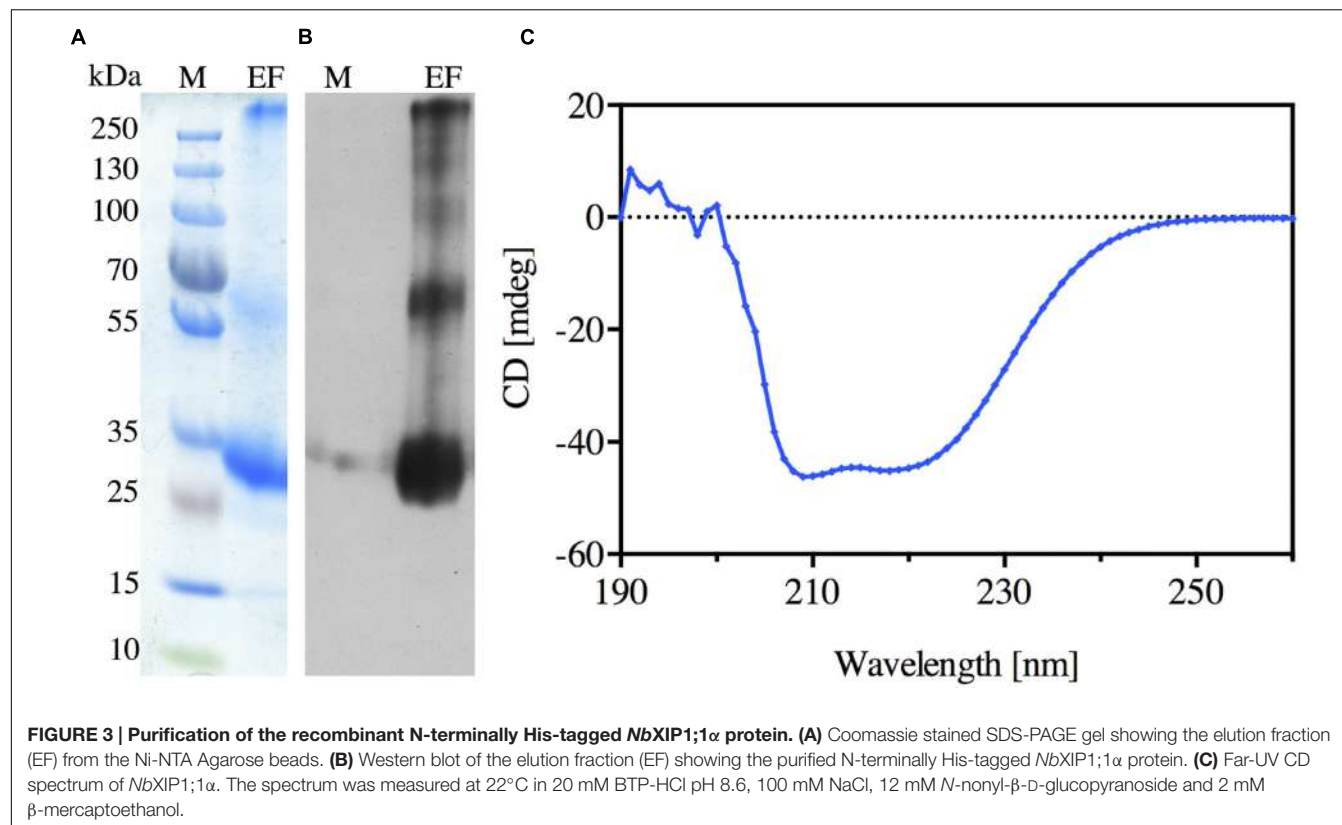


FIGURE 3 | Purification of the recombinant N-terminally His-tagged NbXIP1;1 α protein. (A) Coomassie stained SDS-PAGE gel showing the elution fraction (EF) from the Ni-NTA Agarose beads. **(B)** Western blot of the elution fraction (EF) showing the purified N-terminally His-tagged NbXIP1;1 α protein. **(C)** Far-UVC CD spectrum of NbXIP1;1 α . The spectrum was measured at 22°C in 20 mM BTP-HCl pH 8.6, 100 mM NaCl, 12 mM N-nonyl- β -D-glucopyranoside and 2 mM β -mercaptoethanol.

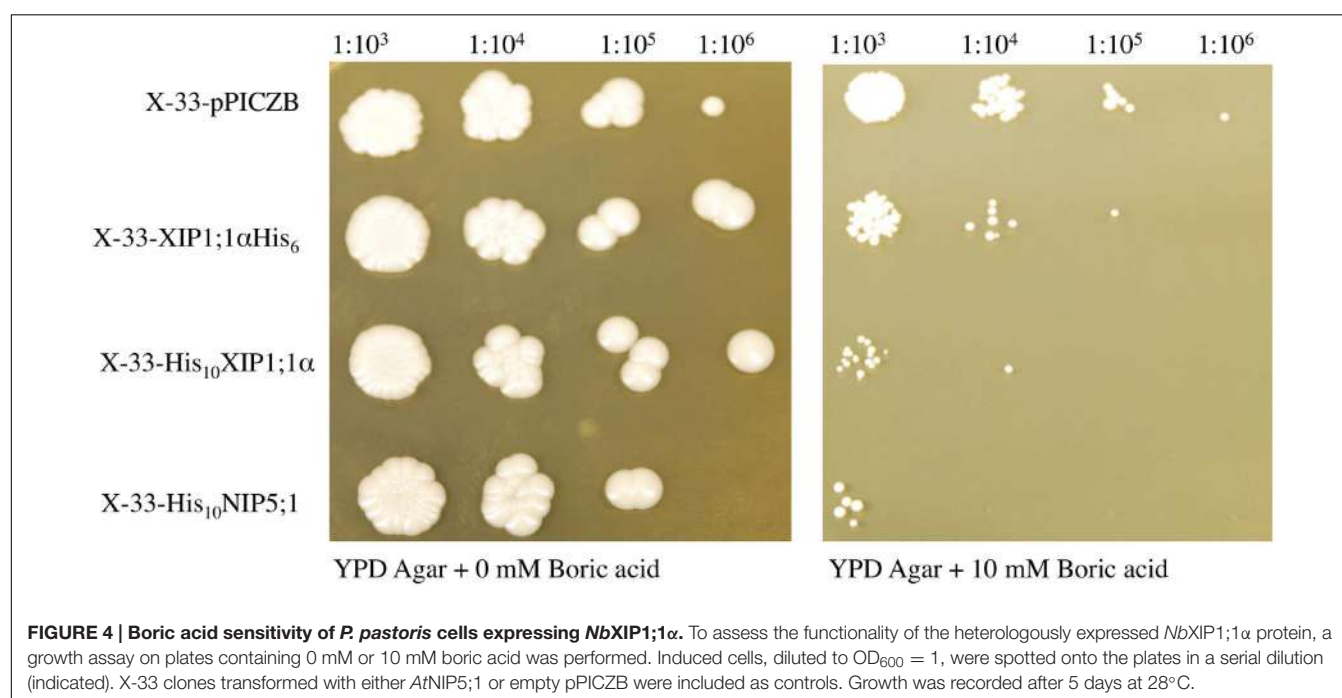
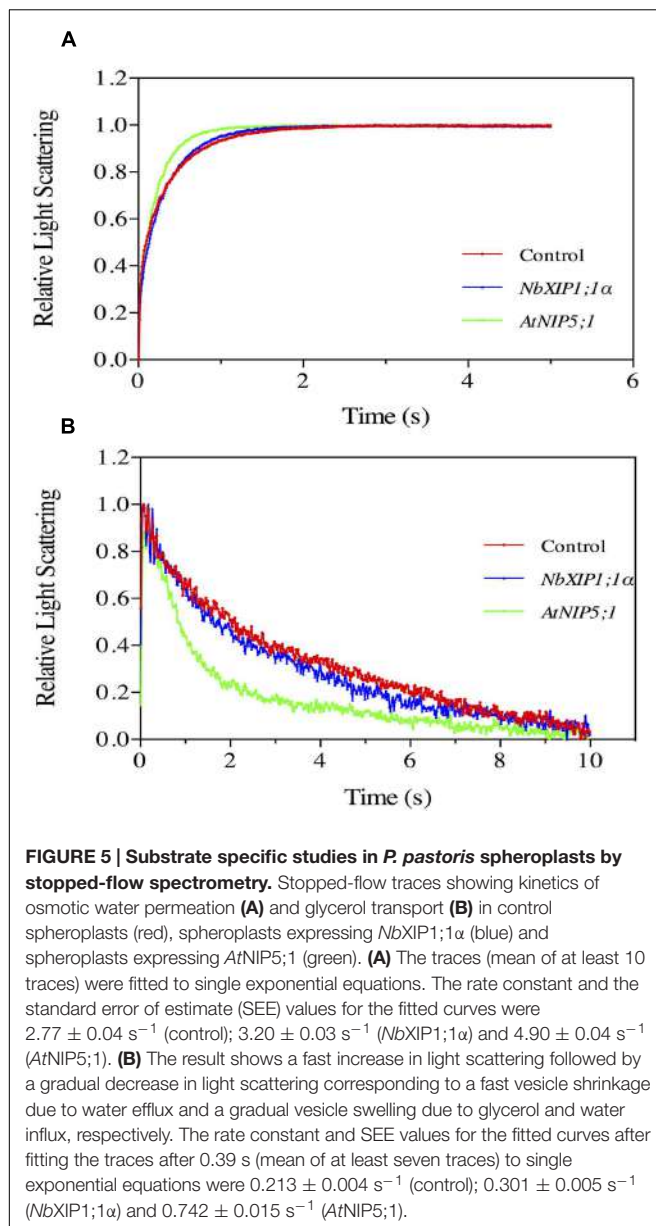


FIGURE 4 | Boric acid sensitivity of *P. pastoris* cells expressing NbXIP1;1 α . To assess the functionality of the heterologously expressed NbXIP1;1 α protein, a growth assay on plates containing 0 mM or 10 mM boric acid was performed. Induced cells, diluted to OD₆₀₀ = 1, were spotted onto the plates in a serial dilution (indicated). X-33 clones transformed with either AtNIP5;1 or empty pPICZB were included as controls. Growth was recorded after 5 days at 28°C.

NbXIP1;1 α in *P. pastoris* spheroplasts was assayed by stopped-flow spectrometry (**Figure 5B**). The result shows a fast increase in light scattering followed by a gradual decrease in light scattering corresponding to a fast vesicle shrinkage

due to water efflux and a gradual vesicle swelling due to glycerol and water influx, respectively. The rate constants for glycerol permeation through the control spheroplasts, spheroplasts expressing NbXIP1;1 α and AtNIP5;1 were calculated



as: $0.213 \pm 0.004 \text{ s}^{-1}$; $0.301 \pm 0.005 \text{ s}^{-1}$; and $0.742 \pm 0.015 \text{ s}^{-1}$, respectively. The result indicated that there was little or no substantial difference in glycerol permeability between the *NbXIP1;1α* and the control spheroplasts as shown in Figure 5B. However, the *AtNIP5;1* had approximately a 3.5-fold increase in glycerol permeation as compared to the control spheroplasts.

Plasma Membrane Localization of *NbXIP1;1α* in *P. pastoris* Cells

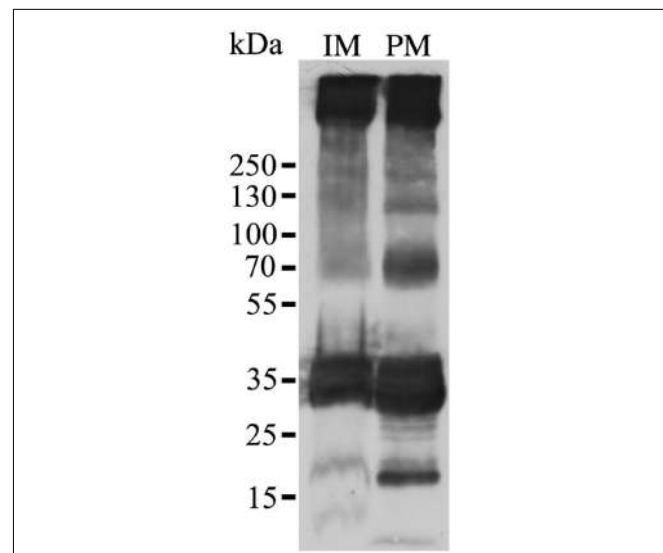
XIP isoforms were predicted (Danielson and Johanson, 2008) and later confirmed to be localized in the plasma membrane of plant cells (Bienert et al., 2011). However, to discard the likelihood that the inability to transport water and glycerol in the *Pichia* spheroplasts was due to lack of expression or to a

disturbance in the trafficking to the plasma membrane in the yeast, the localization of the recombinant N-terminally His₁₀-tagged *NbXIP1;1α* in *P. pastoris* X-33 cells was investigated. Sucrose gradient fractions of cell homogenates of *P. pastoris* cells expressing *NbXIP1;1α* analyzed by western blots indicated that *NbXIP1;1α* was present not only in the internal membranes (including the ER) fraction but also in the plasma membrane fraction as shown in Figure 6. This further indicated that the trafficking of the recombinant *NbXIP1;1α* from the ER to the plasma membrane was not impeded in the *P. pastoris* cells.

Purification and CD Spectrum of Recombinant *NbXIP1;1α*

N-nonyl-β-D-glucopyranoside detergent was used to solubilize *NbXIP1;1α* from urea stripped *P. pastoris* membranes. The solubilized protein was purified further by affinity chromatography, utilizing the His-tag at the N-terminus of the recombinant *NbXIP1;1α*. The elution fraction from the chromatography proved to be highly enriched in *NbXIP1;1α* protein as shown in Figures 3A,B. Using the current optimized protocol, a yield of 0.15 mg protein per gram of yeast cells was routinely obtained.

A CD spectrum of the purified *NbXIP1;1α* protein was recorded to verify that it was intact and correctly folded. CD spectra of AQPs mainly identify the α-helical content of the proteins since AQPs are composed of six α-helices that traverse the membrane with interconnecting loops (Plasencia et al., 2011). As shown in Figure 3C, the characteristic CD pattern at 209 and 222 nm indicated that the purified *NbXIP1;1α* protein was mainly



α -helical and correctly folded, and may therefore be reconstituted into artificial proteoliposomes for substrate specificity studies.

Boric Acid Permeation in Proteoliposomes

Boric acid permeation through the *NbXIP1;1 α* protein reconstituted into *E. coli* polar lipid vesicles supplemented with 20% cholesterol was monitored by stopped-flow spectrometry. An initial inwardly directed boric acid gradient of 100 mM resulted in an initial water efflux followed by boric acid and water influx. This resulted in an initial shrinkage followed by swelling of the vesicles as shown in **Figure 7A**. After fitting the data to a double exponential function, the second rate constants (which estimate the rate at which boric acid permeate through the vesicles) of the control vesicles and proteoliposomes were calculated as $0.11 \pm 0.01 \text{ s}^{-1}$ and $0.20 \pm 0.03 \text{ s}^{-1}$, respectively. This indicated that the purified *NbXIP1;1 α* was not fully active as it could only manage a twofold increase in boric acid permeation through the vesicles.

Recombinant *NbXIP1;1 α* Is Phosphorylated in *P. pastoris*

Attempts to render the recombinant *NbXIP1;1 α* protein fully active led to the investigation of the phosphorylation status of the purified protein, since phosphorylation has previously been shown to regulate AQP function (Kuwahara et al., 1995; Maurel et al., 1995; Johansson et al., 1998). Interestingly, an *in silico* phosphorylation prediction tool NetPhosYeast (Ingrell et al., 2007) revealed that the N-terminal part of *NbXIP1;1 α* harbors six putative phosphorylation sites as shown in **Figure 8**. Probing for phosphorylation with the PhostagTM BTL-111 confirmed that indeed the purified *NbXIP1;1 α* protein was phosphorylated as shown in **Figure 9B**. It is also important to note in **Figure 9A** that alkaline phosphatase dephosphorylated the purified *NbXIP1;1 α* , making the protein bands appear sharper and more homogenous. Dephosphorylation of the purified *NbXIP1;1 α* by alkaline phosphatase had little or no effect on the functionality of the protein as there was no appreciable change in boric acid transport when reconstituted into *E. coli* lipid vesicles as shown by the second rate constants (untreated $0.20 \pm 0.03 \text{ s}^{-1}$, dephosphorylated $0.26 \pm 0.07 \text{ s}^{-1}$; **Figures 7A,B**). A direct interpretation would be that the partially phosphorylated protein is only partly open, or that only a subfraction of *NbXIP1;1 α* is sufficiently phosphorylated to be open.

Phosphorylation Sites in *NbXIP1;1 α* Protein

To identify the sites of phosphorylation in *NbXIP1;1 α* , mass spectrometry (MS) was applied. A sequence coverage of 65% was obtained for *NbXIP1;1 α* in the MS analysis as shown in Supplementary Figure 2. Detected peptides are also shown in Supplementary Table 1. All the five phosphorylation sites [four S(p) and one T(p)] identified were in the N-terminal region of the *NbXIP1;1 α* protein (**Figure 8** and **Table 1**) and four of these coincided with the nine predicted phosphorylation sites. The MS data showed that the purified recombinant *NbXIP1;1 α* protein

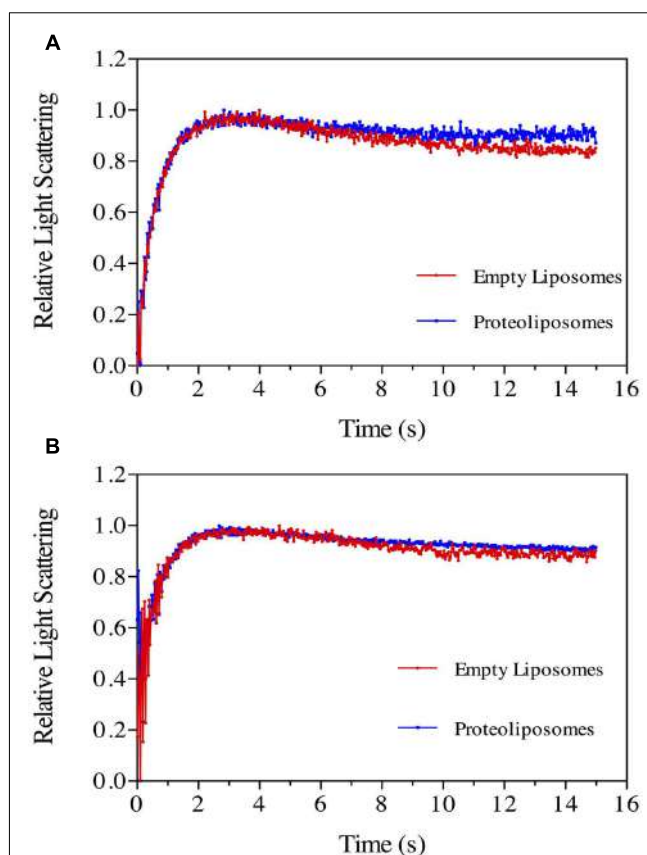


FIGURE 7 | Boric acid permeability in proteoliposomes. Stopped-flow traces showing kinetics of boric acid transport in phosphorylated (A) and dephosphorylated (B) *NbXIP1;1 α* protein reconstituted in *E. coli* lipid vesicles supplemented with 20% cholesterol. Control liposomes (red) and proteoliposomes (blue). (A) The traces (mean of eight traces) were fitted to double exponential equations. The rate constant and SEE values for the fitted curves were control ($R_1 = 1.47 \pm 0.03 \text{ s}^{-1}$; $R_2 = 0.11 \pm 0.01 \text{ s}^{-1}$) and *NbXIP1;1 α* ($R_1 = 1.62 \pm 0.05 \text{ s}^{-1}$; $R_2 = 0.20 \pm 0.03 \text{ s}^{-1}$). (B) The rate constant and SEE values for the fitted curves after fitting the traces (mean of 15 and 29 traces for control liposomes and proteoliposomes, respectively) to double exponential equations were control ($R_1 = 1.44 \pm 0.07 \text{ s}^{-1}$; $R_2 = 0.11 \pm 0.04 \text{ s}^{-1}$) and *NbXIP1;1 α* ($R_1 = 1.02 \pm 0.10 \text{ s}^{-1}$; $R_2 = 0.26 \pm 0.07 \text{ s}^{-1}$).

was partially phosphorylated as identical peptides were found with or without phosphorylation (Supplementary Figure 3).

DISCUSSION

Heterologous Expression

Just as for the *N. tabacum* XIP1;1 splice variants (Bienert et al., 2011), the difference between the two *N. benthamiana* splice variants is that the *NbXIP1;1 β* splice-variant is one amino acid longer as compared to the *NbXIP1;1 α* splice-variant. This is due to the alternative splice site in the first intron either comprised of the donor and acceptor sites GT ... AG for *NbXIP1;1 β* or GT ... (AGC) AG for *NbXIP1;1 α* (Supplementary Figure 4), resulting in the *NbXIP1;1 β* splice-variant being one arginine

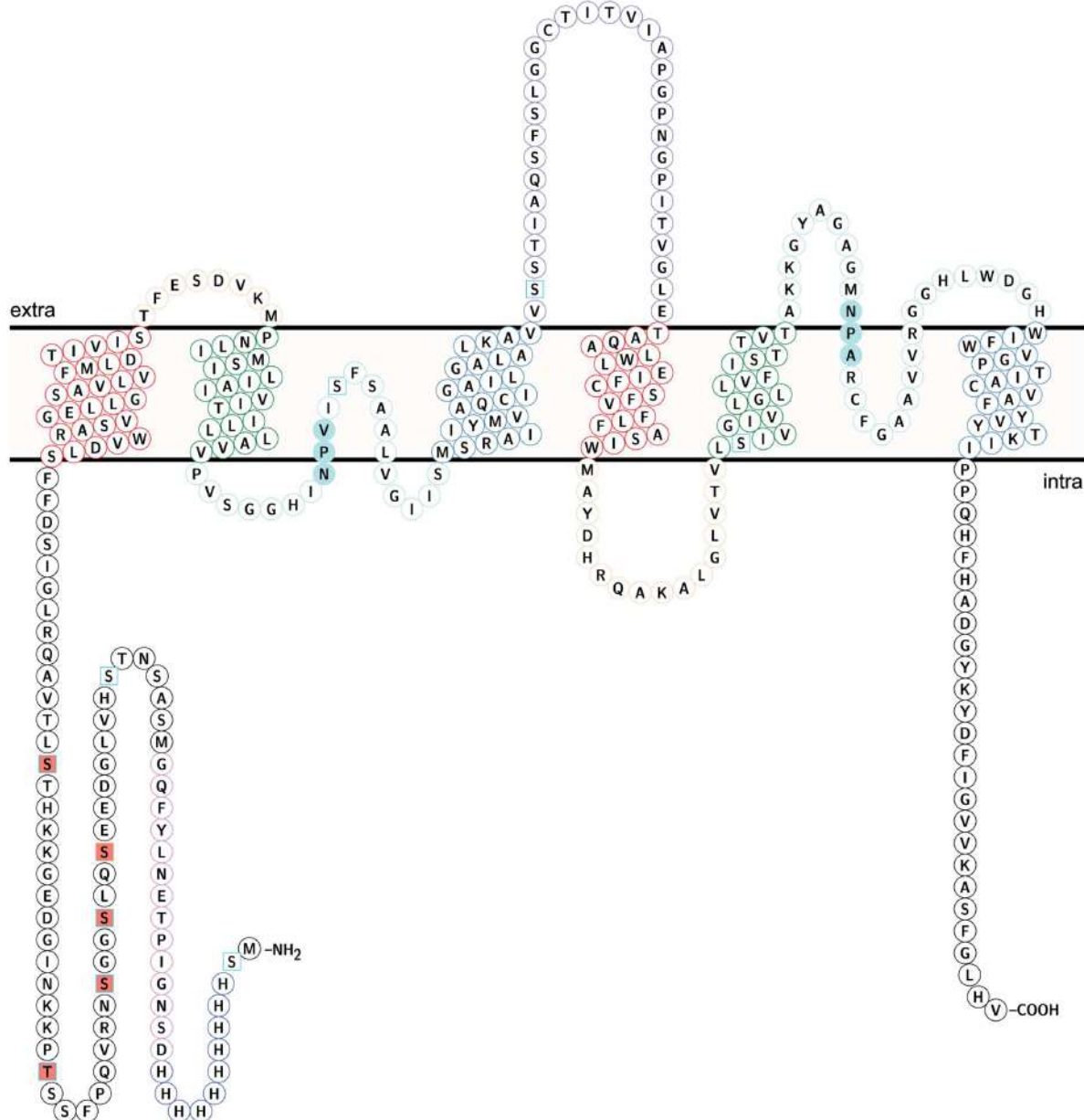
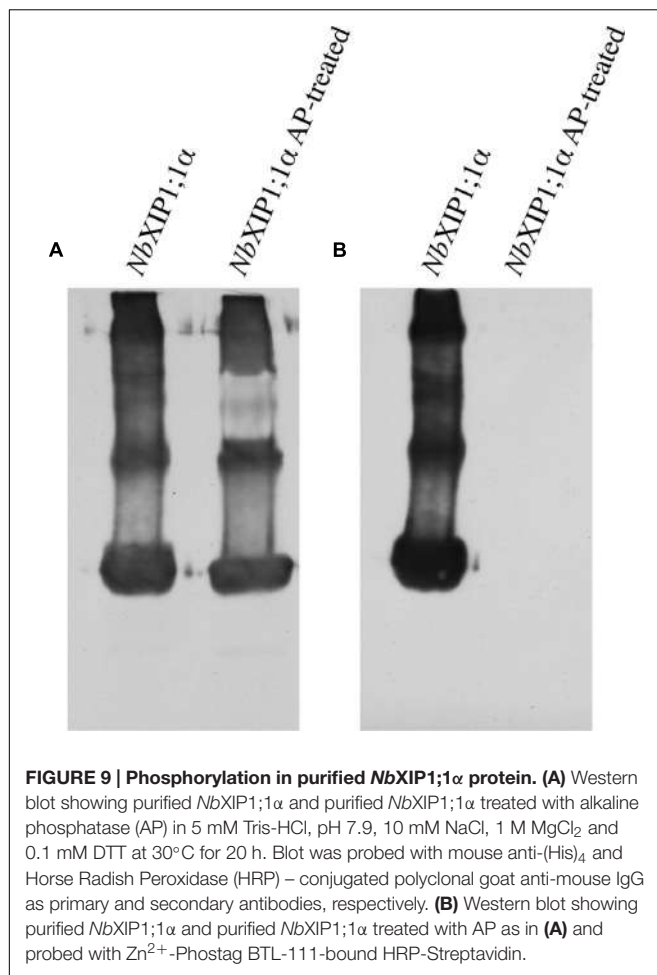


FIGURE 8 | Topology of NbXIP1;1 α protein showing identified phosphorylation sites. Identified phospho sites – square salmon fill. Predicted phospho sites – square frame in sky blue. The coloring of helices and loops reflect a direct repeat in the gene/protein. Transmembrane helix (TM) 1 and TM 4 – frame in red. TM2 and TM 5 – frame in green. TM 3 and TM 6 – frame in steel blue. Loop A and Loop D – frame in peach. Loop B and loop E – frame in pale turquoise. Loop C – frame in medium purple. NPV/NPA box – pale turquoise fill. H3-H12 – Histidine tag in blue. D13-G26 – TEV protease cleavage site and linker in violet. The topology model was done in Protter (Omasits et al., 2014).

longer. The shorter splice-variant *NbXIP1;1 α* loses the arginine and the amino acid upstream in this splice-variant changes from an asparagine to a lysine, with all other amino acids left identical in the two splice variants (Figure 10).

In order to generate enough protein for structural and functional characterizations of the *NbXIP1;1* proteins, cDNAs corresponding to both splice variants were transformed into the yeast *P. pastoris*. After optimizing the protein expression levels,

by screening clones with different gene copy numbers selected at different levels of antibiotic concentration (Nordén et al., 2011), both splice variants expressed at similar protein levels. Not all AQPs express well in *P. pastoris* but for these two isoforms the expression levels were relatively high and comparable to other plant and human AQPs and to other integral membrane proteins that we have managed to express and purify in functional form (Karlsson et al., 2003; Törnroth-Horsefield et al., 2006; Horsefield



et al., 2008; Agemark et al., 2012; Moparthi et al., 2014; Kirscht et al., 2016). Due to a slightly higher expression level, the shorter splice-variant NbXIP1;1 α was selected for further investigations in the present study (Supplementary Figure 1).

In most plant organs and tissues XIP isoforms have been predicted and shown to be located in the plasma membrane (Danielson and Johanson, 2008; Bienert et al., 2011). In order to functionally study NbXIP1;1 α in the cell membrane of *P. pastoris* or purified from a crude membrane fraction from *P. pastoris*, it is necessary to verify that this AQP is correctly targeted to the *P. pastoris* cell membrane. When membrane vesicles from a total membrane fraction (i.e., a microsomal fraction) of *P. pastoris* were separated on a sucrose density gradient, NbXIP1;1 α was shown to be primarily located in the plasma membrane fraction (Figure 6). As expected, the protein was also to a lesser extent present in the internal membrane fraction since NbXIP1;1 α , like all integral proteins of the plasma membrane, is synthesized in the ER.

Substrate Selectivity of NbXIP1;1 α in *P. pastoris*

The orthodox AQPs are only permeable to water, e.g., *HsAQP1* and *SoPIP2;1*, (Preston et al., 1992; Törnroth-Horsefield et al.,

2006), while other AQPs are permeable to water and in addition other small uncharged solutes, e.g., glycerol, (*EcGlpF*; Fu et al., 2000), ammonia (*AtTIP2;1*; Kirscht et al., 2016), and boric acid (*AtNIP5;1*; Takano et al., 2006). The substrate specificity of AQPs is determined by a selectivity filter that consists of two regions in the pore of AQPs.

One is the NPA region that basically prevents protons from going through the pore. The NPA region is formed by two half helices each of which have the amino acids NPA at their N-termini. The N-termini of the two half helices meet and connect in the middle of the membrane spanning AQP creating a partial positive charge in the pore that prevents protons from passing. Based on sequence alignments the XIPs conform to the generic AQP fold with the two half helices and for most XIPs, including the NbXIP1;1s, the NPA boxes are relatively well conserved. It is only in the third position of the first NPA box that the alanine is substituted for a valine (Supplementary Figure 5) or another small uncharged amino acid residue in other plant species (Danielson and Johanson, 2008). Thus it is likely that there is an obstruction for hydronium ion permeation also in the XIPs. This is consistent with our finding that NbXIP1;1 α is tolerated in the plasma membrane where a leakage of protons would be detrimental for the pH and charge gradients that are crucial for nutrient uptake and maintenance of the osmotic balance.

The other region in the pore that determines the substrate specificity of AQPs is the so-called aromatic/arginine (ar/R) region. This region has recently been extended to consist of five amino acids at specific positions in the pore and the identity of these amino acids determine which substrates can pass (Table 2; Kirscht et al., 2016). It should be noted that the sequence divergence of XIPs from other AQPs makes the identity of the amino acid residues at position LC^P in C-loop and H5^P in helix 5 highly uncertain, and it is likely that a structure of a XIP will reveal novel and unpredicted features, as the structure of *AtTIP2;1* did for the TIP subfamily. The amino acids predicted to constitute the ar/R region of NbXIP1;1 α are similar to the amino acids in the ar/R region of some of the AQP isoforms belonging to the NIP subfamily in plants. One of these isoforms is *AtNIP5;1* that has been shown to be permeable to boric acid, as mentioned above (Takano et al., 2006).

Boric Acid

We used a growth assay in *P. pastoris* to investigate whether also NbXIP1;1 α is permeable to boric acid (B[OH]₃) and found that the cells expressing the NbXIP1;1 α AQP were similarly sensitive to boric acid as compared to the cells expressing the *AtNIP5;1*. Thus, NbXIP1;1 α is permeable to boric acid and placing the His-tag at the N-terminal renders the protein slightly more permeable to boric acid as compared to a channel with a C-terminally located His-tag (Figure 4). This result may suggest that the N-terminally His-tagged NbXIP1;1 α is somewhat more open, which might have implications when discussing a putative gating mechanism involving phosphorylation of the protein (see below). However, the difference in sensitivity of the cells may be due to difference in the expression levels of NbXIP1;1 α constructs as the N-terminally His-tagged protein expresses better than the

TABLE 1 | Phosphorylation sites in NbXIP1;1 α identified by mass spectrometry.

Number	Assigned p-sites	Sequence	Mascot Score	Charge	Experimental weight	Theoretical weight
26–49	S41	GMSASNTSHVLGDEES(p)QLSGGSNR	95	3+	2499.0246	2499.0333
28–49	S44	SASNTSHVLGDEESQLS(p)GGSNR	92	3+	2310.9612	2310.9714
32–49	S47	TSHVLGDEESQLSGGS(p)NJR	82	2+	1951.8163	1951.8273
50–58	T56	VQPFSST(p)PK	42	2+	1069.4796	1069.4845
68–76	S70	HTS(p)LTVQR	63	2+	1091.5076	1091.5125

NbXIP1;1 α MASNTSHVLGDEESQLSGGSNRVQPFSSTPK-KNIGDEGKKHTSLTVAQRLG 51
NbXIP1;1 β MASNTSHVLGDEESQLSGGSNRVQPFSSTPKRNIGDEGKKHTSLTVAQRLG 52
NbXIP1;2 α MAATTRDALGDEETQ-----FSSIPKQV-IDGENKKKAPLTLSQRLG 41
NbXIP1;2 β MAATTRDALGDEETQ-----FSSIPKQVRIDGENKKKAPLTLSQRLG 42
NbXIP1;3 MDASNGNVLGDEESQSIS-----FGSSNKIQPITSTQKRYTSLTMAERLG 45

FIGURE 10 | Close up of the splice sites in the amino acid sequences of NbXIP1 splice variants. Splice sites in NbXIP1;1 splice variants and NbXIP1;2 splice variants are in red boxes.

C-terminally His-tagged protein as shown in **Figure 2**. That NbXIP1;1 α in the growth assay is equally permeable to boric acid as compared to AtNIP5;1 also suggests that NbXIP1;1 α is not only correctly targeted to the cell membrane but also correctly folded and functional.

Water and Glycerol

Whether NbXIP1;1 α is permeable to water is possible to investigate using *P. pastoris* spheroplasts and stopped-flow spectrometry. The results suggest that water flow through NbXIP1;1 α do not take place or is very limited (**Figure 5A**),

while the control boric acid-permeable AQP AtNIP5;1 displayed a comparably higher but limited water permeability. However, the sizes of the different spheroplasts were not checked and this may complicate the interpretation of the result. In a previous study, *PtXIP2;1* and *PtXIP3;3* were permeable to water when expressed in *Xenopus oocytes* whereas other *PtXIPs* including *PtXIP1;1* were not permeable to water (Lopez et al., 2012).

Some XIP isoforms have been reported to be permeable to glycerol when transiently expressed in *Xenopus laevis* oocytes (Bienert et al., 2011). Using the *P. pastoris* spheroplast experimental system, we could not detect any glycerol permeability for NbXIP1;1 α while the control AQP AtNIP5;1 showed approximately a fourfold higher glycerol permeability as compared to spheroplasts from *P. pastoris* cells transformed with empty pPICZB plasmid (**Figure 5B**). Our spheroplast results for NbXIP1;1 α are in agreement with previous results showing that XIP1;1 isoforms are not permeable to water when expressed in oocytes (Bienert et al., 2011; Lopez et al., 2012). However, the glycerol permeability that could be seen for XIP1;1 isoforms when expressed in oocytes was not evident using the *P. pastoris* spheroplast experimental system. Whether this discrepancy reflects the choice of the different experimental systems or a difference in the substrate specificity of the different XIP1;1 isoforms from *N. benthamiana*, *N. tabacum*, and *P. trichocarpa*, respectively, remains unclear.

It is quite difficult to visualize how small uncharged substances like boric acid can permeate through an AQP pore without water also being transported. Nevertheless, the inability of NbXIP1;1 α to facilitate the transport of water was not unexpected considering the amino acids defining the selectivity filter, since the amino acid residues constituting its ar/R region are more hydrophobic than the amino acids constituting the ar/R region of orthodox water permeable AQPs (Danielson and Johanson, 2008; Bienert et al., 2011). Based on the above, we suggest that it is unlikely that water is a true *in vivo* substrate for XIP1;1 isoforms and furthermore, that it is still unclear whether glycerol is a true *in vivo* substrate, especially

TABLE 2 | Aromatic arginine (ar/R) selectivity filter of NbXIP isoforms, human and *A. thaliana* aquaporin isoforms.

AQPs	H2 ^P	LC ^P	H5 ^P	LE ^P	HE ^P
NbXIP1;1s	I	C	V/T	A	R
NbXIP1;2s	A	C	V/T	A	R
NbXIP1;3	I	C	V/T	A	R
AtNIP1s, 2;1, 4s	W	S/T	V	A	R
AtNIP3;1	W	T	I	A	R
AtNIP5;1	A	T	I	G	R
AtNIP6;1	A	T	I	A	R
AtNIP7;1	A	T	V	G	R
AtTIP1s	H	F	I	A	V
AtTIP2s	H	H	I	G	R
AtTIP3s	H	F	I	A	R
AtTIP5;1	N	Y	V	G	C
HsAQP8	H	F	I	G	R
AtPIP8	F	N	H	T	R
AtSIP1;1	I	G	V	P	I
AtSIP1;2	V	G	F	P	I
AtSIP2;1	S	K	H	G	A

The ar/R filter is defined by five amino acid residues: one in helix 2 (H2^P), one in loop C (LC^P), one in helix 5 (H5^P), one in loop E (LE^P), and one in helix E (HE^P). ^PThe position of the amino acid residue in the ar/R filter. Due to alternative alignment possibilities, the amino acids in the LC^P and H5^P positions are uncertain.

since the relevance for glycerol transport in plants is limited. This is in contrast to mammalian cells where glycerol from hydrolysed triacylglycerols need to be transported and taken up by liver cells and converted to glucose (Jelen et al., 2011). One instance when triacylglycerols are hydrolysed in plants is during seed germination releasing fatty acids that by β -oxidation provide energy for germination. Another plant developmental state when fatty acids from triacylglycerols provide energy is during pollen tube growth following pollination (Buchanan et al., 2000). Upon triacylglycerol hydrolysis in seeds, the fatty acids and the remaining glycerol are released from the oil bodies into the cytosol. The glycerol may be converted to triose phosphates and subsequently to sucrose, but this takes place inside the cells. Thus, it remains unclear whether glycerol has to be transported between cells and require glycerol-specific protein channels in the plasma membrane of cells.

Characterization of Purified NbXIP1;1 α

The N-terminally His-tagged NbXIP1;1 α solubilized from *Pichia* membranes and Ni-NTA affinity purified, showed a typical AQP banding pattern when separated by SDS-PAGE with the monomeric form as the dominating band (Figures 3A,B). The CD spectrum of NbXIP1;1 α was very similar to that of other AQPs showing a typical CD spectrum of a predominantly α -helical protein, suggesting that the α -helices are intact and that NbXIP1;1 α is correctly folded (Figure 3C). The purified NbXIP1;1 α was reconstituted into proteoliposomes in order to be able to monitor the function of the isolated protein, i.e., XIP1;1 α homotetramers, in contrast to the *P. pastoris* spheroplast experimental set up in which putatively interfering proteins might be present. The stopped-flow spectrometry measurements showed that NbXIP1;1 α conferred a twofold increase in the boric acid permeation as compared to empty liposomes (Figure 7A). This result is in contrast to the apparently highly active boric acid transport by NbXIP1;1 α in the *P. pastoris* cells. This suggests to us that even if NbXIP1;1 α is permeable to boric acid when reconstituted into proteoliposomes, the NbXIP1;1 α pore is most probably not fully open. This could be due to a yet unknown gating mechanism blocking the pore, such that only a subpopulation of the NbXIP1;1 α present in the proteoliposomes have an open pore and that the rest have a closed conformation. The absence of an accessory protein necessary for the pore to be fully open *in vivo* would also result in a low channel activity.

Phosphorylation of NbXIP1;1 α

It is known from other plant AQPs that phosphorylation and dephosphorylation of specific amino acids, such as serines and threonines, is involved in opening and closing the pore (Johansson et al., 1998; Törnroth-Horsefield et al., 2006). In order to discern whether the difference in boric acid permeability of NbXIP1;1 α when present in *P. pastoris* cells as compared to reconstituted into proteoliposomes could be due to different phosphorylation states of the protein, we first investigated whether purified NbXIP1;1 α was phosphorylated. Figure 9 clearly shows that purified NbXIP1;1 α is indeed

phosphorylated and that the phosphate groups can be removed by alkaline phosphatase. To define which specific amino acids are phosphorylated, we used an *in silico* prediction tool in combination with mass spectrometry. The protein was predicted to be phosphorylated at nine different serines and threonines, six in the N-terminal region, one serine in loop B, one serine in loop C and one serine in helix 5 (Figure 8). By mass spectrometry four of these predicted phosphorylation sites were confirmed, all four in the N-terminal region. In addition, the mass spectrometry analysis discerned yet another phosphorylation site, also in the N-terminal region. Thus, NbXIP1;1 α is phosphorylated at altogether five amino acids in the N-terminal region, four serines and one threonine. Since phosphorylation of AQPs has been shown to be important for both gating the channel, as mentioned above, as well as for targeting the AQP to the plasma membrane, phosphorylation of some of the amino acids might have a role in targeting NbXIP1;1 α to the plasma membrane. Interestingly, the N-terminus of AtNIP5;1, an AQP isoform that shares similar substrate specificity with the *Nt*XIPs, needed to be truncated to be active in *S. cerevisiae* yeast cells (Bienert et al., 2008). Here, we show that a full-length version is successfully expressed and active in the plasma membrane of *P. pastoris*. This deviance may be due to the presence of the added N-terminal His-tag or due to differences in trafficking mechanisms in the two yeasts, possibly directed by phosphorylation.

Both phosphorylated and non-phosphorylated, but otherwise identical, NbXIP1;1 α peptides were identified by mass spectrometry (Supplementary Figure 3). This suggests that only a fraction of NbXIP1;1 α was phosphorylated. When a dephosphorylated NbXIP1;1 α was reconstituted into proteoliposomes, no difference in boric acid permeability could be detected compared to phosphorylated NbXIP1;1 α (Figure 7B). We speculate that the dephosphorylated NbXIP1;1 α represents the closed conformation of the protein and the N-terminal region may need to be fully phosphorylated for the channel to open. For other AQPs, it has been shown that amino acids phosphorylated when the proteins were expressed in *P. pastoris* were also phosphorylated *in planta* (Daniels and Yeager, 2005). Thus, the amino acids in the N-terminal region of NbXIP1;1 α shown here to be phosphorylated by kinases in *P. pastoris* would most likely also be accessible for plant kinases. Whether NbXIP1;1 is phosphorylated *in planta* and if this is affected by the alternative splicing, remains to be shown but it could potentially be a mechanism that regulates trafficking or gating of NbXIP1;1.

CONCLUSION

We have shown that XIP1;1 isoforms can be expressed in the heterologous host *P. pastoris*, that the splice variant NbXIP1;1 α is functional and permeable to boric acid in *Pichia* cells and that NbXIP1;1 α is not a water channel. Moreover, we have shown that the N-terminal region of NbXIP1;1 α is phosphorylated. We suggest that NbXIP1;1 α is gated by phosphorylation and that the phosphorylated protein represents the open conformation.

AUTHOR CONTRIBUTIONS

PK and UJ conceived the research. PK and UJ planned the experiments. HA-K, HA, AE, AK, KN, and SK performed the experiments. HA-K wrote the manuscript. PK, UJ, HA-K, KN, and SK revised the manuscript.

FUNDING

This work was supported by the Swedish Research Council (621-2011-5139) to PK.

REFERENCES

- Agemark, M., Kowal, J., Kukulski, W., Nordén, K., Gustavsson, N., Johanson, U., et al. (2012). Reconstitution of water channel function and 2D-crystallization of human aquaporin 8. *Biochim. Biophys. Acta* 1818, 839–850. doi: 10.1016/j.bbamem.2011.12.006
- Agre, P., and Kozono, D. (2003). Aquaporin water channels: molecular mechanisms for human diseases. *FEBS Lett.* 555, 72–78. doi: 10.1016/s0014-5793(03)01083-4
- Anderberg, H. I., Kjellbom, P., and Johanson, U. (2012). Annotation of *Selaginella moellendorffii* major intrinsic proteins and the evolution of the protein family in terrestrial plants. *Front. Plant Sci.* 3:33. doi: 10.3389/fpls.2012.00033
- Ariani, A., and Gepts, P. (2015). Genome-wide identification and characterization of aquaporin gene family in common bean (*Phaseolus vulgaris* L.). *Mol. Genet. Genom.* 290, 1771–1785. doi: 10.1007/s00438-015-1038-2
- Azad, A. K., Katsuhara, M., Sawa, Y., Ishikawa, T., and Shibata, H. (2008). Characterization of four plasma membrane aquaporins in tulip petals: a putative homolog is regulated by phosphorylation. *Plant Cell Physiol.* 49, 1196–1208. doi: 10.1093/pcp/pcn095
- Bienert, G. P., Bienert, M. D., Jahn, T. P., Boutry, M., and Chaumont, F. (2011). Solanaceae XIPs are plasma membrane aquaporins that facilitate the transport of many uncharged substrates. *Plant J.* 66, 306–317. doi: 10.1111/j.1365-313X.2011.04496.x
- Bienert, G. P., Thorsen, M., Schussler, M. D., Nilsson, H. R., Wagner, A., Tamás, M. J., et al. (2008). A subgroup of plant aquaporins facilitate the bi-directional diffusion of As(OH)3 and Sb(OH)3 across membranes. *BMC Biol.* 6:26. doi: 10.1186/1741-7007-6-26
- Buchanan, B. B., Grussem, W., and Jones, R. L. (2000). *Biochemistry and Molecular Biology of Plants*. Derwood, MD: American Society of Plant Physiologists.
- Bushell, M. E., Rowe, M., Avignone-Rossa, C. A., and Wardell, J. N. (2003). Cyclic fed-batch culture for production of human serum albumin in *Pichia pastoris*. *Biotechnol. Bioeng.* 82, 678–683. doi: 10.1002/bit.10616
- Chaumont, F., Barrieu, F., Wojcik, E., Chrispeels, M. J., and Jung, R. (2001). Aquaporins constitute a large and highly divergent protein family in maize. *Plant Physiol.* 125, 1206–1215. doi: 10.1104/pp.125.3.1206
- Daniels, M. J., and Yeager, M. (2005). Phosphorylation of aquaporin PvTIP3;1 defined by mass spectrometry and molecular modeling. *Biochemistry* 44, 14443–14454. doi: 10.1021/bi050565d
- Danielson, J. A., and Johanson, U. (2008). Unexpected complexity of the aquaporin gene family in the moss *Physcomitrella patens*. *BMC Plant Biol.* 8:45. doi: 10.1186/1471-2229-8-45
- Don-Doncow, N., Escobar, Z., Johansson, M., Kjellström, S., Garcia, V., Munoz, E., et al. (2014). Galiellalactone is a direct inhibitor of the transcription factor STAT3 in prostate cancer cells. *J. Biol. Chem.* 289, 15969–15978. doi: 10.1074/jbc.M114.564252
- Edgar, R. C. (2004). MUSCLE: a multiple sequence alignment method with reduced time and space complexity. *BMC Bioinformatics* 5:113. doi: 10.1186/1471-2105-5-113
- Fischer, G., Kosinska-Eriksson, U., Aponte-Santamaría, C., Palmgren, M., Geijer, C., Hedfalk, K., et al. (2009). Crystal structure of a yeast aquaporin at 1.15 Ångström reveals a novel gating mechanism. *PLoS Biol.* 7:e1000130. doi: 10.1371/journal.pbio.1000130
- Fotiadis, D., Jeno, P., Mini, T., Wirtz, S., Muller, S. A., Fraysse, L., et al. (2001). Structural characterization of two aquaporins isolated from native spinach leaf plasma membranes. *J. Biol. Chem.* 276, 1707–1714. doi: 10.1074/jbc.M009383200
- Fu, D., Libson, A., Miercke, L. J., Weitzman, C., Nollert, P., Krucinski, J., et al. (2000). Structure of a glycerol-conducting channel and the basis for its selectivity. *Science* 290, 481–486. doi: 10.1126/science.290.5491.481
- Gomes, D., Agasse, A., Thiébaud, P., Delrot, S., Gerós, H., and Chaumont, F. (2009). Aquaporins are multifunctional water and solute transporters highly divergent in living organisms. *Biochim. Biophys. Acta* 1788, 1213–1228. doi: 10.1016/j.bbamem.2009.03.009
- Gonen, T., Cheng, Y., Sliz, P., Hiroaki, Y., Fujiyoshi, Y., Harrison, S. C., et al. (2005). Lipid-protein interactions in double-layered two-dimensional AQP0 crystals. *Nature* 438, 633–638. doi: 10.1038/nature04321
- Grillitsch, K., Tarazona, P., Klug, L., Wriessnegger, T., Zellnig, G., Leitner, E., et al. (2014). Isolation and characterization of the plasma membrane from the yeast *Pichia pastoris*. *Biochim. Biophys. Acta* 1838, 1889–1897. doi: 10.1016/j.bbamem.2014.03.012
- Guenther, J. F., Chanmanivone, N., Galetovic, M. P., Wallace, I. S., Cobb, J. A., and Roberts, D. M. (2003). Phosphorylation of soybean nodulin 26 on serine 262 enhances water permeability and is regulated developmentally and by osmotic signals. *Plant Cell* 15, 981–991. doi: 10.1105/tpc.009787
- Gupta, A. B., and Sankararamakrishnan, R. (2009). Genome-wide analysis of major intrinsic proteins in the tree plant *Populus trichocarpa*: characterization of XIP subfamily of aquaporins from evolutionary perspective. *BMC Plant Biol.* 9:134. doi: 10.1186/1471-2229-9-134
- Hiroaki, Y., Tani, K., Kamegawa, A., Gyobu, N., Nishikawa, K., Suzuki, H., et al. (2006). Implications of the aquaporin-4 structure on array formation and cell adhesion. *J. Mol. Biol.* 355, 628–639. doi: 10.1016/j.jmb.2005.10.081
- Hori, T., Sato, Y., Takahashi, N., Takio, K., Yokomizo, T., Nakamura, M., et al. (2010). Expression, purification and characterization of leukotriene B(4) receptor, BLT1 in *Pichia pastoris*. *Protein Expr. Purif.* 72, 66–74. doi: 10.1016/j.pep.2010.02.013
- Horsefield, R., Nordén, K., Fellert, M., Backmark, A., Törnroth-Horsefield, S., Terwisscha van Scheltinga, A. C., et al. (2008). High-resolution x-ray structure of human aquaporin 5. *Proc. Natl. Acad. Sci. U.S.A.* 105, 13327–13332. doi: 10.1073/pnas.0801466105
- Ingrell, C. R., Miller, M. L., Jensen, O. N., and Blom, N. (2007). NetPhosYeast: prediction of protein phosphorylation sites in yeast. *Bioinformatics* 23, 895–897. doi: 10.1093/bioinformatics/btm020
- Invitrogen. (2005). *EasySelect Pichia Expression Kit, version G*. Available at: http://tools.invitrogen.com/content/sfs/manuals/easyselect_man.pdf
- Jelen, S., Wacker, S., Aponte-Santamaría, C., Skott, M., Rojek, A., Johanson, U., et al. (2011). Aquaporin-9 protein is the primary route of hepatocyte glycerol

ACKNOWLEDGMENTS

We would like to express our sincere gratitude to Adine Karlsson for her technical assistance in the laboratory. We are also grateful to Katja Bernfur for her immeasurable assistance in creating the in-house Mascot database for *N. benthamiana* XIP1;1 aquaporins.

SUPPLEMENTARY MATERIAL

The Supplementary Material for this article can be found online at: <http://journal.frontiersin.org/article/10.3389/fpls.2016.00862>

- uptake for glycerol gluconeogenesis in mice. *J. Biol. Chem.* 286, 44319–44325. doi: 10.1074/jbc.M111.297002
- Johanson, U., Karlsson, M., Johansson, I., Gustavsson, S., Sjövall, S., Fraysse, L., et al. (2001). The complete set of genes encoding major intrinsic proteins in *Arabidopsis* provides a framework for a new nomenclature for major intrinsic proteins in plants. *Plant Physiol.* 126, 1358–1369. doi: 10.1104/pp.126.4.1358
- Johansson, I., Karlsson, M., Johanson, U., Larsson, C., and Kjellbom, P. (2000). The role of aquaporins in cellular and whole plant water balance. *Biochim. Biophys. Acta* 1465, 324–342. doi: 10.1016/S0005-2736(00)00147-4
- Johansson, I., Karlsson, M., Shukla, V. K., Chrispeels, M. J., Larsson, C., and Kjellbom, P. (1998). Water transport activity of the plasma membrane aquaporin PM28A is regulated by phosphorylation. *Plant Cell* 10, 451–459. doi: 10.1105/tpc.10.3.451
- Karlsson, M., Fotiadis, D., Sjövall, S., Johansson, I., Hedfalk, K., Engel, A., et al. (2003). Reconstitution of water channel function of an aquaporin overexpressed and purified from *Pichia pastoris*. *FEBS Lett.* 537, 68–72. doi: 10.1016/S0014-5793(03)00082-6
- Kinoshita, E., Kinoshita-Kikuta, E., Sugiyama, Y., Fukada, Y., Ozeki, T., and Koike, T. (2012). Highly sensitive detection of protein phosphorylation by using improved Phos-tag Biotin. *Proteomics* 12, 932–937. doi: 10.1002/pmic.201100639
- Kirsch, A., Kapitan, S. S., Bienert, G. P., Chaumont, F., Nissen, P., de Groot, B. L., et al. (2016). Crystal structure of an ammonia-permeable aquaporin. *PLoS Biol.* 14:e1002411. doi: 10.1371/journal.pbio.1002411
- Kistler, J., Goldie, K., Donaldson, P., and Engel, A. (1994). Reconstitution of native-type noncrystalline lens fiber gap junctions from isolated hemichannels. *J. Cell Biol.* 126, 1047–1058. doi: 10.1083/jcb.126.4.1047
- Kuwahara, M., Fushimi, K., Terada, Y., Bai, L., Marumo, F., and Sasaki, S. (1995). cAMP-dependent phosphorylation stimulates water permeability of aquaporin-collecting duct water channel protein expressed in *Xenopus* oocytes. *J. Biol. Chem.* 270, 10384–10387. doi: 10.1074/jbc.270.10.10384
- Lee, J. K., Kozono, D., Remis, J., Kitagawa, Y., Agre, P., and Stroud, R. M. (2005). Structural basis for conductance by the archaeal aquaporin AqpM at 1.68 Å. *Proc. Natl. Acad. Sci. U.S.A.* 102, 18932–18937. doi: 10.1073/pnas.0506144102
- Lee, J. W., Zhang, Y., Weaver, C. D., Shomer, N. H., Louis, C. F., and Roberts, D. M. (1995). Phosphorylation of nodulin 26 on serine 262 affects its voltage-sensitive channel activity in planar lipid bilayers. *J. Biol. Chem.* 270, 27051–27057. doi: 10.1074/jbc.270.45.27051
- Lopez, D., Bronner, G., Brunel, N., Auguin, D., Bourgerie, S., Brignolas, F., et al. (2012). Insights into *Populus* XIP aquaporins: evolutionary expansion, protein functionality, and environmental regulation. *J. Exp. Bot.* 63, 2217–2230. doi: 10.1093/jxb/err404
- Maurel, C., Kado, R. T., Guern, J., and Chrispeels, M. J. (1995). Phosphorylation regulates the water channel activity of the seed-specific aquaporin α-TIP. *EMBO J.* 14, 3028–3035.
- Moparthi, L., Survery, S., Kreir, M., Simonsen, C., Kjellbom, P., Högestätt, E. D., et al. (2014). Human TRPA1 is intrinsically cold- and chemosensitive with and without its N-terminal ankyrin repeat domain. *Proc. Natl. Acad. Sci. U.S.A.* 111, 16901–16906. doi: 10.1073/pnas.1412689111
- Neuhoff, V., Arold, N., Taube, D., and Ehrhardt, W. (1988). Improved staining of proteins in polyacrylamide gels including isoelectric focusing gels with clear background at nanogram sensitivity using Coomassie Brilliant Blue G-250 and R-250. *Electrophoresis* 9, 255–262. doi: 10.1002/elps.1150090603
- Newby, Z. E., O'Connell, J. III, Robles-Colmenares, Y., Khademi, S., Miercke, L. J., and Stroud, R. M. (2008). Crystal structure of the aquaglyceroporin PfAQP from the malarial parasite *Plasmodium falciparum*. *Nat. Struct. Mol. Biol.* 15, 619–625. doi: 10.1038/nsmb.1431
- Nordén, K., Agemark, M., Danielson, J. A., Alexandersson, E., Kjellbom, P., and Johanson, U. (2011). Increasing gene dosage greatly enhances recombinant expression of aquaporins in *Pichia pastoris*. *BMC Biotechnol.* 11:47. doi: 10.1186/1472-6750-11-47
- Nyblom, M., Öberg, F., Lindkvist-Petersson, K., Hallgren, K., Findlay, H., Wikström, J., et al. (2007). Exceptional overproduction of a functional human membrane protein. *Protein Expr. Purif.* 56, 110–120. doi: 10.1016/j.pep.2007.07.007
- Omasits, U., Ahrens, C. H., Müller, S., and Wollscheid, B. (2014). Proter: interactive protein feature visualization and integration with experimental proteomic data. *Bioinformatics* 30, 884–886. doi: 10.1093/bioinformatics/btt607
- Park, W., Scheffler, B. E., Bauer, P. J., and Campbell, B. T. (2010). Identification of the family of aquaporin genes and their expression in upland cotton (*Gossypium hirsutum* L.). *BMC Plant Biol.* 10:142. doi: 10.1186/1471-2229-10-142
- Plasencia, I., Survery, S., Ibragimova, S., Hansen, J. S., Kjellbom, P., Helix-Nielson, C., et al. (2011). Structure and stability of the spinach aquaporin SoPIP2;1 in detergent micelles and lipid membranes. *PLoS ONE* 6:e14674. doi: 10.1371/journal.pone.0014674
- Preston, G. M., Carroll, T. P., Guggino, W. B., and Agre, P. (1992). Appearance of water channels in *Xenopus* oocytes expressing red cell CHIP28 protein. *Science* 256, 385–387. doi: 10.1126/science.256.5055.385
- Reuscher, S. S., Akiyama, M., Mori, C., Aoki, K., Shibata, D., and Shiratake, K. (2013). Genome-wide identification and expression analysis of aquaporins in tomato. *PLoS ONE* 8:e79052. doi: 10.1371/journal.pone.0079052
- Sade, N., Vinocur, B. J., Diber, A., Shatil, A., Ronen, G., Nissan, H., et al. (2009). Improving plant stress tolerance and yield production: is the tonoplast aquaporin SITIP2;2 a key to isohydric to anisohydric conversion? *New Phytol.* 181, 651–661. doi: 10.1111/j.1469-8137.2008.02689.x
- Sakurai, J., Ishikawa, F., Yamaguchi, T., Uemura, M., and Maeshima, M. (2005). Identification of 33 rice aquaporin genes and analysis of their expression and function. *Plant Cell Physiol.* 46, 1568–1577. doi: 10.1093/pcp/pci172
- Savage, D. F., Egea, P. F., Robles-Colmenares, Y., O'Connell, J. D. I. I. I., and Stroud, R. M. (2003). Architecture and selectivity in aquaporins: 2.5 Å X-ray structure of aquaporin Z. *PLoS Biol.* 1:e72. doi: 10.1371/journal.pbio.0000072
- Shevchenko, A., Tomas, H., Havlis, J., Olsen, J. V., and Mann, M. (2006). In-gel digestion for mass spectrometric characterization of proteins and proteomes. *Nat. Protoc.* 1, 2856–2860. doi: 10.1038/nprot.2006.468
- Stratton, J., Chiruvolu, V., and Meagher, M. (1998). High cell-density fermentation. *Methods Mol. Biol.* 103, 107–120.
- Sui, H., Han, B. G., Lee, J. K., Walian, P., and Jap, B. K. (2001). Structural basis of water-specific transport through the AQP1 water channel. *Nature* 414, 872–878. doi: 10.1038/414872a
- Takano, J., Wada, M., Ludewig, U., Schaaf, G., von Wirén, N., and Fujiwara, T. (2006). The *Arabidopsis* major intrinsic protein NIP5;1 is essential for efficient boron uptake and plant development under boron limitation. *Plant Cell* 18, 1498–1509. doi: 10.1105/tpc.106.041640
- Tamura, K., Stecher, G., Peterson, D., Filipski, A., and Kumar, S. (2013). MEGA6: molecular evolutionary genetics analysis version 6.0. *Mol. Biol. Evol.* 30, 2725–2729. doi: 10.1093/molbev/mst197
- Temmei, Y., Uchida, S., Hoshino, D., Kanzawa, N., Kuwahara, M., Sasaki, S., et al. (2005). Water channel activities of *Mimosa pudica* plasma membrane intrinsic proteins are regulated by direct interaction and phosphorylation. *FEBS Lett.* 579, 4417–4422. doi: 10.1016/j.febslet.2005.06.082
- Törnroth-Horsefield, S., Wang, Y., Hedfalk, K., Johanson, U., Karlsson, M., Tajkhorshid, E., et al. (2006). Structural mechanism of plant aquaporin gating. *Nature* 439, 688–694. doi: 10.1038/nature04316
- Venkatesh, J., Yu, J. W., Gaston, D., and Park, S. W. (2015). Molecular evolution and functional divergence of X-intrinsic protein genes in plants. *Mol. Genet. Genom.* 290, 443–460. doi: 10.1007/s00438-014-0927-0
- Zou, Z., Gong, J., An, F., Xie, G., Wang, J., Mo, Y., et al. (2015a). Genome-wide identification of rubber tree (*Hevea brasiliensis* Muell. Arg.) aquaporin genes and their response to ethephon stimulation in the laticifer, a

- rubber-producing tissue. *BMC Genomics* 16:1001. doi: 10.1186/s12864-015-2152-6
- Zou, Z., Gong, J., Huang, Q., Mo, Y., Yang, L., and Xie, G. (2015b). Gene structures, evolution, classification and expression profiles of the aquaporin gene family in castor bean (*Ricinus communis* L.). *PLoS ONE*. 10:e0141022. doi: 10.1371/journal.pone.0141022
- Zou, Z., Yang, L., Gong, J., Mo, Y., Wang, J., Cao, J., et al. (2016). Genomide-wide identification of *Jatropha curcas* aquaporin genes and the comparative analysis provides insights into the gene family expansion and evolution in *Hevea brasiliensis*. *Front. Plant Sci.* 7:395. doi: 10.3389/fpls.2016.00395

Conflict of Interest Statement: The authors declare that the research was conducted in the absence of any commercial or financial relationships that could be construed as a potential conflict of interest.

Copyright © 2016 Ampah-Korsah, Anderberg, Engfors, Kirscht, Nordén, Kjellström, Kjellbom and Johanson. This is an open-access article distributed under the terms of the Creative Commons Attribution License (CC BY). The use, distribution or reproduction in other forums is permitted, provided the original author(s) or licensor are credited and that the original publication in this journal is cited, in accordance with accepted academic practice. No use, distribution or reproduction is permitted which does not comply with these terms.



Mutual Interactions between Aquaporins and Membrane Components

Maria del Carmen Martínez-Ballesta and Micaela Carvajal*

Plant Nutrition Department, Aquaporins Group, Centro de Edafología y Biología Aplicada del Segura-Consejo Superior de Investigaciones Científicas (CEBAS-CSIC), Murcia, Spain

OPEN ACCESS

Edited by:

Richard Belanger,
Laval University, Canada

Reviewed by:

Wei-Jiun Guo,
National Cheng Kung University,
Taiwan

Clay Carter,
University of Minnesota, USA

***Correspondence:**

Micaela Carvajal
mcarvaja@cebas.csic.es

Specialty section:

This article was submitted to
Plant Physiology,
a section of the journal
Frontiers in Plant Science

Received: 25 April 2016

Accepted: 18 August 2016

Published: 30 August 2016

Citation:

Martínez-Ballesta MC and Carvajal M (2016) Mutual Interactions between Aquaporins and Membrane Components. *Front. Plant Sci.* 7:1322.
doi: 10.3389/fpls.2016.01322

In recent years, a number of studies have been focused on the structural evaluation of protein complexes in order to get mechanistic insights into how proteins communicate at the molecular level within the cell. Specific sites of protein-aquaporin interaction have been evaluated and new forms of regulation of aquaporins described, based on these associations. Heterotetramerizations of aquaporin isoforms are considered as novel regulatory mechanisms for plasma membrane (PIPs) and tonoplast (TIPs) proteins, influencing their intrinsic permeability and trafficking dynamics in the adaptive response to changing environmental conditions. However, protein–protein interaction is an extensive theme that is difficult to tackle and new methodologies are being used to study the physical interactions involved. Bimolecular fluorescence complementation and the identification of cross-linked peptides based on tandem mass spectra, that are complementary to other methodologies such as heterologous expression, co-precipitation assays or confocal fluorescence microscopy, are discussed in this review. The chemical composition and the physical characteristics of the lipid bilayer also influence many aspects of membrane aquaporins, including their functionality. The molecular driving forces stabilizing the positions of the lipids around aquaporins could define their activity, thereby altering the conformational properties. Therefore, an integrative approach to the relevance of the membrane-aquaporin interaction to different processes related to plant cell physiology is provided. Finally, it is described how the interactions between aquaporins and copolymer matrixes or biological compounds offer an opportunity for the functional incorporation of aquaporins into new biotechnological advances.

Keywords: aquaporins, lipids, fluidity, micorviscosity, phospholipids, sterols, heterotetramers

INTRODUCTION

The current knowledge of membrane components is rather complete, but the physical and structural aspects of the lipid-protein interactions are still under investigation and underline the complexity of the biological membrane as a whole. Two different approaches have been established to determine the protein and lipid molecules interaction in a membrane: lipid- and protein-based approaches (Lee, 2011). Lipid-based approaches consider the intrinsic physical properties of the membrane, like fluidity, permeability, or viscosity, together with the lipid chemical composition, in regard to the interference with membrane protein function. Protein-based

approaches concern the molecular aspects of the proteins themselves and their interactions with other proteins. In fact, we have to consider an intrinsic membrane protein as a different type of protein, since the comprehensive function of intrinsic membrane proteins can only be understood in conjunction with their interactions with the lipid bilayer and other membrane proteins.

Plants aquaporins (AQPs) are molecular proteinaceous membrane channels that finely control the passage of water through membranes. During the last 20 years, after their discovery, AQPs have been deeply investigated and this has highlighted the difficulty in characterizing an individual role for them. The great number of AQPs in plants, the different substrates that they transport (Li et al., 2014) and the diverse forms of molecular regulation (Yaneff et al., 2015) make the study of the physiological role of AQPs a great challenge. To this complicated landscape, we have to add the recent discovery of AQP-protein and AQP-AQP interaction, which affect the regulation of aquaporin functionality (Fetter et al., 2004; Xin et al., 2014).

Biological membranes are constituted by lipids and proteins that establish physical and chemical communication between cells and their intracellular compartments. The lipid bilayer forms a fluid matrix to hold proteins. However, this lipid bilayer has been widely reported to be more than a passive fluid since it influences many aspects of membrane proteins, including their insertion into the membrane (Marsh, 2008; Dowhan and Bogdanov, 2009), assembly into complexes (Dalbey et al., 2011; Raja, 2011; Vitrac et al., 2011), and activity (Phillips et al., 2009). On the contrary, membrane proteins can alter the physical properties of lipid bilayers – mediating, for instance, pore formation (Brogden, 2005), fusogenicity (Jahn and Scheller, 2006), and membrane bending (Graham and Kozlov, 2010; Qualmann et al., 2011). Detailed knowledge of how lipids and membrane proteins interact with each other is therefore crucial to understand the molecular machinery of biological membranes.

In this review, the regulation of AQP isoforms by the physical and chemical characteristics of the lipid bilayer is considered, together with the interaction of the isoforms with other AQP isoforms and proteins. These characteristics are also described as novel regulators of membrane intrinsic proteins (MIPs), influencing the permeability and trafficking dynamics of the membrane in the adaptive response to changing environmental conditions. The molecular driving forces resulting from the positions of the lipids around AQPs, which modulate their activity, will be discussed in terms of future challenges.

METHODOLOGIES TO STUDY LIPID-PROTEIN AND PROTEIN-PROTEIN INTERACTION

The structures of AQPs and specific lipid-protein interactions have, classically, been determined by electron and X-ray crystallography (Andrews et al., 2008). However, due to the high hydrophobicity of the *trans*-membrane regions of AQPs, lipid-AQP stabilization is an important challenge to these

methodologies. In fact, there is only limited information about pore conformation and this was determined for only two AQPs, AQP0 (Gonen et al., 2004), and the plant AQP SoPIP2;1 (Tönroth-Horsefield et al., 2005); the mechanisms involved in their regulation were not clarified.

The use of bicelles and nanodiscs presents some advantages with respect to the use of liposomes and micelles, since they confer adequate size and stability to the lipid-protein complex (Bayburt and Sligar, 2010). In particular, protein-protein interaction, protein dynamics, and protein-binding sites are addressed by this approach, but it appears to be less effective in transport assays as a consequence of the lack of protein compartmentalization.

Although protein reconstitution in proteoliposomes has been used widely to study AQPs functionality, there is also evidence that AQPs activity may vary depending on the bilayer composition (Tong et al., 2012); this would have physiological consequences for the permeability of cell membranes. In fact, changes in the membrane lipid composition have been related to changes in AQPs permeability (López-Pérez et al., 2009).

Also, the importance of protein-protein interaction with regard to understanding biological processes is clear (Wu et al., 2009) and the functioning and regulation of AQPs in relation to these interactions have been well characterized in different cell based assays. In general, interaction between heterooligomers of AQPs is studied by co-injection of the cRNA of different PIP isoforms in a heterologous system such as *Xenopus* oocytes (Zelazny et al., 2009). However, great variation in the subsequent water permeability has been found, depending on the PIP isoforms, cRNA ratio or the experimental conditions. Complementary approaches, such as localization by confocal fluorescence microscopy, immunohistochemistry, or inhibition by cytosolic acidification, may yield more extensive information. One additional complexity regarding AQPs interaction studies is that the common methodologies have been developed for soluble proteins rather than plasma membrane (PM) proteins.

Among the methods used for protein complementation, yeast two-hybrid interaction is based on the activated expression of a reporter gene that is associated with a characteristic phenotype (Sjöhamn and Hedfalk, 2014). The interactions of AQPs with bacterial and oomycete effectors were described using this methodology (Mukhtar et al., 2011). Constructs with the transcription factor and the interacting proteins allow *in vivo* protein assembly. The method is able to detect tenuous linkages but a high rate of false positives is usual. Co-precipitation assays combined with immunodetection are feasible alternative tools for the determination of protein-protein interaction (Ciruela, 2008). Co-immunoprecipitation may discern the reciprocal actions of the different protein subunits that form a protein conglomerate. However, the main difficulties of this methodology are the cost and the time that is consumed during the design and preparation of the highly specific antibodies needed to bind to the complexes that include the bait protein (Miernyk and Thelen, 2008).

Photobleaching fluorescence resonance energy transfer (FRET) has been applied to demonstrate the physical interaction between the maize AQP isoforms Zm-PIP1s and Zm-PIP2s (Zelazny et al., 2009) as well as between

Zm-PIP2;5 and the SNARE protein SYP121 (Besserer et al., 2012). Another technically demanding method is the use of bimolecular fluorescence complementation (BiFC). BiFC has several advantages in the study of protein–protein interaction (Horstman et al., 2014) and, in combination with fluorescence detection, represents a useful tool for the purification of the intact complex (Murozuka et al., 2013), especially when the proteins have a low affinity for each other. The use of BiFC may maintain the integrity of the complex formed *in vivo* and ensure that the protein targets are localized in their native cellular compartment. In addition, the fluorescence (with GFP or YFP proteins) can be traced during the solubilization or purification steps, which improves the methodology. By contrast, the cellular expression of the fluorescence particles (GFP or YFP) does not always lead to an effective fluorophore; also, protein–protein interaction may impede the correct reconstitution of the fluorescent protein (Citovsky et al., 2008).

Thus, the study of protein–protein interaction partners is a young discipline, while there are a great number of reports concerning the functional and structural information of purified AQPs. The identification and analysis of these proteins which form complexes with other membrane proteins are still a major challenge, but the large number of interacting partners that affect AQP regulation makes this discipline a promising tool in cell biology that can provide a way to answer novel scientific questions.

PROTEIN–PROTEIN INTERACTIONS

Aquaporin–Aquaporin Interaction

Protein interactions, ranging from the formation of stable complexes within the cell to transient complexes involved in cell signaling pathways, determine protein function. Membrane proteins are basic elements of the cell, allowing the transport of molecules across the membrane and communication with the external environment. Among them, the AQPs are transmembrane channels – organized in highly conserved tetrameric structures in the cell membranes – which facilitate the passage of water and/or small solutes (Maurel et al., 2008). The function of AQPs is controlled by physiological signals as well as the interactions between different AQP monomers or binding with other proteins.

The role of hetero-molecular AQP interactions has been described in plants as a mode to control physiological mechanisms (Maurel, 2007). An interesting point of view is that AQP isoforms can act on other AQP isoforms, which could be of remarkable importance in tissues where multiple isoforms are expressed. Heterooligomerization between PIP1 and PIP2 has been shown to modify the characteristics of water channels in plant cells or *Xenopus laevis* oocytes. Thus, co-expression of PIP1 with PIP2 was necessary not only to increase PIP1 water permeability (Fetter et al., 2004; Otto et al., 2010), but also for its displacement from the endoplasmic reticulum to the PM (Zelazny et al., 2007, 2009).

The study of the structural basis for heterooligomers formation is still a challenge. In maize, a conserved cysteine (Cys) residue

in the loop A of PIP1 and PIP2 proteins has been identified as responsible for the formation of a covalent disulfide bond between the monomers of these two subfamilies. Although this Cys did not directly regulate the activity or trafficking of the two PIPs, the residue increased the oligomer stability under unfavorable conditions, hence controlling PIP abundance in plant cells (Bienert et al., 2012). However, in *Beta vulgaris*, BvPIP2;1 was not able to translocate BvPIP1;1 to the PM after the co-expression of both isoforms, whereas BvPIP2;2 was assembled with BvPIP1;1. Differences in the heterooligomerization of the PIPs were attributed to differences in the functionality of loop A (Jozefkowicz et al., 2013). Also, recently, Yaneff et al. (2015) postulated that the abundance of PIPs transcripts regulates the PIP1-PIP2 associations, providing specific combinations of PIP1-PIP2 isoforms when plants are exposed to different environmental conditions and conferring on the PIP1-PIP2 pair a role as a functional unit in the related physiological processes (Figure 1).

Less studied are the interactions between TIP isoforms and there is a lack of information about the function of their association. The putative interactions between TIPs isoforms from *Arabidopsis* have been studied using heterologous expression in yeast (Murozuka et al., 2013). The authors described not only a strong interaction between the TIP1;2, TIP2;1, and TIP3;1 isoforms but also the assembly of TIPs with PIP2;1. Although PIPs were localized in different membranes when compared with TIPs (Maurel et al., 2008), some TIPs were

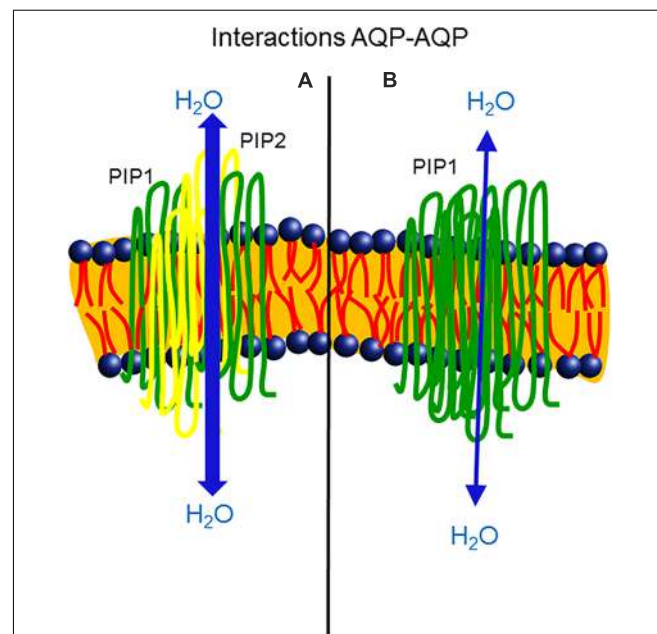


FIGURE 1 | Heterooligomerization of two PIP1 monomers (green color) and two PIP2 monomers (yellow color), isoforms of aquaporins. The co-expression of PIP1 and PIP2 enhanced water permeability across the plasma membrane of *Xenopus* oocytes (**A**). Homotetramer assembly of PIP1 monomers (green color) resulted in a lower capacity to transport water in the membrane (**B**), in comparison with the heterotetramer.

present in the PM (Wienkoop and Saalbach, 2003; Gattolin et al., 2011). In the same way, it has been reported that the form of heterotetramers assembly may condition physiological processes related to plant development. In onion cells, the HvTIP1;2 and HvTIP3;1 isoforms interacted, forming a heterotetramer which increased water permeability in the cells of late ripening seeds. A high level of water permeability was induced in comparison with the expression of HvTIP1;2 homotetramers alone. Thus, tight control of the water status of the cells by HvTIP3;1 was achieved in the seed development and desiccation stages (Utsugi et al., 2015).

In cotton, fiber elongation was found to depend on PIP2s and specific PIP2 isoform combinations markedly enhanced the water permeability in *Xenopus* oocytes (Li et al., 2013). Also, in the halophyte, *Thellungiella halophila*, ThPIP1 interacted with ThPIP2 and a non-specific lipid-transfer protein 2, suggesting a role of ThPIP1 in the response to the external signals that trigger multiple physiological processes when plants are exposed to salinity (Qiang et al., 2015).

Therefore, although the formation and dissociation of the heterotetramers of MIPs represent a mechanism for dynamic changes of the membrane permeability, further studies are necessary to discern these functions of the heterotetramers in plants.

Aquaporin Interaction with other Proteins

Hetero-complexes with AQPs, regulating different biological processes, have been described in several organisms. In humans, 70% of the AQPs interactions are comprised by the C-terminus (Sjöhamn and Hedfalk, 2014), which is the most divergent sequence in the AQP family and frequently appears as the main site of regulation. However, in plants, these interactions are emerging as new mechanisms that determine AQPs functions.

The interaction of AQPs with other proteins or nucleic acids involved in osmotic adjustment processes has been described. Xin et al. (2014) showed that transgenic *Arabidopsis* plants expressing SITIP2;2 possessed enhanced tolerance of salinity. In addition, yeast two-hybrid and BiFC analysis in protoplasts determined the physical binding between SITIP2;2 from tomato (*Solanum lycopersicum*) and the UDP-galactose transporter (Xin et al., 2014).

The functionality of the AQP TsMIP6, from the halophyte *T. salsuginea*, was characterized in transgenic rice (*Oryza sativa*). The expression of this gene was enhanced under salinity (Sun et al., 2015). In addition, TsMIP6 specifically interacted with a member of the glycoside hydrolase family in yeast cells. The authors suggested that the relationship between TsMIP6 and the hydrolase could mediate the osmotic balance in the plant cells and that TsMIP6 could also be involved in the transport of solutes that participate in the maintenance of the osmotic potential.

The pore-gating phosphorylation sites in AQPs were affected in inserted T-DNA mutants for the SIRK1 protein, an active kinase with increased activity in the presence of external sucrose (Wu et al., 2013). Thus, a direct interaction and regulation

of the AQPs *via* phosphorylation by SIRK1 were implicated in this sucrose-specific osmotic response. In maize plants, a physical interaction between the PM syntaxin SYP121, a SNARE protein, and the AQP isoform Zm-PIP2;5 was described, with evidence that the SNAREs coordinated membrane trafficking and the activity of AQPs and plant K⁺ channels (Besserer et al., 2012). This mechanism of coordination may suppose an adjusted regulation of the movement of water and ions in growing cells, guard cells, or cells under drought stress.

Also, in *Arabidopsis*, autophagic degradation of PIP2;7 in the vacuole was regulated by a protein–protein interaction under drought stress. The *Arabidopsis* tryptophan-rich sensory protein/translocator (TSPO), a multi-stress regulator, interacted with the AQP isoform at the level of the endoplasmic reticulum and Golgi membranes, resulting in a decreased abundance of PIP2;7 protein in the PM that prevented cell water loss (Hachez et al., 2014b). The correct delivery of this PIP to the PM involved specific interactions with two syntaxin proteins, SYP61 and SYP121 (Hachez et al., 2014a). An additional anchoring role of PIP2;7 has been suggested by Kriechbaumer et al. (2015); the presence of the AQP in the plasmodesmata proteome and the interaction with the plant reticulum family proteins tubulat (RTNLB) may confirm the connection between the desmotubule and PM. In agreement with this idea, the heterologous expression of the OsPIP1;3 AQP of rice in yeast showed a direct interaction with the hairpin protein Hap1 from *Xanthomonas oryzae* pv. *oryzae* (Xoo), the pathogen that causes bacterial blight of rice. This may favor the virulence of plant pathogenic bacteria, with the AQPs acting as anchor elements (Ji and Dong, 2015). These interaction studies will form the basis for future research related to the AQP–protein interaction network, with implications in cellular functions and pathways.

MEMBRANE PHYSICAL PROPERTIES

Membrane Fluidity

In living organisms, membranes are in the liquid-crystalline phase, in which there is considerable freedom of motion for the phospholipids. The membranes are characterized by high rotation of the C-C bonds of the fatty acyl chains and lateral diffusion of the phospholipids within the phase of the membrane. The amplitude of motion, described by an order-parameter, which describes the time-averaged disposition in space of each group of atoms in the acyl chains (Los and Murata, 2004), is inversely proportional to the fluidity (Laroche et al., 2001).

Membrane fluidity has been associated with many other processes in membranes, like protein activity. The effect of fluidity change on the function of membrane proteins such as ATPase was reported by Cooke and Burden (1990). They used xenobiotics to help elucidate the influence of fluidity on protein activity but encountered difficulties in their search for a direct relationship. Yeagle (1985) observed that high pressure decreased fluidity and stimulated ATPase activity, whereas addition of cholesterol also decreased fluidity but inhibited ATPase activity. Kitagawa et al. (1995) claimed to have demonstrated a correlation between fluidity and membrane-bound enzyme

activity. Subsequently, fluidity changes have been reported to affect the activity of membrane proteins, like P4 ATPases, influencing the ability of the plant to adapt to cold stress (Gomès et al., 2000). In the same way, some investigations have shown that water transport through AQPs can be affected by membrane physical properties such as fluidity (Carvajal et al., 1996; Frick et al., 2013). These reports showed that high fluidity is related to high AQP functionality. Frick et al. (2013) concluded that increased membrane fluidity could affect the conformational state of SoPIP2;1, pushing the equilibrium toward an open conformation. Furthermore, Ho et al. (1994) reported that water in the membrane bilayer was also responsible for modifying fluidity, since increases in membrane water content increased fluidity. Thus, diffusion of water through the bilayer affects its fluidity and the rate of that diffusion depends on the fluidity, as determined by changes in lipid composition (sterols and/or fatty acid saturation). Also, recent findings indicate that membrane hydration increases the space in the acyl chains (Disalvo, 2015). Therefore, due to an increased presence of water molecules at the lipid/protein interface, a consequence of increasing unsaturation, an increase in AQP permeability has been observed (Lee, 2004). In this context, it should always be remembered that the PM is a heterogeneous entity comprising different domains, each with its own fluidity and viscosity (Marrink et al., 2009). Therefore, although it is now possible to obtain a reasonable quantification of the overall motion parameters in terms of membrane structure and mobility, and their influence on AQP functionality, they should be interpreted very carefully.

Viscosity and Microviscosity

Viscosity, as a property of a fluid, is the internal friction a consequence of the cohesive forces between molecules (Lee et al., 1989). The term microviscosity was defined by Shinitzky et al. (1971) as the harmonic mean of the effective viscosities opposing the in- and out-of-plane rotations of the fluorescent probe. An effective definition of these terms that would allow translation of one to the other is, in fact, elusive, especially in those situations where microviscosity values are determined using steady-state fluorescence anisotropy values (Engel and Prendergast, 1981). Thus, in lipid bilayers, it is possible to define a relationship between fluidity and viscosity, both being dynamic parameters. Although studies of microviscosity in relation to AQPs functionality are very scarce, microviscosity has been reported to be involved in the alteration of the conformation of transmembrane channels, changing the activity of the proteins (Foulkes, 1998).

This property, that is dependent on the physical state of the membrane lipid bilayer and on the water in the membrane, has been related to AQPs functionality – its maximum influence being in the response of plants to stress conditions (Carvajal et al., 1998).

The fact that the microviscosity of lipid membranes is higher than that of water bestows on AQPs the critical parameter related to the nearly frictionless transport of water molecules through them. This phase has been identified recently as the possible phase transition temperature, after

selecting specific activation energies and activation volumes for confined (cylindrical) geometry (Kwang-Hua, 2015). With this approach and model-based calculations, the study produced results that can be applied to the diverse fields of research related to transmembrane water transport via AQPs, thereby shedding further light on the microviscosity/fluidity-AQPs relationship.

In a study of the microviscosity of the hydrocarbon zone in the isolated tonoplast and PM, using a fluorescent diphenylhexatriene probe, it was demonstrated that both membranes do not differ in this parameter in the phase state of their lipid bilayer (Trofimova et al., 2001). The study pointed out that the observed difference in water permeability does not depend on the state of the lipid phase and probably reflects the dissimilar functional activity of PM and tonoplast AQPs. However, the study did not take into account that the tonoplast and PM possess different amount of AQPs – that result in differing osmotic water permeabilities (Maurel et al., 2008), independently of the physical properties of the membrane.

LIPIDS

Sterols

It has always been assumed that the lipid composition of the membrane is the major factor determining its physical characteristics. The function of sterols in plants was thought to be related primarily to their ability to affect membrane structure and water permeability (Graziani and Livne, 1972). However, they can also affect the packing of the membrane bilayer, interacting with fatty acid side-chains of phospholipids and integral membrane proteins, increasing fluidity (Cooper, 2000) and bilayer water permeability (Da Silveira et al., 2003). In relation to this, beside the fact that a high sterol content increases fluidity and thereby AQPs functionality, other studies indicate that the highest local concentrations of PIP-AQPs correspond to tightly packed, sterol-enriched domains (Belugin et al., 2011). These domains are correlated with higher water permeability that probably corresponds to both AQPs and the lipid bilayer.

Also, it has been reported that an increase in the proportion of AQPs in the plant DRM (detergent-resistant PM fraction), which is rich in sterols and is considerably different from the total PM fraction, increased the osmotic water permeability of the PM at low and freezing temperatures and, hence, increased cell survival (Minami et al., 2009). Also, discoveries regarding the regulation of AQP intracellular trafficking and sub-cellular localization in response to environmental stresses, like water shortage and salt stress, revealed that sterol-rich domains are crucial in the cell surface dynamics and endocytosis of PM AQPs (for reviews see Hachez et al., 2013 and Luu and Maurel, 2013). Therefore, the interactions between AQPs and sterol-enriched domains seem to be closely related to AQP membrane functionality (Belugin et al., 2011). All these studies have contributed to the deciphering of AQP sub-cellular trafficking, which has been reported to be related to plant growth and development in *Arabidopsis* as a response to environmental changes (Boursiac et al., 2005). In

fact, the content of sterols seems to be related to the higher or lower resistance to salinity that involves AQPs functionality (López-Pérez et al., 2009; Chalbi et al., 2015). High salinity usually produces an increase in total PM sterols (Silva et al., 2007; López-Pérez et al., 2009). However, the results obtained for halophytes revealed that in *Cakile maritima* the total PM sterols decreased, reducing membrane rigidity (Chalbi et al., 2015). This was related to low membrane stability, but not to water permeability. However, rather than total sterols, the stigmasterol/sitosterol ratio should be used as the parameter that indicates a swift increase in water permeability. Sitosterol has been shown to be very efficient regarding the regulation of water permeability in plants grown under salt stress (Silva et al., 2007; Basyuni et al., 2012), and it is related closely to AQP functionality (López-Pérez et al., 2009).

In the same way, the results in animals provide evidence that the sterol content in the membrane could shift the balance toward the transport of other molecules, rather than water, by AQPs. Therefore, it has been concluded that sterols, which impart mechanical stability to the membrane, reduce gas permeability through the lipid bilayer but can markedly raise the gas permeability through AQPs. In this sense, Itel et al. (2012) showed that cholesterol can decrease membrane CO₂ permeability by two orders of magnitude in phospholipid vesicles and intact cells. However, the permeability of CO₂, and possibly other gasses, through AQP1 appeared to be increased by three orders of magnitude. Also, studies with kidney cells revealed that cholesterol depletion reduced the diffusion coefficient of AQP3 but not that of AQP5 (Koffman et al., 2015), suggesting that only a subset of AQPs may be associated with lipid rafts and regulated by cholesterol.

Phospholipids

The phospholipid composition, in terms of the head-group and acyl chains, also seems to be related to membrane physical properties which influence the activity of proteins. In studies of the PM composition of wheat plants grown under drought stress, it was observed that the phosphatidylcholine/phosphatidylethanolamine ratio and the level of unsaturation of the fatty acyl chains increased. It was suggested that this produced a more fluid lipid matrix in order to preserve the physiological function of the lipid bilayer (Vigh et al., 1986). Similar findings, plus an increase in free sterol abundance, were observed in water-stressed sunflower PM (Navarri-Izzo et al., 1993). However, after the discovery of AQPs, it was found that the adaptation to stress was dependent on the AQPs rather than on lipid composition, although the phospholipid composition could modulate AQP functionality through effects on the physical properties of membranes, such as fluidity (Carvajal et al., 1996).

Molecular dynamic simulations and crystallographic refinement to determine the localization of DMPC (dimyristoylphosphatidylcholine) lipids around lens-specific animal water channel aquaporin-0 (AQP0) showed that the positions of the constrained lipids in the 2D crystals are defined by the acyl chains rather than the head groups (Aponte-Santamaría et al., 2012). Furthermore, the positions of these lipids are influenced greatly by the local mobility of the protein, whereas specific hydrogen bonds play a secondary role. Therefore, AQPs follow the general mechanism in which membrane proteins diffuse laterally, associated with the two layers of lipids, with the positions of the lipids in the first solvation shell being modulated also by irregularities in the protein interface (Lindahl and Sansom, 2008).

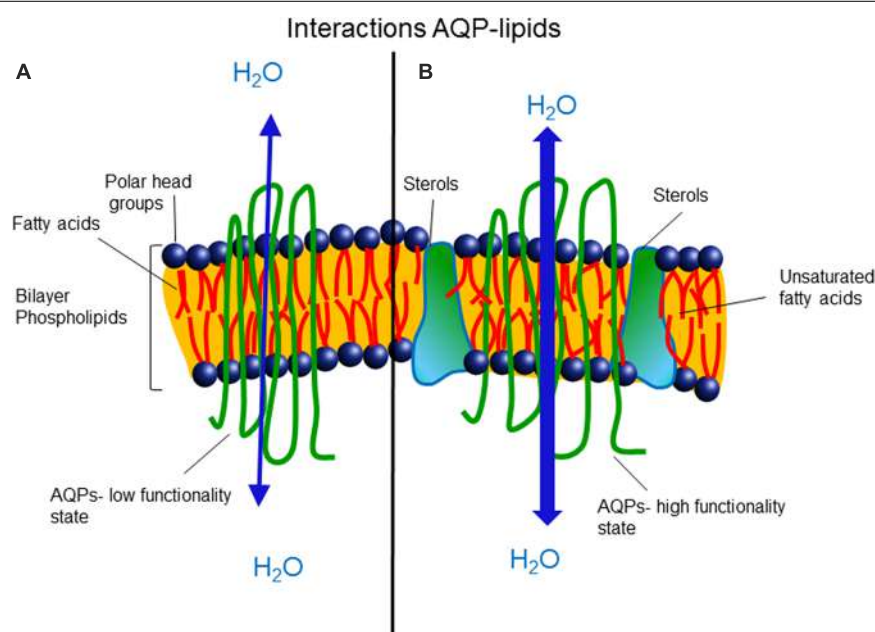


FIGURE 2 | (A) Saturated hydrocarbon fatty acids are related with low membrane fluidity, high microviscosity, and low aquaporin functionality. **(B)** The presence of unsaturated hydrocarbon fatty acids and sterols prevents packing and enhances membrane fluidity, favoring the open state and functionality of aquaporins.

INTERACTION OF AQUAPORINS WITH COPOLYMERS

Supported biomimetic membranes (SBMs) have attracted much interest as enabling components in promising applications such as water purification (Kaufman et al., 2010; Zhong et al., 2012). Hence, AQPs incorporated into SBMs created a potential high-performance water purification membrane with high water permeability and reliable ion rejection, exceeding the yield of commercial polymeric membranes (Kumar et al., 2007). However, two critical aspects should be borne in mind for the design of SBMs containing AQPs (Xie et al., 2013): AQPs must be highly selective to water and show great transport capability, and there is a need for high strength of the membrane matrix. For the first requirement, the influence of the membrane composition is very important. The big challenge is to characterize all AQPs and determine the most suitable lipid surroundings, to maximize water transport. Also, the preparation of stable, functioning SBMs and their integration and interfacing with an appropriate, robust supporting structure still remain highly challenging. Recently, SBMs were successfully prepared on silica using a positively charged, single-chain bolalipid GLH-20 (Kaufman et al., 2013). Unlike common SBM precursors (vesicle-forming lipids), GLH-20 in solution forms micelles, rather than vesicles, which spontaneously form a stable and contiguous supported SBM with a low defect rate.

In the same way, Xie et al. (2013) designed and fabricated a stable and functional polymeric membrane embedded with nano-sized AQP vesicles, through an innovative yet simple and easy-to-implement method based on an AQPz-incorporating biomimetic membrane and surface imprinting polymerization technology. They concluded that the AQPz functionally incorporated into polymer vesicles exhibits high mechanical strength and stability during the water filtration process. Also, the micro-batchwise methodology has been reported to be suitable for the functional reconstitution of rice AQP and other membrane transport proteins (Scalera et al., 2014).

Therefore, the possibility of mimicking biological membranes and the challenges of fabricating separation devices based on such biomimetic membranes have both increased in recent years, which offer an opportunity for the functional incorporation of AQPs in new technologies.

CONCLUDING REMARKS

There is a general understanding that membrane AQP proteins diffuse laterally, associated with several layers of

REFERENCES

- Andrews, S., Reichow, S. L., and Gonen, T. (2008). Electron crystallography of aquaporins. *IUBMB Life* 60, 430–436. doi: 10.1002/iub.53
 Aponte-Santamaría, C., Briones, R., Schenk, A. D., Walz, T., and de Groot, B. L. (2012). Molecular driving forces defining lipid positions around aquaporin-5. *Proc. Natl. Acad. Sci. U.S.A.* 109, 9887–9892. doi: 10.1073/pnas.1121054109

lipids, with the positions of the lipids in the first solvation shell being modulated also by irregularities in the protein interface. Therefore, the physical properties and chemical composition of the membrane will influence the functionality of the AQPs and could regulate their open/closed state (Figure 2). Also, it is becoming increasingly clear that AQP/AQP and AQP/protein interactions represent an important coordination system involved in cellular functions and need to be elucidated.

Another aspect to consider is the mechanical or therapeutic/food uses of vesicles rich in AQPs. Filters with a tremendous potential use in engineering, for water filtration, are being developed. The therapeutic/food aspect has been initiated and will be a very exciting line of plant AQPs exploitation in the future (Martínez-Ballesta et al., 2016). Furthermore, one of the challenges for the next 10 years is to use widely the expected increase in computational resources, due to the ongoing development of both hard- and software, to be able to implement the anticipated possibility of simulating both millisecond events, with all atom models, and truly macroscopic time scales, for simplified models. With the increasing number of particles that can be simulated, we expect studies on membranes to become gradually more dominant. However, the progress that is being made in the investigation of lipid/peptide force fields and protein/protein interactions is still a prerequisite for this.

AUTHOR CONTRIBUTIONS

MM-B her contribution was reviewed the aspect of interactions of aquaporins with aquaporins in the membranes. MC her contribution was reviewed the aspects of interactions of aquaporins with lipids in the membranes. The completed manuscript was corrected as a whole.

FUNDING

This work was funded by the Spanish Ministerio de Economía y Competitividad (AGL2012-40175-C02-01 and RTC-2015-3536-2).

ACKNOWLEDGMENT

The authors thank Dr. D. Walker, for correction of the written English in the manuscript.

- Basyuni, M., Baba, S., Kinjo, Y., and Oku, H. (2012). Salinity increases the triterpenoid content of a salt secretor and a non salt secretor mangrove. *Aquat. Bot.* 97, 17–23. doi: 10.1016/j.aquabot.2011.10.005
 Bayburt, T. H., and Sligar, S. G. (2010). Membrane protein assembly into nanodiscs. *FEBS Lett.* 584, 1721–1727. doi: 10.1016/j.febslet.2009.10.024
 Belugin, B. V., Zhestkova, I. M., and Trofimova, M. S. (2011). Affinity of PIP aquaporins to sterol enriched domains in plasma membrane of the cells of

- etiolated pea seedlings. *Biochem. (Mosc) Suppl. Ser. A Membr. Cell Biol.* 5, 56–63. doi: 10.1134/S1990747810051010
- Besserer, A., Burnotte, E., Bienert, G. P., Chevalier, A. S., Errachid, A., Grefen, C., et al. (2012). Selective regulation of maize plasma membrane aquaporin trafficking and activity by the SNARE SYP121. *Plant Cell* 24, 3463–3481. doi: 10.1105/tpc.112.101758
- Bienert, G. P., Cavez, D., Besserer, A., Berny, M. C., Gilis, D., Rooman, M., et al. (2012). A conserved cysteine residue is involved in disulfide bond formation between plant plasma membrane aquaporin monomers. *Biochem. J.* 445, 101–111. doi: 10.1042/BJ20111704
- Boursiac, Y., Chen, S., Luu, D.-T., Sorieul, M., van den Dries, N., and Maurel, C. (2005). Early effects of salinity on water transport in *Arabidopsis* roots: molecular and cellular features of aquaporin expression. *Plant Physiol.* 139, 790–805. doi: 10.1104/pp.105.065029
- Brogden, K. A. (2005). Antimicrobial peptides: pore formers or metabolic inhibitors in bacteria? *Nat. Rev. Microbiol.* 3, 238–250. doi: 10.1038/nrmicro1098
- Carvajal, M., Cooke, D. T., and Clarkson, D. T. (1996). Response of wheat plants to nutrient deprivation may involve the regulation of water uptake. *Planta* 199, 372–381. doi: 10.1007/BF00195729
- Carvajal, M., Cooke, D. T., and Clarkson, D. T. (1998). Water transport across plant plasma membrane. *Plant Growth Regul.* 25, 89–95. doi: 10.1023/A:100591830552
- Chalbi, N., Martínez-Ballesta, M. C., Youssef, N. B., and Carvajal, M. (2015). Intrinsic stability of Brassicaceae plasma membrane in relation to changes in proteins and lipids as a response to salinity. *J. Plant Physiol.* 175, 148–156. doi: 10.1016/j.jplph.2014.12.003
- Ciruela, F. (2008). Fluorescence-based methods in the study of protein-protein interactions in living cells. *Curr. Opin. Biotech.* 19, 338–343. doi: 10.1016/j.copbio.2008.06.003
- Citovsky, V., Gafni, Y., and Tzfira, T. (2008). Localizing protein-protein interactions by bimolecular fluorescence complementation in planta. *Methods* 45, 196–206. doi: 10.1016/j.ymeth.2008.06.007
- Cooke, D. T., and Burden, R. S. (1990). Lipid modulation of plasma membrane-bound ATPases. *Phys. Plant.* 78, 153–159. doi: 10.1111/j.1399-3054.1990.tb08730.x
- Cooper, G. M. (2000). *The Cell: A Molecular Approach*, 2nd Edn. Sunderland: Sinauer Associates.
- Da Silveira, M. G., Golovina, E. A., Hoekstra, F. A., Rombouts, F. M., and Abee, T. (2003). Membrane fluidity adjustments in ethanol-stressed *Oenococcus oeni*. *Cells Appl. Environ. Microbiol.* 69, 5826–5832. doi: 10.1128/AEM.69.10.5826-5832.2003
- Dalbey, R., Wang, P., and Kuhn, A. (2011). Assembly of bacterial inner membrane proteins. *Annu. Rev. Biochem.* 80, 161–187. doi: 10.1146/annurev-biochem-06409-092524
- Disalvo, E. A. (2015). “Membrane hydration: a hint to a new model for biomembranes,” in *Membrane Hydration. The Role of Water in the Structure and Function of Biological Membranes*, ed. E. A. Disalvo (Berlin: Springer), 1–17.
- Dowhan, W., and Bogdanov, M. (2009). Lipid-dependent membrane protein topogenesis. *Annu. Rev. Biochem.* 78, 515–540. doi: 10.1146/annurev-biochem.77.060806.091251
- Engel, L. W., and Prendergast, F. G. (1981). Values for and significance of order parameter and “cone angles” of fluorophore rotation in lipid bilayers. *Biochemistry* 20, 7338–7345. doi: 10.1021/bi00529a003
- Fetter, K., Van Wilder, V., Moshelion, M., and Chaumont, F. (2004). Interactions between plasma membrane aquaporins modulate their water channel activity. *Plant Cell* 16, 215–228. doi: 10.1105/tpc.017194
- Foulkes, E. C. (1998). *Biological Membranes in Toxicology*. London: Taylor and Francis Ltd, 45.
- Frick, A., Järvinen, M., Ekwall, M., Uzdavinys, P., Nyblom, M., and Törnroth-Horsefield, S. (2013). Mercury increases water permeability of a plant aquaporin through a non-cysteine-related mechanism. *Biochem. J.* 454, 491–499. doi: 10.1042/BJ20130377
- Gattolin, S., Sorieul, M., and Frigerio, L. (2011). Mapping of tonoplast intrinsic proteins in maturing and germinating *Arabidopsis* seeds reveals dual localization of embryonic TIPs to the tonoplast and plasma membrane. *Mol. Plant* 4, 180–189. doi: 10.1093/mp/ssq051
- Gomès, E., Jakobsen, M. K., Axelsen, K. B., Geisler, M., and Palmgren, M. G. (2000). Chilling tolerance in *Arabidopsis* involves ALA1, a member of a new family of putative aminophospholipid translocases. *Plant Cell* 12, 2441–2454. doi: 10.2307/3871240
- Gonen, T., Sliz, P., Kistler, J., Cheng, Y., and Walz, T. (2004). Aquaporin-0 membrane junctions reveal the structure of a closed water pore. *Nature* 429, 193–197. doi: 10.1038/nature02503
- Graham, T. R., and Kozlov, M. M. (2010). Interplay of proteins and lipids in generating membrane curvature. *Curr. Opin. Cell Biol.* 22, 430–436. doi: 10.1016/j.ceb.2010.05.002
- Graziani, Y., and Livne, A. (1972). Water permeability in bilayer lipid membranes: sterol-lipid interaction. *J. Membr. Biol.* 7, 275–284. doi: 10.1007/BF01867920
- Hachez, C., Besserer, A., Chevalier, A. S., and Chaumont, F. (2013). Insights into plant plasma membrane aquaporin trafficking. *Trends Plant Sci.* 18, 344–352. doi: 10.1016/j.tplants.2012.12.003
- Hachez, C., Laloux, T., Reinhardt, H., Cavez, D., Degand, H., Grefen, C., et al. (2014a). *Arabidopsis* SNAREs SYP61 and SYP121 coordinate the trafficking of plasma membrane aquaporin PIP2;7 to modulate the cell membrane water permeability. *Plant Cell* 26, 3132–3147. doi: 10.1105/tpc.114.127159
- Hachez, C., Veljanovski, V., Reinhardt, H., Guillaumot, D., Vanhee, C., Chaumont, F., et al. (2014b). The *Arabidopsis* abiotic stress-induced TSPO-related protein reduces cell-surface expression of the aquaporin PIP2;7 through protein-protein interactions and autophagic degradation. *Plant Cell* 26, 4974–4990. doi: 10.1105/tpc.114.134080
- Ho, C., Kelly, M. B., and Stubbs, C. D. (1994). The effects of phospholipid unsaturation and alcohol perturbation at the protein/lipid interface probed using fluorophore lifetime heterogeneity. *Biochem. Biophys. Acta* 1193, 307–315. doi: 10.1016/0005-2736(94)90167-8
- Horstman, A., Tonaco, I. A. N., Boutilier, K., and Immink, R. G. H. (2014). A cautionary note on the use of split-YFP/BiFC in plant protein-protein interaction studies. *Int. J. Mol. Sci.* 15, 9628–9643. doi: 10.3390/ijms15069628
- Itel, F., Al-Samir, S., Öberg, F., Chami, M., Kumar, M., Supuran, C. T., et al. (2012). CO₂ permeability of cell membranes is regulated by membrane cholesterol and protein gas channels. *FASEB J.* 26, 5182–5191. doi: 10.1096/fj.12-09916
- Jahn, R., and Scheller, R. H. (2006). SNAREs-engines for membrane fusion. *Nat. Rev. Mol. Cell Biol.* 7, 631–643. doi: 10.1038/nrm2002
- Ji, H., and Dong, H. (2015). Biological significance and topological basis of aquaporin-partnering protein-protein interactions. *Plant Signal. Behav.* 10:e1011947. doi: 10.1080/15592324.2015.1011947
- Jozefkowicz, C., Rosi, P., Sigaut, L., Soto, G., Pietrasanta, L. I., Amodeo, G., et al. (2013). Loop A is critical for the functional interaction of two *Beta vulgaris* PIP aquaporins. *PLoS ONE* 8:e57999. doi: 10.1371/journal.pone.0057999
- Kaufman, Y., Berman, A., and Freger, V. (2010). Supported lipid bilayer membranes for water purification by reverse osmosis. *Langmuir* 26, 7388–7395. doi: 10.1021/la904411b
- Kaufman, Y., Grinberg, S., Linder, C., Heldman, E., Gilron, J., and Freger, V. (2013). Fusion of bolaamphiphile micelles: a method to prepare stable supported biomimetic membranes. *Langmuir* 29, 1152–1161. doi: 10.1021/la304484p
- Kitagawa, S., Sugaya, Y., Nishizawa, M., and Hirata, H. (1995). Relationship of alcohol-induced changes in Mg²⁺-ATPase activity of rabbit intestinal brush border membrane with changes in fluidity of its lipid bilayer. *J. Membr. Biol.* 146, 193–199. doi: 10.1007/BF00238008
- Koffman, J. S., Arnspong, E. C., Marlar, S., and Nejsum, L. N. (2015). Opposing effects of cAMP and T259 phosphorylation on plasma membrane diffusion of the water channel aquaporin-5 in madin-darby canine kidney cells. *PLoS ONE* 10:e0133324. doi: 10.1371/journal.pone.0133324
- Kriechbaumer, V., Botchway, S. W., Slade, S. E., Knox, K., Frigerio, L., Oparka, K., et al. (2015). Reticulomics: protein-protein interaction studies with two plasmodesmata-localized reticulon family proteins identify binding partners enriched at plasmodesmata, endoplasmic reticulum, and the plasma membrane. *Plant Physiol.* 169, 1933–1945. doi: 10.1104/pp.15.01153
- Kumar, M., Grzelakowski, M., Zilles, J., Clark, M., and Meier, W. (2007). Highly permeable polymeric membranes based on the incorporation of the functional

- water channel protein aquaporin Z. *Proc. Natl. Acad. Sci.* 104, 20719. doi: 10.1073/pnas.0708762104
- Kwang-Hua, C. R. (2015). Temperature-tuned transport in biomembrane pores. *J. Mol. Liq.* 208, 356–359. doi: 10.1016/j.molliq.2015.05.017
- Laroche, C., Beney, L., Marechal, P. A., and Gervais, P. (2001). The effect of osmotic pressure on the membrane fluidity of *Saccharomyces cerevisiae* at different physiological temperatures. *Appl. Microbiol. Biotechnol.* 56, 249–254. doi: 10.1007/s002530000583
- Lee, A. G. (2004). How lipids affect the activities of integral membrane proteins. *Biochim. Biophys. Acta* 1666, 62–87. doi: 10.1016/j.bbamem.2004.05.012
- Lee, A. G. (2011). Biological membranes: the importance of molecular detail. *Trends Biochem. Sci.* 36, 493–500. doi: 10.1016/j.tibs.2011.06.007
- Lee, A. G., Michelangeli, F., and East, J. M. (1989). Tests for the importance of fluidity for the function of membrane proteins. *Biochem. Soc. Trans.* 17, 962–964. doi: 10.1042/bst0170962
- Li, D. D., Ruan, X. M., Zhang, J., Wu, Y. J., Wang, X. L., and Li, X. B. (2013). Cotton plasma membrane intrinsic protein 2s (PIP2s) selectively interact to regulate their water channel activities and are required for fibre development. *New Phytol.* 199, 695–707. doi: 10.1111/nph.12309
- Li, G., Santoni, V., and Maurel, C. (2014). Plant aquaporins: roles in plant physiology. *Biochim. Biophys. Acta* 1840, 1574–1582. doi: 10.1016/j.bbagen.2013.11.004
- Lindahl, E., and Sansom, M. S. P. (2008). Membrane proteins: molecular dynamics simulations. *Curr. Opin. Struct. Biol.* 18, 425–431. doi: 10.1016/j.sbi.2008.02.003
- López-Pérez, L., Martínez-Ballesta, M. C., Maurel, C., and Carvajal, M. (2009). Changes in plasma membrane lipids, aquaporins and proton pump of broccoli roots, as an adaptation mechanism to salinity. *Phytochem.* 70, 492–500. doi: 10.1016/j.phytochem.2009.01.014
- Los, D. A., and Murata, N. (2004). Membrane fluidity and its roles in the perception of environmental signals. *Biochim. Biophys. Acta* 1666, 142–157. doi: 10.1016/j.bbamem.2004.08.002
- Luu, D.-T., and Maurel, C. (2013). Aquaporin trafficking in plant cells: an emerging membrane-protein model. *Traffic* 14, 629–635. doi: 10.1111/tra.12062
- Marrink, S. J., de Vries, A. H., and Tieleman, D. P. (2009). Lipids on the move: simulations of membrane pores, domains, stalks and curves. *Biochim. Biophys. Acta* 1788, 149–168. doi: 10.1016/j.bbamem.2008.10.006
- Marsh, D. (2008). Protein modulation of lipids, and vice-versa, in membranes. *Biochim. Biophys. Acta* 1778, 1545–1575. doi: 10.1016/j.bbamem.2008.01.015
- Martínez-Ballesta, M. C., Pérez-Sánchez, H., Moreno, D. A., and Carvajal, M. (2016). Plant plasma membrane aquaporins in natural vesicles as potential stabilizers and carriers of glucosinolates. *Coll. Surf. B* 43, 318–326. doi: 10.1016/j.colsurfb.2016.03.056
- Maurel, C. (2007). Plant aquaporins: novel functions and regulation properties. *FEBS Lett.* 581, 2227–2236. doi: 10.1016/j.febslet.2007.03.021
- Maurel, C., Verdoucq, L., Luu, D. T., and Santoni, V. (2008). Plant aquaporins: membrane channels with multiple integrated functions. *Annu. Rev. Plant Biol.* 59, 595–624. doi: 10.1146/annurev.arplant.59.032607.092734
- Miernyk, J. A., and Thelen, J. J. (2008). Biochemical approaches for discovering protein-protein interactions. *Plant J.* 53, 597–609. doi: 10.1111/j.1365-313X.2007.03316.x
- Minami, A., Fujiwara, M., Furuto, A., Fukao, Y., Yamashita, T., Kamo, M., et al. (2009). Alterations in detergent-resistant plasma membrane microdomains in *Arabidopsis thaliana* during cold acclimation. *Plant Cell Physiol.* 50, 341–359. doi: 10.1093/pcp/pcn202
- Mukhtar, M. S., Carvunis, A. R., Dreze, M., Epple, P., Steinbrenner, J., Moore, J., et al. (2011). Independently evolved virulence effectors converge onto hubs in a plant immune system network. *Science* 333, 596–601. doi: 10.1126/science.1203659
- Murozuka, E., Hanisch, S., Pomorski, T. G., Jahn, T. P., and Schjoerring, J. K. (2013). Bimolecular fluorescence complementation and interaction of various *Arabidopsis* major intrinsic proteins expressed in yeast. *Physiol. Plant.* 148, 422–431. doi: 10.1111/ppl.12000
- Navarri-Izzo, F., Quartacci, M. F., Melfi, D., and Izzo, R. (1993). Lipid composition of plasma membranes isolated from sunflower seedlings grown under water stress. *Physiol. Plant.* 87, 508–514. doi: 10.1111/j.1399-3054.1993.tb02500.x
- Ootto, B., Uehlein, N., Sdorra, S., Fischer, M., Ayaz, M., Belastegui-Macadam, X., et al. (2010). Aquaporin tetramer composition modifies the function of tobacco aquaporins. *J. Biol. Chem.* 285, 31253–31260. doi: 10.1074/jbc.M110.15881
- Phillips, R., Ursell, T., Wiggins, P., and Sens, P. (2009). Emerging roles for lipids in shaping membrane-protein function. *Nature* 459, 379–385. doi: 10.1038/nature08147
- Qiang, X. J., Yu, G. H., Jlian, L. L., Sun, L. L., Zhang, S. H., Li, W., et al. (2015). *Thellungiella halophila* ThPIP1 gene enhances the tolerance of the transgenic rice to salt stress. *J. Integr. Agric.* 14, 1911–1922. doi: 10.1016/S2095-3119(15)61045-0
- Qualmann, B., Koch, D., and Kessels, M. M. (2011). Let's go bananas: revisiting the endocytic BAR code. *EMBO J.* 30, 3501–3515. doi: 10.1038/emboj.2011.266
- Raja, M. (2011). The potassium channel KcsA: a model protein in studying membrane protein oligomerization and stability of oligomeric assembly? *Arch. Biochem. Biophys.* 510, 1–10. doi: 10.1016/j.abb.2011.03.010
- Scalera, V., Gena, P., Mastrodonato, M., Kitagawa, Y., Carulli, S., Svelto, M., et al. (2014). Functional reconstitution of a rice aquaporin water channel, PIP1;1, by a micro-batchwise methodology. *Plant Physiol. Biochem.* 85, 78–84. doi: 10.1016/j.plaphy.2014.10.013
- Shinitzky, M., Dianoux, A.-C., Gitler, C., and Weber, G. (1971). Microviscosity and order in the hydrocarbon regions of micelles and membranes determined with fluorescent probes. I. Synthetic micelles. *Biochemistry* 10, 2106–2113.
- Silva, C., Aranda, F. J., Ortiz, A., Carvajal, M., Martínez, V., and Teruel, J. A. (2007). Root plasma membrane lipid changes in relation to water transport in pepper: a response to NaCl and CaCl₂ treatment. *J. Plant Biol.* 50, 650–657. doi: 10.1007/BF03030609
- Sjöhamn, J., and Hedfalk, K. (2014). Unraveling aquaporin interaction partners. *Biochim. Biophys. Acta* 1840, 1614–1623. doi: 10.1016/j.bbagen.2013.11.012
- Sun, L., Yu, G., Han, X., Xin, S., Qiang, X., Jiang, L., et al. (2015). TsMIP6 enhances the tolerance of transgenic rice to salt stress and interacts with target proteins. *J. Plant Biol.* 58, 285–292. doi: 10.1007/s12374-015-0069-x
- Tong, J., Briggs, M. M., and McIntosh, T. J. (2012). Water permeability of aquaporin-4 channel depends on bilayer composition, thickness, and elasticity. *Biophys. J.* 103, 1899–1908. doi: 10.1016/j.bpj.2012.09.025
- Tönroth-Horsefield, S., Wang, Y., Hedfalk, K., Johanson, U., Karlsson, M., Tajkhorshid, E., et al. (2005). Structural mechanism of plant aquaporin gating. *Nature* 439, 688–694. doi: 10.1038/nature04316
- Trofimova, M. S., Zhestkova, I. M., Andreev, I. M., Svinov, M. M., Bobylev, Y. S., and Sorokin, E. M. (2001). Osmotic water permeability of vacuolar and plasma membranes isolated from maize roots. *Russ. J. Plant Physiol.* 48, 287–293. doi: 10.1023/A:1016697813072
- Utsugi, S., Shibasaki, M., Maekawa, M., and Katsuhara, M. (2015). Control of the water transport activity of barley HvTIP3;1 specifically expressed in seeds. *Plant Cell Physiol.* 56, 1831–1840. doi: 10.1093/pcp/pcv104
- Vigh, L., Huitema, H., Woltjes, J., and van Hasselt, P. R. (1986). Drought stress-induced changes in the composition and physical state of phospholipids in wheat. *Physiol. Plant.* 67, 92–96.
- Vitrac, H., Bogdanov, M., Heacock, P., and Dowhan, W. (2011). Lipids and topological rules of membrane protein assembly: balance between long and short range lipid–protein interactions. *J. Biol. Chem.* 286, 15182–15194. doi: 10.1074/jbc.M110.214387
- Wienkoop, S., and Saalbach, G. (2003). Proteome analysis. Novel proteins identified at the peribacteroid membrane from *Lotus japonicus* root nodules. *Plant Physiol.* 131, 1080–1090. doi: 10.1104/pp.102.015362
- Wu, X. N., Sanchez-Rodriguez, C., Pertl-Obermeyer, H., Obermeyer, G., and Schulze, W. X. (2013). Sucrose-induced receptor kinase SIRK1 regulates a plasma membrane aquaporin in *Arabidopsis*. *Mol. Cell. Proteom.* 12, 2856–2873. doi: 10.1074/mcp.M113.029579
- Wu, Z., Zhao, X., and Chen, L. (2009). Identifying responsive functional modules from protein-protein interaction network. *Mol. Cell* 27, 271–277. doi: 10.1007/s10059-009-0035-x

- Xie, W., He, F., Wang, B., Chung, T., Jeyaseelan, K., Armugam, A., et al. (2013). An aquaporin-based vesicle-embedded polymeric membrane for low energy water filtration. *J. Mater. Chem.* 1, 7592–7600. doi: 10.1039/c3ta10731k
- Xin, S. C., Yu, G. H., Sun, L. L., Qiang, X. J., Xu, N., and Cheng, X. G. (2014). Expression of tomato SITIP2;2 enhances the tolerance to salt stress in the transgenic *Arabidopsis* and interacts with target proteins. *J. Plant Res.* 127, 695–708. doi: 10.1007/s10265-014-0658-7
- Yaneff, A., Vitali, V., and Amodeo, G. (2015). PIP1 aquaporins: intrinsic water channels or PIP2 aquaporin modulators? *FEBS Lett.* 589, 3508–3515. doi: 10.1016/j.febslet.2015.10.018
- Yeagle, P. L. (1985). Cholesterol and the cell membrane. *Biochem. Biophys. Acta* 822, 267–287.
- Zelazny, E., Borst, J. W., Muylaert, M., Batoko, H., Hemminga, M. A., and Chaumont, F. (2007). FRET imaging in living maize cells reveals that plasma membrane aquaporins interact to regulate their subcellular localization. *Proc. Natl. Acad. Sci.* 104, 12359–12364. doi: 10.1073/pnas.0701180104
- Zelazny, E., Miecielica, U., Borst, J. W., Hemminga, M. A., and Chaumont, F. (2009). An N-terminal diacidic motif is required for the trafficking of maize aquaporins ZmPIP2;4 and ZmPIP2;5 to the plasma membrane. *Plant J.* 57, 346–355. doi: 10.1111/j.1365-313X.2008.03691.x
- Zhong, P., Chung, T. S., Jeyaseelan, K., and Armugam, A. (2012). Aquaporin-embedded biomimetic membranes for nanofiltration. *J. Membr. Sci.* 407–408, 27–33. doi: 10.1016/j.memsci.2012.03.033

Conflict of Interest Statement: The authors declare that the research was conducted in the absence of any commercial or financial relationships that could be construed as a potential conflict of interest.

Copyright © 2016 Martínez-Ballesta and Carvajal. This is an open-access article distributed under the terms of the Creative Commons Attribution License (CC BY). The use, distribution or reproduction in other forums is permitted, provided the original author(s) or licensor are credited and that the original publication in this journal is cited, in accordance with accepted academic practice. No use, distribution or reproduction is permitted which does not comply with these terms.



Plant Aquaporins: Genome-Wide Identification, Transcriptomics, Proteomics, and Advanced Analytical Tools

Rupesh K. Deshmukh [†], Humira Sonah [†] and Richard R. Bélanger ^{*}

Département de Phytologie–Faculté des Sciences de l’Agriculture et de l’Alimentation, Université Laval, Québec, QC, Canada

OPEN ACCESS

Edited by:

Oscar Vicente,
Polytechnic University of Valencia,
Spain

Reviewed by:

Anton R. Schäffner,
Helmholtz Zentrum München,
Germany

Gheorghe Benga,
Romanian Academy, Romania

*Correspondence:

Richard R. Bélanger
richard.belanger@fsaa.ulaval.ca

[†]These authors have contributed
equally to this work.

Specialty section:

This article was submitted to
Plant Physiology,
a section of the journal
Frontiers in Plant Science

Received: 30 August 2016

Accepted: 30 November 2016

Published: 20 December 2016

Citation:

Deshmukh RK, Sonah H and Bélanger RR (2016) Plant Aquaporins: Genome-Wide Identification, Transcriptomics, Proteomics, and Advanced Analytical Tools. *Front. Plant Sci.* 7:1896.
[doi: 10.3389/fpls.2016.01896](https://doi.org/10.3389/fpls.2016.01896)

Aquaporins (AQPs) are channel-forming integral membrane proteins that facilitate the movement of water and many other small molecules. Compared to animals, plants contain a much higher number of AQPs in their genome. Homology-based identification of AQPs in sequenced species is feasible because of the high level of conservation of protein sequences across plant species. Genome-wide characterization of AQPs has highlighted several important aspects such as distribution, genetic organization, evolution and conserved features governing solute specificity. From a functional point of view, the understanding of AQP transport system has expanded rapidly with the help of transcriptomics and proteomics data. The efficient analysis of enormous amounts of data generated through omic scale studies has been facilitated through computational advancements. Prediction of protein tertiary structures, pore architecture, cavities, phosphorylation sites, heterodimerization, and co-expression networks has become more sophisticated and accurate with increasing computational tools and pipelines. However, the effectiveness of computational approaches is based on the understanding of physiological and biochemical properties, transport kinetics, solute specificity, molecular interactions, sequence variations, phylogeny and evolution of aquaporins. For this purpose, tools like *Xenopus* oocyte assays, yeast expression systems, artificial proteoliposomes, and lipid membranes have been efficiently exploited to study the many facets that influence solute transport by AQPs. In the present review, we discuss genome-wide identification of AQPs in plants in relation with recent advancements in analytical tools, and their availability and technological challenges as they apply to AQPs. An exhaustive review of omics resources available for AQP research is also provided in order to optimize their efficient utilization. Finally, a detailed catalog of computational tools and analytical pipelines is offered as a resource for AQP research.

Keywords: plant aquaporin, omic scale analysis, analytical approaches, yeast assay, *Xenopus* oocytes assay

INTRODUCTION

Aquaporins (AQPs) are channel-forming proteins that facilitate selective transport of water and many other small molecules like urea, silicon (Si) in the form of silicic acid, boron (B) in the form of boric acid, and CO₂ across biological membranes. AQPs are present in almost all living organisms including eukaryotes and prokaryotes (Quigley et al., 2001; Tanghe et al., 2006; Benga and Huber, 2012; Benga, 2013). In animals, minor defects or changes in AQP configuration are known to cause many diseases such as hereditary nephrogenic diabetes insipidus, congenital cataracts and, more commonly, the inability to concentrate solutes in urine (Verkman, 2009; Benga and Huber, 2012). Similarly, plant AQPs have an important role in regulating the overall development of a plant, namely in the maintenance of hydraulic status under extreme conditions. As early as 1986, Benga et al. in a pioneer effort, reported the role of proteins in water transport (Benga et al., 1986a,b). Subsequently, Peter Agre's team proved through cRNA expression studies that those proteins, named aquaporin-1, were specific water channels (Preston et al., 1992), and Agre was awarded the Nobel Prize in chemistry in 2003 for his discovery (Agre, 2004). These findings have sparked a veritable explosion of work that has enhanced our understanding of the importance of AQPs in animals as well as in plants (Papadopoulos and Verkman, 2013; Deshmukh et al., 2015; Kitchen et al., 2015; Maurel et al., 2015; Kirscht et al., 2016; Srivastava et al., 2016).

AQPs from diverse origins have characteristic hourglass-like structures with six transmembrane (TM) alpha helices and two half TM alpha-helices with conserved NPA domains (asparagine–proline–alanine) (Jung et al., 1994; Murata et al., 2000). The two half alpha helices form a constraint in the center of the pore that regulates the selective transport of solutes through the pore. Another constraint known as the aromatic arginine (ar/R) selectivity filter (SF), formed mostly with four amino acid residues, plays also a major role in solute selectivity (Murata et al., 2000; Törnroth-Horsefield et al., 2006). Based on their phylogenetic distribution, plant AQPs are generally categorized into five major subfamilies: plasma membrane intrinsic proteins (PIP), nodulin 26-like intrinsic proteins (NIPs), tonoplast intrinsic proteins (TIPs), small intrinsic proteins (SIPs), and uncharacterized intrinsic proteins (XIPs) (Quigley et al., 2001; Deshmukh et al., 2015). The phylogenetic classification of each group is very well aligned with the functionality and characteristic features of AQPs (Grégoire et al., 2012; Deshmukh et al., 2015).

Availability of whole genome sequences for animal and plant species has facilitated genome-wide identification and classification of AQPs. For instance, compared to animals, plants have a larger number of AQPs ranging from 23 in *Selaginella moellendorffii* to 72 in soybean (Deshmukh et al., 2015). Apart from identifying novel genes, genome-wide studies have contributed to a better understanding of the molecular evolution of the AQP gene families (Gupta and Sankararamakrishnan, 2009; Deshmukh and Bélanger,

2016). Precise identification of conserved features along with their functional relevance has progressed rapidly with the availability of AQP sequences from many plant species. Similarly, transcriptome profiling of AQPs conducted in several plant species has helped to determine that AQPs have expression specific to tissue, growth stage, or environmental conditions (Gupta and Sankararamakrishnan, 2009).

Regulation of solute transport through AQPs is a very complex phenomenon that involves environmental stimuli, transcriptional changes, and post-translational modifications. For a better understanding of AQP-mediated transport systems, integration of information generated through different approaches such as genomics, transcriptomics, and proteomics is required. In addition, information about analytical tools and available resources is also important to properly characterize AQPs. In the present review, we discuss how different approaches and analytical tools exploiting the many available resources can contribute to the study of AQPs.

GENOME-WIDE IDENTIFICATION OF AQPS

The initial genome-wide studies in *Arabidopsis* have paved the way to understand the distribution, characterization, and evolution of gene families in plants. The *Arabidopsis* genome has 35 AQPs that can be classified into four subfamilies based on phylogenetic distribution (Quigley et al., 2001). This classification was found to cluster fairly well with the functionality of AQPs. Subsequently, a second genome-wide study was performed in rice, which is considered as a model cereal crop and also represents a distinct monocot clade (Sakurai et al., 2005). Apart from the phylogenetic classification, solute-based classification of AQPs like aquaporins, aquaglyceroporins and S-aquaporins has also been used, particularly in animals (Benga, 2012). The information of AQPs in rice and *Arabidopsis* facilitated the monocot-dicot comparison that expanded the understanding of AQP gene families in plants. Later on, the genome sequencing of cucumber (*Cucumis sativus*) using next generation sequencing approaches started a new era characterized by a constant flow of reports of plant genome sequences and subsequent genome-wide AQP studies in plants (Huang et al., 2009; Deshmukh et al., 2013; Ariani and Gepts, 2015).

The genome sequences for moss (*Physcomitrella patens*) enabled the identification of 23 AQPs (Danielson and Johanson, 2008). In addition, the study added two new AQP subfamilies: Hybrid Intrinsic Proteins (HIP) and GlpF-like intrinsic proteins (GIPs) (Danielson and Johanson, 2008). Mosses, being primitive plants, are valuable for evolutionary studies, and the features observed in mosses are likely to be present in higher plants. In this regard, the seven AQP subfamilies found in mosses suggest that the diversion of AQPs was an early event and that higher plants lost two sub-families in the course of evolution. Subsequently, tissue-specific expression observed in vascular plants is argued to have evolved after the diversion of subfamilies. A recent study highlighting genome-wide comparison of AQPs in 25 plant species revealed several unique features about the subfamilies

(Deshmukh et al., 2015). For instance, it is now clear that the XIP subfamily has been lost throughout the entire monocots, as well as within the *Brassicaceae*. In addition, *Brassicaceae* have also lost NIP2s from their genome (Deshmukh et al., 2015).

Most of the genome-wide studies have used AQP sequences reported in rice and *Arabidopsis* as a query to perform homology-based searches. However, it would be more accurate if a larger number of AQPs from different species could be included in the query sequences given that some subfamilies and groups are absent from *Arabidopsis* and rice. For example, NIP2s having characteristic G-S-G-R ar/R SF are missing from *Arabidopsis*, and, similarly, the entire XIP subfamily is absent in both *Arabidopsis* and rice (**Table 1**). In this paper, we have described over 1000 aquaporins from 26 plant species representing a wide range of families and clades (Supplementary Dataset 1). This exhaustive list will be useful as a query in genome-wide identification of AQPs in other plant species. The analytical steps

required for genome-wide identification of AQPs are described in **Figure S1**.

TRANSCRIPTOMICS STUDIES FOR AQPS

Transcriptomics progressed initially with the technological improvement in chip-based expression profiling platforms (Schulze and Downward, 2001). Subsequently, the advancements in affordable sequencing technologies have greatly contributed to transcriptome sequencing (Burgess, 2016; Chen et al., 2016). As a result, transcriptomic resources have become widely available with RNA-seq studies performed on many plant species covering major crops, medicinal plants, model species and plant species important for evolutionary studies (www.ncbi.nlm.nih.gov/sra). Available transcriptomic resources are helpful to integrate information with genomics data for a better comprehension of gene functions (Movahedi et al., 2012; Patil et al., 2015; Sonah et al., 2016; Song et al., 2016). For instance, many of the

TABLE 1 | Genome-wide identification and classification of aquaporins in 31 plant species.

Plant species	PIP	TIP	NIP	SIP	XIP	AQP	References
<i>Physcomitrella patens</i>	9	4	5	2	2	23	Danielson and Johanson, 2008
<i>Selaginella moellendorffii</i>	3	3	8	1	3	19	Anderberg et al., 2014; Deshmukh et al., 2015
<i>Picea abies</i>	18	6	13	2	0	39	Deshmukh et al., 2015
<i>Musa acuminata</i>	21	18	9	3	0	51	Deshmukh et al., 2015
<i>Oryza sativa</i>	11	10	11	2	0	34	Sakurai et al., 2005
<i>Brachypodium distachyon</i>	11	10	9	2	0	32	Deshmukh et al., 2015
<i>Sorghum bicolor</i>	14	13	10	3	0	40	Deshmukh et al., 2015
<i>Zea mays</i>	10	13	13	7	0	43	Deshmukh et al., 2015
<i>Setaria italic</i>	16	16	15	3	0	50	Deshmukh et al., 2015
<i>Elaeis guineensis</i>	9	10	9	2	0	30	Deshmukh et al., 2015
<i>Arabidopsis thaliana</i>	13	10	9	3	0	35	Quigley et al., 2001
<i>Arabidopsis lyrata</i>	14	12	10	3	0	39	Deshmukh et al., 2015
<i>Brassica rapa</i>	22	16	15	6	0	59	Deshmukh et al., 2015
<i>Brassica oleracea</i>	25	19	17	6	0	67	Deshmukh et al., 2015
<i>Carica papaya</i>	10	7	7	2	2	28	Deshmukh et al., 2015
<i>Citrus sinensis</i>	11	9	8	3	3	34	Deshmukh et al., 2015
<i>Citrus clementine</i>	14	10	9	3	1	37	Deshmukh et al., 2015
<i>Vitis vinifera</i>	9	9	9	1	2	30	Deshmukh et al., 2015
<i>Glycine max</i>	22	23	17	8	2	72	Deshmukh et al., 2013
<i>Cajanus cajan</i>	12	13	10	4	1	40	Deshmukh et al., 2015
<i>Fragaria vesca</i>	10	9	14	4	2	39	Deshmukh et al., 2015
<i>Prunus persica</i>	7	8	9	3	2	29	Deshmukh et al., 2015
<i>Ricinus communis</i>	10	9	8	4	5	36	Deshmukh et al., 2015
<i>Populus trichocarpa</i>	15	18	11	7	7	58	Gupta and Sankararamakrishnan, 2009
<i>Solanum tuberosum</i>	15	11	11	2	5	44	Deshmukh et al., 2015
<i>Solanum lycopersicum</i>	14	10	11	3	6	44	Deshmukh et al., 2015
<i>Phaseolus vulgaris</i>	12	13	10	4	2	41	Ariani and Gepts, 2015
<i>Hevea brasiliensis Muell. Arg.</i>	15	17	9	4	6	51	Zou et al., 2015
<i>Hordeum vulgare L</i>	11	7	4	2	0	22	Hove et al., 2015
<i>Jatropha curcas</i>	9	9	8	4	2	32	Zou et al., 2016
<i>Phyllostachys edulis</i>	10	6	8	2	0	26	Sun et al., 2016
Total 31 plant species	402	348	316	105	53	1224	

recent studies highlighting genome-wide identification of AQPs have relied on transcriptomic resources to explain tissue-specific expression of those genes (Gupta and Sankararamakrishnan, 2009; Reuscher et al., 2013; Venkatesh et al., 2013; Deshmukh et al., 2015; Hu et al., 2015; Deokar and Tar'an, 2016; Deshmukh and Bélanger, 2016; Zou et al., 2016).

In a study of genome-wide identification of AQPs in soybean, we have used publicly available RNA-seq and microarray data to elucidate the expression profile of AQPs across tissues (Deshmukh et al., 2013). Among particular observations, the study revealed a seed-specific expression for all members of the TIP3 subgroup. A similar type of seed-specific expression for TIP3s has been reported with rice and Arabidopsis, transcriptomic data (Deshmukh et al., 2013). These results suggest an important role of TIP3s in seed development, possibly in the desiccation process required for seed maturation. Similarly, Gupta and Sankararamakrishnan (2009) have used microarray data to perform genome-wide expression profiling of AQPs in poplar, and revealed higher expression of TIPs and PIPs in xylem tissues. Using a publicly available RNA-seq data for barley, Hove et al. (2015) observed a high level of HvNIP4;1 expression in inflorescences. Recently, the tissue-specific expression of NIP4s (AtNIP4;1 and AtNIP4;2) was found to be required for pollen development and pollination in *Arabidopsis thaliana* (Di Giorgio et al., 2016). Such information about expression profile is instrumental in defining substrate specificity and interdependency among AQPs.

Interdependency of AQPs is a well-known phenomenon, particularly in the case of PIP1s and PIP2s (Yaneff et al., 2014). The AQP-mediated transport system is very complex and will rely on the conjugated action of distinct transporters to carry solutes from one tissue to another (Ma et al., 2007; Sakurai et al., 2015). In this context, recent developments in analytical tools offer great opportunities for construction of co-expression networks and several online tools are available for this purpose (Table 2). As an example, Figure 1 describes a co-expression network in rice using the online tool FREND that revealed the concerted role of PIP2-1, PIP1-1, and PIP1-2. Another tool, PlaNet, allows a comparative analysis of co-expression networks across plant species such as rice, soybean, *Brachypodium*, barley, *Medicago*, poplar and wheat. Furthermore, some tools exploit data from the literature, known protein domains, experimentally proven protein-protein interactions, genetic interactions based on QTL/GWAS studies, and information generated through proteomics interactions to infer specific roles of AQPs (Table 2). As part of an integrated omics approach, these tools will provide precise information about AQP-mediated molecular events in plants.

PROTEOMICS CONTRIBUTIONS IN AQP STUDIES

Compared to genomics and transcriptomics, proteomic approaches have contributed limited efforts to the study of AQPs. This is mostly because of the costly and demanding

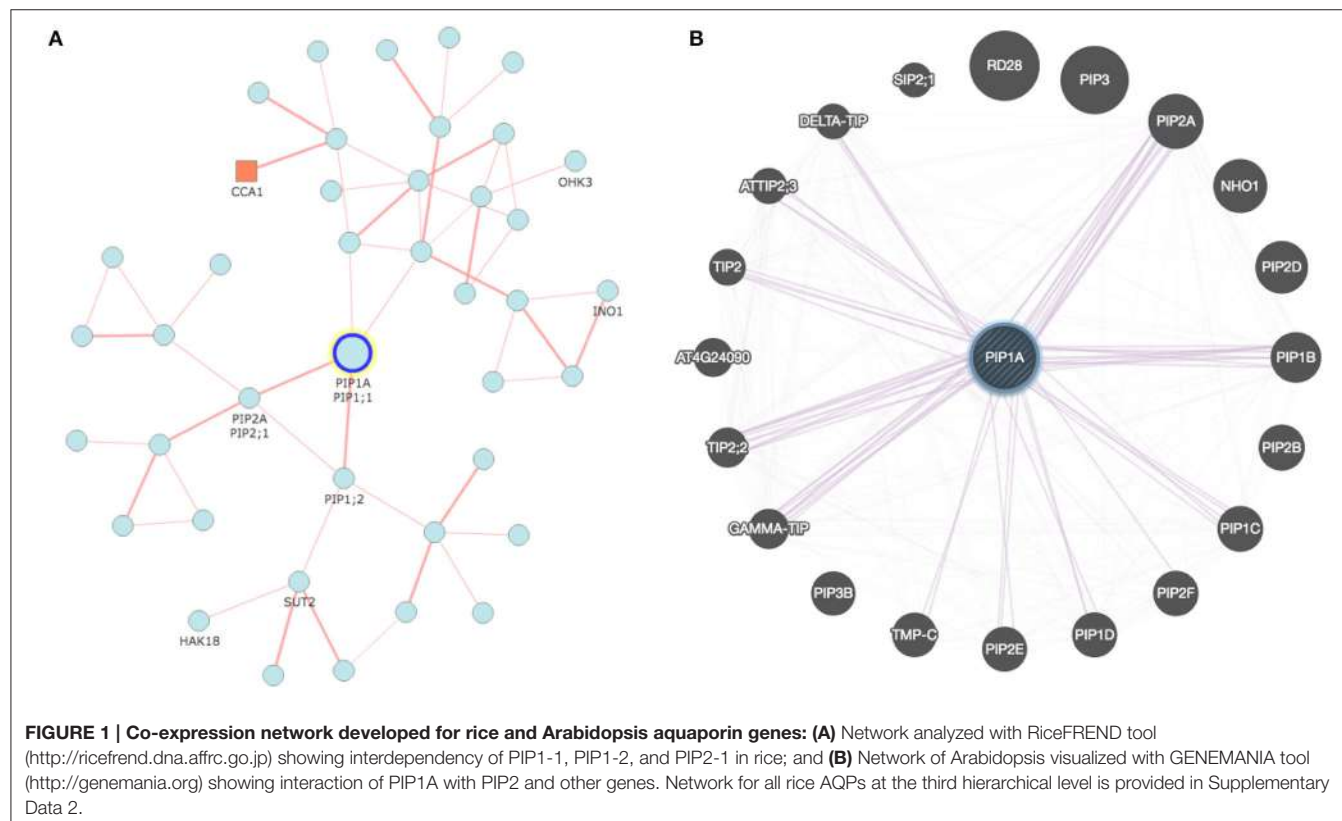


TABLE 2 | Tools available for the development of co-expression network using transcriptomic data from different plant species.

S. no.	Database/ Online tool	Plant species	Website	Other notes/Features
1	PlaNet	Arabidopsis, barley, <i>Medicago truncatula</i> , poplar, rice, soybean, <i>Nicotiana tabacum</i> , and wheat	http://aranet.mpimp-golm.mpg.de	Allows comparative analysis of co-expression networks across plant species
2	PLANEX	<i>Arabidopsis thaliana</i> , soybean, barley, rice, tomato, wheat, grape and maize	http://planex.plantbioinformatics.org	Gene Expression Omnibus (GEO)
3	ATTED-II	Arabidopsis, soybean, maize, rice, tomato, wheat, grape, poplar, and mustard	http://atted.jp	Uses known protein-protein interactions and functional annotations
4	CressExpress	Arabidopsis	http://cressexpress.org	Suitable for downstream data-mining, visualization, and analysis.
5	Genemania	Arabidopsis	http://genemania.org	GeneMANIA's database of 1800+ networks, containing over 500 million interactions across eight organisms
6	CORNET	Maize, Tool	https://bioinformatics.psb.ugent.be/cornet/	Allows co-expression analysis using either predefined or user-defined groups of microarray experiments.
7	VTCdb	Grape	http://vtcdb.adelaide.edu.au/Home.aspx	Retrieves hierarchical optimized Gene Ontology enrichment and tissue/condition specificity genes within the module along with interactive network visualization and analysis via CytoscapeWeb.
8	CORE	Rice	https://core.ac.uk/display/8598313/tab/similar-list	Creates gene co-expression networks using both condition-dependent and condition-independent data
9	Xpressomics	Arabidopsis	https://xpressomics.com/search/	Uses differential expression from expert-curated and analyzed raw data
10	CoP	Arabidopsis, soybean, barley, rice, poplar, wheat, grape, maize	http://webs2.kazusa.or.jp/kagiana/cop0911/	Provides information about gene co-expression, specific gene expression, biological processes, and metabolic pathways that are mutually interconnected
11	RiceFREND	Rice	http://ricefrend.dna.affrc.go.jp/	Based on a large collection of microarray data

methodological requirements of proteomic studies. Most of the large-scale proteomic analyses focusing on AQPs have been conducted with Arabidopsis, and rice (**Table S1**). In general, modern proteomic tools yield an enormous amount of valuable data that can be used to resolve complex molecular mechanisms, more specifically regarding post-translation modifications, protein expression, and protein-protein interactions (Deshmukh et al., 2014). However, relatively limited information is available for membrane proteins including AQPs because of constraints such as limited solubility, low expression and restricted use of restriction enzymes (Tan et al., 2008).

Solubility of AQPs is a very critical issue to perform efficient proteomic studies because of their higher hydrophobicity, difficult extraction, and presence in relatively small amounts. This issue prevents or limits reliance on standard approaches utilizing mass spectrometry (MS), matrix-assisted laser desorption ionization (MALDI), and electrospray ionization (ESI). Some of the pioneer studies, including those of Schindler et al. (1993) and Schey et al. (1992), developed procedures for improving solubilisation of membrane proteins by using organic solvents, acetonitrile, 2-propanol, hexafluoro-2-propanol and detergents. Better solubilisation also helps for a more efficient

digestion. However, problems with dissolving membrane proteins remain even though the amount of AQPs obtained with fractionated plasma membrane was somewhat alleviated with the advancement in instrumentation that works at the nano-scale level (**Table S1**).

Santoni et al. (2003) described the first comprehensive efforts for AQP research using proteomic approaches. They developed an inventory of Arabidopsis AQP isoforms expressed in root tissues that were characterized with MALDI and electro-ionization tandem MS. The study also provided key information about phosphorylation and other post-translational modifications of AQPs, particularly within the PIP subfamily. Nearly a decade after this pioneer work, a study by Mirzaei et al. (2012) demonstrated the effects of environmental factors like drought on AQP regulation in rice. The study described the AQP expression profile at precise physiological stages during the progression of drought over time. For this purpose, the authors used label-free quantitative shotgun proteomic approaches involving nano-LC-MS/MS to identify 1548 proteins including AQPs, and predicted the mechanisms involved in drought stress. Similarly, di Pietro et al. (2013) conducted extensive proteomic studies of

Arabidopsis AQPs under different physiological conditions. They studied nine physiological treatments modulating root hydraulics over different time periods. They observed 55 AQP peptides undergoing significant changes with respect to different physiological conditions, including several post-translational modifications like methylation, acetylation, and phosphorylation.

AQUAPORIN TERTIARY STRUCTURE

The precise definition of the molecular structure of a protein is very important to understand its function. It contributes to the elucidation of the specific activity of a protein and its interaction with other molecules including ligands and inhibitors. Since the discovery of the first AQP in human red blood cells and renal proximal tubules, several attempts have been made to resolve AQP structure (Preston et al., 1992). Initial work by Preston et al. (1994), using a-chymotrypsin digestion of intact oocytes and inside-out membrane vesicles, confirmed the cytoplasmic loops and orientations of the six transmembrane alpha helices predicted by the hydrophathy analysis. In the same year, another study by Jung et al. (1994) predicted the hourglass model for AQPs based on the topological information and the positioning of the loops, more particularly loop B and loop E, which penetrate in the membrane from opposite sides to form a constriction harboring conserved NPA domains. This study was instrumental in predicting for the first time the role of NPA domains in the tight regulation of solute transport. Later, Murata et al. (2000) solved the atomic structure of AQP1 using electron crystallographic analysis that confirmed the earlier predictions. The AQP1 structure has 3.8 Å resolution describing highly conserved amino-acid residues that stabilize the fold, and form the hourglass structure. The structural model presented by Murata et al. (2000) showed the conserved hydrophobic residues lining the water channel at the center of the protein. The structure also showed constrictions with a pore diameter of about 3 Å that provided a clue as to how the AQP was permeable to water but not the proton.

Up to now, about 51 AQP structures have been described using different approaches at varying levels of resolution (**Table S2**). Most of the solved structures belong to human and *Escherichia coli* AQPs representing eukaryotic and prokaryotic models. Apart from human, high-resolution AQP structures are also available from other animals such as rat, sheep, and cattle (**Table S2**). Compared to animals and prokaryotes, very few structures are available for plant AQPs. The first plant AQP structure, common bean TIP, was solved by Daniels et al. (1999) at low resolution (7.7 Å) using electron cryo-crystallography. In spite of the low resolution, the AQP structure showed resemblance with animal AQPs. Törnroth-Horsefield et al. (2006) described the first high resolution plant AQP structure (from spinach, SoPIP2;1) in its closed (2.1 Å resolution) and open conformation (3.9 Å resolution). The structure with closed and open conformation explained the gating mechanism in which loop D, through a displacement of up to 16 Å, widened the pore and acted as molecular gating. The mechanism of gating

is found to be conserved across all plant species (Törnroth-Horsefield et al., 2006). Recently, the structure of Arabidopsis aquaporin AtTIP2;1 was determined at very high resolution (1.18 Å) (Kirscht et al., 2016). Most of the previously reported structures are from water-transporting AQPs (**Table S2**) but AtTIP2;1 is a model AQP for ammonia transport. Interestingly, Kirscht et al. (2016) discovered a fifth amino acid involved in the permeability of ammonia, expanding the complexity of solute specificity from the four amino acids ar/R SF. Owing to the increasing availability of high-resolution AQP structures, homology-based computational approaches used to predict 3D-structure have now become more efficient and sophisticated (**Tables S2, S3**).

Advances in computational methods during the last two decades have made it possible to predict structures more accurately. The success of computational methods can be attributed to the evolutionary conserved features of proteins, the relatively small number of unique protein fold in nature, and the ever increasing number of solved protein structures (www.rcsb.org; Koonin et al., 2002). Compared to proteins that have no similarity with known structures, prediction of structure for candidate AQPs is facilitated by the abundance of resolved AQP structures publicly available (**Table S2**). In addition, several online servers and tools available for the homology-based prediction of protein structures are helpful to pursue more advanced studies in AQPs (**Table S3**).

Molecular dynamics simulations are advanced computational approaches used for *in silico* reconstitution of protein structure in its native environment (Lindahl and Sansom, 2008). Molecular dynamics simulations became more advanced with the availability of very high-resolution 3-D structures, increased computing power, and improvement in the analytical algorithms. In addition, detailed information about the interaction between amino acid residues and the surrounding environment makes it possible to reconstitute protein structures in different environments (Lindahl and Sansom, 2008). More particularly, studies focusing on membrane proteins have provided information about the interaction between individual amino acids with the lipid molecules in the membrane environment. There are several methods and tools available for molecular dynamics simulations of membrane proteins like AQPs (Lindahl and Sansom, 2008). Recently, Sakurai et al. (2015) have performed molecular dynamics simulations to study silicic acid uptake through AQP (OsLsi1) coupled with another active transporter (OsLsi2) in rice roots. They developed a mathematical model using diffusion equation along with the effects of active transport by OsLsi2. The study provides a good example for the utilization of *in vivo* experimental data to calibrate the model.

ANALYTICAL AND FUNCTIONAL APPROACHES

Xenopus Oocyte Assay

Oocytes of *Xenopus laevis* (African clawed frog) are commonly used for the evaluation of solute transport activity by AQPs

and many other transporters. cRNA of foreign proteins can be easily injected and expressed in *X. laevis* oocytes. A cRNA volume of up to 50 nL can be injected in the oocyte, which allows production of large amounts of protein. The simplified steps involved in the *X. laevis* oocyte assay are provided in **Figure 2**. The transport of several different substrates by plant AQPs has been evaluated using *X. laevis* oocyte assay (**Table 3**). The oocyte assay conveniently allows the use of radiolabeled substrates to facilitate a better estimation of transport kinetics and also to increase the sensitivity of the assay (Ma et al., 2006). However, in the case of certain substrates such as silicic acid, many have used ^{68}Ge as silicic acid surrogate, a method often criticized given that ^{68}Ge was never shown to represent a perfectly interchangeable surrogate. In recent studies, silicic acid transport (influx and efflux) in oocytes was measured directly by atomic absorption spectrophotometry, a technical improvement that greatly facilitates the study of silicic acid movement in plants (Ma et al., 2006; Grégoire et al., 2012; Deshmukh et al., 2015; Carpentier et al., 2016; Vivancos et al., 2016). The measurement of change in volume of oocyte in response to osmolality of external solution is a simple and effective measure to study water transport by AQPs. The *X. laevis* oocyte system provides several advantages for the study of transporters. For instance, there is very low transport across the oocyte membrane through the endogenous transporters; therefore there is limited background effect and less ambiguity about solute transport. In addition, the relatively large size of *X. laevis* oocytes facilitates their manipulation and allows studying electrophoretic transporters using the two-electrode voltage clamp technique. Nevertheless, one has to keep in mind that the environment of a plant cell is drastically different from that of the *X. laevis* oocyte. Therefore, results obtained with the *X. laevis* oocyte assay need to be corroborated with the actual activity of the protein in plant cells.

Translation of plant AQP transcripts in the oocyte may be altered by the differential codon preference between plants and *Xenopus*. For this reason, western blotting is often required to confirm protein expression/presence in the oocytes. However, codon optimization is rarely considered for plant AQPs when tested with oocytes, which raises the question, whether codon optimization is really a concern or not. Recently, Feng et al. (2013) reported better nitrate transport in oocytes with codon-optimized rice high affinity nitrate transporter. Similarly Bienert et al. (2014) also observed a significantly higher expression of ZmPIP1 and ZmPIP2 in yeast cells only after optimizing the codons. Nowadays, the use of synthesized DNA for gene-cloning related applications is becoming more common because of reduced costs and codon optimization can be routinely applied while synthesizing the gene for oocyte or yeast assays.

Evaluation of AQPs Using Yeast Assays

Characteristic features of yeasts including ease of growth, short generation time, well established and easy transformation systems, and sequenced genomes, make them amenable as a heterologous system to study eukaryotic proteins. Several yeast species, including *Saccharomyces cerevisiae*, *Schizosaccharomyces pombe*, and *Pichia pastoris* have been used as a tool to study foreign genes.

Numerous AQPs have been studied using a yeast expression system (**Table 4**). The study of water fluxes through AQPs in yeast assays is a particularly easy and affordable option. Water transport in yeast results in measurable cell volume changes (swelling or shrinking) in relatively short periods of time. The water transport through AQPs (as a hydrophilic passage) is much faster than the transport through the hydrophobic lipid bilayer membrane. This allows discrimination between water transport through the foreign AQP expressed in the yeast and the transport through the membrane. The volume change in yeast affects several physical parameters that can be used to make quantitative measurements essential to understand transport kinetics. Light absorption, light scattering or reflection with fluorescent dye are effective variables that are being used to monitor cell volume changes (**Table 4**, **Figure 3**). Given the small size of the yeast that takes milliseconds to change volume in response to osmotic pressure, it requires a method known as stopped-flow spectrometry to take precise measurements. In stopped-flow spectrometry, protoplasts, vesicles or even intact cells are subjected simultaneously to hypotonic and hypertonic buffers. The rapidly mixing hypotonic and hypertonic solution stops transport in milliseconds, which allows taking measurements at the scale required to understand transport kinetics. Use of fluorescent dye in stopped-flow spectrometry increases precision of measurements. Recently, Sabir et al. (2014) evaluated grape AQPs for water conductivity using a stopped-flow fluorescence spectroscopy assay. They pre-loaded yeast cells with the non-fluorescent precursor 5-(and-6)-carboxyfluorescein diacetate (CFDA) that is permeable to membranes, and then intracellularly hydrolyzed CFDA to release the membrane impermeable fluorescent compound. Changes in cell volume in stopped-flow assay in response to osmotic changes resulted in changes in fluorescence intensity that can be measured to deduct transport kinetics.

Apart from water, transport of many other solutes through AQPs is also studied with yeast systems. Commonly, yeast growth and survival are used to study solutes (**Table 4**). For instance, uptake of germanium (Ge), arsenate (As), boric acid and antimonite severely affect yeast growth, and this effect can be measured through heterologous expression of AQPs specific for such solutes. Similarly, mutant strains like YNVW1 carrying the deletion $\Delta dur3$ cannot grow on media with urea as sole nitrogen source, thus making such deletion strains useful to study urea transport by AQPs (**Table 4**).

Recently, To et al. (2015) demonstrated rapid screening of an AQP mutant library to evaluate the effects of amino acid changes on solute transport. The authors developed a novel method that looks promising to study water transport ability for hundreds of AQPs simultaneously. The assay can be used to identify inhibitors as well as co-transporting molecules. The method exploits the property of yeast cells that show increased freezing tolerance with expression of functional AQPs. The rapid transport of water through AQP allows removal of water from freezing yeast cells that avoid formation of ice crystals thus preventing cell damage. With this method, a library of yeasts (preferably AQP mutant strains) transformed with different AQPs can grow in 96-well microplates that are exposed to freeze-thaw cycles. Only the

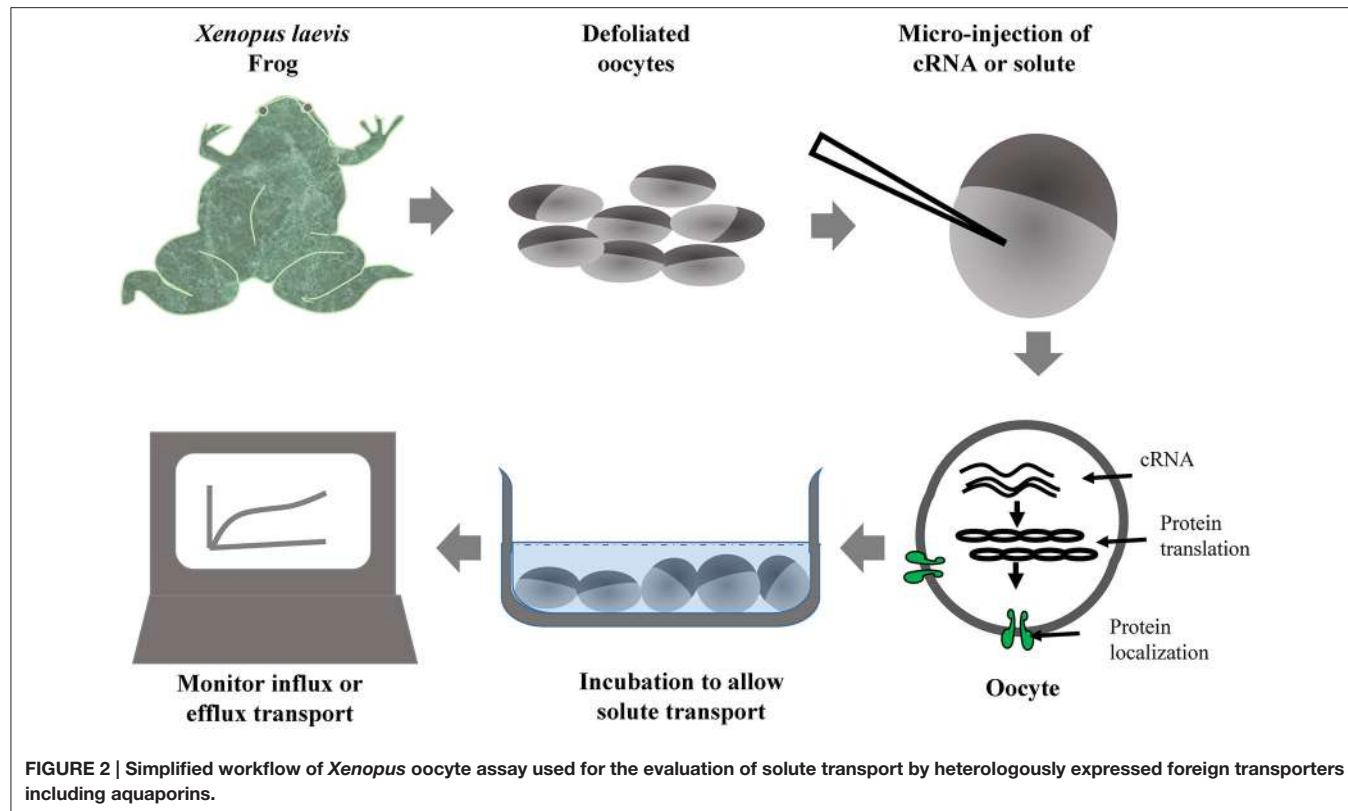


FIGURE 2 | Simplified workflow of *Xenopus* oocyte assay used for the evaluation of solute transport by heterologously expressed foreign transporters including aquaporins.

TABLE 3 | List of important studies performed to evaluate different solutes transported by plant aquaporins using the *Xenopus* oocyte assay.

Plant species	Gene	Solute	References
Arabidopsis	AtTIP2;1, AtTIP2;3	Ammonium	Loqué et al., 2005; Liu et al., 2013
Rice	Lsi1 (OsNIP2;1)	Arsenite	Zhao et al., 2010
Arabidopsis	NIP5;1	Boron	Takano et al., 2006
Arabidopsis	NIP6;1	Boron	Tanaka et al., 2008
<i>Nicotiana tabacum</i>	NtAQP1	CO ₂	Uehlein et al., 2003
<i>Nicotiana tabacum</i>	NtXIP1;1	Glycerol, urea, boric acid	Bienert et al., 2011
Soybean	Nodulin 26	Glycerol, Water	Dean et al., 1999
<i>Nicotiana tabacum</i>	NtAQP1	Glycerol, Water,	Biela et al., 1999
Poplar	PtNIP2-1	Silicic acid	Deshmukh et al., 2015
Tomato	SINIP2-1 (Mutant)	Silicic acid	Deshmukh et al., 2015
Barley	HvLsi1	Silicic acid	Chiba et al., 2009
<i>Equisetum arvense</i>	EaNIP3;1, EaNIP3;3 and EaNIP3;4	Silicic acid	Grégoire et al., 2012
Soybean	GmNIP2-1, GmNIP2-2	Silicic acid	Deshmukh et al., 2013
Rice	Lsi1 (OsNIP2;1)	Silicic acid (⁶⁸ Ge)	Ma et al., 2006
Maize	ZmPIP1-5b	Urea, Water	Bousser et al., 2003
Spinach	PM28A	Water	Johansson et al., 1998
Maize	ZmPIP2a	Water	Chaumont et al., 2000
Rice	OsPIP1;1	Water	Liu et al., 2013
Radish	VM23	Water	Higuchi et al., 1998
Olive	OePIP2.1, OeTIP1.1	Water	Secchi et al., 2007
Tomato	LeAqp2	Water	Werner et al., 2001
Walnut	JrPIP2,1	Water	Sakr et al., 2003
Soybean	GmTIP1-5, GmTIP2-5	Water	Song et al., 2016

TABLE 4 | List of plant aquaporins evaluated for transport of different solutes using yeast assays.

Aquaporin	Plant	Yeast strain	Solute	Yeast assay	References
TIP1;1, TIP1;2	Arabidopsis	$\Delta tsa1;2$, $\Delta skn7$, $\Delta yap1$, $\Delta fsp1$, $\Delta yfl054c$	H_2O_2	Spheroplast Swelling Assay, Survival test, Catalase Activity Assay, Fluorescence Assay, Bioimaging	Bienert et al., 2007
AtNIP1;1, AtNIP2;1, AtNIP5;1, AtNIP6;1, AtNIP7;1	Arabidopsis	W303-1A	As(III), As(V), antimonite	Yeast growth and survival test	Bienert et al., 2008
AtPIP1;2, AtPIP2;3	Arabidopsis	W303	CO_2	Stopped-flow spectrometry	Heckwolf et al., 2011
SIP1;1, SIP1;2, SIP2;1	Arabidopsis	BJ5458	H_2O	Stopped-flow spectrometry	Ishikawa et al., 2005
AtNIP7;1	Arabidopsis	acr3 Δ , fsp1 Δ	As(III), As(V),	Yeast growth and survival test	Isayenkov and Maathuis, 2008
HvNIP2;1	Barley	INVSc2, SY1	Boric acid, Ge, As	Yeast growth and survival test	Schnurbusch et al., 2010
HvNIP1;1, HvNIP1;2, HvNIP2;1, HvNIP2;2	Barley	$\Delta SKN7$, $\Delta ACR3$	H_2O_2 , As(OH) ₃	Yeast growth and survival test	Katsuhara et al., 2014
VvTnPIP2;1, VvTnTIP1;1, VvTnTIP2;2, VvTnPIP1;4, VvTnPIP2;3, VvTnTIP4;1	Grape	10560-6B	H_2O	Stopped-flow fluorescence spectroscopy	Sabir et al., 2014
HaTIP1;1, HaPIP1;1, HaPIP1;2	<i>Helianthemum almeriense</i>	SY1	CO_2 , NH ₃ , H_2O	Stopped-flow spectrometry	Navarro-Ródenas et al., 2013
VALT (TIP), PALT1 (PIP)	Hydrangea (<i>Hydrangea macrophylla</i>)	$\Delta hsp150$, BY4741	Al	Yeast growth and survival test	Negishi et al., 2012
LjNIP5;1, LjNIP6;1	<i>Lotus japonicus</i>	W303-1A	As(III), As(V), antimonite	Yeast growth and survival test	Bienert et al., 2008
LjNIP1	<i>Lotus japonicus</i>	31019b, YNW1	Amonia, Urea, H_2O	Stopped-flow spectrometry, Yeast growth and survival test	Giovannetti et al., 2012
ZmPIP1;2, ZmPIP2;5	Maize	31019b ($\Delta mep1-3$), BY4741	H_2O_2	Yeast growth and survival test, Codon optimization	Bienert et al., 2014
PvTIP4;1	<i>Pteris vittata</i>	$\Delta fsp1$ and $\Delta acr3$	As(III), As(V)	Yeast growth and survival test	He et al., 2016
RsPIP1-2, RsPIP1-3, RsPIP2-1, RsPIP2-2	Radish	BJ5458	H_2O	Stopped-flow spectrophotometry	Suga and Maeshima, 2004
OsNIP1;1, OsNIP1;2, OsNIP2;1, OsNIP2;2, OsNIP3;1, OsNIP3;2, OsNIP3;3, OsNIP4;1	Rice	$\Delta SKN7$, $\Delta ACR3$	H_2O_2 , As(OH) ₃	Yeast growth and survival test	Katsuhara et al., 2014
OsNIP2;1, OsNIP2;2, OsNIP3;2	Rice	W303-1A	As(III), As(V), antimonite	Yeast growth and survival test	Bienert et al., 2008
TsTIP1;2	<i>Thellungiella salsuginea</i>	<i>aqy-null</i> strain	H_2O_2	Fluorescence assays, Yeast growth and survival test	Wang et al., 2014
NtXIP1;1, StXIP1;1	Tobacco	YNW1 ($\Delta dur3$)	Urea	Yeast growth and survival test	Bienert et al., 2011
TaTIP2;2	Wheat	31019b, BJ5458	Ammonia	Stopped-flow spectrometry	Bertl and Kaldenhoff, 2007

yeasts transformed with functional AQPs will survive following freeze-thaw cycles, a quick way to assess AQP properties. Such high-throughput procedures will certainly expand the analytical power required to integrate omics scale research.

Mesophyll Protoplast Assay

Mesophyll protoplasts can be easily obtained for several plant species (Shen et al., 2014). More particularly, the procedure for the evaluation of AQPs using Arabidopsis, tobacco and maize mesophyll protoplasts is well established (Yoo et al., 2007; Besserer et al., 2012; Ma et al., 2015). There are several methods for the delivery of macromolecules into protoplasts including, electroporation, microinjection, and PEG–calcium fusion method (Sade et al., 2009; Shen et al., 2014). Transient

expression of AQPs in plant mesophyll protoplast allows efficient study of solute transport and also the subcellular localization of the protein. Recently, Wang et al. (2015) exploited Arabidopsis protoplasts for the transient expression of an AQP from maize (MzPIP2;1) tagged with a green fluorescent protein to confirm the plasma membrane specific localization. Similarly, Chevalier et al. (2014) used the mesophyll protoplast assay to study subcellular localization of several maize AQPs belonging to the ZmPIP1s and ZmPIP2s subfamilies. They observed efficient localization in plasma membrane only for ZmPIP2s when expressed alone in the mesophyll protoplasts. They further swapped transmembrane domain-3 along with the ER export diacidic motif to demonstrate its requirement in the localization. Another study conducted using tobacco protoplasts showed the

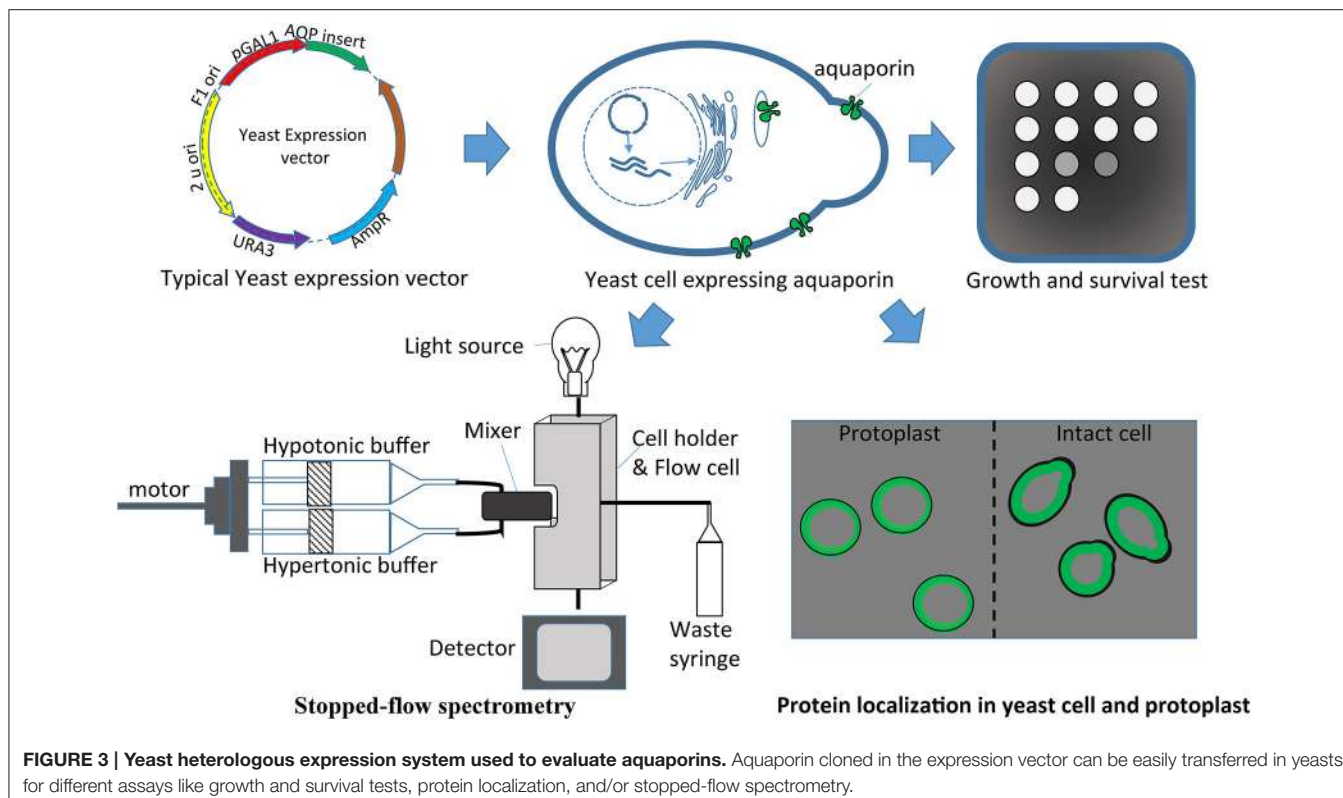


FIGURE 3 | Yeast heterologous expression system used to evaluate aquaporins. Aquaporin cloned in the expression vector can be easily transferred in yeasts for different assays like growth and survival tests, protein localization, and/or stopped-flow spectrometry.

role of phosphoinositides in modulating aquaporin activity (Ma et al., 2015). AQP gene ZmPIP2;4 from maize was transiently expressed in tobacco protoplasts to evaluate phosphoinositides effect on AQP expression and water flux (Ma et al., 2015). In spite of the rather routine application of the mesophyll protoplast assay, a high-throughput method for AQP evaluation using this assay has not been developed yet. Such an assay would allow large-scale exploitation of native rather than surrogate membranes. However, the major limitation with this technique is the requirement of highly skilled expertise to handle protoplasts, and the relatively low rate of success when experiments are replicated across different labs.

Isolated Vesicle Assay: Right-Side Out and Inside-Out

Vesicles isolated from different types of tissues and cell types are being used for the evaluation of AQPs. The vesicles can be easily obtained following ultracentrifugation-based fractioning. After obtaining vesicles separated from the other organelles and cytoplasm, AQPs can be studied with stopped-flow fluorescence spectroscopy that measures shrinking/swelling of the vesicle. Dordas et al. (2000) used plasma membrane vesicles obtained from squash (*Cucurbita pepo*) roots to study the role of AQPs in boric acid transport. They used mercuric chloride and phloretin, a well-known non-specific transporter inhibitor, to conclude that boric acid permeation occurred both through proteinaceous channels and diffusion through the membrane.

Isolated inverted vesicles are useful to measure uptake inside the vesicle by efflux transporter. The reversed membrane vesicle

is known as inside-out where the apoplastic side is inside the vesicle. The inside out vesicles are generally used for the evaluation of efflux transporters and energy dependent transporters. Initially, Palmgren et al. (1990) developed the method to prepare inside-out and right-side-out (apoplastic side out) vesicles using sugar beet (*Beta vulgaris* L.) leaves. They used freezing and thawing to turn vesicles inside-out and subsequently separated the inside-out and right-side-out by repeating the phase partition step. ATPase assay is used to verify the proportion of inside-out vesicles, since the ATPase active site is situated on the cytoplasmic side of the membrane, and only sealed, inside-out vesicles efficiently perform ATP-dependent H⁺ pumping (Palmgren et al., 1990). Similarly, Sutka et al. (2005) used the stopped-flow technique to measure water transport activity of tonoplast vesicles. They were able to conclude that most of the AQPs located in the tonoplast membrane are sensitive to HgCl₂ and few of them are inhibited by pH. Their study expanded the use of isolated vesicle assays to the tonoplast-specific AQPs. However, the major drawback of the system resides in its labor intensive procedure required to isolate plasma membrane vesicle fractions.

TRANSGENIC APPROACHES USED FOR AQUAPORIN RESEARCH

The heterologous expression of AQPs in plants represents a useful approach for functional evaluation of AQPs, even though it can sometimes lead to experimental artifacts. Indeed, transgenic approaches are often criticized over the use of constitutive

or non-specific promoters that express AQPs in tissues where natural expression is not observed. In the case where a plant trait is governed by genotypic variations, complementation assays with a transgenic approach is considered more reliable since expression of the transgenes are evaluated under the same conditions. In addition to contributing to the functional annotation of novel AQPs, transgenic approaches are also being exploited to develop crop plants with agronomically important traits (**Table S4**). Currently, Arabidopsis and tobacco remain the preferred source for the heterologous expression of genes including AQPs. In addition, extensive resource of T-DNA insertion mutant libraries available for Arabidopsis makes it an obvious choice for the functional study of novel AQPs. As a matter of fact, mutants are available for most of the AQPs identified in the Arabidopsis genome, which facilitates evaluation of any native Arabidopsis AQP as well as their homologs in other plant species.

Most of the AQP transgenic studies have evaluated responses against abiotic stresses like high salinity, drought, and cold (**Table S4**). In a notable effort, Jang et al. (2007) analyzed the effect of expression of *AtPIP1;4* and *AtPIP2;5* in Arabidopsis and tobacco transgenic plants under various abiotic stress conditions. They also noticed a change in endogenous AQP genes with the over expression of *AtPIP1;4* and *AtPIP2;5* transgenes. Another study by Peng et al. (2007) reported that the overexpression of *PgTIP1* from *Panax ginseng* in transgenic Arabidopsis plants led to enhanced tolerance against salt-stress and drought, but lowered cold acclimation ability. The contrasting effect of overexpression of an AQP on drought and cold is expected since altered water movement has a contrasting effect over these stresses. However, many contradictory results with the heterologous expression of AQPs in transgenic plants have been reported. For instance, Peng et al. (2008) observed a significantly lowered freezing tolerance with overexpression of *Rhododendron catawbiense* AQP (RcPIP2) in Arabidopsis. Similarly, with the overexpression of a PIP in transgenic tobacco, Aharon et al. (2003) achieved improvement in plant growth under favorable growth conditions but not under drought or salt stress. AQPs are also extensively studied for physiological parameters like CO₂ conductance and photosynthesis efficiency (**Table S4**). For instance, Katsuhara and Hanba (2008) evaluated the effect of *HvPIP2;1*, cloned from barley for the transport of water and CO₂ conductance in a transgenic rice. In a rare study with biotic stress, Vivancos et al. (2015) showed that expression of a wheat *NIP2* in Arabidopsis conferred higher Si absorption and better protection against powdery mildew.

CONCLUSIONS

Enormous progress has been achieved to understand solute transport in plants over last two decades following the discovery of the first AQP. Currently, over 30 plant species have been analyzed for genome-wide identification of AQPs. These efforts have highlighted the distribution and evolution of AQPs in plants and have also defined the phylogeny

of AQPs and subsequent categorization into sub-families and groups. The dataset of over 1000 well-characterized AQPs provided here will be helpful to maximize the use of query sequences in homology-based AQP identification and subsequent characterization. Access to AQPs originating from diverse species is important to insure the identification of the entire set of AQPs in a given genome as well as their proper classification. In addition, the ever-growing resources of transcriptomic data should be exploited to characterize AQPs and refine our understanding of their role in relation with their tissue-specific expression. Integration of omics approaches to complex molecular systems like AQP-mediated transport has been facilitated lately with the development of powerful computational tools. Computational predictions however must be supported and validated by functional studies. For this purpose, biological assays such as *Xenopus* oocytes and yeast systems are now well-established approaches used to study solute specificity and transport kinetics of AQPs. In addition, several novel AQPs identified with omics efforts have been functionally annotated through transgenic approaches that have highlighted their beneficial role. With the current concerns over water resources, it is clear that a better understanding of AQP-mediated transport system in plants can only lead to the development and management of plants better adapted to changing environmental conditions.

AUTHOR CONTRIBUTIONS

RD, HS, and RRB compiled the data, drew the conclusions and wrote the manuscript.

FUNDING

The project was funded by a grant from the Natural Sciences and Engineering Research Council of Canada (NSERC), the Agri-Innovation program Growing Forward 2, SaskCanola and Agriculture and Agri-Food Canada and the Canada Research Chairs Program to RRB.

SUPPLEMENTARY MATERIAL

The Supplementary Material for this article can be found online at: <http://journal.frontiersin.org/article/10.3389/fpls.2016.01896/full#supplementary-material>

Figure S1 | Proposed flowchart procedure for genome-wide identification of AQPs in plant species.

Table S1 | Proteomic approaches applied to the study of plant aquaporins (AQPs).

Table S2 | Details of aquaporin tertiary structures revealed with different methods. The data were obtained by search performed with Protein Data Bank (<http://www.rcsb.org/pdb/home/home.do>) on August 1st 2016.

Table S3 | Online tools and servers available for the prediction of tertiary structures of transmembrane proteins including aquaporins.

Table S4 | List of selected studies describing the effect of heterologous expression of aquaporins in plants.

REFERENCES

- Agre, P. (2004). Aquaporin water channels (Nobel lecture). *Angew. Chem. Int. Ed. Engl.* 43, 4278–4290. doi: 10.1002/anie.200460804
- Aharon, R., Shahak, Y., Wininger, S., Bendov, R., Kapulnik, Y., and Galili, G. (2003). Overexpression of a plasma membrane aquaporin in transgenic tobacco improves plant vigor under favorable growth conditions but not under drought or salt stress. *Plant Cell* 15, 439–447. doi: 10.1105/tpc.009225
- Anderberg, H. I., Kjellbom, P., and Johanson, U. (2014). Annotation of Selaginella moellendorffii major intrinsic proteins and the evolution of the protein family in terrestrial plants. Evolution of transporters in plants *Front. Plant Sci.* 3:33. doi: 10.3389/fpls.2012.00033
- Ariani, A., and Gepts, P. (2015). Genome-wide identification and characterization of aquaporin gene family in common bean (*Phaseolus vulgaris* L.). *Mol. Genet. Genomics* 290, 1771–1785. doi: 10.1007/s00438-015-1038-2
- Benga, G. (2012). On the definition, nomenclature and classification of water channel proteins (aquaporins and relatives). *Mol. Aspects Med.* 33, 514–517. doi: 10.1016/j.mam.2012.04.003
- Benga, G. (2013). Comparative studies of water permeability of red blood cells from humans and over 30 animal species: an overview of 20 years of collaboration with Philip Kuchel. *Eur. Biophys. J.* 42, 33–46. doi: 10.1007/s00249-012-0868-7
- Benga, G., Popescu, O., Borza, V., Pop, V. I., Muresan, A., Mocsy, I., et al. (1986a). Water permeability in human erythrocytes: identification of membrane proteins involved in water transport. *Eur. J. Cell Biol.* 41, 252–262.
- Benga, G., Popescu, O., Pop, V. I., and Holmes, R. P. (1986b). p-(Chloromercuri) benzenesulfonate binding by membrane proteins and the inhibition of water transport in human erythrocytes. *Biochemistry* 25, 1535–1538. doi: 10.1021/bi00355a011
- Benga, O., and Huber, V. J. (2012). Brain water channel proteins in health and disease. *Mol. Aspects Med.* 33, 562–578. doi: 10.1016/j.mam.2012.03.008
- Bertl, A., and Kaldenhoff, R. (2007). Function of a separate NH₃-pore in aquaporin TIP2; 2 from wheat. *FEBS Lett.* 581, 5413–5417. doi: 10.1016/j.febslet.2007.10.034
- Besserer, A., Burnotte, E., Bienert, G. P., Chevalier, A. S., Errachid, A., Grefen, C., et al. (2012). Selective regulation of maize plasma membrane aquaporin trafficking and activity by the SNARE SYP121. *Plant Cell* 24, 3463–3481. doi: 10.1105/tpc.112.101758
- Biela, A., Grote, K., Otto, B., Hoth, S., Hedrich, R., and Kaldenhoff, R. (1999). The Nicotiana tabacum plasma membrane aquaporin NtAQP1 is mercury-insensitive and permeable for glycerol. *Plant J.* 18, 565–570. doi: 10.1046/j.1365-313X.1999.00474.x
- Bienert, G. P., Bienert, M. D., Jahn, T. P., Boutry, M., and Chaumont, F. (2011). Solanaceae XIPs are plasma membrane aquaporins that facilitate the transport of many uncharged substrates. *Plant J.* 66, 306–317. doi: 10.1111/j.1365-313X.2011.04496.x
- Bienert, G. P., Heinen, R. B., Berny, M. C., and Chaumont, F. (2014). Maize plasma membrane aquaporin ZmPIP2; 5, but not ZmPIP1; 2, facilitates transmembrane diffusion of hydrogen peroxide. *Biochim. Biophys. Acta* 1838, 216–222. doi: 10.1016/j.bbamem.2013.08.011
- Bienert, G. P., Møller, A. L., Kristiansen, K. A., Schulz, A., Møller, I. M., Schjoerring, J. K., et al. (2007). Specific aquaporins facilitate the diffusion of hydrogen peroxide across membranes. *J. Biol. Chem.* 282, 1183–1192. doi: 10.1074/jbc.M603761200
- Bienert, G. P., Thorsen, M., Schüssler, M. D., Nilsson, H. R., Wagner, A., Tamás, M. J., et al. (2008). A subgroup of plant aquaporins facilitate the bi-directional diffusion of As(OH)₃ and Sb(OH)₃ across membranes. *BMC Biol.* 6:26. doi: 10.1186/1741-7007-6-26
- Bousser, A., Sisoëff, I., Roche, O., Hoarau, J., and Mahé, A. (2003). Cloning and characterization of ZmPIP1-5b, an aquaporin transporting water and urea. *Plant Sci.* 165, 21–31. doi: 10.1016/S0168-9452(03)00117-1
- Burgess, D. J. (2016). Gene expression: a space for transcriptomics. *Nat. Rev. Genet.* 17, 436–437. doi: 10.1038/nrg.2016.94
- Carpentier, G. A., Garneau, A. P., Marcoux, A.-A., Noël, M., Frenette-Cotton, R., and Isenring, P. (2016). Identification of key residues involved in Si transport by the aquaglyceroporins. *J. Gen. Physiol.* 148, 239–251. doi: 10.1085/jgp.201611598
- Chaumont, F., Barrieu, F., Jung, R., and Chrispeels, M. J. (2000). Plasma membrane intrinsic proteins from maize cluster in two sequence subgroups with differential aquaporin activity. *Plant Physiol.* 122, 1025–1034. doi: 10.1104/pp.122.4.1025
- Chen, W., Yao, Q., Patil, G. B., Agarwal, G., Deshmukh, R. K., Lin, L., et al. (2016). Identification and comparative analysis of differential gene expression in soybean leaf tissue under drought and flooding stress revealed by RNA-Seq. *Front. Plant Sci.* 7:1044. doi: 10.3389/fpls.2016.01044
- Chevalier, A. S., Bienert, G. P., and Chaumont, F. (2014). A new LxxxA motif in the transmembrane Helix3 of maize aquaporins belonging to the plasma membrane intrinsic protein PIP2 group is required for their trafficking to the plasma membrane. *Plant Physiol.* 166, 125–138. doi: 10.1104/pp.114.240945
- Chiba, Y., Mitani, N., Yamaji, N., and Ma, J. F. (2009). HvLs1 is a silicon influx transporter in barley. *Plant J.* 57, 810–818. doi: 10.1111/j.1365-313X.2008.03728.x
- Daniels, M. J., Chrispeels, M. J., and Yeager, M. (1999). Projection structure of a plant vacuole membrane aquaporin by electron cryo-crystallography. *J. Mol. Biol.* 294, 1337–1349. doi: 10.1006/jmbi.1999.3293
- Danielson, J. A., and Johanson, U. (2008). Unexpected complexity of the aquaporin gene family in the moss *Physcomitrella patens*. *BMC Plant Biol.* 8:45. doi: 10.1186/1471-2229-8-45
- Dean, R. M., Rivers, R. L., Zeidel, M. L., and Roberts, D. M. (1999). Purification and functional reconstitution of soybean nodulin 26. An aquaporin with water and glycerol transport properties. *Biochemistry* 38, 347–353. doi: 10.1021/bi982110c
- Deokar, A., and Tar'an, B. (2016). Genome-wide analysis of the aquaporin gene family in chickpea (*Cicer arietinum* L.). *Front. Plant Sci.* 7:1802. doi: 10.3389/fpls.2016.01802
- Deshmukh, R., and Bélanger, R. R. (2016). Molecular evolution of aquaporins and silicon influx in plants. *Funct. Ecol.* 30, 1277–1285. doi: 10.1111/1365-2435.12570
- Deshmukh, R., Sonah, H., Patil, G., Chen, W., Prince, S., Mutava, R., et al. (2014). Integrating omic approaches for abiotic stress tolerance in soybean. *Front. Plant Sci.* 5:244. doi: 10.3389/fpls.2014.00244
- Deshmukh, R. K., Vivancos, J., Guérin, V., Sonah, H., Labbé, C., Belzile, F., et al. (2013). Identification and functional characterization of silicon transporters in soybean using comparative genomics of major intrinsic proteins in *Arabidopsis* and rice. *Plant Mol. Biol.* 83, 303–315. doi: 10.1007/s11103-013-0087-3
- Deshmukh, R. K., Vivancos, J., Ramakrishnan, G., Guérin, V., Carpentier, G., Sonah, H., et al. (2015). A precise spacing between the NPA domains of aquaporins is essential for silicon permeability in plants. *Plant J.* 83, 489–500. doi: 10.1111/tpj.12904
- Di Giorgio, J. A., Bienert, G. P., Ayub, N. D., Yaneff, A., Barberini, M. L., Mecchia, M. A., et al. (2016). Pollen-specific aquaporins NIP4; 1 and NIP4; 2 are required for pollen development and pollination in *Arabidopsis thaliana*. *Plant Cell* 28, 1053–1077. doi: 10.1105/tpc.15.00776
- di Pietro, M., Vialaret, J., Li, G.-W., Hem, S., Prado, K., Rossignol, M., et al. (2013). Coordinated post-translational responses of aquaporins to abiotic and nutritional stimuli in *Arabidopsis* roots. *Molecular & Cellular Proteomics* 12, 3886–3897. doi: 10.1074/mcp.M113.028241
- Dordas, C., Chrispeels, M. J., and Brown, P. H. (2000). Permeability and channel-mediated transport of boric acid across membrane vesicles isolated from squash roots. *Plant physiology* 124, 1349–1362. doi: 10.1104/pp.124.3.1349
- Feng, H., Xia, X., Fan, X., Xu, G., and Miller, A. J. (2013). Optimizing plant transporter expression in *Xenopus* oocytes. *Plant Methods* 9:48. doi: 10.1186/1746-4811-9-48
- Giovannetti, M., Balestrini, R., Volpe, V., Guether, M., Straub, D., Costa, A., et al. (2012). Two putative-aquaporin genes are differentially expressed during arbuscular mycorrhizal symbiosis in *Lotus japonicus*. *BMC Plant Biol.* 12:186. doi: 10.1186/1471-2229-12-186
- Grégoire, C., Rémy-Borel, W., Vivancos, J., Labbé, C., Belzile, F., and Bélanger, R. R. (2012). Discovery of a multigene family of aquaporin silicon transporters in the primitive plant *Equisetum arvense*. *Plant J.* 72, 320–330. doi: 10.1111/j.1365-313X.2012.05082.x
- Gupta, A. B., and Sankararamakrishnan, R. (2009). Genome-wide analysis of major intrinsic proteins in the tree plant *Populus trichocarpa*: characterization of XIP subfamily of aquaporins from evolutionary perspective. *BMC Plant Biol.* 9:134. doi: 10.1186/1471-2229-9-134

- He, Z., Yan, H., Chen, Y., Shen, H., Xu, W., Zhang, H., et al. (2016). An aquaporin PvTIP4; 1 from *Pteris vittata* may mediate arsenite uptake. *New Phytol.* 209, 746–761. doi: 10.1111/nph.13637
- Heckwolf, M., Pater, D., Hanson, D. T., and Kaldenhoff, R. (2011). The *Arabidopsis thaliana* aquaporin AtPIP1; 2 is a physiologically relevant CO₂ transport facilitator. *Plant J.* 67, 795–804. doi: 10.1111/j.1365-313X.2011.04634.x
- Higuchi, T., Suga, S., Tsuchiya, T., Hisada, H., Morishima, S., Okada, Y., et al. (1998). Molecular cloning, water channel activity and tissue specific expression of two isoforms of radish vacuolar aquaporin1. *Plant Cell Physiol.* 39, 905–913. doi: 10.1093/oxfordjournals.pcp.a029453
- Hove, R. M., Zieman, M., and Bhave, M. (2015). Identification and expression analysis of the barley (*Hordeum vulgare* L.) aquaporin gene family. *PLoS ONE* 10:e0128025. doi: 10.1371/journal.pone.0128025
- Hu, W., Hou, X., Huang, C., Yan, Y., Tie, W., Ding, Z., et al. (2015). Genome-wide identification and expression analyses of aquaporin gene family during development and abiotic stress in banana. *Int. J. Mol. Sci.* 16, 19728–19751. doi: 10.3390/ijms160819728
- Huang, S., Li, R., Zhang, Z., Li, L., Gu, X., Fan, W., et al. (2009). The genome of the cucumber, *Cucumis sativus* L. *Nat. Genet.* 41, 1275–1281. doi: 10.1038/ng.475
- Isayenkova, S. V., and Maathuis, F. J. (2008). The *Arabidopsis thaliana* aquaglyceroporin AtNIP7; 1 is a pathway for arsenite uptake. *FEBS Lett.* 582, 1625–1628. doi: 10.1016/j.febslet.2008.04.022
- Ishikawa, F., Suga, S., Uemura, T., Sato, M. H., and Maeshima, M. (2005). Novel type aquaporin SIPs are mainly localized to the ER membrane and show cell-specific expression in *Arabidopsis thaliana*. *FEBS Lett.* 579, 5814–5820. doi: 10.1016/j.febslet.2005.09.076
- Jang, J. Y., Lee, S. H., Rhee, J. Y., Chung, G. C., Ahn, S. J., and Kang, H. (2007). Transgenic *Arabidopsis* and tobacco plants overexpressing an aquaporin respond differently to various abiotic stresses. *Plant Mol. Biol.* 64, 621–632. doi: 10.1007/s11103-007-9181-8
- Johansson, I., Karlsson, M., Shukla, V. K., Chrispeels, M. J., Larsson, C., and Kjellbom, P. (1998). Water transport activity of the plasma membrane aquaporin PM28A is regulated by phosphorylation. *Plant Cell* 10, 451–459. doi: 10.1105/tpc.10.3.451
- Jung, J. S., Preston, G. M., Smith, B. L., Guggino, W. B., and Agre, P. (1994). Molecular structure of the water channel through aquaporin CHIP. The hourglass model. *J. Biol. Chem.* 269, 14648–14654.
- Katsuhara, M., and Hanba, Y. T. (2008). Barley plasma membrane intrinsic proteins (PIP aquaporins) as water and CO₂ transporters. *Pflügers Arch.* 456, 687–691. doi: 10.1007/s00424-007-0434-9
- Katsuhara, M., Sasano, S., Horie, T., Matsumoto, T., Rhee, J., and Shibasaki, M. (2014). Functional and molecular characteristics of rice and barley NIP aquaporins transporting water, hydrogen peroxide and arsenite. *Plant Biotechnol.* 31, 213–219. doi: 10.5511/plantbiotechnology.14.0421a
- Kirsch, A., Kaptan, S. S., Bienert, G. P., Chaumont, F., Nissen, P., de Groot, B. L., et al. (2016). Crystal structure of an ammonia-permeable aquaporin. *PLoS Biol.* 14:e1002411. doi: 10.1371/journal.pbio.1002411
- Kitchen, P., Day, R. E., Salman, M. M., Conner, M. T., Bill, R. M., and Conner, A. C. (2015). Beyond water homeostasis: diverse functional roles of mammalian aquaporins. *Biochim. Biophys. Acta* 1850, 2410–2421. doi: 10.1016/j.bbagen.2015.08.023
- Koonin, E. V., Wolf, Y. I., and Kirev, G. P. (2002). The structure of the protein universe and genome evolution. *Nature* 420, 218–223. doi: 10.1038/nature01256
- Lindahl, E., and Sansom, M. S. (2008). Membrane proteins: molecular dynamics simulations. *Curr. Opin. Struct. Biol.* 18, 425–431. doi: 10.1016/j.sbi.2008.02.003
- Liu, C., Fukumoto, T., Matsumoto, T., Gena, P., Frascaria, D., Kaneko, T., et al. (2013). Aquaporin OsPIP1; 1 promotes rice salt resistance and seed germination. *Plant Physiol. Biochem.* 63, 151–158. doi: 10.1016/j.plaphy.2012.11.018
- Loqué, D., Ludewig, U., Yuan, L., and von Wirén, N. (2005). Tonoplast intrinsic proteins AtTIP2; 1 and AtTIP2; 3 facilitate NH₃ transport into the vacuole. *Plant Physiol.* 137, 671–680. doi: 10.1104/pp.104.051268
- Ma, J. F., Tamai, K., Yamaji, N., Mitani, N., Konishi, S., Katsuhara, M., et al. (2006). A silicon transporter in rice. *Nature* 440, 688–691. doi: 10.1038/nature04590
- Ma, J. F., Yamaji, N., Mitani, N., Tamai, K., Konishi, S., Fujiwara, T., et al. (2007). An efflux transporter of silicon in rice. *Nature* 448, 209–212. doi: 10.1038/nature05964
- Ma, X., Shatil-Cohen, A., Ben-Dor, S., Wigoda, N., Perera, I. Y., Im, Y. J., et al. (2015). Do phosphoinositides regulate membrane water permeability of tobacco protoplasts by enhancing the aquaporin pathway? *Planta* 241, 741–755. doi: 10.1007/s00425-014-2216-x
- Maurel, C., Boursiac, Y., Luu, D.-T., Santoni, V., Shahzad, Z., and Verdoucq, L. (2015). Aquaporins in plants. *Physiol. Rev.* 95, 1321–1358. doi: 10.1152/physrev.00008.2015
- Mirzaei, M., Pascoiu, D., Atwell, B. J., and Haynes, P. A. (2012). Differential regulation of aquaporins, small GTPases and V-ATPases proteins in rice leaves subjected to drought stress and recovery. *Proteomics* 12, 864–877. doi: 10.1002/pmic.201100389
- Movahedi, S., Van Bel, M., Heyndrickx, K. S., and Vandepoele, K. (2012). Comparative co-expression analysis in plant biology. *Plant Cell Environ.* 35, 1787–1798. doi: 10.1111/j.1365-3040.2012.02517.x
- Murata, K., Mitsuoka, K., Hirai, T., Walz, T., Agre, P., Heymann, J. B., et al. (2000). Structural determinants of water permeation through aquaporin-1. *Nature* 407, 599–605. doi: 10.1038/35036519
- Navarro-Ródenas, A., Bárcana, G., Nicolás, E., Carra, A., Schubert, A., and Morte, A. (2013). Expression analysis of aquaporins from desert truffle mycorrhizal symbiosis reveals a fine-tuned regulation under drought. *Mol. Plant-Microbe Interact.* 26, 1068–1078. doi: 10.1094/MPMI-07-12-0178-R
- Negishi, T., Oshima, K., Hattori, M., Kanai, M., Mano, S., Nishimura, M., et al. (2012). Tonoplast-and plasma membrane-localized aquaporin-family transporters in blue hydrangea sepals of aluminum hyperaccumulating plant. *PLoS ONE* 7:e43189. doi: 10.1371/journal.pone.0043189
- Palmgren, M. G., Askerlund, P., Fredrikson, K., Widell, S., Sommarin, M., and Larsson, C. (1990). Sealed inside-out and right-side-out plasma membrane vesicles optimal conditions for formation and separation. *Plant Physiol.* 92, 871–880. doi: 10.1104/pp.92.4.871
- Papadopoulos, M. C., and Verkman, A. S. (2013). Aquaporin water channels in the nervous system. *Nat. Rev. Neurosci.* 14, 265–277. doi: 10.1038/nrn3468
- Patil, G., Valliyodan, B., Deshmukh, R., Prince, S., Nicander, B., Zhao, M., et al. (2015). Soybean (*Glycine max*) SWEET gene family: insights through comparative genomics, transcriptome profiling and whole genome re-sequence analysis. *BMC Genomics* 16:520. doi: 10.1186/s12864-015-1730-y
- Peng, Y., Arora, R., Li, G., Wang, X., and Fessehaie, A. (2008). *Rhododendron catawbiense* plasma membrane intrinsic proteins are aquaporins, and their over-expression compromises constitutive freezing tolerance and cold acclimation ability of transgenic *Arabidopsis* plants. *Plant Cell Environ.* 31, 1275–1289. doi: 10.1111/j.1365-3040.2008.01840.x
- Peng, Y., Lin, W., Cai, W., and Arora, R. (2007). Overexpression of a Panax ginseng tonoplast aquaporin alters salt tolerance, drought tolerance and cold acclimation ability in transgenic *Arabidopsis* plants. *Planta* 226, 729–740. doi: 10.1007/s00425-007-0520-4
- Preston, G. M., Carroll, T. P., Guggino, W. B., and Agre, P. (1992). Appearance of water channels in *Xenopus* oocytes expressing red cell CHIP28 protein. *Science* 256:385. doi: 10.1126/science.256.5055.385
- Preston, G. M., Jung, J. S., Guggino, W. B., and Agre, P. (1994). Membrane topology of aquaporin CHIP. Analysis of functional epitope-scanning mutants by vectorial proteolysis. *J. Biol. Chem.* 269, 1668–1673.
- Quigley, F., Rosenberg, J. M., Shachar-Hill, Y., and Bohnert, H. J. (2001). From genome to function: the *Arabidopsis* aquaporins. *Genome Biol.* 3:research0001.0001–0001.0017. doi: 10.1186/gb-2001-3-1-research0001
- Reuscher, S., Akiyama, M., Mori, C., Aoki, K., Shibata, D., and Shiratake, K. (2013). Genome-wide identification and expression analysis of aquaporins in tomato. *PLoS ONE* 8:e79052. doi: 10.1371/journal.pone.0079052
- Sabir, F., Leandro, M. J., Martins, A. P., Loureiro-Dias, M. C., Moura, T. F., Soveral, G., et al. (2014). Exploring three PIPs and three TIPs of grapevine for transport of water and atypical substrates through heterologous expression in aqy-null yeast. *PLoS ONE* 9:e102087. doi: 10.1371/journal.pone.0102087
- Sade, N., Vinocur, B. J., Diber, A., Shatil, A., Ronen, G., Nissan, H., et al. (2009). Improving plant stress tolerance and yield production: is the tonoplast aquaporin SITIP2; 2 a key to isohydric to anisohydric conversion? *New Phytol.* 181, 651–661. doi: 10.1111/j.1469-8137.2008.02689.x
- Sakr, S., Alves, G., Morillon, R., Maurel, K., Decourteix, M., Guillot, A., et al. (2003). Plasma membrane aquaporins are involved in winter embolism recovery in walnut tree. *Plant Physiol.* 133, 630–641. doi: 10.1104/pp.103.02779

- Sakurai, G., Satake, A., Yamaji, N., Mitani-Ueno, N., Yokozawa, M., Feugier, F. G., et al. (2015). *In silico* simulation modeling reveals the importance of the Casparyan strip for efficient silicon uptake in rice roots. *Plant Cell Physiol.* 56, 631–639. doi: 10.1093/pcp/pcv017
- Sakurai, J., Ishikawa, F., Yamaguchi, T., Uemura, M., and Maeshima, M. (2005). Identification of 33 rice aquaporin genes and analysis of their expression and function. *Plant Cell Physiol.* 46, 1568–1577. doi: 10.1093/pcp/pci172
- Santoni, V., Vinh, J., Pfleiderer, D., Sommerer, N., and Maurel, C. (2003). A proteomic study reveals novel insights into the diversity of aquaporin forms expressed in the plasma membrane of plant roots. *Biochem. J.* 373, 289–296. doi: 10.1042/bj20030159
- Schey, K. L., Papac, D. I., Knapp, D. R., and Crouch, R. K. (1992). Matrix-assisted laser desorption mass spectrometry of rhodopsin and bacteriorhodopsin. *Biophys. J.* 63:1240. doi: 10.1016/s0006-3495(92)81699-5
- Schindler, P. A., Van Dorsselaer, A., and Falick, A. M. (1993). Analysis of hydrophobic proteins and peptides by electrospray ionization mass spectrometry. *Anal. Biochem.* 213, 256–263. doi: 10.1006/abio.1993.1418
- Schnurbusch, T., Hayes, J., Hrmova, M., Baumann, U., Ramesh, S. A., Tyerman, S. D., et al. (2010). Boron toxicity tolerance in barley through reduced expression of the multifunctional aquaporin HvNIP2; 1. *Plant Physiol.* 153, 1706–1715. doi: 10.1104/pp.110.158832
- Schulze, A., and Downward, J. (2001). Navigating gene expression using microarrays—a technology review. *Nat. Cell Biol.* 3, E190–E195. doi: 10.1038/35087138
- Secchi, F., Lovisolo, C., Uehlein, N., Kaldenhoff, R., and Schubert, A. (2007). Isolation and functional characterization of three aquaporins from olive (*Olea europaea* L.). *Planta* 225, 381–392. doi: 10.1007/s00425-006-0365-2
- Shen, J., Fu, J., Ma, J., Wang, X., Gao, C., Zhuang, C., et al. (2014). Isolation, culture, and transient transformation of plant protoplasts. *Curr. Protoc. Cell Biol.* 63, 2.8.1–2.8.17 doi: 10.1002/0471143030.cb0208s63
- Sonah, H., Chavan, S., Katara, J., Chaudhary, J., Kadam, S., Patil, G., et al. (2016). Genome-wide identification and characterization of Xylanase Inhibitor Protein (XIP) genes in cereals. *Indian J. Genet. Plant Breed.* 76, 159–166. doi: 10.5958/0975-6906.2016.000365
- Song, L., Nguyen, N., Deshmukh, R. K., Patil, G. B., Prince, S. J., Valliyodan, B., et al. (2016). Soybean TIP gene family analysis and characterization of GmTIP1; 5 and GmTIP2; 5 in water transport. *Front. Plant Sci.* 7:1564. doi: 10.3389/fpls.2016.01564
- Srivastava, A. K., Penna, S., Nguyen, D. V., and Tran, L.-S. (2016). Multifaceted roles of aquaporins as molecular conduits in plant responses to abiotic stresses. *Crit. Rev. Biotechnol.* 36, 389–398. doi: 10.3109/07388551.2014.973367
- Suga, S., and Maeshima, M. (2004). Water channel activity of radish plasma membrane aquaporins heterologously expressed in yeast and their modification by site-directed mutagenesis. *Plant Cell Physiol.* 45, 823–830. doi: 10.1093/pcp/pch120
- Sun, H., Li, L., Lou, Y., Zhao, H., and Gao, Z. (2016). Genome-wide identification and characterization of aquaporin gene family in moso bamboo (*Phyllostachys edulis*). *Mol. Biol. Rep.* 43, 437–450. doi: 10.1007/s11033-016-3973-3
- Sutka, M., Alleva, K., Parisi, M., and Amodeo, G. (2005). Tonoplast vesicles of *Beta vulgaris* storage root show functional aquaporins regulated by protons. *Biol. Cell* 97, 837–846. doi: 10.1042/BC20040121
- Takano, J., Wada, M., Ludewig, U., Schaaf, G., von Wirén, N., and Fujiwara, T. (2006). The Arabidopsis major intrinsic protein NIP5; 1 is essential for efficient boron uptake and plant development under boron limitation. *Plant Cell* 18, 1498–1509. doi: 10.1105/tpc.106.041640
- Tan, S., Tan, H. T., and Chung, M. (2008). Membrane proteins and membrane proteomics. *Proteomics* 8, 3924–3932. doi: 10.1002/pmic.200800597
- Tanaka, M., Wallace, I. S., Takano, J., Roberts, D. M., and Fujiwara, T. (2008). NIP6; 1 is a boric acid channel for preferential transport of boron to growing shoot tissues in Arabidopsis. *Plant Cell* 20, 2860–2875. doi: 10.1105/tpc.108.058628
- Tanghe, A., Van Dijck, P., and Thevelein, J. M. (2006). Why do microorganisms have aquaporins? *Trends Microbiol.* 14, 78–85. doi: 10.1016/j.tim.2005.12.001
- To, J., Yeo, C. Y., Soon, C. H., and Torres, J. (2015). A generic high-throughput assay to detect aquaporin functional mutants: potential application to discovery of aquaporin inhibitors. *Biochim. Biophys. Acta* 1850, 1869–1876. doi: 10.1016/j.bbagen.2015.05.019
- Törnroth-Horsefield, S., Wang, Y., Hedfalk, K., Johanson, U., Karlsson, M., Tajkhorshid, E., et al. (2006). Structural mechanism of plant aquaporin gating. *Nature* 439, 688–694. doi: 10.1038/nature04316
- Uehlein, N., Lovisolo, C., Siefritz, F., and Kaldenhoff, R. (2003). The tobacco aquaporin NtAQP1 is a membrane CO₂ pore with physiological functions. *Nature* 425, 734–737. doi: 10.1038/nature02027
- Venkatesh, J., Yu, J.-W., and Park, S. W. (2013). Genome-wide analysis and expression profiling of the *Solanum tuberosum* aquaporins. *Plant Physiol. Biochem.* 73, 392–404. doi: 10.1016/j.plaphy.2013.10.025
- Verkman, A. (2009). Aquaporins: translating bench research to human disease. *J. Exp. Biol.* 212, 1707–1715. doi: 10.1242/jeb.024125
- Vivancos, J., Deshmukh, R., Grégoire, C., Rémy-Borel, W., Belzile, F., and Bélanger, R. R. (2016). Identification and characterization of silicon efflux transporters in horsetail (*Equisetum arvense*). *J. Plant Physiol.* 200, 82–89. doi: 10.1016/j.jplph.2016.06.011
- Vivancos, J., Labbé, C., Menzies, J. G., and Bélanger, R. R. (2015). Silicon-mediated resistance of Arabidopsis against powdery mildew involves mechanisms other than the salicylic acid (SA)-dependent defence pathway. *Mol. Plant Pathol.* 16, 572–582. doi: 10.1111/mpp.12213
- Wang, L.-L., Chen, A.-P., Zhong, N.-Q., Liu, N., Wu, X.-M., Wang, F., et al. (2014). The *Thellungiella salsuginea* tonoplast aquaporin TsTIP1; 2 functions in protection against multiple abiotic stresses. *Plant Cell Physiol.* 55, 148–161. doi: 10.1093/pcp/pct166
- Wang, L., Li, Q., Lei, Q., Feng, C., Gao, Y., Zheng, X., et al. (2015). MzPIP2; 1: an aquaporin involved in radial water movement in both water uptake and transportation, altered the drought and salt tolerance of transgenic Arabidopsis. *PLoS ONE* 10:e0142446. doi: 10.1371/journal.pone.0142446
- Werner, M., Uehlein, N., Proksch, P., and Kaldenhoff, R. (2001). Characterization of two tomato aquaporins and expression during the incompatible interaction of tomato with the plant parasite *Cuscuta reflexa*. *Planta* 213, 550–555. doi: 10.1007/s00425-001-00533
- Yaneff, A., Sigaut, L., Marquez, M., Alleva, K., Pietrasanta, L. I., and Amodeo, G. (2014). Heteromerization of PIP aquaporins affects their intrinsic permeability. *Proc. Natl. Acad. Sci. U.S.A.* 111, 231–236. doi: 10.1073/pnas.1316537111
- Yoo, S.-D., Cho, Y.-H., and Sheen, J. (2007). Arabidopsis mesophyll protoplasts: a versatile cell system for transient gene expression analysis. *Nat. Protoc.* 2, 1565–1572. doi: 10.1038/nprot.2007.199
- Zhao, F. J., Ago, Y., Mitani, N., Li, R. Y., Su, Y. H., Yamaji, N., et al. (2010). The role of the rice aquaporin Lsi1 in arsenite efflux from roots. *New Phytol.* 186, 392–399. doi: 10.1111/j.1469-8137.2010.03192.x
- Zou, Z., Gong, J., An, F., Xie, G., Wang, J., Mo, Y., et al. (2015). Genome-wide identification of rubber tree (*Hevea brasiliensis* Muell. Arg.) aquaporin genes and their response to etephon stimulation in the laticifer, a rubber-producing tissue. *BMC Genomics* 16:1001. doi: 10.1186/s12864-015-2152-6
- Zou, Z., Yang, L., Gong, J., Mo, Y., Wang, J., Cao, J., et al. (2016). Genome-wide identification of *Jatropha curcas* aquaporin genes and the comparative analysis provides insights into the gene family expansion and evolution in *Hevea brasiliensis*. *Front. Plant Sci.* 7:395. doi: 10.3389/fpls.2016.00395

Conflict of Interest Statement: The authors declare that the research was conducted in the absence of any commercial or financial relationships that could be construed as a potential conflict of interest.

Copyright © 2016 Deshmukh, Sonah and Bélanger. This is an open-access article distributed under the terms of the Creative Commons Attribution License (CC BY). The use, distribution or reproduction in other forums is permitted, provided the original author(s) or licensor are credited and that the original publication in this journal is cited, in accordance with accepted academic practice. No use, distribution or reproduction is permitted which does not comply with these terms.



Genome-Wide Analysis of the Aquaporin Gene Family in Chickpea (*Cicer arietinum* L.)

Amit A. Deokar and Bunyamin Tar'an *

Department of Plant Sciences, Crop Development Centre, University of Saskatchewan, Saskatoon, SK, Canada

OPEN ACCESS

Edited by:

Rupesh Kailasrao Deshmukh,
Laval University, Canada

Reviewed by:

Swarup Kumar Parida,
National Institute of Plant Genome
Research, India
Suhas B. Kadam,
University of Missouri, USA

*Correspondence:

Bunyamin Tar'an
bunyamin.taran@usask.ca

Specialty section:

This article was submitted to
Plant Physiology,
a section of the journal
Frontiers in Plant Science

Received: 09 August 2016

Accepted: 15 November 2016

Published: 29 November 2016

Citation:

Deokar AA and Tar'an B (2016)
Genome-Wide Analysis of the
Aquaporin Gene Family in Chickpea
(*Cicer arietinum* L.).
Front. Plant Sci. 7:1802.
doi: 10.3389/fpls.2016.01802

Aquaporins (AQPs) are essential membrane proteins that play critical role in the transport of water and many other solutes across cell membranes. In this study, a comprehensive genome-wide analysis identified 40 AQP genes in chickpea (*Cicer arietinum* L.). A complete overview of the chickpea AQP (CaAQP) gene family is presented, including their chromosomal locations, gene structure, phylogeny, gene duplication, conserved functional motifs, gene expression, and conserved promoter motifs. To understand AQP's evolution, a comparative analysis of chickpea AQPs with AQP orthologs from soybean, *Medicago*, common bean, and *Arabidopsis* was performed. The chickpea AQP genes were found on all of the chickpea chromosomes, except chromosome 7, with a maximum of six genes on chromosome 6, and a minimum of one gene on chromosome 5. Gene duplication analysis indicated that the expansion of chickpea AQP gene family might have been due to segmental and tandem duplications. CaAQPs were grouped into four subfamilies including 15 NOD26-like intrinsic proteins (NIPs), 13 tonoplast intrinsic proteins (TIPs), eight plasma membrane intrinsic proteins (PIPs), and four small basic intrinsic proteins (SIPs) based on sequence similarities and phylogenetic position. Gene structure analysis revealed a highly conserved exon-intron pattern within CaAQP subfamilies supporting the CaAQP family classification. Functional prediction based on conserved Ar/R selectivity filters, Froger's residues, and specificity-determining positions suggested wide differences in substrate specificity among the subfamilies of CaAQPs. Expression analysis of the AQP genes indicated that some of the genes are tissue-specific, whereas few other AQP genes showed differential expression in response to biotic and abiotic stresses. Promoter profiling of CaAQP genes for conserved cis-acting regulatory elements revealed enrichment of cis-elements involved in circadian control, light response, defense and stress responsiveness reflecting their varying pattern of gene expression and potential involvement in biotic and abiotic stress responses. The current study presents the first detailed genome-wide analysis of the AQP gene family in chickpea and provides valuable information for further functional analysis to infer the role of AQP in the adaptation of chickpea in diverse environmental conditions.

Keywords: chickpea (*Cicer arietinum* L.), aquaporin gene family, biotic and abiotic stress, genome-wide characterization, gene structure, phylogeny

INTRODUCTION

Chickpea (*Cicer arietinum* L.) is second most important food legume crop grown globally over 13.5 Mha with the production of 13.1 Mt in 2013 (FAOSTAT 2013; <http://faostat.fao.org/site/339/default.aspx>). The productivity of chickpea has been limited by several biotic and abiotic factors, among them drought is one of the major abiotic stress causing a significant reduction in yield in the majority of chickpea growing areas (Krishnamurthy et al., 1999). Soil salinity is another increasing abiotic stress in many of the chickpea growing areas (Flowers et al., 2010). Understanding the genetic and molecular mechanisms of tolerance to drought and salinity will help to improve the adaptation of chickpea to these adverse conditions. Both the drought and salinity stresses cause tissue dehydration instigated by the imbalance between root water uptake and leaf transpiration and modify root water uptake (Wahid and Close, 2007). Water is absorbed by plants through root hairs by apoplastic (passive absorption) and symplastic (active absorption) pathways (Suga et al., 2002; Lian et al., 2004). The later is more active under different abiotic stress conditions and mainly regulated by members of aquaporin family proteins (Amodeo et al., 1999). As a central part of water absorption and transportation, the role of aquaporin (AQP) genes in response to biotic and abiotic stresses has been reported in several plants (Jang et al., 2004; Alexandersson et al., 2005, 2010; Aroca et al., 2012; Zhou et al., 2012). Despite the importance of AQPs in regulating stress tolerance, very limited studies on understanding the role of AQPs in biotic and abiotic stresses were reported in chickpea. Differential regulation of some of the AQP genes under drought stress has been described (Molina et al., 2008; Deokar et al., 2011), suggesting the potential involvement of AQPs in drought and other osmotic related stresses in chickpea.

AQPs are water channel proteins belong to the membrane intrinsic proteins (MIPs) family that facilitate the rapid and selective transport of water and several small molecules, such as glycerol, and urea, dissolved gasses such as carbon dioxide and ammonia, and metalloids such as boron and silicon across plant cell membranes (Chaumont et al., 2001; Kaldenhoff et al., 2008; Hachez and Chaumont, 2010; Maurel et al., 2015). Apart from the water transport, AQPs are also involved in different physiological processes such as seed longevity and seed viability (Mao and Sun, 2015), sexual reproduction/anther dehiscence (Bots et al., 2005), photosynthesis, and stomatal and mesophyll conductance (Perez-Martin et al., 2014), cell elongation (Yang and Cui, 2009), and responses to diverse biotic and abiotic stress treatments (Jang et al., 2004; Peng et al., 2007; Montalvo-Hernández et al., 2008; Aroca et al., 2012; Khan et al., 2015).

Based on their subcellular localization, the AQPs genes are classified into five subfamilies including, the tonoplast intrinsic proteins (TIPs), the plasma membrane intrinsic proteins (PIPs), the nodulin-like plasma membrane intrinsic proteins (NIPs), the small intrinsic proteins (SIPs) and the uncategorized (X) intrinsic proteins (XIPs) (Maurel et al., 2015). These AQP subfamilies were found highly conserved in higher plant species; however, the XIP subfamily is absent in monocots or the Brassicaceae (Deshmukh et al., 2015). Although the AQP were initially classified and

named on the basis of their subcellular localization, recent studies demonstrated complex and highly regulated mechanism of AQP at subcellular localization, such as dual localization of ZmPIP1;2 in the PM and in the ER of root elongating cells (Chaumont et al., 2000) and salt stress condition which regulate Arabidopsis PIPs to relocated to intracellular vesicles (Boursiac et al., 2008).

The tonoplast AtTIP1;1 gene from *Arabidopsis* (*Arabidopsis thaliana*) was the first plant AQP protein characterized for water channel activity (Maurel et al., 1993). After that several plant AQP genes have been identified and characterized using *Xenopus* oocyte, yeast and/or plant protoplast swelling assays for water movement (Kaldenhoff et al., 1998; Sommer et al., 2007, 2008; Gomes et al., 2009). With the availability of whole-genome sequences for several plant species, aquaporin-related sequences were identified using genome-wide analysis. In higher plants depending on the ploidy level, AQP family constitutes from 30 to more than 70 diverse members. 35 AQP homologs from *Arabidopsis* (Johanson et al., 2001; Quigley et al., 2002), 33 from rice (Sakurai et al., 2005; Nguyen et al., 2013), 31 from maize (Chaumont et al., 2001), 37 from tomato (Reuscher et al., 2013), 41 from common bean (Ariani and Gepts, 2015), 72 from soybean (Deshmukh et al., 2013), and 71 in cotton (Park et al., 2010) have been identified. Compared to other plant species, little is known about the AQP genes in chickpea, only a few differentially expressed EST sequences encoding the AQP protein has been identified (Molina et al., 2008; Jain and Chattopadhyay, 2010; Deokar et al., 2011).

The availability of whole genome sequence of chickpea would facilitate genome-wide analysis to identify the complete set of AQPs in chickpea, and comparative analysis to understand the evolutionary relationship of chickpea's AQPs with related plant species. The present study was carried out to identify chickpea AQP genes using genome-wide analysis and to characterize their phylogeny, chromosomal distribution, and structure. Additionally, we also investigated the expression profile of AQP genes in various tissues and in response to biotic and abiotic stresses.

MATERIALS AND METHODS

Identification of Putative Aquaporin Genes in Chickpea Genome

Nucleotide and protein sequences of chickpea genome (assembly ASM33114v1) were retrieved from NCBI and (CDC Frontier genome Cav1.0) from <https://www.coolseasonfoodlegume.org/analysis/105>. Nucleotide and protein sequences of *Medicago* (*Medicago truncatula*), soybean (*Glycine max*) and common bean (*Phaseolus vulgaris* L.) were retrieved from Phytozome database (<http://genome.jgi.doe.gov/pages/dynamicOrganismDownload.jsf?organism=PhytozomeV11>). The four species were selected based on their whole-genome sequence availability, their agricultural importance, as a model legume species and representatives of phaseoloid (common bean and soybean) and galegoid (chickpea and *Medicago*) the two major clades of papilionoideae (grain legume) family. A local nucleotide and protein database of annotated chickpea genes was created

using NCBI command-line BLAST utilities in BioEdit (Version 7.0.9.0). The putative chickpea aquaporin genes were identified with BLASTp using 218 known aquaporin genes as query sequences against the chickpea local database. An e-value of 10^{-5} was used as an initial cut-off to claim significant matches. Then, the BLAST output was tabulated and top hits on the basis of bit scores were selected. BLAST hits with less than a 100 bit-score were removed.

Multiple Sequence Alignments and Phylogenetic Analysis

The predicted Chickpea AQP genes (CaAQPs) were classified into subgroups based on sequence alignment and phylogenetic relationship with clearly classified AQPs from *Arabidopsis* (Quigley et al., 2002). Multiple sequence alignments of amino acid sequences of CaAQPs and those of *Arabidopsis*, *Medicago*, soybean, and common bean were performed using CLUSTALW implemented in MEGA5 software (Tamura et al., 2011). A phylogenetic tree was then constructed using maximum likelihood (ML) method. A bootstrap analysis with 1000 reiterations was conducted to determine the statistical stability of each node. The aquaporin subgroups PIP, TIP, NIP, SIP, and XIP formed in the phylogenetic tree were classified in accordance with the nomenclature of known AQPs that were used as a query in initial BLAST search. The phylogenetic tree was visualized using iTOL (<http://itol.embl.de/help.cgi>).

Protein Characterization and Identification of NPA Motifs and Transmembrane Domains in CaAQPs

Conserved domains within the CaAQP protein sequences were identified using NCBI's Conserved Domain Database (CDD, www.ncbi.nlm.nih.gov/Structure/cdd/cdd.shtml). Transmembrane domains were detected using TMHMM 2.0 (www.cbs.dtu.dk). All results were manually examined to re-confirm the CDD results. NPA motifs, ar/R filters (H2, H5, LE1, LE2), Froger's positions (P1-P5) and specificity-determining positions (SDP1-SDP9) were predicted based on careful visual inspection of multiple sequence alignments of CaAQPs with structure resolved and functionally characterized AQPs as reported earlier (Froger et al., 1998; Wallace and Roberts, 2004; Hove and Bhave, 2011; Zhang da et al., 2013).

The Isoelectric Point (pI), molecular weight and grand average of hydrophytropy (GRAVY) of the amino acid sequences were predicted by Sequence Manipulation Suite (SMS) V2 available at geneinfinity web server (<http://www.geneinfinity.org/index.html?dp=5>). The subcellular localization of CaAQPs was predicted using WoLF PSORT a protein Subcellular Localization Prediction Tool available at <http://www.genscript.com/wolf-psort.html>.

Genomic Organization and Promoter Sequence Profiling of CaAQPs

The physical location of CaAQPs on each chickpea chromosome was detected using BLASTNT search against the local database of the CDC Frontier genome Cav1.0. Starting position of all

CaAQP genes were used as the indicative position of the genes on the chromosome or the scaffold. MapChart was used to plot the chickpea chromosomes and the respective positions of CaAQPs (Voorrips, 2002).

Intron-exon structures of all CaAQPs were retrieved from the gene annotation file (GFF) of the CDC Frontier genome Cav1.0. Intron-exon structures of the genes were visualized using GSDS 2.0 server (<http://gsds.cbi.pku.edu.cn/>).

The core promoter sequence (1 kb upstream region from the predicted transcription start site) for all CaAQPs was extracted from CDC Frontier genome Cav1.0. The PlantCARE (<http://bioinformatics.psb.ugent.be/webtools/plantcare/html/>) database of plant cis-acting regulatory elements was used to find putative cis-acting regulatory elements in the CaAQP promoter sequences.

3D Structure

The three-dimensional (3D) structure of CaAQPs were generated by intensive protein modeling using Phyre2 server (<http://www.sbg.bio.ic.ac.uk/phyre2/html/page.cgi?id=index>) using 'Normal' mode modeling based on alignment to experimentally solved protein structures. Transmembrane helix and topology of the CaAQPs were predicted by MEMSAT-SVM prediction method available in Phyre2 server.

Expression Analysis of CaAQPs

Over the past few years, the number of publicly available transcriptome (RNA-seq) datasets has greatly increased. These publicly available data sets are extremely useful for large-scale gene expression studies. RNA-seq data were downloaded from the NCBI Sequence Read Archive (SRA) database (<http://www.ncbi.nlm.nih.gov/sra/>) and used to analyze the expression pattern of the CaAQPs under different biotic and abiotic stresses. The following Sequence Read Archives were used for fusarium wilt stress (SRX535349, SRX535346, SRX535348, SRX535351, and SRX548566), root drought stress (SRX402840), shoot drought stress (SRX402844), root salinity stress (SRX402841), shoot salinity stress (SRX402845), root cold stress (SRX402842), shoot cold stress (SRX402846), root control (SRX402839) and shoot control (SRX402843). For the tissue-specific expression, RNA-seq data from various plant tissues and development stages including shoot (SRX402843), young leaves (SRX208031), apical meristem (SRX208032), flower (SRX208039, SRX208038, and SRX208037), flower bud (SRX208033, SRX208034, SRX208035, and SRX208036), young pod (SRX361953) and root (SRX402839) were used.

Gene expression of the CaAQP genes was presented as the FPKM (fragments per kilobase of transcript per million mapped reads) values. Hierarchical clustering of the CaAQP genes based on the expression data was performed using Cluster 3.0 software (<http://bonsai.hgc.jp/~mdehoon/software/cluster/software.htm>), using "correlation (uncentered)" as the distance metric and average linkage method. Clustering trees and Heatmaps was visualized using Java TreeView software (<http://jtreeview.sourceforge.net/>).

RESULTS AND DISCUSSION

Aquaporin Gene Family in Chickpea

Whole-genome sequence availability of Kabuli cultivar CDC Frontier (Varshney et al., 2013) provided an opportunity to identify and analyse AQP genes in chickpea. We identified a total of 40 putative aquaporin encoding genes chickpea genome, namely, thereafter, as CaAQPs (**Table 1** and **Supplementary File S1**). The number of AQP identified in this study are slightly higher than the 35 AQP genes reported in Arabidopsis (Johanson et al., 2001), 33 in rice (Sakurai et al., 2005), 35 in Medicago and 30 in lotus genome, then again almost same in number as reported 41 AQP genes in potato (Venkatesh et al., 2013), Sorghum (Reddy et al., 2015), common bean (Ariani and Gepts, 2015), and 40 AQP genes in Pigeonpea (Deshmukh et al., 2015).

A strong correlation between phylogenetic analysis with the gene function has been observed in AQPs (Soto et al., 2012; Perez Di Giorgio et al., 2014), indicating that the amino acid based phylogenetic analysis can be used to predict a putative function of the identified CaAQPs. To investigate the phylogenetic relationships and to predict the functionality of the CaAQPs, we constructed a phylogenetic tree of 223 protein sequences of aquaporin genes from four legumes including Medicago (35), common bean (41), soybean (72), chickpea (40), and 35 sequences from Arabidopsis (**Figure 1**). In accordance with the AQP gene classification in Arabidopsis, the phylogenetic tree was subdivided into five clades with well-supported bootstrap values, representing five distinct AQPs subfamilies. The chickpea AQPs identified in the present study were named according to nomenclature proposed in gene classification of Arabidopsis AQP genes as genus (one letter), species (one letter) i.e., Ca (*Cicer arietinum* L.), gene name (three letter code for AQP subfamily; e.g., PIP) (**Table 1**). All groups contain CaAQP genes, except the XIP group. The XIP group contains two genes from soybean and common bean. In addition to these two members of phaseoloid clade of Papilionoideae family, XIPs have been also reported in other phaseoloids such as pigeon pea (*Cajanus cajan*) (Deshmukh and Bélanger, 2016). However, the XIPs were completely missing or have not yet been reported in species from a galegoid clade of papilionoideae family such as Medicago and *Lotus japonicus* (Deshmukh and Bélanger, 2016). This observation suggests the possibility that the XIPs genes were mainly observed in phaseoloids clade (warm season legumes) and lost from the galegoid species (cool-season legumes) during the evolution of the papilionoideae family. Compared to the 40 CaAQPs, its legume counterparts Medicago, common bean, and soybean have 35, 41, and 72 AQP genes, respectively (**Supplementary File S2**). Multiple copies of AQP genes in soybean could be due to whole-genome duplication (WGD) event occurred twice at approximately 59 and 13 million years ago (mya) (Schmutz et al., 2010). Whole-genome sequence analysis of chickpea also observed a historical genome duplication after the divergence of legumes from Arabidopsis and grape (Varshney et al., 2013). The soybean whole-genome duplication events also occurred in the same period. The observed CaAQPs (40) number is within the range of Medicago,

common bean, and Arabidopsis, but fewer than that of soybean. This could be due to the combination of gene loss and duplication events occurred during chickpea genome evolution.

The CaAQPs were classified in four different subfamilies, PIPs (9 members), TIPs (12), NIPs (16 members), and SIPs (3 members). Further, the subfamilies were sub-grouped based on the analysis of the aromatic/arginine (Ar/R) selective filters and phylogenetic positioning that corroborate each other very well. The CaPIP subfamily was grouped in two subgroups CaPIP1 and CaPIP2 with four and five members in each group, respectively. Similarly, the CaSIP subfamily was also grouped in two subgroups CaSIP1 and CaSIP2 with two and one members in each group, respectively. The CaTIP subfamily was clustered in five subgroups (CaTIPs1-5). The largest subfamily CaNIPs consisted of six subgroups (CaNIPs1-6), with a maximum of nine members in CaNIP1 subgroups (**Figure 2A** and **Table 1**). Among the CaAQPs, CaNIPs were the most diverse subfamily with 47.5% sequence similarity, whereas CaPIPs were the most conserved subfamily with 76.1% sequence similarity at the amino acid level (**Supplementary Table 1**).

Plant AQPs have been shown to have different biochemical properties associated with the function characteristics (Johanson and Gustavsson, 2002; Hove and Bhave, 2011). In order to analyse biochemical properties of the identified genes, we predicted molecular weight, protein Isoelectric Point (pI) and predicted subcellular localization of the CaAQPs. The identified CaAQPs encodes protein ranging from 251 to 335 (average 261) amino acids in length, a molecular weight ranging from 21.8 to 36.2 (average 27.9) kD and a pI value ranging from 4.8 to 9.43 (average 7.4) (**Table 1**). Among the CaAQP subfamilies, the average pI value of CaTIPs (pH 6.0) is less (i.e., more acidic) than the TIPs (pH 8.5) i.e., more basic (**Table 1**). The difference is mainly due to the presence or absence of basic residues in the C-terminal domains of AQP proteins as also observed in Arabidopsis and sweet orange AQPs (Johansson et al., 2000; Martins Cde et al., 2015). A positive grand average of hydropathy (GRAVY) scores of all the identified CaAQP proteins indicated the hydrophobic nature of the CaAQP proteins, which is a key property of aquaporins which facilitates the high water permeability (Murata et al., 2000). Further, among the CaAQPs subfamilies, the PIPs have the lowest average of GRAVY value (0.43) indicating better interaction of CaTIPs with water molecules.

The analysis of the predicted subcellular localization of the CaAQPs showed that all CaPIPs, except CaPIP2-5, are located at the plasma membrane. The CaPIP2-5 has been predicted to localize at cytosol (**Table 1**). Similarly, 12 out of 16 CaNIPs were also predicted to be localized to the plasma membrane. It has been shown that the majority of plants PIPs and some NIPs were preferentially localized at the plasma membrane (Maurel et al., 2008; Xu et al., 2014), however, this is not a general feature of TIPs or PIPs. Some of the Tobacco NtAQP1, a member of PIP group was found in the inner chloroplast membrane and plasma membrane (Uehlein et al., 2008). Similarly, dual localizations of maize PIP gene (ZmPIP1;2) in the plasma membrane and endoplasmic reticulum (ER) have also been observed (Chaumont et al., 2000). The seed specific isoforms of Arabidopsis TIP genes (AtTIP3;1 and AtTIP3;2) were also

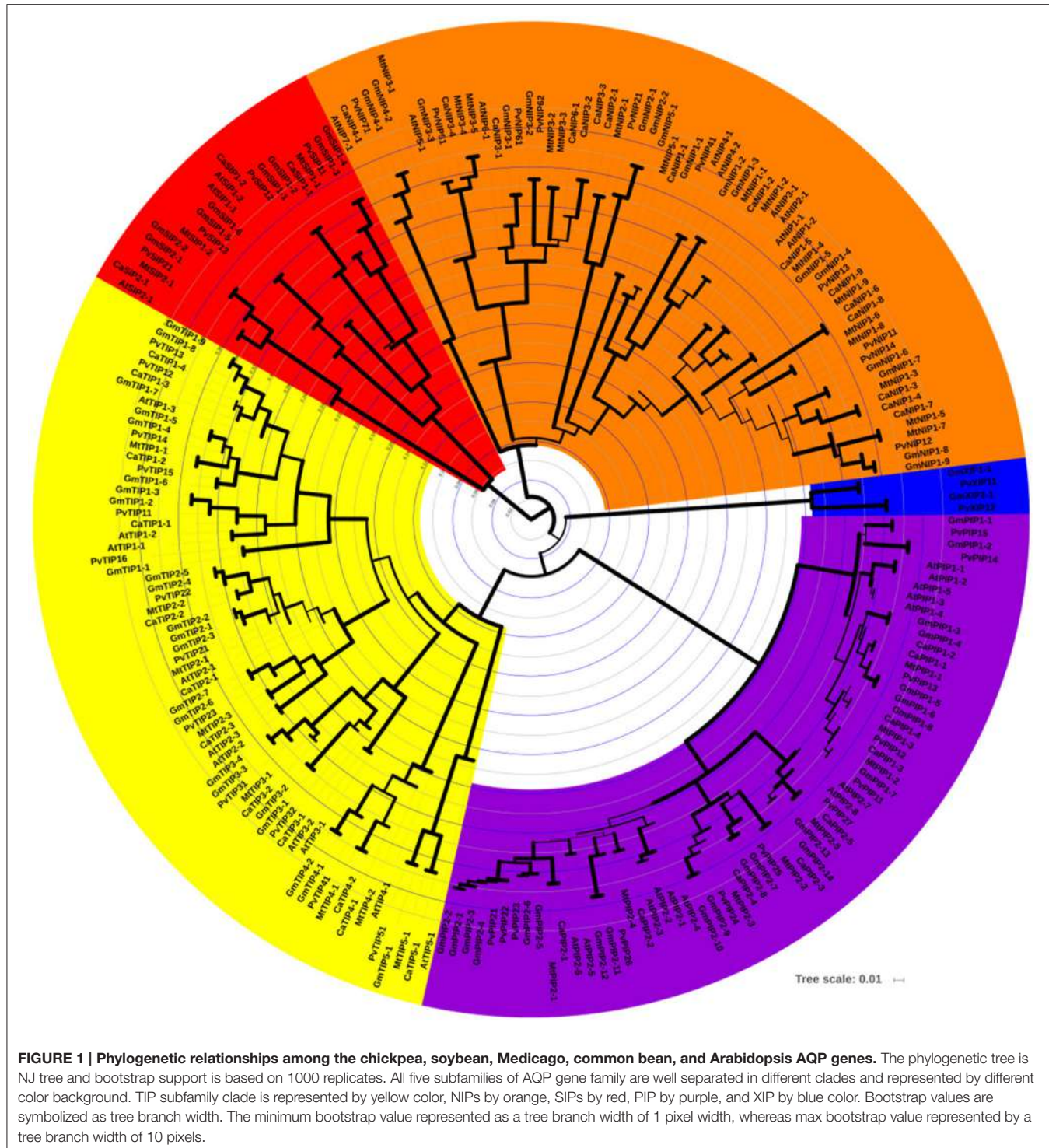
TABLE 1 | Nomenclature and protein properties of chickpea aquaporins.

AQP sub-family	Proposed gene name	Locus ^a	Chromosome location ^a	Protein Isoelectric Point	Protein Molecular Weight (kD)	GRAVY ^b	Predicted subcellular location ^c
PIP	CaPIP1-1	Ca_02435	Ca8:1717936-1719735	9.1	30.75	0.396	plas
	CaPIP1-2	Ca_05754	Ca6:5464092-5465462	9	30.81	0.427	plas
	CaPIP1-3	Ca_10319	Ca6:1932039-1933176	8.68	30.92	0.398	plas
	CaPIP1-4	Ca_12502	Ca2:30479427-30481282	8.7	31.06	0.393	plas
	CaPIP2-5	Ca_04707	Ca5:30303896-30304911	9.14	30.21	0.49	cyto
	CaPIP2-1	Ca_08491	Ca4:10225765-10228793	8.34	30.52	0.588	plas
	CaPIP2-2	Ca_12039	Ca3:32991462-32992568	9.11	30.8	0.406	plas
	CaPIP2-3	Ca_14568	Ca6:27966413-27967838	6.71	30.58	0.375	plas
	CaPIP2-4	Ca_02533	Ca1:12226605-12227713	7.81	30.87	0.382	plas
TIP	CaTIP1-1	Ca_00723	Ca3:34451205-34452295	6.02	25.47	0.88	vacu
	CaTIP1-2	Ca_16712	Ca6:26818668-26820154	5.43	25.82	0.847	vacu
	CaTIP1-3	Ca_18630	Ca4:17906721-17908388	5.61	26.01	0.78	plas
	CaTIP1-4	Ca_19377	Ca3:11393179-11394299	4.94	25.79	0.744	cyto
	CaTIP2-1	Ca_02797	Ca1:9896268-9897261	6.29	25.42	0.745	nucl
	CaTIP2-2	Ca_24137	scaffold1844:60282-61675	5.3	25.32	0.873	vacu
	CaTIP2-3	Ca_02338	Ca8:2481906-2483425	4.8	25.22	0.947	vacu
	CaTIP3-1	Ca_03854	Ca4:3990175-3991038	7.31	27.59	0.565	cyto
	CaTIP3-2	Ca_19737	Ca8:10865608-10867961	6.36	26.92	0.671	mito
	CaTIP4-1	Ca_14915	Ca4:39954258-39957667	7.92	23.85	0.893	cyto
	CaTIP4-2	Ca_14916	Ca4:39950985-39952627	5.51	25.87	0.777	vacu
	CaTIP5-1	Ca_15805	Ca6:34791986-34793660	7.08	26.49	0.731	vacu
NIP	CaNIP1-1	Ca_06493	Ca6:18836478-18837512	5.15	26.59	0.732	plas
	CaNIP1-2	Ca_16129	Ca2:29576437-29578961	7.06	28.53	0.632	plas
	CaNIP1-3	Ca_08631	Ca6:9654827-9656732	8	28.67	0.522	vacu
	CaNIP1-4	Ca_08632	Ca6:9651625-9653530	8	28.67	0.522	vacu
	CaNIP1-5	Ca_08630	Ca6:9661095-9662900	9.15	29.44	0.504	cyto
	CaNIP1-6	Ca_00434	Ca1:3567423-3568768	6.46	27.09	0.761	plas
	CaNIP1-7	Ca_00435	Ca1:3574718-3576622	8.98	29.17	0.421	plas
	CaNIP1-8	Ca_00436	Ca1:3579756-3581062	5.73	25.65	0.822	plas
	CaNIP1-9	Ca_00437	Ca1:3583849-3585825	6.31	29.8	0.501	plas
	CaNIP2-1	Ca_21333	Ca3:3854949-3859331	8.81	28.65	0.354	plas
	CaNIP3-1	Ca_02921	Ca1:8870515-8872730	9.09	31.93	0.361	plas
	CaNIP3-2	Ca_22848	Ca5:17858736-17862203	6.47	26.55	0.713	plas
	CaNIP3-3	Ca_25553	scaffold590:19540-20529	5.44	21.78	0.773	plas
	CaNIP3-4	Ca_04355	Ca4:11227522-11231177	8.56	30.7	0.502	plas
	CaNIP4-1	Ca_07775	Ca4:1463846-1467215	8.72	36.17	0.504	plas
	CaNIP6-1	Ca_22925	Ca6:53303745-53307875	8.49	25.56	0.228	vacu
SIP	CaSIP1-2	Ca_19143	Ca2:6911037-6913006	6.3	22.93	0.979	vacu
	CaSIP1-1	Ca_08262	Ca3:26454060-26457001	8.89	26.44	0.697	vacu
	CaSIP2-1	Ca_08136	Ca3:27710934-27713756	9.43	26.11	0.603	vacu

^aGene IDs and AQP location are based on CDC Frontier genome assembly v1.0.^bGRAVY, Grand Average of Hydropathy.^cPredicted subcellular location of CaAQPs: plas, plasma membrane; cyto, cytosol; vacu, vacuolar; nucl, nuclear; mito, mitochondria.

found in tonoplast and plasma membrane (Gattolin et al., 2011). However, molecular mechanisms underlying the dual localizations of these genes are not yet clear (Luu and Maurel, 2013). With the increasing number of functionally characterized plant aquaporin genes, more diverse patterns of subcellular

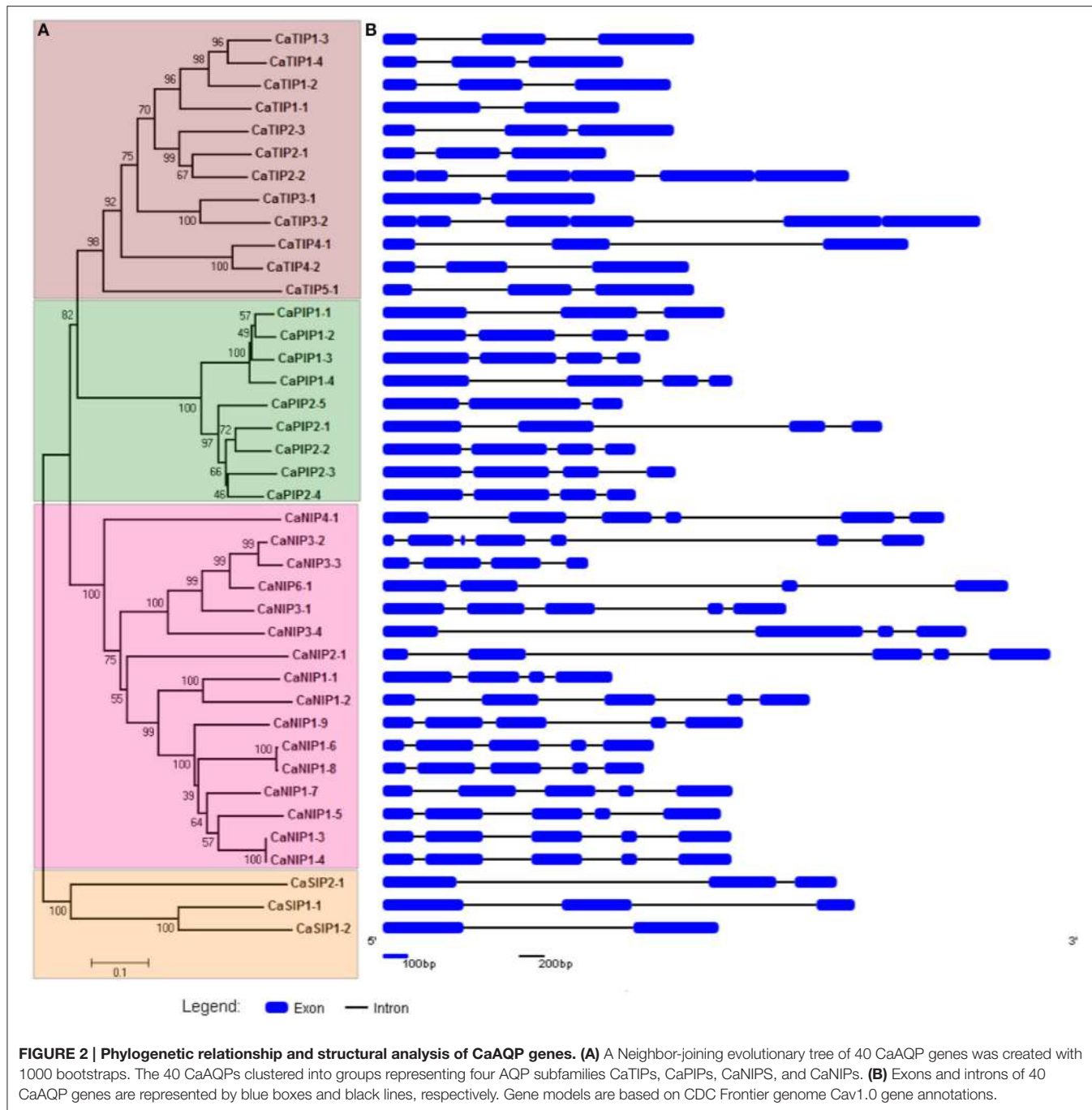
localization and relocalization or redistribution AQPs that were influenced by environmental conditions such as drought and salinity have been also reported (Boursiac et al., 2008; Luu et al., 2012). All these observations indicated that the AQP sub-cellular localization is complex and highly regulated.



Gene Structure and Genomic Distribution of CaAQP

The gene structure analysis showed the distribution of introns and exons in the CaAQP genes, from one to six introns per genes (**Figure 2B**). Variation in the average number of introns between the CaAQP subfamily was also observed. The members of SIPs

and TIPs subfamilies contained a maximum of 2 introns, with an average of 1.7 and 2.0 introns per gene, respectively, whereas the members of PIPs and NIP's subfamily contains a maximum of 4 and 6 introns, with an average of 2.9 and 4 introns per gene. Gene length variation within CaAQP was observed, where CaTIP3-1 (863 bp) was the shortest and CaNIP2-1 (4382 bp) was



the longest AQP in chickpea genome. The length variation in intron size was also observed with the shortest intron size of 76 bp in CaNIP3-1 and CaTIP2-3 genes, whereas the largest intron size of 3118 bp in the CaNIP2-1 gene. With some exceptions, the exon-intron structure is conserved within each AQP subfamily. For example, the CaPIP subfamily contains three introns, except CaPIP1-1 and CaPIP2-5, which contain two introns. Similarly, the majority of the CaTIP subfamily genes contains two introns with the exception of CaTIP1-1 and CaTIP3-1 which contain one intron. Relatively diverse exon-intron pattern was observed for

the CaNIPs subfamily, the majority (10 out of 16 CaNIPs) of the genes contains four introns, four NIPs (CaNIP1-1, CaNIP3-3, CaNIP3-4, CaNIP6-1) contain three introns, CaNIP4-1 contains one intron, and CaNIP3-2 contains six introns. Three members of the CaSIP subfamily contain two introns (CaSIP and CaSIP) and one (CaSIP) intron. Similar exon-intron patterns have been reported in PIP and TIP subfamily of Arabidopsis, soybean, tomato, and orange (Johanson et al., 2001; Deshmukh et al., 2013; Reuscher et al., 2013; Martins Cde et al., 2015). Overall, the gene structure analysis indicated a conserved pattern of intron-exon

within the subfamilies of CaAQPs suggesting the conserved evolution and supporting the CaAQP family classification.

The Physical mapping of the identified CaAQPs on the CDC Frontier kabuli genome assembly indicated the diverse distribution of the genes on chickpea chromosomes, except chromosome seven (**Figure 3**). Chromosome 3 contained the largest number (10; 25%) of the CaAQP genes, followed by chromosome 1 and 4, which both contained six members (17.5%). Chromosome 5 contained only two members (5.0%). Two CaAQP genes (CaTIP2-2 and CaNIP3-3) were located on unplaced scaffold sequences scaffold1844 and scaffold590, respectively. AQP gene density varies on individual chromosomes. The entire chickpea genome has an average of one AQP gene per 13.3 Mb. Further, some of the AQP genes were located in clusters at certain chromosomal regions, especially in the chromosome 1 and 6, and were dispersed in a single manner at other locations. Eight CaAQPs were found to be tandem duplications according to the criteria described in MCScan algorithm implemented in MCScanX software (Wang Y. et al., 2012). These genes included CaNIP1-6, CaNIP1-7, and CaNIP1-8 located on chromosome 1, CaTIP4-2, and CaTIP4-1 located on chromosome 4 and CaNIP1-3, CaNIP1-4, CaNIP1-5 located on chromosome 6. Additionally, 14 CaAQPs were predicted as segmentally or whole-genome duplication (WGD). Fifty percent of CaNIP subfamily members were predicted as either tandem or segmentally duplicated. These results suggested that the larger size of the NIP subfamily in legumes compared to Arabidopsis (16 members in chickpea and Medicago vs. nine members in Arabidopsis) may have evolved from gene duplication events. Expansion of AQP gene families via genome duplication events have been reported in other plants (Abascal et al., 2014). whole-genome sequence analysis also demonstrated

that the significant number (69%) of the annotated chickpea genes have a history of gene duplication after the divergence of the legumes from *Arabidopsis* and grape (Varshney et al., 2013), which also supports our observation of CaAQPs gene duplication in chickpea.

The Conserved and Substrate-Specific Residues of CaAQPs

Several conserved amino acid domains determining substrate specificity by affecting pore diameter and hydrophobicity have been reported in AQP family members (Froger et al., 1998; Hove and Bhave, 2011). The highly conserved features included six transmembrane α helices and two segments responsible for selectivity, the NPA domain (asparagine-proline-alanine) and the ar/R (aromatic arginine) selectivity filter (Kosinska Eriksson et al., 2013; Almasalmeh et al., 2014). Following a conserved domain database (CDD) BLAST search and careful visual inspection of amino acid sequence alignment, we identified conserved NPA domains, an ar/R selectivity filter, and Froger's residues in all 40 CaAQPs (**Table 2**, **Supplementary File S3**). The CaAQP fold is characterized by six transmembrane α -helices that are arranged in a right-handed bundle and five inter-helical loop regions (A-E) that form the extracellular and cytoplasmic vestibules. The majority of CaAQP (32 out of 40) showed six predicted transmembrane domains (TMDs), whereas the remaining eight CaAQPs have seven (CaNIP3-1, and CaTIP5-1), five (CaPIP2-1, CaPIP2-2, and CaSIP1-1) and four (CaNIP3-3, CaNIP6-1, and CaSIP2-1) TMDs. Two of the five interhelical loops, the loop B (LB) and E (LE) contain the highly conserved asparagine-proline-alanine (NPA) motifs that form one of the two major channel construction sites, the NPA region. Most of

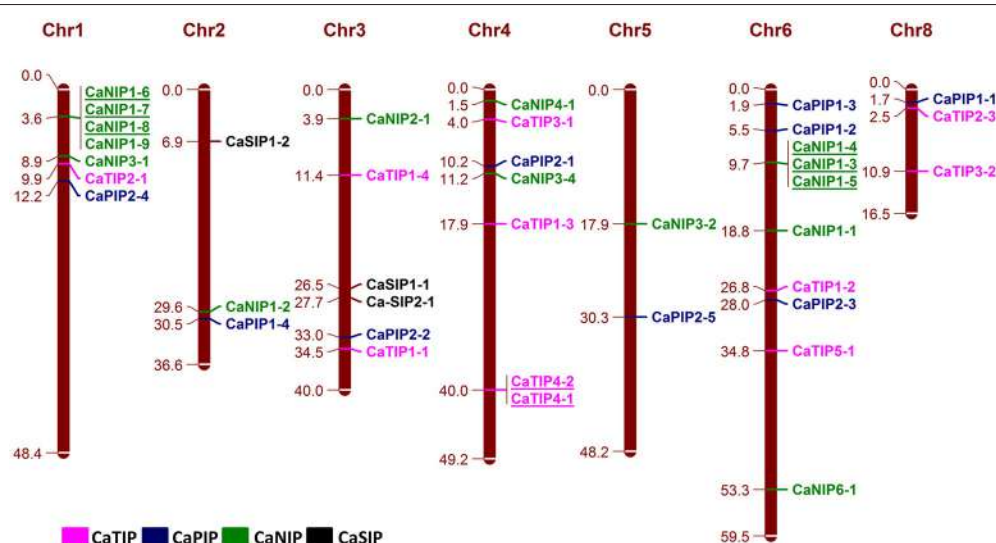


FIGURE 3 | Genomic distribution of CaAQP genes. 38 CaAQP genes are located on all eight chickpea chromosomes, except chromosome 7. The remaining two CaAQP genes are located on scaffolds and not shown in this figure. The numbers at the right side of the chromosomal bar indicate the names of CaAQP genes and the corresponding position on the chromosome (megabase pairs; Mb) are given in left side. The "CaTIP" genes are represented in pink, "CaPIP" genes are in blue, "CaNIP" genes are in green and "CaSIP" genes are in black color. Tandemly duplicated genes are underlined.

TABLE 2 | Amino acid composition of the NPA motifs and ar/R selectivity filter of CaAQPs.

Gene_Id	NPA(LB)	NPA(LE)	Ar/R filters				Froger's residues				
			H2	H5	LE1	LE2	P1	P2	P3	P4	P5
CaNIP1-1	NPA	NPA	W	V	A	R	F	S	A	Y	I
CaNIP1-2	NPA	NPA	W	L	A	R	F	S	A	Y	I
CaNIP1-3	NPA	NPA	W	V	A	R	F	S	A	Y	L
CaNIP1-4	NPA	NPA	W	V	A	R	F	S	A	Y	L
CaNIP1-5	NPA	NPA	W	A	A	R	F	S	A	Y	L
CaNIP1-6	NPA	NPA	W	V	A	R	F	S	A	Y	L
CaNIP1-7	NPA	NPA	W	V	A	R	F	S	A	Y	I
CaNIP1-8	NPA	NPA	W	V	A	R	F	S	A	Y	L
CaNIP1-9	NPA	NPA	W	I	A	R	F	S	A	Y	L
CaNIP2-1	NPA	NPA	G	S	G	R	L	T	A	Y	M
CaNIP3-1	NPA	NPV	S	I	G	R	F	S	A	Y	L
CaNIP3-2	NPA	NPV	S	I	G	R	F	A	A	Y	L
CaNIP3-3	NPA	-	S	I	-	-	F	-	-	-	-
CaNIP3-4	NPS	NPV	A	I	G	R	Y	T	A	Y	L
CaNIP4-1	NPA	NPA	A	V	G	R	Y	S	A	Y	I
CaNIP6-1	NPA	NPV	S	I	G	R	-	T	T	Y	L
CaPIP1-1	NPA	NPA	F	H	T	R	E	S	A	F	W
CaPIP1-2	NPA	NPA	F	H	T	R	E	S	A	F	W
CaPIP1-3	NPA	NPA	F	H	T	R	E	S	A	F	W
CaPIP1-4	NPA	NPA	F	H	T	R	E	S	A	F	W
CaPIP2-1	NPA	NPA	F	H	T	R	Q	S	A	F	W
CaPIP2-2	NPA	NPA	F	H	T	R	Q	S	A	F	W
CaPIP2-3	NPA	NPA	F	H	T	R	Q	S	A	F	W
CaPIP2-4	NPA	NPA	F	H	T	R	Q	S	A	Y	W
CaPIP2-5	NPA	NPA	F	H	T	R	M	S	A	F	W
CaSIP1-1	NPT	NPA	L	V	P	N	I	A	A	Y	W
CaSIP1-2	NPT	NPV	L	I	P	L	I	V	V	-	-
CaSIP2-1	NPL	NPA	F	H	G	A	I	V	A	Y	W
CaTIP1-1	NPA	NPA	H	I	A	V	T	S	A	Y	W
CaTIP1-2	NPA	NPA	H	I	A	V	T	S	A	Y	W
CaTIP1-3	NPA	NPA	H	I	A	V	T	S	A	Y	W
CaTIP1-4	NPA	NPA	H	I	A	V	T	S	A	Y	W
CaTIP2-1	NPA	NPA	H	I	G	R	T	S	A	Y	W
CaTIP2-2	NPA	NPA	H	I	G	R	T	S	A	Y	W
CaTIP2-3	NPA	NPA	H	I	G	R	T	S	A	Y	W
CaTIP3-1	NPA	NPA	H	I	A	R	T	A	A	Y	W
CaTIP3-2	NPA	NPA	H	I	A	L	T	A	S	F	W
CaTIP4-1	NPA	NPA	Q	I	A	R	S	S	A	Y	W
CaTIP4-2	NPA	NPA	H	I	A	R	S	S	A	Y	W
CaTIP5-1	NPA	NPA	N	V	G	C	L	A	A	Y	W

the identified putative CaAQPs also contain two typical NPA domains each one in loop B and loop E. However, six CaNIP and three CaSIP showed variable third residue of NPA motif (LB or LE) in which A is replaced by either L/S/T/V. Several studies also showed that the incompletely conserved NPA motifs also function as water channels (Johanson and Gustavsson, 2002; Yakata et al., 2007). The spacing between the two NPA motifs found essential for the silicon permeability by NIP2s in all silicon transporting plants (Deshmukh et al., 2015). We also

observed diversity in the spacing between two NPA motif in CaAQPs ranging from 108 to 128 amino acids. Although silicon transportation mechanism in chickpea is unknown, it could be possible that the variation in NPA-NPA motif might be associated with permeability and transport of some unknown uncharged solutes.

The second channel construction site known as “ar/R” that consist of tetrad formed by helicase 2 (H2) and 5 (H5) and two LE1 and LE2 residues from loop E. Different combination of

ar/R selectivity filter in CaAQP family and a conserved pattern within the subfamilies were also observed. For example, in the CaPIP subfamily, all the members showed a conserved ar/R filter configuration (F-H-R-T), which was mainly observed in a water transporting AQP, indicating that the CaPIP family members are able to facilitate water and solute transport (Savage et al., 2003). Beside the NPA motif and ar/R selectivity filter, we also analyzed Froger's position P1-P5 the five conserved amino acid residues which discriminated glycerol-transporting aquaglyceroporins (GLPs) from water-conducting AQPs (Froger et al., 1998). The P2, P3, P4 and P5 Froger's positions in the CaPIPs were highly conserved (S-A-F-W), whereas the P1 position varies with either E/Q/M amino acid residue. Froger's positions in the CaNIP subfamily were highly variable in comparison to other subfamilies; however, groups within subfamily showed a conserved pattern. The CaNIP1 group has conserved ar/R filter W-[A/V/L]-A-R and F-S-A-Y-I residue in the P1-P5 positions, which has been predicted as conserved motifs in urea and H₂O₂ transporter NIPs (Hove and Bhave, 2011). The CaNIP3 group have conserved residue A-Y-L in the P2-P5 position, whereas the position P1 (F/Y) and P2 (S/A/T) having variable residues. In the subfamily CaTIP (CaTIP1 and CaTIP2) the ar/R filter H-I-A-V or H-I-G-R and the Froger's positions T-S-A-Y-W residue in the P1-P5 positions were highly conserved and were reported to involve in the transport of urea and H₂O₂ (Hove and Bhave, 2011).

Functional characterization of several AQP genes has shown that the roles of some members of AQP family are not limited to water transport, but also involved in the transport of non-aqua substrates, such as glycerol, CO₂, NH₄⁺/NH₃, urea, silicon, H₂O₂, arsenic, antimony, lactic acid, and boron (Rivers et al., 1997; Biela et al., 1999; Ma et al., 2006, 2008; Takano et al., 2006; Bienert et al., 2008). Based on sequence similarity of the functionally characterized plant AQP genes, Hove and Bhave (Hove and Bhave, 2011) proposed distinct signature sequences and nine specificity-determining positions (SDPs) for each substrate group. To postulate the role of CaAQPs in the transport of non-aqua substrates, we analyzed these conserved SDPs in CaAQPs (**Supplementary File S4**). The members of CaPIP1 and CaPIP2 showed the presence of SDPs deciphered for boric acid (T-I-H-P-E-L/M-L-T-P), CO₂ (ILV-I/M-C-A-I/V-D/H-W) and H₂O₂ (A-G-V-F/L-I-Q/H-F/Y-V-P) transporter. On the other hand, all the CaPIPs and CaTIPs exhibited the H₂O₂ (A/S-G/A-V/L-F/L/A/I-I/V-Q/H/I/L-F/Y-V/A-P) and Urea (H-P-F/F/I/L-L-P/A-G-G/S-N) SDPs.

Molecular Modeling of CaAQP

Molecular dynamics simulations have provided insight into the solute permeation rate and selectivity of AQPs by providing dynamic and energetic information which usually difficult to get experimentally (de Groot and Grubmüller, 2005). In order to understand the structural properties of AQP genes in chickpea, three-dimensional (3D) protein models of all CaAQPs were constructed using phyre2 server and the results are shown in **Figure 4** and **Supplementary File S5**. All the 3D protein models have been constructed with 100% confidence and residue coverage varied from 72 to 98%. Hence, all the predicted 3D

protein structures are considered highly reliable and offer a preliminary basis for understanding the molecular function of Aquaporin genes in chickpea. Broadly, the CaAQP 3D protein structure contains the conserved hour-glass model with a pore-forming integral membrane protein containing α -helical bundle forming six TM helices (H1 to H6) and two additional short (half) helices (HE and HB). The loops HE and HB each containing the conserved NPA motifs get close together in the center of the membrane. Homology-based 3D structure models provided important insights about the boron (B) and silicon (Si) substrate selectivity and passage capabilities of barley and soybean AQPs, respectively (Deshmukh et al., 2013; Tombuloglu et al., 2016). This pointed out that the homology-based 3D modeling of plant AQPs can be effectively used for understanding the substrate specificity and molecular function of AQP genes.

Expression Profile of CaAQP Genes in Different Tissue

Exclusive or highly confined expressions of some of the AQPs in specific tissues such as root or leaf have been observed in several plants. The cell type localization of aquaporin expression profile can provide clues about their potential physiological roles. In order to gather information on the potential role of the CaAQP genes in chickpea, we analyzed RNA-seq data of young leaves, shoot, shoot apical meristem, flower, flower bud, young pod, and root. We observed the expression of all 40 CaAQPs in at least one of the tissue types. The expression of CaAQP varies in tissues and developmental stages. 28 CaAQP genes showed expression in all the tissue types analyzed in this study (**Figure 5A** and **Supplementary Table 2**). From the remaining 12 AQP genes, 10 genes (CaNIP1-1, CaTIP1-3, CaTIP1-4, CaNIP1-5, CaTIP3-2, CaNIP1-2, CaNIP1-8, CaNIP1-9, CaNIP4-1, CaTIP5-1, and CaNIP1-6) were not represented by any sequence reads in either any of the three of the tissue type analyzed, whereas the CaTIP4-1 was only detected in young leaves. Gene clustering and heat map of the CaAQPs showed that the CaPIP1-1, CaPIP2-3, CaPIP1-4, CaPIP2-4, CaPIP2-1, CaPIP1-3 and CaTIP1-1 had high expression in all the eight tissues indicating the constitutive transport process throughout the plant. Gene clustering based on the expression values formed four gene clusters, cluster-I contained seven CaAQP genes that were mainly highly expressed in the shoot, flower, and root, whereas 12 genes in cluster-II genes were mainly highly expressed in the young leaves and roots (**Figure 5A**). Cluster-I contains only CaNIP genes, whereas the cluster-II contains four TIPs and PIPs and two SIP and NIPs. Cluster-III contains four genes (CaNIP1-3, CaNIP1-4, CaNIP1-7, and CaTIP3-1) and mainly highly expressed in flower bud. The cluster-IV contains 13 genes, mainly and highly expressed in the shoot, shoot apical meristem and young pod (**Figure 5A**). Highly expressed CaAQPs in reproductive tissue might be associated with regulation of water and nutrient transport in chickpea as many reproductive development processes in plants involves the movement of water between cells or tissues. Recently, two members of NIP subfamily have been reported to involve in the movement of water in reproductive tissue and in pollen development and pollination (Di Giorgio et al., 2016). We also

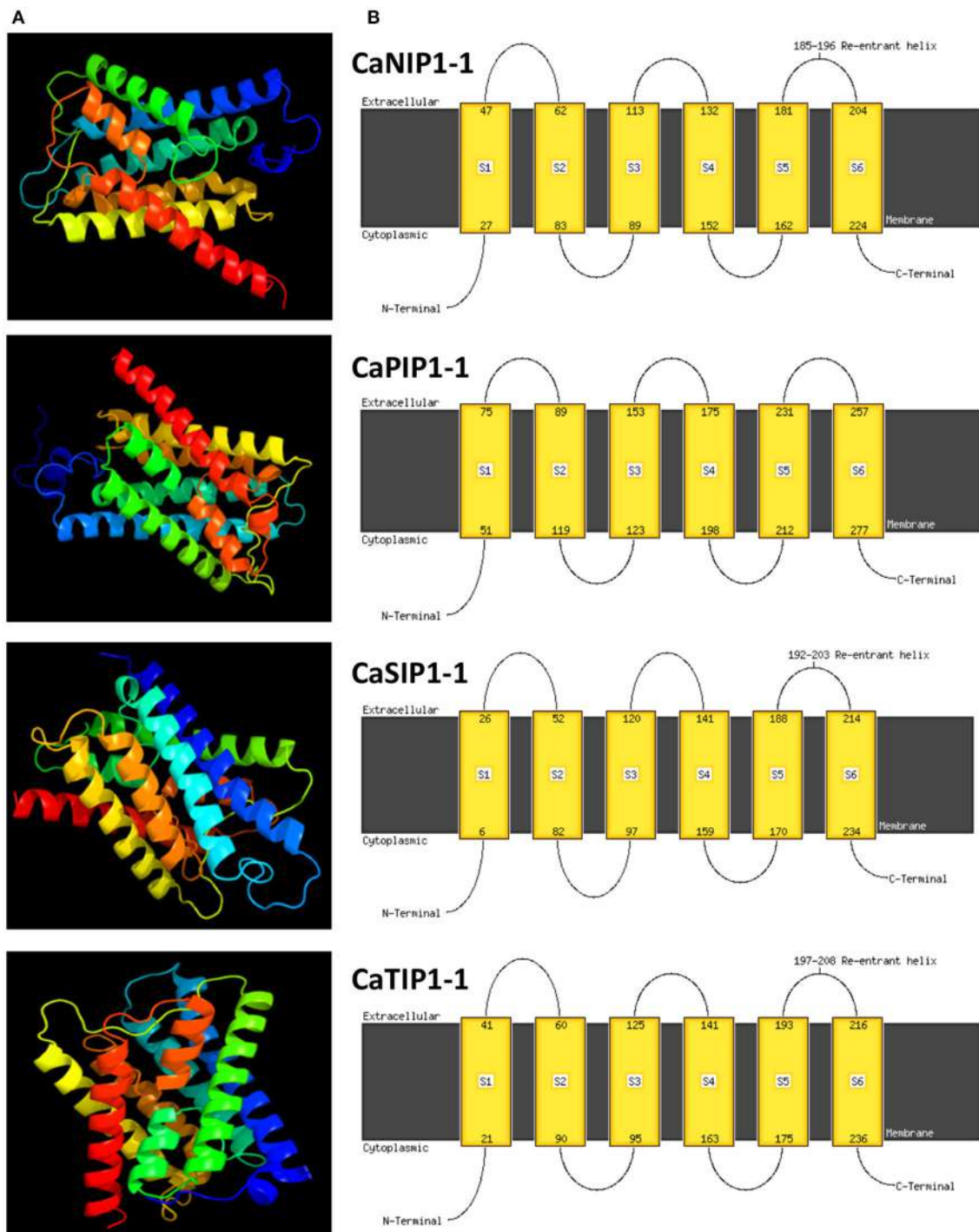
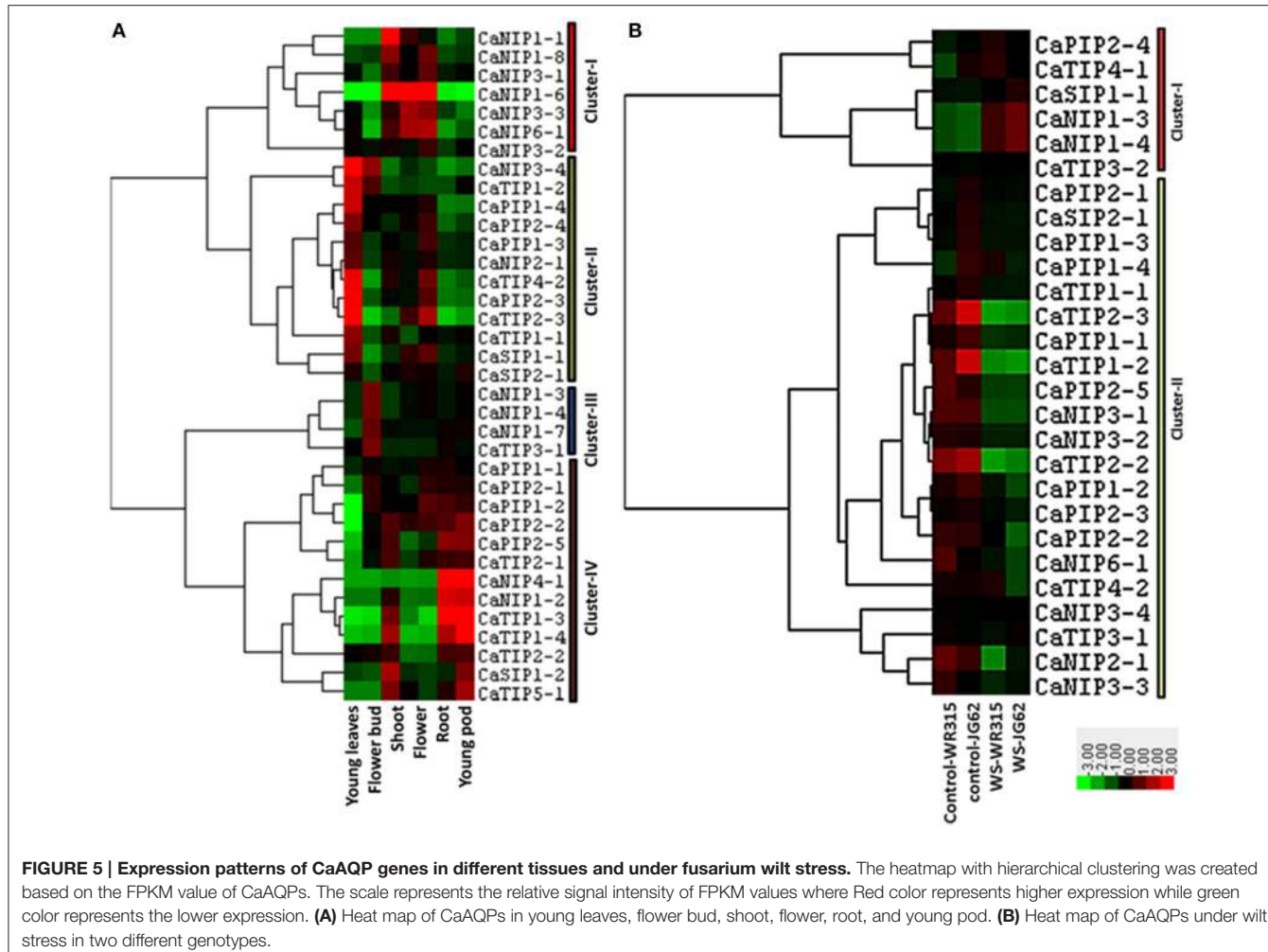


FIGURE 4 | Predicted 3D structures and transmembrane helix of four selected CaAQP proteins. (A) 3D structure and **(B)** TM helix of four CaAQPs representing each subfamily namely CaNIP1-1, CaTIP1-1, CaSIP1-1, and CaPIP1-1, modeled at >90% confidence level by using Phyre2 server. The extracellular and cytoplasmic sides of the membrane are labeled and the beginning and end of each transmembrane helix illustrated with a number indicating the residue index.

observed higher expression of six CaNIPs (cluster-I) in flower tissue sample indicating the potential involvement of these genes in similar function. Higher expression of some of the

chickpea AQPs in tissues with high water fluxes such as fast growing regions in leaf, shoot, and root where actual water uptake occurred have been observed in many other plants. It

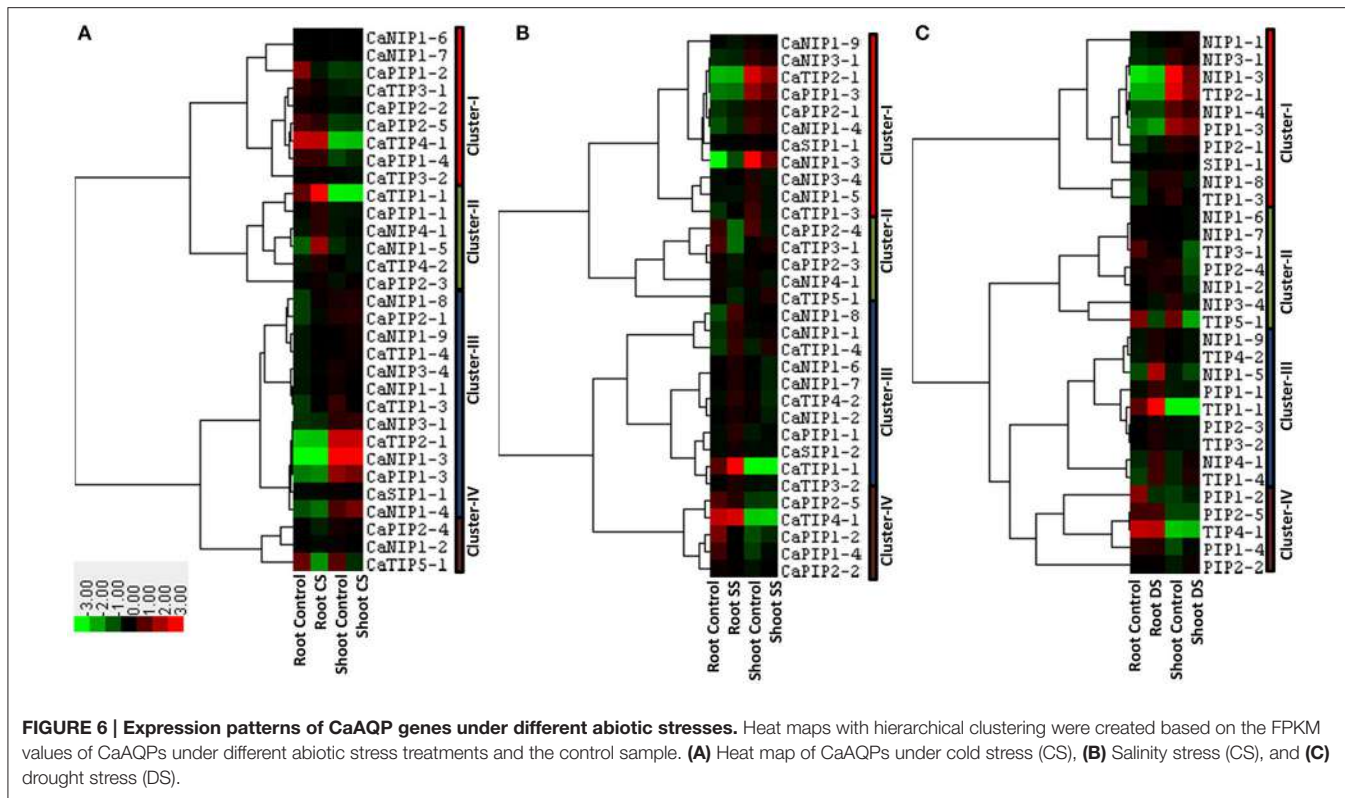


was hypothesized that the high level of expression in these tissues permit osmotic equilibration between the cytosol and the vacuolar content, and permit rapid transcellular water flow when required (Barrieu et al., 1998). All these tissue/organ level expression data suggested that CaAQPs might involve in regulating water transport, physiology and developmental process. To further detail the understanding of the role of CaAQPs in water transport and other developmental process, knowledge of their expression at the cellular level is essential.

Expression Pattern of CaAQP Genes under Biotic and Abiotic Stresses

Expression of several plant AQPs is regulated by abiotic and biotic stresses, and the altered expression can lead to stresses tolerance in plants (Maurel et al., 2008). To predict the potential role of the CaAQPs in chickpea under diverse environmental stresses, RNA-seq dataset of biotic stress (fusarium wilt) and abiotic stress (drought, cold and salinity stress) were analyzed. In total, transcripts of 26 AQP genes were detected in the fusarium wilt expression datasets (Figure 5B and Supplementary Table 3). Two main clusters were formed, Cluster-I contains seven CaAQP genes with high expression levels in wilt stressed condition

as compared to the untreated samples. Cluster-II contains 19 AQP genes with high expression levels in untreated samples as compared to fusarium wilt treated samples. The *Fusarium oxysporum* fungus infects the host plant via the roots or stem and induces wilting of plants due to disruption of water balance. The disturbed water balances resulted in reduced root water uptake, increased resistance to water flow through xylem elements and increased water losses from damaged cells (Wang M. et al., 2012, 2015). This type of physiological alteration in chickpea plants in response to *Fusarium oxysporum* infection likely regulated the expression of some of the observed changes in expression of CaAQP genes. Recently, Tian et al. reported differential expression of 13 Arabidopsis AtPIP1s and the involvement of AtPIP1;4 in the transport pathogen-induced apoplastic H₂O₂ to the cytoplasm of plant cells in response to bacterial pathogen *Pseudomonas syringae* infection (Tian et al., 2016). The cytoplasmic H₂O₂ triggered the pathogen-associated molecular pattern (PAMP)-triggered immunity (PTI) pathway, which conferred resistance to the pathogen. With these increasing evidences of the involvement of AQPs in biotic stress, the CaAQPs and expression profiles presented in present work provide a foundation and resource to study the role of AQPs in



resistance mechanism of two most important diseases of chickpea fusarium wilt and ascochyta blight.

Several pieces of evidence of the AQP involvement in abiotic stress that disturbs plant osmotic balance such as cold, salinity and drought have been reported (Luu and Maurel, 2005). In order to understand the role of CaAQPs in abiotic stress conditions, we analyzed the response of AQPs in root and shoot tissue under cold, salinity and drought stress conditions. Transcripts of 31 AQP genes were detected in shoot and roots of cold stressed (4°C) chickpea seedlings (Figure 6A and Supplementary Table 4). These genes were clustered into four main clusters. Cluster-I contains nine AQPs with high-expression levels in root tissue under both control and cold stress condition as compared to the shoot. Whereas, Cluster-III contains 13 genes with the opposite expression profile of cluster I, i.e., low expression levels in root tissue, but high-expression in the shoot tissue. On average in both of these clusters, AQPs showed constitutive expression profile in control and stress conditions. The cluster-II contain six genes (CaTIP1-1, CaTIP4-2, CaPIP1-1, CaPIP2-3, CaNIP1-5, and CaNIP4-1) and were highly expressed, whereas cluster-IV contained three genes (CaPIP2-4, CaTIP5-1, and CaNIP1-2) under-expressed in root tissue under cold stress (Figure 6A).

Transcripts of 32 CaAQPs were detected in shoot or root or both tissues under salinity stress condition (Figure 6B and Supplementary Table 4). These genes were clustered into four main clusters. Cluster-I contains 11 genes, highly expressed in shoot tissue, whereas cluster-V contains five CaAQPs, highly expressed in root tissue. Cluster-II contains five genes (CaTIP3-1,

CaTIP5-1, CaPIP2-3, CaPIP2-4, and CaNIP4-1) down-regulated under salinity stress, whereas Cluster-III contains three genes (CaTIP1-4, CaNIP1-8, and CaNIP1-4) up-regulated under salinity stress in both root and shoot.

We also analyzed the expression profiles of AQP genes in response to drought stress in root and shoot tissue. Results showed that transcripts of 31 CaAQPs were detected in at least one condition i.e., control/stress of root and shoot (Figure 6C and Supplementary Table 4). Based on their expression values, the CaAQPs were clustered into four main clusters. Cluster-I contains ten genes highly expressed in root tissue as compared to shoot tissue. Cluster-IV contains five CaAQPs and have opposite expression profile as in cluster-I i.e., genes showed low expression in roots as compared to shoot. However, AQPs in cluster I and IV shows constitutive expression pattern under control and stress condition. Cluster III contains seven CaAQPs that were highly expressed in root control and drought stress condition, however under-expressed (down-regulated) in shoot tissue under drought stress conditions. This cluster contains CaTIP3-1, CaTIP5-1, CaPIP2-4, CaNIP1-2, CaNIP1-6, CaNIP1-7, and CaNIP3-4 genes. Cluster-III contains nine CaAQPs low-expressed in the shoot, but high-expressed in roots under drought condition. This cluster mainly contains CaTIPs (CaTIP1-1, CaTIP1-4, CaTIP2-3, and CaTIP3-2), CaPIP1-1, CaPIP2-3, CaNIP1-5, CaNIP1-9, and CaNIP4-1 genes.

Overall expression profiles of CaAQPs in response to all stress indicated that some of the CaAQPs such as CaTIP1-1 and CaPIP1-1 showed up-regulation in cold, drought and salinity stress. Whereas, some of the CaAQP genes also have

an organ-specific response such as CaTIP1-1 and CaPIP2-5 that were highly expressed in root tissue and CaTIP2-1 and CaNIP1-3 that were highly expressed in shoot tissue. Differential expression of 13 unigenes encoding PIPs, TIPs, and NIPs in root tissue under terminal drought stress has been reported (Deokar et al., 2011). The majority of these genes were down-regulation under terminal drought conditions. Similar pattern of aquaporin gene expression under stress condition was also observed in Arabidopsis (Jang et al., 2004; Alexandersson et al., 2005, 2010; Boursiac et al., 2005) and other plant species (Smart et al., 2001; Mahdieu et al., 2008; Secchi and Zwieniecki, 2014), although up-regulation and constitutive expression pattern of some of the aquaporins under stress conditions were also observed. The increase and decrease in expression of AQP under water stress have been associated with a general pattern of AQP regulation under different stress conditions. The decrease in the expression of AQPs under stress can effectively prevent water losses under stress condition, whereas the increase in AQP expression helps plants to direct water flow to specific organ that is critical for plant survival under stress condition or necessary for its rapid recovery upon rehydration (Alexandersson et al., 2005, 2010). Therefore, the observed expression pattern of many of CaAQPs in response to biotic and abiotic stresses suggested the potential role of CaAQPs in biotic and abiotic stress response in chickpea.

Our expression analysis categorized the CaAQPs into different groups based on their expression profiles. This information will be helpful for functional characterization of CaAQP genes in chickpea.

Promoter Profiling of CaAQP

The *cis*-acting regulatory elements (CREs) are DNA region in the promoter, where a number of transcription factors can bind and regulate the transcription of nearby genes. Profiling of the promoter region for the CREs can provide information on gene regulatory networks. To predict the CREs, the promoter sequences (1000 bp upstream DNA sequences) of the predicted transcription initiation site of 40 CaAQP gene were extracted and subjected to promoter profiling using PlantCARE web tool (Lescot et al., 2002). The most common *cis*-acting elements present in CaAQPs were known to involve in light response such as Box-4, G-Box, I-Box, ACE etc., (**Supplementary Table 5**). Among the light responsive elements, the Box-4 is the most abundant and present in almost all CaAQPs, except CaPIP1-3, CaTIP1-2, and CaNIP4-1. The ARE, HSE and I-Box light regulating *cis*-acting element were present in the majority of the members of chickpea aquaporin subfamily, but absent in the members of CasIP subfamily. Light is one of the most important environmental factors that regulate plant growth and development. Besides the source of energy, light regulates gene expression network at many levels (Jiao et al., 2007; Petrillo et al., 2014). Effect of light (quantity and quality) on gene expression and function of individual or subfamily of AQPs has been reported in many plants (Baaaziz et al., 2012). The presence of several light responsive *cis*-active elements in specific chickpea AQPs suggested that some of the chickpea AQPs might be regulated by light-dependent activations.

Plant hormone responsive *cis*-elements such as AuxRR-core, ABRE, ERE, TCA-element, and GARE-motif were also

abundantly found in several chickpea AQPs, suggested that the expression of some of the chickpea AQPs might be regulated by the different type of hormones. Several *cis*-elements responsive to biotic and abiotic stresses such as W-box, TC-rich repeat, HSE, and TCA-element were also found in CaAQPs. The presence of these stress-responsive *cis*-elements in the promoter region of CaAQPs indicated their potential involvement in regulating stress responses in chickpea. Two AQP genes (CaTIP1-4 and CANIP4-1), showed higher expression in both roots and shoot tissues under drought and salinity stresses and root tissue under the cold condition contains stress-responsive *cis*-acting elements ABRE, LTR, and MBS. The presence of these stress-responsive *cis*-elements in CaAQPs correlates to high expression in response to drought, salinity, and cold stress. The ABRE and MBS *cis*-elements have been previously reported to be involved in ABA-mediated osmotic stress signaling in the regulation of drought-inducible gene expressions (Abreu and Aragão, 2007; Hou et al., 2016), whereas *cis*-element LTR is a low-temperature-responsive element and involved in the expression of cold-regulated genes (Brown et al., 2001). The link between the presence of stress-related *cis*-acting elements and the differential expression of aquaporin genes under various stress conditions have been reported in several plants (Alexandersson et al., 2010; Wang L. et al., 2015).

The circadian regulation of aquaporin gene expression and the correlation with the modulation water dynamics have been well demonstrated in several plants (Lopez et al., 2003; Hachez et al., 2008, 2012; Sakurai-Ishikawa et al., 2011; Takase et al., 2011). Promoter analysis these AQP genes also showed the presence of abundant circadian regulatory elements (Liu et al., 2009; Lopez et al., 2013). Similarly, in our analysis, we also observed high representation of circadian (CAANNNNATC) *cis*-acting regulatory element involved in circadian control in the CaAQPs promoter region. The presence of a circadian-related *cis*-acting regulatory element suggested that some of the CaAQPs might be involved in the diurnal transport of water through roots as observed in Arabidopsis and maize plants (Lopez et al., 2003; Takase et al., 2011).

Comparative analysis of promoter sequences of Arabidopsis, rice, maize, grape, poplar, Medicago, and Glycine max also observed the high abundance of the conserved light, hormone, biotic and abiotic stress-related response regulatory elements (Lopez et al., 2013). Previous studies also demonstrated that photosynthesis or protein biosynthesis and defense signaling are largely conserved across the species at the promoter element level (Rushton et al., 2002; Vandepoele et al., 2006; Ravel et al., 2014). Promoter profiling and the conserved regulatory elements identified in chickpea AQPs promoter might have conserved regulatory modules as observed for AQP genes in other model plants.

CONCLUSIONS

This study presents the results of the identification and genome-wide survey of the aquaporin genes in chickpea. A total of 40 AQP genes were identified and characterized for their genomic organization, protein sequence properties, gene duplications, phylogenetic relationships with Arabidopsis and closely related

legumes, homology-based 3D models and promoter sequence profiles for conserved *cis*-acting elements. The expression profiles of CaAQPs in different plant parts and under biotic and abiotic stress conditions provided valuable data to understand the involvement of AQPs under different osmotic stress conditions in chickpea.

AUTHOR CONTRIBUTIONS

AD: Conducted the experiments, analyzed and summarized the data. AD and BT: Wrote and finalized the manuscript; BT: Conceived and directed the project.

FUNDING

The authors were supported by funding from the Saskatchewan Pulse Growers and the Saskatchewan Ministry of Agriculture.

SUPPLEMENTARY MATERIAL

The Supplementary Material for this article can be found online at: <http://journal.frontiersin.org/article/10.3389/fpls.2016.01802/full#supplementary-material>

Supplementary File S1 | Nucleotide and amino acid sequences of 40 CaAQP gene identified in this study.

REFERENCES

- Abascal, F., Irisarri, I., and Zardoya, R. (2014). Diversity and evolution of membrane intrinsic proteins. *Biochimica et Biophysica Acta (BBA) Gen. Subj.* 1840, 1468–1481. doi: 10.1016/j.bbagen.2013.12.001
- Abreu, E. F. M., and Aragão, F. J. L. (2007). Isolation and characterization of a myo-inositol-1-phosphate synthase gene from yellow passion fruit (*Passiflora edulis f. flavicarpa*) expressed during seed development and environmental stress. *Ann. Bot.* 99, 285–292. doi: 10.1093/aob/mcl256
- Alexanderson, E., Danielson, J. A., Råde, J., Moparthi, V. K., Fontes, M., Kjellbom, P., et al. (2010). Transcriptional regulation of aquaporins in accessions of Arabidopsis in response to drought stress. *Plant J.* 61, 650–660. doi: 10.1111/j.1365-313X.2009.04087.x
- Alexanderson, E., Fraysse, L., Sjövall-Larsen, S., Gustavsson, S., Fellert, M., Karlsson, M., et al. (2005). Whole gene family expression and drought stress regulation of aquaporins. *Plant Mol. Biol.* 59, 469–484. doi: 10.1007/s11103-005-0352-1
- Almasalmeh, A., Krenc, D., Wu, B., and Beitz, E. (2014). Structural determinants of the hydrogen peroxide permeability of aquaporins. *FEBS J.* 281, 647–656. doi: 10.1111/febs.12653
- Amodeo, G., Dorr, R., Vallejo, A., Sutka, M., and Parisi, M. (1999). Radial and axial water transport in the sugar beet storage root. *J. Exp. Bot.* 50, 509–516. doi: 10.1093/jxb/50.333.509
- Ariani, A., and Gepts, P. (2015). Genome-wide identification and characterization of aquaporin gene family in common bean (*Phaseolus vulgaris* L.). *Mol. Genet. Genomics* 290, 1771–1785. doi: 10.1007/s00438-015-1038-2
- Aroca, R., Porcel, R., and Ruiz-Lozano, J. M. (2012). Regulation of root water uptake under abiotic stress conditions. *J. Exp. Bot.* 63, 42–57. doi: 10.1093/jxb/err266
- Baaziz, K. B., Lopez, D., Rabot, A., Combes, D., Gousset, A., Bouzid, S., et al. (2012). Light-mediated K(leaf) induction and contribution of both the PIP1s and PIP2s aquaporins in five tree species: walnut (*Juglans regia*) case study. *Tree Physiol.* 32, 423–434. doi: 10.1093/treephys/tps022
- Barrieu, F., Chaumont, F., and Chrispeels, M. J. (1998). High expression of the tonoplast aquaporin ZmTIP1 in epidermal and conducting tissues of maize. *Plant Physiol.* 117, 1153–1163. doi: 10.1104/pp.117.4.1153
- Biel, A., Grote, K., Otto, B., Hoth, S., Hedrich, R., and Kaldenhoff, R. (1999). The *Nicotiana tabacum* plasma membrane aquaporin NtAQP1 is mercury-insensitive and permeable for glycerol. *Plant J.* 18, 565–570. doi: 10.1046/j.1365-313X.1999.00474.x
- Bienert, G. P., Thorsen, M., Schüssler, M. D., Nilsson, H. R., Wagner, A., Tamas, M. J., et al. (2008). A subgroup of plant aquaporins facilitate the bi-directional diffusion of As(OH)3 and Sb(OH)3 across membranes. *BMC Biol.* 6:26. doi: 10.1186/1741-7007-6-26
- Bots, M., Vergeldt, F., Wolters-Arts, M., Weterings, K., van As, H., and Mariani, C. (2005). Aquaporins of the PIP2 class are required for efficient anther dehiscence in tobacco. *Plant Physiol.* 137, 1049–1056. doi: 10.1104/pp.104.056408
- Boursiac, Y., Chen, S., Luu, D. T., Sorieul, M., van den Dries, N., and Maurel, C. (2005). Early effects of salinity on water transport in Arabidopsis roots. Molecular and cellular features of aquaporin expression. *Plant Physiol.* 139, 790–805. doi: 10.1104/pp.105.065029
- Boursiac, Y., Prak, S., Boudet, J., Postaire, O., Luu, D. T., Tournaire-Roux, C., et al. (2008). The response of Arabidopsis root water transport to a challenging environment implicates reactive oxygen species- and phosphorylation-dependent internalization of aquaporins. *Plant Signal. Behav.* 3, 1096–1098. doi: 10.4161/psb.3.12.7002
- Brown, A. P., Dunn, M. A., Goddard, N. J., and Hughes, M. A. (2001). Identification of a novel low-temperature-response element in the promoter of the barley (*Hordeum vulgare* L.) gene blt101.1. *Planta* 213, 770–780. doi: 10.1007/s004250100549
- Chaumont, F., Barrieu, F., Jung, R., and Chrispeels, M. J. (2000). Plasma membrane intrinsic proteins from maize cluster in two sequence subgroups with differential aquaporin activity. *Plant Physiol.* 122, 1025–1034. doi: 10.1104/pp.122.4.1025

Supplementary File S2 | Comparison of number of different AQP subfamily members in chickpea, *Arabidopsis*, *Medicago*, common bean, and soybean.

Supplementary File S3 | Multiple sequence alignment of deduced amino acid sequences of 40 CaAQP genes. Sequence alignment was performed using CLUSATLV. Transmembrane helices (TM1–TM6) and two NPAs (LB and LE) are highlighted in gray color, P1–P5 residues highlighted in blue color, and ar/R selectivity filter residues highlighted in green color. The NPA motifs are shown in red color.

Supplementary File S4 | Summary of specificity-determining positions (SDP) identified in the CaAQPs. SDP positions identified in the present study and not found conserved with the reported SDPs in AQPs are highlighted in red color.

Supplementary File S5 | Predicted 3D structure of the 40 CaAQP protein generated using Phyre 2 server.

Supplementary Table 1 | Protein sequence similarity matrix between members of CaAQP genes. Protein sequence similarity expressed in terms of percentage identity calculated using sequence Identity Matrix option available in Bioedit software.

Supplementary Table 2 | FPKM values for all the detected CaAQP genes in the shoot, young leaves, shoot apical meristem, flower, Flower bud, young pod, and root tissue of chickpea plant.

Supplementary Table 3 | FPKM values for all the detected CaAQP genes in fusarium wilt expression datasets.

Supplementary Table 4 | FPKM values for all the detected CaAQP genes in drought, cold and salinity expression datasets.

Supplementary Table 5 | Analysis of cis-acting elements in the 1000bp sequence upstream of the translation initiation codon of CaAQP genes.

- Chaumont, F., Barrieu, F., Wojcik, E., Chrispeels, M. J., and Jung, R. (2001). Aquaporins constitute a large and highly divergent protein family in maize. *Plant Physiol.* 125, 1206–1215. doi: 10.1104/pp.125.3.1206
- de Groot, B. L., and Grubmüller, H. (2005). The dynamics and energetics of water permeation and proton exclusion in aquaporins. *Curr. Opin. Struct. Biol.* 15, 176–183. doi: 10.1016/j.sbi.2005.02.003
- Deokar, A. A., Kondawar, V., Jain, P. K., Karuppayil, S. M., Raju, N. L., Vadze, V., et al. (2011). Comparative analysis of expressed sequence tags (ESTs) between drought-tolerant and -susceptible genotypes of chickpea under terminal drought stress. *BMC Plant Biol.* 11:1–20. doi: 10.1186/1471-229-11-70
- Deshmukh, R., and Bélanger, R. R. (2016). Molecular evolution of aquaporins and silicon influx in plants. *Funct. Ecol.* 30, 1277–1285. doi: 10.1111/1365-2435.12570
- Deshmukh, R. K., Vivancos, J., Guérin, V., Sonah, H., Labbé, C., Belzile, F., et al. (2013). Identification and functional characterization of silicon transporters in soybean using comparative genomics of major intrinsic proteins in *Arabidopsis* and rice. *Plant Mol. Biol.* 83, 303–315. doi: 10.1007/s11103-013-0087-3
- Deshmukh, R. K., Vivancos, J., Ramakrishnan, G., Guérin, V., Carpentier, G., Sonah, H., et al. (2015). A precise spacing between the NPA domains of aquaporins is essential for silicon permeability in plants. *Plant J.* 83, 489–500. doi: 10.1111/tpj.12904
- Di Giorgio, J. A., Bienert, G. P., Ayub, N. D., Yaneff, A., Barberini, M. L., Mecchia, M. A., et al. (2016). Pollen-specific aquaporins NIP4;1 and NIP4;2 are required for pollen development and pollination in *Arabidopsis thaliana*. *Plant Cell* 28, 1053–1077. doi: 10.1105/tpc.15.00776
- Flowers, T. J., Gaur, P. M., Gowda, C. L. L., Krishnamurthy, L., Samineni, S., Siddique, K. H. M., et al. (2010). Salt sensitivity in chickpea. *Plant Cell amp; Environment* 33, 490–509. doi: 10.1111/j.1365-3040.2009.02051.x
- Froger, A., Thomas, D., Delamarche, C., and Tallur, B. (1998). Prediction of functional residues in water channels and related proteins. *Protein Sci.* 7, 1458–1468. doi: 10.1002/pro.5560070623
- Gattolin, S., Sorieul, M., and Frigerio, L. (2011). Mapping of tonoplast intrinsic proteins in maturing and germinating *Arabidopsis* seeds reveals dual localization of embryonic TIPs to the tonoplast and plasma membrane. *Mol. Plant* 4, 180–189. doi: 10.1093/mp/ssq051
- Gomes, D., Agashe, A., Thiebaud, P., Delrot, S., Gerós, H., and Chaumont, F. (2009). Aquaporins are multifunctional water and solute transporters highly divergent in living organisms. *Biochim. Biophys. Acta* 1788, 1213–1228. doi: 10.1016/j.bbamem.2009.03.009
- Hachez, C., and Chaumont, F. (2010). Aquaporins: a family of highly regulated multifunctional channels. *Adv. Exp. Med. Biol.* 679, 1–17. doi: 10.1007/978-1-4419-6315-4_1
- Hachez, C., Heinen, R. B., Draye, X., and Chaumont, F. (2008). The expression pattern of plasma membrane aquaporins in maize leaf highlights their role in hydraulic regulation. *Plant Mol. Biol.* 68, 337–353. doi: 10.1007/s11103-008-9373-x
- Hachez, C., Veselov, D., Ye, Q., Reinhardt, H., Knipfer, T., Fricke, W., et al. (2012). Short-term control of maize cell and root water permeability through plasma membrane aquaporin isoforms. *Plant Cell Environ.* 35, 185–198. doi: 10.1111/j.1365-3040.2011.02429.x
- Hou, J., Jiang, P., Qi, S., Zhang, K., He, Q., Xu, C., et al. (2016). Isolation and functional validation of salinity and osmotic stress inducible promoter from the maize type-II H(+)–pyrophosphatase gene by deletion analysis in transgenic tobacco plants. *PLoS ONE* 11:e0154041. doi: 10.1371/journal.pone.0154041
- Hove, R. M., and Bhave, M. (2011). Plant aquaporins with non-aqua functions: deciphering the signature sequences. *Plant Mol. Biol.* 75, 413–430. doi: 10.1007/s11103-011-9737-5
- Jain, D., and Chattopadhyay, D. (2010). Analysis of gene expression in response to water deficit of chickpea (*Cicer arietinum* L.) varieties differing in drought tolerance. *BMC Plant Biol.* 10:24. doi: 10.1186/1471-2229-10-24
- Jang, J. Y., Kim, D. G., Kim, Y. O., Kim, J. S., and Kang, H. (2004). An expression analysis of a gene family encoding plasma membrane aquaporins in response to abiotic stresses in *Arabidopsis thaliana*. *Plant Mol. Biol.* 54, 713–725. doi: 10.1023/B:PLAN.0000040900.61345.a6
- Jiao, Y., Lau, O. S., and Deng, X. W. (2007). Light-regulated transcriptional networks in higher plants. *Nat. Rev. Genet.* 8, 217–230. doi: 10.1038/nrg2049
- Johanson, U., and Gustavsson, S. (2002). A new subfamily of major intrinsic proteins in plants. *Mol. Biol. Evol.* 19, 456–461. doi: 10.1093/oxfordjournals.molbev.a004101
- Johanson, U., Karlsson, M., Johansson, I., Gustavsson, S., Sjövall, S., Fraysse, L., et al. (2001). The complete set of genes encoding major intrinsic proteins in *Arabidopsis* provides a framework for a new nomenclature for major intrinsic proteins in plants. *Plant Physiol.* 126, 1358–1369. doi: 10.1104/pp.126.4.1358
- Johansson, I., Karlsson, M., Johanson, U., Larsson, C., and Kjellbom, P. (2000). The role of aquaporins in cellular and whole plant water balance. *Biochim. Biophys. Acta* 1465, 324–342. doi: 10.1016/S0005-2736(00)00147-4
- Kaldenhoff, R., Grote, K., Zhu, J. J., and Zimmermann, U. (1998). Significance of plasmalemma aquaporins for water-transport in *Arabidopsis thaliana*. *Plant J.* 14, 121–128. doi: 10.1046/j.1365-313X.1998.00111.x
- Kaldenhoff, R., Ribas-Carbo, M., Sans, J. F., Lovisolo, C., Heckwolf, M., and Uehlein, N. (2008). Aquaporins and plant water balance. *Plant Cell Environ.* 31, 658–666. doi: 10.1111/j.1365-3040.2008.01792.x
- Khan, K., Agarwal, P., Shanware, A., and Sane, V. A. (2015). Heterologous expression of two jatropha aquaporins imparts drought and salt tolerance and improves seed viability in transgenic *Arabidopsis thaliana*. *PLoS ONE* 10:e0128866. doi: 10.1371/journal.pone.0128866
- Kosinska Eriksson, U., Fischer, G., Friemann, R., Enkavi, G., Tajkhoshrid, E., and Neutze, R. (2013). Subangstrom resolution X-ray structure details aquaporin–water interactions. *Science* 340, 1346–1349. doi: 10.1126/science.1234306
- Krishnamurthy, L., Johansen, C., and Sethi, S. C. (1999). Investigation of factors determining genotypic differences in seed yield of non-irrigated and irrigated chickpeas using a physiological model of yield determination. *J. Agron. Crop Sci.* 183, 9–17. doi: 10.1046/j.1439-037x.1999.00306.x
- Lescot, M., Déhais, P., Thijs, G., Marchal, K., Moreau, Y., Van de Peer, Y., et al. (2002). PlantCARE, a database of plant cis-acting regulatory elements and a portal to tools for *in silico* analysis of promoter sequences. *Nucleic Acids Res.* 30, 325–327. doi: 10.1093/nar/30.1.325
- Lian, H. L., Yu, X., Ye, Q., Ding, X., Kitagawa, Y., Kwak, S. S., et al. (2004). The role of aquaporin RW3C in drought avoidance in rice. *Plant Cell Physiol.* 45, 481–489. doi: 10.1093/pcp/pch058
- Liu, Q., Wang, H., Zhang, Z., Wu, J., Feng, Y., and Zhu, Z. (2009). Divergence in function and expression of the NOD26-like intrinsic proteins in plants. *BMC Genomics* 10:313. doi: 10.1016/j.ygeno.2009.02.005
- Lopez, D., Venisse, J. S., Fumanal, B., Chaumont, F., Guillot, E., Daniels, M. J., et al. (2013). Aquaporins and leaf hydraulics: poplar sheds new light. *Plant Cell Physiol.* 54, 1963–1975. doi: 10.1093/pcp/pct135
- Lopez, F., Bousser, A., Sissoeff, I., Gaspar, M., Lachaise, B., Hoarau, J., et al. (2003). Diurnal regulation of water transport and aquaporin gene expression in maize roots: contribution of PIP2 proteins. *Plant Cell Physiol.* 44, 1384–1395. doi: 10.1093/pcp/pcg168
- Luu, D. T., Martinière, A., Sorieul, M., Runions, J., and Maurel, C. (2012). Fluorescence recovery after photobleaching reveals high cycling dynamics of plasma membrane aquaporins in *Arabidopsis* roots under salt stress. *Plant J.* 69, 894–905. doi: 10.1111/j.1365-313X.2011.04841.x
- Luu, D. T., and Maurel, C. (2013). Aquaporin trafficking in plant cells: an emerging membrane-protein model. *Traffic* 14, 629–635. doi: 10.1111/tra.12062
- Luu, D.-T., and Maurel, C. (2005). Aquaporins in a challenging environment: molecular gears for adjusting plant water status. *Plant Cell Environ.* 28, 85–96. doi: 10.1111/j.1365-3040.2004.01295.x
- Ma, J. F., Tamai, K., Yamaji, N., Mitani, N., Konishi, S., Katsuhara, M., et al. (2006). A silicon transporter in rice. *Nature* 440, 688–691. doi: 10.1038/nature04590
- Ma, J. F., Yamaji, N., Mitani, N., Xu, X. Y., Su, Y. H., McGrath, S. P., et al. (2008). Transporters of arsenite in rice and their role in arsenic accumulation in rice grain. *Proc. Natl. Acad. Sci. U.S.A.* 105, 9931–9935. doi: 10.1073/pnas.0802361105
- Mahdieu, M., Mostajeran, A., Horie, T., and Katsuhara, M. (2008). Drought stress alters water relations and expression of PIP-type aquaporin genes in *Nicotiana tabacum* plants. *Plant Cell Physiol.* 49, 801–813. doi: 10.1093/pcp/pcn054
- Mao, Z., and Sun, W. (2015). *Arabidopsis* seed-specific vacuolar aquaporins are involved in maintaining seed longevity under the control of ABSCISIC ACID INSENSITIVE 3. *J. Exp. Bot.* 66, 4781–4794. doi: 10.1093/jxb/erv244
- Martins Cde, P., Pedrossa, A. M., Du, D., Gonçalves, L. P., Yu, Q., Gmitter, F. G. Jr., et al. (2015). Genome-wide characterization and expression analysis of major

- intrinsic proteins during abiotic and biotic stresses in sweet orange (*Citrus sinensis* L. Osb.). *PLoS ONE* 10:e0138786. doi: 10.1371/journal.pone.0138786
- Maurel, C., Boursiac, Y., Luu, D. T., Santoni, V., Shahzad, Z., and Verdoucq, L. (2015). Aquaporins in plants. *Physiol. Rev.* 95, 1321–1358. doi: 10.1152/physrev.00008.2015
- Maurel, C., Reizer, J., Schroeder, J. I., and Chrispeels, M. J. (1993). The vacuolar membrane protein gamma-TIP creates water specific channels in *Xenopus* oocytes. *EMBO J.* 12, 2241–2247.
- Maurel, C., Verdoucq, L., Luu, D.-T., and Santoni, V. (2008). Plant aquaporins: membrane channels with multiple integrated functions. *Annu. Rev. Plant Biol.* 59, 595–624. doi: 10.1146/annurev.arplant.59.032607.092734
- Molina, C., Rotter, B., Horres, R., Udupa, S. M., Besser, B., Bellarmino, L., et al. (2008). SuperSAGE: the drought stress-responsive transcriptome of chickpea roots. *BMC Genomics* 9:553. doi: 10.1186/1471-2164-9-553
- Montalvo-Hernández, L., Piedra-Ibarra, E., Gómez-Silva, L., Lira-Carmona, R., Acosta-Gallegos, J. A., Vazquez-Medrano, J., et al. (2008). Differential accumulation of mRNAs in drought-tolerant and susceptible common bean cultivars in response to water deficit. *New Phytol.* 177, 102–113. doi: 10.1111/j.1469-8137.2007.02247.x
- Murata, K., Mitsuoka, K., Hirai, T., Walz, T., Agre, P., Heymann, J. B., et al. (2000). Structural determinants of water permeation through aquaporin-1. *Nature* 407, 599–605. doi: 10.1038/35036519
- Nguyen, M. X., Moon, S., and Jung, K. H. (2013). Genome-wide expression analysis of rice aquaporin genes and development of a functional gene network mediated by aquaporin expression in roots. *Planta* 238, 669–681. doi: 10.1007/s00425-013-1918-9
- Park, W., Scheffler, B. E., Bauer, P. J., and Campbell, B. T. (2010). Identification of the family of aquaporin genes and their expression in upland cotton (*Gossypium hirsutum* L.). *BMC Plant Biol.* 10:142. doi: 10.1186/1471-2229-10-142
- Peng, Y., Lin, W., Cai, W., and Arora, R. (2007). Overexpression of a Panax ginseng tonoplast aquaporin alters salt tolerance, drought tolerance and cold acclimation ability in transgenic *Arabidopsis* plants. *Planta* 226, 729–740. doi: 10.1007/s00425-007-0520-4
- Perez Di Giorgio, J., Soto, G., Alleva, K., Jozefkowicz, C., Amodeo, G., Muschietti, J. P., et al. (2014). Prediction of aquaporin function by integrating evolutionary and functional analyses. *J. Membr. Biol.* 247, 107–125. doi: 10.1007/s00232-013-9618-8
- Perez-Martin, A., Michelazzo, C., Torres-Ruiz, J. M., Flexas, J., Fernández, J. E., Sebastiani, L., et al. (2014). Regulation of photosynthesis and stomatal and mesophyll conductance under water stress and recovery in olive trees: correlation with gene expression of carbonic anhydrase and aquaporins. *J. Exp. Bot.* 65, 3143–3156. doi: 10.1093/jxb/eru160
- Petritello, E., Godoy Herz, M. A., Barta, A., Kalyna, M., and Kornblith, A. R. (2014). Let there be light: regulation of gene expression in plants. *RNA Biol.* 11, 1215–1220. doi: 10.4161/rb.15476286.2014.972852
- Quigley, F., Rosenberg, J. M., Sharach-Hill, Y., and Bohnert, H. J. (2002). From genome to function: the *Arabidopsis* aquaporins. *Genome Biol.* 3:research0001.1. doi: 10.1186/gb-2001-3-1-research0001
- Ravel, C., Fiquet, S., Boudet, J., Dardevet, M., Vincent, J., Merlini, M., et al. (2014). Conserved cis-regulatory modules in promoters of genes encoding wheat high-molecular-weight glutenin subunits. *Front. Plant Sci.* 5:621. doi: 10.3389/fpls.2014.00621
- Reddy, P. S., Rao, T. S. R. B., Sharma, K. K., and Vadez, V. (2015). Genome-wide identification and characterization of the aquaporin gene family in *Sorghum bicolor* (L.). *Plant Gene* 1, 18–28. doi: 10.1016/j.plgene.2014.12.002
- Reuscher, S., Akiyama, M., Mori, C., Aoki, K., Shibata, D., and Shiratake, K. (2013). Genome-wide identification and expression analysis of aquaporins in tomato. *PLoS ONE* 8:e79052. doi: 10.1371/journal.pone.0079052
- Rivers, R. L., Dean, R. M., Chandy, G., Hall, J. E., Roberts, D. M., and Zeidel, M. L. (1997). Functional analysis of nodulin 26, an aquaporin in soybean root nodule symbiosomes. *J. Biol. Chem.* 272, 16256–16261. doi: 10.1074/jbc.272.26.16256
- Rushton, P. J., Reinstädler, A., Lipka, V., Lippok, B., and Somssich, I. E. (2002). Synthetic plant promoters containing defined regulatory elements provide novel insights into pathogen- and wound-induced signaling. *Plant Cell* 14, 749–762. doi: 10.1105/tpc.010412
- Sakurai, J., Ishikawa, F., Yamaguchi, T., Uemura, M., and Maeshima, M. (2005). Identification of 33 rice aquaporin genes and analysis of their expression and function. *Plant Cell Physiol.* 46, 1568–1577. doi: 10.1093/pcp/pci172
- Sakurai-Ishikawa, J., Murai-Hatano, M., Hayashi, H., Ahamed, A., Fukushi, K., Matsumoto, T., et al. (2011). Transpiration from shoots triggers diurnal changes in root aquaporin expression. *Plant Cell Environ.* 34, 1150–1163. doi: 10.1111/j.1365-3040.2011.02313.x
- Savage, D. F., Egea, P. F., Robles-Colmenares, Y., O'Connell, J. D. III, and Stroud, R. M. (2003). Architecture and selectivity in aquaporins: 2.5 Å X-ray structure of aquaporin Z. *PLoS Biol.* 1:e72. doi: 10.1371/journal.pbio.0000072
- Schmutz, J., Cannon, S. B., Schlueter, J., Ma, J., Mitros, T., Nelson, W., et al. (2010). Genome sequence of the palaeopolyploid soybean. *Nature* 463, 178–183. doi: 10.1038/nature08670
- Secchi, F., and Zwieniecki, M. A. (2014). Down-regulation of plasma intrinsic protein1 aquaporin in poplar trees is detrimental to recovery from embolism. *Plant Physiol.* 164, 1789–1799. doi: 10.1104/pp.114.237511
- Smart, L. B., Moskal, W. A., Cameron, K. D., and Bennett, A. B. (2001). MIP genes are down-regulated under drought stress in *Nicotiana glauca*. *Plant Cell Physiol.* 42, 686–693. doi: 10.1093/pcp/pce085
- Sommer, A., Geist, B., Da Ines, O., Gehwolf, R., Schaffner, A. R., and Obermeyer, G. (2008). Ectopic expression of *Arabidopsis thaliana* plasma membrane intrinsic protein 2 aquaporins in lily pollen increases the plasma membrane water permeability of grain but not of tube protoplasts. *New Phytol.* 180, 787–797. doi: 10.1111/j.1469-8137.2008.02607.x
- Sommer, A., Mahlknecht, G., and Obermeyer, G. (2007). Measuring the osmotic water permeability of the plant protoplast plasma membrane: implication of the nonosmotic volume. *J. Membr. Biol.* 215, 111–123. doi: 10.1007/s00232-007-9011-6
- Soto, G., Alleva, K., Amodeo, G., Muschietti, J., and Ayub, N. D. (2012). New insight into the evolution of aquaporins from flowering plants and vertebrates: orthologous identification and functional transfer is possible. *Gene* 503, 165–176. doi: 10.1016/j.gene.2012.04.021
- Suga, N., Takada, H., Nomura, A., Ohga, S., Ishii, E., Ihara, K., et al. (2002). Perforin defects of primary haemophagocytic lymphohistiocytosis in Japan. *Br. J. Haematol.* 116, 346–349. doi: 10.1046/j.1365-2141.2002.03266.x
- Takano, J., Wada, M., Ludewig, U., Schaaf, G., von Wirén, N., and Fujiwara, T. (2006). The *Arabidopsis* major intrinsic protein NIP5;1 is essential for efficient boron uptake and plant development under boron limitation. *Plant Cell* 18, 1498–1509. doi: 10.1105/tpc.106.041640
- Takase, T., Ishikawa, H., Murakami, H., Kikuchi, J., Sato-Nara, K., and Suzuki, H. (2011). The circadian clock modulates water dynamics and aquaporin expression in *Arabidopsis* roots. *Plant Cell Physiol.* 52, 373–383. doi: 10.1093/pcp/pcq198
- Tamura, K., Peterson, D., Peterson, N., Stecher, G., Nei, M., and Kumar, S. (2011). MEGA5: molecular evolutionary genetics analysis using maximum likelihood, evolutionary distance, and maximum parsimony methods. *Mol. Biol. Evol.* 28, 2731–2739. doi: 10.1093/molbev/msr121
- Tian, S., Wang, X., Li, P., Wang, H., Ji, H., Xie, J., et al. (2016). Plant aquaporin AtPIP1;4 links apoplastic H2O2 induction to disease immunity pathways. *Plant Physiol.* 171, 1635–1650. doi: 10.1104/pp.15.01237
- Tombuloglu, H., Ozcan, I., Tombuloglu, G., Sakcali, S., and Unver, T. (2016). Aquaporins in boron-tolerant barley: identification, characterization, and expression analysis. *Plant Mol. Biol. Report.* 34, 374–386. doi: 10.1007/s11105-015-0930-6
- Uehlein, N., Otto, B., Hanson, D. T., Fischer, M., McDowell, N., and Kaldenhoff, R. (2008). Function of *Nicotiana tabacum* aquaporins as chloroplast gas pores challenges the concept of membrane CO2 permeability. *Plant Cell* 20, 648–657. doi: 10.1105/tpc.107.054023
- Vandepoele, K., Casneuf, T., and Van de Peer, Y. (2006). Identification of novel regulatory modules in dicotyledonous plants using expression data and comparative genomics. *Genome Biol.* 7:R103. doi: 10.1186/gb-2006-7-11-r103
- Varshney, R. K., Song, C., Saxena, R. K., Azam, S., Yu, S., Sharpe, A. G., et al. (2013). Draft genome sequence of chickpea (*Cicer arietinum*) provides a resource for trait improvement. *Nat. Biotechnol.* 31, 240–246. doi: 10.1038/nbt.2491
- Venkatesh, J., Yu, J. W., and Park, S. W. (2013). Genome-wide analysis and expression profiling of the *Solanum tuberosum* aquaporins. *Plant Physiol. Biochem.* 73, 392–404. doi: 10.1016/j.plaphy.2013.10.025
- Voorrips, R. E. (2002). MapChart: software for the graphical presentation of linkage maps and QTLs. *J. Hered.* 93, 77–78. doi: 10.1093/jhered/93.1.77

- Wahid, A., and Close, T. J. (2007). Expression of dehydrins under heat stress and their relationship with water relations of sugarcane leaves. *Biol. Plant.* 51, 104–109. doi: 10.1007/s10535-007-0021-0
- Wallace, I. S., and Roberts, D. M. (2004). Homology modeling of representative subfamilies of *Arabidopsis* major intrinsic proteins. Classification based on the aromatic/arginine selectivity filter. *Plant Physiol.* 135, 1059–1068. doi: 10.1104/pp.103.033415
- Wang, L., Li, Q., Lei, Q., Feng, C., Gao, Y., Zheng, X., et al. (2015). MzPIP2;1: an aquaporin involved in radial water movement in both water uptake and transportation, altered the drought and salt tolerance of transgenic *Arabidopsis*. *PLoS ONE* 10:e0142446. doi: 10.1371/journal.pone.0142446
- Wang, M., Ling, N., Dong, X., Zhu, Y., Shen, Q., and Guo, S. (2012). Thermographic visualization of leaf response in cucumber plants infected with the soil-borne pathogen *Fusarium oxysporum* f. sp. *cucumerinum*. *Plant Physiol. Biochem.* 61, 153–161. doi: 10.1016/j.plaphy.2012.09.015
- Wang, M., Sun, Y., Sun, G., Liu, X., Zhai, L., Shen, Q., et al. (2015). Water balance altered in cucumber plants infected with *Fusarium oxysporum* f. sp. *cucumerinum*. *Sci Rep.* 5:7722. doi: 10.1038/srep07722
- Wang, Y., Tang, H., Debarry, J. D., Tan, X., Li, J., Wang, X., et al. (2012). MCScanX: a toolkit for detection and evolutionary analysis of gene synteny and collinearity. *Nucleic Acids Res.* 40, e49. doi: 10.1093/nar/gkr1293
- Xu, Y., Hu, W., Liu, J., Zhang, J., Jia, C., Miao, H., et al. (2014). A banana aquaporin gene, MaPIP1;1, is involved in tolerance to drought and salt stresses. *BMC Plant Biol.* 14:59. doi: 10.1186/1471-2229-14-59
- Yakata, K., Hiroaki, Y., Ishibashi, K., Sohara, E., Sasaki, S., Mitsuoka, K., et al. (2007). Aquaporin-11 containing a divergent NPA motif has normal water channel activity. *Biochim. Biophys. Acta* 1768, 688–693. doi: 10.1016/j.bbamem.2006.11.005
- Yang, S., and Cui, L. (2009). The action of aquaporins in cell elongation, salt stress and photosynthesis. *Sheng Wu Gong Cheng Xue Bao* 25, 321–327.
- Zhang da, Y., Ali, Z., Wang, C. B., Xu, L., Yi, J. X., Xu, Z. L., et al. (2013). Genome-wide sequence characterization and expression analysis of major intrinsic proteins in soybean (*Glycine max* L.). *PLoS ONE* 8:e56312. doi: 10.1371/journal.pone.0056312
- Zhou, S., Hu, W., Deng, X., Ma, Z., Chen, L., Huang, C., et al. (2012). Overexpression of the wheat aquaporin gene, TaAQP7, enhances drought tolerance in transgenic tobacco. *PLoS ONE* 7:e52439. doi: 10.1371/journal.pone.0052439

Conflict of Interest Statement: The authors declare that the research was conducted in the absence of any commercial or financial relationships that could be construed as a potential conflict of interest.

Copyright © 2016 Deokar and Tar'an. This is an open-access article distributed under the terms of the Creative Commons Attribution License (CC BY). The use, distribution or reproduction in other forums is permitted, provided the original author(s) or licensor are credited and that the original publication in this journal is cited, in accordance with accepted academic practice. No use, distribution or reproduction is permitted which does not comply with these terms.



Genome-Wide Identification of *Jatropha curcas* Aquaporin Genes and the Comparative Analysis Provides Insights into the Gene Family Expansion and Evolution in *Hevea brasiliensis*

OPEN ACCESS

Edited by:

Rupesh Kailasrao Deshmukh,
Laval University, Canada

Reviewed by:

Gunvant Baliram Patil,
University of Missouri, USA
Amit Atmaram Deokar,
University of Saskatchewan, Canada

***Correspondence:**

Zhi Zou
zouzhi2008@126.com;
Guishui Xie
xie23300459@163.com

[†]These authors have contributed
equally to this work.

Specialty section:

This article was submitted to
Plant Physiology,
a section of the journal
Frontiers in Plant Science

Received: 17 December 2015

Accepted: 14 March 2016

Published: 31 March 2016

Citation:

Zou Z, Yang L, Gong J, Mo Y, Wang J, Cao J, An F and Xie G (2016) Genome-Wide Identification of *Jatropha curcas* Aquaporin Genes and the Comparative Analysis Provides Insights into the Gene Family Expansion and Evolution in *Hevea brasiliensis*. *Front. Plant Sci.* 7:395.
doi: 10.3389/fpls.2016.00395

Zhi Zou ^{†*}, Lifu Yang [†], Jun Gong [†], Yeyong Mo, Jikun Wang, Jianhua Cao, Feng An and Guishui Xie ^{*}

Danzhou Investigation and Experiment Station of Tropical Crops, Ministry of Agriculture, Rubber Research Institute, Chinese Academy of Tropical Agricultural Sciences, Danzhou, China

Aquaporins (AQPs) are channel-forming integral membrane proteins that transport water and other small solutes across biological membranes. Despite the vital role of AQPs, to date, little is known in physic nut (*Jatropha curcas* L., Euphorbiaceae), an important non-edible oilseed crop with great potential for the production of biodiesel. In this study, 32 AQP genes were identified from the physic nut genome and the family number is relatively small in comparison to 51 in another Euphorbiaceae plant, rubber tree (*Hevea brasiliensis* Muell. Arg.). Based on the phylogenetic analysis, the JcAQPs were assigned to five subfamilies, i.e., nine plasma membrane intrinsic proteins (PIPs), nine tonoplast intrinsic proteins (TIPs), eight NOD26-like intrinsic proteins (NIPs), two X intrinsic proteins (XIPs), and four small basic intrinsic proteins (SIPs). Like rubber tree and other plant species, functional prediction based on the aromatic/arginine selectivity filter, Froger's positions, and specificity-determining positions showed a remarkable difference in substrate specificity among subfamilies of JcAQPs. Genome-wide comparative analysis revealed the specific expansion of PIP and TIP subfamilies in rubber tree and the specific gene loss of the XIP subfamily in physic nut. Furthermore, by analyzing deep transcriptome sequencing data, the expression evolution especially the expression divergence of duplicated HbAQP genes was also investigated and discussed. Results obtained from this study not only provide valuable information for future functional analysis and utilization of Jc/HbAQP genes, but also provide a useful reference to survey the gene family expansion and evolution in Euphorbiaceae plants and other plant species.

Keywords: physic nut (*Jatropha curcas* L.), rubber tree (*Hevea brasiliensis* Muell. Arg.), aquaporin, AQP gene family, expansion, evolution

INTRODUCTION

Aquaporins (AQPs) are channel-forming integral membrane proteins that transport water and other small solutes across biological membranes (Maurel et al., 2008; Gomes et al., 2009). Since their first identification and characterization in 1990s, AQPs have been found in all types of organisms, including microbes, animals, and plants (Gomes et al., 2009; Abascal et al., 2014). Although the overall sequence similarity can be low, AQPs are characterized by six transmembrane helices (TM1–TM6) connected by five loops (LA–LE), two half helices (HB and HE) formed by the opposite LB and LE dipping into the membrane, two NPA (Asn-Pro-Ala) motifs (located at the N-termini of HB and HE) and the aromatic/arginine (ar/R) selectivity filter (named H2, H5, LE1, and LE2) that determine the substrate specificity (Fu et al., 2000; Sui et al., 2001; Törnroth-Horsefield et al., 2006). Compared with microbes and animals, genome-wide surveys showed that AQPs are highly abundant and diverse in high plants (Table 1). According to the sequence similarity, plant AQPs can be divided into five main subfamilies, i.e., plasma membrane intrinsic proteins (PIPs), tonoplast intrinsic proteins (TIPs), NOD26-like intrinsic proteins (NIPs), small basic intrinsic proteins (SIPs), and uncategorized X intrinsic proteins (XIPs). Interestingly, the newly identified XIP subfamily has been found only in dicots beyond the Brassicaceae family (Johanson et al., 2001; Gupta and Sankararamakrishnan, 2009; Tao et al., 2014; Diehn et al., 2015). Corresponding to the high degree of compartmentalization of plant cells, plant AQPs are localized in the plasma membrane, tonoplasts/vacuoles, plastids,

mitochondria, endoplasmic reticulum, Golgi apparatus, and in some species, in membrane compartments interacting with symbiotic organisms (Wudick et al., 2009; Udvardi and Poole, 2013). In addition to water, function studies showed that plant AQPs also transport glycerol, urea, ammonia (NH_3), carbon dioxide (CO_2), hydrogen peroxide (H_2O_2), and metalloids such as boron and silicon (Maurel et al., 2008; Gomes et al., 2009; Pommerenig et al., 2015).

Euphorbiaceae is one of the largest plant family, which consists of more than 7000 species characterized with high photosynthesis and high biomass (Endress et al., 2013). There are many economically important species in Euphorbiaceae, such as rubber tree (*Hevea brasiliensis* Muell. Arg.), castor bean (*Ricinus communis* L.) and physic nut (*Jatropha curcas* L.). Rubber tree, also known as Para or Brazilian rubber tree, is a perennial big tree native to the Amazon basin. The natural rubber (*cis*-1,4-polyisoprene), produced by the rubber tree laticifer (a highly differentiated single-cell-type tissue located in the secondary phloem of the tree trunk), is an essential industrial raw materials for tires and other products (Zou et al., 2009; Prabhakaran Nair, 2010). Castor bean is a perennial shrub that originated from Africa. The oil extracted from castor seeds is mainly composed of the unusual hydroxylated fatty acid ricinoleic acid and thus widely used for industrial, medicinal, and cosmetic purposes (Ogunniyi, 2006). Physic nut is a perennial shrub or small tree native to central America and now is widely cultivated in many tropical and subtropical countries in Asia and Africa (Montes Osorio et al., 2014). As a non-food oilseed crop, physic nut has great potential for the production of biodiesel, which features

TABLE 1 | Diversity of AQP gene family in high plants.

Species	Common name	Family	Type of organism	PIPs	TIPs	NIPs	SIPs	XIPs	Total	References
<i>Oryza sativa</i>	Rice	Poaceae	Monocot	11	10	10	2	0	33	Sakurai et al., 2005
<i>Zea mays</i>	Maize	Poaceae	Monocot	13	12	5	3	0	33	Chaurand et al., 2001
<i>Hordeum vulgare</i>	Barley	Poaceae	Monocot	20	11	8	1	0	40	Hove et al., 2015
<i>Musa acuminata</i>	Banana	Musaceae	Monocot	18	17	9	3	0	47	Hu W. et al., 2015
<i>Arabidopsis thaliana</i>	Arabidopsis	Brassicaceae	Dicot	13	10	9	3	0	35	Johanson et al., 2001; Quigley et al., 2002;
<i>Brassica rapa</i>	Chinese cabbage	Brassicaceae	Dicot	23	16	15	6	0	60	Tao et al., 2014; Diehn et al., 2015
<i>Brassica oleracea</i>	Cabbage	Brassicaceae	Dicot	25	19	17	6	0	67	Diehn et al., 2015
<i>Solanum tuberosum</i>	Pomato	Solanaceae	Dicot	15	11	10	3	8	47	Venkatesh et al., 2013
<i>Solanum lycopersicum</i>	Garden tomato	Solanaceae	Dicot	14	11	12	4	6	47	Reuscher et al., 2013
<i>Glycine max</i>	Soybean	Fabaceae	Dicot	22	23	17	8	2	72	Deshmukh et al., 2013; Zhang et al., 2013
<i>Gossypium hirsutum</i>	Upland cotton	Malvaceae	Dicot	28	23	12	7	1	71	Park et al., 2010
<i>Vitis vinifera</i>	Grapevine	Vitaceae	Dicot	8	11	9	2	2	32	Jaillon et al., 2007; Shelden et al., 2009
<i>Citrus sinensis</i>	Sweet orange	Rutaceae	Dicot	8	11	9	3	3	34	de Paula Santos Martins et al., 2015
<i>Phaseolus vulgaris</i>	Common bean	Fabaceae	Dicot	12	13	10	4	2	41	Ariani and Gepts, 2015
<i>Jatropha curcas</i>	Physic nut	Euphorbiaceae	Dicot	9	9	8	4	2	32	This study
<i>Ricinus communis</i>	Castor bean	Euphorbiaceae	Dicot	10	9	8	4	6	37	Zou et al., 2015b
<i>Hevea brasiliensis</i>	Rubber tree	Euphorbiaceae	Dicot	15	17	9	4	6	51	Zou et al., 2015a
<i>Populus trichocarpa</i>	Poplar	Salicaceae	Dicot	15	17	11	6	6	55	Gupta and Sankararamakrishnan, 2009

high seed oil content (up to 50%), fossil fuel-like oil composition (unsaturated fatty acids >75%) and adaptation to semiarid and barren soil environments (Fairless, 2007; Montes Osorio et al., 2014). Thus far, the genome sequences of these three diploid plant species (Arumuganathan and Earle, 1991; Leitch et al., 1998; Carvalho et al., 2008) were all obtained through whole genome sequencing (Chan et al., 2010; Sato et al., 2011; Rahman et al., 2013; Wu et al., 2015). The genome size of castor bean is approximate 400 Mb, and the 4.6 × draft genome available consists of 25,878 scaffolds containing 31,221 putative protein-coding genes (Chan et al., 2010). The genome size of physic nut is about 350 Mb, and two assembled genomes of a line originating from the Palawan Island and an inbred cultivar GZQX0401 have been reported (Sato et al., 2011; Wu et al., 2015). The draft genome reported by Sato et al. (2011) is 285,858,490 bp consisting of 120,586 contigs and 29,831 singlets, and a number of 40,929 complete and partial structures of protein encoding genes have been deduced. Later, 537 million paired-end Illumina reads were integrated and the length of the upgraded genome sequences reached 297,661,187 bp consisting of 39,277 scaffolds (Hirakawa et al., 2012). The more complete genome assembly reported by Wu et al. (2015) is 320,546,307 bp consisting of 72,474 contigs longer than 100 bp, and the contigs were further assembled into 23,125 scaffolds with an N50 of 0.746 Mbp which is considerably longer than that of the previous reported one (0.016 Mbp). As a result, the number of putative protein-encoding genes was reduced from 30,203 (Hirakawa et al., 2012) to 27,172 (Wu et al., 2015) since more genes are complete. By comparison, the genome size of rubber tree is considerably larger and the reported assembly spans about 1.1 Gb of the estimated 2.15 Gb haploid genome (Bennett and Leitch, 1997; Rahman et al., 2013). In agreement with this, the number of predicted gene models in rubber tree is 68,955, which is more than two-folds of that in castor bean and physic nut (Chan et al., 2010; Rahman et al., 2013; Wu et al., 2015). Since both castor bean and physic nut underwent no recent whole-genome duplication (WGD) event (Chan et al., 2010; Wu et al., 2015), the duplicated rubber tree genes are more likely to be resulted from an unknown recent doubling event. Lately, two papers reported the identification of AQP genes encoded in the genomes of rubber tree and castor bean (Zou et al., 2015a,b). The family number of 51 in rubber tree (Zou et al., 2015a) is comparable to 55 in poplar (Gupta and Sankararamakrishnan, 2009), a Salicaceae tree species also belongs to Malpighiales which was shown to undergo a recent doubling event (Tuskan et al., 2006). In contrast, castor bean contains as few as 37 family members. Although the evolutionary relationship of AQPs between rubber tree and castor bean is not investigated yet, the classification of subfamily and even subfamily into subgroups was shown to be the same: the PIP subfamily contains two subgroups; the TIP subfamily contains five subgroups; the NIP subfamily contains seven subgroups; the SIP subfamily contains two subgroups; and the XIP subfamily contains three subgroups (Zou et al., 2015a,b). Compared with rubber tree and castor bean, the molecular characterization of physic nut AQPs (JcAQPs) is still in its infancy. As of Sep 2015, only two full-length AQP cDNAs have been reported (Zhang et al., 2007; Jang et al., 2013; Khan et al., 2015). The available

genome and several tissue transcriptome datasets (King et al., 2011; Natarajan and Parani, 2011; Sato et al., 2011; Hirakawa et al., 2012; Jiang et al., 2012; Wang H. et al., 2013; Juntawong et al., 2014; Pan et al., 2014; Zhang et al., 2014, 2015; Wu et al., 2015) provide an opportunity to analyze the physic nut AQP gene family from a global view.

In this study, a genome-wide search was carried out to identify the physic nut AQP genes. Functional prediction was performed based on the ar/R filter (i.e., H2 in TM2, H5 in TM5, LE1 and LE2 in LE) (Törnroth-Horsefield et al., 2006), Froger's positions (five conserved amino acid residues named P1–5 for discriminating glycerol-transporting aquaglyceroporins from water-conducting AQPs) (Froger et al., 1998) and specificity-determining positions (SDP1–SDP9, important for determining the specificity of non-aqua substrates) (Hove and Bhave, 2011), and their expression profiles were examined using deep transcriptome sequencing data. Furthermore, their evolutionary relationships with HbAQPs and RcAQPs as well as the expression evolution of the duplicated HbAQP genes were also investigated.

MATERIALS AND METHODS

Identification of JcAQP Genes

The AQPs in *Arabidopsis* (Johanson et al., 2001), poplar (Gupta and Sankararamakrishnan, 2009), rubber tree (Zou et al., 2015a), and castor bean (Zou et al., 2015b) described before were obtained according to the literatures (the accession number can be found in Supplementary Table S1). The genome sequences, nucleotides, Sanger ESTs (expressed sequence tags), and raw RNA sequencing reads were downloaded from NCBI GenBank or SRA (sequence read archive) databases, respectively (<http://www.ncbi.nlm.nih.gov/>). The deduced amino acid sequences of published JcAQP genes (Zhang et al., 2007; Jang et al., 2013) were used as queries to search the physic nut genome (Sato et al., 2011; Wu et al., 2015) for homologs. Sequences with an $E < 1e^{-5}$ in the tBlastn search (Altschul et al., 1997) were selected for further analysis. The predicted gene models were checked with ESTs and RNA sequencing reads, and the gene structures were displayed using GSDS (Hu B. et al., 2015). Homology search was performed using Blastn (Altschul et al., 1997) and ESTs with the identity of more than 98% were taken into account. RNA sequencing data from callus, root, leaf, flower, inflorescence meristem, seed, and embryo described before (King et al., 2011; Natarajan and Parani, 2011; Sato et al., 2011; Hirakawa et al., 2012; Jiang et al., 2012; Wang H. et al., 2013; Juntawong et al., 2014; Pan et al., 2014; Zhang et al., 2014, 2015; Wu et al., 2015) were also adopted for the expression annotation to determine whether genes are expressed. The clean reads were obtained by removing adaptor sequences, adaptor-only reads, and low quality reads containing more than 50% bases with $Q \leq 5$. Read mapping was performed using Bowtie 2 (Langmead and Salzberg, 2012) with default parameters, and mapped read number of more than one was counted as expressed. The alternative splicing isoforms were identified using Cufflinks (v2.2.1) (Trapnell et al., 2012). The ortholog of each JcAQP in *Arabidopsis*, poplar, rubber tree, and castor bean was identified using Blastp (Altschul et al., 1997) (E -value, $1e^{-20}$) against

AtAQPs, PtAQPs, HbAQPs, and RcAQPs, and the best hit was collected.

Sequence Alignments, Phylogenetic Analysis, and Classification

Multiple sequence alignments of deduced peptides were carried out using ClustalX (Thompson et al., 1994), and the unrooted phylogenetic tree was constructed using MEGA6 (Tamura et al., 2013) with the maximum likelihood method (bootstrap: 1000). Classification of AQPs into subfamilies and subgroups was done as described before (Zou et al., 2015a) and the systematic names were assigned based on their evolutionary relationships.

Structural Features of JcAQPs

Protein properties such as the molecular weight (MW) and isoelectric point (*pI*), were calculated using ProtParam (<http://web.expasy.org/protparam/>). The subcellular localization and transmembrane regions were predicted using WoLF PSORT (Horton et al., 2007) and TOPCONS (Bersnel et al., 2009), respectively. Functional prediction was performed based on dual NPA motifs, the ar/R filter, five Froger's positions and nine SDPs from alignments with the structure resolved *Spinacia oleracea* PIP2;1 and functionally characterized AQPs (Froger et al., 1998; Törnroth-Horsefield et al., 2006; Hove and Bhave, 2011).

Gene Expression Analysis

To investigate the global gene expression profiles among different tissues, Illumina RNA sequencing data derived from physic nut root (NCBI SRA accession number SRX750579), leaf (SRX750580), and seed (SRX750581) (Wu et al., 2015) as well as rubber tree laticifer (SRX278514), bark (SRX278513), and leaf (SRX278515) (Chow et al., 2014) described before was examined. The obtained clean reads were mapped to the CDS of 32 *JcAQPs* and 51 *HbAQPs* as well as available transcripts using Bowtie 2 (Langmead and Salzberg, 2012), and the FPKM (fragments per kilobase of exon per million fragments mapped) method (Mortazavi et al., 2008) was used for the determination of transcript levels. Unless specific statements, the tools used in this study were performed with default parameters.

RESULTS

Identification and Classification of JcAQP Genes

The homology search resulted in 32 loci putatively encoding AQP-like genes from both assembled physic nut genomes. Since all AQP-encoding loci identified in the Palawan genome were found in the genome of GZQX0401 but some genes from Palawan are incomplete, the AQP genes from GZQX0401 were selected for further analyses (Table 2). Among them, 31 loci were predicted by the automatic genome annotation (Wu et al., 2015), whereas one more locus putatively encodes a SIP subfamily member (i.e., *JcSIP1;1*) was identified from the scaffold2033 (GenBank accession number KK916495). Read alignments indicated that the transcriptional region of this gene is 5368 bp, including two introns (590 and 3167 bp, respectively), 329-bp 5' UTR and 562-bp 3' UTR (see Supplementary File S1). The gene structure

is also supported by two ESTs (GenBank accession numbers, FM894285 and GW875379). Sequence alignments showed that most predicted gene models of JcAQPs were validated with ESTs and/or RNA sequencing reads (Table 2), however, three loci (i.e., JCGZ_02114, JCGZ_19604, and JCGZ_01828) seem not to be properly annotated. The locus JCGZ_02114 (*JcNIP7;1*) was predicted to harbor four introns encoding 618 residues (Wu et al., 2015) which is considerably longer than that of any other NIP subfamily members, however, sequence alignment showed that the N- and C-termini of the deduced protein are homologous with eukaryotic aspartyl protease family proteins and NOD26-like intrinsic proteins, i.e., AT1G03220 and AT3G06100 (*AtNIP7;1*) in *Arabidopsis*, respectively. Further read alignments supported the existence of two genes: the first one contains no intron and putatively encodes an aspartyl protease of 451 residues, and the second one harbors four introns encoding an NIP of 265 residues (Supplementary File S2). The locus JCGZ_19604 (*JcXIP1;1*) was predicted to encode 271 residues, which is relatively shorter than 289 residues of its ortholog in rubber tree (Zou et al., 2015a), thus we carefully investigated these two genes and found that a number of 67-bp sequences toward the 5' of the CDS missed from the genome annotation (Supplementary File S3). Thereby, the CDS length of this locus was extended to 885 bp putatively encoding 294 residues (Supplementary File S3). The locus JCGZ_01828 (*JcSIP1;2*) was predicted to contain no intron encoding 235 residues, however, read alignments showed that the transcriptional region of this gene is 992 bp putatively encoding 242 residues (Supplementary File S4).

The 32 identified JcAQP genes were found to be distributed across 26 scaffolds. Although most scaffolds harbor only one AQP gene, five scaffolds (i.e., scaffold660, scaffold473, scaffold595, scaffold1149, and scaffold18) were shown to have two or three AQP genes (Table 2). All JcAQP genes can be further assigned to the 11 chromosomes (Wu et al., 2015). Although all these chromosomes contain at least one AQP gene, the distribution of AQP loci seems unevenly. Among six chromosomes encoding more than one AQP locus, chromosome 2 occupies the largest number of 8 (Table 2).

Along with the genome sequences, as of Sep 2015, 46,865 Sanger ESTs derived from cDNA libraries (including flower, seed, endosperm, embryo, and root) and deep transcriptome sequencing data of several tissues such as callus, root, leaf, flower, inflorescence meristem, seed, and embryo were also available in NCBI. Sequence alignments showed that 15 out of 32 JcAQP genes had EST hits in GeneBank, and *JcTIP1;1* matched the maximum number of 186 ESTs. Except for *JcPIP1;3* and *JcXIP1;1*, read alignments further supported the expression of other 15 JcAQP genes. With the exception of *JcPIP1;3*, *JcXIP1;1*, and *JcNIP4;1*, the transcriptional region of other JcAQP genes was extended. In addition, alternative splicing isoforms existing in 15 AQP-encoding loci were supported by RNA sequencing reads, and four even by Sanger ESTs (i.e., *JcPIP1;2*, *JcTIP1;1*, *JcTIP2;2*, and *JcNIP6;1*) (Table 2).

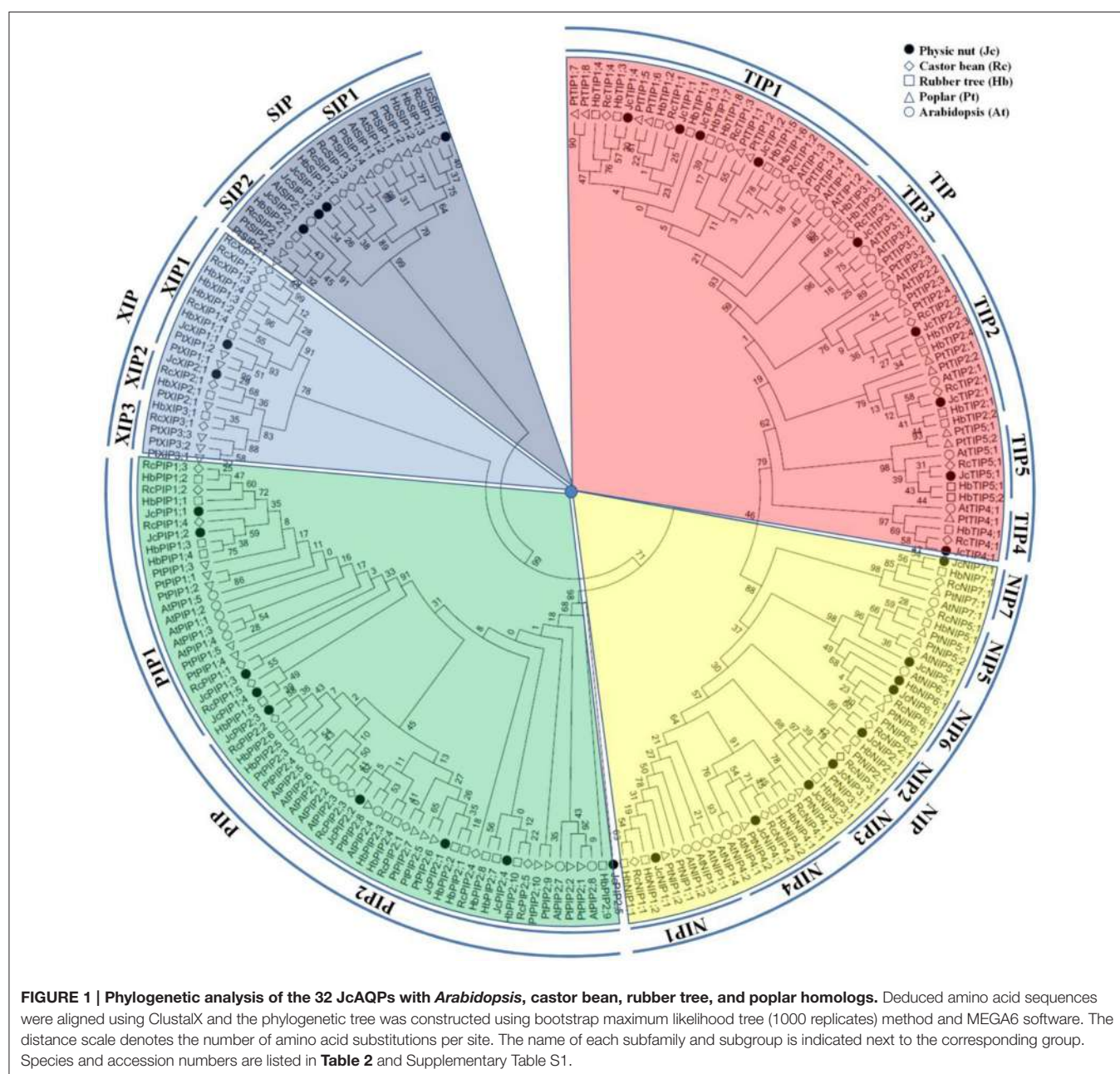
To reveal the evolutionary relationship and gain more information about their putative function, an unrooted phylogenetic tree was constructed using MEGA6 from the

TABLE 2 | List of the 32 JcAQPs genes identified in this study.

Name	Scaffold ID	Locus ID	Predicted position	Identified position	Chr	Nucleotide length (bp, from start to stop codons)	EST hits	Expressed	Alternative splicing	AtAQPs ortholog		PtaAQPs ortholog		RcAQPs ortholog		HbAQPs ortholog	
										CDS	Gene	EST	Read	EST	Read	EST	Read
JcPIP1;1	Scaffold11	JCGZ_01316	1070240-1071401	1069930-1071930	LG10	864	1162	66	Yes	-	-	AtPIP1;1	PtPIP1;3	RcPIP1;3	HbPIP1;2		
JcPIP1;2	Scaffold660	JCGZ_20680	1435150-1432165	1435625-1431654	LG9	864	2986	26	Yes	Yes	Yes	AtPIP1;1	PtPIP1;3	RcPIP1;4	HbPIP1;4		
JcPIP1;3	Scaffold843	JCGZ_25040	422332-423912	422332-423912	LG6	639	1581	-	-	-	-	AtPIP1;1	PtPIP1;5	RcPIP1;1	HbPIP1;5		
JcPIP1;4	Scaffold392	JCGZ_14388	3034258-3032720	3034588-3032444	LG8	861	1539	1	Yes	-	Yes	AtPIP1;1	PtPIP1;5	RcPIP1;5	HbPIP1;5		
JcPIP2;1	Scaffold473	JCGZ_16499	528238-527109	528393-526820	LG6	855	1185	17	Yes	-	-	AtPIP2;4	PtPIP2;7	RcPIP2;1	HbPIP2;1		
JcPIP2;2	Scaffold18	JCGZ_05520	1671011-1673093	1670693-1673533	LG2	861	1654	9	Yes	-	Yes	AtPIP2;4	PtPIP2;8	RcPIP2;3	HbPIP2;4		
JcPIP2;3	Scaffold63	JCGZ_20043	224967-221774	225179-220824	LG10	858	3194	7	Yes	-	Yes	AtPIP2;5	PtPIP2;4	RcPIP2;2	HbPIP2;6		
JcPIP2;4	Scaffold540	JCGZ_18836	689605-690883	689338-691284	LG2	843	1939	50	Yes	-	Yes	AtPIP2;8	PtPIP2;2	RcPIP2;4	HbPIP2;7		
JcPIP2;5	Scaffold872	JCGZ_25357	143964-140778	144178-140525	LG9	852	3187	4	Yes	-	Yes	AtPIP2;8	PtPIP2;9	RcPIP2;4	HbPIP2;9		
JcTIP1;1	Scaffold473	JCGZ_16577	1075843-1074990	1076252-1074449	LG6	759	854	186	Yes	Yes	Yes	AtTIP1;1	PtTIP1;6	RcTIP1;1	HbTIP1;2		
JcTIP1;2	Scaffold528	JCGZ_18448	657196-655908	657291-655693	LG10	759	1289	-	Yes	-	Yes	AtTIP1;3	PtTIP1;1	RcTIP1;2	HbTIP1;5		
JcTIP1;3	Scaffold18	JCGZ_05655	2916885-2918031	2916391-2919915	LG2	759	1070	-	Yes	-	Yes	AtTIP1;3	PtTIP1;1	RcTIP1;3	HbTIP1;7		
JcTIP1;4	Scaffold18	JCGZ_05430	531115-532094	531009-532425	LG2	765	980	-	Yes	-	Yes	AtTIP1;1	PtTIP1;7	RcTIP1;4	HbTIP1;3		
JcTIP2;1	Scaffold191	JCGZ_06324	1941464-1942389	1941333-1942205	LG2	747	1304	40	Yes	-	Yes	AtTIP2;1	PtTIP2;2	RcTIP2;1	HbTIP2;1		
JcTIP2;2	Scaffold137	JCGZ_03415	265803-267097	265749-267564	LG9	753	1295	3	Yes	Yes	Yes	AtTIP2;2	PtTIP2;4	RcTIP2;2	HbTIP2;3		
JcTIP3;1	Scaffold23	JCGZ_08448	71937-71012	72143-70768	LG8	774	927	28	Yes	-	-	AtTIP3;2	PtTIP3;2	RcTIP3;1	HbTIP3;1		
JcTIP4;1	Scaffold211	JCGZ_07757	4725255-4724215	4725438-4724041	LG11	744	1041	1	Yes	-	-	AtTIP4;1	PtTIP4;1	RcTIP4;1	HbTIP4;1		
JcTIP5;1	Scaffold906	JCGZ_26261	21389472-2140440	2138913-2140560	LG5	759	969	-	Yes	-	-	AtTIP5;1	PtTIP5;2	RcTIP5;1	HbTIP5;1		
JcNIP1;1	Scaffold684	JCGZ_21622	2673636-2675513	2673356-2675705	LG3	828	1878	-	Yes	-	-	AtNIP1;2	PtNIP1;1	RcNIP1;1	HbNIP1;1		
JcNIP2;1	Scaffold617	JCGZ_19849	96979-94697	97540-94138	LG9	876	2283	-	Yes	-	-	AtNIP2;1	PtNIP2;1	RcNIP2;1	HbNIP2;1		
JcNIP3;1	Scaffold46	JCGZ_15791	1520636-1519402	1520800-1519402	LG4	834	1235	-	Yes	-	-	AtNIP3;1	PtNIP3;1	RcNIP3;1	HbNIP3;1		
JcNIP3;2	Scaffold8	JCGZ_24027	126258-127532	126113-127676	LG7	843	1275	-	Yes	-	-	AtNIP3;1	PtNIP3;1	RcNIP3;1	HbNIP3;1		
JcNIP4;1	Scaffold1210	JCGZ_02488	12952-14295	12952-14295	LG9	792	1344	1	Yes	-	-	AtNIP4;2	PtNIP4;2	RcNIP4;2	HbNIP4;2		
JcNIP5;1	Scaffold660	JCGZ_20348	126085-128887	124382-130375	LG9	897	2803	2	Yes	-	-	AtNIP5;1	PtNIP5;1	RcNIP5;1	HbNIP5;1		
JcNIP6;1	Scaffold96	JCGZ_27003	2282049-2284301	2281766-2285794	LG2	924	2253	-	Yes	Yes	Yes	AtNIP6;1	PtNIP6;1	RcNIP6;1	HbNIP6;1		
JcNIP7;1	Scaffold119	JCGZ_02114	698621-702542	701200-702613	LG1	798	1124	-	Yes	-	-	AtNIP7;1	PtNIP7;1	RcNIP7;1	HbNIP7;1		
JcXIP1;1	Scaffold595	JCGZ_19604	291308-292309	291239-292309	LG2	885	1071	-	-	-	-	PtXIP1;1	RcXIP1;3	HbXIP1;1			
JcXIP2;1	Scaffold595	JCGZ_19603	2883337-289806	288124-289999	LG2	912	1470	-	Yes	-	-	PtXIP2;1	RcXIP2;1	HbXIP2;1			
JcSIP1;1	Scaffold2033	-	-	-	LG6	720	4477	-	Yes	-	Yes	AtSIP1;1	PtSIP1;2	RcSIP1;1	HbSIP1;3		
JcSIP1;2	Scaffold149	JCGZ_01828	248685-247978	248898-247991	LG7	729	-	-	Yes	-	-	AtSIP1;1	PtSIP1;4	RcSIP1;3	HbSIP1;1		
JcSIP1;3	Scaffold1149	JCGZ_01827	247059-246328	247514-246040	LG7	732	-	-	Yes	-	-	AtSIP1;1	PtSIP2;1	RcSIP2;1	HbSIP2;1		
JcSIP2;1	Scaffold407	JCGZ_14885	34721-215023	35046-24630	LG6	726	6716	-	Yes	-	Yes	AtSIP2;1	PtSIP2;1	RcSIP2;1	HbSIP2;1		

deduced amino acid sequences of JcAQPs together with that from castor bean (RcAQPs), rubber tree (HbAQPs) and two well-studied model plant species, *Arabidopsis* (AtAQPs) and poplar (PtAQPs) (**Figure 1**). According to the phylogenetic analysis, the identified JcAQPs were grouped into five subfamilies, i.e., PIP (9), TIP (9), NIP (8), SIP (4), and XIP (2) (**Table 2** and **Figure 1**). Following the nomenclature of rubber tree, the JcPIP subfamily was further divided into two phylogenetic subgroups (4 JcPIP1s and 5 JcPIP2s), the JcTIP subfamily into five subgroups (4 JcTIP1s, 2 JcTIP2s, 1 JcTIP3, 1 JcTIP4, and 1 JcTIP5), the JcNIP subfamily into seven subgroups (1 JcNIP1, 1 JcNIP2, 2 JcNIP3s, 1 JcNIP4, 1 JcNIP5, 1 JcNIP6, and 1

JcNIP7), the JcSIP subfamily into two subgroups (3 JcSIP1s and 1 JcSIP2), and the JcXIP subfamily into two subgroups (1 JcXIP1 and 1 JcXIP2) (**Figure 1**). It's worth noting that AtNIP2;1 and AtNIP3;1 were assigned into the NIP1 subgroup in this study (Supplementary Table S1), mainly for their closer cluster with the NIP1 subgroup and sharing the highest similarity with NIP1s from physic nut, castor bean, rubber tree, and poplar (**Figure 1**). Thereby, *Arabidopsis* is shown to lose the NIP2 and NIP3 subgroups as well as the XIP subfamily in comparison to other four plant species (**Figures 1, 2**). Homology analysis indicated that the 32 JcAQPs have 30 counterparts in rubber tree, 29 in castor bean and 27 in poplar, whereas only 27 out of



them have orthologs with a number of 18 in *Arabidopsis* (Table 2 and Figure 1), indicating the expansion and loss of certain AQP genes in castor bean, rubber tree, poplar, and *Arabidopsis*. Indeed, as shown in Figure 1, a high number of *Arabidopsis* (11), poplar (23), and rubber tree (17) AQP genes were grouped in pairs, corresponding to the occurrence of more than one WGD events in these plants (Bowers et al., 2003; Tuskan et al., 2006; Zou et al., 2015a). In contrast, very few AQP gene pairs were identified in physic nut (2) and castor bean (5) (Figure 1), which is consistent with no recent WGD event occurred in these two plant species (Chan et al., 2010; Wu et al., 2015). Besides gene expansion, gene loss was also observed in physic nut as seen in *Arabidopsis*. For example, castor bean, rubber tree and poplar harbor three XIP subgroups, whereas physic nut only contains the subgroups XIP1 and XIP2 (Figures 1, 2); castor bean, rubber tree and poplar have two NIP4s that are clustered with their counterparts, respectively; however, physic nut only contains the ortholog of *RcNIP4;2/HbNIP4;2/PtNIP4;2*; the ortholog of *RcPIP1;2/HbPIP1;3* was also lost in physic nut (Figure 1). In addition, compared with physic nut and castor bean, the PIP and TIP subfamilies in rubber tree are shown to be highly expanded (Figure 2).

Analysis of Exon-Intron Structure

The exon-intron structures of 32 *JcAQPs* were analyzed based on the optimized gene models. Although the ORF (open reading frame) length of each gene is consistent (639–924 bp, similar to 627–830 bp in castor bean, and 684–927 bp in rubber tree), the gene size (from start to stop codons) is distinct (729–6716 bp, longer than 705–4934 bp in castor bean and shorter than 720–13,833 bp in rubber tree) (Table 2 and Figure 3; Zou et al., 2015a,b). The *JcAQP* introns have an average length of about

380 bp (same as that in castor bean but relatively shorter than 404 bp in rubber tree), with the minimum of 63 bp in *JcNIP4;1* (corresponding to 46 bp in *RcPIP2;5* and 71 bp in *HbNIP2;1*) and the maximum of 5879 bp in *JcSIP2;1* (corresponding to 3360 bp in *RcNIP5;1* and 13,000 bp in *HbSIP2;1*) (Figure 3; Zou et al., 2015a,b). Like observed in rubber tree and castor bean (Zou et al., 2015a,b), AQP genes in different subfamilies harbor distinct exon-intron structures. Except for *JcPIP1;3* that contains four introns, other *JcPIP* subfamily members feature three introns (83–481, 90–1751, and 87–487 bp, respectively). It is worth noting that *JcPIP1;3* is more likely to be a pseudogene, because no evidence is available for its expression and a C deletion at the 82th position and an A/T mutation at the 456th position were observed when compared with other *JcPIP1* genes. Most *JcTIPs* contain two introns (75–302 bp and 77–372 bp, respectively), while *JcTIP1;1* and *JcTIP1;4* contain only one intron. Most *JcNIPs* harbor four introns (70–1063, 72–957, 79–980, and 88–262 bp, respectively), whereas *JcNIP5;1* contain three introns instead. Two out of three *JcSIP1s* don't contain introns, in contrast, *JcSIP1;3* and the only *JcSIP2* subgroup member *JcSIP2;1* harbor two introns. The two identified *JcXIP* subfamily members *JcXIP1;1* and *JcXIP2;1* contain one or two introns, respectively (Figure 3).

Subcellular Localization, Structural Features, and Functional Inference

Sequence analysis showed that the 32 deduced *JcAQPs* range from 212 to 307 amino acids, with the theoretical molecular weight of 22.57 to 32.29 kDa and the pI value of 4.96 to 10.02. Homology analysis of these deduced proteins revealed a high sequence diversity existing within and between the five subfamilies. The sequence similarities of 57.6–92.9% were

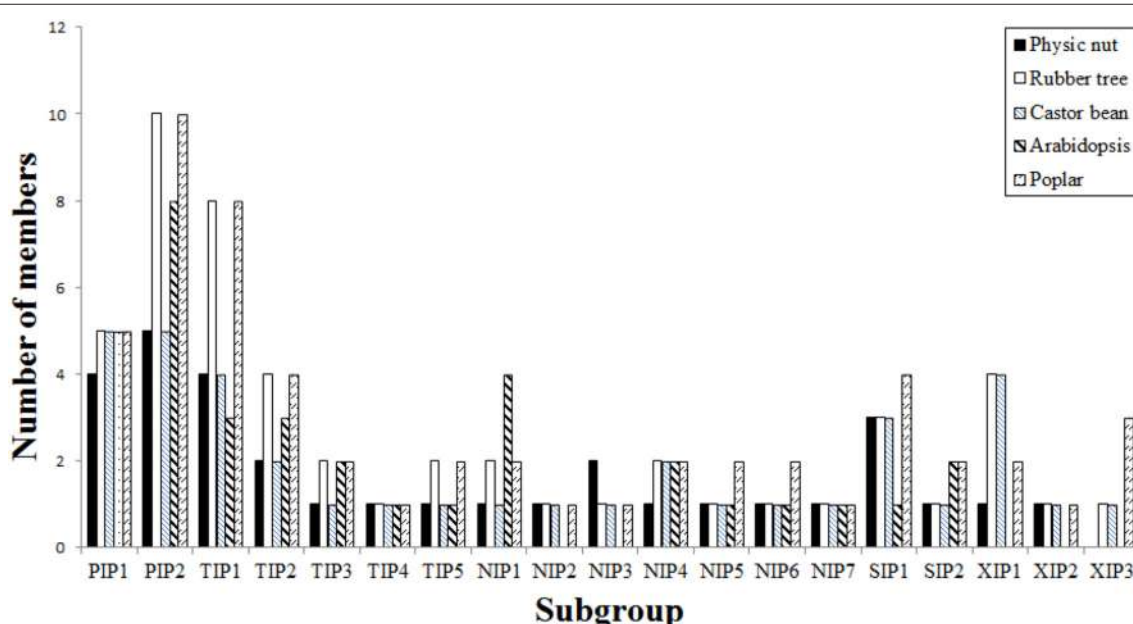


FIGURE 2 | Distribution of the 32 *JcAQP* genes and their *Arabidopsis*, castor bean, rubber tree, and poplar homologs in subgroups.

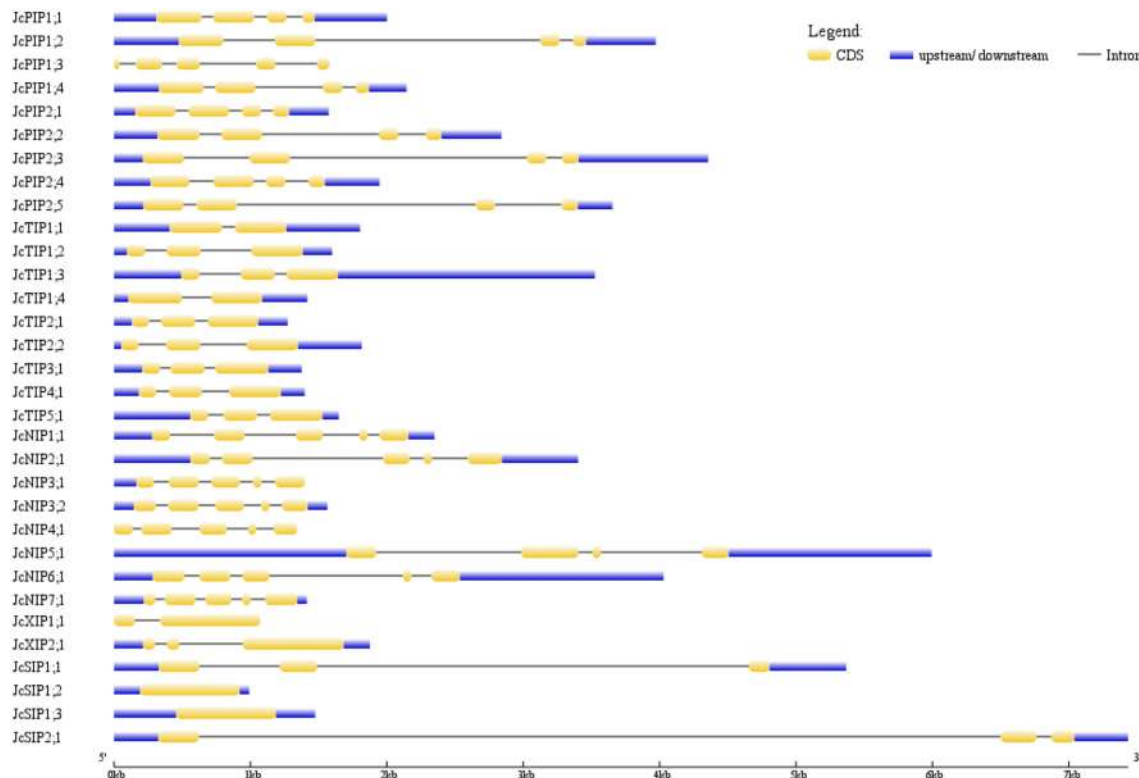


FIGURE 3 | Exon-intron structures of the 32 JcAQP genes. The graphic representation of the gene models is displayed using GSDS.

found within JcTIPs, 56.5–94.4% within JcPIPs, 43.5–81.1% within JcSIPs, 42.4–73.3% within JcNIPs, and 49.5% within JcXIPs. JcPIPs share sequence similarities of 32.1–47.9, 29.9–41.0, 24.8–37.8, or 23.4–31.6% with JcTIPs, JcXIPs, JcNIPs, and JcSIPs, respectively. JcTIPs show 30.3–40.9, 29.9–37.3, or 29.5–35.6% sequence similarities with JcNIPs, JcSIPs, and JcXIPs, respectively. JcNIPs share sequence similarities of 29.4–36.7 or 23.9–32.0% with JcXIPs and JcSIPs, respectively, whereas JcSIPs share the lowest sequence similarity of 22.6–27.3% with JcXIPs (Supplementary Table S2). These results indicated that the SIP subfamily has formed an outstanding group to other subfamilies, and the XIP subfamily share a closer evolutionary relationship with the PIP subfamily than with other subfamilies. Despite the overall sequence similarities between different subfamily members are relatively low, topological analyses showed that all JcAQPs were predicted to harbor six transmembrane helical domains, which is consistent with the results from multiple alignments with structure proven AQPs (Table 3 and Supplementary File S5).

As the names suggested, JcPIPs with an average *pI* value of 8.56 and JcTIPs with an average *pI* value of 5.95 were predicted to localize to the plasma membrane or vacuole, respectively, though several PIPs in other plant species were also shown to target the chloroplast membrane (Ferro et al., 2003; Uehlein et al., 2008; Beebo et al., 2013). NIPs were determined to localize to the plasma membrane, endoplasmic reticulum or peribacteroid membrane of root nodules in other organisms (Ma

et al., 2006; Mizutani et al., 2006; Takano et al., 2006), whereas our *in silico* predictions indicated that JcNIPs with an average *pI* value of 7.82 are mainly localized to the plasma membrane except for the vacuole prediction of JcNIP3;2. JcSIPs with an average *pI* value of 9.73 were predicted to localize to the plasma membrane and vacuole, however, *Arabidopsis* and grapevine SIPs were shown to be localized to the endoplasmic reticulum (Ishikawa et al., 2005; Noronha et al., 2014). Two JcXIPs with an average *pI* value of 6.32 were predicted to localize to the plasma membrane, which is consistent with the experimental results (Bienert et al., 2011). Nevertheless, thus far, only the plasma membrane localization of JcPIP2;4 and the vacuole localization of JcTIP1;2 have been confirmed by experimental means yet (Khan et al., 2015).

Although AQPs were first identified for their high water permeability, accumulating evidence shows that some of them also transport glycerol, urea, boric acid, silicic acid, NH₃, CO₂, H₂O₂, etc. Atomic resolution and molecular dynamics stimulations indicated that the ar/R filter, NPA motifs and Froger's positions all affect the substrate specificity: the two opposite NPA motifs create an electrostatic repulsion of protons and act as a size barrier; the ar/R filter renders the pore constriction site diverse in both size and hydrophobicity; the residues at Froger's positions are helpful for discriminating aquaglyceroporins from AQPs, since aquaglyceroporins usually feature an aromatic residue at P1, an acidic residue at P2, a basic residue at P3, a proline followed by a nonaromatic residue

TABLE 3 | Structural and subcellular localization analysis of the JcAQPs.

Name	Len	Mw (kDa)	pI	TM ^a	Loc ^b	Ar/R selectivity filter				NPA motifs		Froger's positions				
						H2	H5	LE1	LE2	LB	LE	P1	P2	P3	P4	P5
JcPIP1;1	287	30.73	8.60	6	Plas	F	H	T	R	NPA	NPA	E	S	A	F	W
JcPIP1;2	287	30.54	8.62	6	Plas	F	H	T	R	NPA	NPA	E	S	A	F	W
JcPIP1;3	212	22.57	8.53	6	Plas	F	H	T	R	NPA	NPA	E	S	A	F	W
JcPIP1;4	286	30.46	8.72	6	Plas	F	N	A	R	NPA	NPA	Q	S	A	F	W
JcPIP2;1	284	30.35	8.20	6	Plas	F	H	T	R	NPA	NPA	Q	S	A	F	W
JcPIP2;2	286	30.60	7.62	6	Plas	F	H	T	R	NPA	NPA	Q	S	A	F	W
JcPIP2;3	285	30.33	8.67	6	Plas	F	H	T	R	NPA	NPA	Q	S	A	F	W
JcPIP2;4	280	29.91	8.97	6	Plas	F	H	T	R	NPA	NPA	M	S	A	F	W
JcPIP2;5	283	29.67	9.10	6	Plas	F	H	T	R	NPA	NPA	V	S	A	F	W
JcTIP1;1	252	25.97	5.91	6	Plas	H	I	A	V	NPA	NPA	T	S	A	Y	W
JcTIP1;2	252	25.79	4.96	6	Vacu	H	I	A	V	NPA	NPA	T	S	A	Y	W
JcTIP1;3	252	25.79	5.13	6	Vacu	H	I	A	V	NPA	NPA	T	S	A	Y	W
JcTIP1;4	254	26.39	5.83	6	Vacu	H	V	A	V	NPA	NPA	T	S	A	Y	W
JcTIP2;1	248	25.26	5.59	6	Vacu	H	I	G	R	NPA	NPA	T	S	A	Y	W
JcTIP2;2	250	25.34	5.69	6	Vacu	H	I	G	R	NPA	NPA	T	S	A	Y	W
JcTIP3;1	257	27.34	6.49	6	Vacu	H	I	A	R	NPA	NPA	T	A	A	Y	W
JcTIP4;1	247	25.97	6.12	6	Vacu	H	I	A	R	NPA	NPA	T	S	A	Y	W
JcTIP5;1	252	26.01	7.85	6	Vacu	N	V	G	S	NPA	NPA	I	A	A	Y	W
JcNIP1;1	275	29.27	9.21	6	Plas	W	V	A	R	NPA	NPA	F	S	A	Y	L
JcNIP2;1	291	30.80	8.85	6	Plas	G	S	G	R	NPA	NPA	L	T	A	Y	I
JcNIP3;1	277	30.04	8.50	6	Plas	W	V	A	R	NPA	NPA	F	S	A	F	L
JcNIP3;2	280	30.04	5.52	6	Vacu	W	M	A	R	NPA	NPA	F	S	A	Y	I
JcNIP4;1	263	27.82	5.89	6	Plas	W	V	A	R	NPA	NPA	F	S	A	Y	I
JcNIP5;1	298	30.85	8.87	6	Plas	S	I	A	R	NPA	NPV	F	T	A	Y	L
JcNIP6;1	307	31.37	8.71	6	Plas	S	I	A	R	NPS	NPV	L	T	A	Y	L
JcNIP7;1	265	28.17	7.00	6	Plas	A	V	G	R	NPA	NPA	Y	S	A	Y	I
JcXIP1;1	294	32.27	6.05	6	Plas	I	I	V	R	SPI	NPA	M	C	A	F	W
JcXIP2;1	303	32.29	6.59	6	Plas	I	T	V	R	NPV	NPA	L	C	A	F	W
JcSIP1;1	239	25.79	9.58	6	Plas	V	L	P	N	NPT	NPA	I	A	A	Y	W
JcSIP1;2	242	26.01	9.73	6	Vacu	A	L	P	N	NPT	NPA	M	A	A	Y	W
JcSIP1;3	243	26.00	10.02	6	Extr	S	L	P	N	NPT	NPA	M	A	A	Y	W
JcSIP2;1	241	26.37	9.57	6	Vacu	S	L	G	S	NPL	NPA	F	V	A	Y	W

^aRepresenting the numbers of transmembrane helices predicted by TOPCONS.^bBest possible subcellular localization prediction by the WoLF PSORT (Chla, chloroplast; Cyto, cytosol; ER, endoplasmic reticulum; Plas, plasma membrane; Vacu, vacuolar membrane).

at P4 and P5 (Froger et al., 1998; Törnroth-Horsefield et al., 2006). In addition, nine SDPs pivotal for the transport of non-aqua substrates (i.e., urea, boric acid, silicic acid, NH₃, CO₂, and H₂O₂) were also proposed by Hove and Bhave (2011). To learn more about the putative function of JcAQPs, the residues at these conserved positions were carefully identified based on the multiple alignments with structure/function characterized AQPs (Supplementary File S6). As shown in **Table 3**, most JcAQPs exhibit an AqpZ-like Froger's positions (A¹⁰³-S¹⁹⁰-A¹⁹⁴-F²⁰⁸-W²⁰⁹) to favor the permeability of water, which is consistent with the high water transport activity of JcPIP2;4 and JcTIP1;2 (Khan et al., 2015). In contrast, JcSIP2;1 and NIP subfamily members possess mixed key residues of GlpF (Y¹⁰⁸-D²⁰⁷-K²¹¹-P²³⁶-L²³⁷) for P1 and P5, and AqpZ for P2–P4. Given the glycerol permease activity of soybean NOD26 and *Arabidopsis*

NIPs (Dean et al., 1999; Wallace and Roberts, 2005), JcNIPs are more likely to transport glycerol and may play a role in oil formation/translocation.

Besides high permeability to water, plant PIPs were shown to transport urea, boric acid, CO₂, and H₂O₂ (Eckert et al., 1999; Uehlein et al., 2008; Fitzpatrick and Reid, 2009; Bienert et al., 2014). As shown in **Table 3**, except for JcPIP1;4 that harbors an ar/R filter of F-N-A-R, all other JcPIPs represent the F-H-T-R ar/R filter as observed in AqpZ (Savage et al., 2003), indicating their high water permeability. According to the SDP analysis, all JcPIPs except for JcPIP1;3 represent urea-type SDPs (H-P-F-F/L-L-P-G-G-N); JcPIP1;1, JcPIP1;2, and JcPIP1;3 represent boric acid-type SDPs (T-I-H-P-E-L-L-T-P); JcPIP1;2 represents CO₂-type SDPs (L-I-C-A-I-D-W-D-W), whereas JcPIP1;1, JcPIP1;4, JcPIP2;1, JcPIP2;2, and JcPIP2;4 may

represent novel SDPs of I/L-M-C-A-I/V-D-W-D-W; all JcPIPs except for JcPIP1;3 represent H₂O₂-type SDPs (A-G-V-F/L-I-H/Q-F-V-P) (**Table 4** and Supplementary File S6), supporting their similar functionality.

Although highly variable in the ar/R filter, plant TIPs were shown to transport water as efficiently as PIPs. Additionally, they also allow urea, NH₃ and H₂O₂ through (Dynowski et al., 2008a,b). As shown in **Table 4** and Supplementary File S6, all JcTIPs except for JcTIP3;1 represent urea-type SDPs (H-P-F/L-A/F/L-L-A/P-G-S-N); JcTIP1;2, JcTIP3;1, and JcTIP5;1 represent H₂O₂-type SDPs (S-A-L-A/V-I-H/Q-Y-V-P), indicating similar functionality.

In addition to glycerol and water, plant NIPs have been found to transport urea, boric acid, silicic acid, NH₃, and H₂O₂ (Ma et al., 2006; Dynowski et al., 2008a,b). As shown in **Table 4** and Supplementary File S6, JcNIP1;1 is promised to be an NH₃ and urea transporter with nine SDPs of F-K-F-T-A-D-L-E-T or H-P-L-A-L-P-G-S-N, respectively; JcNIP3;1 is promised to be a urea transporter with SDPs of H-P-I-A-L-P-G-S-N; JcNIP4;1 is promised to be an H₂O₂ and urea transporter with SDPs of S-A-L-L-V-L-Y-A-P or H-P-I-A-L-P-G-S-N, respectively; JcNIP5;1 is promised to be a boric acid, H₂O₂ and urea transporter with SDPs of T-I-H-P-E-L-L-A-P, S-A-L-V-V-I-Y-V-P or H-P-I-A-L-P-G-S-N, respectively; JcNIP6;1 is promised to be a boric acid and urea transporter with SDPs of T-I-H-P-E-L-L-A-P or H-P-I-A-L-P-G-S-N, respectively; JcNIP2;1 represent typical boric acid SDPs (V-V-H-P-E-I-I-A-P), NH₃ SDPs (A-A-L-L-V-I-Y-V-P), and urea SDPs (H-P-T-A-M-P-G-S-N), however, whether it represents a novel silicic acid SDPs (G-F-V-H-G-N-R-T-K with the substitution of G for C/S at SDP1 and V for A/E/L at SDP3) needs to be experimentally validated. Nevertheless, JcNIP2;1 possesses a distance of 108 amino acids between two NPA motifs, which was shown to be a feature specific to silicon transporters (Deshmukh et al., 2015).

According to phylogenetic relationships, the newly identified XIPs can be divided into five subgroups (XIP1–5) and XIP1–3 were found in poplar, castor bean and rubber tree (Lopez et al., 2012; Zou et al., 2015a,b). Functional analysis indicated that XIPs are able to transport water, glycerol, urea, boric acid, and H₂O₂ (Bienert et al., 2011; Lopez et al., 2012). The physic nut harbors one XIP1 and one XIP2. Exhibiting an AqpZ-like Froger's positions, two JcXIPs are more likely to transport water. In addition, JcXIP2;1 is promised to be an H₂O₂ transporter with SDPs of A-G-L-V-L-H-F-V-P (**Table 4** and Supplementary File S6).

Tissue-Specific Expression Profiles of JcAQP Genes

As a part of the genome sequencing, the transcriptomes of three important tissues (i.e., root, leaf, and seed) of cultivar GZQX0401 were also deeply sequenced (all counting about 30 M 75-nt paired-end reads): roots were collected from 15-day old seedlings, whereas half expanded leaves and seeds from fruits harvested 19–28 DAP (days after pollination) were obtained from 4-year-old plants (Wu et al., 2015). Expression profiling indicated that, except for JcPIP1;3, JcNIP4;1, JcNIP7;1, and

JcXIP1;1, other 28 JcAQP genes were all detected in one of the examined tissues (**Figure 4**). In contrast to JcPIP1;3 and JcXIP1;1 that the expression was not supported by currently available transcriptome data, JcNIP7;1 was detected in roots after 24 h waterlogging stress (Juntawong et al., 2014), whereas JcNIP4;1 was shown to be expressed in flowers as supported by one EST (GW619951), which is consistent with the flower-specific expression of its ortholog in castor bean (*RcNIP4;1*) (Zou et al., 2015b). According to the FPKM annotation, the JcAQP genes were shown to be expressed most in roots, which exhibited about 2.95 and 6.30 folds than that in seeds and leaves. PIPs represented the most abundant subfamily in all examined tissues, followed by TIPs, SIPs, NIPs, and XIPs: in roots, the total expression level of PIP members was about 1.55, 58.23, 74.51, and 2707.81 folds more than the TIP, SIP, NIP and XIP members, respectively; 1.42, 33.17, 105.01, and 17,702.00 folds in seeds, respectively; and 7.45, 13.85, 23.26, and 54.58 folds in leaves, respectively (**Figure 4**), indicating a crucial role of the PIP subfamily in the water balance of these tissues. In tissues such as roots and seeds with a large central vacuole, the plasma membrane-located JcPIPs facilitate the water transport from the extracellular space to the cell cytoplasm, whereas the vacuole-targeted JcTIPs play an essential role in maintaining the cell osmotic balance (Hunter et al., 2007). In contrast, in immature tissues characterized by polydispersed microvacuoles, the role of JcTIPs is less important. Indeed, as shown in **Figure 4**, the total TIP transcript level in half expanded leaves was considerably lower than that in roots and seeds, only counting about 4.37 or 12.28%, respectively; by contrast, the PIP transcripts counted 20.96 or 64.31%, respectively.

Different JcAQP members exhibited distinct expression profiles in a certain tissue. In roots, two most highly abundant PIP members (*JcPIP1;1* and *JcPIP2;1*) occupied 71.15% of the total PIP transcripts; *JcTIP1;1* and *JcTIP2;1* counted 76.13% of the total TIP transcripts; *JcNIP5;1* and *JcNIP2;1* counted 78.42% of the total NIP transcripts; *JcSIP1;1* counted 70.73% of the total SIP transcripts. In seeds, *JcPIP2;4* and *JcPIP1;1* counted 69.36% of the total PIP transcripts; *JcTIP1;1* and *JcTIP2;1* counted 98.59% of the total TIP transcripts; *JcNIP5;1*, *JcNIP6;1*, and *JcNIP1;1* counted 98.56% of the total NIP transcripts; *JcSIP1;1* counted 71.48% of the total SIP transcripts. In leaves, *JcPIP2;5* and *JcPIP1;1* counted 74.51% of the total PIP transcripts; *JcTIP1;1* and *JcTIP2;1* counted 76.86% of the total TIP transcripts; *JcNIP5;1* counted 69.20% of the total NIP transcripts; *JcSIP1;1* and *JcSIP2;1* counted 91.27% of the total SIP transcripts. Except for the JcXIP subfamily, more than one subfamily members were detected in a certain tissue. Compared with roots and seeds, *JcXIP2;1* was shown to be expressed considerably higher in leaves. Among 26 JcAQP genes detected in roots (excluding *JcPIP2;5* and *JcNIP3;1*), *JcPIP1;1*, *JcTIP1;1*, *JcNIP5;1*, and *JcSIP1;1* represented the most abundant PIP, TIP, NIP, and SIP subfamily members, respectively. Except for *JcTIP3;1*, *JcNIP3;1*, and *JcNIP3;2*, other 25 members were shown to be expressed in seeds and *JcPIP2;4*, *JcTIP1;1*, *JcNIP5;1*, and *JcSIP1;1* represented the most abundant PIP, TIP, NIP, and SIP subfamily members, respectively. In leaves, 25 JcAQP genes (excluding *JcTIP2;2*, *JcTIP5;1*, and *JcNIP3;2*) were detected and *JcPIP2;5*, *JcTIP1;1*, *JcNIP5;1*, and *JcSIP1;1* represented the most abundant PIP, TIP, NIP, and

TABLE 4 | Summary of typical SDPs and those identified in the JcAQPs^a.

Aquaporin	SD position	SDP1	SDP2	SDP3	SDP4	SDP5	SDP6	SDP7	SDP8	SDP9
Typical NH₃ transporter		F/T	K/L/N/V	F/T	V/L/T	A	D/S	A/H/L	E/P/S	A/R/T
JcNIP1;1		F	K	F	T	A	D	L	E	T
Typical boric acid transporter		T/V	I/V	H/I	P	E	I/L	I/L/T	A/T	A/G/K/P
JcPIP1;1		T	I	H	P	E	L	L	T	P
JcPIP1;2		T	I	H	P	E	L	L	T	P
JcPIP1;3		T	I	H	P	E	L	L	T	P
JcNIP2;1		V	V	H	P	E	I	I	A	P
JcNIP5;1		T	I	H	P	E	L	L	A	P
JcNIP6;1		T	I	H	P	E	L	L	A	P
Typical CO₂ transporter		I/L/V	I	C	A	I/V	D	W	D	W
JcPIP1;1		I	M	C	A	I	D	W	D	W
JcPIP1;2		L	I	C	A	I	D	W	D	W
JcPIP1;4		I	M	C	A	I	D	W	D	W
JcPIP2;1		I	M	C	A	V	D	W	D	W
JcPIP2;2		L	M	C	A	V	D	W	D	W
JcPIP2;4		L	M	C	A	I	D	W	D	W
Typical H₂O₂ transporter		A/S	A/G	L/V	A/F/L/T/V	I/L/V	H/I/L/Q	F/Y	A/V	P
JcPIP1;1		A	G	V	F	I	H	F	V	P
JcPIP1;2		A	G	V	F	I	H	F	V	P
JcPIP1;4		A	G	V	F	I	H	F	V	P
JcPIP2;1		A	G	V	F	I	Q	F	V	P
JcPIP2;2		A	G	V	F	I	Q	F	V	P
JcPIP2;3		A	G	V	F	I	Q	F	V	P
JcPIP2;4		A	G	V	F	I	H	F	V	P
JcPIP2;5		A	G	V	L	I	H	F	V	P
JcTIP1;2		S	A	L	A	I	H	Y	V	P
JcTIP3;1		S	A	L	V	I	H	Y	V	P
JcTIP5;1		S	A	L	A	I	Q	Y	V	P
JcNIP2;1		A	A	L	L	V	I	Y	V	P
JcNIP4;1		S	A	L	L	V	L	Y	A	P
JcNIP5;1		S	A	L	V	V	I	Y	V	P
JcXIP2;1		A	G	L	A	V	H	F	V	P
Typical silicic acid transporter		C/S	F/Y	A/E/L	H/R/Y	G	K/N/T	R	E/S/T	A/K/P/T
JcNIP2;1		G	F	V	H	G	N	R	T	K
Typical urea transporter		H	P	F/I/L/T	A/C/F/L	L/M	A/G/P	G/S	G/S	N
JcPIP1;1		H	P	F	F	L	P	G	G	N
JcPIP1;2		H	P	F	F	L	P	G	G	N
JcPIP1;4		H	P	F	F	L	P	G	G	N
JcPIP2;1		H	P	F	F	L	P	G	G	N
JcPIP2;2		H	P	F	F	L	P	G	G	N
JcPIP2;3		H	P	F	F	L	P	G	G	N
JcPIP2;4		H	P	F	F	L	P	G	G	N
JcPIP2;5		H	P	F	L	L	P	G	G	N
JcTIP1;1		H	P	F	F	L	A	G	S	N
JcTIP1;2		H	P	F	F	L	A	G	S	N
JcTIP1;3		H	P	F	F	L	A	G	S	N
JcTIP1;4		H	P	F	F	L	A	G	S	N
JcTIP2;1		H	P	F	A	L	P	G	S	N
JcTIP2;2		H	P	F	A	L	P	G	S	N
JcTIP4;1		H	P	L	L	L	A	G	S	N

(Continued)

TABLE 4 | Continued

Aquaporin	SD position	SDP1	SDP2	SDP3	SDP4	SDP5	SDP6	SDP7	SDP8	SDP9
JcTIP5;1		H	P	F	A	L	P	G	S	N
JcNIP1;1		H	P	L	A	L	P	G	S	N
JcNIP2;1		H	P	T	A	M	P	G	S	N
JcNIP3;1		H	P	I	A	L	P	G	S	N
JcNIP4;1		H	P	I	A	L	P	G	S	N
JcNIP5;1		H	P	I	A	L	P	G	S	N
JcNIP6;1		H	P	I	A	L	P	G	S	N

^aThe SDP residues in the physic nut AQPs differing from the typical SDPs determined in this study are highlighted in red.

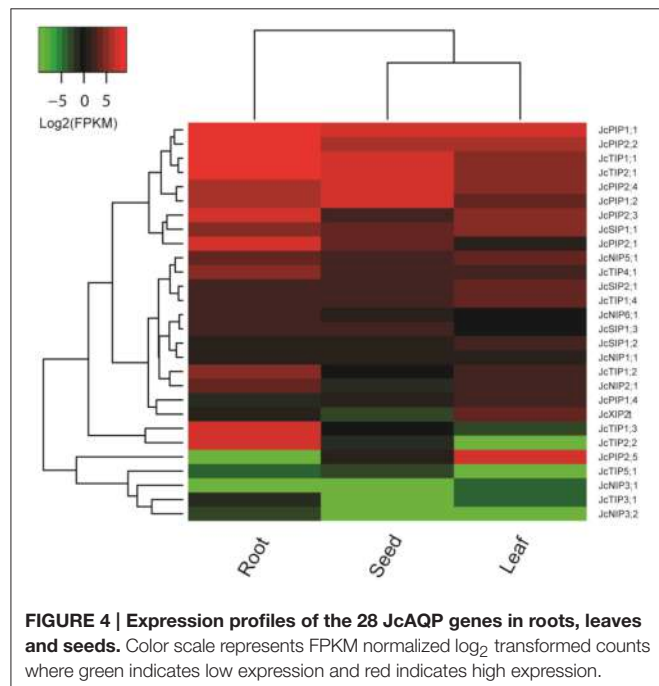


FIGURE 4 | Expression profiles of the 28 JcAQP genes in roots, leaves and seeds. Color scale represents FPKM normalized \log_2 transformed counts where green indicates low expression and red indicates high expression.

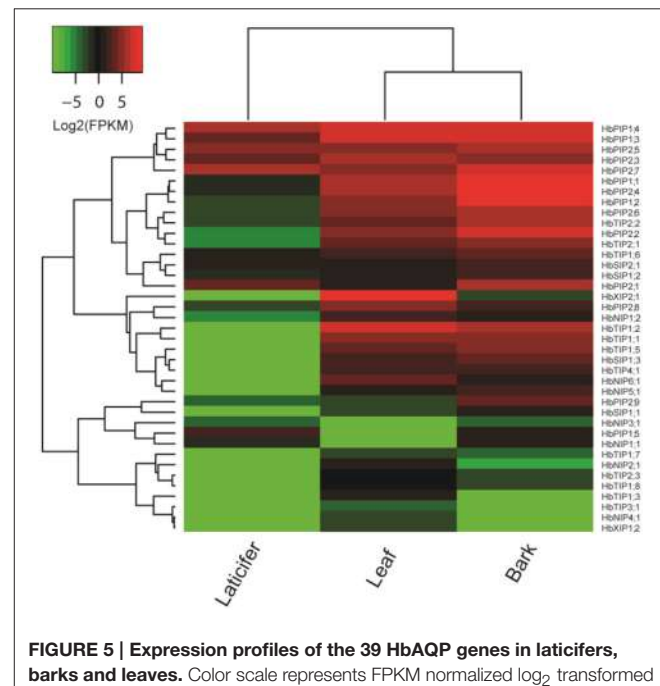


FIGURE 5 | Expression profiles of the 39 HbAQP genes in laticifers, barks and leaves. Color scale represents FPKM normalized \log_2 transformed counts where green indicates low expression and red indicates high expression.

SIP subfamily members, respectively. In contrast to the highly abundant and constitutive expression of *JcPIP1;1*, *JcPIP2;2*, *JcTIP1;1* and *JcTIP2;1*, *JcPIP1;2* and *JcPIP2;4* preferred to express in roots and seeds; *JcPIP2;1*, *JcPIP2;3*, *JcTIP1;2*, *JcTIP1;3*, and *JcTIP2;2* preferred to express in roots; *JcPIP2;5* preferred to express in leaves. In addition, *JcNIP3;1* and *JcNIP3;2*, two orthologs of castor bean *RcNIP3;1*, exhibited an organ-specific expression pattern. *RcNIP3;1* was shown to be expressed in leaves but not in seeds (Zou et al., 2015b), whereas *JcNIP3;1* and *JcNIP3;2* was expressed only in leaves and roots, respectively (Figure 4).

Tissue-Specific Expression Profiles of HbAQP Genes

In the previous study, we reported the identification of 51 AQP genes from rubber tree genome, and focused on their response to ethephon stimulation in the rubber-producing tissue termed laticifer (Zou et al., 2015a) which is not found in physic nut

and castor bean. To gain insights into the expression evolution of duplicated HbAQP genes, in the present study, we take advantage of deep transcriptome sequencing data to investigate their expression profiles in two more important tissues, i.e., bark and leaf (all counting about 25 M 100-nt paired-end reads). As shown in Figure 5, 39 out of 51 HbAQP genes representing all five subfamilies were detected in at least one of the examined tissues, though the expression of the XIP subfamily members was not observed in the laticifer. FPKM annotation indicated HbAQP genes were expressed most in barks, exhibiting 1.79 and 11.49 folds more than that in leaves and laticifers, respectively. As observed in castor bean and physic nut, PIPs represented the most abundant subfamily in all examined tissues: in barks, the total expression level of PIP members was 8.77, 95.51, 235.92, and 12,090.95 folds more than the TIP, SIP, NIP, or XIP members, respectively; 1.20, 2.70, 36.52, and 80.52 folds more than the XIP,

TIP, NIP, or SIP members in leaves, respectively; and 116.11, 122.84, and 752.87 folds more than the SIP, TIP, or NIP members in laticifers, respectively (**Figure 5**). Nevertheless, compared with laticiferous cells that are characterized by a high number of polydispersed microvacuoles (Wang X. C. et al., 2013), cells of bark and mature leaf usually contain a large central vacuole and the role of HbPIPs is less important. Instead, the total TIP transcripts in barks and leaves were 147.25 and 135.28 folds more than that in laticifers, respectively. Compared with the PIPs, TIPs, and SIPs expressed more in barks, NIPs and XIPs were shown to be expressed more in leaves (**Figure 5**). It is worth noting that the expression level of *HbXIP2;1* was particularly high in leaves, counting 99.98% of the total XIP transcripts. Similar expression pattern was also observed in physic nut and castor bean, where its orthologs *JcXIP2;1* and *RcXIP2;1* were shown to be preferentially expressed in leaves (**Figure 4**; Zou et al., 2015b). Compared with laticifers where three highly abundant PIP members (i.e., *HbPIP2;7*, *HbPIP1;4*, and *HbPIP2;5*) occupied 80.99% of the total PIP transcripts, seven PIPs (i.e., *HbPIP1;2*, *HbPIP1;1*, *HbPIP2;4*, *HbPIP1;4*, *HbPIP2;7*, *HbPIP1;3*, and *HbPIP2;2*) occupied 89.53% of the total PIP transcripts in barks, and seven abundant PIPs (i.e., *HbPIP1;4*, *HbPIP1;3*, *HbPIP2;3*, *HbPIP2;4*, *HbPIP1;1*, *HbPIP2;6*, and *HbPIP1;2*) occupied 83.57% of the total PIP transcripts in leaves. In barks, *HbTIP1;2*, *HbTIP2;2*, and *HbTIP2;1* counted 73.04% of the total TIP transcripts; *HbNIP5;1* and *HbNIP1;2* counted 67.31% of the total NIP transcripts; *HbSIP1;3* counted 56.32% of the total SIP transcripts. In leaves, *HbTIP1;2*, and *HbTIP1;1* counted 81.44% of the total TIP transcripts; *HbNIP6;1*, *HbNIP1;2*, and *HbNIP5;1* counted 92.39% of the total NIP transcripts; *HbSIP1;3* and *HbSIP2;1* counted 78.49% of the total SIP transcripts. Among 35 HbAQP genes detected in barks, *HbPIP1;2*, *HbTIP1;2*, *HbNIP5;1*, *HbXIP2;1*, and *HbSIP1;3* represented the most abundant PIP, TIP, NIP, XIP, and SIP subfamily members, respectively. Among 36 HbAQP genes detected in leaves, *HbPIP1;4*, *HbTIP1;2*, *HbNIP6;1*, *HbXIP2;1*, and *HbSIP1;3* represented the most abundant PIP, TIP, NIP, XIP, and SIP subfamily members, respectively (**Figure 5**).

DISCUSSION

Gene duplication is a major mechanism for acquiring new genes and creating genetic novelty in eukaryotes. Gene duplicates may originate from single gene duplications such as local (tandem or proximal), dispersed and transposed duplications, or large-scale duplications such as WGDs and segmental duplications (Wang et al., 2012). WGDs are widespread and play an important role in the origin and diversification of the angiosperms (Bowers et al., 2003). According to the comparative genomics analysis, all core eudicot plant species including *Arabidopsis*, poplar, rubber tree, castor bean, and physic nut underwent one so-called γ whole-genome triplication event occurred at about 117 million years ago (Mya) (Jiao et al., 2012). Moreover, it is well established that poplar and *Arabidopsis* underwent one or two recent doubling events, respectively (Bowers et al., 2003; Tuskan et al., 2006). The doubling event occurred in poplar was shown to be specific to

Salicaceae date to about 60–65 Mya (Tuskan et al., 2006), whereas the β and α WGDs occurred in *Arabidopsis* are Brassicaceae-specific and not distantly separated, probably date to 20–40 Mya (Blanc and Wolfe, 2004). By contrast, like castor bean, physic nut didn't undergo any recent WGD (Chan et al., 2010; Wu et al., 2015). From this perspective, the recently available physic nut genome may provide a good chance to analyze the lineage-specific expansion and evolution of certain gene families in Euphorbiaceae.

Physic Nut Encodes Fewer AQP Genes than Other Plants Including Rubber Tree

Our genome-wide survey indicated that physic nut encodes 32 AQP genes, and 30 out of them were shown to be expressed. To our knowledge, this family number is the fewest in high plants reported to date (**Table 1** and references as in). Nevertheless, physic nut contains members representing all five subfamilies (i.e., PIP, TIP, NIP, XIP, and SIP) found in high plants. In contrast, monocot, and Brassicaceae plants are shown to have lost the XIP subfamily (**Table 1** and references as in).

The phylogenetic analysis further divided the JcAQP subfamilies into subgroups. Except for the XIP subfamily, the classification is shown to be the same as that in castor bean, rubber tree, and poplar (Zou et al., 2015a,b). The XIPs in the above three Malpighiales plants can be divided into three subgroups, which is supported by the sequence similarity and the ar/R filter (Zou et al., 2015a,b). By contrast, physic nut only retains the XIP1 and XIP2 subgroups.

In addition to gene loss, the comparative analysis also revealed the expansion of specific JcAQP genes, i.e., two gene pairs (*JcNIP3;1/JcNIP3;2* and *JcSIP1;2/JcSIP1;3*) as shown in **Figure 1**. *JcNIP3;1/JcNIP3;2* can be defined as dispersed duplicate genes for their distribution on two different chromosomes, whereas *JcSIP1;2/JcSIP1;3* as well as five *RcAQP* gene pairs can be classed as tandem duplicates since they are characterized by same-direction neighbors (foot-to-head order) on the same scaffolds. Thereby, tandem duplications act as the main force for the expansion of AQP genes in physic nut and castor bean. By contrast, in *Arabidopsis*, poplar and rubber tree, WGDs seem to play a more important role in the family expansion. For example, studies showed that the 35 AtAQP genes are more likely to be derived from 17 parents, including 9, 3, and 1 genes resulted from α , β , or γ WGDs, respectively (Wang Y. et al., 2013).

Consistent with that all HbAQPs have orthologs in poplar (Zou et al., 2015a), all Jc/RcAQPs are shown to have orthologs in rubber tree and poplar (**Table 1** and Zou et al., 2015b). By using poplar as an outgroup, we estimate that there are 31 AQP family members in the ancestral Euphorbiaceae species, including 3 PIP1s, 5 PIP2s, 4 TIP1s, 2 TIP2s, 1 TIP3, 1 TIP4, 1 TIP5, 1 NIP1, 1 NIP2, 1 NIP3, 2 NIP4, 1 NIP5, 1 NIP6, 1 NIP7, 1 XIP1, 1 XIP2, 1 XIP3, 2 SIP1s, and 1 SIP2. After a round of a recent WGD and subsequent chromosomal rearrangement, rubber tree preferred to retain the genes of the PIP (especially the PIP2 subgroup) and TIP (especially the subgroups TIP1, TIP2, TIP3, and TIP5) subfamilies, corresponding to their high water permeability (e.g.,

HbPIP2;1, *HbPIP2;5*, and *HbTIP1;1*), the particular importance of water balance in a big tree, and a highly differentiated laticifer tissue which is tapped for the cytoplasm in the form of aqueous latex (Tungngoen et al., 2009; An et al., 2015; Zou et al., 2015a). In fact, as a big tree, poplar implemented a very similar strategy, though relatively more NIP5s, NIP6s, and XIP3s have been preserved (Figure 2).

Since the majority of *Jc/Rc/HbAQP* sequences were confirmed with available cDNAs, ESTs, and/or RNA sequencing read (Table 1 and Zou et al., 2015a,b), we are allowed to investigate the structural divergence of AQP genes in these plant species. As shown in Supplementary Table S3, the comparative analysis indicated that most orthologous genes exhibit the same exon-intron structures. However, *JcPIP1;3* and *RcPIP2;5* harbor four introns instead of the usual three, and *RcXIP1;3* seems to have lost the intron shared by its orthologs and paralogs. In addition, *JcPIP1;3*, *HbPIP1;5*, *RcPIP2;5*, *HbTIP1;4*, *JcNIP7;1*, and *RcXIP1;4* encode relatively fewer amino acids than their orthologs (Supplementary Table S3), suggesting the occurrence of insertions/deletions in their coding-regions as well as the usual nucleotide substitution. In fact, the comparative analysis revealed that nucleotide substitution have played an important role on the diversification of conserved residues that determine the substrate specificity, and the situation is particularly universal in members of NIP, XIP, and SIP subfamilies (Supplementary Table S4), reflecting a variety of their substrate transport capacity.

Expression Divergence of Duplicated HbAQP Genes

In addition to structural divergence, expression divergence also plays a key role in the evolution of duplicate genes. Microarray has been frequently used to study the gene expression evolution in model species such as *Arabidopsis* and rice (Blanc and Wolfe, 2004; Li et al., 2009). With the development of the second generation sequencing technologies, RNA sequencing provides an alternative method for such studies (Harikrishnan et al., 2015). Based on the transcriptional profiling of *Hb/Jc/RcAQP* genes in several important tissues, the expression evolution patterns of duplicated *HbAQP* genes are discussed as follows.

Among 17 *HbAQP* gene pairs, *HbPIP1;1/HbPIP1;2* exhibited similar expression profiles in all tissues examined, which is consistent with that of *RcPIP1;2/RcPIP1;3*, their orthologs in castor bean (Figure 5; Zou et al., 2015b). Nevertheless, the expression levels of *HbPIP1;1* and *HbPIP1;2* were extremely low in laticifers (Figure 5), though they were highly abundant in barks and leaves and their orthologs in physic nut (*JcPIP1;1*) and castor bean were also constitutively expressed in tested tissues (Figure 4; Zou et al., 2015b). *HbPIP1;3* and *HbPIP1;4* showed similar expression profiles in barks and leaves and their high abundance was also similar to that of *JcPIP1;2* and *RcPIP1;4*, their orthologs in physic nut and castor bean, respectively (Figures 4, 5; Zou et al., 2015b). In contrast, the transcript level of *HbPIP1;4* was relatively higher than that of *HbPIP1;3* in laticifers (Figure 5). *HbPIP2;5/HbPIP2;6* exhibited similar evolution pattern to that of *HbPIP1;3/HbPIP1;4*, and *HbPIP2;5* was expressed considerably more than that of

HbPIP2;6 in laticifers (Figure 5). Although both *HbPIP2;1* and *HbPIP2;2* were highly abundant in barks, *HbPIP2;1* preferred to express in laticifers whereas *HbPIP2;2* preferred to express in leaves (Figure 5). The moderate expression of *HbPIP2;2* in leaves was similar to that of their orthologs in physic nut and castor bean, i.e., *JcPIP2;1* and *RcPIP2;1*, respectively (Figures 4, 5; Zou et al., 2015b). Like the high abundance of their orthologs in physic nut (*JcPIP2;2*) and castor bean (*RcPIP2;3*) in leaves (Figure 4; Zou et al., 2015b), both *HbPIP2;3* and *HbPIP2;4* were highly expressed in rubber tree leaves, however, *HbPIP2;3* was preferentially expressed in laticifers while *HbPIP2;4* was preferentially expressed in barks (Figure 5). Similar to *HbPIP2;3/HbPIP2;4*, *HbPIP2;7/HbPIP2;8* were highly abundant in leaves as their orthologs in physic nut (*JcPIP2;4*) and castor bean (*RcPIP2;4*), however, the transcript level of *HbPIP2;7* was considerably higher than that of *HbPIP2;8* in both barks and laticifers (Figure 5). Like the high abundance of *RcTIP1;1* and *JcTIP1;1* in various tissues tested, *HbTIP1;1/HbTIP1;2* were highly expressed in rubber tree barks and leaves, though the transcript level of *HbTIP1;2* was relatively higher than that of *HbTIP1;1* (Figure 5). Nevertheless, their expression was not detected in laticifers. In contrast to *HbTIP1;4* whose expression was not detected in all tissues tested, *HbTIP1;3* was only lowly expressed in rubber tree leaves (Figure 5). However, their orthologs in physic nut (*JcTIP1;4*) and castor bean (*RcTIP1;4*) were shown to be expressed in all tested tissues and the transcript levels in leaves were relatively high (Figure 4; Zou et al., 2015b). Similar to *JcTIP1;2* and *RcTIP1;2* (Figure 4; Zou et al., 2015b), both *HbTIP1;5* and *HbTIP1;6* were moderately expressed in leaves as well as in barks, though the transcript level of *HbTIP1;5* was relatively higher than that of *HbTIP1;6*. In addition, the expression of *HbTIP1;5* was not detected in laticifers, whereas *HbTIP1;6* represented the most abundant TIP member (Figure 5). Similar to *JcTIP1;3* and *RcTIP1;3* (Figure 4; Zou et al., 2015b), both *HbTIP1;7* and *HbTIP1;8* were lowly expressed in leaves as well as in barks. Nevertheless, the transcript level of *HbTIP1;8* was considerably higher than that of *HbTIP1;7* (Figure 5). Similar to *JcTIP2;1* and *RcTIP2;1* (Figure 4; Zou et al., 2015b), both *HbTIP2;1* and *HbTIP2;2* represented two of the most abundant TIP members in leaves as well as in barks. However, the transcript level of *HbTIP2;2* was shown to be relatively higher than that of *HbTIP2;1* in both barks and laticifers, though their expression levels in laticifers were extremely low (Figure 5). In contrast to *HbTIP2;4* whose expression was not detected in all tissues tested, *HbTIP2;3* was only lowly expressed in rubber tree leaves and barks (Figure 5). Similar expression profiles were also observed in physic nut and castor bean, their orthologs *JcTIP2;2* and *RcTIP2;2* were lowly expressed in all tested tissues except for physic nut roots (Figure 4; Zou et al., 2015b). *HbTIP3;1/HbTIP3;2* exhibited similar evolution pattern to that of *HbTIP2;3/HbTIP2;4* and the only detected *HbTIP3;1* was shown to be lowly expressed in leaves (Figure 5). Except for *RcTIP3;1* that was highly abundant in endosperms, the low expression of their orthologs in physic nut (*JcTIP3;1*) and castor bean was also observed in tested tissues (Figure 4; Zou et al., 2015b). The expression of both *HbTIP5;1* and *HbTIP5;2* was not detected

in all tested tissues (**Figure 5**). In contrast, their orthologs in physic nut (*JcTIP5;1*) and castor bean (*RcTIP5;1*) were shown to be lowly expressed in tested tissues except for physic nut leaves (**Figure 4**; Zou et al., 2015b). Similar to *JcNIP1;1* and *RcNIP1;1* (**Figure 4**; Zou et al., 2015b), in leaves, *HbNIP1;2* was shown to be moderately expressed, whereas the expression of *HbNIP1;1* was not detected. In addition, *HbNIP1;1* preferred to express in laticifers whereas *HbNIP1;2* preferred to express in barks (**Figure 5**). *HbSIP1;2/HbSIP1;3* exhibited similar evolution pattern to that of *HbNIP1;1/HbNIP1;2*, where *HbSIP1;2* was shown to be expressed more in laticifers and *HbSIP1;3* was expressed more in barks and leaves. In contrast to the high abundance of *RcXIP1;1* in castor bean leaves (Zou et al., 2015b), the expression of both *HbXIP1;3* and *HbXIP1;4* was not detected in all tested tissues (**Figure 5**).

CONCLUSIONS

Our paper presents the first genome-wide study of the physic nut AQP gene family and using systematic nomenclature assigned 32 *JcAQPs* into five subfamilies. Furthermore, their structural and functional properties were investigated and the global expression profiles of 32 *JcAQPs* and 51 *HbAQPs* were examined with deep transcriptome sequencing data, which provides insights into the evolution of the duplicated *HbAQP* genes. Results obtained from this study not only provide valuable information for future functional analysis and utilization of *Jc/HbAQP* genes, but also

provide a useful reference to survey the gene family expansion and evolution in Euphorbiaceae plants and other plant species.

AUTHOR CONTRIBUTIONS

The study was conceived and directed by ZZ. All the experiments and analysis were directed by ZZ and carried out by ZZ, LY, JG, YM, JW, JC, and FA. ZZ and GX wrote the paper. All the authors read and approved the final manuscript.

ACKNOWLEDGMENTS

The authors are grateful to those contributors who make the physic nut genome and transcriptome data accessible in public databases. This work was supported by the National Natural Science Foundation of China (31371556), the Fundamental Research Funds for Rubber Research Institute CATAS (1630022015004 and 1630022015013) and the Earmarked Fund for Modern Agro-industry Technology Research System (CARS-34-GW5).

SUPPLEMENTARY MATERIAL

The Supplementary Material for this article can be found online at: <http://journal.frontiersin.org/article/10.3389/fpls.2016.00395>

REFERENCES

- Abascal, F., Irisarri, I., and Zardoya, R. (2014). Diversity and evolution of membrane intrinsic proteins. *Biochim. Biophys. Acta* 1840, 1468–1481. doi: 10.1016/j.bbagen.2013.12.001
- Altschul, S. F., Madden, T. L., Schaffer, A. A., Zhang, J., Zhang, Z., Miller, W., et al. (1997). Gapped BLAST and PSI-BLAST: a new generation of protein database search programs. *Nucleic Acids Res.* 25, 3389–3401. doi: 10.1093/nar/25.17.3389
- An, F., Zou, Z., Cai, X. Q., Wang, J., Rookes, J., Lin, W., et al. (2015). Regulation of *HbPIP2;3*, a latex-abundant water transporter, is associated to the latex dilution and latex yield in rubber trees (*Hevea brasiliensis* Muell. Arg.). *PLoS ONE* 10:e0125595. doi: 10.1371/journal.pone.0125595
- Ariani, A., and Gepts, P. (2015). Genome-wide identification and characterization of aquaporin gene family in common bean (*Phaseolus vulgaris* L.). *Mol. Genet. Genomics* 290, 1771–1785. doi: 10.1007/s00438-015-1038-2
- Arumuganathan, K., and Earle, E. D. (1991). Nuclear DNA content of some important plant species. *Plant Mol. Biol. Rep.* 9, 208–218. doi: 10.1007/BF02672069
- Beebo, A., Mathai, J. C., Schoefs, B., and Spetea, C. (2013). Assessment of the requirement for aquaporins in the thylakoid membrane of plant chloroplasts to sustain photosynthetic water oxidation. *FEBS Lett.* 587, 2083–2089. doi: 10.1016/j.febslet.2013.05.046
- Bennett, M. D., and Leitch, I. J. (1997). Nuclear DNA amounts in angiosperms—583 new estimates. *Ann. Bot.* 80, 169–196. doi: 10.1006/anbo.1997.0415
- Bernsel, A., Viklund, H., Hennerdal, A., and Elofsson, A. (2009). TOPCONS: consensus prediction of membrane protein topology. *Nucleic Acids Res.* 37, W465–W468. doi: 10.1093/nar/gkp363
- Bienert, G. P., Bienert, M. D., Jahn, T. P., Boutry, M., and Chaumont, F. (2011). Solanaceae XIPs are plasma membrane aquaporins that facilitate the transport of many uncharged substrates. *Plant J.* 66, 306–317. doi: 10.1111/j.1365-313X.2011.04496.x
- Bienert, G. P., Heinen, R. B., Berny, M. C., and Chaumont, F. (2014). Maize plasma membrane aquaporin *ZmPIP2;5*, but not *ZmPIP1;2*, facilitates transmembrane diffusion of hydrogen peroxide. *Biochim. Biophys. Acta* 1838, 216–222. doi: 10.1016/j.bbagen.2013.08.011
- Blanc, G., and Wolfe, K. H. (2004). Functional divergence of duplicated genes formed by polyploidy during *Arabidopsis* evolution. *Plant Cell* 16, 1679–1691. doi: 10.1105/tpc.021410
- Bowers, J. E., Chapman, B. A., Rong, J., and Paterson, A. H. (2003). Unravelling angiosperm genome evolution by phylogenetic analysis of chromosomal duplication events. *Nature* 422, 433–438. doi: 10.1038/nature01521
- Carvalhoa, C. R., Clarindo, W. R., Praça, M. M., Araújoa, F. S., and Carels, N. (2008). Genome size, base composition and karyotype of *Jatropha curcas* L., an important biofuel plant. *Plant Sci.* 174, 613–617. doi: 10.1016/j.plantsci.2008.03.010
- Chan, A. P., Crabtree, J., Zhao, Q., Lorenzi, H., Orvis, J., Puiu, D., et al. (2010). Draft genome sequence of the oilseed species *Ricinus communis*. *Nat. Biotechnol.* 28, 951–956. doi: 10.1038/nbt.1674
- Chaumont, F., Barrieu, F., Wojcik, E., Chrispeels, M. J., and Jung, R. (2001). Aquaporins constitute a large and highly divergent protein family in maize. *Plant Physiol.* 125, 1206–1215. doi: 10.1104/pp.125.3.1206
- Chow, K. S., Ghazali, A. K., Hoh, C. C., and Mohd-Zainuddin, Z. (2014). RNA sequencing read depth requirement for optimal transcriptome coverage in *Hevea brasiliensis*. *BMC Res. Notes* 7:69. doi: 10.1186/1756-0500-7-69
- de Paula Santos Martins, C., Pedrosa, A. M., Du, D., Gonçalves, L. P., Yu, Q., Gmitter, F. G. Jr., et al. (2015). Genome-wide characterization and expression analysis of major intrinsic proteins during abiotic and biotic stresses in sweet orange (*Citrus sinensis* L. Osb.). *PLoS ONE* 10:e0138786. doi: 10.1371/journal.pone.0138786
- Dean, R. M., Rivers, R. L., Zeidel, M. L., and Roberts, D. M. (1999). Purification and functional reconstitution of soybean nodulin 26. An aquaporin with water and glycerol transport properties. *Biochemistry* 38, 347–353. doi: 10.1021/bi982110c

- Deshmukh, R. K., Vivancos, J., Guérin, V., Sonah, H., Labbé, C., Belzile, F., et al. (2013). Identification and functional characterization of silicon transporters in soybean using comparative genomics of major intrinsic proteins in *Arabidopsis* and rice. *Plant Mol. Biol.* 83, 303–315. doi: 10.1007/s11103-013-0087-3
- Deshmukh, R. K., Vivancos, J., Ramakrishnan, G., Guérin, V., Carpentier, G., Sonah, H., et al. (2015). A precise spacing between the NPA domains of aquaporins is essential for silicon permeability in plants. *Plant J.* 83, 489–500. doi: 10.1111/tpj.12904
- Diehn, T. A., Pomerrenig, B., Bernhardt, N., Hartmann, A., and Bienert, G. P. (2015). Genome-wide identification of aquaporin encoding genes in *Brassica oleracea* and their phylogenetic sequence comparison to *Brassica* crops and *Arabidopsis*. *Front Plant Sci.* 6:166. doi: 10.3389/fpls.2015.00166
- Dynowski, M., Mayer, M., Moran, O., and Ludewig, U. (2008a). Molecular determinants of ammonia and urea conductance in plant aquaporin homologs. *FEBS Lett.* 582, 2458–2462. doi: 10.1016/j.febslet.2008.06.012
- Dynowski, M., Schaaf, G., Loque, D., Moran, O., and Ludewig, U. (2008b). Plant plasma membrane water channels conduct the signalling molecule H₂O₂. *Biochem. J.* 414, 53–61. doi: 10.1042/BJ20080287
- Eckert, M., Biela, A., Siefritz, F., and Kaldenhoff, R. (1999). New aspects of plant aquaporin regulation and specificity. *J. Exp. Bot.* 50, 1541–1545. doi: 10.1093/jxb/50.339.1541
- Endress, P. K., Davis, C. C., and Matthews, M. L. (2013). Advances in the floral structural characterization of the major subclades of Malpighiales, one of the largest orders of flowering plants. *Ann. Bot.* 111, 969–985. doi: 10.1093/aob/mct056
- Fairless, D. (2007). Biofuel: the little shrub that could—maybe. *Nature* 449, 652–655. doi: 10.1038/449652a
- Ferro, M., Salvi, D., Brugière, S., Miras, S., Kowalski, S., Louwagie, M., et al. (2003). Proteomics of the chloroplast envelope membranes from *Arabidopsis thaliana*. *Mol. Cell. Proteomics* 2, 325–345. doi: 10.1074/mcp.m300030-mcp200
- Fitzpatrick, K. L., and Reid, R. (2009). The involvement of aquaglyceroporins in transport of boron in barley root. *Plant Cell Environ.* 32, 1357–1365. doi: 10.1111/j.1365-3040.2009.02003.x
- Froger, A., Tallur, B., Thomas, D., and Delamarche, C. (1998). Prediction of functional residues in water channels and related proteins. *Protein Sci.* 7, 1458–1468. doi: 10.1002/pro.5560070623
- Fu, D., Libson, A., Miercke, L. J. W., Weitzman, C., Nollert, P., Krucinski, J., et al. (2000). Structure of a glycerol-conducting channel and the basis for its selectivity. *Science* 290, 481–486. doi: 10.1126/science.290.5491.481
- Gomes, D., Agasse, A., Thiébaud, P., Delrot, S., Gerós, H., and Chaumont, F. (2009). Aquaporins are multifunctional water and solute transporters highly divergent in living organisms. *Biochim. Biophys. Acta* 1788, 1213–1228. doi: 10.1016/j.bbamem.2009.03.009
- Gupta, A. B., and Sankararamakrishnan, R. (2009). Genome-wide analysis of major intrinsic proteins in the tree plant *Populus trichocarpa*: characterization of XIP subfamily of aquaporins from evolutionary perspective. *BMC Plant Biol.* 20:134. doi: 10.1186/1471-2229-9-134
- Harikrishnan, S. L., Pucholt, P., and Berlin, S. (2015). Sequence and gene expression evolution of paralogous genes in willows. *Sci. Rep.* 5, 18662. doi: 10.1038/srep18662
- Hirakawa, H., Tsuchimoto, S., Sakai, H., Fukai, E., Watanabe, A., Kato, M., et al. (2012). Upgraded genomic information of *Jatropha curcas* L. *Plant Biotechnol.* 29, 123–130. doi: 10.5511/plantbiotechnology.12.0515a
- Horton, P., Park, K. J., Obayashi, T., Fujita, N., Harada, H., Adams-Collier, C. J., et al. (2007). WoLF PSORT: protein localization predictor. *Nucleic Acids Res.* 35, W585–W587. doi: 10.1093/nar/gkm259
- Hove, R. M., and Bhave, M. (2011). Plant aquaporins with non-aqua functions: deciphering the signature sequences. *Plant Mol. Biol.* 75, 413–430. doi: 10.1007/s11103-011-9737-5
- Hove, R. M., Ziemann, M., and Bhave, M. (2015). Identification and expression analysis of the barley (*Hordeum vulgare* L.) aquaporin gene family. *PLoS ONE* 10:e0128025. doi: 10.1371/journal.pone.0128025
- Hu, B., Jin, J., Guo, A., Zhang, H., Luo, J., and Gao, G. (2015). GS2D 2.0: an upgraded gene feature visualization server. *Bioinformatics* 31, 1296–1297. doi: 10.1093/bioinformatics/btu817
- Hu, W., Hou, X., Huang, C., Yan, Y., Tie, W., Ding, Z., et al. (2015). Genome-wide identification and expression analyses of aquaporin gene family during development and abiotic stress in banana. *Int. J. Mol. Sci.* 16, 19728–19751. doi: 10.3390/ijms160819728
- Hunter, P. R., Craddock, C. P., Di Benedetto, S., Roberts, L. M., and Frigerio, L. (2007). Fluorescent reporter proteins for the tonoplast and the vacuolar lumen identify a single vacuolar compartment in *Arabidopsis* cells. *Plant Physiol.* 145, 1371–1382. doi: 10.1104/pp.107.103945
- Ishikawa, F., Suga, S., Uemura, T., Sato, M. H., and Maeshima, M. (2005). Novel type aquaporin SIPs are mainly localized to the ER membrane and show cell specific expression in *Arabidopsis thaliana*. *FEBS Lett.* 579, 5814–5820. doi: 10.1016/j.febslet.2005.09.076
- Jaillon, O., Aury, J. M., Noel, B., Policriti, A., Clepet, C., Casagrande, A., et al. (2007). The grapevine genome sequence suggests ancestral hexaploidization in major angiosperm phyla. *Nature* 449, 463–467. doi: 10.1038/nature06148
- Jang, H. Y., Yang, S. W., Carlson, J. E., Ku, Y. G., and Ahn, S. J. (2013). Two aquaporins of *Jatropha* are regulated differentially during drought stress and subsequent recovery. *J. Plant Physiol.* 170, 1028–1038. doi: 10.1016/j.jplph.2013.03.001
- Jiang, H., Wu, P., Zhang, S., Song, C., Chen, Y., Li, M., et al. (2012). Global analysis of gene expression profiles in developing physic nut (*Jatropha curcas* L.) seeds. *PLoS ONE* 7:e36522. doi: 10.1371/journal.pone.0036522
- Jiao, Y., Leebens-Mack, J., Ayyampalayam, S., Chanderbali, A. S., Landherr, L., Ralph, P. E., et al. (2012). A genome triplication associated with early diversification of the core eudicots. *Genome Biol.* 13, R3. doi: 10.1186/gb-2012-13-1-r3
- Johanson, U., Karlsson, M., Johansson, I., Gustavsson, S., Slovall, S., Fraysse, L., et al. (2001). The complete set of genes encoding major intrinsic proteins in *Arabidopsis* provides a framework for a new nomenclature for major intrinsic proteins in plants. *Plant Physiol.* 126, 1358–1369. doi: 10.1104/pp.126.4.1358
- Juntawong, P., Sirikhachornkit, A., Pimjan, R., Sonthirod, C., Sangsrakru, D., Yoocha, T., et al. (2014). Elucidation of the molecular responses to waterlogging in *Jatropha* roots by transcriptome profiling. *Front Plant Sci.* 5:658. doi: 10.3389/fpls.2014.00658
- Khan, K., Agarwal, P., Shanware, A., and Sane, V. A. (2015). Heterologous expression of two *Jatropha* aquaporins imparts drought and salt tolerance and improves seed viability in transgenic *Arabidopsis thaliana*. *PLoS ONE* 10:e0128866. doi: 10.1371/journal.pone.0128866
- King, A. J., Li, Y., and Graham, I. A. (2011). Profiling the developing *Jatropha curcas* L. seed transcriptome by pyrosequencing. *Bioenergy Res.* 4, 211–221. doi: 10.1007/s12155-011-9114-x
- Langmead, B., and Salzberg, S. L. (2012). Fast gapped-read alignment with Bowtie 2. *Nat. Methods* 9, 357–359. doi: 10.1038/nmeth.1923
- Leitch, A. R., Lim, K. Y., Leitch, I. J., O'Neill, M., Chye, M. L., and Low, F. C. (1998). Molecular cytogenetic studies in rubber, *Hevea brasiliensis* Muell. Arg. (Euphorbiaceae). *Genome* 41, 464–467.
- Li, Z., Zhang, H., Ge, S., Gu, X., Gao, G., and Luo, J. (2009). Expression pattern divergence of duplicated genes in rice. *BMC Bioinformatics* 6:S8. doi: 10.1186/1471-2105-10-S6-S8
- Lopez, D., Bronner, G., Brunel, N., Auguin, D., Bourgerie, S., Brignolas, F., et al. (2012). Insights into *Populus* XIP aquaporins: evolutionary expansion, protein functionality, and environmental regulation. *J. Exp. Bot.* 63, 2217–2230. doi: 10.1093/jxb/err404
- Ma, J. F., Tamai, K., Yamaji, N., Mitani, N., Konishi, S., Katsuhara, M., et al. (2006). A silicon transporter in rice. *Nature* 440, 688–691. doi: 10.1038/nature04590
- Maurel, C., Verdoucq, L., Luu, D. T., and Santoni, V. (2008). Plant aquaporins: membrane channels with multiple integrated functions. *Annu. Rev. Plant Biol.* 59, 595–624. doi: 10.1146/annurev.aplant.59.032607.092734
- Mizutani, M., Watanabe, S., Nakagawa, T., and Maeshima, M. (2006). Aquaporin NIP2;1 is mainly localized to the ER membrane and shows root-specific accumulation in *Arabidopsis thaliana*. *Plant Cell Physiol.* 47, 1420–1426. doi: 10.1093/pcp/pcl004
- Montes Osorio, L. R., Torres Salvador, A. F., Jongschaap, R. E., Azurdia Perez, C. A., Berduo Sandoval, J. E., Trindade, L. M., et al. (2014). High level of molecular and phenotypic biodiversity in *Jatropha curcas* from Central America

- compared to Africa, Asia and South America. *BMC Plant Biol.* 14:77. doi: 10.1186/1471-2229-14-77
- Mortazavi, A., Williams, B. A., McCue, K., Schaeffer, L., and Wold, B. (2008). Mapping and quantifying mammalian transcriptomes by RNA-seq. *Nat. Methods* 5, 621–628. doi: 10.1038/nmeth.1226
- Natarajan, P., and Parani, M. (2011). *De novo* assembly and transcriptome analysis of five major tissues of *Jatropha curcas* L. using GS FLX titanium platform of 454 pyrosequencing. *BMC Genomics* 12:191. doi: 10.1186/1471-2164-12-191
- Noronha, H., Agasse, A., Martins, A. P., Berny, M. C., Gomes, D., Zarrouk, O., et al. (2014). The grape aquaporin VvSIP1 transports water across the ER membrane. *J. Exp. Bot.* 65, 981–993. doi: 10.1093/jxb/ert448
- Ogunnyi, D. S. (2006). Castor oil: a vital industrial raw material. *Bioresour. Technol.* 97, 1086–1091. doi: 10.1016/j.biortech.2005.03.028
- Pan, B. Z., Chen, M. S., Ni, J., and Xu, Z. F. (2014). Transcriptome of the inflorescence meristems of the biofuel plant *Jatropha curcas* treated with cytokinin. *BMC Genomics* 15:974. doi: 10.1186/1471-2164-15-974
- Park, W., Scheffler, B. E., Bauer, P. J., and Campbell, B. T. (2010). Identification of the family of aquaporin genes and their expression in upland cotton (*Gossypium hirsutum* L.). *BMC Plant Biol.* 10:142. doi: 10.1186/1471-2229-10-142
- Pommerenig, B., Diehn, T. A., and Bienert, G. P. (2015). Metalloido-porins: Essentiality of Nodulin 26-like intrinsic proteins in metalloid transport. *Plant Sci.* 238, 212–227. doi: 10.1016/j.plantsci.2015.06.002
- Prabhakaran Nair, K. P. (2010). “Rubber (*Hevea brasiliensis*),” in *The Agronomy and Economy of Important Tree Crops of the Developing World*, ed K. P. Prabhakaran Nair (London: Elsevier Press), 237–273. doi: 10.1016/B978-0-12-384677-8.00008-4
- Quigley, F., Rosenberg, J. M., Shachar-Hill, Y., and Bohnert, H. J. (2002). From genome to function: the *Arabidopsis* aquaporins. *Genome Biol.* 3, research0001.1–research0001.17.
- Rahman, A. Y., Usharraj, A. O., Misra, B. B., Thottathil, G. P., Jayasekaran, K., Feng, Y., et al. (2013). Draft genome sequence of the rubber tree *Hevea brasiliensis*. *BMC Genomics* 14:75. doi: 10.1186/1471-2164-14-75
- Reuscher, S., Akiyama, M., Mori, C., Aoki, K., Shibata, D., and Shiratake, K. (2013). Genome-wide identification and expression analysis of aquaporins in tomato. *PLoS ONE* 8:e79052. doi: 10.1371/journal.pone.0079052
- Sakurai, J., Ishikawa, F., Yamaguchi, T., Uemura, M., and Maeshima, M. (2005). Identification of 33 rice aquaporin genes and analysis of their expression and function. *Plant Cell Physiol.* 46, 1568–1577. doi: 10.1093/pcp/pci172
- Sato, S., Hirakawa, H., Isobe, S., Fukai, E., Watanabe, A., Kato, M., et al. (2011). Sequence analysis of the genome of an oil-bearing tree, *Jatropha curcas* L. *DNA Res.* 18, 65–76. doi: 10.1093/dnare/dsq030
- Savage, D. F., Egea, P. F., Robles-Colmenares, Y., O’Connell, J. D. III, and Stroud, R. M. (2003). Architecture and selectivity in aquaporins: 2.5 Å structure of aquaporin Z. *PLoS Biol.* 1:e72. doi: 10.1371/journal.pbio.0000072
- Sheldén, M., Howitt, S., Kaiser, B., and Tyerman, S. (2009). Identification and functional characterisation of aquaporins in the grapevine, *Vitis vinifera*. *Funct. Plant. Biol.* 36, 1065–1078. doi: 10.1071/FP09117
- Sui, H., Han, B. G., Lee, J. K., Walian, P., and Jap, B. K. (2001). Structural basis of water specific transport through the AQP1 water channel. *Nature* 414, 872–878. doi: 10.1038/414872a
- Takano, J., Wada, M., Ludewig, U., Schaaf, G., von Wirén, N., and Fujiwara, T. (2006). The *Arabidopsis* major intrinsic protein NIP5;1 is essential for efficient boron uptake and plant development under boron limitation. *Plant Cell* 18, 1498–1509. doi: 10.1105/tpc.106.041640
- Tamura, K., Stecher, G., Peterson, D., Filipski, A., and Kumar, S. (2013). MEGA6: Molecular evolutionary genetics analysis version 6.0. *Mol. Biol. Evol.* 30, 2725–2729. doi: 10.1093/molbev/mst197
- Tao, P., Zhong, X., Li, B., Wang, W., Yue, Z., Lei, J., et al. (2014). Genome-wide identification and characterization of aquaporin genes (AQPs) in Chinese cabbage (*Brassica rapa* ssp. *pekinensis*). *Mol. Genet. Genomics* 289, 1131–1145. doi: 10.1007/s00438-014-0874-9
- Thompson, J. D., Higgins, D. G., and Gibson, T. J. (1994). CLUSTAL W: improving the sensitivity of progressive multiple sequence alignment through sequence weighting, position-specific gap penalties and weight matrix choice. *Nucleic Acids Res.* 22, 4673–4680. doi: 10.1093/nar/22.22.4673
- Törnroth-Horsefield, S., Wang, Y., Hedfalk, K., Johanson, U., Karlsson, M., Tajkhorshid, E., et al. (2006). Structural mechanism of plant aquaporin gating. *Nature* 439, 688–694. doi: 10.1038/nature04316
- Trapnell, C., Roberts, A., Goff, L., Pertea, G., Kim, D., Kelley, D. R., et al. (2012). Differential gene and transcript expression analysis of RNA-seq experiments with TopHat and Cufflinks. *Nat. Protoc.* 7, 562–578. doi: 10.1038/nprot.2012.016
- Tungnagoen, K., Kongswadworakul, P., Viboonjun, U., Katsuhara, M., Brunel, N., Sakr, S., et al. (2009). Involvement of HbPIP2;1 and HbTIP1;1 aquaporins in ethylene stimulation of latex yield through regulation of water exchanges between inner liber and latex cells in *Hevea brasiliensis*. *Plant Physiol.* 151, 843–856. doi: 10.1104/pp.109.140228
- Tuskan, G. A., Difazio, S., Jansson, S., Bohlmann, J., Grigoriev, I., Hellsten, U., et al. (2006). The genome of black cottonwood, *Populus trichocarpa* (Torr. & Gray). *Science* 313, 1596–1604. doi: 10.1126/science.1128691
- Udvardi, M., and Poole, P. S. (2013). Transport and metabolism in legume-rhizobia symbioses. *Annu. Rev. Plant Biol.* 64, 781–805. doi: 10.1146/annurev-arplant-050312-120235
- Uehlein, N., Otto, B., Hanson, D. T., Fischer, M., McDowell, N., and Kaldenhoff, R. (2008). Function of *Nicotiana tabacum* aquaporins as chloroplast gas pores challenges the concept of membrane CO₂ permeability. *Plant Cell* 20, 648–657. doi: 10.1105/tpc.107.054023
- Venkatesh, J., Yu, J. W., and Park, S. W. (2013). Genome-wide analysis and expression profiling of the *Solanum tuberosum* aquaporins. *Plant Physiol. Biochem.* 73, 392–404. doi: 10.1016/j.plaphy.2013.10.025
- Wallace, I. S., and Roberts, D. M. (2005). Distinct transport selectivity of two structural subclasses of the nodulin-like intrinsic protein family of plant aquaglyceroporin channels. *Biochemistry* 44, 16826–16834. doi: 10.1021/bi0511888
- Wang, H., Zou, Z., Wang, S., and Gong, M. (2013). Global analysis of transcriptome responses and gene expression profiles to cold stress of *Jatropha curcas* L. *PLoS ONE* 8:e82817. doi: 10.1371/journal.pone.0082817
- Wang, X. C., Shi, M., Wang, D., Chen, Y., Cai, F., Zhang, S., et al. (2013). Comparative proteomics of primary and secondary laticoids reveals that chitinase and glucanase play a crucial combined role in rubber particle aggregation in *Hevea brasiliensis*. *J. Proteome Res.* 12, 5146–5159. doi: 10.1021/pr400378c
- Wang, Y., Tan, X., and Paterson, A. H. (2013). Different patterns of gene structure divergence following gene duplication in *Arabidopsis*. *BMC Genomics* 14:652. doi: 10.1186/1471-2164-14-652
- Wang, Y., Wang, X., and Paterson, A. H. (2012). Genome and gene duplications and gene expression divergence: a view from plants. *Ann. N. Y. Acad. Sci.* 1256, 1–14. doi: 10.1111/j.1749-6632.2011.06384.x
- Wu, P., Zhou, C., Cheng, S., Wu, Z., Lu, W., Han, J., et al. (2015). Integrated genome sequence and linkage map of physic nut (*Jatropha curcas* L.), a biodiesel plant. *Plant J.* 81, 810–821. doi: 10.1111/tpj.12761
- Wudick, M. M., Luu, D. T., and Maurel, C. (2009). A look inside: localization patterns and functions of intracellular plant aquaporins. *New Phytol.* 184, 289–302. doi: 10.1111/j.1469-8137.2009.02985.x
- Zhang, C., Zhang, L., Zhang, S., Zhu, S., Wu, P., Chen, Y., et al. (2015). Global analysis of gene expression profiles in physic nut (*Jatropha curcas* L.) seedlings exposed to drought stress. *BMC Plant Biol.* 15:17. doi: 10.1186/s12870-014-0397-x
- Zhang, D. Y., Ali, Z., Wang, C. B., Xu, L., Yi, J. X., Xu, Z. L., et al. (2013). Genome-wide sequence characterization and expression analysis of major intrinsic proteins in soybean (*Glycine max* L.). *PLoS ONE* 8:e56312. doi: 10.1371/journal.pone.0056312
- Zhang, L., Zhang, C., Wu, P., Chen, Y., Li, M., Jiang, H., et al. (2014). Global analysis of gene expression profiles in physic nut (*Jatropha curcas* L.) seedlings exposed to salt stress. *PLoS ONE* 9:e97878. doi: 10.1371/journal.pone.0097878
- Zhang, Y., Wang, Y., Jiang, L., Xu, Y., Wang, Y., Lu, D., et al. (2007). Aquaporin JcPIP2 is involved in drought responses in *Jatropha curcas*. *Acta Biochim. Biophys. Sin. (Shanghai)* 39, 787–794. doi: 10.1111/j.1745-7270.2007.00334.x

- Zou, Z., Gong, J., An, F., Xie, G. S., Wang, J. K., Mo, Y. Y., et al. (2015a). Genome-wide identification of rubber tree (*Hevea brasiliensis* Muell. Arg.) aquaporin genes and their response to ethephon stimulation in the laticifer, a rubber-producing tissue. *BMC Genomics* 16:1001. doi: 10.1186/s12864-015-2152-6
- Zou, Z., Gong, J., Huang, Q. X., Mo, Y. Y., Yang, L. F., and Xie, G. S. (2015b). Gene structures, evolution, classification and expression profiles of the aquaporin gene family in castor bean (*Ricinus communis* L.). *PLoS ONE* 10:e0141022. doi: 10.1371/journal.pone.0141022
- Zou, Z., Yang, L. F., Wang, Z. H., and Yuan, K. (2009). Biosynthesis and regulation of natural rubber in *Hevea*. *Plant Physiol. J.* 45, 1231–1238.

Conflict of Interest Statement: The authors declare that the research was conducted in the absence of any commercial or financial relationships that could be construed as a potential conflict of interest.

Copyright © 2016 Zou, Yang, Gong, Mo, Wang, Cao, An and Xie. This is an open-access article distributed under the terms of the Creative Commons Attribution License (CC BY). The use, distribution or reproduction in other forums is permitted, provided the original author(s) or licensor are credited and that the original publication in this journal is cited, in accordance with accepted academic practice. No use, distribution or reproduction is permitted which does not comply with these terms.



The Eucalyptus Tonoplast Intrinsic Protein (TIP) Gene Subfamily: Genomic Organization, Structural Features, and Expression Profiles

Marcela I. Rodrigues¹, Agnes A. S. Takeda^{2,3}, Juliana P. Bravo¹ and Ivan G. Maia^{1*}

¹ Department of Genetics, Institute of Biosciences of Botucatu, São Paulo State University, Botucatu, Brazil, ² Department of Physics and Biophysics, Institute of Biosciences of Botucatu, São Paulo State University, Botucatu, Brazil, ³ Institute of Biotechnology, São Paulo State University, Botucatu, Brazil

OPEN ACCESS

Edited by:

Rupesh Kailasrao Deshmukh,
Laval University, Canada

Reviewed by:

P. Kannapiran,
Mepco Schlenk Engineering College,
India
B. N. Devanna,
National Research Centre on Plant
Biotechnology, India

*Correspondence:

Ivan G. Maia
igmaia@ibb.unesp.br

Specialty section:

This article was submitted to
Plant Physiology,
a section of the journal
Frontiers in Plant Science

Received: 15 August 2016

Accepted: 16 November 2016

Published: 30 November 2016

Citation:

Rodrigues MI, Takeda AAS, Bravo JP and Maia IG (2016)
The Eucalyptus Tonoplast Intrinsic Protein (TIP) Gene Subfamily:
Genomic Organization, Structural Features, and Expression Profiles.
Front. Plant Sci. 7:1810.
doi: 10.3389/fpls.2016.01810

Plant aquaporins are water channels implicated in various physiological processes, including growth, development and adaptation to stress. In this study, the Tonoplast Intrinsic Protein (TIP) gene subfamily of Eucalyptus, an economically important woody species, was investigated and characterized. A genome-wide survey of the *Eucalyptus grandis* genome revealed the presence of eleven putative TIP genes (referred as *EgTIP*), which were individually assigned by phylogeny to each of the classical TIP1–5 groups. Homology modeling confirmed the presence of the two highly conserved NPA (Asn-Pro-Ala) motifs in the identified *EgTIPs*. Residue variations in the corresponding selectivity filters, that might reflect differences in *EgTIP* substrate specificity, were observed. All *EgTIP* genes, except *EgTIP5.1*, were transcribed and the majority of them showed organ/tissue-enriched expression. Inspection of the *EgTIP* promoters revealed the presence of common *cis*-regulatory elements implicated in abiotic stress and hormone responses pointing to an involvement of the identified genes in abiotic stress responses. In line with these observations, additional gene expression profiling demonstrated increased expression under polyethylene glycol-imposed osmotic stress. Overall, the results obtained suggest that these novel *EgTIPs* might be functionally implicated in eucalyptus adaptation to stress.

Keywords: aquaporin, tonoplast intrinsic protein, gene structure, gene expression, abiotic stress, Eucalyptus

INTRODUCTION

Aquaporins are membrane channels implicated in the transfer of water and small solutes across cell membranes (reviewed in Maurel et al., 2015). In plants, aquaporins fall into at least seven different subfamilies that reflect their main subcellular localization (reviewed in Maurel et al., 2015). Members of the Tonoplast Intrinsic Protein (TIP) subfamily are generally targeted to the vacuolar membrane and known to facilitate water transport across this subcellular compartment. Parallel to their role as water channels, TIP isoforms can also translocate glycerol, hydrogen peroxide (H_2O_2) (reviewed in Maeshima, 2001) and urea (Liu et al., 2003), and enhance vacuolar membrane permeability to ammonia (Loqué et al., 2005; Kirscht et al., 2016). Specificity of substrate transport is mainly determined by four amino acid (aa) residues present at specific positions of the so-called aromatic/arginine (ar/R) selectivity filter, which acts as a size-exclusion barrier (Sui et al., 2001; Wu et al., 2009).

Reports on the expression of a set of TIP genes revealed differential regulation in response to environmental constraints, especially drought and salinity, and to abscisic acid (ABA) (Alexandersson et al., 2005; Bouriac et al., 2005; Rodrigues et al., 2013; Regon et al., 2014). Supporting the importance of these proteins in plant stress adaptation, TIPs were shown to improve drought and salt tolerance when overexpressed in transgenic plants (Peng et al., 2007; Khan et al., 2015; Li and Cai, 2015). Intriguingly, TIP overexpression also positively affected plant growth and biomass production (Lin et al., 2007; Peng et al., 2007; Sade et al., 2009; Khan et al., 2015; Li and Cai, 2015). Although some discrepancies exist, since overexpression phenotypes displaying sensitivity to abiotic stress have been observed (Wang et al., 2011), the current consensus is that TIPs are engaged in the regulation of important physiological processes that contributes to plant growth and adaptation to stress (reviewed in Afzal et al., 2016). In this context, a recent role for different TIP isoforms in facilitating lateral root emergence in *Arabidopsis thaliana* was demonstrated (Reinhardt et al., 2016).

A systematic genome-wide analysis conducted in 10 different plant species, including both monocots and dicots, identified at least 100 genes encoding TIPs (Regon et al., 2014). In *A. thaliana*, the TIP subfamily is composed of 10 members that are phylogenetically classified into five subgroups (Johanson et al., 2001). In forest and fruit tree species, genome-wide surveys revealed the presence of 17 TIP genes in *Populus trichocarpa* (Gupta and Sankararamakrishnan, 2009) and *Hevea brasiliensis* (Zou et al., 2015a), while 10 and 11 genes were identified in *Vitis vinifera* and *Citrus sinensis*, respectively (Shelden et al., 2009; Martins et al., 2015). Intriguingly, a preliminary study identified a relatively small number of TIP genes (five in total) in the Eucalyptus genome (Rodrigues et al., 2013). Taking into consideration the evolutionary history of the eucalyptus genome (Myburg et al., 2014), such a comparatively low number of genes is unexpected and requires additional investigation.

To gain further insights into the functional/structural attributes of the TIP subfamily of Eucalyptus, in the present study we undertook a genomic survey for additional members. This effort led to the identification of six novel genes (referred to as *EgTIP*), indicating that the *EgTIP* subfamily encompasses 11 members. In parallel, we investigated the phylogeny, structural features and expression patterns across different eucalyptus organs/tissues and in response to osmotic stress of the entire gene subfamily. The results obtained provide an interesting framework for future studies aiming to elucidate the roles of TIPs in woody species.

MATERIALS AND METHODS

Plant Material

Freshly harvested vegetative and reproductive organs/tissues (1 month-old plantlets; pool of leaves of different ages; roots from 1 and 6 month-old plantlets; stems from 1 and 6 month-old plantlets; vascular cambium samples from 6 year-old trees; flower; flower buds; and fruits) were obtained from *Eucalyptus grandis* essentially as described previously (Rodrigues et al.,

2013). After harvesting, fresh samples were frozen immediately in liquid nitrogen until total RNA extraction. Two-month-old plantlets of a commercial clone of *E. grandis*, kindly provided by Suzano Papel e Celulose SA, Brazil, were used in the osmotic stress assays.

In silico Identification and Characterization of the Eucalyptus TIP Genes (*EgTIP*)

To identify members of the TIP gene subfamily in Eucalyptus, annotated TIP sequences from *Arabidopsis* (Johanson et al., 2001; Alexandersson et al., 2005) were used as queries in BLAST searches against the *E. grandis* BRASUZ1 genome assembly (v2.0) available at Phytozome¹. To refine our analysis, additional BLAST searches were performed using previously identified poplar TIP sequences (Gupta and Sankararamakrishnan, 2009) as drivers. The identified gene products were subsequently validated using the Pfam domain annotation (Finn et al., 2016). The exon/intron organization of the mined *EgTIP* genes was determined using the Eucalyptus gene models annotated in Phytozome and the Gene Structure Display Server² (GSDS v2.0). The existence of duplication of the *EgTIP* genes was investigated using the locus-search module of the Plant Genome Duplication Database³ (PGDD). The ratio of non-synonymous (Ka) to synonymous (Ks) substitution rates of evolution were also calculated using PGDD. Searches for the presence of putative *cis*-regulatory elements within the *EgTIP* promoter regions were carried out using the Plant Care and PLACE databases. Predictions of the subcellular location of the *EgTIP* proteins were performed using Plant-mPLoc⁴ (Chou and Shen, 2010).

Phylogenetic Analyses

The deduced aa sequences of the identified *EgTIPs* were aligned with known TIPs from *A. thaliana*, *P. trichocarpa*, *Quercus petraea*, and *V. vinifera* using CLUSTALX2⁵. Phylogenetic relationships were inferred using the neighbor-joining method with 1000 bootstrap replicates implemented by the MEGA 7 software package⁶. Branches with <50% bootstrap support were collapsed. Accession numbers of the sequences used in the phylogenetic analyses are as follows: AtTIP1.1 (At2g36830), AtTIP1.2 (At3g26520), AtTIP1.3 (At4g01470), AtTIP2.1 (At3g16240), AtTIP2.2 (At4g17340), AtTIP2.3 (At5g47450), AtTIP3.1 (At1g73190), AtTIP3.2 (At1g17810), AtTIP4.1 (At2g25810), AtTIP5.1 (At3g47440), QqTIP1.1 (JQ846274), QqTIP2.1 (JQ846275), QqTIP2.2 (JQ846276), VvTIP1.1 (GSVIVP 00018548001), VvTIP1.2 (GSVIVP 00000605001), VvTIP1.3 (GSVIVP00022146001), VvTIP1.4 (GSVIVP00024394001), VvTIP2.1 (GSVIVP00034350001), VvTIP2.2 (GSVIVP00012703001), VvTIP3.1 (GSVIVP00013854001), VvTIP4.1 (GSVIVP00032441001), VvTIP5.1 (GSVIVP000299

¹<http://www.phytozome.net/>

²<http://gsds.cbi.pku.edu.cn/>

³<http://chibba.agtec.uga.edu/duplication/>

⁴<http://www.csbio.sjtu.edu.cn/bioinf/plant-multi/#>

⁵<http://www.clustal.org/>

⁶<http://www.megasoftware.net/>

46001), VvTIP5.2 (GSVIVP00019170001), PtTIP1.1 (549212), PtTIP1.2 (833283), PtTIP1.3 (822504), PtTIP1.4 (656044), PtTIP1.5 (667870), PtTIP1.6 (589502), PtTIP1.7 (558321), PtTIP1.8 (828458), PtTIP2.1 (548890), PtTIP2.2 (645978), PtTIP2.3 (817166), PtTIP2.4 (676397), PtTIP3.1 (584517), PtTIP3.2 (811826), PtTIP4.1 (561759), PtTIP5.1 (414059), PtTIP5.2 (423803). The Phytozome IDs of the mined *E. grandis* TIPs are: EgTIP1.1 (Eucgr.K02438), EgTIP1.2 (Eucgr.J00051), EgTIP1.3 (Eucgr.B02403), EgTIP1.4 (Eucgr.J02074) EgTIP2.1 (Eucgr.F03054), EgTIP2.2 (Eucgr.D02090), EgTIP2.3 (Eucgr.D02507), EgTIP3.1 (Eucgr.K02339), EgTIP3.2 (Eucgr.H00668), EgTIP4.1 (Eucgr.C02914), and EgTIP5.1 (Eucgr.K00164).

Molecular Modeling

The deduced aa sequences of EgTIPs representing each TIP group (EgTIP1.1; EgTIP2.1; EgTIP3.1; EgTIP4.1, and EgTIP5.1) were employed for the construction of the models. These structures were predicted based on the alignment data generated by the program Phyre2 that uses homology detection methods to build 3D models (Kelley et al., 2015). Considering the quality of the structure, the crystallographic structure of the *A. thaliana* aquaporin TIP2.1 (AtTIP2.1) at 1.18 Å resolution (PDB ID: 5I32, Chain A) (Kirscht et al., 2016) was chosen as template. The program MODELLER 9v16 (Sali and Blundell, 1993; Marti-Renom et al., 2000) was used to generate the protein models and rank them according to the DOPE (Discrete Optimized Protein Energy) score. The best TIP models were selected based on the stereochemical parameters using the program RAMPAGE (Lovell et al., 2003). The ConSurf Server (Landau et al., 2005; Ashkenazy et al., 2010) was used for conservation analysis and all images were generated using the PyMOL program (Schrödinger, 2011).

PEG-Imposed Osmotic Stress

The Eucalyptus plantlets (two months old) were transferred to hydroponic culture by means of a floating system and maintained in an aerated Hoagland's nutrient solution (75%) at pH 6.0 (osmotic potential of -0.1 MPa) before stress imposition. After an acclimatization period, 50% of the tested plantlets were stressed by adding 215 g of polyethylene glycol 8000 (PEG; Sigma, USA) to 1 L of culture medium to induce osmotic stress, while the remaining were maintained in Hoagland's nutrient solution (75%) throughout the assay as control. The osmotic potential of the PEG 8000-treated solution was -0.6 MPa (WP4-T, Decagon Devices, Inc., England). A compressed air system was used to homogenize the solutions in both the tray and the PEG container to avoid anoxia of the roots.

Both control and stress treatments comprised 15 plantlets per tray, and three trays per treatment (control/treated plantlets), representing three biological replications. To carry out the gene expression analyses, the roots, stems and leaves from three randomized plantlets per tray were collected after 6 h (short-term), 12 h (medium-term), and 24 h (long-term) of PEG-treatment. Organ samples from untreated control plantlets were simultaneously collected at each time-point. To reduce plant-to-plant variation, each collected group of organ samples was pooled before RNA extraction.

EgTIP Expression Analyses

The relative expression of the *EgTIP* genes was assessed using quantitative real-time RT-PCR (RT-qPCR). Total RNA extraction and cDNA synthesis were performed as previously described (Rodrigues et al., 2013). The qPCR analyses were carried out using Power SYBR Green Master Mix (Applied Biosystems) and a StepOnePlus Real Time PCR System (Applied Biosystems). The cycling conditions were as follows: 5 min at 95°C, followed by 45 cycles of 15 s at 95°C and 60 s at 60°C. Each reaction was performed in triplicate in a total volume of 10 µl, and contained 20 ng of cDNA and 0.2 µM of each *EgTIP*-specific primer (Supplementary Table S1). Among five selected *E. grandis* reference genes (*Actin*, *GAPDH*, *Cdk8*, *Transcription elongation factor s-II*, and *Aspartyl-tRNA synthetase*; de Oliveira et al., 2012) tested, *actin* was the most stable and thus employed as endogenous control (Supplementary Table S1; Goicoechea et al., 2005). Cycle threshold (Ct) values were obtained for each sample, and relative quantification was determined using the $2^{-\Delta\Delta Ct}$ method as described (Livak and Schmittgen, 2001). Amplification efficiencies were derived from the amplification plots using the program LinRegPCR (Ramakers et al., 2003). A value of two was used in calculations. For the expression analysis under osmotic stress, the relative expression of each *EgTIP* at a given time point was determined as the fold change of its expression under treated condition relative to its expression under control condition.

Relative expression data were analyzed using the Relative expression software tool (REST 2009) and differences with *p*-values <0.05 were considered statistically significant. The heatmaps were created using the function heatmap.2 from plot package at R environment. For the organ/tissue-specific gene expression analyses, normalization was performed using 1-month-old plantlets as control sample as previously reported (Yu et al., 2014). According to Yu et al. (2014), these plantlets represent a highly stable and less variable sample that contain the main investigated organs/tissues. Additional expression analyses were performed using publicly available RNA-Seq data⁷ generated for six different vegetative organs/tissues (young and mature leaves, shoot tips, phloem, immature xylem and xylem) from a 6-year-old *E. grandis* X *E. urophylla* hybrid clone (Mizrachi et al., 2010). In this case, transcript abundances were expressed as units of normalized FPKM (fragments per kilobase of exon per million fragments mapped), that were used for heatmap construction.

RESULTS

Identification and Analysis of the Eucalyptus TIP Genes

BLAST searches in the *E. grandis* genome identified 11 putative TIP coding sequences (Table 1), thus indicating that the Eucalyptus TIP subfamily has 11 members (referred as *EgTIP*) and not 5 as previously suggested (Rodrigues et al., 2013). To analyze in more detail, the evolutionary relationships

⁷www.phytozome.net

TABLE 1 | Structural and subcellular localization analysis of the EgTIPs.

Protein	Ch ^a	Size	pI	MW (kDa)	TM ^b	Loc ^c	Ar/R selectivity filter*					NPA motif**					Froger's positions				
							H2	LC	H5	LE1	LE2	LB	LE	P1	P2	P3	P4	P5			
EgTIP1.1	3	260	5.56	26	6	Vacuole	H	F	—	A	V	NPA	NPA	T	S	A	Y	W			
EgTIP1.2	10	252	4.68	26	6	Vacuole	H	F	—	A	A	NPA	NPA	T	S	A	Y	W			
EgTIP1.3	2	252	4.79	26	6	Vacuole	H	F	—	A	A	NPA	NPA	T	S	A	Y	W			
EgTIP1.4	10	251	5.16	25.8	6	Vacuole	H	F	—	A	A	NPA	NPA	T	S	A	Y	W			
EgTIP2.1	6	248	5.52	25	6	Vacuole	H	H	—	G	R	NPA	NPA	T	S	A	Y	W			
EgTIP2.2	4	250	5.12	25	6	Vacuole	H	H	—	G	R	NPA	NPA	T	S	A	Y	W			
EgTIP2.3	4	259	6.78	26.4	6	Cell membrane/vacuole	G	F	—	G	R	NPA	NPA	A	S	A	H	W			
EgTIP3.1	11	262	6.7	27.5	6	Vacuole	F	—	A	L	NPA	NPA	T	A	A	A	Y	W			
EgTIP3.2	8	259	6.04	27.8	6	Vacuole	S	L	—	A	R	NPA	NPA	T	S	A	Y	W			
EgTIP4.1	3	243	5.91	25.3	6	Vacuole	H	H	—	A	R	NPA	NPA	T	S	A	Y	W			
EgTIP5.1	11	256	6.81	25.7	6	Cell membrane/vacuole	N	F	—	G	C	NPA	NPA	T	S	A	Y	W			

* Ar/R: aromatic/arginine; H2: transmembrane helix 2; LC: loop C; H5: transmembrane helix 5; LE: loop E; ** NPA: Asn-Pro-Ala. ^aChromosome location of the corresponding gene. ^bNumber of transmembrane (TM) helices predicted by TMpred. ^cBest possible subcellular localization predicted by Plant-mPloc.

between the identified EgTIPs and those present in other plant species, an unrooted phylogenetic tree was constructed using the predicted protein sequences (**Figure 1**). Based on their phylogenetic relationships, the EgTIPs could be individually assigned to each of the classical TIP1–5 groups (Johanson et al., 2001), and were named accordingly (EgTIP1.1, EgTIP1.2, EgTIP1.3 and EgTIP1.4; EgTIP2.1, EgTIP2.2 and EgTIP2.3; EgTIP3.1 and EgTIP3.2; EgTIP4.1; and EgTIP5.1). In general, the corresponding groups, with the exception of group 1, were supported by moderate to high bootstrap values. The identity at the aa level varied according to the TIP group considered: 79–88% identity between EgTIP1s, 76%–47% identity between EgTIP2s and 77% between EgTIP3s. Taking into account the tree topology, EgTIP2.3 was grouped with known TIP5 isoforms, being closely related to VvTIP5.2 (61% identity at the aa level). Nevertheless, the inspection of the ar/R selectivity residues of both VvTIP5.2 and EgTIP2.3 (see below) revealed a closer relationship with TIP2 isoforms. Therefore, based on its selectivity filter, EgTIP2.3 was assigned here as a TIP2 as originally proposed in Phytozome instead of a TIP5. In fact, the small subgroup formed by VvTIP5.2 and EgTIP2.3 is branched between the groups encompassing TIP5.1 and TIP2 isoforms. In this regard, EgTIP2.3 shares 44 and 47% aa sequence identity with EgTIP5.1 and EgTIP2.2, respectively. As observed in other plant species, the majority of the identified EgTIPs belongs to group 1 (four members) followed by group 2, 3, and 5 with two members each. The phylogenetic tree also revealed the presence of closely related gene pairs (*EgTIP1.3/EgTIP1.4* and *EgTIP3.1/EgTIP3.2*, for example), suggesting possible gene duplication events.

Analysis of the genomic structure of the annotated *EgTIP* genes revealed a two-intron/three-exon organization, except for *EgTIP1.1* that contained two exons disrupted by a single intron (**Figure 2**). These introns showed variations in length and position. Consistent with this, most members of the TIP subfamily of dicot species share such a well-conserved two-intron/three-exon pattern (Regon et al., 2014). Regarding their chromosomal distribution, the *EgTIP* genes are located on seven (2, 3, 4, 6, 8, 10, and 11) out of the eleven eucalyptus chromosomes (**Table 1**). In general, one or two genes are found per chromosome. In this context, *EgTIP1.1* and *EgTIP4.1* (on 3), *EgTIP1.2* and *EgTIP1.4* (on 10), *EgTIP2.2* and *EgTIP2.3* (on 4) and *EgTIP3.1* and *EgTIP5.1* (on 11) are among those located on the same chromosome.

An additional locus search at the PGDD website was performed to evaluate possible *EgTIP* gene duplication. According to the resulting data, the following gene pairs were observed: *EgTIP1.3/EgTIP1.4*, *EgTIP2.1/EgTIP4*, *EgTIP3.1/EgTIP3.2*, and *EgTIP2.2/EgTIP2.3*. Among them, only *EgTIP2.2* and *EgTIP2.3* are located on the same chromosome (4), and may possibly represent tandemly duplicated genes. To investigate the mechanisms involved in gene duplication evolution after divergence, we calculated the Ka/Ks ratio of each *EgTIP* gene pairs. The results (Supplementary Table S2) revealed that the Ka/Ks ratios of all four *EgTIP* gene pairs were less than 0.4, implying that these genes had undergone purifying selection pressure with limited functional divergence after duplication.

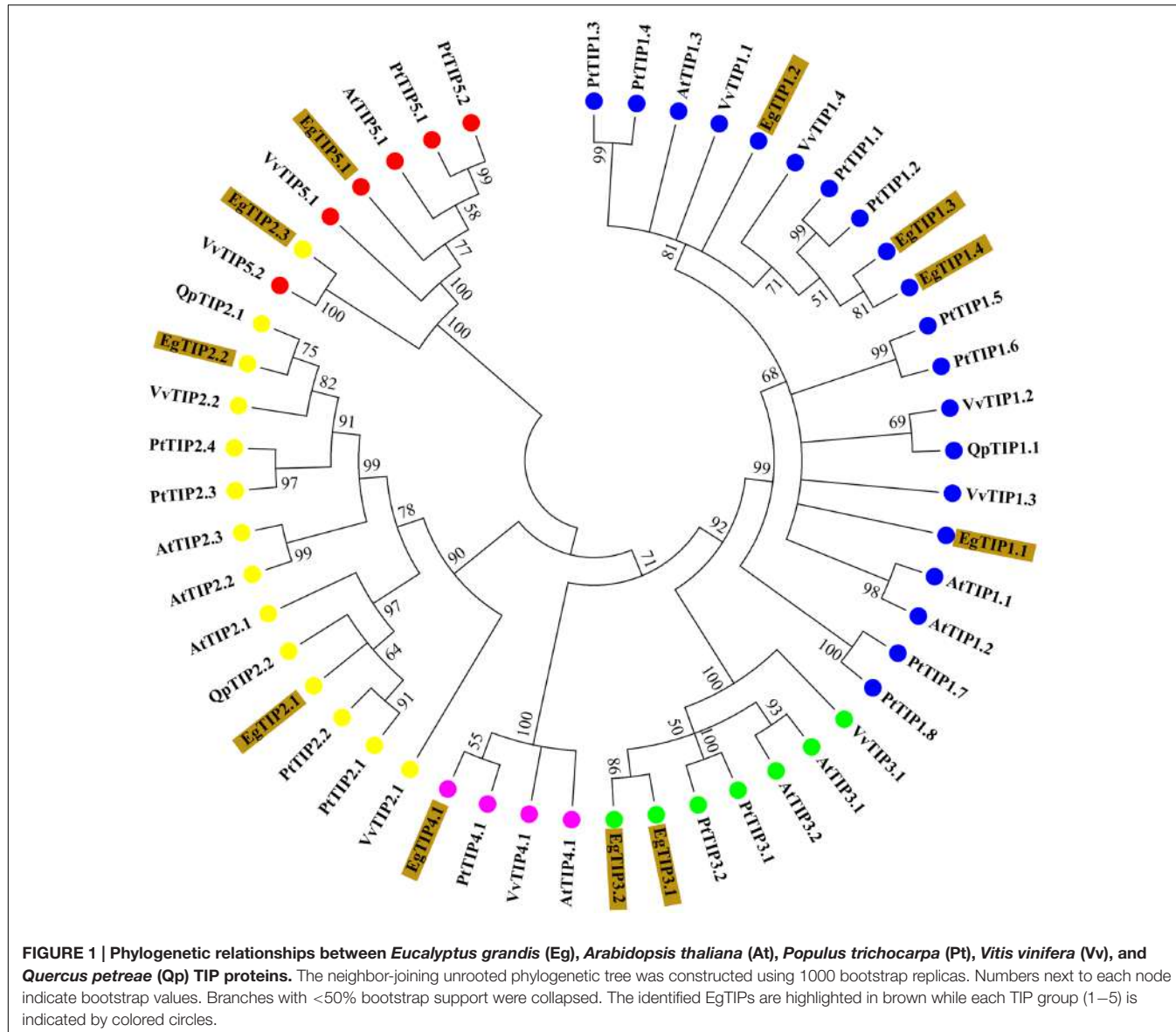


FIGURE 1 | Phylogenetic relationships between *Eucalyptus grandis* (Eg), *Arabidopsis thaliana* (At), *Populus trichocarpa* (Pt), *Vitis vinifera* (Vv), and *Quercus petraea* (Qp) TIP proteins. The neighbor-joining unrooted phylogenetic tree was constructed using 1000 bootstrap replicas. Numbers next to each node indicate bootstrap values. Branches with <50% bootstrap support were collapsed. The identified EgTIPs are highlighted in brown while each TIP group (1–5) is indicated by colored circles.

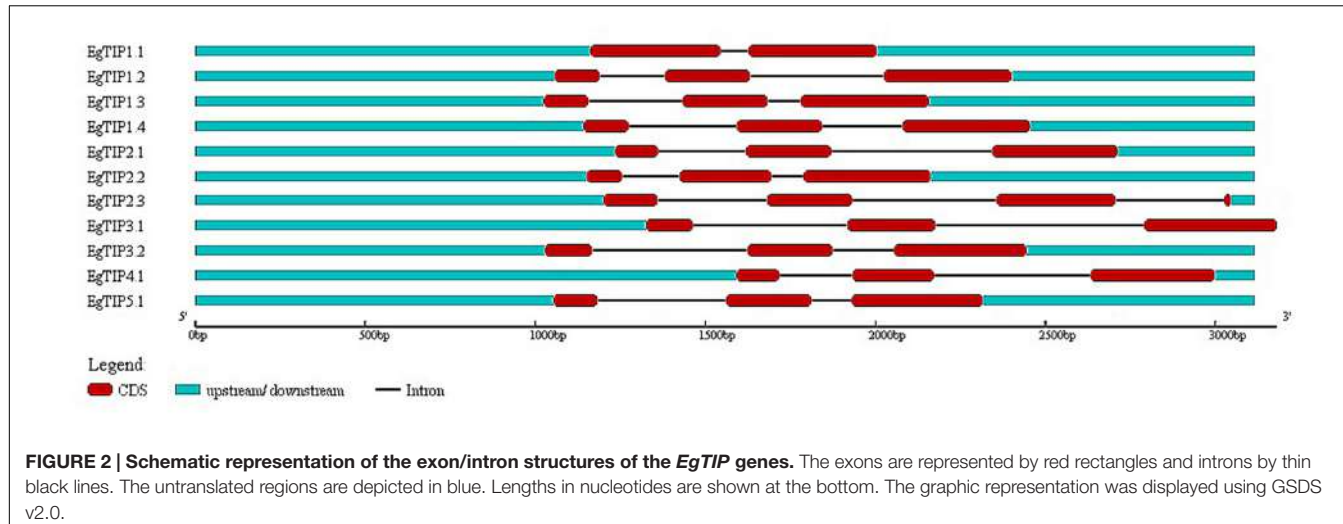
Structural Features of the Identified EgTIPs

The deduced EgTIP proteins ranged in size from 243 (EgTIP4.1) to 262 (EgTIP3.1) aa residues, with molecular weights (MW) and theoretical isoelectric point (pI) values ranging between 25 and 27.8 kDa and 4.68 and 6.81, respectively (Table 1). These proteins are all predicted to contain six transmembrane α -helices (H1–H6) and five loops. Concerning their sub-cellular localization, all EgTIPs are predicted to be located in the vacuole, with the exception of EgTIP5.1 and EgTIP2.3, that are also localized at the cell membrane (Table 1).

To evaluate structural similarities and differences, theoretical models for EgTIPs representing each classical TIP group were constructed using a comparative modeling approach and the crystallography structure of AtTIP2.1 at 1.18 Å resolution (Kirscht et al., 2016) as a template. The sequences shared 53–85%

aa identity and 90–95% of coverage. As expected, all models contained the six α -helices and interhelical loop regions as seen throughout the aquaporin family. The best models showed good stereochemical quality with 96.9% of the residues in favored regions, 2.6–1.7% and 0–0.9% (corresponding to two residues) in allowed and disallowed regions, respectively (Supplementary Table S3).

Residue conservation was reflected by surface mapping of the aa sequences of several plant TIPs over the generated EgTIP1.1 model (Figure 3). An overall evaluation of the EgTIP models detected the dual NPA (Asn-Pro-Ala) motifs conserved in all structures (Figures 3A,C; Supplementary Figure S1). In contrast, the key residues of the selectivity filter (positions H2, H5, LE1, and LE2) displayed some variations between the modeled proteins (Table 1; Figures 3B,C; Supplementary Figure S1). In all EgTIP1 and EgTIP2, the tetrad of the



ar/R selectivity filter was composed of HIAV and HIGR, respectively (**Table 1**; Supplementary Figure S1). Despite showing phylogenetic relationships with TIP5 isoforms (**Figure 1**), the selectivity filter of EgTIP2.3 (HIGR) resembles the one found overall in group 2 members (HIGR; **Figure 3E**). Remarkably, EgTIP2.3 lacks the I residue in the H5 position, but has instead an F residue that preserves the hydrophobicity. Interestingly, the closest homologue of EgTIP2.3, VvTIP5.2, also harbors a classical TIP2-like selectivity filter (HIGR). For the other EgTIPs, slight residue variations at specific positions were observed (**Table 1**; **Figure 3D**). According to previous reports, a V residue is typically found at the LE2 position of TIPs from group 1, while an R is found in TIPs from groups 2, 3, and 4, whereas a C residue is present in all group 5 TIPs (Wallace and Roberts, 2004; Gupta and Sankararamakrishnan, 2009). In this regard, EgTIP3.1 harbors an atypical L residue in this position, while an R residue in EgTIP2.3 replaces the usual C residue (**Table 1**; **Figure 3D**). In addition, compared to the other EgTIPs, EgTIP3.2 and EgTIP5.1 harbor changes in the H2 position (S and N, respectively, instead of H), while EgTIP5.1 and EgTIP2.3 display variations in H5 (V and F, respectively, instead of I) (**Table 1**; **Figure 3D**).

Further comparison of the EgTIP-deduced aa sequences with those of other plant TIPs revealed that TIP members of groups 1 and 2 have the most conserved selectivity filters, including the H residue located in loop C (LC) of the proposed extended ar/R filter (Kirscht et al., 2016) (**Figures 3D,E**). VvTIP1.3 from *V. vinifera*, that possesses an M residue instead of a V in the LE2 position, is the only exception. The members of group 3 have most conserved residues in the H5 and LE1 positions and small variations in the H2 and LE2 positions. On the other hand, group 4 members have differences mainly in the LC and H5 positions, while EgTIP5.1 have the most variable LC positions.

The *EgTip* Genes Show Enriched Organ/Tissues Profiles

To investigate the spatiotemporal expression profiles of the identified *EgTIP* genes, we first assessed their relative expression

over a panel of different Eucalyptus organs/tissues using RT-qPCR. As shown in **Figure 4**, all members of the *EgTIP* subfamily, except *EgTIP5.1*, were transcribed. Among the genes investigated, solely *EgTIP1.1* had a relatively broad distribution among organs/tissues, being expressed at moderate levels in the roots, stems, flowers and flower buds. In contrast, the other *EgTIP* genes surveyed showed distinctive organ/tissue-enriched expression. Of the genes grouped in the so-called group 1, *EgTIP1.3* was preferentially expressed in vascular cambium and stems, *EgTIP1.4* in flowers and flower buds, and *EgTIP1.2* in leaves and stems. Of group 2, *EgTIP2.1*, and *EgTIP2.2* were both moderately expressed in flowers and flower buds, but recapitulating previous data (Rodrigues et al., 2013), *EgTIP2.2* was also highly expressed in roots. Of note, *EgTIP2.3* was barely detected in leaves and stems and was not included in the heatmap. The duplicated gene pair *EgTIP3.1* and *EgTIP3.2* shared a similar fruit-enriched expression, but *EgTIP3.2* was also detected at moderate levels in leaves. Finally, *EgTIP4.1* was prominent in the stems.

EgTIP spatial expression patterns were further examined employing publicly available RNA-Seq data (FPKM values) from six different organs/tissues of a hybrid clone of Eucalyptus (Mizrachi et al., 2010). Interestingly, this dataset included vegetative and vascular tissue samples (such as phloem, xylem, and shoot tips) that were not represented in the previously performed RT-qPCR assays. According to the digital expression profiles generated (**Figure 5**), a wide expression pattern was observed for *EgTIP2.1* and *EgTIP1.1*, which were detected at moderate to high levels in all organs/tissues examined. A similar pattern was observed for *EgTIP1.2*, except for its very low expression level in the phloem. According to our RT-qPCR assays, this gene was predominantly expressed in leaves (**Figure 4**). On the other hand, *EgTIP4.1* was detected at moderate levels in mature leaves and at lower levels in young leaves and in shoot tips, while *EgTIP4.1* was prominent in vascular tissues (phloem and xylem). This is consistent with the preferential expression of *EgTIP4.1* in the stems as indicated by RT-qPCR (**Figure 4**). Contrasting with *EgTIP5.1* that was not expressed,

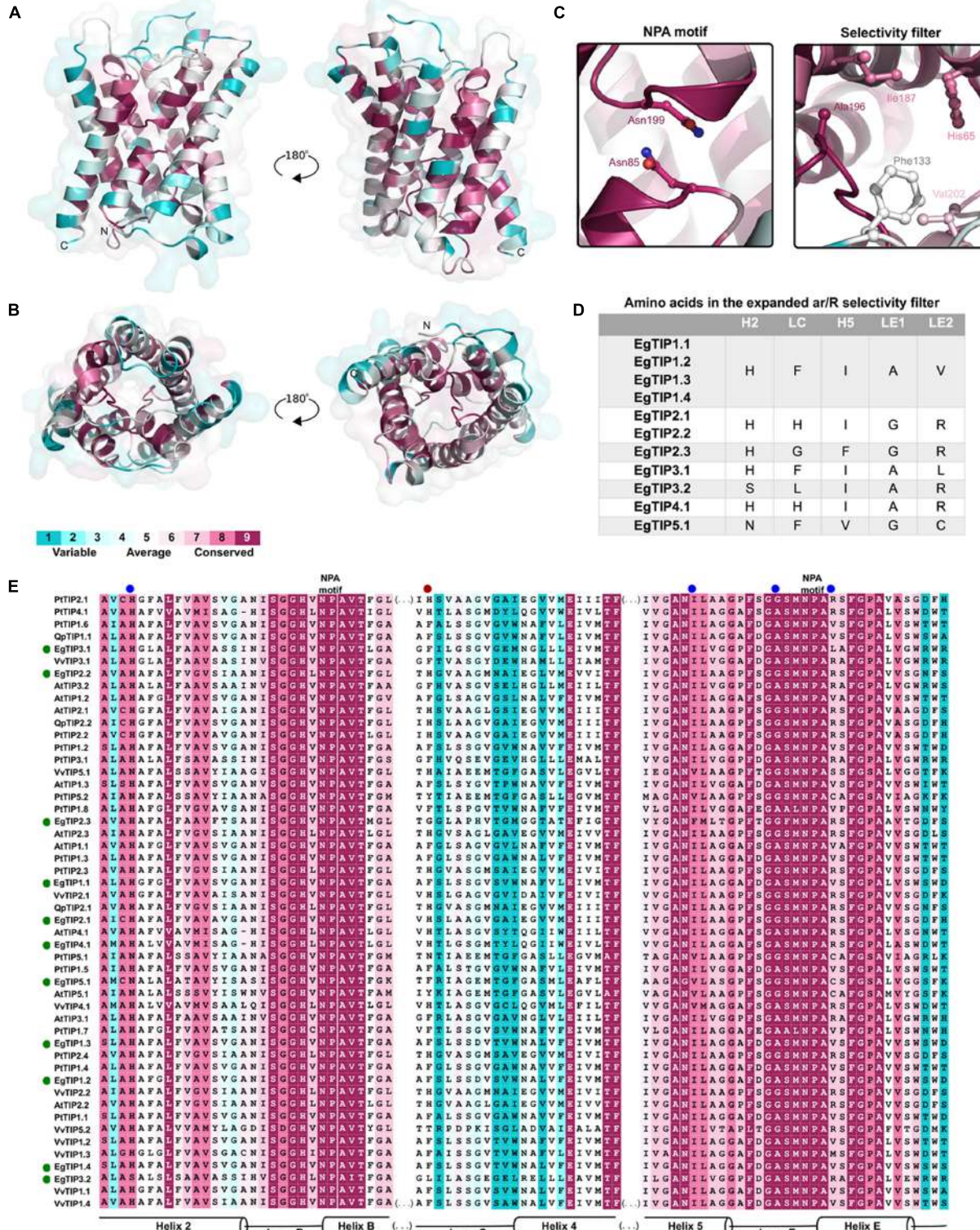


FIGURE 3 | Conservation of the EgTIP proteins. The protein sequences employed for the construction of the phylogenetic tree were used and residues were colored according to conservation. **(A)** Lateral view of EgTIP1.1 shown in ribbon representation in two positions. **(B)** Top and bottom views of EgTIP1.1. **(C)** Residues of the NPA motif and selectivity filter shown in stick representation. **(D)** Residues of the expanded selectivity filter. **(E)** Multiple sequence alignment colored according to the surfacing mapping of the EgTIP1.1 model. The green and blue dots indicate EgTIP sequences and residues of the selectivity filter, respectively. The red dot corresponds to the residue from the expanded selectivity filter.

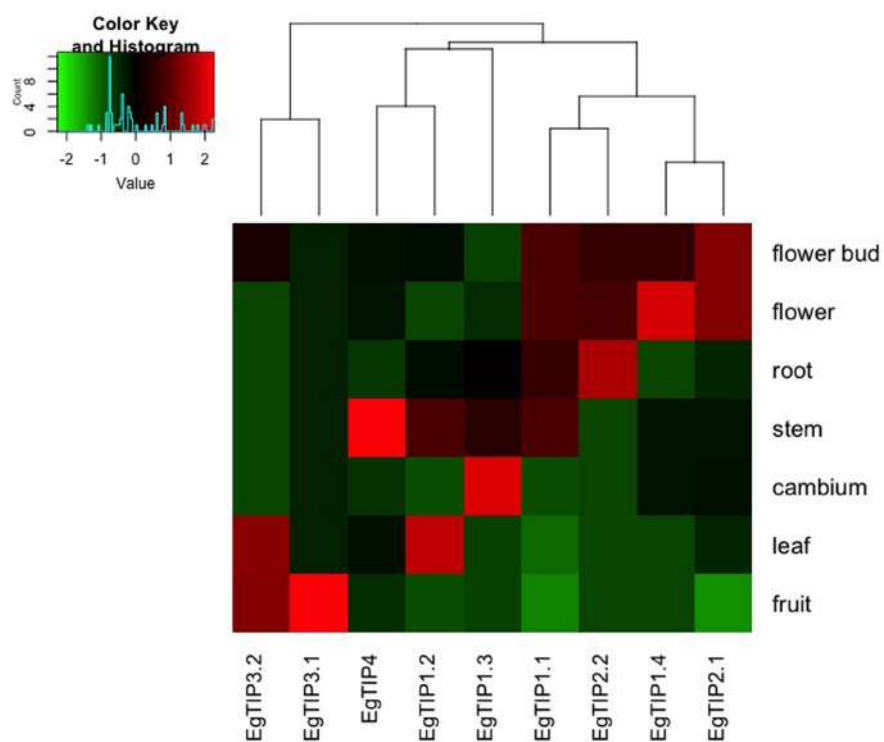


FIGURE 4 | Expression profiles of *EgTIP* genes in different *E. grandis* organs/tissues. The heatmap was generated employing the relative expression of each *EgTIP* as determined by RT-qPCR normalized with the control sample (1-month-old plantlets). Red and green colors denote relatively high and lower expression compared to control, respectively. Genes were clustered according to their expression profiles. All samples were analyzed in triplicate.

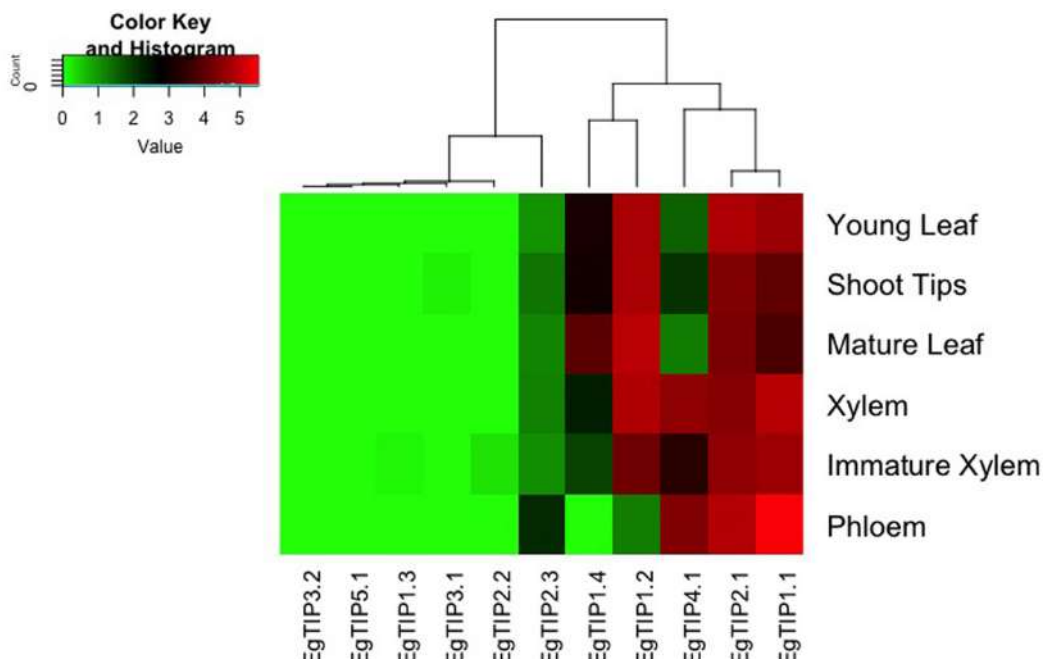


FIGURE 5 | *EgTIP* expression profiles determined using the RNA-Seq data from different *E. grandis* organs/tissues. The heatmap was generated employing normalized FPKM values available at Phytozome. The color scale is the same as in Figure 4.

EgTIP2.3 was observed at very low levels in the phloem. The other *EgTIP* genes, including those mainly expressed in reproductive organs as determined by RT-qPCR, were almost undetectable in the RNA-Seq data surveyed. In this regard, the absence of *EgTIP3.2* expression was particularly intriguing, especially because its transcripts were readily detectable in leaves by RT-qPCR (Figure 4). Overall, these results reveal a distinctive spatial distribution of the *EgTIP* genes, indicating that certain isoforms may act in a relatively organ-specific manner.

***EgTIP* Promoter Analysis Reveals the Presence of Stress-Related Regulatory Elements**

Inspection of the 5' upstream regions (1200 bp) of the *EgTIP* genes revealed the presence of several putative *cis*-regulatory elements mainly implicated in phytohormone and abiotic stress responses (Table 2). In this context, all *EgTIP* promoter regions, with the exception of *EgTIP1.2*, contained more than one ABA-responsive element (ABRE), involved in hormone responsiveness and in ABA-mediated abiotic stress signaling (Yamaguchi-Shinozaki and Shinozaki, 2005). The presence of ABRE in the promoters investigated suggests a possible role of ABA in the control of *EgTIP* expression as already reported for *HvTIP1.2* and *HvTIP3.1* in barley (Lee et al., 2015). Another well-represented regulatory element found in all the promoters investigated, except *EgTIP2.3*, was the TGACG-motif implicated in plant responses to methyl jasmonate (MeJA), a well-known primary signal in plant defense responses. Most *EgTIP* promoters (9 out of 11) also contained a MBS (MYB-binding site) motif generally recognized by MYB transcription factors implicated in drought and salt inducible gene expression. The circadian and SP1 elements known to play a role in circadian control and in light responses, respectively, were also detected in the majority of the *EgTIP* promoters. The circadian element is similarly over-represented in the promoter regions of aquaporin genes from sorghum (Reddy et al., 2015). Additional stress-related regulatory elements found in a small number of *EgTIP* promoters include TC-rich motifs, LTR, HSE and C-repeat/DRE (Table 2). Overall, these findings indicate that the *EgTIP* genes are regulated by phytohormones such as ABA and MeJA and differentially responsive to a set of abiotic stimuli. This prediction is supported by a previous study showing the modulation of *EgTIP2.2* promoter activity by osmotic stress and ABA (Rodrigues et al., 2013). However, the functionality of such predicted elements requires further validation.

***EgTIP* Expression Profiles Under PEG-Imposed Osmotic Stress**

Taking into account the aforementioned promoter analysis, we decided to evaluate the stress-responsive expression of each *EgTIP* gene. For this, total RNA extracted from roots, stems and leaves of Eucalyptus plantlets treated with PEG 8000 for 6, 12, and 24 h was employed. Relative to the untreated control, the majority of the investigated *EgTIPs*, with the obvious exception of the fruit-enriched *EgTIP3.1* and *EgTIP3.2* genes (not shown), showed increased expression upon PEG-induced osmotic stress

at one or more time points (Figure 6). The timing and magnitude of the observed changes in gene expression were quite diverse among the investigated organs. In roots, most *EgTIPs* showed moderate fold-changes and reached peak expression levels mainly at 12 h of stress imposition (Figure 6A). In contrast, the timing of maximal expression in the stems varied between the investigated genes and was most evident at 6 and 12 h of PEG treatment (Figure 6B). *EgTIP1.2* showed maximum stress-induced fold-change in this organ at 12 h of PEG treatment. Compared to roots and stems, *EgTIP* expression was increased in leaves. In this organ, significant fold-changes were observed at 6 h, and more substantially, at 24 h of stress imposition (Figure 6C). At this time point, *EgTIP1.1*, *EgTIP1.2*, *EgTIP1.3*, and *EgTIP2.3* appeared as the most responsive genes. Interestingly, despite being barely detectable in leaves and stems, *EgTIP2.3* was moderately and highly induced by osmotic stress in the investigated organs. In addition, the expression of *EgPIP2*, which was used as an inducible control (Rodrigues et al., 2013), was monitored in parallel and shown to be induced by PEG in all organs examined.

DISCUSSION

Although described throughout all kingdoms, aquaporins show a particularly high diversity and abundance in plants. Among the plant aquaporins, the members of the TIP subfamily are implicated in the control of tonoplast permeability to water and other solutes. Despite the accumulated knowledge in model species, much less is known about the organization of the TIP subfamily in woody species, especially in Eucalyptus, an economically important and high water-demanding forest tree.

In this study, we show that 11 members, which have been assigned to the five classical TIP groups of higher plants, compose the TIP subfamily of Eucalyptus. These data expand the results of Rodrigues et al. (2013), revealing the presence of six additional TIP genes in *E. grandis*. When compared to other woody species, the Eucalyptus TIP subfamily is almost the same size as those described in *V. vinifera* (10 genes) and *C. sinensis* (11 genes), but possess less members than *Populus* and rubber tree (17 genes each). The number of TIP genes in the Eucalyptus genome is also well conserved among other well-studied model species such as *Arabidopsis* (10 genes) and rice (10 genes). Thus, despite the occurrence of a whole-genome duplication (WGD) event and the reported large number of tandem duplications (Myburg et al., 2014), no major expansion of the eucalyptus TIP subfamily relatively to other woody and non-woody species was observed. This is in clear contrast with *Populus*, in which the expansion of the MIP superfamily, including the acquisition of several TIP genes, has been attributed to gene retention after a recent WGD event (Gupta and Sankararamakrishnan, 2009).

Concerning their structure, the *EgTIP* genes showed a similar pattern of exon/intron organization as reported for other TIP genes from dicot species that normally harbor three exons separated by two introns. The only exception is the single intron-containing *EgTIP1.1* gene, which probably evolved from sequential loss of introns as previously suggested (Regon et al., 2014).

TABLE 2 | Main *cis*-regulatory elements found in the *EgTIP* promoters.

<i>EgTIP</i> genes	Element	Sequence	Function
1.1, 1.3, 1.4, 2.1, 2.2, 2.3, 3.1, 3.2, 4.1, 5.1	ABRE	ACGTG	Cis-acting element involved in the abscisic acid responsiveness
1.1, 1.2, 1.4, 2.1, 2.2, 2.3, 4.1	TC-RICH REPEATS	ATTTCCTTCA	Cis-acting element involved in defense and stress responsiveness
1.1, 1.2, 1.3, 1.4, 2.2, 4.1, 5.1	O2-SITE	GATGATGTGG	Element involved in metabolism regulation
1.1, 1.2, 1.3, 1.4, 2.1, 5.1	LTR	CCGAAA	Element involved in low-temperature responsiveness
1.1, 1.2, 2.1, 4.1	P-BOX	CCTTTG	Gibberellin-responsive element
1.2, 1.4, 1.3, 3.2, 5.1	ATCT-motif	AATCTGATCG	Part of a conserved DNA module involved in light responsiveness
1.1, 1.2, 1.3, 1.4, 2.1, 2.2, 3.2, 4.1	CIRCADIAN	CAANNNNATC	Element involved in circadian control
1.1, 3.2, 5.1	HSE	AGAAAATTCG	Element involved in heat stress responsiveness
1.1, 1.2, 1.3, 1.4, 2.1, 2.3, 3.1, 4.1, 5.1	MBS	CAACTG	MYB binding site involved in drought-induction
1.1, 2.1, 2.2, 3.2	TCA-ELEMENT	CCATCTTTT	Element involved in salicylic acid (SA) responsiveness
4.1, 5.1	SARE	TTCGACCTCCTT	Element involved in SA responsiveness
1.4, 2.1, 2.2, 2.3	TGA-ELEMENT	AACGAC	Auxin-responsive element
1.1, 1.4, 2.1, 3.2	ACE	AAACACGTTA	Element involved in light responsiveness
1.4	C-repeat/DRE	TGGCCGAC	Element involved in cold and dehydration-responsiveness
1.2, 4.1, 5.1	Box-W1	TTGACC	Fungal elicitor responsive element
1.1, 1.2, 1.3, 1.4, 2.1, 2.2, 3.1, 3.2, 4.1, 5.1	TGACG-motif	TGACG	Element involved in the MeJA-responsiveness
1.1, 1.2, 1.3, 1.4, 2.1, 2.2, 3.1, 3.2, 4.1, 5.1	SP1	CC(G/A)CCC	Light responsive element

***EgTIP* Expression Patterns and Possible Functional Diversification**

Based on our results, distinct organ/tissue expression profiles were observed for the *EgTIP* genes identified. Among them, *EgTIP1.1* was the most widely expressed, indicating that it might play a more generalized role throughout the plant. This is in line with previous reports showing that TIP1.1 is widely distributed and the most abundantly expressed TIP isoform (Alexandersson et al., 2005; Knipfer et al., 2011; Regon et al., 2014). Conversely, the other *EgTIP* genes showed enriched-organ/tissue expression, a feature that was particularly evident in wood-related and reproductive organs/tissues. The only exception was *EgTIP5.1*, which appears to be nonfunctional since no transcripts or expression sequence tag evidences could be found for this gene. Interestingly, none of the identified *EgTIP* genes was found to be exclusively expressed in a specific organ/tissue.

Despite some partial overlaps, the observed divergences in their spatial expression patterns indicate that *EgTIPs* may have undergone functional diversification. This fact also suggests that certain isoforms might have acquired specific organ/tissue roles. Evidence from poplar trees, however, indicate that, in spite of their elevated tissue-specificity, a high level of functional redundancy exists amongst *PtTIP* members (Cohen et al., 2013). In this respect, the existence of functional redundancy between TIP genes was postulated in previous studies employing insertional *Arabidopsis* mutants (Schüssler et al., 2008). In general, current evidences indicate that TIP isoforms act redundantly to regulate water and solute transport. In contrast with this, Gattolin et al. (2009) demonstrated the existence of tissue- and cell-specific patterns of expression of some *AtTIP* genes in *Arabidopsis* roots. Similarly, a specific and developmentally regulated leaf expression pattern of some *HvTIP* subfamily members was observed in barley (Besse et al., 2011). These results highlight the existence of possible specialization

of TIP isoforms, but further investigations are required to uncover possible functional specificity of the identified *EgTIP* genes.

In trees, the modulation of *TIP* expression in response to abiotic stress has been documented (Cohen et al., 2013; Rodrigues et al., 2013; Martins et al., 2015; Regon et al., 2014), and the major evidences point to a role for these proteins in stress adaptation. It is noteworthy that most of the *EgTIP* genes analyzed here displayed osmotic stress-responsive transcriptional profiles in three different organs. Although the timing and extent of their expression varied, these results indicate that the Eucalyptus responses to osmotic stress require the coordinated transcriptional regulation of most *EgTIPs*. The existence of *cis*-regulatory elements related to hormone and abiotic stress response in the *EgTIP* promoter regions lend further support to this idea. Consistently, we have previously shown the induction and repression of the *EgTIP2.2* promoter activity by osmotic stress and ABA, respectively (Rodrigues et al., 2013). However, despite these reported evidences of transcriptional regulation, the possible contribution of the different *EgTIP* isoforms in the control of water flow under stress conditions requires further investigation.

***EgTIP* Substrate Selectivity**

The selectivity filter of aquaporins comprises four residues located at the non-cytosolic portion of the pore. These residues are implicated in water translocation and in the selection of other substrate molecules such as glycerol, ammonia, boric acid, CO₂, H₂O₂, and urea (reviewed in Maurel et al., 2015). Previous data have indicated that TIP subfamily members show the highest level of sequence divergence in the ar/R region among known plant aquaporins (Wallace and Roberts, 2004; Azad et al., 2012). Despite this, some residues are well conserved, particularly in the LE1 position, in which an A or G is present, and in the H₂ position, in which an H residue has

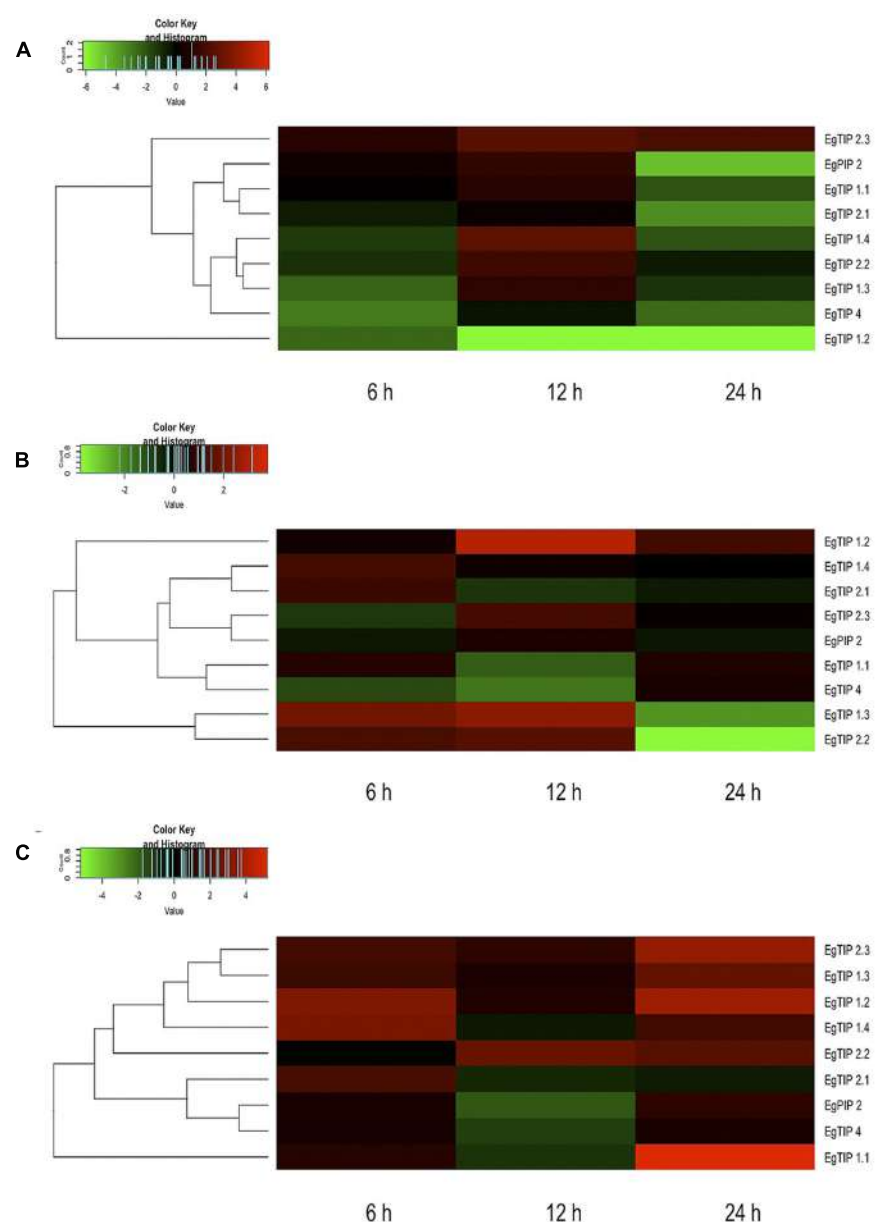


FIGURE 6 | Expression patterns of *EgTIP* genes under osmotic stress. (A) Roots; **(B)** Stems; and **(C)** Leaves. The normalized fold change (\log_2 transformed) of *EgTIP* expression at each time point after PEG treatment was calculated relative to that of the untreated control at the same time point. The color scale is the same as in **Figure 4**. Genes were clustered according to their expression profiles. All samples were analyzed in triplicate.

been associated with water specificity (Sui et al., 2001; Kirscht et al., 2016). Remarkably, this conserved H residue is found in most identified EgTIPs, with the exception of EgTIP3.2 and EgTIP5.1.

Concerning LE2, an R residue known to contribute to the mechanism of proton exclusion is usually present at this position (Wu et al., 2009; Kirscht et al., 2016). In TIPs, however, this residue can be replaced by polar residues such as C or nonpolar residues such as V, a feature that is observed in some EgTIPs. Intriguingly, a nonpolar L residue is found in this position in EgTIP3.1. According to Azad et al. (2012), the presence of a

hydrophobic residue in this position in TIP1 homologs renders the proteins multifunctional aqua-glyceroporins. Thus, changes in aa charge and side chains lead to modifications in pore size and hydrophobicity that have direct consequences in TIP transport selectivity.

A still unresolved question concerns EgTIP2.3. Due to its clustering with known TIP5 isoforms, EgTIP2.3 could be also assigned as a member of group 5. However, EgTIP2.3 lack the tetrad NVGC commonly found in the ar/R filter of most TIP5 isoforms. Instead, it harbors a selectivity filter that resembles the one present in TIP2 isoforms, an attribute that justifies its

nomination as a TIP2 in Phytozome. The closest homologue of EgTIP2.3, VvTIP5.2, also harbors a canonic TIP2-like ar/R filter (HIGR). Intriguingly, such an ambiguous classification was also observed for certain NOD26-like intrinsic proteins from different plant species (Zou et al., 2015b). Overall, our results suggest that both EgTIP2.3 and VvTIP5.2 represent unusual isoforms sharing phylogenetic relationships with TIP5s but transport selectivity of TIP2s.

Several studies have demonstrated that additional residues may contribute to TIP preference for the transport of other substrates than water (Froger et al., 1998; Hove and Bhave, 2011). A recent study that elucidated the crystal structure of AtTIP2.1 proposed the expansion of the selectivity filter with the inclusion of a flexible H residue in loop C (Kirscht et al., 2016), that has been implicated in ammonia transport. In this respect, EgTIP2.1, EgTIP2.2, and EgTIP4.1 have the same H residue in loop C as AtTIP2.1. Comparatively, several TIP2 orthologs from other plant species also have an AtTIP2.1-like extended selectivity filter (Zou et al., 2015a,b, 2016), thus suggesting that these proteins may be able to transport ammonia. Moreover, in view of the predictions for non-aqua transport profiles proposed by Azad et al. (2016), both EgTIP2 and EgTIP4.1 as well as all EgTIP1 fulfill the requirements to act as H₂O₂ transporters.

Previous reports have also included the analysis of nine specificity-determining positions (SDPs) to predict non-aqua substrates (Hove and Bhave, 2011) as well as the Froger's positions (P1–P5) to discriminate TIP-mediated glycerol transport (Froger et al., 1998). All these positions were evaluated in the EgTIPs investigated in order to address possible transport specificity. Although the Froger's positions remained highly conserved in EgTIPs compared to TIPs found in other plant species (Table 1), they do not fit the requirements for glycerol transport. Noteworthy, as reported earlier for TIPs from *Ricinus communis* and *Jatropha curcas* (Zou et al., 2015b, 2016), the SDP analysis indicated the presence of residues typically associated with urea transport in all EgTIPs (Supplementary Table S4). In particular, EgTIP1.1, EgTIP4.1, and EgTIP5.1 have classical urea-type SDPs (Supplementary Table S4). Overall, these results are valuable for future studies on the structure–function relationships of the identified EgTIPs.

REFERENCES

- Afzal, Z., Howton, T. C., Sun, Y., and Mukhtar, M. S. (2016). The roles of aquaporins in plant stress responses. *J. Dev. Biol.* 4, 9. doi: 10.3390/jdb4010009
 Alexandersson, E., Fraysse, L., Sjövall-Larsen, S., Gustavsson, S., Fellert, M., Karlsson, M., et al. (2005). Whole gene family expression and drought stress regulation of aquaporins. *Plant Mol. Biol.* 59, 469–484. doi: 10.1007/s11103-005-0352-1
 Ashkenazy, H., Erez, E., Martz, E., Pupko, T., and Ben-Tal, N. (2010). ConSurf 2010: calculating evolutionary conservation in sequence and structure of proteins and nucleic acids. *Nucleic Acids Res.* 38, W529–33. doi: 10.1093/nar/gkq399
 Azad, A. K., Ahmed, J., Alum, M. A., Hasan, M. M., Ishikawa, T., Sawa, Y., et al. (2016). Genome-wide characterization of major intrinsic proteins in four grass plants and their non-Aqua transport selectivity profiles with comparative perspective. *PLoS ONE* 11:e0157735. doi: 10.1371/journal.pone.0157735
 Azad, A. K., Yoshikawa, N., Ishikawa, T., Sawa, Y., and Shibata, H. (2012). Substitution of a single amino acid residue in the aromatic/arginine selectivity

CONCLUSION

In this work, an in depth analysis of the Eucalyptus TIP subfamily was performed using different molecular approaches. Eleven genes were identified based upon sequence similarity and phylogenetic relationships with known TIPs from other plant species. Among them, only *EgTIP5.1* was not expressed and seems not to be functional. The structural and functional properties of the EgTIP isoforms were further investigated using bioinformatics tools, and their capacities to transport water and other substrates were predicted and discussed. Interestingly, distinctive spatial expression patterns and inducible expression under osmotic stress were observed. Although to be taken with caution, a possible involvement of the *EgTIP* products in abiotic stress responses was envisaged. The genes identified in this study represent an important resource for further functional analyses and use in biotechnological programs aiming Eucalyptus genetic improvement.

AUTHOR CONTRIBUTIONS

Conceived and designed the experiments: MR, AT, and IM; performed the experiments: MR and AT; analyzed the data: JB and IM; wrote the paper: MR, AT, and IM.

ACKNOWLEDGMENTS

We thank Dr. Paulo E. M. Ribolla (IBTEC – UNESP) for his precious help with heatmap construction. MR is a recipient of a Ph.D. fellowship from CNPq. AT is a recipient of a PNPD/CAPES postdoctoral fellowship. IM is recipient of a research fellowship from CNPq.

SUPPLEMENTARY MATERIAL

The Supplementary Material for this article can be found online at: <http://journal.frontiersin.org/article/10.3389/fpls.2016.01810/full#supplementary-material>

- filter alters the transport profiles of tonoplast aquaporin homologs. *Biochim. Biophys. Acta* 1818, 1–11. doi: 10.1016/j.bbamem.2011.09.014
 Besse, M., Knipfer, T., Miller, A. J., Verdeil, J. L., Jahn, T. P., and Fricke, W. (2011). Developmental pattern of aquaporin expression in barley (*Hordeum vulgare* L.) leaves. *J. Exp. Bot.* 62, 4127–4142. doi: 10.1093/jxb/err175
 Boursiac, Y., Chen, S., Luu, D. T., Sorieul, M., Van den Dries, N., and Maurel, C. (2005). Early effects of salinity on water transport in *Arabidopsis* roots: molecular cellular features of aquaporin expression. *Plant Physiol.* 139, 790–805.
 Chou, K.-C., and Shen, H.-B. (2010). Plant-mPLoc: a top-down strategy to augment the power for predicting plant protein subcellular localization. *PLoS ONE* 5:e11335. doi: 10.1371/journal.pone.0011335
 Cohen, D., Bogaert-Triboullet, M. B., Vialet-Chabrand, S., Merret, R., County, P. E., Moretti, S., et al. (2013). Developmental and environmental regulation of Aquaporin gene expression across *Populus* species: divergence or redundancy? *PLoS ONE* 8:e55506. doi: 10.1371/journal.pone.0055506

- de Oliveira, L. A., Breton, M. C., Bastolla, F. M., Camargo Sda, S., Margis, R., Frazzon, J., et al. (2012). Reference genes for the normalization of gene expression in eucalyptus species. *Plant Cell Physiol.* 53, 405–422. doi: 10.1093/pcp/pcr187
- Finn, R. D., Coggill, P., Eberhardt, R. Y., Eddy, S. R., Mistry, J., Mitchell, A. L., et al. (2016). The Pfam protein families database: towards a more sustainable future. *Nucleic Acids Res.* 44, D279–D285. doi: 10.1093/nar/gkv1344
- Froger, A. C., Tallur, B. C., Thomas, D. C., and Delamarche, C. (1998). Prediction of functional residues in water channels and related proteins. *Protein Sci.* 7, 1458–1468. doi: 10.1002/pro.5560070623
- Gattolin, S., Sorieul, M., Hunter, P. R., Khonsari, R. H., and Frigerio, L. (2009). In vivo imaging of the tonoplast intrinsic protein family in *Arabidopsis* roots. *BMC Plant Biol.* 9:133. doi: 10.1186/1471-2229-9-133
- Goicoechea, M., Lacombe, E., Legay, S., Mihaljevic, S., Rech, P., Jauneau, A., et al. (2005). EgMYB2, a new transcription activator from *Eucalyptus* xylem, regulates secondary cell wall formation and lignin biosynthesis. *Plant J.* 43, 553–567. doi: 10.1111/j.1365-313X.2005.02480.x
- Gupta, A. B., and Sankararamakrishnan, R. (2009). Genome-wide analysis of major intrinsic proteins in the tree plant *Populus trichocarpa*: characterization of XIP subfamily of aquaporins from evolutionary perspective. *BMC Plant Biol.* 9:134. doi: 10.1186/1471-2229-9-134
- Hove, R. M., and Bhave, M. (2011). Plant aquaporins with non-aqua functions: deciphering the signature sequences. *Plant Mol. Biol.* 75, 413–430. doi: 10.1007/s11103-011-9737-5
- Johanson, U., Karlsson, M., Johansson, I., Gustavsson, S., Sjövall, S., Fraysse, L., et al. (2001). The complete set of genes encoding major intrinsic proteins in *Arabidopsis* provides a framework for a new nomenclature for major intrinsic proteins in plants. *Plant Physiol.* 126, 1358–1369. doi: 10.1104/pp.126.4.1358
- Kelley, L. A., Mezulis, S., Yates, C. M., Wass, M. N., and Sternberg, M. J. E. (2015). The Phyre2 web portal for protein modeling, prediction and analysis. *Nat. Protoc.* 10, 845–858. doi: 10.1038/nprot.2015.053
- Khan, K., Agarwal, P., Shanware, A., and Sane, V. A. (2015). Heterologous expression of two *Jatropha* aquaporins imparts drought and salt tolerance and improves seed viability in transgenic *Arabidopsis thaliana*. *PLoS ONE* 10:e0128866. doi: 10.1371/journal.pone.0128866
- Kirscht, A., Kaptan, S. S., Bienert, G. P., Chaumont, F., Nissen, P., de Groot, B. L., et al. (2016). Crystal structure of an ammonia-permeable aquaporin. *PLoS Biol.* 14:e1002411. doi: 10.1371/journal.pbio.1002411
- Knipfer, T., Besse, M., Verdeil, J. L., and Fricke, W. (2011). Aquaporin-facilitated water uptake in barley (*Hordeum vulgare* L.) roots. *J. Exp. Bot.* 62, 4115–4126. doi: 10.1093/jxb/err075
- Landau, M., Mayrose, I., Rosenberg, Y., Glaser, F., Martz, E., Pupko, T., et al. (2005). ConSurf 2005: the projection of evolutionary conservation scores of residues on protein structures. *Nucleic Acids Res.* 33, W299–W302. doi: 10.1093/nar/gki370
- Lee, S. E., Yim, H. K., Lim, M. N., Yoon, I. S., Kim, J. H., and Hwang, Y. S. (2015). Abscisic acid prevents the coalescence of protein storage vacuoles by upregulating expression of a tonoplast intrinsic protein gene in barley aleurone. *J. Exp. Bot.* 66, 1191–1203. doi: 10.1093/jxb/eru467
- Li, J., and Cai, W. (2015). A ginseng PgTIP1 gene whose protein biological activity related to Ser(128) residue confers faster growth and enhanced salt stress tolerance in *Arabidopsis*. *Plant Sci.* 234, 74–85. doi: 10.1016/j.plantsci.2015.02.001
- Lin, W., Peng, Y., Li, G., Arora, R., Tang, Z., Su, W., et al. (2007). Isolation and functional characterization of PgTIP1, a hormone-autotrophic cells-specific tonoplast aquaporin in ginseng. *J. Exp. Bot.* 58, 947–956. doi: 10.1093/jxb/erl255
- Liu, L. H., Ludewig, U., Gassert, B., Frommer, W. B., and von Wirén, N. (2003). Urea transport by nitrogen-regulated tonoplast intrinsic proteins in *Arabidopsis*. *Plant Physiol.* 133, 1220–1228. doi: 10.1104/pp.103.027409
- Livak, K., and Schmittgen, T. D. (2001). Analysis of relative gene expression data using real time quantitative PCR and the $2^{-\Delta\Delta Ct}$ method. *Methods* 25, 402–408. doi: 10.1006/meth.2001.1262
- Loqué, D., Ludewig, U., Yuan, L., and von Wirén, N. (2005). Tonoplast intrinsic proteins AtTIP2;1 and AtTIP2;3 facilitate NH₃ transport into the vacuole. *Plant Physiol.* 137, 671–680. doi: 10.1104/pp.104.051268
- Lovell, S. C., Davis, I. W., Arendall III, W. B., de Bakker, P. I. W., Word, J. M., Prisant, M. G., et al. (2003). Structure validation by Calpha geometry: phi, psi and Cbeta deviation. *Proteins* 50, 437–450. doi: 10.1002/prot.10286
- Maeshima, M. (2001). TONOPLAST TRANSPORTERS: organization and function. *Annu. Rev. Plant Physiol. Plant Mol. Biol.* 52, 469–497. doi: 10.1146/annurev.arplant.52.1.469
- Martins, C., de, P., Pedrosa, A. M., Du, D., Gonçalves, L. P., Yu, Q., et al. (2015). Genome-wide characterization and expression analysis of major intrinsic proteins during abiotic and biotic stresses in sweet orange (*Citrus sinensis* L. Osb.). *PLoS ONE* 10:e0138786. doi: 10.1371/journal.pone.0138786
- Marti-Renom, M. A., Stuart, A., Fiser, A., Sánchez, R., Melo, F., and Sali, A. (2000). Comparative protein structure modeling of genes and genomes. *Annu. Rev. Biophys. Biomol. Struct.* 29, 291–325. doi: 10.1146/annurev.biophys.29.1.291
- Maurel, C., Boursiac, Y., Luu, D. T., Santoni, V., Shahzad, Z., and Verdoucq, L. (2015). Aquaporins in plants. *Physiol. Rev.* 95, 1321–1358. doi: 10.1152/physrev.00008.2015
- Mizrahi, E., Hefer, C. A., Ranik, M., Joubert, F., and Myburg, A. A. (2010). De novo assembled expressed gene catalog of a fast-growing *Eucalyptus* tree produced by Illumina mRNA-Seq. *BMC Genomics* 11:681. doi: 10.1186/1471-2164-11-681
- Myburg, A. A., Grattapaglia, D., Tuskan, G. A., Hellsten, U., Hayes, R. D., Grimwood, J., et al. (2014). The genome of *Eucalyptus grandis*. *Nature* 510, 356–362. doi: 10.1038/nature13308
- Peng, Y., Lin, W., Cai, W., and Arora, R. (2007). Overexpression of a *Panax ginseng* tonoplast aquaporin alters salt tolerance, drought tolerance and cold acclimation ability in transgenic *Arabidopsis* plants. *Planta* 226, 729–740. doi: 10.1007/s00425-007-0520-4
- Ramakers, C., Ruijter, J. M., Ronald, H., Lekanne, D., and Moormana, A. F. M. (2003). Assumption-free analysis of quantitative real-time polymerase chain reaction (PCR) data. *Neurosci. Lett.* 339, 62–66. doi: 10.1016/S0304-3940(02)01423-4
- Reddy, P. S., Rao, T. S. R. B., Sharma, K. K., and Vadez, V. (2015). Genome-wide identification and characterization of the aquaporin gene family in *Sorghum bicolor* (L.). *Plant Gene.* 1, 18–28. doi: 10.1016/j.plgene.2014.12.002
- Regon, P., Panda, P., Kshetrimayum, E., and Panda, S. K. (2014). Genome-wide comparative analysis of tonoplast intrinsic protein (TIP) genes in plants. *Funct. Integr. Genomics* 14, 617–629. doi: 10.1007/s10142-014-0389-9
- Reinhardt, H., Hachez, C., Bienert, M. D., Beebo, A., Swarup, K., Voß, U., et al. (2016). Tonoplast aquaporins facilitate lateral root emergence. *Plant Physiol.* 170, 1640–1654. doi: 10.1104/pp.15.01635
- Rodrigues, M. I., Bravo, J. P., Sasaki, F. T., Severino, F. E., and Maia, I. G. (2013). The tonoplast intrinsic aquaporin (TIP) subfamily of *Eucalyptus grandis*: characterization of EgTIP2, a root-specific and osmotic stress-responsive gene. *Plant Sci.* 213, 106–113. doi: 10.1016/j.plantsci.2013.09.005
- Sade, N., Vinocur, B. J., Diber, A., Shatil, A., Ronen, G., Nissan, H., et al. (2009). Improving plant stress tolerance and yield production: is the tonoplast aquaporin SITIP2;2 a key to isohydric to anisohydric conversion? *New Phytol.* 181, 651–661. doi: 10.1111/j.1469-8137.2008.02689.x
- Sali, A., and Blundell, T. L. (1993). Comparative protein modelling by satisfaction of spatial restraints. *J. Mol. Biol.* 234, 779–815. doi: 10.1006/jmbi.1993.1626
- Schrödinger, L. C. C. (2011). *The PyMol Molecular Graphics System*. Version 1.3. Available at: <http://www.pymol.org/>
- Schüssler, M. D., Alexandersson, E., Bienert, G. P., Kichey, T., Laursen, K. H., Johanson, U., et al. (2008). The effects of the loss of TIP1;1 and TIP1;2 aquaporins in *Arabidopsis thaliana*. *Plant J.* 56, 756–767. doi: 10.1111/j.1365-313X.2008.03632.x
- Shelden, M. C., Howitt, S. M., Kaiser, B. N., and Tyerman, S. D. (2009). Identification and functional characterisation of aquaporins in the grapevine, *Vitis vinifera*. *Funct. Plant Biol.* 36, 1065–1078. doi: 10.1071/FP09011
- Sui, H., Han, B. G., Lee, J. K., Walian, P., and Jap, B. K. (2001). Structural basis of water-specific transport through the AQP1 water channel. *Nature* 414, 872–878. doi: 10.1038/414872a
- Wallace, I. S., and Roberts, D. M. (2004). Homology modeling of representative subfamilies of *Arabidopsis* major intrinsic proteins. Classification based on the aromatic/arginine selectivity filter. *Plant Physiol.* 135, 1059–1068. doi: 10.1104/pp.103.033415
- Wang, X., Li, Y., Ji, W., Bai, X., Cai, H., Zhu, D., et al. (2011). A novel *Glycine soja* tonoplast intrinsic protein gene responds to abiotic stress and depresses salt and dehydration tolerance in transgenic *Arabidopsis thaliana*. *J. Plant Physiol.* 168, 1241–1248. doi: 10.1016/j.jplph.2011.01.016

- Wu, B., Steinbronn, C., Alsterfjord, M., Zeuthen, T., and Beitz, E. (2009). Concerted action of two cation filters in the aquaporin water channel. *EMBO J.* 28, 2188–2194. doi: 10.1038/embj.2009.182
- Yamaguchi-Shinozaki, K., and Shinozaki, K. (2005). Organization of cis-acting regulatory elements in osmotic- and cold-stress-responsive promoters. *Trends Plant Sci.* 10, 88–94. doi: 10.1016/j.tplants.2004.12.012
- Yu, H., Soler, M., Mila, I., San Clemente, H., Savelli, B., Dunand, C., et al. (2014). Genome-wide characterization and expression profiling of the AUXIN RESPONSE FACTOR (ARF) gene family in *Eucalyptus grandis*. *PLoS ONE* 9:e108906. doi: 10.1371/journal.pone.0108906
- Zou, Z., Gong, J., An, F., Xie, G., Wang, J., Mo, Y., et al. (2015a). Genome-wide identification of rubber tree (*Hevea brasiliensis* Muell. Arg.) aquaporin genes and their response to ethephon stimulation in the laticifer, a rubber-producing tissue. *BMC Genomics* 16:1001. doi: 10.1186/s12864-015-2152-6
- Zou, Z., Gong, J., Huang, Q., Mo, Y., Yang, L., and Xie, G. (2015b). Gene structures, evolution, classification and expression profiles of the aquaporin gene family in castor bean (*Ricinus communis* L.). *PLoS ONE* 10:e0141022. doi: 10.1371/journal.pone.0141022
- Zou, Z., Yang, L., Gong, J., Mo, Y., Wang, J., Cao, J., et al. (2016). Genome-wide identification of *Jatropha curcas* aquaporin genes and the comparative analysis provides insights into the gene family expansion and evolution in *Hevea brasiliensis*. *Front. Plant Sci.* 7:395. doi: 10.3389/fpls.2016.00395

Conflict of Interest Statement: The authors declare that the research was conducted in the absence of any commercial or financial relationships that could be construed as a potential conflict of interest.

Copyright © 2016 Rodrigues, Takeda, Bravo and Maia. This is an open-access article distributed under the terms of the Creative Commons Attribution License (CC BY). The use, distribution or reproduction in other forums is permitted, provided the original author(s) or licensor are credited and that the original publication in this journal is cited, in accordance with accepted academic practice. No use, distribution or reproduction is permitted which does not comply with these terms.



Characterization and Regulation of Aquaporin Genes of Sorghum [*Sorghum bicolor* (L.) Moench] in Response to Waterlogging Stress

Suhas Kadam¹, Alejandra Abril², Arun P. Dhanapal¹, Robert P. Koester¹, Wilfred Vermerris^{3,4}, Shibu Jose⁵ and Felix B. Fritsch^{1*}

¹ Division of Plant Sciences, University of Missouri, Columbia, MO, United States, ² Graduate Program in Plant Molecular and Cellular Biology, University of Florida, Gainesville, FL, United States, ³ Department of Microbiology and Cell Science – Institute of Food and Agricultural Sciences, University of Florida, Gainesville, FL, United States, ⁴ University of Florida Genetics Institute, University of Florida, Gainesville, FL, United States, ⁵ The Center for Agroforestry, University of Missouri, Columbia, MO, United States

OPEN ACCESS

Edited by:

Richard Belanger,
Laval University, Canada

Reviewed by:

Rivka Elbaum,
Hebrew University of Jerusalem, Israel
Angelika Mustroph,
University of Bayreuth, Germany

*Correspondence:

Felix B. Fritsch
fritsch@missouri.edu

Specialty section:

This article was submitted to
Plant Physiology,
a section of the journal
Frontiers in Plant Science

Received: 01 September 2016

Accepted: 09 May 2017

Published: 30 May 2017

Citation:

Kadam S, Abril A, Dhanapal AP, Koester RP, Vermerris W, Jose S and Fritsch FB (2017) Characterization and Regulation of Aquaporin Genes of Sorghum [*Sorghum bicolor* (L.) Moench] in Response to Waterlogging Stress. *Front. Plant Sci.* 8:862.
doi: 10.3389/fpls.2017.00862

Waterlogging is a significant environmental constraint to crop production, and a better understanding of plant responses is critical for the improvement of crop tolerance to waterlogged soils. Aquaporins (AQPs) are a class of channel-forming proteins that play an important role in water transport in plants. This study aimed to examine the regulation of AQP genes under waterlogging stress and to characterize the genetic variability of AQP genes in sorghum (*Sorghum bicolor*). Transcriptional profiling of AQP genes in response to waterlogging stress in nodal root tips and nodal root basal regions of two tolerant and two sensitive sorghum genotypes at 18 and 96 h after waterlogging stress imposition revealed significant gene-specific pattern with regard to genotype, root tissue sample, and time point. For some tissue sample and time point combinations, *PIP2-6*, *PIP2-7*, *TIP2-2*, *TIP4-4*, and *TIP5-1* expression was differentially regulated in tolerant compared to sensitive genotypes. The differential response of these AQP genes suggests that they may play a tissue specific role in mitigating waterlogging stress. Genetic analysis of sorghum revealed that AQP genes were clustered into the same four subfamilies as in maize (*Zea mays*) and rice (*Oryza sativa*) and that residues determining the AQP channel specificity were largely conserved across species. Single nucleotide polymorphism (SNP) data from 50 sorghum accessions were used to build an AQP gene-based phylogeny of the haplotypes. Phylogenetic analysis based on single nucleotide polymorphisms of sorghum AQP genes placed the tolerant and sensitive genotypes used for the expression study in distinct groups. Expression analyses suggested that selected AQPs may play a pivotal role in sorghum tolerance to water logging stress. Further experimentation is needed to verify their role and to leverage phylogenetic analyses and AQP expression data to improve waterlogging tolerance in sorghum.

Keywords: sorghum, waterlogging, aquaporin, expression, haplotypes, phylogenetic

Abbreviations: AQP, aquaporin; ML, maximum likelihood; NIP, NOD26-like intrinsic protein; PIP, plasma membrane intrinsic protein; qRT-PCR, quantitative real time PCR; SIP, small basic protein; TIP, tonoplast intrinsic protein.

INTRODUCTION

Aquaporins are integral membrane proteins that form channels that allow water to move from one plant compartment to another. They exist in all plants and animals and play important roles in different developmental and physiological processes of living organisms, including stomatal movement, photosynthesis, germination, cell elongation, reproduction, and responses to diverse abiotic stress conditions (Ariani and Gepts, 2015). In particular, AQPs play important roles in the regulation of plant water uptake, hydraulic conductivity, and water loss, and as such are critically involved in regulating tissue and whole-plant water relations (Chaumont and Tyerman, 2014). Other than water, AQPs can transport a variety of molecules including ammonia, CO₂, boron, and silicon (Dordas et al., 2000; Terashima and Ono, 2002; Jahn et al., 2004; Ma et al., 2006). Plant AQPs were originally classified into four subfamilies: PIPs, TIPs, NIPs, and SIPs (Johanson et al., 2001; Zardoya, 2005). More recently, three additional AQP subfamilies, including glycerol facilitator (GlpF)-like intrinsic proteins (GIPs), hybrid intrinsic proteins (HIPs), and X (unrecognized) intrinsic proteins (XIPs) have been described. However, unlike PIPs, TIPs, NIPs, and SIPs which are present in all land plants, GIPs and HIPs have only been identified in algae and moss, and XIPs only in moss and several dicots (Danielson and Johanson, 2008; Venkatesh et al., 2013; Zhang et al., 2013). Two of the AQP subfamilies, the PIPs, which are usually localized in the plasma membrane, and the TIPs, which are generally localized in the vacuolar membranes, have been investigated intensively in regard to their functions and regulation as related to plant water relations.

Aquaporins have been studied extensively in order to understand the complex mechanisms of solute permeation and selectivity (Törnroth-Horsefield et al., 2005; Eriksson et al., 2013). AQPs are small proteins that are highly conserved in plants and animals and contain six transmembrane α -helix domains that form a pore. Two of the loops are characterized by NPA motifs (Asp-Pro-Ala) which, together with an aromatic/Arg filter (ar/R), act as a size-exclusion barrier and regulate the transport specificity of these proteins (Murata et al., 2000; Hub and De Groot, 2008; Mitani-Ueno et al., 2011).

As hypoxic or even anoxic conditions develop in the rhizosphere in response to waterlogging, growth of most plants is impaired. An early response to waterlogging is reduced water uptake by roots (Schildwacht, 1989; Else et al., 1995) caused by a reduction in root hydraulic conductance (Araki, 2006). A decrease in the root hydraulic conductance may result from a disruption of AQP function as a result of cytosol acidification (Tournaire-Roux et al., 2003) and may trigger water deficit stress leading to partial stomatal closure (Else et al., 2009). Additional responses to waterlogging include synthesis of the phytohormone ethylene, formation of aerenchyma in the root cortex facilitating oxygen diffusion, initiation and growth of adventitious roots, and development of radial oxygen loss barriers (Shaw, 2015). Numerous expression profiling studies have been conducted to elucidate molecular responses associated with low oxygen stress, including for *Arabidopsis* (Liu et al., 2005; Hsu et al., 2011; Van Veen et al., 2016), rice (*Oryza sativa* L.) (Lasanthi-Kudahettige

et al., 2007), poplar (*Populus alba*) (Kreuzwieser and Gessler, 2010), sesame (*Sesamum indicum* L.) (Wang et al., 2012), and brassica (*Brassica napus* L.) (Zou et al., 2013). However, none of these studies focused on the impact of waterlogging on AQP transcript abundance in roots.

Many AQPs are known to be highly expressed in roots (Sakurai et al., 2005; Monneuse et al., 2011), supporting a role of AQPs in root water transport. Numerous recent studies have investigated the association between water relations and gene expression and/or protein levels of AQPs under various environmental conditions and in a range of plant species, providing information that may open the door to manipulating AQP expression to alter plant water-use efficiency (Moshelion et al., 2015). While AQP genes have been characterized in several plant species using genome-wide analyses (Matsuo et al., 2012; Deshmukh et al., 2015), information on AQPs in sorghum [*Sorghum bicolor* (L.) Moench] is sparse, particularly as related to waterlogging stress.

In low-lying areas along rivers in the United States Midwest, periodic short-term waterlogging is common and can cause significant biomass and yield losses. In the United States, losses in crop production due to flooding were second only to drought in many of the past years (Bailey-Serres et al., 2012). Waterlogging-prone land that is deemed too risky for the production of traditional row crops may be useful for the production of sorghum, a hardy C4 grass that originated in Africa. Sorghum is currently grown in the United States on >2.9 million ha¹, mainly for the production of grain for use as animal feed, and, more recently, as bioenergy feedstock (Regassa and Wortmann, 2014). Cultivation of sorghum for the production of lignocellulosic biomass on waterlogging-prone land is of particular interest because this land is not used for the production of food crops, thus it would not redirect farmland normally used for food production for the production of biofuel (Leakey, 2009). This, coupled with only limited knowledge about sorghum responses to waterlogging (Zhang et al., 2016), highlights the need for research to elucidate the physiological and molecular responses of sorghum to waterlogging. Given the direct impact of waterlogging on plant roots, examination of root responses is of particular interest.

Sorghum's seminal root system consists of the primary root and lateral branches that form on the primary root as the plant develops (Singh et al., 2010). In sorghum, nodal roots start to appear when plants have four to five fully expanded leaves. Nodal roots develop sequentially from shoot nodes in flushes that approximate the rate of new leaf appearance (Singh et al., 2010). As cereals develop from seedlings into mature plants, their nodal root systems develop into the dominant root system and provide most of the water and nutrients that are required (Krassovsky, 1926; Sallans, 1942; Shane and McCully, 1999). The limited information available in the literature indicates that continuous waterlogging of sorghum causes an increase in the number of nodal root axes, but not in their total length. Other root system components, such as nodal root laterals and the seminal root and its laterals, are restricted in number and length as a result

¹<http://www.nass.usda.gov>

of waterlogging (Pardales et al., 1991). Despite the availability of powerful genomic resources and techniques, the importance of AQPs in plant water relations, and the limited understanding of sorghum root responses to waterlogging, analyses of AQP gene expression in sorghum nodal roots are lacking.

Consequently, to better understand AQP gene expression in sorghum nodal roots in response to waterlogging stress we examined the transcript levels of selected sorghum AQP (*SbAQP*) genes in nodal root tips and root bases in genotypes contrasting in their response to waterlogging stress. Additionally, to gain a better understanding of *SbAQPs* and provide insights into the genetic variation as well as the association between single nucleotide polymorphism (SNP) haplotypes and waterlogging tolerance in sorghum, we established the phylogenetic relationship of sorghum AQPs with those of maize, rice, and *Arabidopsis*, assigned putative functions of *SbAQPs*, and performed haplotype analysis of AQP genes based on SNP data from 50 sorghum accessions.

MATERIALS AND METHODS

Plant Culture and Waterlogging Stress Imposition

Mexico silt loam soil (fine, smectitic, mesic Aeris Vertic Epiqualfs) was collected at the Bradford Research Center near Columbia, MO, United States. The soil obtained from the top 0.15 m of the profile was homogenized in a soil mixer and autoclaved before filling the pots (20 cm diameter; 32 cm tall). Three subsamples of soil were collected and submitted for analysis at the University of Missouri Soil and Plant Testing Laboratory. Test results indicated a salt pH of 6.5, 1.8% organic matter, 10 meq 100 g⁻¹ cation exchange capacity, 58 kg P ha⁻¹, 169 kg K ha⁻¹, 3580 kg Ca ha⁻¹, and 474 kg Mg ha⁻¹. No fertilizer was applied during the experiment. Two waterlogging-tolerant and two waterlogging-sensitive sorghum genotypes from the ICRISAT mini-core collection (Upadhyaya et al., 2009) were selected for this study based on preliminary screening of the collection under waterlogging and control conditions in the field and follow-up characterization of selected entries under greenhouse conditions. Relative growth and leaf chlorosis of plants grown under waterlogged *versus* well-watered conditions were used as primary criteria to differentiate between waterlogging-tolerant and waterlogging-sensitive genotypes in the preliminary experiments (data not shown). Based on these experiments, genotypes IS 7131 and IS 10969 were characterized as tolerant and genotypes IS 12883 and IS 19389 were characterized as sensitive and were used for this study. Three seeds from each of these genotype were sown in 12 pots to accommodate four treatments and three replications. After sowing, one pot of each genotype was placed into a plastic tub (34 cm × 48 cm × 59 cm) to facilitate waterlogging treatment imposition. The resulting 12 tubs, each with one pot of each genotype, were arranged in three blocks of four tubs. After emergence, pots were thinned to one plant, and plants were watered regularly to maintain well-watered conditions until 30 days after sowing. At 30 days after sowing, plants had reached

the V5 stage (Vanderlip, 1993) and waterlogging treatments were initiated by filling two tubs per replication with water, while maintaining the plants in the other two tubs well-watered. The water levels in the waterlogging treatments were maintained at 5 cm above the soil surface. Following the initiation of waterlogging, the redox potential at 5 cm soil depth was measured in each pot with a Pt electrode (HI3214P, Hanna instruments, Melrose, MA, United States) at 1, 18, and 96 h of waterlogging stress. At 18 h (short) and 96 h (long) post waterlogging treatment initiation, root tip and root base samples from control and waterlogged plants were harvested. To this end, plants were cut at the soil surface and roots were immediately removed from pots and washed by gentle agitation in a large, 30-L tub of water to remove all soil particles. Roots were quickly blotted dry with paper towels, weighed, and root tips (0 to 12 mm) and basal portions (20 mm region closest to the root-shoot junction) of second-whorl nodal roots were excised, immediately frozen in liquid N₂, and stored at -80°C until RNA extraction. Care was taken to ensure that all root tip and basal tissue samples destined for quantification of transcript abundance were immersed in liquid N₂ within 2 min following cutting of the shoot.

RNA Isolation and qRT-PCR

A total of 96 root tissue samples were collected: four genotypes (two tolerant and two sensitive), two conditions (well-watered and waterlogged), two time points (18 and 96 h), two root regions (root tip and root base), and three biological replications. Tissue samples were ground with mortar and pestle in liquid N₂, and RNA was extracted using the RNeasy Plant Mini kit (Qiagen, Germantown, MD, United States) according to manufacturer's instructions. Extracted RNA was analyzed on a NanoDrop spectrophotometer (ND-1000, Thermo Scientific, Wilmington, DE, United States) to assess quantity and on a 1% (w/v) agarose gel to check quality. Template cDNA samples were prepared using Superscript II reverse transcriptase (Invitrogen, Carlson, CA, United States) with 500 ng of total RNA. Primers for reverse transcription PCR (RT-PCR) for nine *SbAQP* genes and actin were designed using Primer3 software² to have a melting temperature between 58 and 62°C and to produce PCR products between 75 and 150 bp (Supplementary Table S1). The nine *SbAQP* genes included in this study were selected based on expression pattern revealed by RNAseq analysis of sorghum root tip and root base tissues in response to waterlogging (Supplementary Table S2, Kadam et al. unpublished results). The sorghum actin gene Sb01g0112600 was used to normalize gene expression, as its expression was found to be stable in root RNA extracted from different sorghum genotypes (Gelli et al., 2014). Transcript abundance was assayed using SYBR green PCR Master Mix (Applied Biosystems, Inc., Foster City, CA, United States) with 2 µl of 10-fold diluted cDNA and 1 µl of the primers (10 µM). The PCR program used was as follows: initial denaturation for 2 min at 95°C, followed by 40 PCR cycles consisting of 95°C for 15 s and 60°C for 60 s using an ABI 7500 thermal cycler (Applied Biosystems, United States). For each product, the threshold cycle (*C_t*) where the amplification

²<http://frodo.wi.mit.edu>

reaction enters the exponential phase, was determined for three independent biological replicates per genotype. The comparative C_t method was used to quantify the relative transcript abundance (Pfaffl, 2001). Gene expression data were analyzed by ANOVA using the GLM procedure in SAS 9.4 (SAS Institute, Cary, NC, United States). Mean separation was conducted by Tukey's test at $\alpha = 0.05$ and $n = 3$.

Phylogenetic Analysis of AQP Proteins and Identification of NPA Motifs and ar/R Selectivity Filters

To identify putative AQP genes in sorghum, the protein sequences of all identified *Arabidopsis*, maize and rice AQPs were used as queries in BLASTX and BLASTP with default parameters from the NCBI and Phytozome databases. After filtering sorghum AQPs with at least 50% identity with the query sequence, the candidate AQP genes were aligned to ensure that no gene was represented multiple times. Multiple sequence alignments of AQPs identified by BLAST were performed using CLUSTALW implemented in MEGA7 (Kumar et al., 2016). The AQP alignments were used to construct a phylogenetic tree with the ML method using MEGA version 7. The stability of branch nodes in the ML-tree was measured by performing 1000 bootstraps and remaining parameters were kept at the default settings. The AQP subgroups PIP, TIP, NIP, and SIP formed in the phylogenetic tree were classified in accordance with the nomenclature of known AQPs, which were used as query in initial BLAST searches.

The conserved NPA domain and ar/R selectivity filter of the different subfamilies of sorghum AQPs were identified by multiple sequence alignment using the SeaView software (Gouy et al., 2010) with MUSCLE using default parameters.

SNP Haplotype Analysis of *SbAPQ* Genes

A total of 50 sorghum accessions were used for SNP haplotype analysis. The SNP information of 48 sorghum accessions (46 *Sorghum bicolor* landraces, improved varieties, wild and weedy entries, and two *S. propinquum*) were obtained from a sorghum genome SNP database (Luo et al., 2016). In addition, the SNPs from the tolerant (IS 7131) and the sensitive (IS 12883) genotypes used in this study were obtained from RNAseq data (Kadam et al., unpublished). The SNP haplotype analysis was conducted using MEGA version 7 (Kumar et al., 2016) and complemented by manual analysis in Microsoft Excel. The ML method was used for the construction of trees and a bootstrap with 1,000 replicates was used to establish confidence in the branches.

RESULTS AND DISCUSSION

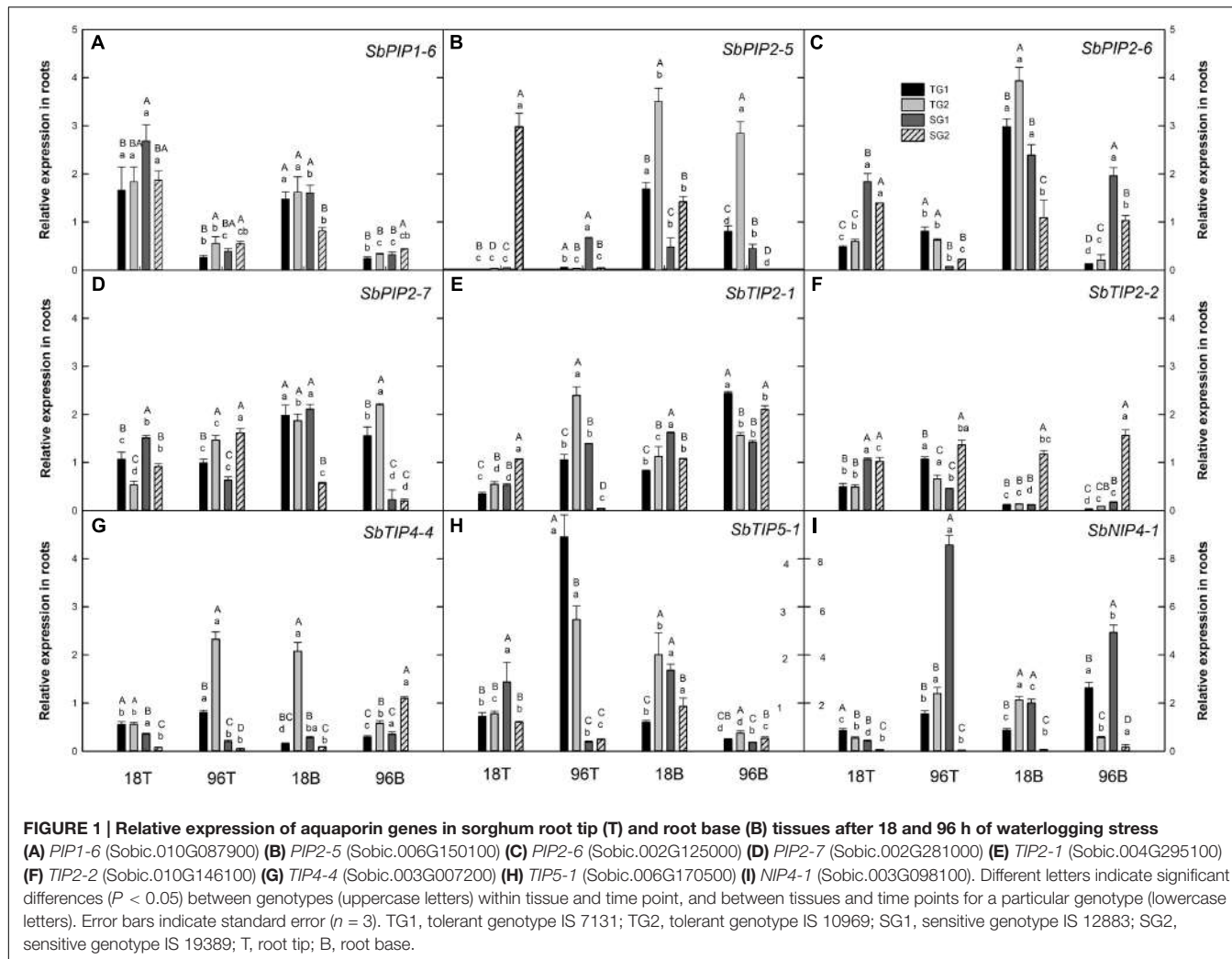
Transcript Abundance of *SbAQPs* in Response to Waterlogging

Aquaporins play a major role in controlling hydraulic conductivity in leaves and roots (Chaumont and Tyerman, 2014; Sade et al., 2015). Consequently, the identification of

physiologically important members and characterization of the regulation of their expression in response to waterlogging stress could be very helpful for crop improvement efforts. Analyses of RNAseq data (Supplementary Table S2, Kadam et al. unpublished) indicated that transcript abundance of the *SbAQP* genes encoding PIP1-6, PIP2-5, PIP2-6, PIP2-7, TIP2-1, TIP2-2, TIP4-4, TIP5-1, and NIP4-1 was influenced by waterlogging stress in sorghum roots. To further explore the expression of these genes, qRT-PCR analyses were conducted to quantify transcript abundance in root tips (0–12 mm region of the root apex) and root bases (20 mm region closest to the root–shoot junction) in two waterlogging-tolerant and two waterlogging-sensitive genotypes. Specifically, transcript abundance was examined in tissue samples collected from roots that developed from the second below-ground node in response to 18 and 96 h of waterlogging stress. The root tip samples were collected to represent the growing region of the second nodal root, thus including the root apical meristem as well as cells that are expanding. In contrast, the samples collected from the base of the root consist of mature cells. As such, the two regions represent tissues that differ substantially in anatomy, physiology, and biochemistry, as well as in their response to waterlogging stress (Xu et al., 2013).

Analysis of variance indicated significant differences in transcript abundance between control and waterlogged treatments for all nine *SbAQP* genes in tolerant as well as in sensitive genotypes and in root tips as well as root bases. However, the responses to waterlogging stress differed depending on *SbAQP* gene, genotype, tissue type, and waterlogging stress duration (Figure 1 and Supplementary Table S3). Further, strong effects of waterlogging stress duration (18 h vs. 96) on transcript abundance were observed, for most *SbAQP* genes regardless of tissue type and genotype. Similarly, waterlogging treatment effects on transcript abundance was often different between root tip and root base samples. These results are consistent with measurements of AQP transcript abundance in response to waterlogging stress in two *Quercus* species in that distance of the collected sample from the root apex, stress duration, and species all influenced transcript levels of different AQPs (Rasheed-Depardieu et al., 2015).

In the present study, among all *SbAQP* genes examined, the expression pattern of *SbPIP1-6* was the most consistent among genotypes. It was the only gene which was upregulated in both root tip and root base samples at 18 h and downregulated at 96 h in all genotypes (except IS 19389 at 18 h in the root base) (Figure 1A). Previously, expression of *SbPIP1-6* in sorghum leaves was found to be downregulated as a result of 4 h cold and heat stress, 24 h salt stress and 5 days drought stress (Reddy et al., 2015). In roots, the observed initial upregulation of *SbPIP1-6* expression in response to short-term exposure to stress may enhance water uptake to maintain the plant water status, while reduced expression after prolonged exposure to stress may reduce hydraulic conductivity. Based on the MOROKOSHI sorghum transcriptome database (Makita et al., 2014), the expression of *SbPIP1-6* in roots is responsive to a range of treatments including nitrogen, polyethylene glycol, abscisic acid, and NaOH. Together, these results indicate that consistent with an important role



of *SbPIP1-6*, expression of *SbPIP1-6* in roots is responsive to changes in a broad range of environmental conditions, but the expression pattern observed in this study does not indicate an association between *SbPIP1-6* transcript abundance and the waterlogging tolerance or sensitivity of the four sorghum genotypes.

While differences among the four genotypes were common, transcript abundance of specific *SbAQPs* genes often did not display consistent contrasts between the tolerant and the sensitive genotypes. That said, instances of expression pattern that were associated with tolerance/sensitivity of the genotypes were found for *SbPIP2-6*, *SbPIP2-7*, *SbTIP2-2*, *SbTIP4-4*, and *SbTIP5-1*. In particular, transcript abundance of *SbPIP2-6* in root tips was significantly different between the tolerant and the sensitive genotypes at both 18 and 96 h (Figure 1C). At 18 h, *SbPIP2-6* expression was upregulated in the sensitive genotypes but not in the tolerant genotypes, while at 96 h it was downregulated in all genotypes but to a greater extent in the sensitive genotypes than the tolerant genotypes. Interestingly, *SbPIP2-6* expression was also upregulated in the sensitive and downregulated in the tolerant genotypes in the root bases

in response to prolonged stress, while its expression was upregulated in the root bases of all genotypes at 18 h. Aside from *SbPIP2-6*, consistent significant differences in transcript abundance between sensitive and tolerant genotypes at more than one time point within the same tissue were only found for *SbTIP4-4* (Figure 1G). The expression of *SbTIP4-4* was downregulated in both sensitive genotypes in root tips collected at 18 and 96 h of waterlogging, and the transcript abundance was significantly lower than in the two tolerant genotypes. In the case of *SbPIP2-7*, *SbTIP2-2*, and *SbTIP5-1*, one time point and tissue combination each was found for which the sensitive and tolerant genotypes exhibited consistent expression patterns. In response to prolonged waterlogging stress, expression of *SbPIP2-7* and *SbTIP5-1*, were upregulated in the tolerant and downregulated in the sensitive genotypes in root bases and root tips, respectively (Figures 1D,H). In the root base at 96 h, *SbTIP5-1* was not only downregulated in the sensitive genotypes but also in the tolerant genotypes. Tolerant genotypes downregulated the expression of *SbTIP2-2* in root tips in response to 18 h of waterlogging stress while the transcript abundance in sensitive genotypes changed little compared to the control treatment (Figure 1F).

The expression of *SbTIP2-2* in the root bases of three of the four genotypes was strongly downregulated in response to 18 h as well as 96 h of waterlogging, and the changes in transcript abundance in response to waterlogging stress were much greater than in the root tips. Downregulation of expression in the root base may be correlated with aerenchyma formation due to cortical cells death in waterlogging stress. A greater degree of root aerenchyma formation in the root base has been reported for maize and sorghum compared to root tips in response to waterlogging stress (Mano et al., 2006; Promkhambut et al., 2011). While significant differences between genotypes and/or time points were observed for transcript abundance of *SbTIP2-1* and *SbNIP4-1*, the only consistent response to waterlogging that was observed for these genes was that *SbNIP4-1* expression in one of the susceptible genotypes (IS 19389) was strongly downregulated in both tissues at both time points (Figure 1I). Given the recent finding *SbNIP4-2* can transport silicon (Markovich et al., 2015), it is possible that the distinct expression pattern of *SbNIP4-1* in IS 19389 (SG2) may also result in silicon accumulation differences in comparison with the other three genotypes. Interestingly, in flood-stressed Arabidopsis, NIP2-1 was induced and may play a role in adaptation to lactic fermentation (Choi and Roberts, 2007).

Diverse patterns in transcript abundance such as those documented here for different AQP genes are not surprising and consistent with AQP expression responses to abiotic stresses, including waterlogging stress, that have been observed by others (Weig et al., 1997; Mariaux et al., 1998; Jang et al., 2004; Ge et al., 2014; Rasheed-Depardieu et al., 2015), as well as differences in cellular location and transport functions that have been documented for AQPs (Hu et al., 2015; Reddy et al., 2015; Deshmukh et al., 2016). Additionally, given the distinct developmental age and associated physiology of the root tip vs. root base tissues, distinct expression pattern and transcript abundance among *SbAQP* genes between the tissues could be expected and have also been observed by others (Rasheed-Depardieu et al., 2015).

Differences in gene expression between tolerant and sensitive genotypes may or may not be linked to their performance under waterlogged conditions. Nonetheless, here, genes for which the expression pattern of the two tolerant genotypes were similar and different from the two sensitive genotypes were regarded as more likely to be functionally associated with sensitivity or susceptibility to waterlogging stress. Such expression patterns were observed for *SbPIP2-6*, *SbTIP2-2*, *SbTIP4-4*, and *SbTIP5-1* in root tips and for *SbPIP2-6* and *SbPIP2-7* in root bases (Figure 1). Recently, Sutka et al. (2011) reported that the transcript abundance of several *PIP*s (*AtPIP1;1*, *AtPIP1;2*, *AtPIP1;4*, *AtPIP2;1*, *AtPIP2;3*, *AtPIP2;4* and *AtPIP2;5*) in Arabidopsis roots is positively correlated with hydraulic conductivity; and, increased expression levels may regulate the uptake of water into cells (Suga et al., 2002). As such, the above-described contrasts in *SbPIP2-6* and *SbPIP2-7* transcript abundance between sensitive and tolerant genotypes may be associated with differences in hydraulic conductivity. Interestingly, opposing expression pattern were observed for these two members of the *SbPIP* family in the

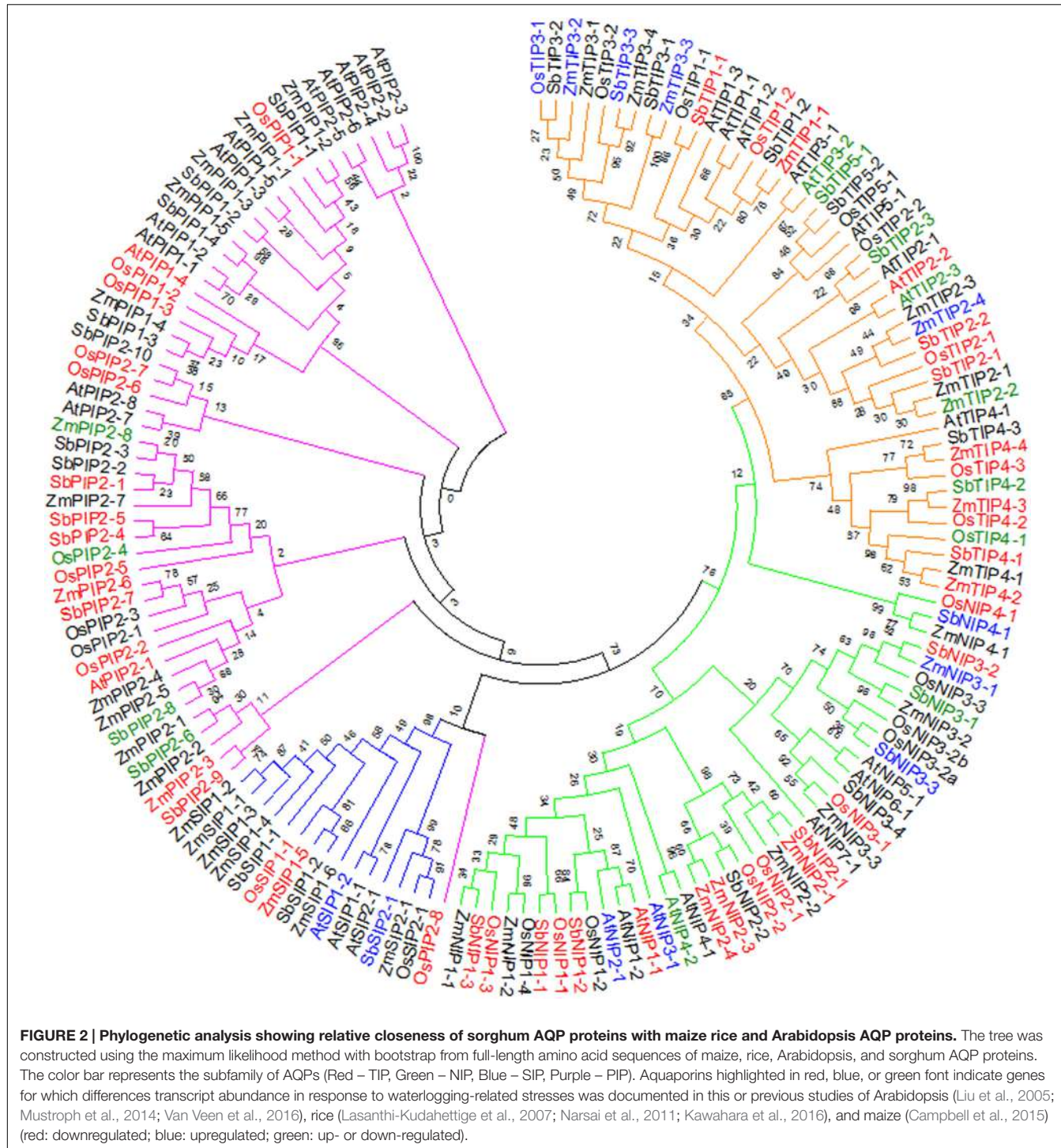
root base tissues of susceptible and tolerant genotypes at 96 h, in that *SbPIP2-7* was upregulated in the tolerant but downregulated in the susceptible genotypes while *SbPIP2-6* was downregulated in the tolerant but upregulated in the susceptible genotypes. In any case, the relevance of these genes and the associated expression differences with regard to waterlogging tolerance/sensitivity as well as hydraulic conductivity remain to be examined.

Three members of the *SbTIP* family, namely *SbTIP2-2*, *SbTIP4-4*, and *SbTIP5-1*, exhibited expression pattern differences between sensitive and tolerant genotypes in root types at 18 and/or 96 h (Figures 1F,G,H). In Arabidopsis, AtTIP facilitates the transport of water, hydrogen peroxide, and urea (Bienert et al., 2007), and SbTIPs likely have similar functions in sorghum. It is interesting to speculate whether the observed gene expression responses primarily influence water transport or whether they may play an important role relative to hydrogen peroxide transport under waterlogged conditions. Hydrogen peroxide is known to be involved in the regulation of root growth, probably acting downstream of auxin (Ivanchenko et al., 2013), and is produced in cortical cells in wheat seminal roots undergoing aerenchyma formation in response to waterlogging (Xu et al., 2013). Thus, different expression pattern of *SbTIP2-2*, *SbTIP4-4*, and *SbTIP5-1* in root tips of sensitive and tolerant genotypes may result in contrasting hydraulic conductivity and/or may alter the distribution of hydrogen peroxide in root tip cells. In root base tissues, no consistent differences in the expression of *SbTIPs* were found between sensitive and tolerant genotypes, but *SbTIP2-1* was upregulated in three of the four genotypes at 18 h as well as 96 h of waterlogging stress (Figure 1E). Further research is needed to examine whether the greater abundance of *SbTIP2-1* transcripts in the root base tissue is associated with hydrogen peroxide formation and the development of aerenchyma in these samples.

The impact of waterlogging stress on transcript abundance in nodal roots was dependent on the position of the root tissue sample, duration of stress imposition, and the sorghum genotype, and differed among the examined *SbAQP* genes. Although some consistent responses across the sensitive and the tolerant genotypes were detected for some of the genes, tissues, and/or time points, it remains unclear whether any of the observed responses reflect differences in AQP abundance and/or are functionally related to the tolerance/sensitivity of the genotypes.

Phylogenetic Analysis of the AQP Family

The differential regulation of the AQP genes as established above, raises questions about how sorghum AQP genes relate to those of other plant species. Advances in plant genome sequencing have enabled the identification and characterization of AQPs in several crop species including rice, maize, and soybean (*Glycine max* L.) (Chaumont et al., 2001; Sakurai et al., 2005; Zhang et al., 2013), facilitating comparative analyses with sorghum AQPs. To study the relationships among AQP proteins from sorghum, maize, rice, and Arabidopsis, a phylogenetic tree was created based on amino acid sequence alignments (Figure 2). Consistent with previous reports for AQPs in rice, Arabidopsis, and maize,



sorghum AQPs grouped into PIP, TIP, NIP, and SIP subfamilies (Weig et al., 1997; Chaumont et al., 2001; Sakurai et al., 2005). The SbPIP subfamily was the largest, with 14 members divided into two groups: PIP1, with 4 members and PIP2, with 10 members. Five groups were found for the SbTIP subfamily (TIP1 to TIP5), with two members in the TIP1 group, three each in groups TIP2 to TIP4 and two members in the TIP5 group. Sorghum NIPs were

divided into NIP1 with three members, NIP2 with two members, NIP3 with four members, and NIP4 with one member. With only three members, the SbSIP subfamily was the smallest and had two SIP1 members and one SIP2 member (Figure 2). Among the four species compared in this study, the number of PIPs was greatest in sorghum and the number of SIPs was greatest in maize. Examination of protein sequences revealed higher levels

of similarity of SbPIP members with maize, rice, and Arabidopsis PIP families, than between SbTIP, SbNIP, and SbSIP members and their respective families in maize, rice, and Arabidopsis. Information on differential expression of AQP genes response to waterlogging, submergence and hypoxic stress obtained from the public domain (Supplementary Table S4) (Liu et al., 2005; Lasanthi-Kudahettige et al., 2007; Narsai et al., 2011; Mustroph et al., 2014; Campbell et al., 2015; Kawahara et al., 2016; Van Veen et al., 2016)³, indicates that waterlogging influences transcript abundance of many AQPs (Figure 2). As in the present study, it appears that the transcript abundance of most AQP genes is lower in roots from waterlogged compared to control treatments.

Analysis of Conserved and Substrate Specific Residues in AQP Proteins

The two NPA motifs found in AQPs are critical for water transport and selectivity (Murata et al., 2000). In addition, the ar/R selectivity filter is essential in determining transport specificity of AQPs. Point mutations or other sequence variations in these residues confer different substrate specificities to AQPs (Beitz et al., 2006; Hub and De Groot, 2008; Mitani-Ueno et al., 2011). To understand the possible physiological role and substrate specificity of sorghum AQPs, we identified and examined the NPA motifs and ar/R selectivity filter sequences (Table 1). The two NPA domains were conserved in the SbPIP and SbTIP AQP subfamilies, except for SbTIP5-2. In SbTIP5-2, the asparagine was replaced by a threonine residue in the first NPA domain (NPA to TPA) and the second NPA domain was replaced by HEP (His-Glu-Pro) (Table 1). Interestingly, this change in both NPA domains of SbTIP5-2 was not observed in maize, rice, and Arabidopsis (Supplementary Table S5).

Except for SbNIP3-4 and SbNIP4-1, both NPA domains were conserved in all members of the SbNIP subfamily. In SbNIP3-4, the alanine in the first NPA domain was substituted with a serine, and in the second NPA domain it was substituted with a valine. While the first NPA domain was conserved in SbNIP4-1, the alanine was substituted with isoleucine in the second domain (Table 1). AQPs in the SbSIP subfamily had a conserved NPA motif in the second domain, but the alanine in the first domain was replaced with either a threonine (SbSIP1-1 and SbSIP1-2) or a leucine (SbSIP2-1) (Table 1). Further research is needed to understand the implications associated with the modified NPA domains in SbTIP5-2, SbNIP3-4, SbNIP4-1, and the SbSIPs.

All but one (PIP2-5) identified SbPIPs contained the ar/R selectivity filter that is highly conserved and typical of water-transporting AQPs (F/H/T/R) (Table 1). The same ar/R selectivity filter sequence is shared by the PIP subfamily in different plant species including maize, Arabidopsis, white poplar, tomato (*Solanum lycopersicum*), soybean, and canola (*Brassica rapa*) (Chaumont et al., 2001; Johanson et al., 2001; Gupta and Sankararamakrishnan, 2009; Reuscher et al., 2013; Zhang et al., 2013; Tao et al., 2014). Evidence is mounting that PIP AQPs are actively involved in regulating root and leaf hydraulic conductivity (Javot et al., 2003; Sutka et al., 2011; Sade et al., 2014; Grondin et al., 2016; Vitali et al., 2016). In

addition to water transport, PIP AQPs in Arabidopsis, tobacco (*Nicotiana tabacum*), and barley (*Hordeum vulgare*) have been shown to facilitate diffusion of CO₂ in leaf mesophyll cells and can directly affect photosynthesis (Flexas et al., 2006; Heckwolf et al., 2011). The conservation of NPA motifs and ar/R residues in sorghum PIPs suggests that they are involved in regulating water absorption, plant hydraulics, and/or CO₂ diffusion (Reddy et al., 2015).

Aquaporins of the TIP subfamily are found mostly in vacuolar membranes and are involved in the control of osmotic potential and water flow across this plant subcellular compartment (Maurel et al., 1993; Pou et al., 2013). A number of studies revealed that TIPs can transport a variety of small solutes, such as NH₄⁺, hydrogen peroxide, and urea, in addition to water (Liu et al., 2003; Holm et al., 2005; Loqué et al., 2005; Bienert et al., 2007). The conserved ar/R residues and NPA motifs of SbTIPs compared with those of other species, suggest a conserved function for these proteins in sorghum (Supplementary Table S5). Waterlogged conditions have been shown to promote the production of reactive oxygen species including hydrogen peroxide in roots and leaves of barley (Kalashnikov et al., 1994) and roots of wheat (Biemelt et al., 2000). Consequently, differences in transcript abundance of SbTIP2-2, SbTIP4-4, and SbTIP5-1 between tolerant and sensitive sorghum genotypes (Figure 1) may point to distinct hydrogen peroxide distribution and/or production in roots of these genotypes.

For the SbNIPs, six distinct ar/R selectivity filters were identified. All three SbNIP1 members had the residues W/V/A/R typical of the subgroup I of plant NIP AQPs (Table 1 and Supplementary Table S4). These NIPs are able to transport uncharged solutes like glycerol and formamide but have low water permeability (Wallace and Roberts, 2005). The structural similarities of the SbNIP1 group with those of other plant species suggest analogous transport specificity. Rice NIP2-1 is a silicon transporter characterized by a double NPA motif and a G/S/G/R ar/R selectivity filter (Ma et al., 2006), and is able to transport arsenite and boric acid when expressed in Xenopus oocytes (Mitani-Ueno et al., 2011). Since the SbNIP2-1 sequence is similar to that of OsNIP2-1, it may be involved in both silicon and boric acid homeostasis in sorghum (Table 1). The Arabidopsis boric acid transporter NIP5-1 is characterized by an NPS/NPV aqueous pore and an A/I/G/R selectivity filter (Takano et al., 2006), and modifications in the protein sequence alter the transport capability of this AQP. Given that AtNIP5-1 and its sorghum homolog SbNIP3-4, share the same domain and selectivity filter, SbNIP3-4 may be involved in boron transport in sorghum. Comparison of NPA and ar/R motifs between the tolerant (IS 7131) and sensitive (IS 12883) sorghum genotypes, did not reveal any non-synonymous SNPs in the NPA and ar/R motifs (Supplementary Table S6).

Haplotype Analysis of SbAQP Genes

Reduced cost of next-generation sequencing has opened the door for the generation of high-density SNP information of sorghum accessions (Morris et al., 2013; Luo et al., 2016), and for the detection of rare alleles which can be used to differentiate sorghum accessions. Haplotype analysis of SbAQP

³<http://tenor.dna.affrc.go.jp/>

genes was accomplished using 50 sorghum accessions. The SNP information of 48 accessions was obtained from the sorghum SNP database (Luo et al., 2016) and the SNP information for the remaining two accessions was based on sequence information resulting from the RNAseq analysis of a waterlogging-tolerant (IS 7131) and a waterlogging-sensitive (IS 10969) genotype (Kadam et al. unpublished data). Sequence comparison between the waterlogging tolerant and sensitive genotype identified SNPs in six out of nine selected *SbAQP* genes [Sobic.002G125000 (*PIP2-6*), Sobic.002G281000 (*PIP2-7*), Sobic.003G098100 (*NIP4-1*), Sobic.006G170500 (*TIP5-1*), Sobic.010G146100 (*TIP2-2*), and

Sobic.010G087900 (*PIP1-6*)]. No SNPs were identified for Sobic.06G150100 (*PIP2-5*), Sobic.003G007200 (*TIP4-4*), and Sobic.04G295100 (*TIP2-1*) (Supplementary Table S6). Most of the SNPs were present in the 3' and 5' UTR. The haplotype range was 5 to 35 (Table 2), with the fewest haplotypes present in *TIP4-4* (Sobic.003G007200) and the most in *NIP4-1* (Sobic.003G098100) (Table 2). For *SbPIP1-6* (Sobic.010G087900.1) a total of 27 haplotypes were present among the 50 sorghum accessions, and in the cluster analysis the tolerant (IS 7131) and sensitive (IS 12883) genotypes were assigned into separate groups (Figure 3 and Supplementary Table S6). Interestingly, in root tips sampled

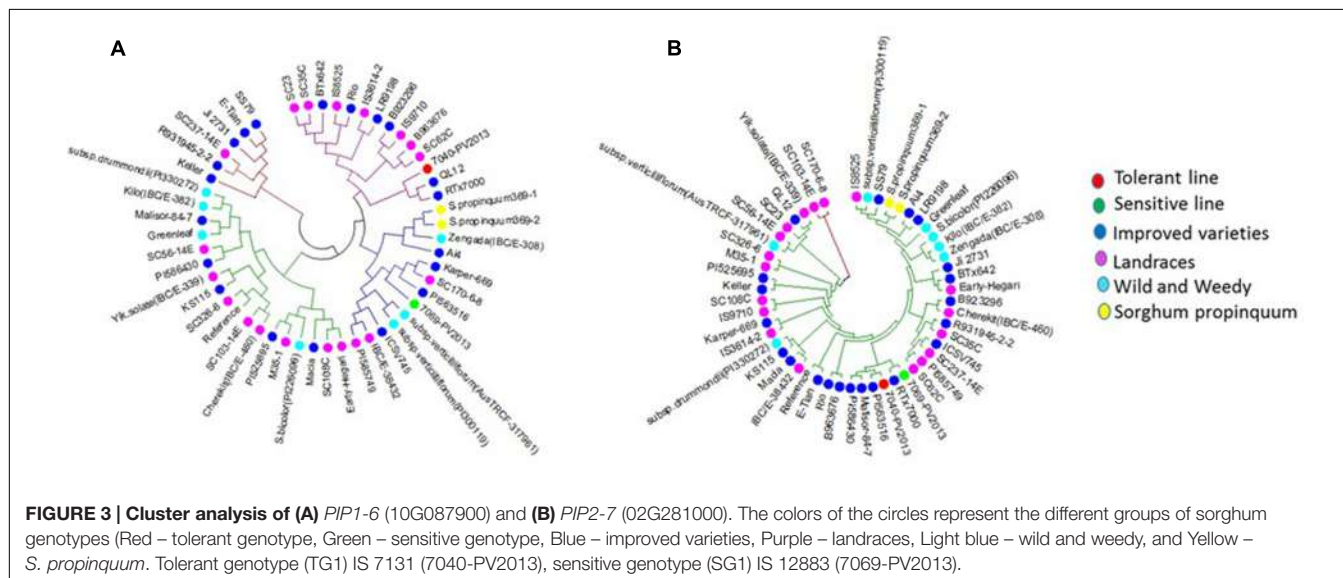
TABLE 1 | Details of NPA domains, ar/R filters and Froger's residues identified using protein sequence alignment in 40 sorghum aquaporins.

S. No.	Gene_Id	NPA (I)	NPA (II)	ar/R filters				Froger's residues				
				H2	H5	LE1	LE2	P1	P2	P3	P4	P5
1	<i>SbPIP1-1</i>	NPA	NPA	F	H	T	R	Q	S	A	F	W
2	<i>SbPIP1-2</i>	NPA	NPA	F	H	T	R	Q	S	A	F	W
3	<i>SbPIP1-3</i>	NPA	NPA	F	H	T	R	Q	S	A	F	W
4	<i>SbPIP1-4</i>	NPA	NPA	F	H	T	R	V	S	A	F	W
5	<i>SbPIP2-1</i>	NPA	NPA	F	H	T	R	Q	S	A	F	W
6	<i>SbPIP2-2</i>	NPA	NPA	F	H	T	R	Q	S	A	F	W
7	<i>SbPIP2-3</i>	NPA	NPA	F	H	T	R	Q	S	A	F	W
8	<i>SbPIP2-4</i>	NPA	NPA	F	H	T	R	Q	S	A	F	W
9	<i>SbPIP2-5</i>	NPA	NPA	-	H	T	R	Q	S	A	F	W
10	<i>SbPIP2-6</i>	NPA	NPA	F	H	T	R	Q	S	A	F	W
11	<i>SbPIP2-7</i>	NPA	NPA	F	H	T	R	Q	S	A	F	W
12	<i>SbPIP2-8</i>	NPA	NPA	F	H	T	R	Q	S	A	F	W
13	<i>SbPIP2-9</i>	NPA	NPA	F	H	T	R	H	S	A	F	W
14	<i>SbPIP2-10</i>	NPA	NPA	F	H	T	R	M	S	A	F	W
15	<i>SbTIP1-1</i>	NPA	NPA	H	I	A	V	T	S	A	Y	W
16	<i>SbTIP1-2</i>	NPA	NPA	H	I	A	V	T	S	A	Y	W
17	<i>SbTIP2-1</i>	NPA	NPA	R	I	G	R	T	S	A	Y	W
18	<i>SbTIP2-2</i>	NPA	NPA	H	I	G	R	T	S	A	Y	W
19	<i>SbTIP2-3</i>	NPA	NPA	H	I	G	R	T	S	A	Y	W
20	<i>SbTIP3-1</i>	NPA	NPA	H	V	A	R	T	A	A	Y	W
21	<i>SbTIP3-2</i>	NPA	NPA	H	V	A	R	T	V	A	Y	W
22	<i>SbTIP3-3</i>	NPA	NPA	H	I	A	R	S	A	A	Y	W
23	<i>SbTIP4-1</i>	NPA	NPA	H	S	A	R	S	S	A	Y	W
24	<i>SbTIP4-2</i>	NPA	NPA	Q	S	A	R	T	S	A	Y	W
25	<i>SbTIP4-3</i>	NPA	NPA	H	V	A	R	T	S	A	Y	W
26	<i>SbTIP5-1</i>	NPA	NPA	Q	V	A	R	S	S	A	Y	W
27	<i>SbTIP5-2</i>	TPA	HEP	Q	V	G	G	S	-	A	Y	W
28	<i>SbNIP1-1</i>	NPA	NPA	W	V	A	R	F	S	A	Y	V
29	<i>SbNIP1-2</i>	NPA	NPA	W	V	A	R	F	T	A	Y	M
30	<i>SbNIP1-3</i>	NPA	NPA	W	V	A	R	F	T	A	Y	F
31	<i>SbNIP2-1</i>	NPA	NPA	G	S	G	R	L	T	A	Y	F
32	<i>SbNIP2-2</i>	NPA	NPA	G	S	G	R	L	T	A	Y	F
33	<i>SbNIP3-1</i>	NPA	NPA	A	A	A	R	Y	T	A	Y	V
34	<i>SbNIP3-2</i>	NPA	NPA	A	-	P	R	Y	T	A	Y	L
35	<i>SbNIP3-3</i>	NPA	NPA	A	A	-	R	Y	T	A	Y	M
36	<i>SbNIP3-4</i>	NPS	NPV	A	I	G	R	F	T	A	Y	L
37	<i>SbNIP4-1</i>	NPA	NPI	C	G	G	R	M	T	A	Y	L
38	<i>SbSIP1-1</i>	NPT	NPA	L	I	P	N	S	A	A	Y	W
39	<i>SbSIP1-2</i>	NPT	NPA	L	V	P	N	S	A	A	Y	W
40	<i>SbSIP2-1</i>	NPL	NPA	S	H	G	S	V	A	A	Y	W

TABLE 2 | Number of SNPs in selected nine AQP genes with their distribution in non-synonyms, synonyms, 3' UTR, and 5' UTR regions of the genes.

Sorghum gene ID	AQPs	Haplotypes	Total SNPs	3' UTR	Non-syn	Syn	5' UTR	Start lost or splice region variant
Sobic.002G125000	<i>PIP2-6</i>	11	45	25	3	6	11	0
Sobic.002G281000	<i>PIP2-7</i>	16	20	9	2	2	6	1
Sobic.003G007200	<i>TIP4-4</i>	5	5	1	1	2	1	0
Sobic.003G098100	<i>NIP4-1</i>	35	74	7	7	13	36	11
Sobic.004G295100	<i>TIP2-1</i>	6	18	6	1	6	5	0
Sobic.006G150100	<i>PIP2-5</i>	16	50	9	0	3	38	0
Sobic.006G170500	<i>TIP5-1</i>	6	12	5	1	2	4	0
Sobic.010G087900	<i>PIP1-6</i>	27	23	13	4	3	3	0
Sobic.010G146100	<i>TIP2-2</i>	29	30	17	0	6	7	0

Haplotype number represents analysis based on 50 sorghum accessions.



18 h into the waterlogging treatment, transcript levels of *SbPIP1-6* were significantly higher in IS 12883 (sensitive; SG1) than IS 7131 (tolerant; TG1). Whether the majority of the 50 sorghum accessions which have the same haplotype as the waterlogging-tolerant genotype also exhibit similar expression pattern for *PIP1-6* as IS 7131, remains to be examined. For *SbPIP2-7*, a total of 16 haplotypes were present, and, although the tolerant and sensitive genotypes had different haplotypes (Supplementary Table S6), they were assigned to the same group based on the cluster analysis. While no consistent expression patterns were observed for sensitive and tolerant genotypes in root tips and in the root base at 18 h, *SbPIP2-7* expression was upregulated in the tolerant and downregulated in the sensitive genotypes in the basal root region at 96 h of waterlogging (Figure 1D). Only one SNP was present in the 3' UTR of *SbPIP2-7* between the sensitive and tolerant genotypes. Additional studies are needed to determine whether this SNP is causing the differential expression observed in the basal root region at 96 h. Seven *SbTIP5-1* haplotypes were identified among the 50 examined accessions (Supplementary Table S6). The tolerant and sensitive genotypes differed by one nucleotide in the 3' UTR of *SbTIP5-1* which may underlie differential expression of this gene between these genotypes. In

the tolerant genotype, *SbTIP5-1* expression increased in root tips with prolonged (96 h) exposure to waterlogging (Figure 1E). In contrast, in root tips of the sensitive genotype, *SbTIP5-1* transcript abundance was greater at 18 h compared to 96 h. Increased expression of this gene has also been reported in leaves in response to drought stress in sorghum and banana (*Musa acuminata* L.) (Hu et al., 2015; Reddy et al., 2015). While four haplotypes were observed for *SbTIP4-4*, no sequence differences were present between the tolerant and sensitive genotype for this gene, and thus, differences in transcript abundance for this gene were not associated with differences in its sequence (Figure 1G and Supplementary Table S6). Analysis of *SbTIP2-2* sequences revealed 29 haplotypes as well as differences in three nucleotides between the tolerant and sensitive genotype. Despite these three differences, the two genotypes were assigned to the same cluster.

Different expression pattern of some of the AQP genes in tolerant as compared to sensitive genotypes under waterlogging stress, and SNPs that may underlie these expression differences may be associated with the tolerance phenotype, and, if so, could prove useful for the development of molecular markers to screen populations of sorghum for waterlogging tolerance.

Phylogenetic analysis on the basis of gene-based haplotypes is useful for the selection of tolerant genotypes (Kadam et al., 2016) because characterization of plant sensitivity or tolerance to waterlogging stress is time-consuming and costly. However, additional research is needed to determine the relevance of SNPs in AQP genes relative to waterlogging tolerance and could be coupled with efforts to identify genetic markers for waterlogging tolerance using bi-parental populations or diversity panels.

CONCLUSION

In this study, 40 AQP genes were identified in the *Sorghum bicolor* genome and were phylogenetically grouped into four subfamilies. Phylogenetic comparisons of rice, maize, *Arabidopsis*, and sorghum AQP proteins showed that homologous pairs were clustered together into a single class. Expression profiling of AQP genes revealed differences in transcript abundance between plants subjected to waterlogging and well-watered control plants in a tissue-type and sampling-time dependent manner. Further, the expression pattern of specific AQP genes often differed based on genotype, independent of the genotype's sensitivity to waterlogging. However, transcript abundance of *PIP2-6*, *PIP2-7*, *TIP2-2*, *TIP4-4*, and *TIP5-1* exhibited contrasting pattern in tolerant and sensitive genotypes for some tissue-type and sampling-time combinations, and thus may in part contribute to the differences in performance of these genotypes under waterlogged conditions. SNP identification and haplotype analysis within a diverse set of sorghum genotypes identified genic variation in AQP genes, which may be useful in sorghum

breeding efforts. Further studies are required to ascertain the relevance and specific functions of the different genes in terms of waterlogging stress tolerance.

AUTHOR CONTRIBUTIONS

SK: Designed the study, performed data analysis, and wrote the manuscript; AD: participated in the data analysis; RK and AA: participated in experiment setup and measurements; WV and SJ: participated in the design and editing of the manuscript; FF: designed and supervised the research and contributed to the writing of the manuscript. All the authors read and approved the final version of the manuscript.

ACKNOWLEDGMENTS

This work was supported by funding from the U.S. Department of Energy's Office of Energy Efficiency and Renewable Energy, Bioenergy Technologies Office and sponsored by the U.S. Department of Energy's International Affairs under award number DE-PI0000031.

SUPPLEMENTARY MATERIAL

The Supplementary Material for this article can be found online at: <http://journal.frontiersin.org/article/10.3389/fpls.2017.00862/full#supplementary-material>

REFERENCES

- Araki, H. (2006). Water uptake of soybean (*Glycine max* L. Merr.) during exposure to O₂ deficiency and field level CO₂ concentration in the root zone. *Field Crops Res.* 96, 98–105. doi: 10.1016/j.fcr.2005.05.007
- Ariani, A., and Gepts, P. (2015). Genome-wide identification and characterization of aquaporin gene family in common bean (*Phaseolus vulgaris* L.). *Mol. Genet. Genom.* 290, 1771–1785. doi: 10.1007/s00438-015-1038-2
- Bailey-Serres, J., Lee, S. C., and Brinton, E. (2012). Waterproofing crops: effective flooding survival strategies. *Plant Physiol.* 160, 1698–1709. doi: 10.1104/pp.112.208173
- Beitz, E., Wu, B., Holm, L. M., Schultz, J. E., and Zeuthen, T. (2006). Point mutations in the aromatic/arginine region in aquaporin 1 allow passage of urea, glycerol, ammonia, and protons. *Proc. Natl. Acad. Sci. U.S.A.* 103, 269–274. doi: 10.1073/pnas.0507225103
- Biemelt, S., Keetman, U., Mock, H. P., and Grimm, B. (2000). Expression and activity of isoenzymes of superoxide dismutase in wheat roots in response to hypoxia and anoxia. *Plant Cell Environ.* 23, 135–144. doi: 10.1046/j.1365-3040.2000.00542.x
- Bienert, G. P., Møller, A. L., Kristiansen, K. A., Schulz, A., Møller, I. M., Schjoerring, J. K., et al. (2007). Specific aquaporins facilitate the diffusion of hydrogen peroxide across membranes. *J. Biol. Chem.* 282, 1183–1192. doi: 10.1074/jbc.M603761200
- Campbell, M. T., Proctor, C. A., Dou, Y., Schmitz, A. J., Phansak, P., Kruger, G. R., et al. (2015). Genetic and molecular characterization of submergence response identifies Subtol6 as a major submergence tolerance locus in maize. *PLoS ONE* 10:e0120385. doi: 10.1371/journal.pone.0120385
- Chaumont, F., Barrieu, F., Wojcik, E., Chrispeels, M. J., and Jung, R. (2001). Aquaporins constitute a large and highly divergent protein family in maize. *Plant Physiol.* 125, 1206–1215. doi: 10.1104/pp.125.3.1206
- Chamont, F., and Tyerman, S. D. (2014). Aquaporins: highly regulated channels controlling plant water relations. *Plant Physiol.* 164, 1600–1618. doi: 10.1104/pp.113.233791
- Choi, W.-G., and Roberts, D. M. (2007). *Arabidopsis NIP2; 1*, a major intrinsic protein transporter of lactic acid induced by anoxic stress. *J. Biol. Chem.* 282, 24209–24218. doi: 10.1074/jbc.M700982200
- Danielson, J. Å., and Johanson, U. (2008). Unexpected complexity of the aquaporin gene family in the moss *Physcomitrella patens*. *BMC Plant Biol.* 8:45. doi: 10.1186/1471-2229-8-45
- Deshmukh, R. K., Sonah, H., and Bélanger, R. R. (2016). Plant Aquaporins: genome-wide identification, transcriptomics, proteomics, and advanced analytical tools. *Front. Plant Sci.* 7:1896. doi: 10.3389/fpls.2016.01896
- Deshmukh, R. K., Vivancos, J., Ramakrishnan, G., Guérin, V., Carpentier, G., Sonah, H., et al. (2015). A precise spacing between the NPA domains of aquaporins is essential for silicon permeability in plants. *Plant J.* 83, 489–500. doi: 10.1111/tpj.12904
- Dordas, C., Chrispeels, M. J., and Brown, P. H. (2000). Permeability and channel-mediated transport of boric acid across membrane vesicles isolated from squash roots. *Plant Physiol.* 124, 1349–1362. doi: 10.1104/pp.124.3.1349
- Else, M. A., Hall, K. C., Arnold, G. M., Davies, W. J., and Jackson, M. B. (1995). Export of abscisic acid, 1-aminocyclopropane-1-carboxylic acid, phosphate, and nitrate from roots to shoots of flooded tomato plants (accounting for effects of xylem sap flow rate on concentration and delivery). *Plant Physiol.* 107, 377–384. doi: 10.1104/pp.107.2.377
- Else, M. A., Janowiak, F., Atkinson, C. J., and Jackson, M. B. (2009). Root signals and stomatal closure in relation to photosynthesis, chlorophyll a fluorescence and adventitious rooting of flooded tomato plants. *Ann. Bot.* 103, 313–323. doi: 10.1093/aob/mcn208

- Eriksson, U. K., Fischer, G., Friemann, R., Enkavi, G., Tajkhorshid, E., and Neutze, R. (2013). Subangstrom resolution X-Ray structure details aquaporin-water interactions. *Science* 340, 1346–1349. doi: 10.1126/science.1234306
- Flexas, J., Bota, J., Galmes, J., Medrano, H., and Ribas-Carbó, M. (2006). Keeping a positive carbon balance under adverse conditions: responses of photosynthesis and respiration to water stress. *Physiol. Plant* 127, 343–352. doi: 10.1111/j.1399-3054.2006.00621.x
- Ge, F., Tao, P., Zhang, Y., and Wang, J. (2014). Characterization of AQP gene expressions in *Brassica napus* during seed germination and in response to abiotic stresses. *Biol. Plant.* 58, 274–282. doi: 10.1007/s10535-013-0386-1
- Gelli, M., Duo, Y., Konda, A. R., Zhang, C., Holding, D., and Dweikat, I. (2014). Identification of differentially expressed genes between sorghum genotypes with contrasting nitrogen stress tolerance by genome-wide transcriptional profiling. *BMC Genomics* 15:179. doi: 10.1186/1471-2164-15-179
- Gouy, M., Guindon, S., and Gascuel, O. (2010). SeaView version 4: a multiplatform graphical user interface for sequence alignment and phylogenetic tree building. *Mol. Biol. Evol.* 27, 221–224. doi: 10.1093/molbev/msp259
- Grondin, A., Mauleon, R., Vadez, V., and Henry, A. (2016). Root aquaporins contribute to whole plant water fluxes under drought stress in rice (*Oryza sativa* L.). *Plant Cell Environ.* 39, 347–365. doi: 10.1111/pce.12616
- Gupta, A., and Sankararamakrishnan, R. (2009). Genome-wide analysis of major intrinsic proteins in the tree plant *Populus trichocarpa*: characterization of XIP subfamily of aquaporins from evolutionary perspective. *BMC Plant Biology* 9:134. doi: 10.1186/1471-2229-9-134
- Heckwolf, M., Pater, D., Hanson, D. T., and Kaldenhoff, R. (2011). The *Arabidopsis thaliana* aquaporin AtPIP1; 2 is a physiologically relevant CO₂ transport facilitator. *Plant J.* 67, 795–804. doi: 10.1111/j.1365-313X.2011.04634.x
- Holm, L. M., Jahn, T. P., Møller, A. L., Schjoerring, J. K., Ferri, D., Klaerke, D. A., et al. (2005). NH₃ and NH 4+ permeability in aquaporin-expressing *Xenopus oocytes*. *Pflügers Archiv.* 450, 415–428. doi: 10.1007/s00424-005-1399-1
- Hsu, F.-C., Chou, M.-Y., Peng, H.-P., Chou, S.-J., and Shih, M.-C. (2011). Insights into hypoxic systemic responses based on analyses of transcriptional regulation in *Arabidopsis*. *PLoS ONE* 6:e28888. doi: 10.1371/journal.pone.0028888
- Hu, W., Hou, X., Huang, C., Yan, Y., Tie, W., Ding, Z., et al. (2015). Genome-wide identification and expression analyses of aquaporin gene family during development and abiotic stress in banana. *Int. J. Mol. Sci.* 16, 19728–19751. doi: 10.3390/ijms160819728
- Hub, J. S., and De Groot, B. L. (2008). Mechanism of selectivity in aquaporins and aquaglyceroporins. *Proc. Natl. Acad. Sci. U.S.A.* 105, 1198–1203. doi: 10.1073/pnas.0707662104
- Ivanchenko, M. G., den Os, D., Monshausen, G. B., Dubrovsky, J. G., Bednářová, A., and Krishnan, N. (2013). Auxin increases the hydrogen peroxide (H₂O₂) concentration in tomato (*Solanum lycopersicum*) root tips while inhibiting root growth. *Ann. Bot.* 112, 1107–1116. doi: 10.1093/aob/mct181
- Jahn, T. P., Møller, A. L., Zeuthen, T., Holm, L. M., Klaerke, D. A., Mohsin, B., et al. (2004). Aquaporin homologues in plants and mammals transport ammonia. *FEBS Lett.* 574, 31–36. doi: 10.1016/j.febslet.2004.08.004
- Jang, A.-S., Lee, J.-U., Choi, I.-S., Park, K.-O., Lee, J. H., Park, S.-W., et al. (2004). Expression of nitric oxide synthase, aquaporin 1 and aquaporin 5 in rat after bleomycin inhalation. *Intensive Care Med.* 30, 489–495. doi: 10.1007/s00134-003-2129-9
- Javot, H., Lauvergeat, V., Santoni, V., Martin-Laurent, F., Güçlü, J., Vinh, J., et al. (2003). Role of a single aquaporin isoform in root water uptake. *Plant Cell* 15, 509–522. doi: 10.1105/tpc.008888
- Johanson, U., Karlsson, M., Johansson, I., Gustavsson, S., Sjövall, S., Fraysse, L., et al. (2001). The complete set of genes encoding major intrinsic proteins in *Arabidopsis* provides a framework for a new nomenclature for major intrinsic proteins in plants. *Plant Physiol.* 126, 1358–1369. doi: 10.1104/pp.126.4.1358
- Kadam, S., Vuong, T. D., Qiu, D., Meinhardt, C. G., Song, L., Deshmukh, R., et al. (2016). Genomic-assisted phylogenetic analysis and marker development for next generation soybean cyst nematode resistance breeding. *Plant Sci.* 242, 342–350. doi: 10.1016/j.plantsci.2015.08.015
- Kalashnikov, J. E., Balakhnina, T., and Zakrzhevsky, D. (1994). Effect of soil hypoxia on activation of oxygen and the system of protection from oxidative destruction in roots and leaves of *Hordeum vulgare*. *Russ. J. Plant Physiol.* 41, 583–588.
- Kawahara, Y., Oono, Y., Wakimoto, H., Ogata, J., Kanamori, H., Sasaki, H., et al. (2016). TENOR: database for comprehensive mRNA-Seq experiments in rice. *Plant Cell Physiol.* 57:e7. doi: 10.1093/pcp/pcv179
- Krassovsky, I. (1926). Physiological activity of the seminal and nodal roots of crop plants. *Soil Sci.* 21:307. doi: 10.1097/00010694-192604000-00006
- Kreuzwieser, J., and Gessler, A. (2010). Global climate change and tree nutrition: influence of water availability. *Tree Physiol.* 30, 1221–1234. doi: 10.1093/treephys/tpq055
- Kumar, S., Stecher, G., and Tamura, K. (2016). MEGA7: molecular evolutionary genetics analysis version 7.0 for bigger datasets. *Mol. Biol. Evol.* 33, 1870–1874. doi: 10.1093/molbev/msw054
- Lasanthi-Kudahettige, R., Magneschi, L., Loretto, E., Gonzali, S., Licausi, F., Novi, G., et al. (2007). Transcript profiling of the anoxic rice coleoptile. *Plant Physiol.* 144, 218–231. doi: 10.1104/pp.106.093997
- Leakey, A. D. (2009). Rising atmospheric carbon dioxide concentration and the future of C4 crops for food and fuel. *Proc. R. Soc. Lond. B* 276, 2333–2343. doi: 10.1098/rspb.2008.1517
- Liu, F., VanToai, T., Moy, L. P., Bock, G., Linford, L. D., and Quackenbush, J. (2005). Global transcription profiling reveals comprehensive insights into hypoxic response in *Arabidopsis*. *Plant Physiol.* 137, 1115–1129. doi: 10.1104/pp.104.055475
- Liu, L.-H., Ludewig, U., Gassert, B., Frommer, W. B., and von Wirén, N. (2003). Urea transport by nitrogen-regulated tonoplast intrinsic proteins in *Arabidopsis*. *Plant Physiol.* 133, 1220–1228. doi: 10.1104/pp.103.027409
- Loqué, D., Ludewig, U., Yuan, L., and von Wirén, N. (2005). Tonoplast intrinsic proteins AtTIP2; 1 and AtTIP2; 3 facilitate NH₃ transport into the vacuole. *Plant Physiol.* 137, 671–680. doi: 10.1104/pp.104.051268
- Luo, H., Zhao, W., Wang, Y., Xia, Y., Wu, X., Zhang, L., et al. (2016). SorGSD: a sorghum genome SNP database. *Biotechnol. Biofuels* 9:6. doi: 10.1186/s13068-015-0415-8
- Ma, J. F., Tamai, K., Yamaji, N., Mitani, N., Konishi, S., Katsuhara, M., et al. (2006). A silicon transporter in rice. *Nature* 440, 688–691. doi: 10.1038/nature04590
- Makita, Y., Shimada, S., Kawashima, M., Kondou-Kuriyama, T., Toyoda, T., and Matsui, M. (2014). MOROKOSH: transcriptome database in *Sorghum bicolor*. *Plant Cell Physiol.* 56:e6. doi: 10.1093/pcp/pcu187
- Mano, Y., Omori, F., Takamizo, T., Kindiger, B., Bird, R. M., and Loaisiga, C. (2006). Variation for root aerenchyma formation in flooded and non-flooded maize and teosinte seedlings. *Plant Soil* 281, 269–279. doi: 10.1007/s11104-005-4268-y
- Mariaux, J.-B., Bockel, C., Salamini, F., and Bartels, D. (1998). Desiccation- and abscisic acid-responsive genes encoding major intrinsic proteins (MIPs) from the resurrection plant *Craterostigma plantagineum*. *Plant Mol. Biol.* 38, 1089–1099. doi: 10.1023/A:1006013130681
- Markovich, O., Kumar, S., Cohen, D., Addadi, S., Fridman, E., and Elbaum, R. (2015). Silicification in leaves of sorghum mutant with low silicon accumulation. *Silicon* 1–7. doi: 10.1007/s12633-015-9348-x
- Matsuo, N., Nanjo, Y., Tougou, M., Nakamura, T., Nishizawa, K., Komatsu, S., et al. (2012). Identification of putative aquaporin genes and their expression analysis under hypoxic conditions in soybean [*Glycine max* (L.) Merr.]. *Plant Prod. Sci.* 15, 278–283. doi: 10.1626/pps.15.278
- Maurel, C., Reizer, J., Schroeder, J. I., and Chrispeels, M. J. (1993). The vacuolar membrane protein gamma-TIP creates water specific channels in *Xenopus oocytes*. *EMBO J.* 12, 2241–2247.
- Mitani-Ueno, N., Yamaji, N., Zhao, F.-J., and Ma, J. F. (2011). The aromatic/arginine selectivity filter of NIP aquaporins plays a critical role in substrate selectivity for silicon, boron, and arsenic. *J. Exp. Bot.* 62, 4391–4398. doi: 10.1093/jxb/err158
- Monneuse, J. M., Sugano, M., Becue, T., Santoni, V., Hem, S., and Rossignol, M. (2011). Towards the profiling of the *Arabidopsis thaliana* plasma membrane transportome by targeted proteomics. *Proteomics* 11, 1789–1797. doi: 10.1002/pmic.201000660
- Morris, G. P., Ramu, P., Deshpande, S. P., Hash, C. T., Shah, T., Upadhyaya, H. D., et al. (2013). Population genomic and genome-wide association studies of agroclimatic traits in sorghum. *Proc. Natl. Acad. Sci. U.S.A.* 110, 453–458. doi: 10.1073/pnas.1215985110
- Moshelion, M., Halperin, O., Wallach, R., Oren, R., and Way, D. A. (2015). Role of aquaporins in determining transpiration and photosynthesis in water-stressed

- plants: crop water-use efficiency, growth and yield. *Plant Cell Environ.* 38, 1785–1793. doi: 10.1111/pce.12410
- Murata, K., Mitsuoka, K., Hirai, T., Walz, T., Agre, P., Heymann, J. B., et al. (2000). Structural determinants of water permeation through aquaporin-1. *Nature* 407, 599–605. doi: 10.1038/35036519
- Mustroph, A., Kaiser, K. A., Larive, C. K., and Bailey-Serres, J. (2014). Characterization of distinct root and shoot responses to low-oxygen stress in *Arabidopsis* with a focus on primary C-and N-metabolism. *Plant Cell Environ.* 37, 2366–2380. doi: 10.1111/pce.12282
- Narsai, R., Rocha, M., Geigenberger, P., Whelan, J., and van Dongen, J. T. (2011). Comparative analysis between plant species of transcriptional and metabolic responses to hypoxia. *New Phytol.* 190, 472–487. doi: 10.1111/j.1469-8137.2010.03589.x
- Pardales, J., Kono, Y., and Yamauchi, A. (1991). Response of the different root system components of sorghum to incidence of waterlogging. *Environ. Exp. Bot.* 31, 107–115. doi: 10.1016/0098-8472(91)90013-E
- Pfaffl, M. W. (2001). A new mathematical model for relative quantification in real-time RT-PCR. *Nucleic Acids Res.* 29:e45. doi: 10.1093/nar/29.9:e45
- Pou, A., Medrano, H., Flexas, J., and Tyerman, S. D. (2013). A putative role for TIP and PIP aquaporins in dynamics of leaf hydraulic and stomatal conductances in grapevine under water stress and re-watering. *Plant Cell Environ.* 36, 828–843. doi: 10.1111/pce.12019
- Promkhambut, A., Polthanee, A., Akksaeng, C., and Younger, A. (2011). Growth, yield and aerenchyma formation of sweet and multipurpose sorghum (*Sorghum bicolor* L. Moench) as affected by flooding at different growth stages. *Aust. J. Crop Sci.* 5:954.
- Rasheed-Depardieu, C., Parelle, J., Tatin-Froux, F., Parent, C., and Capelli, N. (2015). Short-term response to waterlogging in *Quercus petraea* and *Quercus robur*: a study of the root hydraulic responses and the transcriptional pattern of aquaporins. *Plant Physiol. Biochem.* 97, 323–330. doi: 10.1016/j.plaphy.2015.10.016
- Reddy, P. S., Rao, T. S. R. B., Sharma, K. K., and Vadez, V. (2015). Genome-wide identification and characterization of the aquaporin gene family in *Sorghum bicolor* (L.). *Plant Gene* 1, 18–28. doi: 10.1016/j.jplgene.2014.12.002
- Regassa, T. H., and Wortmann, C. S. (2014). Sweet sorghum as a bioenergy crop: literature review. *Biomass Bioenergy* 64, 348–355. doi: 10.1007/s10295-007-0296-3
- Reuscher, S., Akiyama, M., Mori, C., Aoki, K., Shibata, D., and Shiratake, K. (2013). Genome-wide identification and expression analysis of aquaporins in tomato. *PLoS ONE* 8:e79052. doi: 10.1371/journal.pone.0079052
- Sade, N., Gallé, A., Flexas, J., Lerner, S., Peleg, G., Yaaran, A., et al. (2014). Differential tissue-specific expression of NtAQP1 in *Arabidopsis thaliana* reveals a role for this protein in stomatal and mesophyll conductance of CO₂ under standard and salt-stress conditions. *Planta* 239, 357–366. doi: 10.1007/s00425-013-1988-8
- Sade, N., Shatil-Cohen, A., and Moshelion, M. (2015). Bundle-sheath aquaporins play a role in controlling *Arabidopsis* leaf hydraulic conductivity. *Plant Signal. Behav.* 10:e1017177. doi: 10.1080/15592324.2015.1017177
- Sakurai, J., Ishikawa, F., Yamaguchi, T., Uemura, M., and Maeshima, M. (2005). Identification of 33 rice aquaporin genes and analysis of their expression and function. *Plant Cell Physiol.* 46, 1568–1577. doi: 10.1093/pcp/pci172
- Sallans, B. (1942). The importance of various roots to the wheat plant. *Sci. Agric.* 23, 17–26.
- Schildwacht, P. M. (1989). Is a decreased water potential after withholding oxygen to roots the cause of the decline of leaf-elongation rates in *Zea mays* L. and *Phaseolus vulgaris* L.? *Planta* 177, 178–184. doi: 10.1007/BF00392806
- Shane, M., and McCully, M. (1999). Root xylem embolisms: implications for water flow to the shoot in single-rooted maize plants. *Aust. J. Plant Physiol.* 26, 107–114. doi: 10.1071/PP98060
- Shaw, R. E. (2015). *Plant Waterlogging: Causes, Responses, Adaptations and Crop Models*. Adelaide SA: The University of Adelaide.
- Singh, V., van Oosterom, E. J., Jordan, D. R., Messina, C. D., Cooper, M., and Hammer, G. L. (2010). Morphological and architectural development of root systems in sorghum and maize. *Plant Soil* 333, 287–299. doi: 10.1007/s11104-010-0343-0
- Suga, S., Komatsu, S., and Maeshima, M. (2002). Aquaporin isoforms responsive to salt and water stresses and phytohormones in radish seedlings. *Plant Cell Physiol.* 43, 1229–1237. doi: 10.1093/pcp/pcf148
- Sutka, M., Li, G., Boudet, J., Boursiac, Y., Doumas, P., and Maurel, C. (2011). Natural variation of root hydraulics in *Arabidopsis* grown in normal and salt-stressed conditions. *Plant Physiol.* 155, 1264–1276. doi: 10.1104/pp.110.163113
- Takano, J., Wada, M., Ludewig, U., Schaaf, G., Von Wirén, N., and Fujiwara, T. (2006). The *Arabidopsis* major intrinsic protein NIP5; 1 is essential for efficient boron uptake and plant development under boron limitation. *Plant Cell* 18, 1498–1509. doi: 10.1105/tpc.106.041640
- Tao, P., Zhong, X., Li, B., Wang, W., Yue, Z., Lei, J., et al. (2014). Genome-wide identification and characterization of aquaporin genes (AQPs) in Chinese cabbage (*Brassica rapa* ssp. *pekinensis*). *Mol. Genet. Genomics* 289, 1131–1145. doi: 10.1007/s00438-014-0874-9
- Terashima, I., and Ono, K. (2002). Effects of HgCl₂ on CO₂ dependence of leaf photosynthesis: evidence indicating involvement of aquaporins in CO₂ diffusion across the plasma membrane. *Plant Cell Physiol.* 43, 70–78. doi: 10.1093/pcp/pcf001
- Törnroth-Horsefield, S., Wang, Y., Hedfalk, K., Johanson, U., Karlsson, M., Tajkhorshid, E., et al. (2005). Structural mechanism of plant aquaporin gating. *Nature* 439, 688–694. doi: 10.1038/nature04316
- Tournaire-Roux, C., Sutka, M., Javot, H., Gout, E., Gerbeau, P., Luu, D.-T., et al. (2003). Cytosolic pH regulates root water transport during anoxic stress through gating of aquaporins. *Nature* 425, 393–397. doi: 10.1038/nature01853
- Upadhyaya, H., Pandir, R., Dwivedi, S., Gowda, C., Reddy, V. G., and Singh, S. (2009). Developing a mini core collection of sorghum for diversified utilization of germplasm. *Crop Sci.* 49, 1769–1780. doi: 10.2135/cropsci2009.01.0014
- Van Veen, H., Vashisth, D., Akman, M., Girke, T., Mustroph, A., Reinen, E., et al. (2016). Transcriptomes of eight *Arabidopsis thaliana* accessions reveal core conserved, genotype-and organ-specific responses to flooding stress. *Plant physiol.* 172, 668–689. doi: 10.1104/pp.16.00472
- Vanderlip, R. (1993). *How a Grain Sorghum Plant Develops*. Manhattan, KS: Kansas State University.
- Venkatesh, J., Yu, J.-W., and Park, S. W. (2013). Genome-wide analysis and expression profiling of the *Solanum tuberosum* aquaporins. *Plant Physiol. Biochem.* 73, 392–404. doi: 10.1016/j.plaphy.2013.10.025
- Vitali, M., Cochard, H., Gambino, G., Ponomarenko, A., Perrone, I., and Lovisolo, C. (2016). VvPIP2; 4N aquaporin involvement in controlling leaf hydraulic capacitance and resistance in grapevine. *Physiol. Plant.* 158, 284–296. doi: 10.1111/plp.12463
- Wallace, I. S., and Roberts, D. M. (2005). Distinct transport selectivity of two structural subclasses of the nodulin-like intrinsic protein family of plant aquaglyceroporin channels. *Biochemistry* 44, 16826–16834. doi: 10.1021/bi0511888
- Wang, L., Zhang, Y., Qi, X., Li, D., Wei, W., and Zhang, X. (2012). Global gene expression responses to waterlogging in roots of sesame (*Sesamum indicum* L.). *Acta Physiol. Plant.* 34, 2241–2249. doi: 10.1007/s11738-012-1024-9
- Weig, A., Deswarte, C., and Chrispeels, M. J. (1997). The major intrinsic protein family of *Arabidopsis* has 23 members that form three distinct groups with functional aquaporins in each group. *Plant Physiol.* 114, 1347–1357. doi: 10.1104/pp.114.4.1347
- Xu, Q., Yang, L., Zhou, Z., Mei, F., Qu, L., and Zhou, G. (2013). Process of aerenchyma formation and reactive oxygen species induced by waterlogging in wheat seminal roots. *Planta* 238, 969–982. doi: 10.1007/s00425-013-1947-4
- Zardoya, R. (2005). Phylogeny and evolution of the major intrinsic protein family. *Biol. Cell* 97:397–414. doi: 10.1042/BC20040134
- Zhang, D. Y., Ali, Z., Wang, C. B., Xu, L., Yi, J. X., Xu, Z. L., et al. (2013). Genome-wide sequence characterization and expression analysis of major intrinsic proteins in soybean (*Glycine max* L.). *PLoS ONE* 8:e56312. doi: 10.1371/journal.pone.0056312
- Zhang, F., Wang, Y., Yu, H., Zhu, K., Zhang, Z., and Zou, F. L. J. (2016). Effect of excessive soil moisture stress on sweet sorghum: physiological changes and productivity. *Pak. J. Bot.* 48, 1–9.

Zou, X., Tan, X., Hu, C., Zeng, L., Lu, G., Fu, G., et al. (2013). The transcriptome of *Brassica napus* L. roots under waterlogging at the seedling stage. *Int. J. Mol. Sci.* 14, 2637–2651. doi: 10.3390/ijms14022637

Conflict of Interest Statement: The authors declare that the research was conducted in the absence of any commercial or financial relationships that could be construed as a potential conflict of interest.

Copyright © 2017 Kadam, Abril, Dhanapal, Koester, Vermerris, Jose and Fritsch. This is an open-access article distributed under the terms of the Creative Commons Attribution License (CC BY). The use, distribution or reproduction in other forums is permitted, provided the original author(s) or licensor are credited and that the original publication in this journal is cited, in accordance with accepted academic practice. No use, distribution or reproduction is permitted which does not comply with these terms.



Root ABA Accumulation Enhances Rice Seedling Drought Tolerance under Ammonium Supply: Interaction with Aquaporins

Lei Ding^{1,2†}, Yingrui Li^{1†}, Ying Wang¹, Limin Gao¹, Min Wang¹, François Chaumont², Qirong Shen¹ and Shiwei Guo^{1*}

¹ Jiangsu Key Lab for Organic Waste Utilization, Nanjing Agricultural University, Nanjing, China, ² Institut des Sciences de la Vie, Université catholique de Louvain, Louvain-la-Neuve, Belgium

OPEN ACCESS

Edited by:

Rupesh Kailasrao Deshmukh,
Université Laval, Canada

Reviewed by:

Lars Hendrik Wegner,
Karlsruhe Institute of Technology,
Germany

Amit Atmaram Deokar,
University of Saskatchewan, Canada
Arun Prabhu Dhanapal,
University of Missouri, USA

*Correspondence:

Shiwei Guo
sguo@njau.edu.cn

[†]These authors have contributed
equally to this work.

Specialty section:

This article was submitted to
Plant Physiology,
a section of the journal
Frontiers in Plant Science

Received: 16 May 2016

Accepted: 29 July 2016

Published: 10 August 2016

Citation:

Ding L, Li Y, Wang Y, Gao L, Wang M, Chaumont F, Shen Q and Guo S (2016) Root ABA Accumulation Enhances Rice Seedling Drought Tolerance under Ammonium Supply: Interaction with Aquaporins. *Front. Plant Sci.* 7:1206.
doi: 10.3389/fpls.2016.01206

In previous studies, we demonstrated that ammonium nutrition enhances the drought tolerance of rice seedlings compared to nitrate nutrition and contributes to a higher root water uptake ability. It remains unclear why rice seedlings maintain a higher water uptake ability when supplied with ammonium under drought stress. Here, we focused on the effects of nitrogen form and drought stress on root *abscisic acid* (ABA) concentration and aquaporin expression using hydroponics experiments and stimulating drought stress with 10% PEG6000. Drought stress decreased the leaf photosynthetic rate and stomatal conductivity and increased the leaf temperature of plants supplied with either ammonium or nitrate, but especially under nitrate supply. After 4 h of PEG treatment, the root protoplast water permeability and the expression of root *PIP* and *TIP* genes decreased in plants supplied with ammonium or nitrate. After 24 h of PEG treatment, the root hydraulic conductivity, the protoplast water permeability, and the expression of some aquaporin genes increased in plants supplied with ammonium compared to those under non-PEG treatment. Root ABA accumulation was induced by 24 h of PEG treatment, especially in plants supplied with ammonium. The addition of exogenous ABA decreased the expression of *PIP* and *TIP* genes under non-PEG treatment but increased the expression of some of them under PEG treatment. We concluded that drought stress induced a down-regulation of aquaporin expression, which appeared earlier than did root ABA accumulation. With continued drought stress, aquaporin expression and activity increased due to root ABA accumulation in plants supplied with ammonium.

Keywords: rice, water uptake, ABA, aquaporin, drought stress

INTRODUCTION

Previous studies demonstrated that ammonium nitrogen (NH_4^+) enhances rice seedling drought tolerance due to a higher root water uptake ability (Gao et al., 2010; Yang et al., 2012) compared to that of seedlings under nitrate nitrogen (NO_3^-) supply. Under drought stress, Yang et al. (2012) reported decreased root hydraulic conductivity in rice plants supplied with nitrate, illustrated by

Abbreviations: AN, ammonium; ANP, ammonium with PEG; AQP, aquaporin; NN, nitrate; NNP, nitrate with PEG; PEG, polyethylene glycol; PIP, plasma membrane intrinsic protein; TIP, tonoplast membrane intrinsic protein.

the down-regulation of aquaporin activity and the increased formation of root cortical aerenchyma. It was found that short-term simulated drought stress could increase root AQP expression, activity and root hydraulic conductivity under NH_4^+ supply but not under nitrate supply (Ding et al., 2015).

Abscisic acid (ABA) potentially plays important roles in AQP regulation and root water uptake in plants facing different nitrogen forms and/or drought stress (Schraut et al., 2005; Parent et al., 2009). In most studies, application of exogenous ABA increased the root *PIP* gene expression under normal water conditions (Jang et al., 2004; Zhu et al., 2005; Lian et al., 2006). Under drought stress, root ABA accumulation was indispensable for regulating AQP expression (Kaldenhoff et al., 2008; Parent et al., 2009) and for enhancing plant growth (Sharp, 2002; Zhang et al., 2006). Actually, in these conditions, roots-perceived water deficit and accumulated ABA, which would be transported to the leaves to regulate stomatal closure (Zhang and Davies, 1990; Davies and Zhang, 1991; Sengupta et al., 2011). A positive correlation has been observed between drought stress and root ABA accumulation in beans (Puertolas et al., 2013), potato (Puertolas et al., 2015), maize (Zhang and Davies, 1989), rice and *Arabidopsis* (Xu et al., 2013). Using ‘one shoot-two roots’ potato under partial root-zone drying (PRD), Puertolas et al. (2015) also showed that ABA only accumulated in dry-side roots, which further illustrated this positive correlation. In addition, plant aerial parts accumulated ABA under drought stress in tomato (Perez-Perez and Dodd, 2015), wheat (Guóth et al., 2009), and hops (Korovetska et al., 2014).

However, it remains unclear how nitrogen form affects ABA dynamics, such as how changes in ABA amount regulate root AQP expression and water uptake in plants under drought stress. It was reported that root and aerial tissues accumulated more ABA when NH_4^+ is supplied as a sole nitrogen source in castor bean (Peuke et al., 1994), pea (Zdunek and Lips, 2001), and tomato (Rahayu et al., 2005). We hypothesized that rice roots could accumulate more ABA and further stimulate AQP expression under drought stress with NH_4^+ supply. In the present study, we aimed to determine (1) how nitrogen form and drought stress affect ABA dynamics and (2) the potential correlation between ABA change and AQP regulation in roots under drought stress.

MATERIALS AND METHODS

Plant Material and Growth Conditions

Rice seeds (*Oryza sativa* L., cv. ‘Shanyou 63’ hybrid *indica* China) were disinfected in 10% H_2O_2 (W/W) for 30 min and then germinated in a plastic basket (25 cm × 18 cm) with mesh. After the seedlings had developed an average of 2.5 visible leaves, they were transplanted to a 7-L plastic box containing a quarter-strength mixture of NH_4^+ and NO_3^- (ANN) nutrient solution (Ding et al., 2015). After 3 days, the rice seedlings were transferred to half-strength ANN for 5 days and then supplied with full-strength ANN for 1 week, after which the seedlings were supplied with either NH_4^+ (AN) or NO_3^- (NN) nutrient solution. After an additional week, the seedlings were subjected

to simulated drought stress by the addition of 10% PEG (10% w/v, MW 6000) to the nutrient solutions (−0.15 MPa). Four treatments were applied: AN, NN, NH_4^+ plus 10% PEG 6000 (ANP) and NO_3^- plus 10% PEG 6000 (NNP). For exogenous ABA treatment, 5 μM ABA in nutrient solution was added.

Cucumber plants were cultured identically to rice plants with the same nutrient solution in 1-L plastic cup. For simulating drought stress, 2% (w/v) PEG6000 was added into the nutrient solution.

The temperature in the glasshouse was maintained at 30°C during the day and 18°C at night. Light was supplied by SON-T AGRO 400 W bulbs; the light intensity was maintained at a minimum of 1000 μmol photons $\text{m}^{-2} \text{s}^{-1}$ (photosynthetically active radiation) at the leaf level using a 14-h photoperiod.

Gas-Exchange Measurement and Thermo Imaging

After 24 h of treatment with PEG, the light-saturated photosynthesis of newly expanded leaves was measured from 09:00 to 11:00 using the Li-Cor 6400 portable photosynthesis system. The leaf temperature during measurement was maintained at 28°C, and the photosynthetic photon flux density (PPFD) was 1500 $\mu\text{mol m}^{-2} \text{s}^{-1}$.

Meanwhile, infrared images were obtained using an infrared camera (SC620, FLIR Systems, Inc., USA) with a spectral sensitivity ranging from 7.5 to 13 mm and a spatial resolution of 0.65 mrad.

Root Hydraulic Conductivity Measurement and Root Protoplast Swelling Analysis

After 24 h of treatment with PEG, root hydraulic conductance was measured using a high-pressure flow meter (HPFM; Decagon Devices, Pullman, WA, USA) according to Ding et al. (2015). Root protoplasts were isolated after 4 and 24 h of PEG treatment, and a swelling assay was conducted to analyze the water permeability coefficient P_{os} according to a previous method (Ding et al., 2015).

RNA Isolation and Quantitative Real Time PCR (RT-qPCR)

Root samples were harvested after 4 and 24 h of PEG and ABA treatments, immediately frozen in liquid nitrogen, and then stored at −70°C until RNA isolation. The total RNA was extracted with TRIzol reagent (Invitrogen, USA) according to the manufacturer’s instructions. cDNA was synthesized using the PrimeScript™ RT reagent Kit with gDNA Eraser (Takara, Dalian, China). Reverse transcription quantitative real time polymerase chain reaction (RT-qPCR) was performed using the ABI 7500 Real-Time PCR system, and the products were labeled using the SYBR Green master mix (SYBR® Premix Ex Taq™ II (Tli RNaseH Plus); TaKaRa, Dalian, China). The primers for RT-qPCR were according to Sakurai-Ishikawa et al. (2011), and the 18 sRNA was used as a housekeeping gene. Genes identifiers were listed in Supplementary Table S1. The relative gene expression was calculated with the $2^{-\Delta Ct}$ method.

ABA Detection in Roots, Leaves, and Xylem Sap

Root samples were harvested after PEG treatment for 2, 4, 12 and 24 h, followed by storage at -70°C . Leaf samples were harvested after 24 h of PEG treatment. Both the roots and leaves were freeze dried and extracted in glass-distilled water using approximately 1.2 ml per 40 mg dry weight, boiled for 1–2 min, and shaken at 4°C overnight. The extracts were centrifuged, and the supernatants were assayed with an enzyme-linked immunosorbent assay (ELISA; Plant hormone ABA; ELISA Kit, CUSABIO, USA).

To detect xylem sap ABA, xylem sap was collected after 24 h of PEG treatment. The plants were de-topped approximately 2 cm above the interface of the roots and shoots, and the exudation was immediately cleaned with filter paper to avoid contamination. Absorbent cotton was placed on the top of each piece of de-topped xylem and covered with plastic film to avoid evaporation. Xylem sap was collected from the cotton with a syringe and then frozen at -20°C for the ABA assay. Frozen xylem sap was allowed to thaw for approximately 45 min before being assayed.

Statistics

A one-way analysis of variance (ANOVA) was used to assess the differences in each parameter among the treatments using the JMP 9 statistical software package (SAS Institute, Cary, NC, USA). For gene expression analysis, R software package¹ was used to generate a hierarchical cluster heat map and cluster tree. The significant differences ($P < 0.05$) among the treatments as determined by Student's *t*-test are indicated with different letters.

RESULTS

Effect of Nitrogen Form and Drought Stress on Leaf Gas Exchange and Temperature

Under non-PEG treatment, no significant differences in the photosynthetic rate (Pn), stomatal conductivity (g_s), or transpiration (Tr) were observed between NH_4^+ - and NO_3^- -supplied plants (Figure 1). After 24 h of PEG treatment, g_s and Tr significantly decreased in plants supplied with either nitrogen form, and Pn decreased in NO_3^- -supplied plants. In plants supplied with NO_3^- , the g_s decreased from 0.32 to 0.17 mol $\text{m}^{-2} \text{s}^{-1}$ and the Pn decreased by approximately 30% by PEG treatment from 22.9 to 16.1 $\mu\text{mol CO}_2 \text{ m}^{-2} \text{ s}^{-1}$ (Figure 1).

To investigate how drought stress affected leaf temperature, an infrared camera was used. A thermograph was used to determine the temperature difference. Leaves showed the highest temperature when supplied with NO_3^- under PEG treatment (Figures 2A,B). There was a significant negative correlation between stomatal conductivity and leaf temperature (Figure 2C).

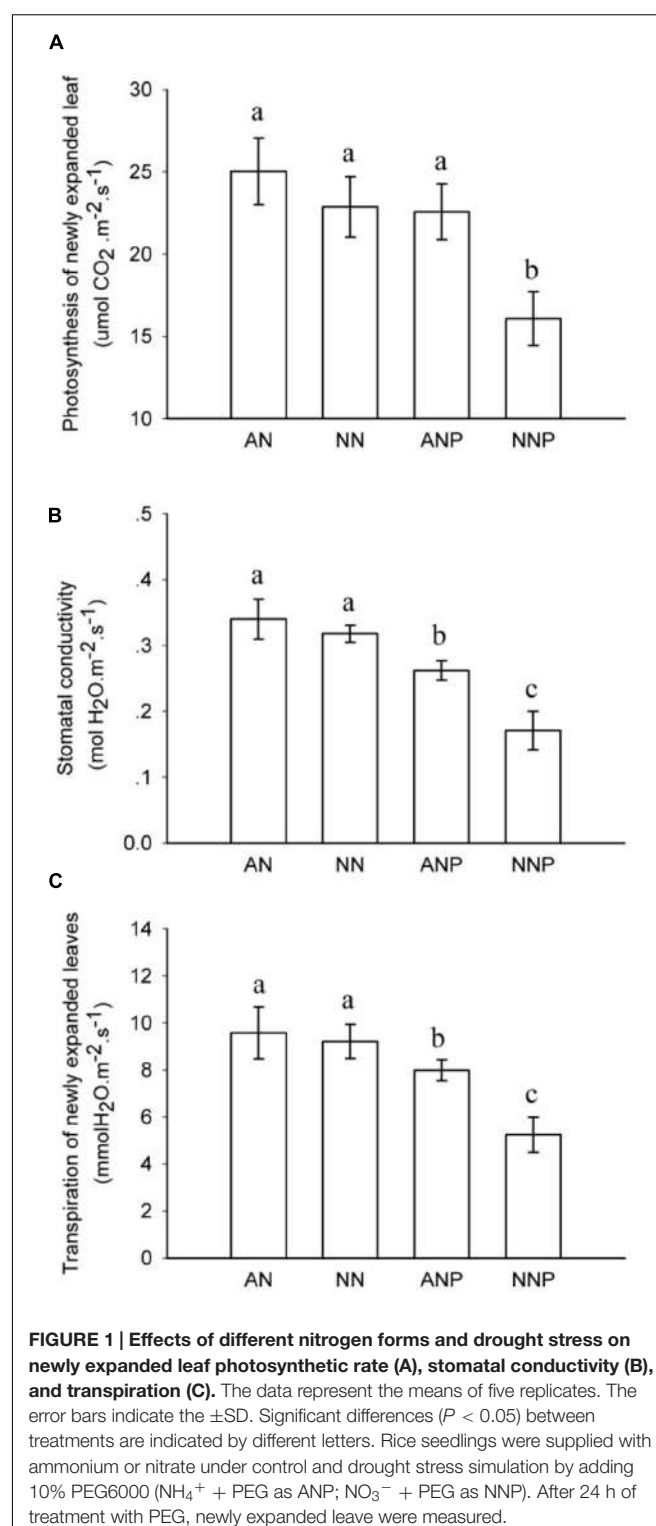


FIGURE 1 | Effects of different nitrogen forms and drought stress on newly expanded leaf photosynthetic rate (A), stomatal conductivity (B), and transpiration (C). The data represent the means of five replicates. The error bars indicate the $\pm\text{SD}$. Significant differences ($P < 0.05$) between treatments are indicated by different letters. Rice seedlings were supplied with ammonium or nitrate under control and drought stress simulation by adding 10% PEG6000 ($\text{NH}_4^+ + \text{PEG}$ as ANP; $\text{NO}_3^- + \text{PEG}$ as NNP). After 24 h of treatment with PEG, newly expanded leaves were measured.

Effect of Nitrogen Form and Drought Stress on Root Water Uptake Ability

After 24 h of PEG treatment, the root hydraulic conductivity increased significantly in plants supplied with NH_4^+ . Compared

¹<http://www.r-project.org/>

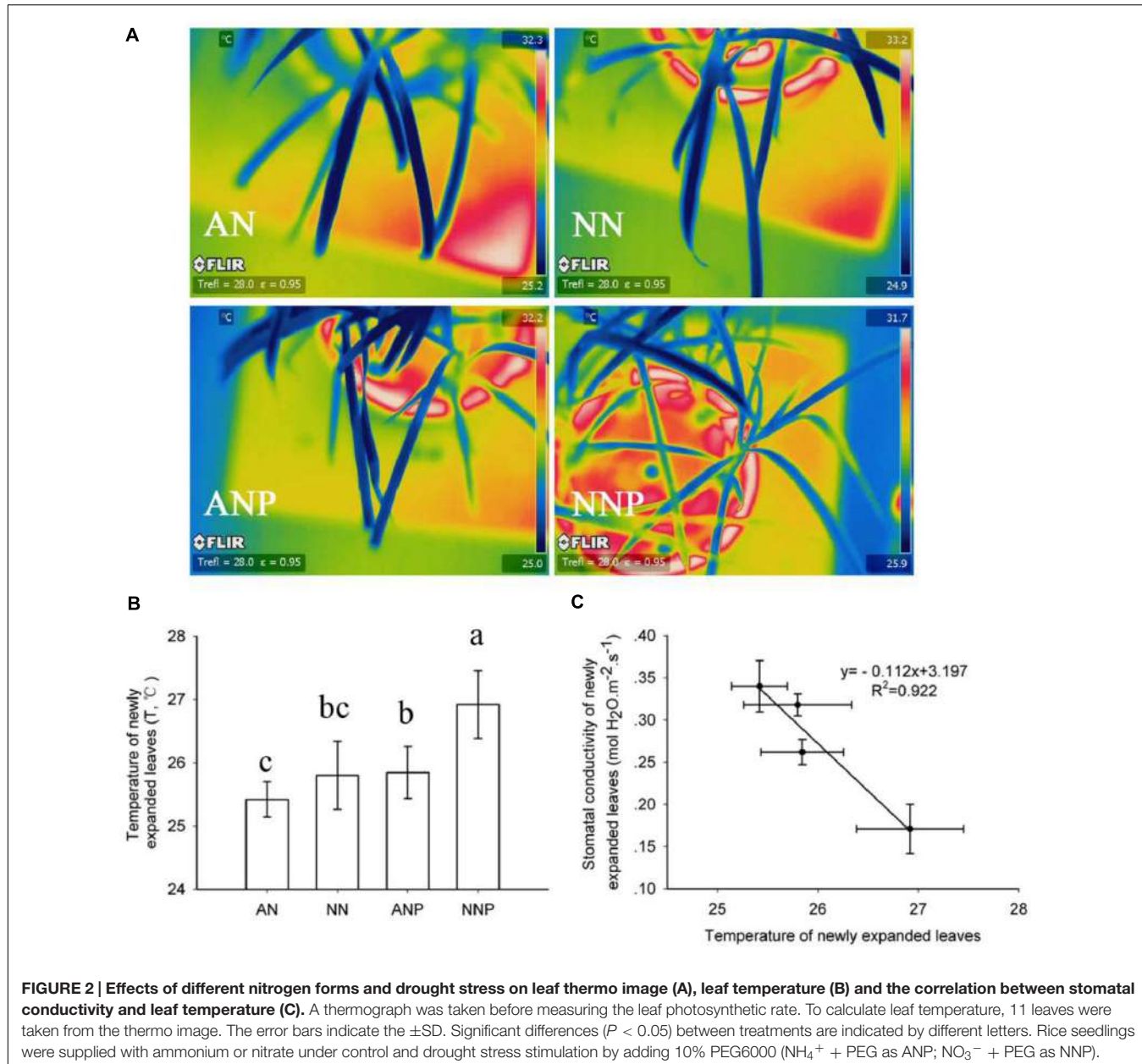


FIGURE 2 | Effects of different nitrogen forms and drought stress on leaf thermo image (A), leaf temperature (B) and the correlation between stomatal conductivity and leaf temperature (C). A thermograph was taken before measuring the leaf photosynthetic rate. To calculate leaf temperature, 11 leaves were taken from the thermo image. The error bars indicate the \pm SD. Significant differences ($P < 0.05$) between treatments are indicated by different letters. Rice seedlings were supplied with ammonium or nitrate under control and drought stress stimulation by adding 10% PEG6000 (NH_4^+ + PEG as ANP; NO_3^- + PEG as NNP).

to non-PEG treatment, drought stress enhanced the root hydraulic conductivity approximately twofold when the plants were fed NH_4^+ (Figure 3A). Similar results were not observed in plants supplied with NO_3^- .

To further investigate the effect of nitrogen form and drought stress on root cell water permeability, a root protoplast swelling assay was performed. After 4 h of PEG treatment, the water permeability P_{os} of protoplasts obtained from roots supplied with either nitrogen form decreased (Figure 3B). However, the P_{os} increased when the plants grew in presence of NH_4^+ supply after 24 h of PEG treatment compared with the P_{os} of cells coming from non-PEG treated plants; no change in P_{os} was observed when the plants were supplied with NO_3^- (Figure 3C).

Effect of Nitrogen Form and Drought Stress on Root *PIP* and *TIP* Gene Expression

To investigate how the expression of the aquaporin genes was affected in roots by drought stress, we measured the mRNA level of nine *PIP* genes (*PIP1;1* to *PIP1;3*, *PIP2;1* to *PIP2;6*), including *PIP1;1* to *1;3* and *PIP2;1* to *2;6*, and four *TIP* genes (*TIP1;1*, *TIP1;2*, *TIP2;1*, and *TIP2;2*) by the RT-qPCR. Under non-PEG treatment, the expression of almost all the *PIP* and *TIP* genes was higher in plants supplied with NH_4^+ than that in those supplied with NO_3^- (Figure 4). After 4 h of PEG treatment, the expression of all genes dramatically decreased in plants supplied with either nitrogen forms compared to that of

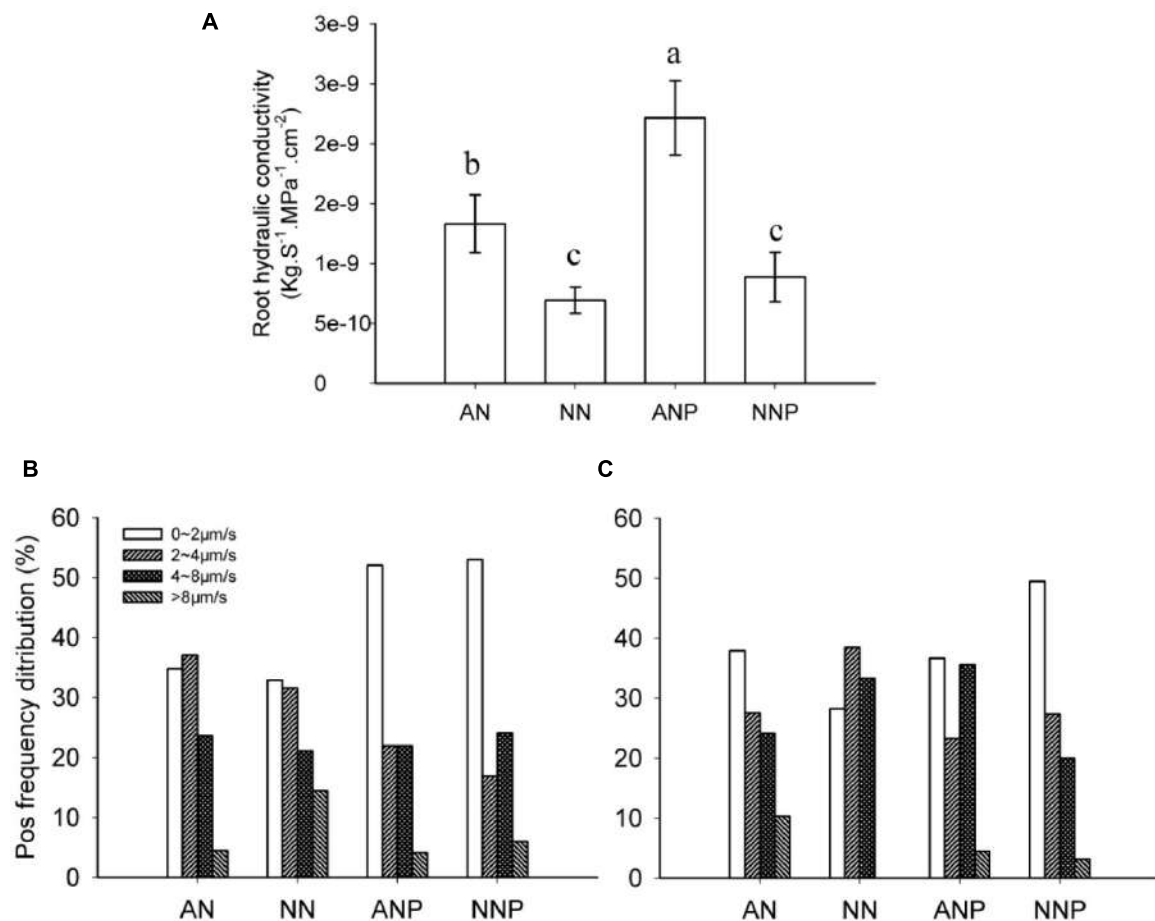


FIGURE 3 | Effects of different nitrogen forms and drought stress on root hydraulic conductivity (A) and the root protoplast water permeability coefficient P_{0s} (B,C). Root hydraulic conductivity was measured after 24 h of PEG treatment. Root protoplasts were isolated after 4 h (B) and 24 h (C) of PEG treatment. The data represent the means of four replicates. The error bars indicate the $\pm \text{SD}$. Significant differences ($P < 0.05$) between treatments are indicated by different letters. Rice seedlings were supplied with ammonium or nitrate under control and drought stress stimulation by adding 10% PEG6000 (NH_4^+ + PEG as ANP; NO_3^- + PEG as NNP).

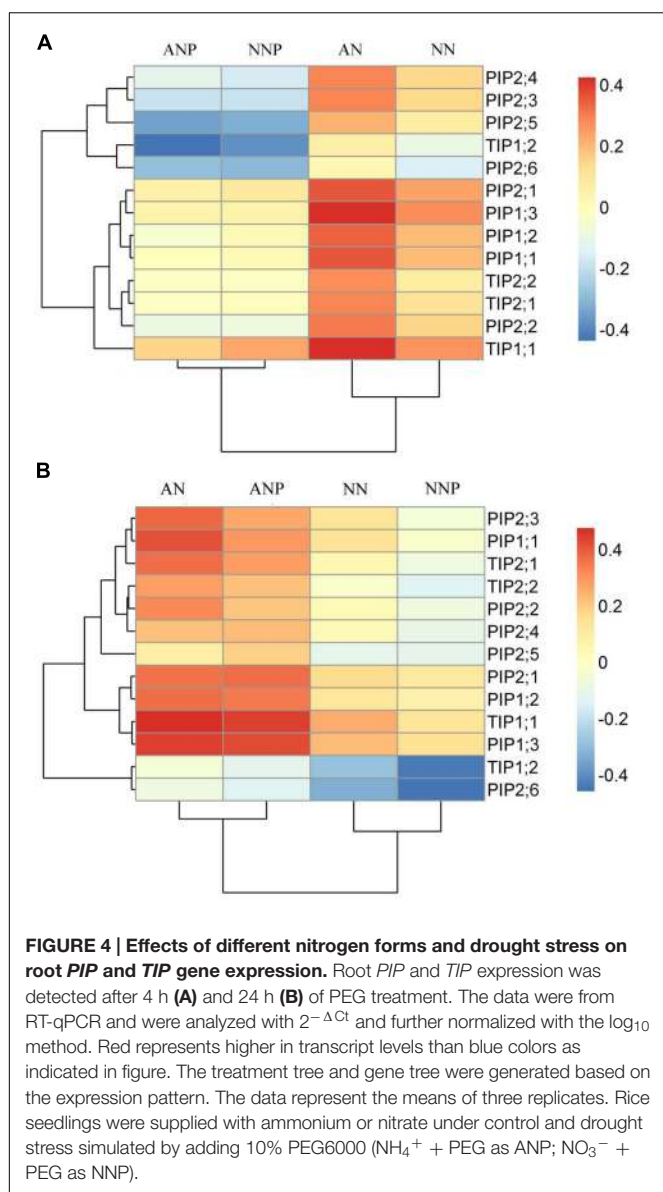
non-PEG treatment, especially that of *PIP2;5*, *PIP2;6*, and *TIP1;2*. In contrast, after 24 h of PEG treatment, the expression of these genes showed different levels of increase compared to those under 4 h PEG treatment, especially in plants supplied with NH_4^+ . Compared to non-PEG treatment, *PIP2;5* expression was higher under NH_4^+ supply after 24 h of PEG treatment (Figure 4).

Effect of Nitrogen Form and Drought Stress on Root Endogenous Abscisic Acid (ABA), Xylem Sap ABA, and Leaf ABA

To investigate the potential relationship between aquaporin and ABA under drought stress, ABA concentration was measured after 2, 4, 12, and 24 h of PEG treatment. Under non-PEG treatment, the root ABA concentration was higher in plants supplied with NH_4^+ compared with the plants supplied with NO_3^- (Figure 5). The ABA concentration was significantly higher in plants supplied with NH_4^+ after 12 h of PEG treatment

than in plants under non-PEG treatment. In particular, after 24 h of treatment, the ABA concentration increased 10-fold from 0.13 to 1.2 $\mu\text{g g}^{-1}$. In plants supplied with NO_3^- , PEG treatment increased the ABA concentration from 0.09 to 0.33 $\mu\text{g g}^{-1}$. After 24 h of PEG treatment, the root ABA concentration was fourfold higher under NH_4^+ supply than that under NO_3^- supply.

In the aerial parts under non-PEG treatment, both xylem sap and leaf ABA concentrations were higher when supplied with NO_3^- , but not significantly different than supplied with NH_4^+ (Figure 6A). However, 24 h of PEG treatment significantly increased the xylem sap ABA concentration, which was threefold higher than that in non-PEG-treated plant supplied with NH_4^+ . There was no increase in the xylem ABA concentration by PEG treatment in plants supplied with NO_3^- , which was significantly lower than that in plants supplied with NH_4^+ (Figure 6A). Compared to the xylem sap ABA change, the ABA concentration in the leaves showed the same tendency, increasing by PEG treatment from 2.24 to 8.33 $\mu\text{g g}^{-1}$ in plants supplied with NH_4^+ (Figure 6B).



Effect of Exogenous Abscisic Acid (ABA) on Root AQP Gene Expression

To further investigate the regulation by ABA of root AQP gene expression, exogenous ABA was applied to the roots. Under non-PEG treatment, exogenous ABA applied for 4 h decreased the expression of all PIP and TIP genes in plants supplied with either NH_4^+ or NO_3^- . Under PEG treatment, the application of exogenous ABA for 4 h increased *PIP1;1*, *PIP1;2*, *PIP1;3*, *PIP2;1*, *TIP1;1*, *TIP2;1*, and *TIP2;2* mRNA levels compared to that in non-ABA-applied plants (Figure 7) supplied with either NH_4^+ or NO_3^- , but especially under NH_4^+ supply. After 24 h of ABA treatment, no increase in gene expression was observed compared with non-ABA application under PEG treatment, and the expression of some genes decreased (Supplementary Figure S2).

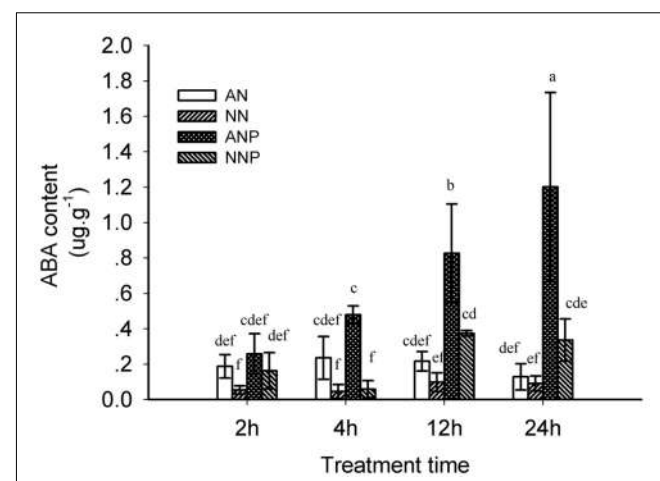


FIGURE 5 | Effects of different nitrogen forms and drought stress on the root ABA concentration. Root ABA dynamics were detected after 2, 4, 12, and 24 h of PEG treatment. The data represent the means of three replicates. The error bars indicate the $\pm\text{SD}$. Significant differences ($P < 0.05$) between treatments are indicated by different letters. Rice seedlings were supplied with ammonium (AN) or nitrate (NN) under control and drought stress simulation by adding 10% PEG6000 (NH_4^+ + PEG as ANP; NO_3^- + PEG as NNP).

DISCUSSION

Effect of Drought Stress on Root Water Uptake

Drought stress increased the root hydraulic conductivity (Lpr) in plants supplied with ammonium (Figure 3). Numerous studies have reported Lpr was regulated by drought stress in different plant species, e.g., maize (Hachez et al., 2012), cucumber (Qian et al., 2015), tobacco (Mahdiah et al., 2008), grapevine (Vandeleur et al., 2009), and rice (Yang et al., 2012; Grondin et al., 2016). In these studies, regulation of the Lpr was shown to be dependent on the duration of the stress, the species and even the cultivars. First, long-term drought stress decreases Lpr compared to short-term stress, which might increase Lpr. Grondin et al. (2016) analyzed the Lpr of six different rice cultivars under long term drought stress, and five of them showed obvious conductivity decrease. Our previous results demonstrated no significant difference in the Lpr during several weeks of drought stress compared with normal water treatment in rice plants supplied with ammonium, while Lpr decreased in plants supplied with nitrate under the same conditions (Yang et al., 2012). It is possible that the roots Lpr decreased to avoid water depletion when the plant suffers long-term drought stress. Considering short-term PEG stress (24 h), Lpr increased in plants supplied with ammonium (Figure 3). Compared to our results, Hachez et al. (2012) reported that cell hydraulic conductivity increased approximately fourfold when maize plants stressed with 10% PEG for 2 h. Second, the Lpr varied according to the species under drought stress. Qian et al. (2015) reported that both root and cell hydraulic conductivity decreased in cucumber upon 140 mM PEG treatment for 2 and 24 h, while in tobacco, the root water uptake ability decreased

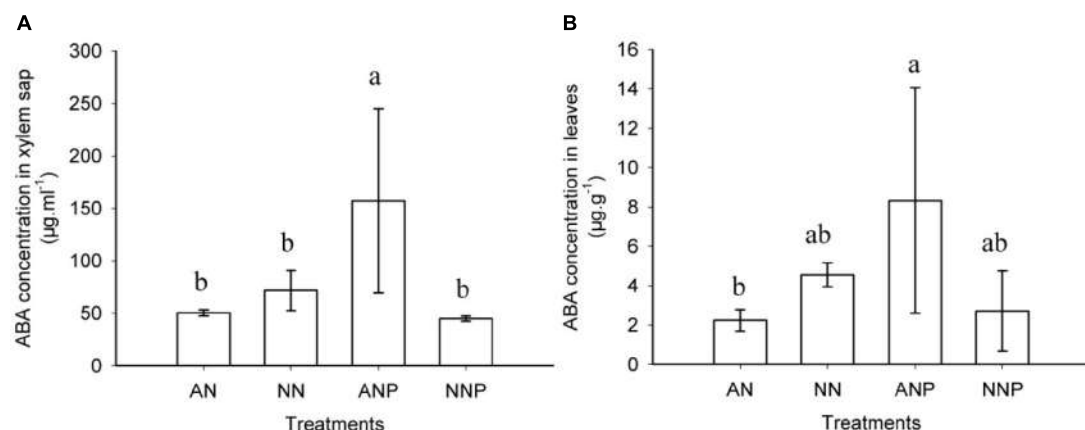


FIGURE 6 | Effects of different nitrogen forms and drought stress on xylem (A) and leaf (B) ABA concentration. After 24 h of PEG treatment, xylem sap and leaves were harvested for ABA detection. The data represent the means of three replicates. The error bars indicate the $\pm\text{SD}$. Significant differences ($P < 0.05$) between treatments are indicated by different letters. Rice seedlings were supplied with ammonium or nitrate under control and drought stress simulation by adding 10% PEG6000 ($\text{NH}_4^+ + \text{PEG}$ as ANP; $\text{NO}_3^- + \text{PEG}$ as NNP).

upon PEG treatment ($\Psi = -0.35$ MPa) for 24 h (Mahdieu et al., 2008). In maize and rice plants, the hydraulic conductivity was increased by short-term drought stress. Both increased and decreased Lpr could enhance drought tolerance, representing different regulation strategies.

Increasing evidence indicates that aquaporin plays vital roles in the process of root radial water transport and affect Lpr, for review see (Chaumont and Tyerman, 2014). The contribution of aquaporin to Lpr is generally high, up to 79% under well-watered conditions and 85% under drought stress in rice plants (Grondin et al., 2016). In the present study, we investigated root protoplast water permeability and *PIP* and *TIP* genes expression in response to PEG treatment in presence of different nitrogen forms. We observed that 4 h of drought stress decreased root protoplast P_{os} in plants supplied with either ammonium or nitrate, while 24 h of drought stress increased P_{os} in plants supplied with ammonium (Figures 3B,C), which is consistent with previous result (Ding et al., 2015). Interestingly, this is in accordance with the decreased expression of all *PIP* and *TIP* genes observed upon 4 h of drought stress in plants supplied with either ammonium or nitrate and the dramatic increase in expression in plants supplied with ammonium after 24 h of stress (Figure 4).

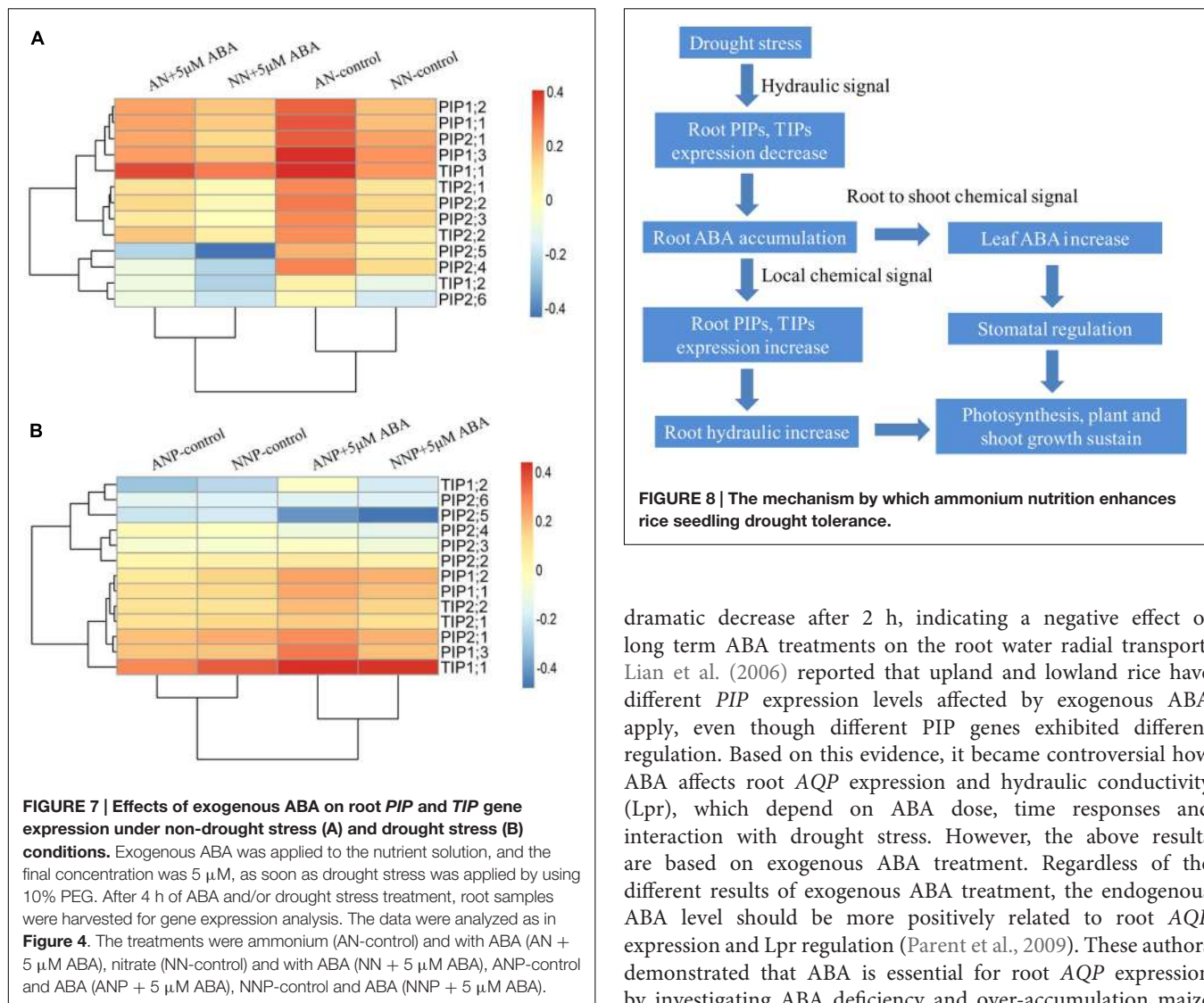
In the present study, drought stress in presence of ammonium induced a decrease in *PIP2;5* gene expression after 4 h of treatment and an increase in its expression after 24 h (Figure 4). This flexible shift suggested that *PIP2;5* plays an important role in regulating radial water transport under drought stress. Sakurai-Ishikawa et al. (2011) reported that *OsPIP2;5* contributed significantly to water radial water movement during diurnal changes and mainly accumulated on the proximal end of the endodermis and in xylem parenchyma cells, where transport resistance is high. In maize plants, both 2 and 8 h of 10% PEG treatment increased *ZmPIP2;5* gene expression and protein content (Hachez et al., 2012). Considering *TIP* genes, Li et al. (2008) found them to be tightly related to tolerance to various stresses, including dehydration, salinity, ABA and seed

germination in rice plants. *TIP1;2* and *TIP2;2* facilitated water transport when expressed in *Xenopus* oocytes. In addition, a 10 h 15% PEG treatment increased significantly *OsTIP1;1* expression, while in our study the expression of four *TIP* genes significantly increased after 24 h of PEG treatment compared to that after 4 h.

In conclusion, short-term 24 h PEG treatment increased root hydraulic conductivity, root protoplast water permeability and the expression of *PIP* and *TIP* genes, which might facilitate the water transport in and out the cells and the whole plant metabolism in plants supplied ammonium. However, after 4 h of PEG treatment, *AQP* expression and activity decreased to avoid cell dehydration in plants supplied with either ammonium or nitrate (Figure 4).

The Interaction between ABA Change and Aquaporin Expression Regulation in Roots under Drought Stress

We observed that root ABA accumulation peaked after 24 h of PEG treatment in plants supplied with ammonium and increased by approximately 10-fold (Figure 5). In xylem sap and leaves, drought stress also induced ABA accumulation under ammonium supply (Figure 6). However, there is limited evidence suggesting how nitrogen form and drought stress affect the root ABA concentration. Our results showed that there was a greater ABA concentration in rice plants supplied with ammonium rather than with nitrate under drought stress, while no significant difference was observed under normal water condition (Figure 5). In wheat, there was no difference in root ABA concentration between plants supplied with ammonium and those supplied with nitrate (Chen et al., 1998). Root or aerial tissues accumulate more ABA when NH_4^+ supplied as a sole nitrogen source under non-drought stress in castor bean (Peuke et al., 1994), pea (Zdunek and Lips, 2001), and tomato (Rahayu et al., 2005). In cucumber, a higher but not significant root ABA concentration was observed when supplied with nitrate



compared with the ammonium supply. Under drought stress, ABA change varied with duration of stress and nitrogen form (Supplementary Figure S1). It was therefore speculated that plant ABA is dynamically dependent on the nitrogen form, the species and the water status.

In roots, ABA plays important roles in regulating radial water transport and AQP gene expression, and in most cases, ABA increases root AQP gene expression and Lpr (Jang et al., 2004; Zhu et al., 2005; Mahdieu and Mostajeran, 2009; Parent et al., 2009). We observed an expression decrease in *PIP* and *TIP* genes by when the plants are incubated with 5 µM ABA under non-drought stress (**Figure 7A**; Supplementary Figure S2A). Consistent with this result, Beaudette et al. (2007) reported that 0.01 and 100 µM ABA incubation for 24 h decreased *PsPIP2;1* expression. However, they also demonstrated that 1 and 10 µM exogenous ABA increased *PsPIP2;1* expression. In maize plants, 1 µM ABA increased root cell hydraulic conductivity from 10 min to 1 h incubation, followed by a

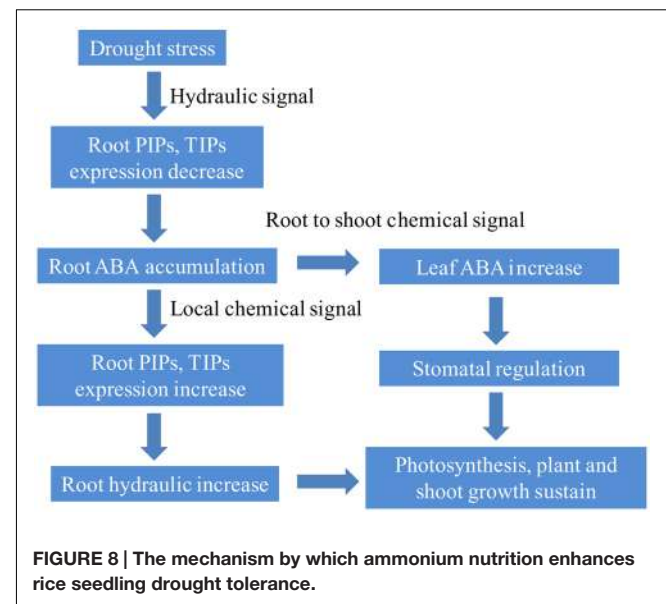


FIGURE 8 | The mechanism by which ammonium nutrition enhances rice seedling drought tolerance.

dramatic decrease after 2 h, indicating a negative effect of long term ABA treatments on the root water radial transport. Lian et al. (2006) reported that upland and lowland rice have different *PIP* expression levels affected by exogenous ABA apply, even though different *PIP* genes exhibited different regulation. Based on this evidence, it became controversial how ABA affects root AQP expression and hydraulic conductivity (Lpr), which depend on ABA dose, time responses and interaction with drought stress. However, the above results are based on exogenous ABA treatment. Regardless of the different results of exogenous ABA treatment, the endogenous ABA level should be more positively related to root AQP expression and Lpr regulation (Parent et al., 2009). These authors demonstrated that ABA is essential for root AQP expression by investigating ABA deficiency and over-accumulation maize plants; ABA-accumulated maize plants showed higher root AQP expression, while ABA deficient plants showed lower root AQP expression.

Under drought stress, 5 µM exogenous ABA induced an up-regulation of *PIP1;1*, *PIP1;2*, *PIP1;3*, *PIP2;1*, *TIP1;1*, *TIP2;1* and *TIP2;2* genes, especially in plants supplied with ammonium (**Figure 7B**). Moreover, drought stress induced more ABA accumulation in roots supplied with ammonium after 24 h of treatment, when root *PIP* and *TIP* expression was up-regulated (**Figure 5**). Our results showed that root ABA accumulation increase AQP expression induced by drought stress. Meanwhile, the AQP expression decreased by 4 h of drought stress independent of ABA regulation. In addition, we observed a higher ABA level, which could explain why the Pos was higher under drought stress in cucumber supplied with nitrate than in that supplied with ammonium (Supplementary Figure S1B). Despite the different effects of nitrogen form and drought stress on rice and cucumber root water uptake, ABA accumulation increased the root and/or cell water hydraulics under drought stress.

In aerial xylem sap and leaves, we observed that ABA levels increased when the plants are supplied with ammonium under drought stress (**Figure 6**), in which root ABA accumulated 10-fold after 24 h of drought stress (**Figure 5**). Under drought stress, the stomatal conductivity decreased in leaves supplied with either nitrogen form, especially in plants supplied with nitrate (**Figure 1**). In previous study, digital infrared thermography (DIT) was employed to detect changes in leaf temperature, which negative associated with leaf transpiration rate (Wang et al., 2012). However, the leaf transpiration was regulated by stomatal conductivity, and therefore thermo image could be an indicator for leaf stomatal opening (**Figure 2**).

Interestingly, there were higher levels of ABA and stomatal conductivity under drought stress in plants supplied with ammonium rather than with nitrate, indicating that ABA is indispensable for plants under drought stress. Two factors might simultaneously explain the higher stomatal conductivity and ABA under drought stress in plants supplied with ammonium rather than nitrate. First, drought stress could induce the alkalinization of apoplastic sap; this process has a crosstalk with nitrate metabolism (Ehlert et al., 2011; Korovetska et al., 2014). Under low pH, most of the leaf ABA was stored in the symplast (inactivation), while drought stress increased the pH, activating ABA, which would reside in the apoplast and enter the stomata (Wilkinson et al., 2007). In the present study, more ABA was stored in the symplast under drought stress in plants supplied with ammonium; in contrast, as most of the ABA resides in the apoplast under nitrate supply, even less ABA could induce the stomatal closure. To support this, plants fertilized with nitrate will tend to show high xylem and apoplastic pH (Supplementary Figure S3; Mengel et al., 1994; Muhling and Lauchli, 2001). Second, ABA accumulation is essential for shoots growing under drought stress (Koornneef et al., 1998; Sharp, 2002). Under drought stress, ABA-deficient mutants wilt and die. As a result, a higher ABA concentration might induce partial stomatal closure, further reducing water loss under drought stress in plant supplied with ammonium. Consistently, Li et al. (2012) showed that drought stress decreased the leaf water

potential under nitrate supply, further inducing chloroplast down-sizing.

CONCLUSION

Taken together, one of the possible mechanism of “ABA accumulation in enhanced seedling stage drought tolerance” is given in **Figure 8**. First, under drought stress, root *PIP* and *TIP* expression decreased immediately and intensely, while root ABA tended to accumulate. Second, root *PIP* and *TIP* expression increased with stress extension, resulting from endogenous ABA accumulation and further increasing root hydraulic conductivity. Third, root ABA accumulation induced aboveground ABA level increase, including in the leaves, as a result of stomatal closure (partially closure). Photosynthetic CO₂ assimilation was maintained under drought stress in rice plants supplied with ammonium.

AUTHOR CONTRIBUTIONS

SG and LD designed the experiment. LD, YL, YW, and LG performed the experiments. LD analyzed the data. LD, MW, FC, QS, and SG wrote the paper.

ACKNOWLEDGMENTS

This work was supported by the National Basic Research Program of China (2013CB127403), the National Natural Science Foundation of China (31172020 and 31272236), China Postdoctoral Science Foundation (2015M571768) and Jiangsu Postdoctoral Science Foundation (1402148C).

SUPPLEMENTARY MATERIAL

The Supplementary Material for this article can be found online at: <http://journal.frontiersin.org/article/10.3389/fpls.2016.01206>

REFERENCES

- Beaudette, P. C., Chlup, M., Yee, J., and Emery, R. J. (2007). Relationships of root conductivity and aquaporin gene expression in *Pisum sativum*: diurnal patterns and the response to HgCl₂ and ABA. *J. Exp. Bot.* 58, 1291–1300. doi: 10.1093/jxb/erl289
- Chaumont, F., and Tyerman, S. D. (2014). Aquaporins: highly regulated channels controlling plant water relations. *Plant Physiol.* 164, 1600–1618. doi: 10.1104/pp.113.233791
- Chen, J. G., Cheng, S. H., Cao, W., and Zhou, X. (1998). Involvement of endogenous plant hormones in the effect of mixed nitrogen source on growth and tillering of wheat. *J. Plant Nutr.* 21, 87–97. doi: 10.1080/01904169809365385
- Davies, W. J., and Zhang, J. (1991). Root signals and the regulation of growth and development of plants in drying soil. *Annu. Rev. Plant Biol.* 42, 55–76. doi: 10.1146/annurev.pp.42.060191.000415
- Ding, L., Gao, C., Li, Y., Li, Y., Zhu, Y., Xu, G., et al. (2015). The enhanced drought tolerance of rice plants under ammonium is related to aquaporin (AQP). *Plant Sci.* 234, 14–21. doi: 10.1016/j.plantsci.2015.01.016
- Ehlert, C., Plassard, C., Cookson, S. J., Tardieu, F., and Simonneau, T. (2011). Do pH changes in the leaf apoplast contribute to rapid inhibition of leaf elongation rate by water stress? Comparison of stress responses induced by polyethylene glycol and down-regulation of root hydraulic conductivity. *Plant Cell Environ.* 34, 1258–1266. doi: 10.1111/j.1365-3040.2011.02326.x
- Gao, Y. X., Li, Y., Yang, X. X., Li, H. J., Shen, Q. R., and Guo, S. W. (2010). Ammonium nutrition increases water absorption in rice seedlings (*Oryza sativa* L.) under water stress. *Plant Soil* 331, 193–201. doi: 10.1007/s11104-009-0245-1
- Grondin, A., Mauleon, R., Vadez, V., and Henry, A. (2016). Root aquaporins contribute to whole plant water fluxes under drought stress in rice (*Oryza sativa* L.). *Plant Cell Environ.* 39, 347–365. doi: 10.1111/pce.12616
- Guóth, A., Tari, I., Csizsár, J., Pécsvárdi, A., Cseuz, L., and Erdei, L. (2009). Comparison of the drought stress responses of tolerant and sensitive wheat cultivars during grain filling: changes in flag leaf photosynthetic activity, ABA levels, and grain yield. *J. Plant Growth Regul.* 28, 167–176. doi: 10.1007/s00344-009-9085-8
- Hachez, C., Veselov, D., Ye, Q., Reinhardt, H., Knipfer, T., Fricke, W., et al. (2012). Short-term control of maize cell and root water permeability through

- plasma membrane aquaporin isoforms. *Plant Cell Environ.* 35, 185–198. doi: 10.1111/j.1365-3040.2011.02429.x
- Jang, J. Y., Kim, D. G., Kim, Y. O., Kim, J. S., and Kang, H. (2004). An expression analysis of a gene family encoding plasma membrane aquaporins in response to abiotic stresses in *Arabidopsis thaliana*. *Plant Mol. Biol.* 54, 713–725. doi: 10.1023/B:PLAN.0000040900.61345.6a
- Kaldenhoff, R., Ribas-Carbo, M., Flexas, J., Lovisolo, C., Heckwolf, M., and Uehlein, N. (2008). Aquaporins and plant water balance. *Plant Cell Environ.* 31, 658–666. doi: 10.1111/j.1365-3040.2008.01792.x
- Koornneef, M., Léon-Kloosterziel, K. M., Schwartz, S. H., and Zeevaart, J. A. (1998). The genetic and molecular dissection of abscisic acid biosynthesis and signal transduction in *Arabidopsis*. *Plant Physiol. Biochem.* 36, 83–89. doi: 10.1016/S0981-9428(98)80093-4
- Korovetska, H., Novák, O., Juža, O., and Gloser, V. (2014). Signalling mechanisms involved in the response of two varieties of *Humulus lupulus* L. to soil drying: i. changes in xylem sap pH and the concentrations of abscisic acid and anions. *Plant Soil* 380, 375–387.
- Li, G. W., Peng, Y. H., Yu, X., Zhang, M. H., Cai, W. M., Sun, W. N., et al. (2008). Transport functions and expression analysis of vacuolar membrane aquaporins in response to various stresses in rice. *J. Plant Physiol.* 165, 1879–1888. doi: 10.1016/j.jplph.2008.05.002
- Li, Y., Ren, B. B., Yang, X. X., Xu, G. H., Shen, Q. R., and Guo, S. W. (2012). Chloroplast downscaling under nitrate nutrition restrained mesophyll conductance and photosynthesis in rice (*Oryza sativa* L.) Under Drought Conditions. *Plant Cell Physiol.* 53, 892–900. doi: 10.1093/pcp/pcs032
- Lian, H. L., Yu, X., Lane, D., Sun, W. N., Tang, Z. C., and Su, W. A. (2006). Upland rice and lowland rice exhibited different PIP expression under water deficit and ABA treatment. *Cell Res.* 16, 651–660. doi: 10.1038/sj.cr.7310068
- Mahdieu, M., and Mostajeran, A. (2009). Abscisic acid regulates root hydraulic conductance via aquaporin expression modulation in *Nicotiana tabacum*. *J. Plant Physiol.* 166, 1993–2003. doi: 10.1016/j.jplph.2009.06.001
- Mahdieu, M., Mostajeran, A., Horie, T., and Katsuhara, M. (2008). Drought stress alters water relations and expression of PIP-type aquaporin genes in *Nicotiana tabacum* plants. *Plant Cell Physiol.* 49, 801–813. doi: 10.1093/pcp/pcn054
- Mengel, K., Planker, R., and Hoffmann, B. (1994). Relationship between leaf apoplast Ph and iron chlorosis of sunflower (*Helianthus-Annuus* L.). *J. Plant Nutr.* 17, 1053–1065. doi: 10.1080/01904169409364787
- Muhling, K. H., and Lauchli, A. (2001). Influence of chemical form and concentration of nitrogen on apoplastic pH of leaves. *J. Plant Nutr.* 24, 399–411. doi: 10.1081/PLN-100104968
- Parent, B., Hachez, C., Redondo, E., Simonneau, T., Chaumont, F., and Tardieu, F. (2009). Drought and abscisic acid effects on aquaporin content translate into changes in hydraulic conductivity and leaf growth rate: a trans-scale approach. *Plant Physiol.* 149, 2000–2012. doi: 10.1104/pp.108.130682
- Perez-Perez, J. G., and Dodd, I. C. (2015). Sap fluxes from different parts of the rootzone modulate xylem ABA concentration during partial rootzone drying and re-wetting. *J. Exp. Bot.* 66, 2315–2324. doi: 10.1093/jxb/erv029
- Peuke, A. D., Jeschke, W. D., and Hartung, W. (1994). The uptake and flow of C. *J. Exp. Bot.* 45, 741–747.
- Puertolas, J., Alcobendas, R., Alarcon, J. J., and Dodd, I. C. (2013). Long-distance abscisic acid signalling under different vertical soil moisture gradients depends on bulk root water potential and average soil water content in the root zone. *Plant Cell Environ.* 36, 1465–1475. doi: 10.1111/pce.12076
- Puertolas, J., Conesa, M. R., Ballester, C., and Dodd, I. C. (2015). Local root abscisic acid (ABA) accumulation depends on the spatial distribution of soil moisture in potato: implications for ABA signalling under heterogeneous soil drying. *J. Exp. Bot.* 66, 2325–2334. doi: 10.1093/jxb/eru501
- Qian, Z. J., Song, J. J., Chaumont, F., and Ye, Q. (2015). Differential responses of plasma membrane aquaporins in mediating water transport of cucumber seedlings under osmotic and salt stresses. *Plant Cell Environ.* 38, 461–473. doi: 10.1111/pce.12319
- Rahayu, Y. S., Walch-Liu, P., Neumann, G., Romheld, V., Von Wieren, N., and Bangerth, F. (2005). Root-derived cytokinins as long-distance signals for NO₃-induced stimulation of leaf growth. *J. Exp. Bot.* 56, 1143–1152. doi: 10.1093/jxb/eri107
- Sakurai-Ishikawa, J., Murai-Hatano, M., Hayashi, H., Ahamed, A., Fukushi, K., Matsumoto, T., et al. (2011). Transpiration from shoots triggers diurnal changes in root aquaporin expression. *Plant Cell Environ.* 34, 1150–1163. doi: 10.1111/j.1365-3040.2011.02313.x
- Schraut, D., Heilmeier, H., and Hartung, W. (2005). Radial transport of water and abscisic acid (ABA) in roots of Zea mays under conditions of nutrient deficiency. *J. Exp. Bot.* 56, 879–886. doi: 10.1093/jxb/eri080
- Sengupta, D., Kannan, M., and Reddy, A. R. (2011). A root proteomics-based insight reveals dynamic regulation of root proteins under progressive drought stress and recovery in *Vigna radiata* (L.) Wilczek. *Planta* 233, 1111–1127. doi: 10.1007/s00425-011-1365-4
- Sharp, R. E. (2002). Interaction with ethylene: changing views on the role of abscisic acid in root and shoot growth responses to water stress. *Plant Cell Environ.* 25, 211–222. doi: 10.1046/j.1365-3040.2002.00798.x
- Vandeleur, R. K., Mayo, G., Shelden, M. C., Gillham, M., Kaiser, B. N., and Tyerman, S. D. (2009). The role of plasma membrane intrinsic protein aquaporins in water transport through roots: diurnal and drought stress responses reveal different strategies between isohydric and anisohydric cultivars of grapevine. *Plant Physiol.* 149, 445–460. doi: 10.1104/pp.108.128645
- Wang, M., Ling, N., Dong, X., Zhu, Y., Shen, Q., and Guo, S. (2012). Thermographic visualization of leaf response in cucumber plants infected with the soil-borne pathogen *Fusarium oxysporum* f. sp. *cucumerinum*. *Plant Physiol. Biochem.* 61, 153–161. doi: 10.1016/j.plaphy.2012.09.015
- Wilkinson, S., Bacon, M. A., and Davies, W. J. (2007). Nitrate signalling to stomata and growing leaves: interactions with soil drying, ABA, and xylem sap pH in maize. *J. Exp. Bot.* 58, 1705–1716.
- Xu, W. F., Jia, L. G., Shi, W. M., Liang, J. S., Zhou, F., Li, Q. F., et al. (2013). Abscisic acid accumulation modulates auxin transport in the root tip to enhance proton secretion for maintaining root growth under moderate water stress. *New Phytol.* 197, 139–150. doi: 10.1111/nph.12004
- Yang, X. X., Li, Y., Ren, B. B., Ding, L., Gao, C. M., Shen, Q. R., et al. (2012). Drought-induced root aerenchyma formation restricts water uptake in rice seedlings supplied with nitrate. *Plant Cell Physiol.* 53, 495–504. doi: 10.1093/pcp/pcs003
- Zdunek, E., and Lips, S. H. (2001). Transport and accumulation rates of abscisic acid and aldehyde oxidase activity in *Pisum sativum* L. in response to suboptimal growth conditions. *J. Exp. Bot.* 52, 1269–1276. doi: 10.1093/jexbot/52.359.1269
- Zhang, J., and Davies, W. (1989). Abscisic acid produced in dehydrating roots may enable the plant to measure the water status of the soil. *Plant Cell Environ.* 12, 73–81. doi: 10.1111/j.1365-3040.1989.tb01918.x
- Zhang, J., and Davies, W. (1990). Does ABA in the xylem control the rate of leaf growth in soil-dried maize and sunflower plants? *J. Exp. Bot.* 41, 1125–1132. doi: 10.1093/jxb/41.9.1125
- Zhang, J., Jia, W., Yang, J., and Ismail, A. M. (2006). Role of ABA in integrating plant responses to drought and salt stresses. *Field Crops Res.* 97, 111–119. doi: 10.1007/s11103-015-0327-9
- Zhu, C., Schraut, D., Hartung, W., and Schäffner, A. R. (2005). Differential responses of maize MIP genes to salt stress and ABA. *J. Exp. Bot.* 56, 2971–2981. doi: 10.1093/jxb/eri294

Conflict of Interest Statement: The authors declare that the research was conducted in the absence of any commercial or financial relationships that could be construed as a potential conflict of interest.

Copyright © 2016 Ding, Li, Wang, Gao, Wang, Chaumont, Shen and Guo. This is an open-access article distributed under the terms of the Creative Commons Attribution License (CC BY). The use, distribution or reproduction in other forums is permitted, provided the original author(s) or licensor are credited and that the original publication in this journal is cited, in accordance with accepted academic practice. No use, distribution or reproduction is permitted which does not comply with these terms.



Overexpression of a Barley Aquaporin Gene, *HvPIP2;5* Confers Salt and Osmotic Stress Tolerance in Yeast and Plants

Hemasundar Alavilli¹, Jay Prakash Awasthi², Gyana R. Rout³, Lingaraj Sahoo⁴,
Byeong-ha Lee^{1*} and Sanjib Kumar Panda^{2*}

¹ Department of Life Science, Sogang University, Seoul, Korea, ² Plant Molecular Biotechnology Laboratory, Department of Life Science and Bioinformatics, Assam University, Silchar, India, ³ Department of Agricultural Biotechnology, Orissa University of Agriculture and Technology, Bhubaneswar, India, ⁴ Department of Bioscience and Biotechnology, Indian Institute of Technology, Guwahati, India

OPEN ACCESS

Edited by:

Henry T. Nguyen,
University of Missouri, USA

Reviewed by:

Han Asard,
University of Antwerp, Belgium
Woo Taek Kim,
Yonsei University, South Korea

*Correspondence:

Byeong-ha Lee
byeongha@sogang.ac.kr
Sanjib Kumar Panda
drskpanda@gmail.com

Specialty section:

This article was submitted to
Plant Physiology,
a section of the journal
Frontiers in Plant Science

Received: 03 May 2016

Accepted: 05 October 2016

Published: 21 October 2016

Citation:

Alavilli H, Awasthi JP, Rout GR, Sahoo L, Lee B-h and Panda SK (2016) Overexpression of a Barley Aquaporin Gene, *HvPIP2;5* Confers Salt and Osmotic Stress Tolerance in Yeast and Plants. *Front. Plant Sci.* 7:1566.
doi: 10.3389/fpls.2016.01566

We characterized an aquaporin gene *HvPIP2;5* from *Hordeum vulgare* and investigated its physiological roles in heterologous expression systems, yeast and *Arabidopsis*, under high salt and high osmotic stress conditions. In yeast, the expression of *HvPIP2;5* enhanced abiotic stress tolerance under high salt and high osmotic conditions. *Arabidopsis* plants overexpressing *HvPIP2;5* also showed better stress tolerance in germination and root growth under high salt and high osmotic stresses than the wild type (WT). *HvPIP2;5* overexpressing plants were able to survive and recover after a 3-week drought period unlike the control plants which wilted and died during stress treatment. Indeed, overexpression of *HvPIP2;5* caused higher retention of chlorophylls and water under salt and osmotic stresses than did control. We also observed lower accumulation of reactive oxygen species (ROS) and malondialdehyde (MDA), an end-product of lipid peroxidation in *HvPIP2;5* overexpressing plants than in WT. These results suggest that *HvPIP2;5* overexpression brought about stress tolerance, at least in part, by reducing the secondary oxidative stress caused by salt and osmotic stresses. Consistent with these stress tolerant phenotypes, *HvPIP2;5* overexpressing *Arabidopsis* lines showed higher expression and activities of ROS scavenging enzymes such as catalase (CAT), superoxide dismutase (SOD), glutathione reductase (GR), and ascorbate peroxidase (APX) under salt and osmotic stresses than did WT. In addition, the proline biosynthesis genes, Δ^1 -Pyrroline-5-Carboxylate Synthase 1 and 2 (*P5CS1* and *P5CS2*) were up-regulated in *HvPIP2;5* overexpressing plants under salt and osmotic stresses, which coincided with increased levels of the osmoprotectant proline. Together, these results suggested that *HvPIP2;5* overexpression enhanced stress tolerance to high salt and high osmotic stresses by increasing activities and/or expression of ROS scavenging enzymes and osmoprotectant biosynthetic genes.

Keywords: yeast, *Arabidopsis*, aquaporin, barley, *HvPIP2;5*, overexpression, stress tolerance

INTRODUCTION

Aquaporins belong to major intrinsic proteins (MIPs) that are present from prokaryotes to plants and animals. These proteins facilitate the transport of water and small uncharged molecules across biological membranes (Park and Saier, 1996; Heymann and Engel, 1999; Engel and Stahlberg, 2002; Zardoya et al., 2002; Maurel et al., 2008, 2015). MIPs are categorized into two groups: aquaporins that show water-specific channel activity and glycerol-uptake facilitators (GLPs or aquaglyceroporins) that have channel activity for additional small molecules such as glycerol or urea (Park and Saier, 1996; Heymann and Engel, 1999; Engel and Stahlberg, 2002; Zardoya et al., 2002; Zardoya, 2005; Maurel et al., 2008). In plants, all MIPs, except for GlpF-like intrinsic proteins (GIPs), exhibit water-specific channel activity; therefore, most plant MIPs are collectively called aquaporins (Maurel et al., 2008, 2015). Recently, it has been shown that plant MIPs can transport other small molecules such as CO₂ and ammonia (Uehlein et al., 2003; Jahn et al., 2004).

Compared to genomes of other organisms, plant genomes contain a higher number of aquaporins (Wang et al., 2014). For instance, there are 35 aquaporin genes in *Arabidopsis thaliana* (Maurel, 2007), 22 in *Jatropha curcas* (Khan et al., 2015), 36 in *Zea maize* (Chaumont et al., 2001) and over 40 in *Hordeum vulgare* (Hove et al., 2015) while *Escherichia coli* (Gomes et al., 2009), *Caenorhabditis elegans* (Ishibashi et al., 2011), *Drosophila melanogaster* (Spring et al., 2009), and *Homo sapiens* (Day et al., 2014) contain 2, 11, 7, and 12, respectively.

The high diversity in plant aquaporins suggests variation of their physiological roles. Indeed, aquaporins were shown to be associated with vital physiological processes such as photosynthesis, nitrogen fixation, nutrient uptake and other environmental stress responses (Li et al., 2014; Hove et al., 2015; Sun et al., 2015). Plant aquaporins are classified into five subgroups, i.e.: the plasma membrane intrinsic proteins (PIPs), tonoplast intrinsic proteins (TIPs), nodulin26-like intrinsic proteins (NIPs), small basic intrinsic proteins (SIPs) and the recently identified uncategorized (X) intrinsic proteins (XIP) (Maurel et al., 2015). Based on sequence divergence, PIPs are further divided into PIP1 and PIP2 subclasses each consisting of several isoforms which play important roles in determining hydraulic conductivity particularly in roots (Martre et al., 2002; Siefritz et al., 2002; Javot et al., 2003; Postaire et al., 2010). Analyses on PIP1 and PIP2 from barley and maize revealed that the PIP2 proteins had higher water transport activity than PIP1 proteins in *Xenopus oocytes* (Chaumont et al., 2000; Horie et al., 2011). When PIP2 was co-expressed with functional or even nonfunctional PIP1 proteins, water transport activity of PIP2 was enhanced (Chaumont et al., 2000; Fetter et al., 2004; Horie et al., 2011). This enhanced water transport was attributed to their ability to form heterotetramers for proper trafficking to the plasma membrane (Fetter et al., 2004; Zelazny et al., 2007).

Dynamic changes in the expression levels of many *PIP* genes were observed in response to drought stress, suggesting their involvement in stress responses by regulating water balance (Afzal et al., 2016). Studies with *PIP*-defective mutants or overexpressing plants also linked the roles of *PIP* proteins to

water-deficit stress tolerance. For example, when expression of a tobacco *PIP1* member (*NtAQP1*) was reduced by antisense technology, the *NtAQP1*-downregulated tobacco plants showed reduced root hydraulic conductivity and wilting phenotypes under water stress (Siefritz et al., 2002). *Physcomitrella patens* *PIP2;1* or *PIP2;2* knockouts showed low water permeability with drought-sensitive phenotypes (Lienard et al., 2008). Reduction in water permeability of protoplasts and root hydraulic conductivity were observed respectively in *Arabidopsis* *PIP1;2* and *PIP2;2*-defective mutants but without clear developmental defects (Kaldenhoff et al., 1998; Javot et al., 2003). Overexpression of several *PIP* genes from various plants including *Oryza sativa*, *Vicia faba*, *Nicotiana tabacum*, and *Triticum aestivum* successfully enhanced water stress tolerance in transgenic plants (Lian et al., 2004; Cui et al., 2008; Sade et al., 2010; Zhou et al., 2012). Interestingly, some contrasting results (i.e., stress sensitive phenotypes in *PIP* overexpressing plants) have also been reported, implying the complexity of *PIP* function in plants (Aharon et al., 2003; Katsuhara et al., 2003; Jang et al., 2007; Li et al., 2015).

Barley (*Hordeum vulgare* L.) is one of the most agronomically cultivated crops; it is more adaptable to drought, salinity and cold than other cereal crops (Katsuhara et al., 2014; Hove et al., 2015). These characteristics would possibly make the barley gene pool, including barley aquaporins, as one of stress-adaptive genetic resources. Although, several *PIPs* have been identified in barley, only few of them have been functionally characterized thus far.

In this study, we overexpressed barley *PIP2;5* (*HvPIP2;5*) in yeast and *Arabidopsis* and characterized these lines to understand the functions of the barley *PIP* gene under high salt and high osmotic stress conditions.

MATERIALS AND METHODS

HvPIP2;5 Expression Vector Construction

Barley (*Hordeum vulgare* cv. NP21) cDNA was prepared using superscriptTM III reverse transcriptase (Invitrogen, USA), and total RNA was extracted with TRIzol® Reagent (Ambion, USA). A 873 bp-length *HvPIP2;5* coding sequence (GenBank Accession number: AB377270.1) was cloned into TA cloning vector pTOPO2.1 (Invitrogen, Carlsbad, CA, USA) using gene specific primers (Supplementary Table 1). The coding sequences of *HvPIP2;5* was cloned into yeast expression vector pYES2.0 (Invitrogen, USA) at the EcoRI site and named pYES2: *HvPIP2;5*. For plant transformation, *HvPIP2;5* coding sequence was cloned into a standard plant binary vector pCAMBIA2301. The resulting overexpression construct was named pCAMBIA2301-35S:*HvPIP2;5*.

Transformation of Yeast and Stress Analysis

The *HvPIP2;5* coding sequence under control of GAL1 promoter in pYES2 yeast expression vector was introduced into yeast FY3 cells. As controls, FY3 cells containing pYES2 vector only (vector control) and FY3 strain only were used in stress assays. The yeast strain FY3 was transformed with a pYES2 empty vector or pYES2:*HvPIP2;5* recombinant vector by lithium acetate method

(Kawai et al., 2010) and selected on SC medium devoid of uracil. Yeast cells expressing *HvPIP2;5* along with control cells were grown on YPD solid medium (1% Yeast extract, 2% peptone, and 2% glucose).

For stress analysis, transformed yeast cells were propagated in SC-U medium containing 2% galactose for 12 h and cell density was adjusted to 1.0 of OD600 followed by serial dilutions. Yeast cell were spotted on YPD medium supplemented with PEG (4%) or NaCl (200 mM), respectively. Plates were maintained at 30°C and growth was monitored after 2 days.

Generation of *HvPIP2;5* Overexpressing *Arabidopsis* Lines and Stress Analysis

Using *Agrobacterium tumefaciens* GV3101 harboring pCAMBIA2301-35S:*HvPIP2;5*, *Arabidopsis Columbia-0* plants were transformed via floral dipping method (Clough and Bent, 1998). Homozygote for 35S:*HvPIP2;5* insertion was selected at T4 generation by analyzing kanamycin resistance at each generation.

For germination analysis, the seeds of WT and homozygote *HvPIP2;5* OE *Arabidopsis* lines were plated on half strength Murashige Skoog (MS) media and allowed to germinate at 22°C and 60% relative humidity with a 16/8 h light-dark photo cycle after 3 day stratification at 4°C.

Final concentration of 100–200 mM NaCl (for high salt stress) or 10–20% PEG (for high osmotic stress) was supplemented to the MS media for stress administration. Hereby salt stress or osmotic stress indicates high salt stress or high osmotic stress, respectively. Emergence of cotyledons was used as a germination criterium. The number of germinated seeds was expressed as a percentage of total number of seeds planted after 7 days. For root elongation analysis, vertically grown seedlings with 1–1.5 cm long root were transferred onto a MS vertical plate supplemented with or without stress agents (200 mM NaCl and 20% PEG). Root length was measured 15 days after transfer. Root length of seedlings under stress conditions was expressed as a percentage of their respective controls grown on normal MS medium. All stress analysis experiments were conducted three times and each contained 3 biological repeats. For drought test with soil-grown plants, 4 week old seedlings were subjected to drought stress by withholding water supply for 21 days and then re-watered. For salt and osmotic stress, 3 week old plants were irrigated with either half strength MS liquid (control) or half strength MS liquid supplemented either with 200 mM NaCl or 20% PEG to impose stress for 15 days at 2 day intervals and then harvested for analysis. The chlorophyll, proline, and malondialdehyde (MDA) content in control or stress treated plants were determined by the methods reported previously by Lichtenthaler (1987), Bates et al. (1973), and Heath and Packer (1968), respectively.

Water Loss and Relative Water Content Analysis

Rosette leaves of 3 week old seedlings were detached, weighed and placed on paper under the fume hood to administrate drought stress. Fresh weights of rosette leaves were measured each hour for 5 h. Water loss was calculated as the loss in fresh weight

of the samples. For relative water content analysis, the root from WT and the *HvPIP2;5* OE lines were excised and treated either with 200 mM NaCl or 20% PEG or deionized water after measuring the fresh weight. After 24 h of incubation, the tissues were weighed again for their turgid weight and then dried completely to obtain dry weight. The root RWC was calculated by the following formula; RWC (%) = [(fresh weight – dry weight)/(turgid weight – dry weight)] × 100 (Weatherley, 1950).

Reactive Oxygen Species Analysis and Antioxidant Enzyme Activity Assay

In situ detection of superoxide by nitro blue tetrazolium (NBT) staining and hydrogen peroxide by 3, 3'diaminobenzidine (DAB) staining was performed according to methods previously described by Rao and Davis (1999) and Ramel et al. (2009). For this, 3 week old seedlings were grown on MS medium with 0, 100, 200 mM NaCl and the third leaf from the top was used. Superoxide radicals were visualized as blue color produced by NBT precipitation while hydrogen peroxide spots were visualized as brown color due to DAB polymerization.

For ROS quantification and antioxidant enzyme activity assay, 3 week old plants were irrigated with either half strength MS liquid (control) or half strength MS liquid supplemented either with 200 mM NaCl or 20% PEG to impose stress for 15 days at 2 day intervals and then harvested for analysis. Contents of superoxide and hydrogen peroxide were estimated by methods previously described by Elstner and Heupel (1976) and Sagisaka (1976), respectively. For antioxidant enzyme assay, the samples (200 mg tissue) were homogenized in 1.5 mL of 0.1 M phosphate buffer (pH 6.8) containing 1 mM ethylenediamine tetra-acetic acid (EDTA) and 1% polyvinylpyrrolidone (PVP) in a chilled pestle and mortar. The homogenate was then centrifuged at 17,000 g for 15 min at 4°C. The supernatant was quantified by the Bradford method (Bradford, 1976) and used for the assay of catalase (CAT), superoxide dismutase (SOD) and glutathione reductase (GR) (Chance and Maehly, 1955; Smith et al., 1988; Gupta et al., 1993). For the ascorbate peroxidase (APX) activity assay, a final concentration of 1 mM ascorbic acid was added to the assay buffer (Nakano and Asada, 1981).

Gene Expression Analysis

Plants were treated with water for control or 300 mM NaCl for 6 h or 20% PEG for 6 h, and total RNAs were extracted using RNeasy Plant mini Kit (Qiagen, Germany). cDNA was synthesized using RevertAid First Strand cDNA Synthesis Kit (ThermoFisher, USA), and resulting cDNAs were used for semi-quantitative RT or qRT-PCR experiments for selected genes. Primer pairs used in experiments are shown in **Supplementary Table 1**.

Statistical Analysis

All statistical comparisons between variances were determined by ANOVA (Analysis of variance) and least significant differences (LSD) between variants were calculated using Statistix 8.1 computation software. Statistically significant mean values were denoted as * ($P \leq 0.05$).

RESULTS

Sequence Analysis of *HvPIP2;5*

Previously, we identified several barley plasma membrane intrinsic protein (*HvPIP*) genes and examined their expressions under salt and osmotic stress conditions (Horie et al., 2011; Katsuhara et al., 2014). For further functional and physiological characterization, we selected *HvPIP2;5* (Genbank #AB377270), one of the *HvPIP2* genes that possesses abundant transcripts and demonstrates down-regulation of gene expression under salt and osmotic stresses (Horie et al., 2011; Katsuhara et al., 2014). The *HvPIP2;5* gene encodes a polypeptide of 291 amino acids with an estimated molecular mass of 30.3 kDa and an isoelectric point of 8.28 as predicted by ExPaSy bioinformatics tools for protein structure analysis (http://web.expasy.org/compute_pi/). *HvPIP2;5* protein shares 81% identity with Arabidopsis PIP2;5 protein (AtPIP2;5, AT3G54820). As shown in **Supplementary Figure 1A**, both *HvPIP2;5* and AtPIP2;5 harbor two Asn-Pro-Ala (NPA) motifs in addition to the highly conserved amino acid sequence “HINPAVTGF” which is reportedly conserved among all the MIP superfamily proteins (Li et al., 2009; Zhou et al., 2012). Conserved phosphorylation-target serine residues were also found in the C-termini of both PIP2;5

orthologs (**Supplementary Figure 1A**; Hove et al., 2015). The predicted *HvPIP2;5* protein contained aquaporin-characteristic six transmembrane spanning α -helices (H1-H6) with presence of 35.17% alpha helix, 30% random coil, 24.48% random coil, and 10.34% beta turn (**Supplementary Figures 1B,C**).

It has been recently reported that the barley genome comprises at least 40 aquaporin genes with 5 PIP1 genes and 9 PIP2 genes (Hove et al., 2015). Multiple sequence alignment using all reported *HvPIP2* isoforms was performed using Mega 6 software (<http://www.megasoftware.net>). As expected, *HvPIP2* proteins showed high degree of homology among them, and *HvPIP2;5* was located in the same clade as *HvPIP2;1* with 85% identity to *HvPIP2;1* (**Supplementary Figure 1D**).

Increased Tolerance of *HvPIP2;5*-Expressing Yeast under High Salt and Osmotic Stresses

A yeast expression system was employed to examine the functions of the *HvPIP2;5* gene under high saline and high osmotic conditions. As shown in **Figure 1A**, yeast strains transformed with *HvPIP2;5* or empty vector and FY3 cells could grow up to 10^{-6} dilution on YPD plates. In the

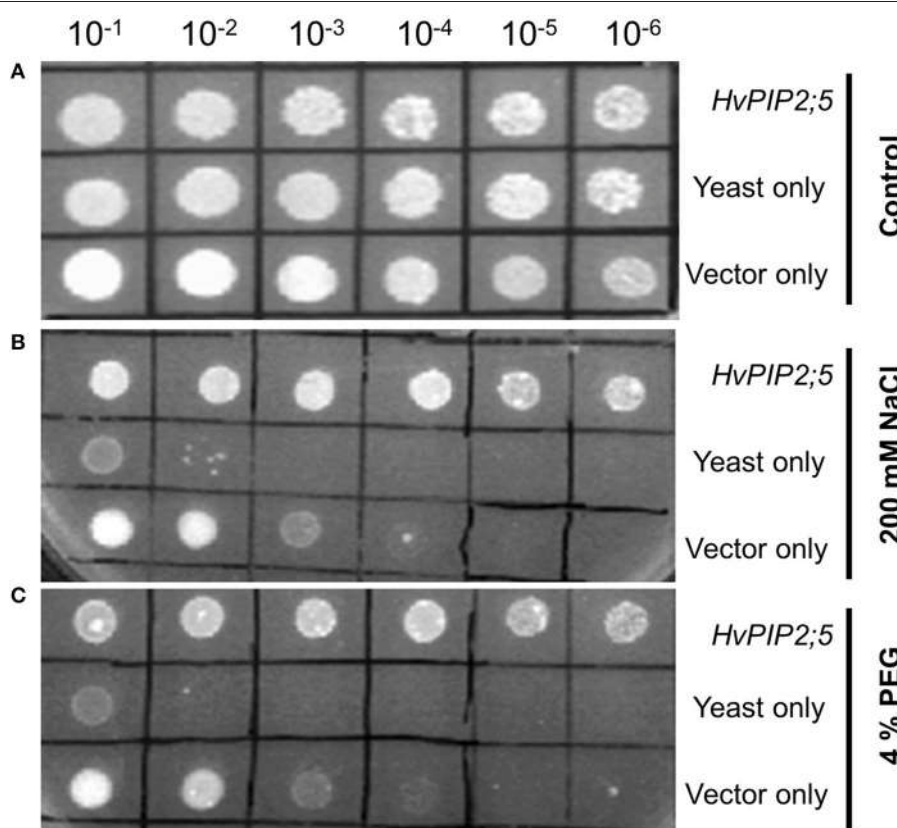


FIGURE 1 | Effect of *HvPIP2;5* expression in yeast under salt and osmotic stresses. Yeast cells harboring the *HvPIP2;5* expressing construct (*HvPIP2;5*), yeast cells only (yeast), and yeast cells with the vector pYES2 only (vector only) were subjected to 200 mM NaCl and 4% PEG. Cell density was adjusted to OD-600 at 1.0 and serial dilutions were made at each step. Ten microliter of each dilution was spotted on **(A)** YPD plates without stress. **(B)** YPD plates supplemented with 200 mM NaCl. **(C)** Supplemented with 4% PEG. Photographs were taken after 48 h of incubation at 30°C.

presence of 200 mM NaCl, pYES2 vector-containing FY3 cells grew only until 10^{-3} dilution, whereas the yeast strain transformed with *HvPIP2;5* was able to grow until 10^{-6} dilution (**Figure 1B**). Similarly, empty vector containing cells grew only to 10^{-3} dilution on the YPD medium supplemented with 4% polyethylene glycol (PEG), while yeast cells with *HvPIP2;5* displayed growth until 10^{-6} dilution under the same condition (**Figure 1C**). Taken together, these results showed that *HvPIP2;5* expression in yeast resulted in increased stress tolerance under high salt and high osmotic conditions.

Enhanced Stress Tolerance of *HvPIP2;5*-Overexpressing *Arabidopsis*

To investigate the functional roles of *HvPIP2;5* in *planta*, we expressed *HvPIP2;5* in *Arabidopsis* under the control of CaMV 35S promoter (**Supplementary Figure 2A**). Two independent homozygous *HvPIP2;5* overexpressing (OE) lines were selected. PCR analysis confirmed the presence of the *HvPIP2;5* gene in transgenic plants (data not shown) and semi quantitative RT-PCR for *HvPIP2;5* expression analysis demonstrated that transgenic lines were overexpressing *HvPIP2;5* gene (**Supplementary Figure 2B**).

Germination under 200 mM NaCl (high salt stress) and 20% PEG (high osmotic stress) was first tested for two independent *HvPIP2;5* OE lines along with WT. On the control medium, all lines germinated successfully after 7 days of planting. On the medium supplemented with 200 mM NaCl, WT germination ratios were decreased to about 50%, whereas *HvPIP2;5* OE lines displayed a 59–60% germination ratio on salt medium (**Figures 2A,D**). Also, *HvPIP2;5* OE lines displayed a 41–44% germination ratio in MS medium with 20% PEG whereas WT germination was reduced to 18% (**Figures 2A,D**).

Root growth under salt and osmotic stress conditions was also compared. In root growth assays, we observed increased tolerance of *HvPIP2;5* OE lines under salinity and osmotic stresses compared to WT. The relative root length of *HvPIP2;5* OE lines was significantly higher in the presence of 200 mM NaCl (59–62% vs. 34%) or 20% PEG (47–50% vs. 28%) compared to that of WT (**Figures 2B,E**).

We further evaluated growth performance of WT and *HvPIP2;5* OE lines during drought stress. WT and *HvPIP2;5* OE plants were grown in well-watered conditions for 4 weeks and then subjected to drought conditions. After 21 days of water withdrawal, WT lines became wilted with retarded growth, whereas *HvPIP2;5* OE lines did not wilt as severely as WT. Upon re-watering, WT plants were so severely damaged that they were unable to resume growth. In contrast, the transgenic lines were able to recover and retained survival upon rehydration (**Figure 2C**).

Chlorophyll degradation is among the changes caused by salt and osmotic stresses. No remarkable differences were observed between WT and *HvPIP2;5* OE lines grown under control conditions; however, after stress treatments with 200 mM NaCl or 20% PEG, *HvPIP2;5* OE lines showed less chlorophyll degradation when compared with WT. Measurement of chlorophyll contents of stress-treated plants confirmed the

better retention of chlorophyll A in OE lines than in WT (**Figure 2F**). WT under salinity stress with 200 mM NaCl contained only 23% of chlorophyll A levels under normal conditions, while OE lines under salt stress had largely higher levels of chlorophyll A retention (27–43%). Additionally, osmotic stress with 20% PEG caused 51 and 25–31% chlorophyll A loss in WT and *HvPIP2;5* OE, respectively (**Figure 2F**).

Low Water Loss and High Water Retention in *HvPIP2;5* Overexpressing Lines under Stresses

Dehydration tolerance in *HvPIP2;5* lines was assessed by measuring the water loss percentage. For this, rosette leaves from WT and *HvPIP2;5* OE lines were detached, placed on paper for dehydration and fresh weight measured. After 5 h of dehydration, the leaves of WT plants lost ~45% of their original fresh weight, whereas leaves of the *HvPIP2;5* OE lines lost only about 30–35% from their initial fresh weight (**Figure 3A**).

In addition, relative water content (RWC) was measured from the root tissues of WT and *HvPIP2;5* OE lines under salt or osmotic stress. Under salt stress with 200 mM NaCl, WT lines held 68.1% RWC, whereas *HvPIP2;5* OE lines kept 75–77% RWC (**Figure 3B**). Likewise, OE lines contained largely higher RWC than did WT under osmotic stress with 20% PEG (**Figure 3B**).

Reduction of Oxidative Stress in *HvPIP2;5* Overexpressing Lines under stresses

Reactive oxygen species (ROS) are generated in plants under drought, salt, and temperature stresses. Using nitro blue tetrazolium (NBT) staining for superoxide and diaminobenzidine (DAB) staining for hydrogen peroxide, we measured the levels of ROS in WT and *HvPIP2;5* OE lines under high salt (200 mM NaCl) and high osmotic stress (20% PEG). Compared to WT, the *HvPIP2;5* OE lines showed significantly weaker NBT staining and less O_2^- amount under osmotic or salt stress conditions (**Figures 4A,B**). Similarly, DAB staining and quantification of H_2O_2 content revealed lower amounts of H_2O_2 in the OE lines than in WT after NaCl treatment (**Figures 4C,D**). However, *HvPIP2;5* OE lines did not seem to display very significant reduction in H_2O_2 levels after PEG treatment when compared to WT.

Malondialdehyde (MDA) is an end product of lipid peroxidation of cell membrane lipids and a good indicator of oxidative damage (Diao et al., 2011). After salt stress (200 mM NaCl) and osmotic stress (20% PEG), MDA content was significantly lower in *HvPIP2;5* OE lines than in WT, which implicates lesser membrane damage in *HvPIP2;5* OE lines (**Figure 4E**). These results suggested that enhanced stress tolerance in *HvPIP2;5* OE lines might be due, at least in part, to reduced levels of oxidative stress caused by salt and osmotic stresses.

Increased Activities of ROS Scavenging Enzymes in *HvPIP2;5* Overexpressing Lines

To assess the contribution of ROS scavenging enzymes in reduction of oxidative stress caused by salt and osmotic stresses,

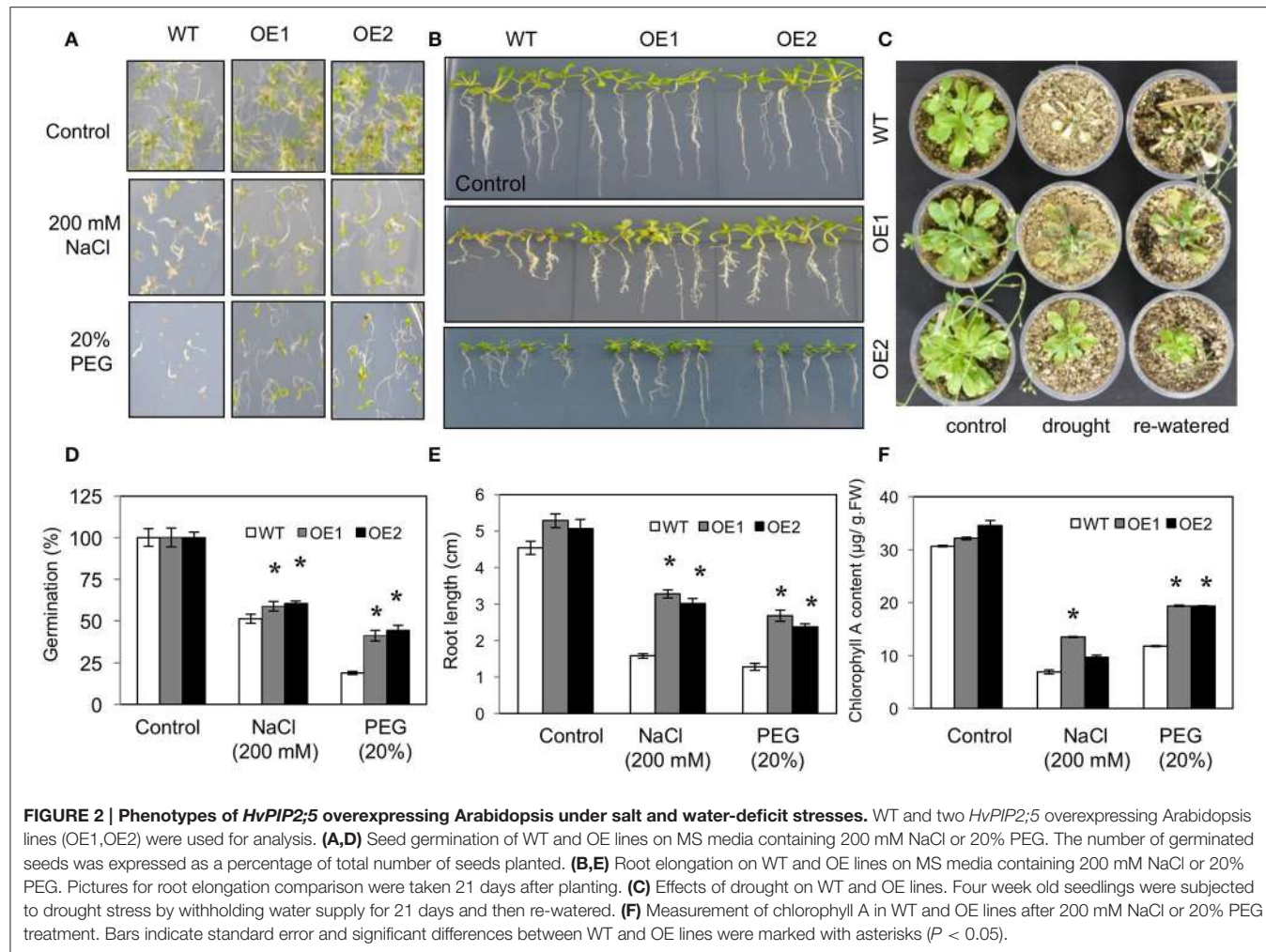


FIGURE 2 | Phenotypes of *HvPIP2;5* overexpressing Arabidopsis under salt and water-deficit stresses. WT and two *HvPIP2;5* overexpressing Arabidopsis lines (OE1, OE2) were used for analysis. **(A,D)** Seed germination of WT and OE lines on MS media containing 200 mM NaCl or 20% PEG. The number of germinated seeds was expressed as a percentage of total number of seeds planted. **(B,E)** Root elongation on WT and OE lines on MS media containing 200 mM NaCl or 20% PEG. Pictures for root elongation comparison were taken 21 days after planting. **(C)** Effects of drought on WT and OE lines. Four week old seedlings were subjected to drought stress by withholding water supply for 21 days and then re-watered. **(F)** Measurement of chlorophyll A in WT and OE lines after 200 mM NaCl or 20% PEG treatment. Bars indicate standard error and significant differences between WT and OE lines were marked with asterisks ($P < 0.05$).

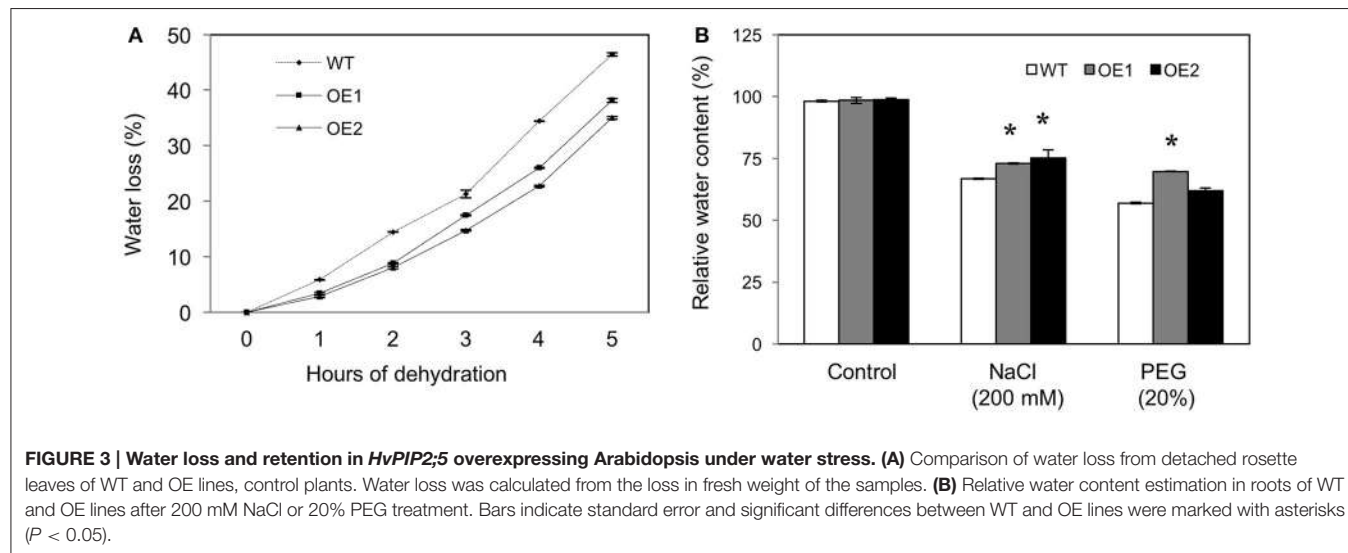
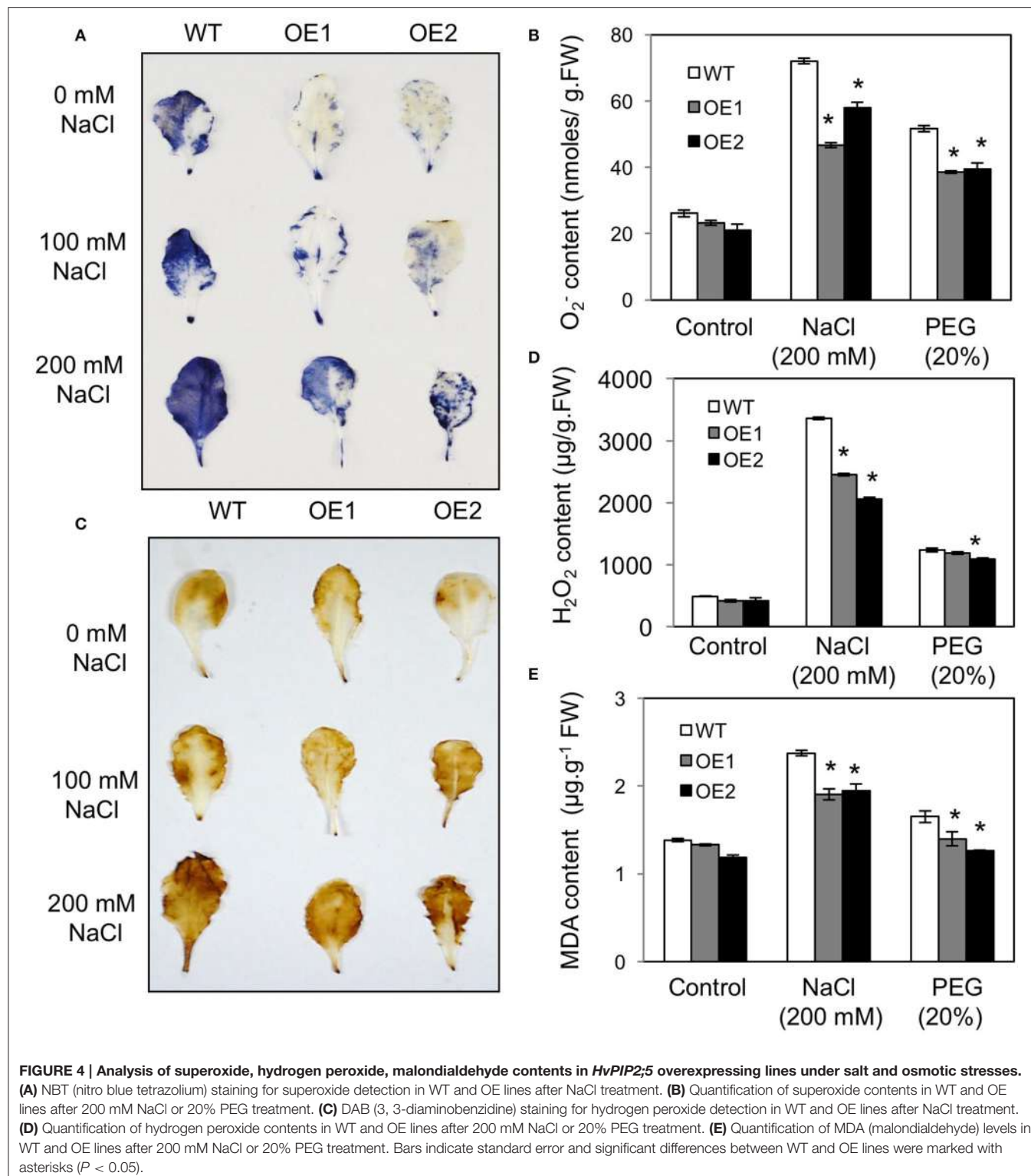


FIGURE 3 | Water loss and retention in *HvPIP2;5* overexpressing Arabidopsis under water stress. **(A)** Comparison of water loss from detached rosette leaves of WT and OE lines, control plants. Water loss was calculated from the loss in fresh weight of the samples. **(B)** Relative water content estimation in roots of WT and OE lines after 200 mM NaCl or 20% PEG treatment. Bars indicate standard error and significant differences between WT and OE lines were marked with asterisks ($P < 0.05$).

we measured the activities of catalase (CAT) and superoxide dismutase (SOD) in WT and *HvPIP2;5* OE lines under salt and osmotic stress conditions. Although, CAT activity was elevated

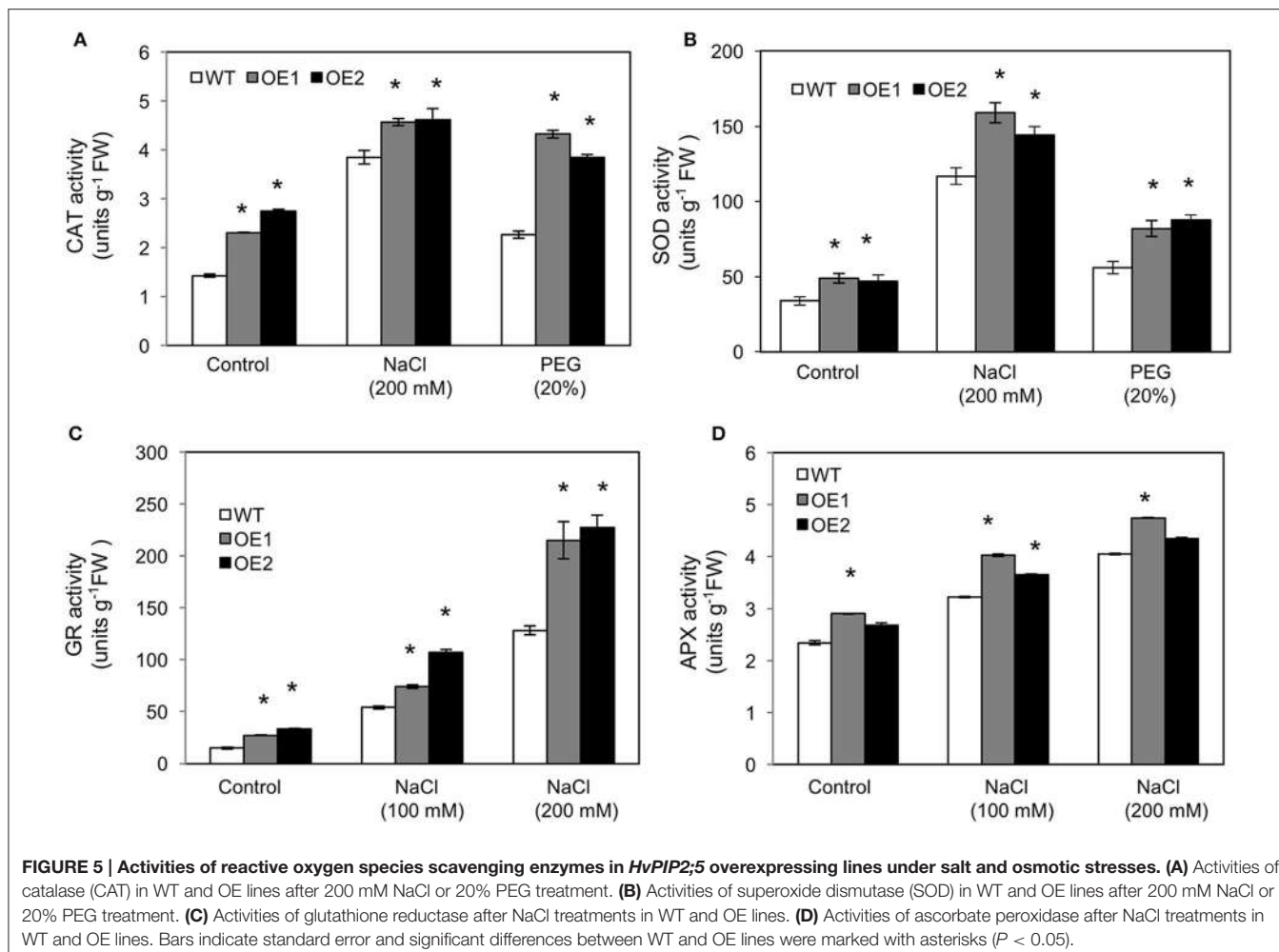
in both WT and *HvPIP2;5* OE lines, consistent with increase of osmotic and saline stresses (Figure 5A), the level of increase of CAT activity was significantly higher in *HvPIP2;5* OE lines



than in WT. Patterns largely similar to those found in the CAT activity assay were observed in SOD activity assay. SOD activity in *HvPIP2;5* OE lines were higher than those in WT under salt and osmotic stresses (Figure 5B). Interestingly, both CAT and

SOD activities in *HvPIP2;5* OE lines were generally higher than those of WT even under normal conditions.

In addition, we measured the activities of glutathione reductase (GR) and ascorbate peroxidase (APX) in *HvPIP2;5* OE



lines under 100 and 200 mM NaCl conditions. GR and APX are major enzymes for the ascorbate-glutathione cycle which is an important component of the ROS scavenging system in plants (Pang and Wang, 2010). Generally, elevated activities of APX and GR have been shown to correlate with increased salt tolerance in plants (Pang and Wang, 2010). The activities of GR were higher in *HvPIP2;5* OE lines than in WT under both normal and salt conditions (Figure 5C). The activities of APX were also largely higher in *HvPIP2;5* OE lines than in WT under normal and salt conditions (Figure 5D).

Taken together, these results indicated that reduction of oxidative stress in *HvPIP2;5* OE lines under salt and osmotic stresses is possibly related to enhanced activities of ROS scavenging enzymes.

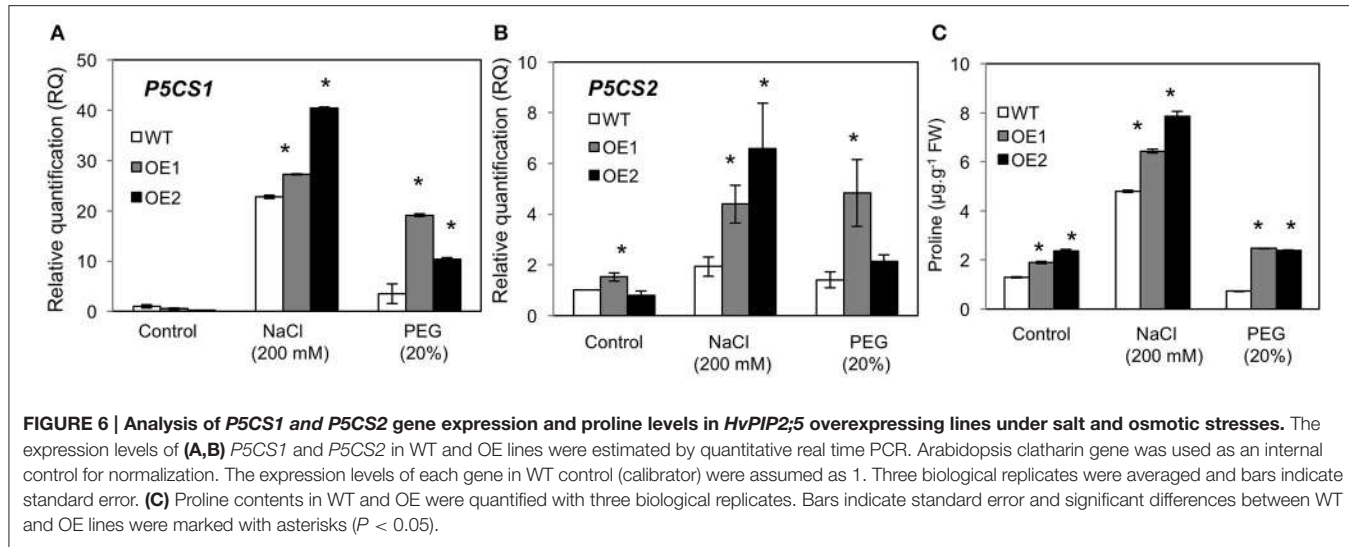
Increased Levels of Proline in *HvPIP2;5* Overexpressing Lines

The amino acid proline acts as an osmolytes and an antioxidant, and high levels of proline enhance stress adaptation under unfavorable conditions (Bates et al., 1973; Hayat et al., 2012). Thus, we investigated expression patterns of the *Arabidopsis* proline biosynthesis genes, Δ^1 -Pyrroline-5-Carboxylate Synthase

1 and 2 (*P5CS1* and *P5CS2*) in WT and *HvPIP2;5* OE lines. Real time PCR analysis revealed that gene expression levels of *P5CS1* and *P5CS2* were higher in *HvPIP2;5* OE lines than in WT under salt and osmotic stresses (Figures 6A,B). We also measured proline levels in WT and *HvPIP2;5* OE lines and found that even under normal conditions, *HvPIP2;5* OE lines demonstrated slightly higher proline levels than WT (Figure 6C). After salt treatment, proline levels were increased in both WT and *HvPIP2;5* OE lines with much higher increase in OE lines than in WT (Figure 6C). Interestingly, our PEG treatment did not seem to induce proline accumulation. Still, proline levels remained higher in the *HvPIP2;5* OE lines than in WT (Figure 6C). This salt-induced proline accumulation correlated with the up-regulation of *P5CS1* and *P5CS2* expression in *HvPIP2;5* OE lines, suggesting a possible molecular mechanism behind the enhanced stress tolerance in *HvPIP2;5* OE lines.

DISCUSSION

Water-deficit stress such as salt and osmotic stress and impede plant growth and development by affecting plant water balance. Aquaporins play important roles as water channels in regulating



plant water status; thus, many aquaporin genes from diverse plant species have been used in transgenic research to improve water-deficit stress tolerance in plants (Martre et al., 2002; Cui et al., 2008; Khan et al., 2015).

We found that overexpression of barley *PIP2;5* (*HvPIP2;5*) in both yeast and Arabidopsis improved tolerance to high salt and high osmotic stresses (Figures 1–3). These improved tolerances in *HvPIP2;5* overexpressing Arabidopsis were also observed in milder stress conditions (100 mM NaCl and 10% PEG) (Supplementary Figures 3, 4). Increased stress tolerance in *HvPIP2;5* overexpressing Arabidopsis was correlated with lower levels of stress-induced ROS (Figure 4 and Supplementary Figure 5), high activity of ROS scavenging enzymes (Figure 5), higher induction of proline biosynthetic gene expression and high levels of osmoprotectant proline (Figure 6). In particular, *HvPIP2;5* overexpressing Arabidopsis displayed lower water loss in shoots and higher relative water contents in roots than did WT under salt and osmotic stresses.

While *HvPIP2;5* overexpression improved water-stress tolerance in both yeast and Arabidopsis, Arabidopsis *PIP2;5* (*AtPIP2;5*) overexpression brought about reduced osmotic stress tolerance in Arabidopsis and tobacco (Jang et al., 2007). These seemingly contradicting results are not uncommon. In fact, many aquaporin overexpression studies have produced contrasting results—aquaporin-overexpressing plants have shown either positive or negative effects on stress tolerance (Maurel et al., 2008; Martinez-Ballesta and Carvajal, 2014; Zhou et al., 2014). Even overexpression of aquaporins with high homology has resulted in different sensitivities to dehydration stress. For example, Arabidopsis *AtPIP1;2*, rice *RWC3*, and tobacco *NtAQP1* share approximately 80% sequence identity. Despite this, overexpression of *AtPIP1;2* in tobacco has caused reduced stress tolerance (Aharon et al., 2003) while *RWC3* overexpression in rice and *NtAQP1* overexpression in tomato have shown enhanced tolerance under drought and salt stress, respectively (Lian et al., 2004; Sade et al., 2010). In addition, Arabidopsis *pip2;2* mutants display defects in hydraulic

conductivity despite the expression of a very close homolog *AtPIP2;3* which shares >96% homology, demonstrating that close aquaporin homologs could not function redundantly even within the same plant (Javot et al., 2003).

Although, *HvPIP2;5* and *AtPIP2;5* share high sequence homology, there are differences in gene regulation. *AtPIP2;5* expression levels remain low in Arabidopsis and are only up-regulated by drought and cold (Jang et al., 2007). However, *HvPIP2;5* is one of the highly expressed *PIPs* in barley which is down-regulated by osmotic stress (Katsuhara et al., 2014). These different patterns of gene expression might indicate the divergent functions of *PIP2;5* in Arabidopsis and barley, and may be attributed to contrasting stress responses in *HvPIP2;5* and *AtPIP2;5* overexpressors.

Another explanation for the contrasting results might lie in the difference in protein sequence between *HvPIP2;5* and *AtPIP2;5* proteins. Amino acid sequence differences are mainly found in the N-terminus which is expected to be exposed on the cytosol side (Walz et al., 1997; Supplementary Figures 1A, 6). Thus, it is tempting to speculate that contrasting stress phenotypes may be due to differences in the N-termini of *PIP2;5* proteins which may contain important motifs such as for activity regulation, protein stability, protein interaction, or even subcellular localization. Although transcriptional control of aquaporins appeared to be important for physiological functions (Alexandersson et al., 2005; Guo et al., 2006; Jiang et al., 2016), aquaporin activity is also post-translationally regulated by protein modification including phosphorylation (Johansson et al., 1998; Santoni et al., 2003; Daniels and Yeager, 2005). We have found some differences in phosphorylation sites at the N-terminus of two *PIP2;5* proteins (Supplementary Figure 6) which might be important for *PIP2;5* function. This differential protein modification might cause variable functional activities of *PIP2;5* in plant tissue, particularly where proteins are ectopically expressed due to constant promoter activity. It is interesting to note that Arabidopsis *PIP2;1*, an *AtPIP2;5* close homolog was shown to be a drought response-negative regulator which

is a target of ubiquitination and degradation by a RING membrane-anchor 1 E3 ubiquitin ligase (Lee et al., 2009). Thus, it might be possible that this kind of Arabidopsis regulation system might function differently on the endogenous PIP2;5 (AtPIP2;5) and the heterologous PIP2;5 (HvPIP2;5) due to the different amino acid residues in the N-termini.

We found, in *HvPIP2;5* overexpressing Arabidopsis, up-regulation of *P5CS2*, high levels of proline, and increased activities of SOD, CAT, GR, and APX with reduced levels of ROS under drought and salt stress conditions. Particularly, up-regulation of the key proline biosynthetic *P5CS* genes coincided with increased levels of osmoprotectant proline under salt stress (Figure 6). Proline mainly functions in defense and turgor pressure maintenance against water-deprived conditions (Oregan et al., 1993; Kishor et al., 1995; Khedr et al., 2003). Thus, enhanced stress tolerance in *HvPIP2;5* overexpressing plants seemed to result, at least in part, from increased expression of proline biosynthetic genes and elevated activities of ROS scavenging enzymes. Similar to our findings, the overexpression of wheat *TaAQP7*, one of the closest homologs of *HvPIP2;5*, in tobacco enhanced drought tolerance in correlation with decreased levels of MDA and H₂O₂ and increased activities of SOD and CAT enzymes (Zhou et al., 2012). Improved osmotic stress tolerance by up-regulation of stress-induced genes and an increase of ROS scavenging enzyme activity suggest that *HvPIP2;5* overexpression might sensitize transgenic plants, making the overexpressors react faster to osmotic stress signals and eventually induce enhanced stress defense. Thus, one might speculate that *HvPIP2;5* aquaporins in transgenic plants might activate osmotic and salt stress sensing or upstream steps in signaling pathways to induce better stress-tolerance mechanism than WT under stress conditions. Consistent with our speculation, it has been suggested that aquaporins may be part of an osmotic stress signaling cascade (Maurel et al., 2008); additionally, it has even been proposed that aquaporins may act as osmosensors (Hill et al., 2004). Further, study will be required to investigate this possibility.

In conclusion, we have shown that *HvPIP2;5* can improve tolerance to salt and osmotic stresses when overexpressed in yeast and Arabidopsis. Our results contrast with a previous *AtPIP2;5* overexpression study where osmotic stress sensitive phenotypes in *AtPIP2;5* overexpressing plants were reported (Jang et al., 2007). These results suggest the diversity of PIP regulation and function in acquiring stress tolerance in plants. Further studies should be conducted to understand the functional differences among aquaporins for crop improvement under abiotic stress.

AUTHOR CONTRIBUTIONS

HA, BhL, and SKP designed the experiments; HA, JPA performed the experiments; GR, LS, BhL, and SKP advised the research; HA, BhL, and SKP discussed the results and wrote the paper.

ACKNOWLEDGMENTS

Authors thank the lab members for advice and help. The research was supported by Next-Generation BioGreen21 Program (PJ011006), Rural Development Administration, Republic of Korea.

SUPPLEMENTARY MATERIAL

The Supplementary Material for this article can be found online at: <http://journal.frontiersin.org/article/10.3389/fpls.2016.01566>

Supplementary Table 1 | Sequences of primers used in the study.

Supplementary Figure 1 | Sequence analysis and structure prediction of HvPIP2;5 protein. **(A)** Alignment of full-length deduced amino acid sequences of HvPIP2;5 and its Arabidopsis homolog, AtPIP2;5. Asterisks below the alignment indicate identical amino acids. The MIPS domain is marked with a black bar below the alignment. The highly conserved amino acid sequence “HINPAVTFG” and two NPA motifs are marked with a solid-line box and a dotted-line box, respectively. The conserved phosphorylation-target serine residues in the C-termini were shown in bold. **(B)** Six predicted transmembrane helical regions (H1–H6) were indicated with boxes in the protein sequence alignments in HvPIP2;5 and AtPIP2;5 sequences. The prediction was made by TMpred online software. **(C)** HvPIP2;5 secondary structure prediction using SOPMA online program. **(D)** Phylogenetic analysis of members of barley PIP2 clade aquaporins. GenBank accession numbers for barley PIP2 clade proteins are as follows: HvPIP2;1 (BAE02729.1), HvPIP2;2 (BAG06230.1), HvPIP2;3 (BAF33069.1), HvPIP2;4 (BAE06148.1), HvPIP2;5 (BAG06231.1), HvPIP2;7 (ADW85675.1), HvPIP2;8 (BAJ90410.1), HvPIP2;9 (BAJ92749.1), HvPIP2;10 (BAK04917.1). Neighbor-end joining (NJ) method was applied using MEGA6 with a tree file produced by Clustal omega. The scale bar indicates 0.2 substitutions per site.

Supplementary Figure 2 | Generation of *HvPIP2;5* overexpressing Arabidopsis. **(A)** Schematic illustration of the binary vector region used for *HvPIP2;5* overexpression in Arabidopsis. The complete ORF of *HvPIP2;5* was cloned in pCAMBIA-2301 vector carrying CaMV35s promoter. **(B)** Detection of the *HvPIP2;5* transcripts from the *HvPIP2;5* overexpressing Arabidopsis lines by semi-quantitative RT-PCR. Ubiquitin gene was used as an internal control.

Supplementary Figure 3 | Seed germination and root growth of *HvPIP2;5* overexpressing lines. **(A,C)** Seed germination of WT and OE lines on MS media containing 100 mM NaCl or 10% PEG. **(B,D)**, Root elongation on WT and OE lines on MS media containing 100 mM NaCl or 10% PEG.

Supplementary Figure 4 | Chlorophyll and relative water contents in *HvPIP2;5* overexpressing lines. **(A)** Chlorophyll A contents under salt (100 mM) or osmotic stress (10% PEG) conditions. **(B)** Relative water contents under salt (100 mM) or osmotic stress (10% PEG) conditions. Bars represent means \pm SE and values with asterisks indicate significance at $P < 0.05$.

Supplementary Figure 5 | Analysis of superoxide, hydrogen peroxide, malondialdehyde contents in *HvPIP2;5* overexpressing lines under salt and osmotic stresses. **(A)** Quantification of superoxide contents in WT and OE lines after 100 mM NaCl or 10% PEG treatments. **(B)** Quantification of hydrogen peroxide contents in WT and OE lines after 100 mM NaCl or 10% PEG treatments. **(C)** Quantification of MDA (malondialdehyde) levels in WT and OE lines after 100 mM NaCl or 10% PEG treatments. Bars indicate standard error and significant differences between WT and OE lines were marked with asterisks ($P < 0.05$).

Supplementary Figure 6 | Predicted phosphorylation sites in PIP2;5 proteins. Predicted phosphorylation sites in **(A)** HvPIP2;5 and **(B)** AtPIP2;5 (At3554820). Phosphorylation site prediction was carried out using NetPhos 2.0 (<http://www.cbs.dtu.dk/services/NetPhos/>). Peaks above the threshold line (red) indicate the phosphorylation sites with high probability.

REFERENCES

- Afzal, Z., Howton, T., Sun, Y., and Mukhtar, M. (2016). The roles of aquaporins in plant stress responses. *J. Develop. Biol.* 4:9. doi: 10.3390/jdb4010009
- Aharon, R., Shahak, Y., Wininger, S., Bendov, R., Kapulnik, Y., and Galili, G. (2003). Overexpression of a plasma membrane aquaporin in transgenic tobacco improves plant vigor under favorable growth conditions but not under drought or salt stress. *Plant Cell* 15, 439–447. doi: 10.1105/tpc.009225
- Alexandersson, E., Fraysse, L., Sjövall-Larsen, S., Gustavsson, S., Fellert, M., Karlsson, M., et al. (2005). Whole gene family expression and drought stress regulation of aquaporins. *Plant Mol. Biol.* 59, 469–484. doi: 10.1007/s11103-005-0352-1
- Bates, L. S., Waldren, R. P., and Teare, I. D. (1973). Rapid determination of free proline for water-stress studies. *Plant Soil* 39, 205–207. doi: 10.1007/BF00018060
- Bradford, M. M. (1976). A rapid and sensitive method for the quantitation of microgram quantities of protein utilizing the principle of protein-dye binding. *Anal. Biochem.* 72, 248–254. doi: 10.1016/0003-2697(76)90527-3
- Chance, B. A., and Maehly, A. C. (1955). "Assay of catalases and peroxidases," in *Methods in Enzymology*, Vol. 2, eds S. P. Colowick and N. O. Kaplan (Cambridge, MA: Academic Press), 764–775. doi: 10.1016/S0076-6879(55)02300-8
- Chaumont, F., Barrieu, F., Jung, R., and Chrispeels, M. J. (2000). Plasma membrane intrinsic proteins from maize cluster in two sequence subgroups with differential aquaporin activity. *Plant Physiol.* 122, 1025–1034. doi: 10.1104/pp.122.4.1025
- Chaumont, F., Barrieu, F., Wojcik, E., Chrispeels, M. J., and Jung, R. (2001). Aquaporins constitute a large and highly divergent protein family in maize. *Plant Physiol.* 125, 1206–1215. doi: 10.1104/pp.125.3.1206
- Clough, S. J., and Bent, A. F. (1998). Floral dip: a simplified method for Agrobacterium-mediated transformation of *Arabidopsis thaliana*. *Plant J.* 16, 735–743. doi: 10.1046/j.1365-313x.1998.00343.x
- Cui, X. H., Hao, F. S., Chen, H., Chen, J., and Wang, X. C. (2008). Expression of the *Vicia faba* VfPIP1 gene in *Arabidopsis thaliana* plants improves their drought resistance. *J. Plant Res.* 121, 207–214. doi: 10.1007/s10265-007-0130-z
- Daniels, M. J., and Yeager, M. (2005). Phosphorylation of aquaporin PvTIP3;1 defined by mass spectrometry and molecular modeling. *Biochemistry* 44, 14443–14454. doi: 10.1021/bi050565d
- Day, R. E., Kitchen, P., Owen, D. S., Bland, C., Marshall, L., Conner, A. C., et al. (2014). Human aquaporins: regulators of transcellular water flow. *Biochim. Biophys. Acta Gen. Subjects* 1840, 1492–1506. doi: 10.1016/j.bbagen.2013.09.033
- Diao, G. P., Wang, Y. C., Wang, C., and Yang, C. P. (2011). Cloning and functional characterization of a Novel Glutathione S-Transferase Gene from Limonium bicolor. *Plant Mol. Biol. Report.* 29, 77–87. doi: 10.1007/s11105-010-0212-2
- Elstner, E. F., and Heupel, A. (1976). Formation of hydrogen peroxide by isolated cell walls from horseradish (*Armoracia lapathifolia* Gilib.). *Planta* 130, 175–180. doi: 10.1007/BF00384416
- Engel, A., and Stahlberg, H. (2002). "Aquaglyceroporins: channel proteins with a conserved core, multiple functions, and variable surfaces," in *International Review of Cytology*, Vol. 215, eds W. D. Stein and T. Zeuthen (Cambridge, MA: Academic Press), 75–104. doi: 10.1016/S0074-7696(02)15006-6
- Fetter, K., Van Wilder, V., Moshelion, M., and Chaumont, F. (2004). Interactions between plasma membrane aquaporins modulate their water channel activity. *Plant Cell* 16, 215–228. doi: 10.1105/tpc.017194
- Gomes, D., Agasse, A., Thiébaud, P., Delrot, S., Gerós, H., and Chaumont, F. (2009). Aquaporins are multifunctional water and solute transporters highly divergent in living organisms. *Biochim. Biophys. Acta* 1788, 1213–1228. doi: 10.1016/j.bbamem.2009.03.009
- Guo, L., Wang, Z. Y., Lin, H., Cui, W. E., Chen, J., Liu, M., et al. (2006). Expression and functional analysis of the rice plasma-membrane intrinsic protein gene family. *Cell Res.* 16, 277–286. doi: 10.1038/sj.cr.7310035
- Gupta, A. S., Webb, R. P., Holaday, A. S., and Allen, R. D. (1993). Overexpression of superoxide dismutase protects plants from oxidative stress (Induction of Ascorbate Peroxidase in Superoxide Dismutase-Overexpressing plants). *Plant Physiol.* 103, 1067–1073.
- Hayat, S., Hayat, Q., Alyemeni, M. N., Wani, A. S., Pichtel, J., and Ahmad, A. (2012). Role of proline under changing environments: a review. *Plant Signal. Behav.* 7, 1456–1466. doi: 10.4161/psb.21949
- Heath, R. L., and Packer, L. (1968). Photoperoxidation in isolated chloroplasts. *Arch. Biochem. Biophys.* 125, 189–198. doi: 10.1016/0003-9861(68)90654-1
- Heymann, J. B., and Engel, A. (1999). Aquaporins: phylogeny, structure, and physiology of water channels. *Physiology* 14, 187–193.
- Hill, A. E., Shachar-Hill, B., and Shachar-Hill, Y. (2004). What are aquaporins for? *J. Membr. Biol.* 197, 1–32. doi: 10.1007/s00232-003-0639-6
- Horie, T., Kaneko, T., Sugimoto, G., Sasano, S., Panda, S. K., Shibasaki, M., et al. (2011). Mechanisms of water transport mediated by PIP aquaporins and their regulation via phosphorylation events under salinity stress in Barley roots. *Plant Cell Physiol.* 52, 663–675. doi: 10.1093/pcp/pcr027
- Hove, R. M., Zieman, M., and Bhave, M. (2015). Identification and expression analysis of the Barley (*Hordeum vulgare* L.) Aquaporin gene family. *PLoS ONE* 10:e0128025. doi: 10.1371/journal.pone.0128025
- Ishibashi, K., Kondo, S., Hara, S., and Morishita, Y. (2011). The evolutionary aspects of aquaporin family. *Am. J. Physiol. Regul. Integr. Comparat. Physiol.* 300, R566–R576. doi: 10.1152/ajpregu.90464.2008
- Jahn, T. P., Moller, A. L. B., Zeuthen, T., Holm, L. M., Klaerke, D. A., Mohsin, B., et al. (2004). Aquaporin homologues in plants and mammals transport ammonia. *FEBS Lett.* 574, 31–36. doi: 10.1016/j.febslet.2004.08.004
- Jang, J. Y., Lee, S. H., Rhee, J. Y., Chung, G. C., Ahn, S. J., and Kang, H. (2007). Transgenic *Arabidopsis* and tobacco plants overexpressing an aquaporin respond differently to various abiotic stresses. *Plant Mol. Biol.* 64, 621–632. doi: 10.1007/s11103-007-9181-8
- Javot, H., Lauvergeat, V., Santoni, V., Martin-Laurent, F., Güçlü, J., Vinh, J., et al. (2003). Role of a single aquaporin isoform in root water uptake. *Plant Cell* 15, 509–522. doi: 10.1105/tpc.008888
- Jiang, Y., Liu, H., Liu, W.-J., Tong, H.-B., Chen, C.-J., Lin, F.-G., et al. (2016). Endothelial Aquaporin-1 (AQP1) expression is regulated by transcription factor Mef2c. *Mol. Cells* 39, 292–298. doi: 10.14348/molcells.2016.2223
- Johansson, I., Karlsson, M., Shukla, V. K., Chrispeels, M. J., Larsson, C., and Kjellbom, P. (1998). Water transport activity of the plasma membrane aquaporin PM28A is regulated by phosphorylation. *Plant Cell* 10, 451–459. doi: 10.1105/tpc.10.3.451
- Kaldenhoff, R., Grote, K., Zhu, J. J., and Zimmermann, U. (1998). Significance of plasmalemma aquaporins for water-transport in *Arabidopsis thaliana*. *Plant J.* 14, 121–128. doi: 10.1046/j.1365-313X.1998.00111.x
- Katsuhara, M., Koshio, K., Shibasaki, M., Hayashi, Y., Hayakawa, T., and Kasamo, K. (2003). Over-expression of a barley aquaporin increased the shoot/root ratio and raised salt sensitivity in transgenic rice plants. *Plant Cell Physiol.* 44, 1378–1383. doi: 10.1093/pcp/pcg167
- Katsuhara, M., Tsuji, N., Shibasaki, M., and Panda, S. K. (2014). Osmotic stress decreases PIP aquaporin transcripts in barley roots but H₂O₂ is not involved in this process. *J. Plant Res.* 127, 787–792. doi: 10.1007/s10265-014-0662-y
- Kawai, S., Hashimoto, W., and Murata, K. (2010). Transformation of *Saccharomyces cerevisiae* and other fungi: Methods and possible underlying mechanism. *Bioeng. Bugs* 1, 395–403. doi: 10.4161/bbug.1.6.13257
- Khan, K., Agarwal, P., Shanware, A., and Sane, V. A. (2015). Heterologous expression of two *Jatropha* Aquaporins imparts drought and salt tolerance and improves seed viability in Transgenic *Arabidopsis thaliana*. *PLoS ONE* 10:e0128866. doi: 10.1371/journal.pone.0128866
- Khedr, A. H. A., Abbas, M. A., Wahid, A. A. A., Quick, W. P., and Abogadallah, G. M. (2003). Proline induces the expression of salt-stress-responsive proteins and may improve the adaptation of *Pancratium maritimum* L. to salt-stress. *J. Exp. Bot.* 54, 2553–2562. doi: 10.1093/jxb/erg277
- Kishor, P. B. K., Hong, Z., Miao, G. H., Hu, C. A. A., and Verma, D. P. S. (1995). Overexpression of Delta-Pyrroline-5-Carboxylate synthetase increases proline production and confers osmotolerance in transgenic plants. *Plant Physiol.* 108, 1387–1394.
- Lee, H. K., Cho, S. K., Son, O., Xu, Z., Hwang, I., and Kim, W. T. (2009). Drought Stress-Induced Rma1H1, a RING Membrane-Anchor E3 Ubiquitin Ligase Homolog, Regulates Aquaporin Levels via Ubiquitination in Transgenic *Arabidopsis* Plants. *Plant Cell* 21, 622–641. doi: 10.1105/tpc.108.061994
- Li, D. D., Wu, Y. J., Ruan, X. M., Li, B., Zhu, L., Wang, H., et al. (2009). Expressions of three cotton genes encoding the PIP proteins are regulated in

- root development and in response to stresses. *Plant Cell Rep.* 28, 291–300. doi: 10.1007/s00299-008-0626-6
- Li, G., Santoni, V., and Maurel, C. (2014). Plant aquaporins: roles in plant physiology. *Biochim. Biophys. Acta Gen. Subjects* 1840, 1574–1582. doi: 10.1016/j.bbagen.2013.11.004
- Li, J., Ban, L., Wen, H., Wang, Z., Dzyubenko, N., Chapurin, V., et al. (2015). An aquaporin protein is associated with drought stress tolerance. *Biochem. Biophys. Res. Commun.* 459, 208–213. doi: 10.1016/j.bbrc.2015.02.052
- Lian, H.-L., Yu, X., Ye, Q., Ding, X.-S., Kitagawa, Y., Kwak, S. S., et al. (2004). The role of aquaporin RWC3 in drought avoidance in rice. *Plant Cell Physiol.* 45, 481–489. doi: 10.1093/pcp/pch058
- Lichtenthaler, H. K. (1987). Chlorophyll Fluorescence Signatures of Leaves during the Autumnal Chlorophyll Breakdown. *J. Plant Physiol.* 131, 101–110. doi: 10.1016/S0176-1617(87)80271-7
- Liénard, D., Durambur, G., Kiefer-Meyer, M. C., Nogué, F., Menu-Bouaouiche, L., Charlot, F., et al. (2008). Water transport by aquaporins in the extant plant *Physcomitrella patens*. *Plant Physiol.* 146, 1207–1218. doi: 10.1104/pp.107.111351
- Martinez-Ballesta, M. D. C., and Carvajal, M. (2014). New challenges in plant aquaporin biotechnology. *Plant Sci.* 217–218, 71–77. doi: 10.1016/j.plantsci.2013.12.006
- Martre, P., Morillon, R., Barrieu, F., North, G. B., Nobel, P. S., and Chrispeels, M. J. (2002). Plasma membrane Aquaporins play a significant role during recovery from water deficit. *Plant Physiol.* 130, 2101–2110. doi: 10.1104/pp.009019
- Maurel, C. (2007). Plant aquaporins: novel functions and regulation properties. *FEBS Lett.* 581, 2227–2236. doi: 10.1016/j.febslet.2007.03.021
- Maurel, C., Boursiac, Y., Luu, D. T., Santoni, V., Shahzad, Z., and Verdoucq, L. (2015). Aquaporins in plants. *Physiol. Rev.* 95, 1321–1358. doi: 10.1152/physrev.00008.2015
- Maurel, C., Verdoucq, L., Luu, D. T., and Santoni, V. (2008). Plant aquaporins: membrane channels with multiple integrated functions. *Annu. Rev. Plant Biol.* 59, 595–624. doi: 10.1146/annurev.arplant.59.032607.092734
- Nakano, Y., and Asada, K. (1981). Hydrogen Peroxide is Scavenged by Ascorbate-specific Peroxidase in Spinach Chloroplasts. *Plant Cell Physiol.* 22, 867–880.
- Oregan, B. P., Cress, W. A., and Vanstaden, J. (1993). Root-growth, water relations, abscisic-acid and proline levels of drought-resistant and drought-sensitive maize cultivars in response to water-stress. *South Afr. J. Bot.* 59, 98–104. doi: 10.1016/S0254-6299(16)30780-3
- Pang, C.-H., and Wang, B.-S. (2010). “Role of ascorbate peroxidase and glutathione reductase in Ascorbate–Glutathione cycle and stress tolerance in plants,” in *Ascorbate–Glutathione Pathway and Stress Tolerance in Plants*, eds A. N. Anjum, M.-T. Chan, and S. Umar (Dordrecht: Springer), 91–113.
- Park, J. H., and Saier, M. H. Jr. (1996). Phylogenetic characterization of the MIP family of transmembrane channel proteins. *J. Membrane Biol.* 153, 171–180. doi: 10.1007/s00239900120
- Postaire, O., Tournaire-Roux, C., Grondin, A., Boursiac, Y., Morillon, R., Schäffner, A. R., et al. (2010). A PIP1 aquaporin contributes to hydrostatic pressure-induced water transport in both the root and rosette of Arabidopsis. *Plant Physiol.* 152, 1418–1430. doi: 10.1104/pp.109.145326
- Ramel, F., Sulmon, C., Bogard, M., Couée, I., and Gouesbet, G. (2009). Differential patterns of reactive oxygen species and antioxidative mechanisms during atrazine injury and sucrose-induced tolerance in *Arabidopsis thaliana* plantlets. *BMC Plant Biol.* 9:28. doi: 10.1186/1471-2229-9-28
- Rao, M. V., and Davis, K. R. (1999). Ozone-induced cell death occurs via two distinct mechanisms in Arabidopsis: the role of salicylic acid. *Plant J.* 17, 603–614. doi: 10.1046/j.1365-313X.1999.00400.x
- Sade, N., Gebretsadik, M., Seligmann, R., Schwartz, A., Wallach, R., and Moshelion, M. (2010). The role of tobacco aquaporin1 in improving water use efficiency, hydraulic conductivity, and yield production under salt stress. *Plant Physiol.* 152, 245–254. doi: 10.1104/pp.109.145854
- Sagisaka, S. (1976). The Occurrence of Peroxide in a Perennial Plant, Populus gelrica. *Plant Physiol.* 57, 308–309. doi: 10.1104/pp.57.2.308
- Santoni, V., Vinh, J., Pfleiger, D., Sommerer, N., and Maurel, C. (2003). A proteomic study reveals novel insights into the diversity of aquaporin forms expressed in the plasma membrane of plant roots. *Biochem. J.* 373, 289–296. doi: 10.1042/bj20030159
- Siefritz, F., Tyree, M. T., Lovisolo, C., Schubert, A., and Kaldenhoff, R. (2002). PIP1 plasma membrane aquaporins in tobacco: from cellular effects to function in plants. *Plant Cell* 14, 869–876. doi: 10.1105/tpc.000901
- Smith, I. K., Vierheller, T. L., and Thorne, C. A. (1988). Assay of glutathione reductase in crude tissue homogenates using 5,5'-dithiobis(2-nitrobenzoic acid). *Anal. Biochem.* 175: 408–413. doi: 10.1016/0003-2697(88)90564-7
- Spring, J. H., Robichaux, S. R., and Hamlin, J. A. (2009). The role of aquaporins in excretion in insects. *J. Exp. Biol.* 212, 358–362. doi: 10.1242/jeb.024794
- Sun, L., Yu, G., Han, X., Xin, S., Qiang, X., Jiang, L., et al. (2015). TsMIP6 enhances the tolerance of transgenic rice to salt stress and interacts with target proteins. *J. Plant Biol.* 58, 285–292. doi: 10.1007/s12374-015-0069-x
- Uehlein, N., Lovisolo, C., Siefritz, F., and Kaldenhoff, R. (2003). The tobacco aquaporin NtAQP1 is a membrane CO₂ pore with physiological functions. *Nature* 425, 734–737. doi: 10.1038/nature02027
- Walz, T., Hirai, T., Murata, K., Heymann, J. B., Mitsuoka, K., Fujiyoshi, Y., et al. (1997). The three-dimensional structure of aquaporin-1. *Nature* 387, 624–627. doi: 10.1038/42512
- Wang, L. L., Chen, A. P., Zhong, N. Q., Liu, N., Wu, X. M., Wang, F., et al. (2014). The *Thellungiella salsuginea* tonoplast aquaporin TsTIP1;2 functions in protection against multiple abiotic stresses. *Plant Cell Physiol.* 55, 148–161. doi: 10.1093/pcp/pct166
- Weatherley, P. E. (1950). Studies in the water relations of the cotton plant. *New Phytol.* 49, 81–97. doi: 10.1111/j.1469-8137.1950.tb05146.x
- Zardoya, R. (2005). Phylogeny and evolution of the major intrinsic protein family. *Biol. Cell* 97, 397–414. doi: 10.1042/BC20040134
- Zardoya, R., Ding, X., Kitagawa, Y., and Chrispeels, M. J. (2002). Origin of plant glycerol transporters by horizontal gene transfer and functional recruitment. *Proc. Natl. Acad. Sci. U.S.A.* 99, 14893–14896. doi: 10.1073/pnas.19257399
- Zelazny, E., Borst, J. W., Muylaert, M., Batoko, H., Hemminga, M. A., and Chaumont, F. (2007). FRET imaging in living maize cells reveals that plasma membrane aquaporins interact to regulate their subcellular localization. *Proc. Natl. Acad. Sci. U.S.A.* 104, 12359–12364. doi: 10.1073/pnas.0701180104
- Zhou, L., Wang, C., Liu, R., Han, Q., Vandeleur, R. K., Du, J., et al. (2014). Constitutive overexpression of soybean plasma membrane intrinsic protein GmPIP1;6 confers salt tolerance. *BMC Plant Biol.* 14:181. doi: 10.1186/1471-2229-14-181
- Zhou, S., Hu, W., Deng, X., Ma, Z., Chen, L., Huang, C., et al. (2012). Overexpression of the wheat aquaporin gene, TaAQPT7, enhances drought tolerance in Transgenic Tobacco. *PLoS ONE* 7:e52439. doi: 10.1371/journal.pone.0052439

Conflict of Interest Statement: The authors declare that the research was conducted in the absence of any commercial or financial relationships that could be construed as a potential conflict of interest.

Copyright © 2016 Alavilli, Awasthi, Rout, Sahoo, Lee and Panda. This is an open-access article distributed under the terms of the Creative Commons Attribution License (CC BY). The use, distribution or reproduction in other forums is permitted, provided the original author(s) or licensor are credited and that the original publication in this journal is cited, in accordance with accepted academic practice. No use, distribution or reproduction is permitted which does not comply with these terms.



Pollen Aquaporins: The Solute Factor

Juliana A. Pérez Di Giorgio^{1†}, Gabriela C. Soto², Jorge P. Muschietti^{1,3} and Gabriela Amodeo^{3,4*}

¹ Instituto de Investigaciones en Ingeniería Genética y Biología Molecular – Consejo Nacional de Investigaciones Científicas y Técnicas, Buenos Aires, Argentina, ² Instituto de Genética Ewald A. Favret – Centro de Investigación en Ciencias Veterinarias y Agronómicas – Instituto Nacional de Tecnología Agropecuaria – Consejo Nacional de Investigaciones Científicas y Técnicas, Buenos Aires, Argentina, ³ Departamento de Biodiversidad y Biología Experimental, Facultad de Ciencias Exactas y Naturales, Universidad de Buenos Aires, Buenos Aires, Argentina, ⁴ Instituto de Biodiversidad y Biología Experimental y Aplicada – Universidad de Buenos Aires–Consejo Nacional de Investigaciones Científicas y Técnicas, Buenos Aires, Argentina

OPEN ACCESS

Edited by:

Richard Belanger,
Laval University, Canada

Reviewed by:

Ian S. Wallace,
University of Nevada, Reno, USA
Gaurav Zinta,
Shanghai Center for Plant Stress
Biology (CAS), China

***Correspondence:**

Gabriela Amodeo
amodeo@bg.fcen.uba.ar

†Present address:

Juliana A. Pérez Di Giorgio,
Department of Biochemistry
and Molecular Medicine, Université
de Montréal, Montréal, QC, Canada

Specialty section:

This article was submitted to
Plant Physiology,
a section of the journal
Frontiers in Plant Science

Received: 28 June 2016

Accepted: 21 October 2016

Published: 09 November 2016

Citation:

Pérez Di Giorgio JA, Soto GC,
Muschietti JP and Amodeo G (2016)
Pollen Aquaporins: The Solute Factor.
Front. Plant Sci. 7:1659.
doi: 10.3389/fpls.2016.01659

In the recent years, the biophysical properties and presumed physiological role of aquaporins (AQPs) have been expanded to specialized cells where water and solute exchange are crucial traits. Complex but unique processes such as stomatal movement or pollen hydration and germination have been addressed not only by identifying the specific AQP involved but also by studying how these proteins integrate and coordinate cellular activities and functions. In this review, we referred specifically to pollen-specific AQPs and analyzed what has been assumed in terms of transport properties and what has been found in terms of their physiological role. Unlike that in many other cells, the AQP machinery in mature pollen lacks plasma membrane intrinsic proteins, which are extensively studied for their high water capacity exchange. Instead, a variety of TIPs and NIPs are expressed in pollen. These findings have altered the initial understanding of AQPs and water exchange to consider specific and diverse solutes that might be critical to sustaining pollen's success. The spatial and temporal distribution of the pollen AQPs also reflects a regulatory mechanism that allowing a properly adjusting water and solute exchange.

Keywords: aquaporin, fertilization, membrane intrinsic protein, solute permeability, plant fitness, pollen germination, water channel, water and solute transport

INTRODUCTION

Over the last 25 years overwhelming evidence has been gathered indicating that the role of certain members of a complex superfamily of major intrinsic proteins (MIPs) known as aquaporins (AQPs) is to facilitate the permeation of water and small uncharged solutes (including gasses) through biological membranes (Bienert and Chaumont, 2014; Kitchen et al., 2015; Maurel et al., 2015; Pommerenig et al., 2015). The first water channel -CHIP28, later named AQP1- confirmed not only the appearance of an unequivocally facilitated water path in a cell membrane (Preston et al., 1992) but also the role of the membrane osmotic permeability (P_f), i.e., that the membrane expressing these proteins can increase their capacity to exchange water 10- to 100-fold, reflected in a change in this parameter. The “simple permeability hypothesis” holds that AQPs act as key modulators of the P_f of membranes and sustains that the change in the rate of water transport is the critical trait for certain biological processes (Hill et al., 2004; Hill and Shachar-Hill, 2015).

Unlike ion channels, AQPs are small (~30 kDa) tetramers in which each monomer is a functional unit. Although assembled primarily as homotetramers, certain groups in

both animals and plants can form heterotetramers (Verbavatz et al., 1993; Neely et al., 1999; Fetter et al., 2004; Yaneff et al., 2014). The integral membrane region of each monomer is composed of six transmembrane α -helices, three extracellular loops (A, C, E) and two intracellular ones (B, D). The channel “signature” is two opposing and highly conserved NPA motifs (Asn-Pro-Ala) near the center of the molecule resulting from the dipping of two inverted hemi-helices on loops B and E (Murata et al., 2000; Ho et al., 2009; Tani et al., 2009; Wree et al., 2011). While this constriction zone is associated with the single-file conductance of water, a second constriction -typically composed of aromatic residues and an arginine known as the ar/R zone, is located in the outer channel vestibule and forms a strong selectivity filter that determines the solutes that can permeate through the pore (Fu et al., 2000; Sui et al., 2001; Beitz et al., 2006; Fu and Lu, 2007; Almasalmeh et al., 2014). Recent structural studies of AQPs from a diverse range of organisms have revealed new insights into selectivity and modes of regulation, including gating and trafficking (Kreida and Törnroth-Horsefield, 2015).

Genome and transcriptome sequencing data available from all kingdoms have confirmed a vast number of orthologous channels, challenging the classical outlook to address water/solute transport through biological membranes (Gupta et al., 2011; Alleva et al., 2012; Soto et al., 2012; Pérez Di Giorgio et al., 2014). MIP genes are particularly prevalent in the plant kingdom with 35–60 MIP isoforms in vascular plants compared to 10 in mammals including humans. Moreover, compared to other kingdoms, plants show not only a strong diversification (seven major classes have been distinguished: PIP, HIP, XIP, TIP, NIP, GIP, and SIP; this number is reduced to five or four in higher plants) but also higher gene copy numbers within certain species. Because “orthodox” AQPs were first suggested to facilitate the passive transport of water across cell membranes in response to osmotic gradients, paradigms to explore plant water hydraulics were opened. New research shed light on their impact on plant transpiration (Maurel et al., 2016; Yaaran and Moshelion, 2016), on solute transport including toxic metalloids (Bienert and Jahn, 2010; Pommerenig et al., 2015) and gas transport (Herrera and Garvin, 2011; Bienert and Chaumont, 2014; Kaldenhoff et al., 2014).

In this context, the study of plant AQPs has been expanded to include specialized and symplastically isolated cells such as guard cells or pollen tubes in which the rate of water and solute exchange is critical to accomplishing their physiological task (volume change strategy: to swell or to grow). In the particular case of pollen tubes, growth is fast and complex, reflected by a spatial and temporal regulation tightly linked to the cellular process. Thus, pollen water status can be addressed as a structural, physiological and molecularly coordinated mechanism. It has been proposed that the identification of potential “water homeostasis control points” might improve our understanding of pollen quality and function upon exposure to environmental stresses (Firon et al., 2012).

Under this scenario, AQPs were considered natural candidates for controlling and fine tuning these control points. Analysis of *Arabidopsis* gene expression has helped to identify the genes responsible for pollen hydration and growth. Interestingly,

pollen exhibits a fewer number and more exclusive types of AQP-expressed genes when compared to other single cell transcriptional profiles (Soto et al., 2008). Unlike many other cells, the AQP machinery in *Arabidopsis* mature pollen lacks plasma membrane intrinsic proteins and is restricted to a limited variety of members of other MIP subfamilies: tonoplast intrinsic proteins (TIPs) and NOD26-like intrinsic proteins (NIPs) (Honys and Twell, 2004; Pina et al., 2005; Wang et al., 2008; Qin et al., 2009; Lorraine et al., 2013).

The aim of this review is focused on integrating information provided by available data in the field of pollen AQPs not only to highlight their physiological role but also to contribute to the understanding of their intrinsic properties.

POLLEN HYDRATION AND GERMINATION

Pollen grains undergo a sophisticated developmental program that includes internal cell adjustments during the different phases of dehydration and rehydration. These processes allow it not only to achieve fertilization as a final goal but also to cope with hostile environmental conditions. When a compatible pollen grain contacts the suitable stigma surface, it rapidly germinates and turns into an elongating pollen tube that will search for the ovules. Signaling molecules and ion channels act as pacemakers of the growth rate as well as controllers of the direction of the pollen tubes (Guan et al., 2013). Changes during germination and pollen tube growth result in mechanical stress sustained by the coordinated activity of the protoplasm and barriers (membranes and cell wall). Water uptake is thus critical during pollination: i.e., rehydration on the stigma surface and pollen tube growth, not only because they demand water entry but also because pollen tube growth is a very fast process within plant cells. Volume increase is a consequence of water and nutrient uptake. The process is osmoregulated and pollen tube growth is so tightly synchronized to the osmolality of the medium (Benkert et al., 1997) that it can be completely arrested if osmolality is changed (Pierson et al., 1994). Inappropriate pollen hydration inhibits fertilization triggered by premature germination within the anther (Johnson and McCormick, 2001) or landing on an incorrect surface (Lolle et al., 1998). Despite the evidence for water uptake and osmoregulation during this process, data on water transport or on the specific role of AQP-mediated water transport were acknowledged much later than ion and solute transport (Sommer et al., 2008).

POLLEN AQUAPORINS: ONLY FOUR AQP GENES ARE POLLEN-SPECIFIC

The first reports in the literature describing putative pollen water channels were performed in *Brassica*, *Nicotiana*, and *Lilium* (Marin-Olivier et al., 2000; Dixit et al., 2001; Bots et al., 2005a,b; Sommer et al., 2008). Interestingly, these first reports did not conclusively demonstrate that PIPs, the better-described “orthodox” water channels, were highly represented.

Two PIPs were found differentially expressed in *Nicotiana* anther and stigma (Bots et al., 2005a,b). In *Brassica* pollen, the presence of PIPs was not clear (Marin-Olivier et al., 2000; Dixit et al., 2001). Comparative analysis of pistil transcriptomes revealed the expression of *PIP1* and *PIP2* in species with dry and semi-dry stigmas (*Oryza sativa*, *Crocus sativus*, *Arabidopsis thaliana*, and *S. squalidus*), but not with wet stigmas (*Nicotiana tabacum*) (Allen et al., 2010). Recently, stigmatic papilla cells transcriptome analysis in *A. thaliana* ecotype Oldenburg (Old-1), which still retains the female SI function, showed that *PIP1;4* is up-regulated in compatible pollinations (using wild-type Old-1 pollen), whereas *PIP2;1* and *PIP2;7* are down-regulated in incompatible pollinations (using transgenic self-incompatible Old-1 pollen) (Matsuda et al., 2015). These studies support the hypothesis of pistil AQP potentially regulating pollen hydration in dry stigmas but not in wet stigmas, since the presence of the stigmatic exudate obviates the control of water flow to pollen grains.

Analysis performed at four pollen *Arabidopsis* developmental stages confirmed that only TIPs and NIPs, but not PIPs are preferentially expressed in mature pollen (Honys and Twell, 2004; Bock et al., 2006) and pollen tubes (Wang et al., 2008; Qin et al., 2009). Genome-wide analysis¹ of *Arabidopsis* AQP genes showed that only four (out of 35 loci) are preferentially expressed in mature pollen and/or pollen tubes: *TIP5;1*, *TIP1;3*, *NIP4;1*, and *NIP4;2*. In addition, *AtSIP1;1* and *AtSIP1;2* show both high expression levels in pollen as well as in other sporophytic tissues (Ishikawa et al., 2005), and are therefore not considered to be pollen-specific. *AtPIP2;7/2;8* is expressed during pollen development but has very low levels at maturity, and in turn, shows higher expression levels in sporophytic tissue. *AtTIP1;1* has very low levels of expression in mature pollen, and higher levels in sporophytic tissues. *AtNIP2;1* shows low constitutive levels in pollen and sporophytic tissues, but its expression sharply increase under hypoxic conditions (Choi and Roberts, 2007). It has been demonstrated by *in situ* hybridization and GUS activity assays that *AtNIP7;1* is expressed during pollen development and also in other sporophytic tissues (Li et al., 2011). **Figure 1** shows a heatmap representation of AQP expression, which highlights the distinctive repertoire of *Arabidopsis* pollen AQPs.

SEEKING THEIR PHYSIOLOGICAL ROLE

TIP1;3 and TIP5;1

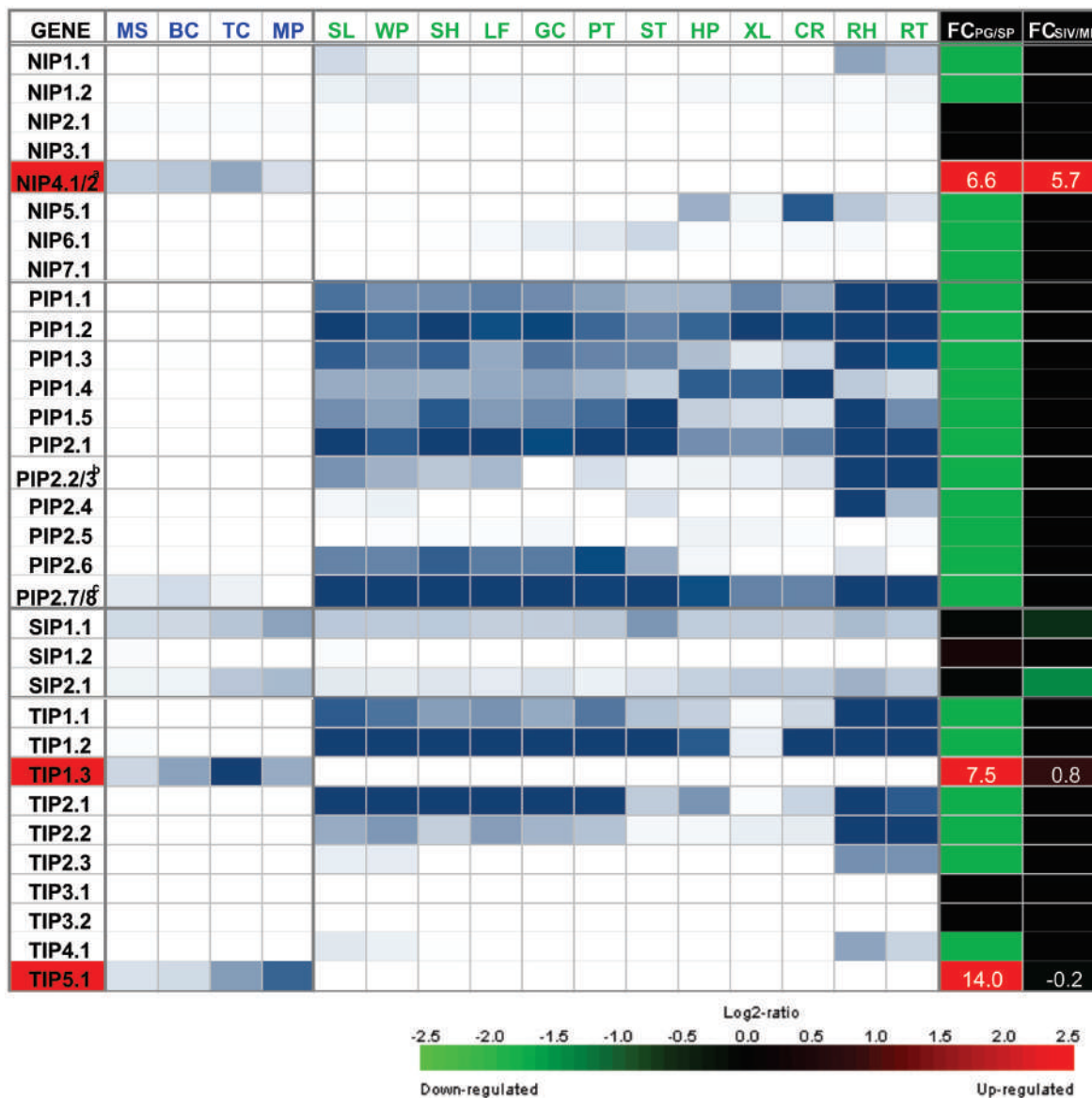
Arabidopsis TIP1;3 and *TIP5;1* are among the most highly expressed genes in mature pollen. *TIP1;3* is expressed in vesicles and vacuoles of vegetative cells while *TIP5;1* is expressed in vacuoles of sperm cells when expressed under its own promoter (Wudick et al., 2014), or in the mitochondria of vegetative cells when heterologously expressed under the control of the LAT52 promoter (Soto et al., 2010). Single *tip1;3* and *tip5;1* mutant plants showed no apparent phenotypic defects in pollen development and no significant reduction in fertility (Soto et al.,

2010). However, double *tip1;3 tip5;1* mutant plants showed an abnormal incidence of sterile pods under water- or nitrogen-deficient conditions and heat stress (Wudick et al., 2014). TIP1;3 and TIP5;1 are bi-functional AQPs with intermediate levels of permeability to water and high permeability to urea when expressed in *Xenopus* oocytes (Soto et al., 2008). Interestingly, Soto et al. (2010) showed that TIP5;1 water transport activity is significantly inhibited by an acidic external pH, and therefore proposed that His131, located in extracellular loop C in TIP5;1 and not present in other *Arabidopsis* TIPs, acts as the pH-sensing amino acid. In addition, it was shown that single *tip1;3* and *tip5;1* and double *tip1;3 tip5;1* mutant plants showed shorter pollen tubes only when they were germinated *in vitro* under nitrogen-deficient conditions (Soto et al., 2010). These results suggested that TIP5;1 and TIP1;3 are involved in the nitrogen metabolic pathway during pollen tube growth (Soto et al., 2008, 2010).

NIP4;1 and NIP4;2

Arabidopsis NIP4;1 and *NIP4;2* have two distinct features: both are paralog genes found exclusively in the angiosperm lineage and, although they share 84% amino acid identity, they display different expression patterns. Pérez Di Giorgio et al. (2016) found that *NIP4;1* is modestly expressed from the unicellular microspore to the mature pollen stage, and functions in pollen development and germination. In turn, *NIP4;2* is highly expressed following pollen germination, and functions exclusively during pollen tube growth. *NIP4;1* and *NIP4;2* are localized in the plasma membrane and internal vesicles of pollen tubes when expressed under their own promoters. In addition, a dynamic cycling between both sub-cellular compartments was observed for *NIP4;1*. Single *nip4;1* mutant plants showed reduced fertility due to defective pollen development (higher percentages of immature pollen, arrested in uni- or bi-cellular stages, losing viability and collapsing in some cases), pollination and germination; single *nip4;2* mutant plants showed defective pollen tube growth. Double knockdown plants displayed an abnormal incidence of sterile and stunted siliques with fewer seeds as a result of reduced fertilization, owing to defective pollen germination and pollen tube growth. Swelling assays in *Xenopus* oocytes showed that *NIP4;1* and *NIP4;2* function as water and glycerol channels. In addition, *NIP4;1* and *NIP4;2* C-termini were found to be phosphorylated by a pollen-specific CPK, modifying their water permeability. Survival assays in yeast indicated that *NIP4;1* also transports ammonia, urea, H₂O₂ and boric acid. One of the primary functions of boron in plants is to serve in the cross-linking of rhamnogalacturonan-II (RG-II), a component of cell wall pectic polysaccharides, and thus is an essential micronutrient required for plant growth and reproduction (Blevins and Lukaszewski, 1998). Indeed, double knockdown *nip4;1nip4;2* pollen showed shorter pollen tubes, particularly under boron deficient conditions, suggesting that *NIP4;1* and *NIP4;2* might be involved in boric acid uptake. Likewise, *Arabidopsis NIP7;1*, which is selectively expressed at the microspore stage, was also identified as a boric acid channel, and *nip7;1* mutant plants showed defects in

¹<https://genestigator.com/gv/>

**FIGURE 1 | Heatmap representation of the expression of NIP, PIP, SIP, and TIP genes in gametophytic and sporophytic tissues of *Arabidopsis*.**

Microarray data for MS, microspore; BC, bicellular pollen; TC, tricellular pollen; and MP, mature pollen; and for sporophytic organ or tissue, SL, seedlings; WP, whole plants; SH, shoots; LF, leave; GC, guard cell-enriched leaf extracts; PT, petioles; ST, stems; HP, hypocotyls; XL, xylem; CR, cork; RH, root hair zone; RT, roots, was obtained from Bock et al. (2006). Scale: white, 10th percentile, blue, 19th percentile. To identify AQP genes that show specific or preferential expression in pollen, fold change (FC) of the maximum expression from the four pollen grain stages (PG) and the maximum expression from the 12 sporophytic tissues (SP) was calculated as the log2 of the ratio of PG/SP. Microarray data for SIV, pollen tubes grown semi *in vivo*; and MP, mature pollen grains, was obtained from Qin et al. (2009). To identify AQP genes that are differentially expressed upon pollen germination, FC was calculated as the log2 of the ratio of SIV/MP. FC scale: green = -2.5 (down-regulated genes), black = 0, red = 2.5 (up-regulated genes). FC values for pollen specific AQPs NIP4;1, TIP1;3, and TIP5;1 are indicated in white. ^aNIP4;1 and NIP4;2 are promiscuously detected by the same probe set 249584_s_at. Based on RNA-seq data (Lorraine et al., 2013) and qRT-PCR assays (Pérez Di Giorgio et al., 2016), pollen grain expression corresponds to NIP4;1; whereas NIP4;2 is only expressed in pollen tubes. ^bPIP2;2 and PIP2;3 are promiscuously detected by the same probe set 265444_s_at. Based on RNA-seq data (Lorraine et al., 2013) none of them are expressed in mature pollen. ^cPIP2;7 and PIP2;8 are promiscuously detected by the same probe set 266533_s_ during pollen development at BC stage, but based on RNA-seq data (Lorraine et al., 2013), they are not expressed in mature pollen.

pollen tube growth in the absence of boric acid (Li et al., 2011). Considering that NIP4;1 and NIP4;2 are exclusive to angiosperms (Anderberg et al., 2012; Abascal et al., 2014) and that flowering plants are thought to have evolved under

selection for a faster reproductive cycle (Williams, 2008, 2012; Abercrombie et al., 2011), NIP4;1 and NIP4;2 might contribute to improved pollen germination and pollen tube growth in angiosperms.

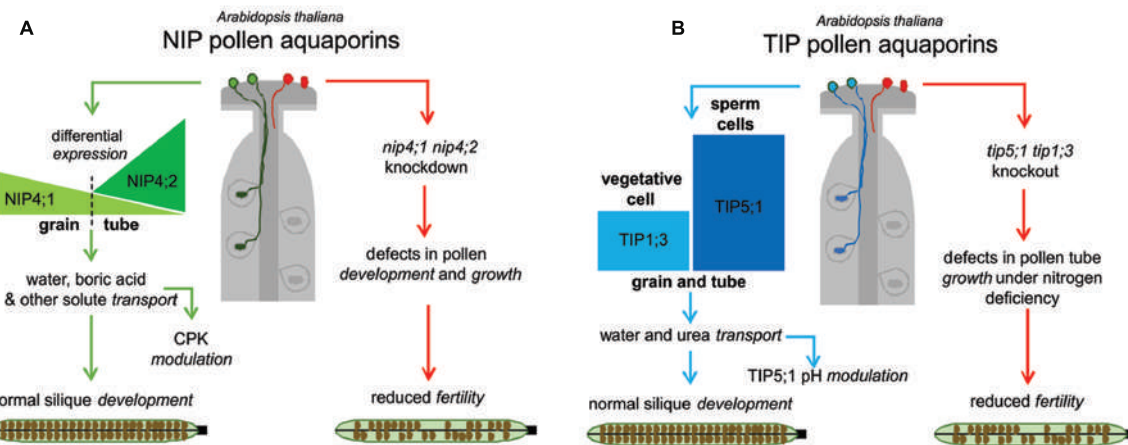


FIGURE 2 | Global models for the roles of pollen specific aquaporins (AQPs) in reproduction. (A) In the presence of NIP4;1 and NIP4;2, plant fitness is normal (left, green pathway). NIP4;1 and NIP4;2 expression peaks differ temporally. In the absence of NIPs AQPs, (right, red pathway) plant fitness is reduced (fewer seeds and shorter siliques due to non-fertilized ovules). The *nip4;1nip4;2* knockdown showed defects in pollen development, maturation, germination, and pollen tube growth. **(B)** In the presence of TIP1;3 and TIP5;1 there is normal fertilization (left, blue pathway). TIP1;3 and TIP5;1 expression patterns are also differentially localized in vegetative and sperm cells, respectively. In the absence of both TIPs (right, red pathway), plant fitness is reduced under nitrogen deficiency (in accordance with their substrate specificity) due to defects in pollen tube growth.

The Working Hypothesis: Relevance of Aquaporins in Plant Fitness

Current evidence from the literature shows that specific AQPs are part of the machinery of pollen physiology. The fact that *nip4;1* and *nip4;2* mutant phenotypes were evident under normal growth conditions (and not when they are limited) reflects the relevance of these two specific NIPs in reproduction. Although most of the described defects in pollen development, germination and pollen tube elongation are mild at the physiological level, they somehow reveal reduced plant fitness. A model that reflects this hypothesis is proposed in Figure 2: when the four AQPs are following their normal pattern of expression, plant fertility is not affected. In panel A, NIP4;1 is expressed at relatively low levels in mature pollen, while NIP4;2 expression peaks only after pollen germination. Both NIPs transport water and glycerol (in *Xenopus* oocytes), and in particular NIP4;1 can also transport other solutes such as boric acid, ammonia, H₂O₂ and urea in yeast assays. Besides, the water transport capacity of both NIPs is regulated by phosphorylation at Ser267. In the absence of both NIP AQPs plant fitness is reduced (less seeds and shorter siliques due to non-fertilized ovules). Single *nip4;1* mutant show defects in pollen development, maturation and germination, while *nip4;2* mutant only in pollen tube growth. In panel B, when TIP1;3 and TIP5;1 are normally expressed, there is also normal fertilization. TIP1;3 is expressed at medium levels in the vegetative cell, while TIP5;1 is the highest gene expressed in sperm cells, where it is the one of the top 200 expressed genes on pollen sperm transcriptomic analysis (Borges et al., 2008). Both TIPs transport water and urea in *Xenopus* oocytes, and water transport of TIP5;1 is regulated by pH. In the absence of both TIPs, plant fitness under nitrogen deficiency is reduced (in accordance with their substrate specificity), due to defects in pollen tube growth.

Another important feature described in certain AQPs is the transport of gas molecules, including carbon dioxide and hydrogen peroxide (Herrera and Garvin, 2011; Bienert and Chaumont, 2014; Kaldenhoff et al., 2014). The physiological relevance of AQP-facilitated gas diffusion includes both the exchange capacity and the signaling process. For instance, hydrogen peroxide (H₂O₂), acts as a signaling molecule at lower concentrations, maintaining normal plant growth and development, but it produces toxic effects at higher levels. Specific AQP isoforms are proposed to be critical in the H₂O₂ signaling network (Bienert and Chaumont, 2014). Importantly, abiotic stress induces excess accumulation of ROS leading to pollen abortion and programmed cell death of microspores in developing anthers, and consequently resulting in male sterility (Zinta et al., 2016). In this regard, pollen-specific NIP4;1 and other pollen-expressed AQPs, such as TIP1;1, NIP2;1, and NIP7;1 have been shown to transport H₂O₂ (revised in Pérez Di Giorgio et al., 2014), and therefore potentially play a role in the redox control of pollen development.

In addition, H₂O₂ was shown to mediate redox signaling in pollen-pistil interactions (Sharma and Bhatla, 2013). Considering AtPIP1;4 was found to be up-regulated in stigmas upon compatible pollination (Matsuda et al., 2015) and has a role in H₂O₂ transport for signal transduction in immunity pathways (Tian et al., 2016), we could speculate a role of this AQP in ROS signaling during pollination.

UNCERTAIN ISSUES THAT STILL NEED TO BE ADDRESSED

The paradox in the analysis of the pollen specific AQPs is that none is an “orthodox” water AQP. Although they differ

substantially, TIP5;1, TIP1;3, NIP4;1, and NIP4;2 are solute and water transporters. These findings are consistent with other NIPs and TIPs described in the literature in other organs and/or tissues (Pérez Di Giorgio et al., 2014). In particular, NIPs are considered AQPs with poor water permeability but capacity to transport glycerol, formamide, urea, ammonia or metalloids (Wallace et al., 2002; Danielson and Johanson, 2010; Mitani-Ueno et al., 2011). In agreement with these observations, it was recently proposed that certain NIP channel proteins should be considered metalloido-porins and not AQPs (Pommerrenig et al., 2015).

Even if the analysis of a complete set of pollen AQPs is broadened to include the non-specific SIP1;1 and SIP2;1, it should be emphasized that these two SIPs are preferentially expressed in the endoplasmic reticulum of stems of *Arabidopsis* plants (Maeshima and Ishikawa, 2008).

Thus, pollen tube growth employs a tightly regulated and complex machinery to rapidly coordinate water and solute exchange. Pollen tube growth depends on plasma membrane polarization at the tip involving a strong and rapid membrane recycling to the secretory system (Hepler et al., 2001; Hellung et al., 2006). Recently, a highly expressed K⁺ channel (LilKT1) in *Lilium* pollen was found to include a strong endocytic recycling mechanism (Safarian et al., 2015). The authors propose that this feature could be a way to adjust the number of inward K⁺ channels in the pollen plasma membrane in order to sustain the correct water influx (driven by the raising cytosolic K⁺ concentrations). The fact that the described AQPs move uncharged solutes broadens the discussion of the controlled driving forces

that operate in pollen tube growth. Mechano-sensitive channels have also been considered to be potential components in sensing osmotic changes (Zerzour et al., 2009; Kurusu et al., 2013), and these type of channels had already been described in pollen protoplasts (Dutta and Robinson, 2004). A recent study has identified and characterized a pollen-specific membrane tension-gated ion channel, MscS-like 8 (MSL8), which is critical both for pollen survival during the hypoosmotic shock of rehydration and for sustaining full male fertility (Hamilton et al., 2015). There is also new evidence in the literature that certain AQPs are mechanosensitive (human AQP1, described in Ozu et al., 2013). The possibility of analyzing these AQPs as components of an osmosensor system that regulates this machinery might be reasonable but remains speculative (Hill and Shachar-Hill, 2015).

AUTHOR CONTRIBUTIONS

GA and JM conceived the idea of this work, JPDG and GA planned and wrote the manuscript, and JM and GS contributed with discussion and critical comments. All authors approved the final version.

ACKNOWLEDGMENTS

Our work was supported by grants PICT2011-1698, PICT2012-0007, and PICT2014-0423 to JM and PICT2014-0744, PIP2012-2014, and UBACyT12014-2017 to GA.

REFERENCES

- Abascal, F., Irisarri, I., and Zardoya, R. (2014). Diversity and evolution of membrane intrinsic proteins. *Biochim. Biophys. Acta* 1840, 1468–1481. doi: 10.1016/j.bbagen.2013.12.001
- Abercrombie, J. M., O'Meara, B. C., Moffatt, A. R., and Williams, J. H. (2011). Developmental evolution of flowering plant pollen tube cell walls: callose synthase (CalS) gene expression patterns. *Evodevo* 2:14. doi: 10.1186/2041-9139-2-14
- Allen, A. M., Lexer, C., and Hiscock, S. J. (2010). Comparative analysis of pistil transcriptomes reveals conserved and novel genes expressed in dry, wet, and semidry stigmas. *Plant Physiol.* 154, 1347–1360. doi: 10.1104/pp.110.162172
- Alleva, K., Chara, O., and Amodeo, G. (2012). Aquaporins: another piece in the osmotic puzzle. *FEBS Lett.* 586, 2991–2999. doi: 10.1016/j.febslet.2012.06.013
- Almasalmeh, A., Krenc, D., Wu, B., and Beitz, E. (2014). Structural determinants of the hydrogen peroxide permeability of aquaporins. *FEBS J.* 281, 647–656. doi: 10.1111/febs.12653
- Anderberg, H. I., Kjellbom, P., and Johanson, U. (2012). Annotation of *Selaginella moellendorffii* major intrinsic proteins and the evolution of the protein family in terrestrial plants. *Front. Plant Sci.* 20:33. doi: 10.3389/fpls.2012.00033
- Beitz, E., Wu, B., Holm, L. M., Schultz, J. E., and Zeuthen, T. (2006). Point mutations in the aromatic/arginine region in aquaporin 1 allow passage of urea, glycerol, ammonia, and protons. *Proc. Natl. Acad. Sci. U.S.A.* 103, 269–274. doi: 10.1073/pnas.0507225103
- Benkert, R., Obermeyer, G., and Bentrup, F. W. (1997). The turgor pressure of growing lily pollen tubes. *Protoplasma*. 198, 1–8. doi: 10.1007/BF01282125
- Bienert, G. P., and Chaumont, F. (2014). Aquaporin-facilitated transmembrane diffusion of hydrogen peroxide. *Biochim. Biophys. Acta* 1840, 1596–1604. doi: 10.1016/j.bbagen.2013.09.017
- Bienert, G. P., and Jahn, T. P. (2010). Major intrinsic proteins and arsenic transport in plants: new players and their potential role. *Adv. Exp. Med. Biol.* 679, 111–125. doi: 10.1007/978-1-4419-6315-4_9
- Blevins, D. G., and Lukaszewski, K. M. (1998). Boron in plant structure and function. *Annu. Rev. Plant Physiol. Plant Mol. Biol.* 49, 481–500. doi: 10.1146/annurev.arplant.49.1.481
- Bock, K. W., Honys, D., Ward, J. M., Padmanaban, S., Nawrocki, E. P., Hirschi, K. D., et al. (2006). Integrating membrane transport with male gametophyte development and function through transcriptomics. *Plant Physiol.* 140, 1151–1168. doi: 10.1104/pp.105.074708
- Borges, F., Gomes, G., Gardner, R., Moreno, N., McCormick, S., Feijó, J. A., et al. (2008). Comparative transcriptomics of *Arabidopsis* sperm cells. *Plant Physiol.* 148, 1168–1181. doi: 10.1104/pp.108.125229
- Bots, M., Feron, R., Uehlein, N., Weterings, K., Kaldenhoff, R., and Mariani, T. (2005a). PIP1 and PIP2 aquaporins are differentially expressed during tobacco anther and stigma development. *J. Exp. Bot.* 56, 113–121.
- Bots, M., Vergeldt, F., Wolters-Arts, M., Weterings, K., van As, H., and Mariani, C. (2005b). Aquaporins of the PIP2 class are required for efficient anther dehiscence in tobacco. *Plant Physiol.* 137, 1049–1056. doi: 10.1104/pp.104.056408.1
- Choi, W. G., and Roberts, D. M. (2007). *Arabidopsis* NIP2;1, a major intrinsic protein transporter of lactic acid induced by anoxic stress. *J. Biol. Chem.* 282, 24209–24218. doi: 10.1074/jbc.M700982200
- Danielson, J. H., and Johanson, U. (2010). “Phylogeny of major intrinsic proteins,” in *MIPs and Their Role in the Exchange of Metalloids*, Vol. 679, eds T. Jahn and G. Bienert (New York, NY: Springer), 19–31. doi: 10.1007/978-1-4419-6315-4_2
- Dixit, R., Rizzo, C., Nasrallah, M., and Nasrallah, J. (2001). The Brassica MIP-MOD gene encodes a functional water channel that is expressed in the stigma epidermis. *Plant Mol. Biol.* 45, 51–62. doi: 10.1023/A:1006428007826

- Dutta, R., and Robinson, K. R. (2004). Identification and characterization of stretch-activated ion channels in pollen protoplasts. *Plant Physiol.* 135, 1398–1406. doi: 10.1104/pp.104.041483
- Fetter, K., Van Wilder, V., Moshelion, M., and Chaumont, F. (2004). Interactions between plasma membrane aquaporins modulate their water channel activity. *Plant Cell* 16, 215–228. doi: 10.1105/tpc.017194
- Firon, N., Nepi, M., and Pacini, E. (2012). Water status and associated processes mark critical stages in pollen development and functioning. *Ann. Bot.* 109, 1201–1214. doi: 10.1093/aob/mcs070
- Fu, D., Libson, A., Miercke, L. J., Weitzman, C., Nollert, P., Krucinski, J., et al. (2000). Structure of a glycerol-conducting channel and the basis for its selectivity. *Science* 290, 481–486. doi: 10.1126/science.290.5491.481
- Fu, D., and Lu, M. (2007). The structural basis of water permeation and proton exclusion in aquaporins (review). *Mol. Membr. Biol.* 24, 366–374. doi: 10.1080/09687680701446965
- Guan, Y., Guo, J., Li, H., and Yang, Z. (2013). Signaling in pollen tube growth: crosstalk, feedback, and missing links. *Mol. Plant* 6, 1053–1064. doi: 10.1093/mp/sst070
- Gupta, A. B., Verma, R. K., Agarwal, V., Vajpai, M., Bansal, V., and Sankararamakrishnan, R. (2011). MIPModDB: a central resource for the superfamily of major intrinsic proteins. *Nucleic Acids Res.* 40, D362–D369. doi: 10.1093/nar/gkr914
- Hamilton, E. S., Jensen, G. S., Maksaev, G., Katims, A., Sherp, A. M., and Haswell, E. S. (2015). Mechanosensitive channel MSL8 regulates osmotic forces during pollen hydration and germination. *Science* 350, 438–441. doi: 10.1126/science.aac6014
- Helling, D., Possart, A., Cottier, S., Klahre, U., and Kost, B. (2006). Pollen tube tip growth depends on plasma membrane polarization mediated by Tobacco PLC3 activity and endocytic membrane recycling. *Plant Cell* 18, 3519–3534. doi: 10.1105/tpc.106.047373
- Hepler, P. K., Vidali, L., and Cheung, A. Y. (2001). Polarized cell growth in higher plants. *Annu. Rev. Cell Dev. Biol.* 17, 159–187. doi: 10.1146/annurev.cellbio.17.1.159
- Herrera, M., and Garvin, J. L. (2011). Aquaporins as gas channels. *Pflugers. Arch.* 462, 623–630. doi: 10.1007/s00424-011-1002-x
- Hill, A. E., Shachar-Hill, B., and Shachar-Hill, Y. (2004). What are aquaporins for? *J. Membr. Biol.* 197, 1–32. doi: 10.1007/s00232-003-0639-6
- Hill, A. E., and Shachar-Hill, Y. (2015). Are aquaporins the missing transmembrane osmosensors? *J. Membr. Biol.* 248, 753–765. doi: 10.1007/s00232-015-9790-0
- Ho, J. D., Yeh, R., Sandstrom, A., Chorniy, I., Harries, W. E., Robbins, R. A., et al. (2009). Crystal structure of human aquaporin 4 at 1.8 Å and its mechanism of conductance. *Proc. Natl. Acad. Sci. U.S.A.* 106, 7437–7442. doi: 10.1073/pnas.0902725106
- Honyes, D., and Twell, D. (2004). Transcriptome analysis of haploid male gametophyte development in *Arabidopsis*. *Genome Biol.* 5:R85. doi: 10.1186/gb-2004-5-11-r85
- Ishikawa, F., Suga, S., Uemura, T., Sato, M. H., and Maeshima, M. (2005). Novel type aquaporin SIPs are mainly localized to the ER membrane and show cell-specific expression in *Arabidopsis thaliana*. *FEBS Lett.* 579, 5814–5820. doi: 10.1016/j.febslet.2005.09.076
- Johnson, S., and McCormick, S. (2001). Pollen germinates precociously in the anthers of raring-to-go, an *Arabidopsis* gametophytic mutant. *Plant Physiol.* 126, 685–695. doi: 10.1104/pp.126.2.685
- Kaldenhoff, R., Kai, L., and Uehlein, N. (2014). Aquaporins and membrane diffusion of CO₂ in living organisms. *Biochim. Biophys. Acta* 1840, 1592–1595. doi: 10.1016/j.bbagen.2013.09.037
- Kitchen, P., Day, R. E., Salman, M. M., Conner, M. T., Bill, R. M., and Conner, A. C. (2015). Beyond water homeostasis: diverse functional roles of mammalian aquaporins. *Biochim. Biophys. Acta* 1850, 2410–2421. doi: 10.1016/j.bbagen.2015.08.023
- Kreida, S., and Törnroth-Horsefield, S. (2015). Structural insights into aquaporin selectivity and regulation. *Curr. Opin. Struct. Biol.* 33, 126–134. doi: 10.1016/j.sbi.2015.08.004
- Kurusu, T., Kuchitsu, K., Nakano, M., Nakayama, Y., and Iida, H. (2013). Plant mechanosensing and Ca²⁺ transport. *Trends Plant Sci.* 18, 227–233. doi: 10.1016/j.tplants.2012.12.002
- Li, T., Choi, W., Wallace, I. S., Baudry, J., and Roberts, D. M. (2011). AtNIP7;1: an anther-specific boric acid transporter of the AQP superfamily regulated by an unusual Tyrosine in Helix 2 of the transport pore. *Biochemistry* 50, 6633–6641. doi: 10.1021/bi2004476
- Lolle, S. J., Hsu, W., and Pruitt, R. E. (1998). Genetic analysis of organ fusion in *Arabidopsis thaliana*. *Genetics* 149, 607–619.
- Lorraine, A. E., McCormick, S., Estrada, A., Patel, K., and Qin, P. (2013). P. RNA-Seq of *Arabidopsis* pollen uncovers novel transcription and alternative splicing. *Plant Physiol.* 162, 1092–1109. doi: 10.1104/pp.112.211441
- Maeshima, M., and Ishikawa, F. (2008). ER membrane aquaporins in plants. *Pflugers Arch. Eur. J. Physiol.* 456, 709–716. doi: 10.1007/s00424-007-0363-7
- Marin-Olivier, M., Chevalier, T., Fobis-Loisy, I., Dumas, C., and Gaude, T. (2000). Aquaporin PIP genes are not expressed in the stigma papillae in *Brassica oleracea*. *Plant J.* 2, 231–240. doi: 10.1046/j.1365-313x.2000.00874.x
- Matsuda, T., Matsushima, M., Nabemoto, M., Osaka, M., Sakazono, S., Masuko-Suzuki, H., et al. (2015). Transcriptional characteristics and differences in *Arabidopsis* stigmatic papilla cells pre- And post-pollination. *Plant Cell Physiol.* 56, 663–673. doi: 10.1093/pcp/pcu209
- Maurel, C., Boursiac, Y., Luu, D. T., Santoni, V., Shahzad, Z., and Verdoucq, L. (2015). Aquaporins in plants. *Physiol. Rev.* 95, 1321–1358. doi: 10.1152/physrev.00008.2015
- Maurel, C., Verdoucq, L., and Rodrigues, O. (2016). Aquaporins and plant transpiration. *Plant Cell Environ.* 39, 2580–2587. doi: 10.1111/pce.12814
- Mitani-Ueno, N., Yamaji, N., Zhao, F. J., and Ma, J. F. (2011). The aromatic/arginine selectivity filter of NIP aquaporins plays a critical role in substrate selectivity for silicon, boron, and arsenic. *J. Exp. Bot.* 62, 4391–4398. doi: 10.1093/jxb/err158
- Murata, K., Mitsuoka, K., Hirai, T., Walz, T., et al. (2000). Structural determinants of water permeation through aquaporin-1. *Nature* 407, 599–605.
- Neely, J. D., Christensen, B. M., Nielsen, S., and Agre, P. (1999). Heterotetrameric composition of aquaporin-4 water channels. *Biochemistry* 38, 11156–11163. doi: 10.1021/bi990941s
- Ozu, M., Dorr, R. A., Gutiérrez, F., Politi, M. T., and Toriano, R. (2013). Human AQP1 is a constitutively open channel that closes by a membrane-tension-mediated mechanism. *Biophys. J.* 104, 85–95. doi: 10.1016/j.bpj.2012.11.3818
- Pérez Di Giorgio, J., Bienert, G. P., Ayub, N., Yaneff, A., Barberini, M. L., Mecchia, M. A., et al. (2016). Pollen-specific aquaporins NIP4;1 and NIP4;2 are required for pollen development and pollination in *Arabidopsis thaliana*. *Plant Cell* 28, 1053–1077. doi: 10.1105/tpc.15.00776
- Pérez Di Giorgio, J., Soto, G., Alleva, K., Jozefkowicz, C., Amodeo, G., Muschietti, J. P., et al. (2014). Prediction of aquaporin function by integrating evolutionary and functional analyses. *J. Membr. Biol.* 247, 107–125. doi: 10.1007/s00232-013-9618-8
- Pierson, E. S., Miller, D. D., Callahan, D. A., Shipley, A. M., Rivers, B. A., Cresti, M., et al. (1994). Pollen tube growth is coupled to the extracellular calcium ion flux and the intracellular calcium gradient: effect of BAPTA-type buffers and hypertonic media. *Plant Cell* 6, 1815–1828. doi: 10.2307/3869910
- Pina, C., Pinto, F., Feijo, J. A., and Becker, J. D. (2005). Gene family analysis of the *Arabidopsis* pollen transcriptome reveals biological implications for cell growth, division control, and gene expression regulation. *Plant Physiol.* 138, 744–756. doi: 10.1104/pp.104.057935
- Pommerrenig, B., Diehn, T. A., and Bienert, G. P. (2015). Metalloido-porins: essentiality of Nodulin 26-like intrinsic proteins in metalloid transport. (2015). *Plant Sci.* 238, 212–227. doi: 10.1016/j.plantsci.2015.06.002
- Preston, G. M., Carroll, T. P., Guggino, W. B., and Agre, P. (1992). Appearance of water channels in *Xenopus* oocytes expressing red cell CHIP28 protein. *Science* 256, 385–387. doi: 10.1126/science.256.5055.385
- Qin, Y., Leydon, A. R., Manziello, A., Pandey, R., Mount, D., Denic, S., et al. (2009). Penetration of the stigma and style elicits a novel transcriptome in pollen tubes, pointing to genes critical for growth in a pistil. *PLoS Genet.* 5:e1000621. doi: 10.1371/journal.pgen.1000621
- Safarian, M. J., Pertl-Obermeyer, H., Lughofer, P., Hude, R., Bertl, A., and Obermeyer, G. (2015). Lost in traffic? The K⁺ channel of lily pollen, LilKT1, is detected at the endomembranes inside yeast cells, tobacco leaves, and lily pollen. *Plant Traffic Transp.* 10:47. doi: 10.3389/fpls.2015.00047
- Sharma, B., and Bhatla, S. C. (2013). Accumulation and scavenging of reactive oxygen species and nitric oxide correlate with stigma maturation and pollen-stigma interaction in sunflower. *Acta Physiol. Plant.* 35, 2777–2787. doi: 10.1007/s11738-013-1310-1

- Sommer, A., Geist, B., Da Ines, O., Gehwolf, R., Schäffner, A. R., and Obermeyer, G. (2008). Ectopic expression of *Arabidopsis thaliana* plasma membrane intrinsic protein 2 aquaporins in lily pollen increases the plasma membrane water permeability of grain but not of tube protoplasts. *New Phytol.* 180, 787–797. doi: 10.1111/j.1469-8137.2008.02607.x
- Soto, G., Alleva, K., Amodeo, G., Muschietti, J., and Ayub, N. D. (2012). New insight into the evolution of aquaporins from flowering plants and vertebrates: orthologous identification and functional transfer is possible. *Gene* 503, 165–176. doi: 10.1016/j.gene.2012.04.021
- Soto, G., Alleva, K., Mazzella, M. A., Amodeo, G., and Muschietti, J. P. (2008). AtTIP1;3 and AtTIP5;1, the only highly expressed *Arabidopsis* pollen-specific aquaporins, transport water and urea. *FEBS Lett.* 582, 4077–4082. doi: 10.1016/j.febslet.2008.11.002
- Soto, G., Fox, R., Ayub, N., Alleva, K., Guaimas, F., Erijman, E. J., et al. (2010). TIP5;1 is an aquaporin specifically targeted to pollen mitochondria and is probably involved in nitrogen remobilization in *Arabidopsis thaliana*. *Plant J.* 64, 1038–1047. doi: 10.1111/j.1365-313X.2010.04395.x
- Sui, H., Han, B. G., Lee, J. K., Walian, P., and Jap, B. K. (2001). Structural basis of water-specific transport through the AQP1 water channel. *Nature* 414, 872–878. doi: 10.1038/414872a
- Tani, K., Mitsuma, T., Hiraoki, Y., Kamegawa, A., Nishikawa, K., Tanimura, Y., et al. (2009). Mechanism of aquaporin-4's fast and highly selective water conduction and proton exclusion. *J. Mol. Biol.* 389, 694–706. doi: 10.1016/j.jmb.2009.04.049
- Tian, S., Wang, X., Li, P., Wang, H., Ji, H., Xie, J., et al. (2016). Plant aquaporin AtPIP1;4 links apoplastic H₂O₂ induction to disease immunity pathways. *Plant Physiol.* 17, 1635–1650. doi: 10.1104/pp.15.01237
- Verbavatz, J. M., Brown, D., Sabolič, I., Valenti, G., Ausiello, D. A., Van Hoek, A. N., et al. (1993). Tetrameric assembly of CHIP28 water channels in liposomes and cell membranes: a freeze fracture study. *J. Cell Biol.* 123, 605–618. doi: 10.1083/jcb.123.3.605
- Wallace, I. S., Wills, D. M., Guenther, J. F., and Roberts, D. M. (2002). Functional selectivity for glycerol of the nodulin 26 subfamily of plant membrane intrinsic proteins. *FEBS Lett.* 523, 109–112. doi: 10.1016/S0014-5793(02)02955-1
- Wang, Y., Zhang, W. Z., Song, L. F., Zou, J. J., Su, Z., and Wu, W. H. (2008). Transcriptome analyses show changes in gene expression to accompany pollen germination and tube growth in *Arabidopsis*. *Plant Physiol.* 148, 1201–1211. doi: 10.1104/pp.108.126375
- Williams, J. H. (2008). Novelties of the flowering plant pollen tube underlie diversification of a key life history stage. *Proc. Natl. Acad. Sci. U.S.A.* 105, 11259–11263. doi: 10.1073/pnas.0800036105
- Williams, J. H. (2012). The evolution of pollen germination timing in flowering plants: *Austrobailey ascendens* (Austrobaileyaceae). *AoB Plants* 2012, ls010. doi: 10.1093/aobpla/pls010
- Wree, D., Wu, B., Zeuthen, T., and Beitz, E. (2011). Requirement for asparagine in the aquaporin NPA sequence signature motifs for cation exclusion. *FEBS J.* 278, 740–748. doi: 10.1111/j.1742-4658.2010.07993.x
- Wudick, M. M., Luu, D.-T., Tournaire-Roux, C., Sakamoto, W., and Maurel, C. (2014). Vegetative and sperm cell-specific aquaporins of *Arabidopsis thaliana* highlight the vacuolar equipment of pollen and contribute to plant reproduction. *Plant Physiol.* 164, 1697–1706. doi: 10.1104/pp.113.228700
- Yaaran, A., and Moshelion, M. (2016). Role of aquaporins in a composite model of water transport in the leaf. *Int. J. Mol. Sci.* 17:E1045. doi: 10.3390/ijms17071045
- Yaneff, A., Sigaut, L., Marquez, M., Alleva, K., Pietrasanta, L. I., and Amodeo, G. (2014). Heteromerization of PIP aquaporins affects their intrinsic permeability. *Proc. Natl. Acad. Sci. U.S.A.* 111, 231–236. doi: 10.1073/pnas.1316537111
- Zerzour, R., Kroeger, J., and Geitmann, A. (2009). Polar growth in pollen tubes is associated with spatially confined dynamic changes in cell mechanical properties. *Dev. Biol.* 334, 437–446. doi: 10.1016/j.ydbio.2009.07.044
- Zinta, G., Khan, A., AbdElgawad, H., Verma, V., and Srivastava, A. K. (2016). Unveiling the redox control of plant reproductive development during abiotic stress. *Front. Plant. Sci.* 7:700. doi: 10.3389/fpls.2016.00700

Conflict of Interest Statement: The authors declare that the research was conducted in the absence of any commercial or financial relationships that could be construed as a potential conflict of interest.

Copyright © 2016 Pérez Di Giorgio, Soto, Muschietti and Amodeo. This is an open-access article distributed under the terms of the Creative Commons Attribution License (CC BY). The use, distribution or reproduction in other forums is permitted, provided the original author(s) or licensor are credited and that the original publication in this journal is cited, in accordance with accepted academic practice. No use, distribution or reproduction is permitted which does not comply with these terms.



Roles of Aquaporins in *Setaria viridis* Stem Development and Sugar Storage

Samantha A. McGaughey^{1,2}, Hannah L. Osborn³, Lily Chen^{1,3}, Joseph L. Pegler¹, Stephen D. Tyerman², Robert T. Furbank³, Caitlin S. Byrt^{2*} and Christopher P. L. Grof[†]

¹ Centre for Plant Science, School of Environmental and Life Sciences, University of Newcastle, Callaghan, NSW, Australia

² Australian Research Council Centre of Excellence in Plant Energy Biology, Waite Research Institute and School of

Agriculture, Food and Wine, University of Adelaide, Glen Osmond, SA, Australia, ³ Australian Research Council Centre of Excellence for Translational Photosynthesis, College of Medicine, Biology and Environment, Australian National University, Canberra, ACT, Australia

OPEN ACCESS

Edited by:

Rupesh Kailasrao Deshmukh,
Laval University, Canada

Reviewed by:

Manoj Prasad,

National Institute of Plant Genome
Research, India

Kapil Kumar Tiwari,

Sardarkrushinagar Dantwada
Agricultural University, India

*Correspondence:

Caitlin S. Byrt

caitlin.byrt@adelaide.edu.au

[†]These authors have contributed
equally to this work.

Specialty section:

This article was submitted to

Plant Physiology,

a section of the journal

Frontiers in Plant Science

Received: 15 August 2016

Accepted: 17 November 2016

Published: 01 December 2016

Citation:

McGaughey SA, Osborn HL, Chen L, Pegler JL, Tyerman SD, Furbank RT, Byrt CS and Grof CPL (2016) Roles of Aquaporins in *Setaria viridis* Stem Development and Sugar Storage. *Front. Plant Sci.* 7:1815. doi: 10.3389/fpls.2016.01815

Setaria viridis is a C₄ grass used as a model for bioenergy feedstocks. The elongating internodes in developing *S. viridis* stems grow from an intercalary meristem at the base, and progress acropetally toward fully expanded cells that store sugar. During stem development and maturation, water flow is a driver of cell expansion and sugar delivery. As aquaporin proteins are implicated in regulating water flow, we analyzed elongating and mature internode transcriptomes to identify putative aquaporin encoding genes that had particularly high transcript levels during the distinct stages of internode cell expansion and maturation. We observed that *SvPIP2;1* was highly expressed in internode regions undergoing cell expansion, and *SvNIP2;2* was highly expressed in mature sugar accumulating regions. Gene co-expression analysis revealed *SvNIP2;2* expression was highly correlated with the expression of five putative sugar transporters expressed in the *S. viridis* internode. To explore the function of the proteins encoded by *SvPIP2;1* and *SvNIP2;2*, we expressed them in *Xenopus laevis* oocytes and tested their permeability to water. *SvPIP2;1* and *SvNIP2;2* functioned as water channels in *X. laevis* oocytes and their permeability was gated by pH. Our results indicate that *SvPIP2;1* may function as a water channel in developing stems undergoing cell expansion and *SvNIP2;2* is a candidate for retrieving water and possibly a yet to be determined solute from mature internodes. Future research will investigate whether changing the function of these proteins influences stem growth and sugar yield in *S. viridis*.

Keywords: aquaporin, stem, water transport, sugar accumulation, grasses

INTRODUCTION

The panicoid grasses sugarcane (*Saccharum officinarum*), sorghum (*Sorghum bicolor*), switchgrass (*Panicum virgatum*), and miscanthus (*Miscanthus X giganteum*) provide the majority of soluble sugars and lignocellulosic biomass used for food and biofuel production worldwide (Somerville et al., 2010; Waclawovsky et al., 2010). A closely related grass with a smaller genome, *Setaria viridis*, is used as a model for these crops in photosynthesis research and for the study of biomass generation and sugar accumulation (Li and Brutnell, 2011; Bennetzen et al., 2012; Brutnell et al., 2015; Martin et al., 2016). The mechanisms that regulate cell expansion and photoassimilate delivery in

the stems of these grasses are of interest because they influence the yields of soluble sugars and cell wall biomass produced (Byrt et al., 2011).

Grass stems have repeating units consisting of an internode positioned between two nodes that grow from intercalary meristems at the base; sugar, primarily sucrose, accumulates and is stored in mature cells at the top of the internode (Grof et al., 2013). Along this developmental gradient there is also a transition from synthesis and deposition of primary cell walls through to establishment of thicker secondary cell walls. Sucrose that is not used for growth and maintenance is primarily accumulated intracellularly in the vacuoles of storage parenchyma cells that surround the vasculature (Glasziou and Gayler, 1972; Hoffmann-Thoma et al., 1996; Rae et al., 2005) or in the apoplasm (Tarpley et al., 2007). The mature stems of grasses such as sugarcane can accumulate up to 1M sucrose, with up to 428 mM sucrose stored in the apoplasm (Hawker, 1985; Welbaum and Meinzer, 1990). In addition to a high capacity for soluble sugar storage, carbohydrates are also stored in cell walls of stem parenchyma cells (Botha and Black, 2000; Ermawar et al., 2015; Byrt et al., 2016a).

Historically, increases in sugar yields in the stems of panicoid grasses have been achieved by increasing sugar concentration in stem cells without increasing plant size (McCormick et al., 2009). Sugarcane and sorghum stem sugar content has been increased by years of selecting varieties with the highest culm sucrose content, but these gains have begun to plateau (Grof and Campbell, 2001; Pfeiffer et al., 2010). It may be that we are approaching a physiological ceiling that limits the potential maximum sucrose concentration in the stems of these grasses. Increasing the size of grass stems as a sink may be an effective strategy to increase stem biomass and the potential for greater soluble sugar yield as a relationship exists between stem size and capacity to import and accumulate photoassimilates (sink strength) as soluble sugars or cell wall carbohydrates. Hence, improved stem sugar yields have also been achieved in some sorghum hybrids by expanding stem volume through increased plant height and stem diameter (Pfeiffer et al., 2010; Slewinski, 2012).

In elongating stems, water and dissolved photoassimilates are imported from the phloem into the stem by bulk-flow, or translocation, to drive cell expansion or otherwise be used for growth, development and storage (Schmalstig and Cosgrove, 1990; Wood et al., 1994). In non-expanding storage sinks, water delivering sucrose is likely to be effluxed to the apoplasm and then recycled into the xylem transportation stream to be exported to other tissues (Lang and Thorpe, 1989; Lang, 1990). In addition to vacuolar accumulation of sugars delivered for storage, sugars may also accumulate in the apoplasm with apoplastic barriers preventing leakage back into the vasculature (Moore, 1995; Patrick, 1997).

The flow of water from the phloem into growth and storage sinks involves the diffusion of water across plant cell membranes facilitated by aquaporins (Kaldenhoff and Fischer, 2006; Zhang et al., 2007). Aquaporins are a highly conserved family of transmembrane channel proteins that enable plants to rapidly and reversibly alter their membrane water permeability or permeability to other solutes depending on

the isoform. In maize (*Zea mays*) and rice (*Oryza sativa*) genomes 30–70 aquaporin homologs have been identified, respectively (Chaumont et al., 2001; Sakurai et al., 2005). These large numbers of isoforms can be divided into five sub-families by sequence homology; plasma membrane intrinsic proteins (PIPs), tonoplast intrinsic proteins (TIPs), nodulin-like intrinsic proteins (NIPs), and small basic intrinsic proteins (SIPs; Johanson and Gustavsson, 2002). In dicotyledonous plants but not monocotyledonous plants there is also a group referred to as X intrinsic proteins (XIPs; Danielson and Johanson, 2008).

As aquaporins have important roles in controlling water potential, they are prospective targets for manipulating stem biomass and sugar yields (Maurel, 1997). The crucial role of aquaporins in water delivery to expanding tissues and water recycling in mature tissues is indicated by their high expression in these regions (Barrieu et al., 1998; Chaumont et al., 1998; Wei et al., 2007). Here, we explore the transcriptional regulation of aquaporins in meristematic, expanding, transitional and mature *S. viridis* internodal tissues to identify candidate water channels involved in cell expansion and water recycling after sugar delivery in mature internode tissues.

MATERIALS AND METHODS

Phylogenetic Tree

Setaria viridis aquaporins were identified from *S. italica* (Azad et al., 2016), *Arabidopsis* (Johanson et al., 2001), rice (Sakurai et al., 2005), barley (Hove et al., 2015) and maize (Chaumont et al., 2001) aquaporins, and predicted *S. viridis* aquaporins from transcriptomic data (Martin et al., 2016) (Supplementary Table S1) using the online HMMER tool phmmmer (Finn et al., 2015¹). Protein sequences used to generate the phylogenetic tree were obtained for *S. viridis* and *Z. mays* from Phytozome 11.0.5 (*S. viridis* v1.1, DOE-JGI²; last accessed July 19, 2016) (Supplementary Table S2). The phylogenetic tree was generated using the neighbor-joining method in the Geneious Tree Builder program (Geneious 9.0.2).

Elongating Internode Transcriptome Analysis and Aquaporin Candidate Selection

Expression data on identified *S. viridis* aquaporins was obtained from a transcriptome generated from *S. viridis* internode tissue (Martin et al., 2016). Protein sequences of selected putative aquaporin candidates expressed in the elongating *S. viridis* transcriptome were analyzed by HMMscan (Finn et al., 2015¹).

Plant Growth Conditions

Seeds of *S. viridis* (Accession-10; A10) were grown in 2 L pots, two plants per pot, in a soil mixture that contained one part

¹<http://www.ebi.ac.uk/Tools/hmmer/>

²<http://phytozome.jgi.doe.gov/>

coarse river sand, one part perlite, and one part coir peat. The temperatures in the glasshouse, located at the University of Newcastle (Callaghan, NSW, Australia) were 28°C during the day (16 h) and 20°C during the night (8 h). The photoperiod was artificially extended from 5 to 8 am and from 3 to 9 pm by illumination with 400 W metal halide lamps suspended ~40 cm above the plant canopy. Water levels in pots were maintained with an automatic irrigation system that delivered water to each pot for 2 min once a day. Osmocote® exact slow release fertilizer (Scotts Australia Pty Ltd, Sydney, NSW, Australia) was applied at 20 g per pot, 2 weeks post-germination. Additional fertilization was applied using Wuxal® liquid foliar nutrient and Wuxal® calcium foliar nutrient (AgNova Technologies, Box Hill North, VIC, Australia) alternately each week.

Harvesting Plant Tissues, RNA Extraction, and cDNA Library Synthesis

Harvesting of plant material from a developing internode followed Martin et al. (2016). Total RNA was isolated from plant material ground with mortar and pestle cooled with liquid nitrogen, using Trizol® Reagent (Thermo Fisher Scientific, Scoresby, VIC, Australia) as per manufacturer's instruction. Genomic DNA was removed using an Ambion TURBO DNase Kit (Thermo Fisher Scientific) following the manufacturer's instructions. cDNA was synthesized from 230 ng of isolated RNA from the cell expansion, transitional, and maturing developmental zones as described in Martin et al. (2016) using the Superscript III cDNA synthesis kit (Thermo Fisher Scientific) with an oligo d(T) primer and an extension temperature of 50°C as per the manufacturer's instructions.

Reverse-Transcriptase Quantitative PCR (RT-qPCR)

Reverse-transcriptase-qPCR was performed using a Rotor-Gene Q (QIAGEN, Venlo, Netherlands) and GoTaq® Green Master Mix 2x (Promega, Madison, WI, USA). A two-step cycling program was used following the manufacturer's instructions. The green channel was used for data acquisition. Gene expression of the candidate genes was measured as relative to the housekeeper *S. viridis* PP2A (*SvPP2A*; accession no.: Sevir.2G128000). The *PP2A* gene was selected as a housekeeper gene because it is established as a robust reference gene in many plant species (Czechowski et al., 2005; Klie and Debener, 2011; Bennetzen et al., 2012) and it was consistently expressed across the developmental internode gradient in the transcriptome and cDNA libraries (Martin et al., 2016; Supplementary Figure S1). The forward (F) and reverse (R) primers used for RT-qPCR for were: *SvPIP2;1-F* (5'-CTCTACATCGTGGCGCAGT-3') and *SvPIP2;1-R* (5'-ACGAAGGTGCCGATGATCT-3'), and *SvNIP2;2-F* (5'-AGTCACGGGAGCGATGT-3') and *SvNIP2;2-R* (5'-CTAACCCGGCCAATCAC-3'). *SvPIP2;1* and *SvNIP2;2* primer sets amplified 161 and 195 base pair fragments from the CDS, respectively. *SvPP2A* primer set sequences were *SvPP2A-F* (5'-GGCAACAAGAAGCTCACTCC-3') and *SvPP2A-R* (5'-TTGCACATCAATGGAATCGT-3') and amplified a 164 base pair fragment from the 3'UTR.

Gene Co-expression Network Analysis

Raw FPKM values of putative aquaporins and sugar transporters were extracted from the *S. viridis* elongating internode transcriptome (Martin et al., 2016). Putative *S. viridis* sugar transporters from the Sucrose Transporter (SUT), Sugar Will Eventually be Exported Transporter (SWEET), and Tonoplast Monosaccharide Transporter (TMT) families were identified by homology to rice SUT, SWEET, and TMT genes (Supplementary Table S3; Supplementary Figures S2–S4). FPKM values were normalized by Log₂ transformation and Pearson's correlation coefficients calculated by Metscape (Karnovsky et al., 2012). A gene network was generated for Pearson's correlation coefficients between 0.8 and 1.0 and visualized with the Metscape app in Cytoscape v3.4.0. Significance of Pearson's correlation coefficients were calculated using SPSS (IBM Corp. Released 2013. IBM SPSS Statistics for Windows, Version 22.0. Armonk, NY, USA) (Supplementary Table S4). The 1.5Kb 5' promoter region, directly upstream of the transcriptional start site, of the two aquaporin candidates and the highly correlated putative sugar transporter genes were screened for the presence of *cis*-acting regulatory elements registered through the PlantCARE online database (Lescot et al., 2002³) and *cis*-acting elements of *Arabidopsis* and rice SUT genes reported by Ibraheem et al. (2010).

Photometric Swelling Assay

Extracted consensus coding sequences for *SvPIP2;1* and *SvNIP2;2*, from *S. viridis* transcriptome data (Martin et al., 2016), were synthesized commercially by GenScript (Piscataway, NJ, USA). *SvPIP2;1* and *SvNIP2;2* cDNA fragments were inserted into a gateway enabled pGEMHE vector. pGEMHE constructs were linearized using NheI (New England Biolabs, Ipswich, MA, USA) and purified using the MinElute PCR Purification Kit (QIAGEN). Complimentary RNA (cRNA) for *SvPIP2;1* and *SvNIP2;2* was transcribed using the Ambion mMessage mMachine Kit (Life Technologies, Carlsbad, CA, USA).

Xenopus laevis oocytes were injected with 46 ng of *SvPIP2;1* or *SvNIP2;2* cRNA in 46 µL of water, or 46 µL of water alone as a control. Injected oocytes were incubated for 72 h in Ca-Ringer's solution. Prior to undertaking permeability assays oocytes were transferred into ND96 solution pH 7.4 (96 mM NaCl, 2 mM KCl, 1.8 mM CaCl₂, 1 mM MgCl₂, 500 µg.mL⁻¹ Streptomycin, 500 µg.mL⁻¹ Tetracycline; 204 osmol/L) and allowed to acclimate for 30 min. Oocytes were then individually transferred into a 1:5 dilution of ND96 solution (42 osmol/L), pH 7.4, and swelling was measured for 1 min for *SvPIP2;1* injected oocytes and 2 min for *SvNIP2;2* injected oocytes. Oocytes were viewed under a dissecting microscope (Nikon SMZ800 light microscope, Japan) at 2× magnification. The changes in volume were captured with a Vicam color camera (Pacific Communications, Australia) at 2× magnification and recorded with IC Capture 2.0 software (The Imagine Source, US) as AVI format video files. Images were acquired every 2.5 s for 2 min measurements and every 2 s for 1 min measurements. The osmotic permeability (*P_f*) was calculated for water injected

³<http://bioinformatics.psb.ugent.be/webtools/plantcare/html/>

and cRNA injected oocytes from the initial rate of change in relative volume (dV_{rel}/dt)_I determined from the cross sectional area images captured assuming the oocytes were spherical:

$$P_f = \frac{V_i \times (dV_{rel}/dt)_i}{A_i \times V_w \times \Delta C_0},$$

Where V_i and A_i are the initial volume and area of the oocyte, respectively, V_w is the partial molar volume of water and ΔC_0 is the change in external osmolality. The osmolality of each solution was determined using a Fiske® 210 Micro-Sample freezing point osmometer (Fiske, Norwood, MA, USA). pH inhibition of oocyte osmotic permeability was determined as above where oocytes were bathed in 1:5 diluted ND96 solution with the addition of 50 mM Na-Acetate, pH 5.6. Topological prediction models of SvPIP2;1 and SvNIP2;2 were generated in TMHMM⁴ (Krogh et al., 2001) and TMRPres-2D (Spyropoulos et al., 2004) to assess potential mechanisms of pH gating.

RESULTS

Identification of Putative *Setaria viridis* Aquaporins

Previously published *S. viridis* elongating internode transcriptome data (Martin et al., 2016), and protein sequences of aquaporins identified in *Arabidopsis*, *S. italica*, barley, maize and rice were used to identify genes predicted to encode aquaporins that were highly expressed in stages of cell expansion and sugar accumulation. The nomenclature assigned to the putative aquaporins followed their relative homology to previously named maize aquaporins determined by phylogenetic analysis of protein sequences (Chaumont et al., 2001; Figure 1). *S. viridis* 41 full length aquaporins were identified: 12 PIPs, 14 TIPs, 12 NIPs, and three SIPs. One predicted aquaporin identified in the genome, transcript Sevir.6G061300.1, has very high similarity to SvNIP5;3 (Sevir.6G06000.1) but may be a pseudogene as it has two large deletions in the transcript relative to SvNIP5;3. Sevir.6G061300.1 only encodes for two out of the typical six transmembrane domains characteristic of aquaporins, and no transcripts have been detected in any of the *S. viridis* RNA-seq libraries available through the Joint Genome Institute (JGI) Plant Gene Atlas Project (Grigoriev et al., 2011). Another truncated NIP-like transcript, Sevir.5G141800.1, was identified. It is predicted to encode a protein 112 amino acids in length with only two transmembrane domains. As it is unlikely to generate an individually functioning aquaporin it has not been named. However, unlike Sevir.6G061300.1, Sevir.5G141800.1 was included in the phylogenetic tree as it was shown to be highly expressed in several tissue types in *S. viridis* RNA-seq libraries available through the JGI Plant Gene Atlas Project (Grigoriev et al., 2011) and may be of interest to future studies of *Setaria* aquaporin-like genes.

⁴<http://www.cbs.dtu.dk/services/TMHMM/>

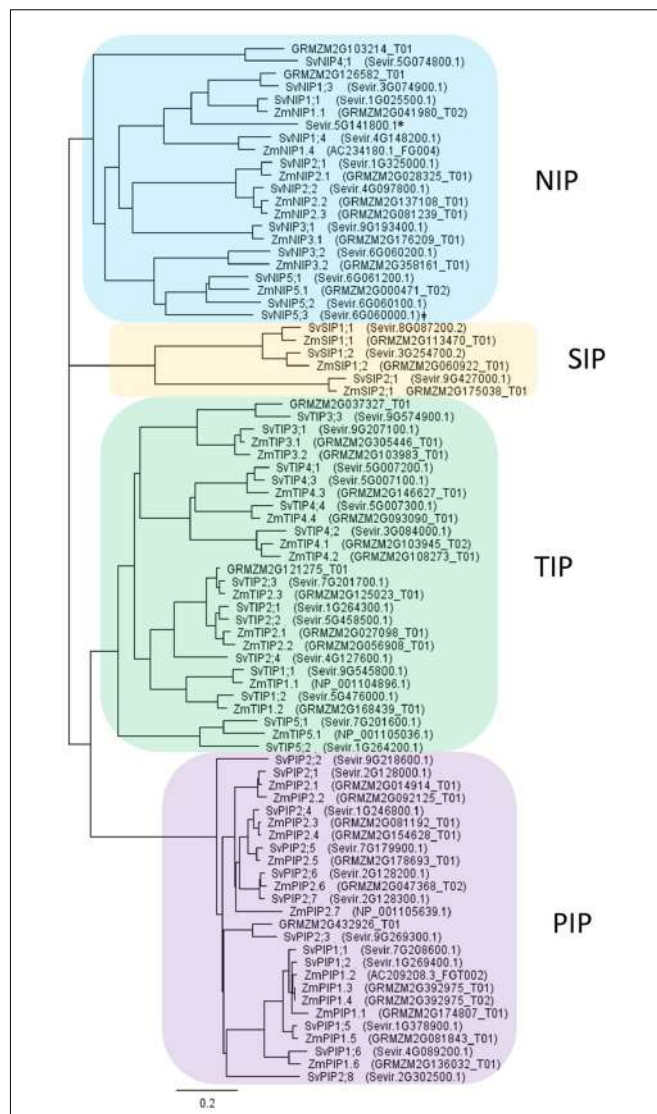


FIGURE 1 | Phylogenetic tree based on protein sequences of aquaporins from *Setaria viridis* and *Zea mays*. *S. viridis* aquaporins were identified in the genome via HMMER search using aquaporin sequences from *Arabidopsis*, barley, maize, and rice. Maize aquaporins were included in the phylogenetic tree for ease of interpretation. The addition of aquaporin sequences from other grasses did not change the groupings. Tree was generated by neighbor-joining method using the Geneious Tree Builder program, Geneious 9.0.2. The scale bar indicates the evolutionary distance, expressed as changes per amino acid residue. Aquaporins can be grouped into four subfamilies: PIPs (plasma membrane intrinsic proteins), NIPs (nudlin-like intrinsic proteins), and SIPs (small basic intrinsic proteins). *Sevir.5G141800.1 protein sequence is truncated, 112 amino acids in length. [†]SvNIP5;3 (Sevir.6G06000.1) may have a related pseudogene Sevir.6G061300.1.

Analysis of *Setaria viridis* Aquaporin Transcripts in Stem Regions

We compared the relative transcript levels of putative *S. viridis* aquaporin encoding genes in the different developmental regions of an elongating internode (Figure 2). We observed that SvPIP1;2

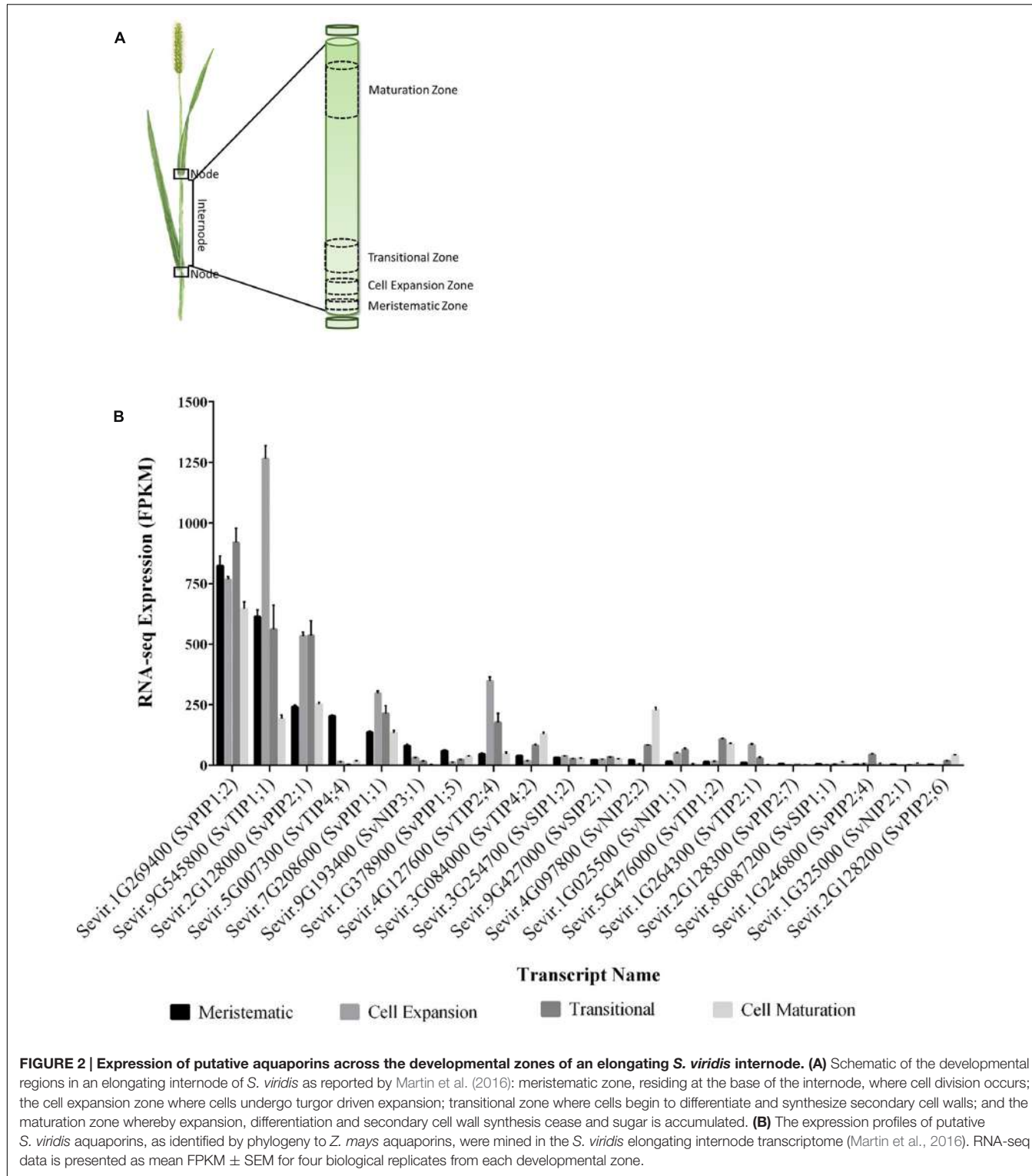


FIGURE 2 | Expression of putative aquaporins across the developmental zones of an elongating *S. viridis* internode. (A) Schematic of the developmental regions in an elongating internode of *S. viridis* as reported by Martin et al. (2016): meristematic zone, residing at the base of the internode, where cell division occurs; the cell expansion zone where cells undergo turgor driven expansion; transitional zone where cells begin to differentiate and synthesize secondary cell wall synthesis cease and sugar is accumulated. **(B)** The expression profiles of putative *S. viridis* aquaporins, as identified by phylogeny to *Z. mays* aquaporins, were mined in the *S. viridis* elongating internode transcriptome (Martin et al., 2016). RNA-seq data is presented as mean FPKM \pm SEM for four biological replicates from each developmental zone.

transcripts were abundant in all regions; and *SvTIP1;1* transcripts were also abundant, particularly in cell expansion regions. *SvPIP2;1*, *SvPIP1;1*, *SvTIP2;2*, and *SvTIP2;1* transcripts were detected in all regions with the highest transcript levels in cell expansion and transitional regions. Transcripts for *SvTIP4;4*,

SvNIP3;1, and *SvPIP1;5* were highest in the meristem relative to other regions; whereas *SvTIP4;2*, *SvNIP2;2*, and *SvTIP1;2* transcripts were at their highest in transitional or mature regions. Low transcript levels were observed for *SvSIP1;2*, *SvNIP1;1*, and *SvPIP2;4* in all regions, with maximum transcripts for

SvNIP1;1 and *SvPIP2;4* detected in the transitional region, and very low transcript levels were detected for *SvPIP2;6*, *SvSIP1;1*, and *SvNIP2;1*.

Overall the highest aquaporin transcript levels detected across the internode developmental zones were those of *SvPIP1;2* (**Figure 2**). Previous research has indicated that the related *ZmPIP1;2* interacts with PIP2 subgroup proteins targeting PIP2s to plasma membrane, and a number of PIP1 aquaporins are not associated with osmotic water permeability when expressed alone in oocytes (Fetter et al., 2004; Luu and Maurel, 2005; Zelazny et al., 2007). Our interest lay in identifying water permeable aquaporins that might be preferentially involved in delivering water to the growing stem cells and in sucrose accumulation in mature stem regions. As candidates *SvPIP2;1* and *SvNIP2;2* met these criteria we focussed on these two genes. *SvPIP2;1* had the high transcript levels in the region of cell expansion and transcript levels of *SvNIP2;2* were highest in mature stem regions (**Figure 2B**). The protein sequences of *SvPIP2;1* and *SvNIP2;2* were analyzed by the HMMER tool HMMscan which identified these candidates as belonging to the aquaporin (Major Intrinsic Protein) protein family.

To confirm our RNA-seq expression profile observations, we measured the transcript levels of *SvPIP2;1* and *SvNIP2;2* in the *S. viridis* internode regions by RT-qPCR. Stem samples were harvested from *S. viridis* plants grown under glasshouse conditions with the light period artificially supplemented by use of metal halide lamps to replicate as closely as possible the conditions used by Martin et al. (2016) for the RNA-seq analysis. We assessed the relative fold change of gene expression normalized to the cell expansion zone and similar trends were observed for the RT-qPCR expression data compared to the RNA-seq transcriptome data (**Figure 3**). *SvPIP2;1* transcript levels were high in the cell expansion region and decreased toward the maturation region and *SvNIP2;2* transcript levels were highest in mature stem tissues.

We are interested in the coordination of water and sugar transport related processes in developing grass stems. As a tool to investigate this, we further analyzed the stem transcriptome data to test whether any aquaporin and sugar transport related genes were co-expressed. Putative *S. viridis* sugar transporters were identified from the internode transcriptome (Martin et al., 2016) by homology to the rice sugar transporter families: SUTs, SWEETs, and TMTs (Supplementary Figures S2–S4). A co-expression gene network of the aquaporins and sugar transporters expressed in the *S. viridis* stem was generated in Cytoscape v3.4.0 using Pearson's correlation coefficients calculated by MetScape (Karnovsky et al., 2012) (**Figure 4**). This analysis revealed that for a number of aquaporins and sugar transport related genes there was a high correlation in expression: *SvPIP2;1* expression correlated with the expression of *SvPIP2;3*, *SvTIP2;1*, and *SvNIP1;1* (0.8–0.9); and the correlation coefficients for co-expression of *SvPIP2;1* with *SvPIP2;5*, *SvTIP4;1*, *SvTIP1;2*, and *SWEET1a* were in the range of 0.8–0.9. Most notable was the high correlation (0.95–1.0) of expression of *SvNIP2;2* with sugar transport related genes *SvSUT5*, *SvSUT1*, *SvSWEET4a* and with *SvTIP4;2* and *SvPIP2;6*. The correlation between expression of *SvNIP2;2* and *SvSWEET13b* and *SvSWEET16* was also high

(0.9–0.95). The *cis*-acting regulatory elements of the promoter regions of the aquaporin candidates *SvNIP2;2* and *SvPIP2;1*, and the putative sugar transporter genes *SvSUT1*, *SvSUT5*, and *SvSWEET4a* were analyzed (Supplementary Figure S5). There was no obvious relationship between the correlation of expression of *SvNIP2;2* and *SvSUT1*, *SvSUT5* and *SvSWEET4a* and their *cis*-acting regulatory elements.

Characterisation of *Setaria viridis* PIP2;1 and NIP2;2 in *Xenopus laevis* Oocytes

To explore whether the proteins encoded by *SvPIP2;1* and *SvNIP2;2* function as water channels they were expressed in the heterologous *X. laevis* oocytes system. Water with or without 46 ng of *SvPIP2;1* and *SvNIP2;2* cRNA was injected into oocytes and the swelling of these oocytes in response to bathing in a hypo-osmotic solution (pH 7.4) was measured (**Figure 5A**). The osmotic permeability (P_f) of cRNA injected oocytes was calculated and compared to the osmotic permeability of water injected oocytes. Water injected oocytes had a P_f of $0.60 \pm 0.08 \times 10^{-2}$ mm s $^{-1}$. Relative to water injected control oocytes *SvPIP2;1* and *SvNIP2;2* cRNA injected oocytes had significantly higher P_f of $14.13 \pm 1.66 \times 10^{-2}$ mm s $^{-1}$ and $3.22 \pm 0.28 \times 10^{-2}$ mm s $^{-1}$, respectively ($p < 0.05$).

The effect of lowering oocyte cytosolic pH was determined by bathing oocytes in an external hypo-osmotic solution at pH 5.6 with the addition of Na-Acetate (**Figure 5B**). Reduced osmotic permeability of the cRNA injected oocyte membrane was observed in response to the low pH treatment. A reduction in P_f was observed for *SvPIP2;1* and *SvNIP2;2* cRNA injected oocytes bathed in an external hypo-osmotic solution at pH 5.6 relative to the pH 7.4 solution indicating that *SvPIP2;1* and *SvNIP2;2* have pH gating mechanisms (**Figure 5B**). Water injected oocytes in the pH 5.6 Na-Acetate solution had P_f of $0.84 \pm 0.13 \times 10^{-2}$ mm s $^{-1}$. *SvNIP2;2* and *SvPIP2;1* cRNA injected oocytes in the pH 5.6 solution had significantly lower P_f of $2.46 \pm 0.32 \times 10^{-2}$ mm s $^{-1}$ and $0.97 \pm 0.13 \times 10^{-2}$ mm s $^{-1}$, respectively, compared to those in pH 7.4 solution ($p < 0.05$). *SvPIP2;1* and *SvNIP2;2* associated osmotic permeability and pH gating observations indicate that these proteins can function as water channels. The mechanism of pH gating for other plant aquaporins is the protonation of a Histidine residue in the Loop D structure; topological modeling of *SvPIP2;1* and *SvNIP2;2* predicted that the Loop D of *SvPIP2;1* contains a Histidine residue while *SvNIP2;2* Loop D does not contain a His residue (Supplementary Figure S6).

DISCUSSION

Roles of Aquaporins in Grass Stem Development

On the basis of amino acid sequence comparison with known aquaporins in *Arabidopsis*, rice and maize, the genomes of sugarcane, sorghum and *S. italica* include 42, 41, and 42 predicted aquaporin encoding genes, respectively (da Silva et al., 2013; Reddy et al., 2015; Azad et al., 2016). In *S. viridis* 41 aquaporin encoding genes were identified that group into four clades

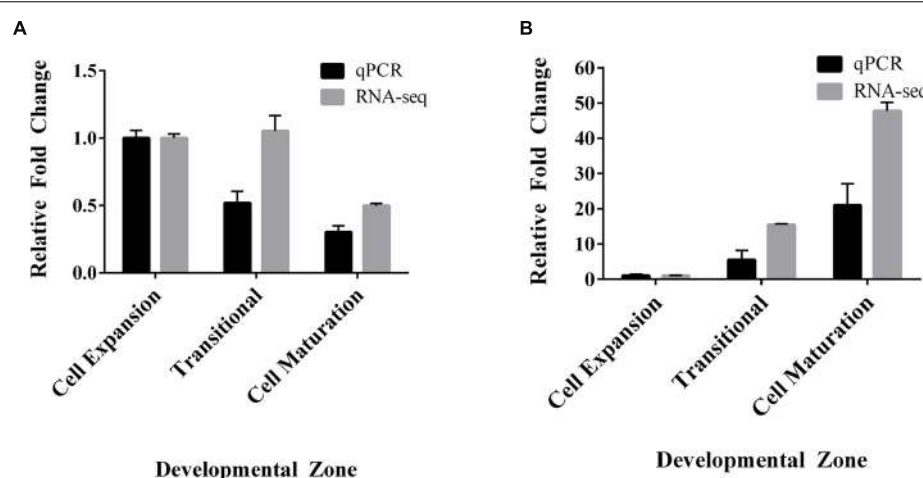


FIGURE 3 | Comparison of relative fold changes between RNA-seq and RT-qPCR of *SvPIP2;1* and *SvNIP2;2* in an elongating internode of *S. viridis*. (A) *SvPIP2;1*. (B) *SvNIP2;2*. Data is mean relative fold change in expression \pm SEM. Data for RNA-seq and RT-qPCR was normalized relative to the cell expansion zone expression level.

corresponding to NIPs, TIPs, SIPs, and PIPs (Figure 1). We note that Azad et al. (2016) named the *Setaria* aquaporins in an order consecutive with where they are found in the genome. For ease of comparing related aquaporins in C₄ grasses of interest, we named the *Setaria* aquaporins based on their homology to previously named maize aquaporins (Figure 1) (Chaumont et al., 2001), of course high homology and the same name does not infer the same function. In the *S. viridis* elongating internode transcriptome, we detected transcripts for 19 putative aquaporin encoding genes, including 5 NIPs, 6 TIPs, 2 SIPs, and 6 PIPs (Figures 2 and 3; Martin et al., 2016). In mature *S. viridis* internode tissues, the transcript levels of TIPs and NIPs was generally low with the exception of *SvNIP2;2*, *SvTIP4;2*, and *SvTIP1;2*. In a sorghum stem transcriptome report investigating SWEET gene involvement in sucrose accumulation, we note that transcripts for all 41 sorghum aquaporins were detected in pith and rind tissues in 60-day-old plants (Reddy et al., 2015; Mizuno et al., 2016). Of those 41 aquaporins the expression of 16, primarily NIPs and TIPs, was relatively low. However, *PIP1;2*, *PIP2;1*, and *NIP2;2* homologs were all highly expressed in pith and rind of sorghum plants after heading, which is consistent with our findings for the *S. viridis* homologs of these genes (Figure 2; Mizuno et al., 2016). Comparisons with other gene expression studies for C₄ grass stem tissues were not possible as in most studies the internode tissue has not been separated into different developmental zones or the study has not reported aquaporin expression (Carson and Botha, 2000, 2002; Casu et al., 2007).

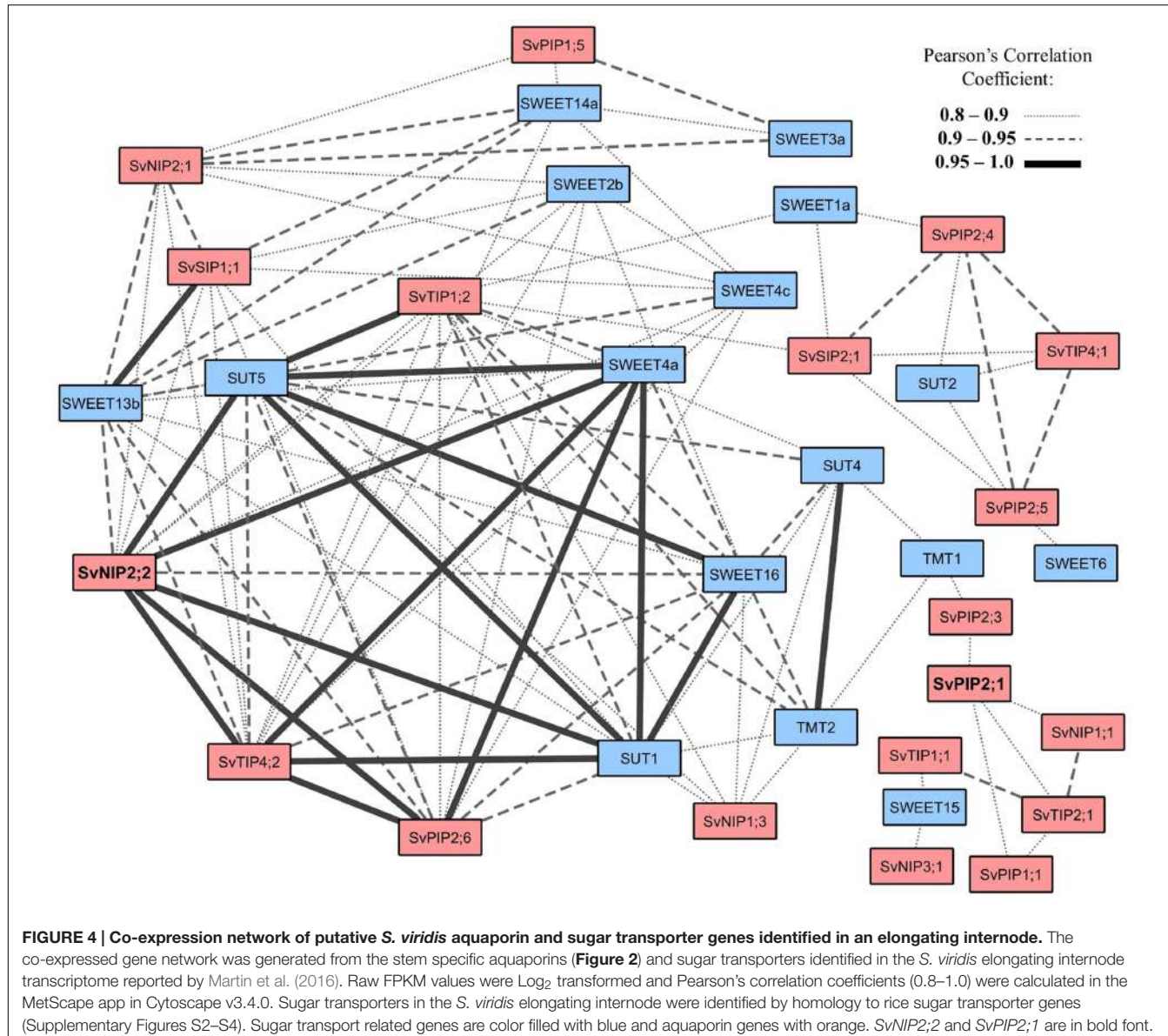
Relationships between Sink Strength, Sink Size, Water Flow, and the Function of Aquaporins

The molecular and physiological mechanisms that determine stem cell number and cell size in turn determine the capacity of the stem as a sink (Ho, 1988; Herbers and Sonnewald, 1998).

Examples have been reported in the literature where stem volume and sucrose concentration has been increased, in sugarcane and sorghum, by increasing cell size (Slewinski, 2012; Patrick et al., 2013). Larger cell size may improve sink strength by increasing membrane surface area available to sucrose transport (increasing import capacity), increasing single cell capacity to accumulate greater concentrations of sucrose in parenchyma cell vacuoles due to increased individual cell volume (increasing storage capacity), and increasing lignocellulosic biomass.

Cell expansion and growth are highly sensitive to water potential. This is because expansion requires a continuous influx of water into the cell to maintain turgor pressure (Hsiao and Acevedo, 1974; Cosgrove, 1986, 2005). The diffusion of water across a plant cell membrane is facilitated by aquaporins (Kaldenhoff and Fischer, 2006). Aquaporins function throughout all developmental stages, but several PIP aquaporins have been found to be particularly highly expressed in regions of cell expansion (Chaumont et al., 1998; Maurel et al., 2008; Besse et al., 2011). Here, we report that in the *S. viridis* internode, *SvPIP2;1* was highly expressed in regions undergoing cell expansion (Figure 2). Positive correlations have been reported for the relationship between PIP mRNA and protein expression profiles of PIP isoforms in the expanding regions of embryos, roots, hypocotyls, leaves, and reproductive organs indicating that gene expression is a key mechanism to regulate PIP function (Maurel et al., 2002; Hachez et al., 2008; Liu et al., 2008). Therefore, high expression of *SvPIP2;1* in the expanding zone of *S. viridis* internodes indicates that this gene may be involved in the process of water influx in this tissue to maintain turgor pressure for growth.

The roles of a number of PIP proteins in hydraulic conductivity in plant roots and leaves have been reported but PIP function in stems is largely unexplored. The regulation of the hydraulic properties of expanding root tissues by PIP expression was analyzed by Péret et al. (2012) and they reported



that auxin mediated reduction of *Arabidopsis thaliana* (At) PIP gene expression resulted in delayed lateral root emergence. Previously AtPIP2;2 anti-sense mutants were reported to have lower (25–30%) hydraulic conductivity of root cortex cells than control plants (Javot et al., 2003). PIP2 family aquaporins, involved in cellular water transport in roots have also been linked to water movement in leaves, seeds, and reproductive organs (Schuurmans et al., 2003; Bots et al., 2005). The roles of PIP proteins in maintenance of hydraulic conductivity and cell expansion in stems are likely to be equally as important as the roles reported for PIPs in the expanding tissues of roots and leaves. One study in rice reported OsPIP1;1 and OsPIP2;1 as being highly expressed in the zone of cell expansion in rapidly growing internodes (Malz and Sauter, 1999). Expression analysis of sugarcane genes associated with sucrose content identified that some unnamed PIP isoforms were highly expressed in

immature internodes, and in high sugar yield cultivars (Papini-Terzi et al., 2009). Proteins from the PIP2 subfamily in particular in maize, spinach and *Arabidopsis* have been shown to be highly permeable to water (Johansson et al., 1998; Chaumont et al., 2000; Kaldenhoff and Fischer, 2006). Here, we demonstrate, by expression of *SvPIP2;1* in *Xenopus* oocytes and analysis of water permeability, that this protein functions as a water channel (**Figure 5A**).

Aquaporin Function and Sugar Accumulation in Mature Grass Stems

The accumulation of sucrose to high concentrations in panicle stems rapidly increases with the cessation of cell expansion, which is also associated with the deposition of secondary cell walls (Hoffmann-Thoma et al., 1996). In the mature regions of the stem internodes, imported sucrose is no longer required for

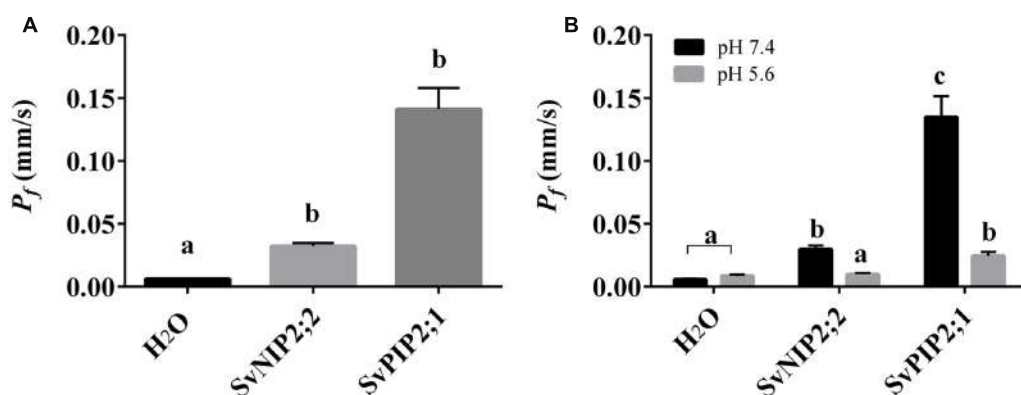


FIGURE 5 | Osmotic permeability (P_f) of *Xenopus laevis* oocytes injected with *SvNIP2;2* and *SvPIP2;1* cRNA. (A) Osmotic permeability (P_f) of water (H_2O) injected and *SvNIP2;2* and *SvPIP2;1* cRNA (46 ng) injected oocytes. Oocytes were transferred into a hypo-osmotic solution, pH 7.4, and P_f was calculated by video monitoring of the rate of oocyte swelling. **(B)** Effect of lowering oocyte cytosolic pH on osmotic permeability (P_f) of H_2O and *SvNIP2;2* and *SvPIP2;1* cRNA injected oocytes by bathing in hypo-osmotic solution supplemented with 50 mM Na-acetate, pH 5.6. $n = 12\text{--}14$; a = non-significant; b = $p < 0.05$; c = $p < 0.005$.

growth, development, or as a necessary precursor to structural elements and it is stored in the vacuoles of ground parenchyma cells or the apoplasm (Rae et al., 2009). Phloem unloading and the delivery of sucrose to these storage cells may occur via an apoplastic pathway as in sorghum or a symplasmic pathway as in sugarcane (Welbaum and Meinzer, 1990; Walsh et al., 2005). The degree of suberisation and/or lignification of cell walls surrounding the phloem may influence stem sucrose storage traits by restricting apoplastic pathways of sucrose transport. In potato tubers and *Arabidopsis* ovules a switch between apoplastic and symplasmic pathways of delivering sucrose to storage sites has been reported (Viola et al., 2001; Werner et al., 2011). Similarly, a switch from symplasmic to apoplastic transport pathways has been proposed for sorghum as internodes approach maturity (Tarpley et al., 2007; Milne et al., 2015). Both apoplastic and symplasmic mechanisms of phloem unloading require the maintenance of low sugar concentration in the cytoplasm of parenchymal storage cells. Control of hydrostatic pressure is facilitated by the sequestration of sucrose into the vacuole by tonoplast localized SUTs or into the apoplasm by plasma membrane localized SUTs (Slewinski, 2011). Members of the SUT and TMT families have been shown to function on the tonoplast to facilitate sucrose accumulation in the vacuole (Reinders et al., 2008; Wingenter et al., 2010; Bihmidine et al., 2016). In mature stem tissue plasma membrane localized SWEETs, SUTs, and possibly some NIPs may have a role in transporting sugar into the apoplasm (Milne et al., 2013; Chen, 2014).

The cell maturation zone is characterized by cells that have ceased expansion and differentiation and have realized their sugar accumulation capacity (Rohwer and Botha, 2001; McCormick et al., 2009). In mature sink tissues, the movement of water and dissolved photoassimilates from the phloem to storage parenchyma cells may be driven by differences in solute concentration and hydrostatic pressure (Turgeon, 2010; De Schepper et al., 2013). However, the movement of water and sucrose by diffusion or bulk-flow requires the

continued maintenance of low cytosolic sucrose concentrations by accumulation of sucrose into the vacuole or efflux into the apoplasm for storage (Grof et al., 2013). Throughout internode development, the internal cell pressure of storage parenchyma cells in sugarcane remains relatively constant despite increasing solute concentrations toward maturation (Moore and Cosgrove, 1991). As mature cells tend to have heavily lignified cell walls that limit the ability of the protoplast to expand in response to water flux the equilibration of storage parenchyma cell turgor is likely to be achieved by the partitioning of sucrose into the vacuole and apoplasm, and efflux of water into the apoplasm (Moore and Cosgrove, 1991; Vogel, 2008; Keegstra, 2010; Moore and Botha, 2013). Phloem water effluxed into the apoplasm may then be recycled back to the vascular bundles (Welbaum et al., 1992).

Members of the NIPs are candidates for water and neutral solute permeation, and some NIPs could have a role in water and solute efflux to the apoplasm in mature stem cells (Takano et al., 2006; Kamiya et al., 2009; Li et al., 2009; Hanaoka et al., 2014). The NIP subfamily is divided into the subgroups NIP I, NIP II, and NIP III based on the composition of the ar/R selectivity filter (Liu and Zhu, 2010). NIP III subgroup homologs have reported permeability to water, urea, boric acid, and silicic acid (Bienert et al., 2008; Ma et al., 2008; Ma and Yamaji, 2008; Li et al., 2009). In grasses NIP2;2 homologs, from the NIP III subgroup, have been shown to localize to the plasma membrane (Ma et al., 2006).

In the *S. viridis* internode, *SvNIP2;2* had relatively high transcript levels in mature stem tissue where sugar accumulates, and it can function as a water channel, although with a relatively low water permeability compared to *SvPIP2;1* (Figures 2 and 5A). Our analysis of gene co-expression in stem tissues revealed high correlation between the expression of *SvNIP2;2* and five putative *S. viridis* sugar transporter genes (Figure 4). Co-expression can indicate that genes are controlled by the same transcriptional regulatory program, may be functionally related, or be members of the same pathway or protein complex (Eisen et al., 1998;

Yonekura-Sakakibara and Saito, 2013). The strong correlation between expression of *SvNIP2;2* and key putative sugar transport related genes such as *SvSUT5*, *SvSUT1*, *SvSWEET4a*, *SvSWEET13b*, and *SvSWEET16* indicates that they may be involved in a related biological process such as stem sugar accumulation. It is likely that one or more of the SWEETs have roles in transporting sugars out of the stem parenchyma cells into the apoplasm. *SvNIP2;2* may be permeable to neutral solutes as well as water and the role of this protein in the mature stem could be in effluxing a solute to adjust osmotic pressure allowing for greater sugar storage capacity. The rice and soybean (*Glycine max* L.) NIP2;2 proteins are permeable to silicic acid and silicon, respectively (Ma et al., 2006; Zhao et al., 2010; Deshmukh et al., 2013). The deposition of silicic acid into the apoplasm, where it associates with the cell wall matrix as a polymer of hydrated amorphous silica (Epstein, 1994; Ma et al., 2004; Coskun et al., 2016), strengthens the culm to reduce lodging events, and increases plant resistance to pathogens and abiotic stress factors (Mitani, 2005).

SvNIP2;2 water permeability was gated by pH (Figure 5B). Gating of water channel activity has been reported for PIPs, including *SvPIP2;1* (Figure 5B), and for the TIP2;1 isoform found in grapevine (Törnroth-Horsefield et al., 2006; Leitao et al., 2012; Frick et al., 2013). The mechanism of pH gating for these AQPs is the protonation of a Histidine residue located on the cytoplasmic Loop D where site-directed mutagenesis studies of the Loop D His residue results in a loss of pH dependent water permeability (Tournaire-Roux et al., 2002; Leitao et al., 2012; Frick et al., 2013). However, although *SvNIP2;2* water permeability was pH dependent the predicted Loop D structure does not contain a His residue (Supplementary Figure S5), hence for *SvNIP2;2* the mechanism for pH gating is not clear.

CONCLUSION

Our observations of high transcript levels of *SvPIP2;1* in expanding *S. viridis* stem regions and high transcript levels of *SvNIP2;2* in mature stems inspired us to test the function of the proteins encoded by these genes. We found that *SvPIP2;1* and *SvNIP2;2* can function as pH gated water channels. We hypothesize that in stem tissues *SvPIP2;1* is involved in cell growth and that *SvNIP2;2* may facilitate water movement and potentially the flow of other solutes into the apoplasm to sustain solute transportation by bulk-flow, and possibly ‘recycle’ water used for solute delivery back to the xylem. It is expected

REFERENCES

- Azad, A. K., Ahmed, J., Alum, A., Hasan, M., Ishikawa, T., Sawa, Y., et al. (2016). Genome-wide characterization of major intrinsic proteins in four grass plants and their non-aqua transport selectivity profiles with comparative perspective. *PLoS ONE* 11:e0157735. doi: 10.1371/journal.pone.0157735
- Barrieu, F., Chaumont, F., and Chrispeels, M. J. (1998). High expression of the tonoplast aquaporin ZmTIP1 in epidermal and conducting tissues of maize. *Plant Physiol.* 117, 1153–1163. doi: 10.1104/pp.117.4.1153
- Bennetzen, J. L., Schmutz, J., Wang, H., Percifield, R., Hawkins, J., Pontaroli, A. C., et al. (2012). Reference genome sequence of the model plant *Setaria*. *Nat. Biotechnol.* 30, 555–564. doi: 10.1038/nbt.2196
- Besse, M., Knipfer, T., Miller, A. J., Verdeil, J.-L., Jahn, T. P., and Fricke, W. (2011). Developmental pattern of aquaporin expression in barley (*Hordeum vulgare* L.) leaves. *J. Exp. Bot.* 62, 4127–4142. doi: 10.1093/jxb/err175
- Bienert, G. P., and Chaumont, F. (2014). Aquaporin-facilitated transmembrane diffusion of hydrogen peroxide. *Biochim. Biophys. Acta.* 1840, 1596–1604. doi: 10.1016/j.bbagen.2013.09.017
- Bienert, G. P., Thorsen, M., Schüssler, M. D., Nilsson, H. R., Wagner, A., Tamás, M. J., et al. (2008). A subgroup of plant aquaporins facilitate the bi-directional

that *SvPIP2;1* could have additional roles, as other PIP water channels have been shown to also be permeable to CO₂, hydrogen peroxide, urea, sodium and arsenic (Siefritz et al., 2001; Uehlein et al., 2003; Mosa et al., 2012; Bienert and Chaumont, 2014; Byrt et al., 2016b). *SvNIP2;2* could have roles such as transporting neutral solutes to the apoplasm, as previous studies report silicic acid, urea, and boric acid permeability for other NIPs (Bienert et al., 2008; Ma et al., 2008; Ma and Yamaji, 2008; Li et al., 2009; Deshmukh et al., 2013). Transporting solutes other than sucrose into the apoplasm in mature stem tissues may be an important part of the processes that supports high sucrose accumulation capacity in grass stem parenchyma cells. The next steps in establishing the respective functions of *SvPIP2;1* and *SvNIP2;2* in stem growth and sugar accumulation in *S. viridis* will require testing of the permeability of these proteins to a range of other solutes and modification of their function *in planta*.

AUTHOR CONTRIBUTIONS

CG conceived and designed the work. SM, HO, LC, and JP acquired the data. SM, ST, CB, and CG analyzed and interpreted the data. SM and CB drafted and revised the work. All authors commented on the manuscript. SM, ST, RF, CB, and CG revised the work critically for intellectual content.

FUNDING

This research was supported by The Australian Research Council (ARC) Centre of Excellence in Plant Energy Biology (CE140100008) and CB (ARC DE150100837).

ACKNOWLEDGMENT

We thank Wendy Sullivan for preparation of oocytes. We thank Kate Hutcheon for advice on qPCR and Antony Martin for comments on early planning documents and cloning plans.

SUPPLEMENTARY MATERIAL

The Supplementary Material for this article can be found online at: <http://journal.frontiersin.org/article/10.3389/fpls.2016.01815/full#supplementary-material>

- diffusion of As(OH)3 and Sb(OH)3 across membranes. *BMC Biol.* 6:26. doi: 10.1186/1741-7007-6-26
- Bihmidine, S., Julius, B. T., Dweikat, I., and Braun, D. M. (2016). Tonoplast sugar transporters (SbTSTs) putatively control sucrose accumulation in sweet sorghum stems. *Plant Signal. Behav.* 11:e1117721. doi: 10.1080/15592324.2015.1117721
- Botha, F. C., and Black, K. G. (2000). Sucrose phosphate synthase and sucrose synthase activity during maturation of internodal tissue in sugarcane. *Aust. J. Plant Physiol.* 27, 81–85.
- Bots, M., Feron, R., Uehlein, N., Weterings, K., Kaldenhoff, R., and Mariani, T. (2005). PIP1 and PIP2 aquaporins are differentially expressed during tobacco anther and stigma development. *J. Exp. Bot.* 56, 113–121.
- Brutnell, T. P., Bennetzen, J. L., and Vogel, J. P. (2015). Brachypodium distachyon and *Setaria viridis*: Model genetic systems for the grasses. *Annu. Rev. Plant Biol.* 66, 465–485. doi: 10.1146/annurev-aplant-042811-105528
- Byrt, C. S., Betts, N. S., Tan, H.-T., Lim, W. L., Ermawar, R. A., Nguyen, H. Y., et al. (2016a). Prospecting for energy-rich renewable raw materials: sorghum stem case study. *PLoS ONE* 11:e0156638. doi: 10.1371/journal.pone.0156638
- Byrt, C. S., Grof, C. P. L., and Furbank, R. T. (2011). C4 plants as biofuel feedstocks: optimising biomass production and feedstock quality from a lignocellulosic perspective. *J. Integr. Plant Biol.* 53, 120–135. doi: 10.1111/j.1744-7909.2010.01023.x
- Byrt, C. S., Zhao, M., Kourghi, M., Bose, J., Henderson, S. W., Qiu, J., et al. (2016b). Non-selective cation channel activity of aquaporin AtPIP2;1 regulated by Ca²⁺ and pH. *Plant Cell Environ.* doi: 10.1111/pce.12832 [Epub ahead of print].
- Carson, D., and Botha, F. (2002). Genes expressed in sugarcane maturing internodal tissue. *Plant Cell Rep.* 20, 1075–1081. doi: 10.1007/s00299-002-0444-1
- Carson, D. L., and Botha, F. C. (2000). Preliminary analysis of expressed sequence tags for sugarcane. *Crop Sci.* 40:1769. doi: 10.2135/cropsci2000.4061769x
- Casu, R. E., Jarmey, J. M., Bonnett, G. D., and Manners, J. M. (2007). Identification of transcripts associated with cell wall metabolism and development in the stem of sugarcane by Affymetrix GeneChip sugarcane genome array expression profiling. *Funct. Integr. Genomics* 7, 153–167. doi: 10.1007/s10142-006-0038-z
- Chaumont, F., Barrieu, F., Herman, E. M., and Chrispeels, M. J. (1998). Characterization of a maize tonoplast aquaporin expressed in zones of cell division and elongation. *Plant Physiol.* 117, 1143–1152. doi: 10.1104/pp.117.4.1143
- Chaumont, F., Barrieu, F., Jung, R., and Chrispeels, M. J. (2000). Plasma membrane intrinsic proteins from Maize cluster in two sequence subgroups with differential aquaporin activity. *Plant Physiol.* 122, 1025–1034. doi: 10.1104/pp.122.4.1025
- Chaumont, F., Barrieu, F., Wojcik, E., Chrispeels, M. J., and Jung, R. (2001). Aquaporins constitute a large and highly divergent protein family in Maize. *Plant Physiol.* 125, 1206–1215. doi: 10.1104/pp.125.3.1206
- Chen, L.-Q. (2014). SWEET sugar transporters for phloem transport and pathogen nutrition. *New Phytol.* 201, 1150–1155. doi: 10.1111/nph.12445
- Cosgrove, D. (1986). Biophysical control of plant growth. *Ann. Rev. Plant Physiol.* 37, 377–405. doi: 10.1146/annurev.pp.37.060186.002113
- Cosgrove, D. J. (2005). Growth of the plant cell wall. *Nat. Rev. Mol. Cell Biol.* 6, 850–861. doi: 10.1038/nrm1746
- Coskun, D., Britto, D. T., Huynh, W. Q., and Kronzucker, H. J. (2016). The role of silicon in higher plants under salinity and drought stress. *Front. Plant Sci.* 7:1072. doi: 10.3389/fpls.2016.01072
- Czechowski, T., Stitt, M., Altmann, T., Udvardi, M. K., and Scheible, W.-R. (2005). Genome-wide identification and testing of superior reference genes for transcript normalization in *Arabidopsis*. *Plant Physiol.* 139, 5–17. doi: 10.1104/pp.105.063743
- da Silva, M. D., Silva, R. L. D. O., Costa Ferreira Neto, J. R., Guimarães, A. C. R., Veiga, D. T., Chabregas, S. M., et al. (2013). Expression analysis of Sugarcane aquaporin genes under water deficit. *J. Nucleic Acids* 2013, 1–14. doi: 10.1155/2013/763945
- Danielson, J. Å., and Johanson, U. (2008). Unexpected complexity of the Aquaporin gene family in the moss *Physcomitrella patens*. *BMC Plant Biol.* 8:45. doi: 10.1186/1471-2229-8-45
- De Schepper, V., De Swaef, T., Bauweraerts, I., and Steppe, K. (2013). Phloem transport: a review of mechanisms and controls. *J. Exp. Bot.* 64, 4839–4850. doi: 10.1093/jxb/ert302
- Deshmukh, R. K., Vivancos, J., Guerin, V., Sonah, H., Labbe, C., Belzile, F., et al. (2013). Identification and functional characterization of silicon transporters in soybean using comparative genomics of major intrinsic proteins in *Arabidopsis* and rice. *Plant Mol. Biol.* 83, 303–315. doi: 10.1007/s11103-013-0087-3
- Eisen, M. B., Spellman, P. T., Brown, P. O., and Botstein, D. (1998). Cluster analysis and display of genome-wide expression patterns. *Genetics* 95, 14863–14868.
- Epstein, E. (1994). The anomaly of silicon in plant biology. *Proc. Natl. Acad. Sci. U.S.A.* 91, 11–17. doi: 10.1073/pnas.91.1.11
- Ermawar, R. A., Collins, H. M., Byrt, C. S., Henderson, M., O'Donovan, L. A., Shirley, N. J., et al. (2015). Genetics and physiology of cell wall polysaccharides in the model C4 grass, *Setaria viridis* spp. *BMC Plant Biol.* 15:236. doi: 10.1186/s12870-015-0624-0
- Fetter, K., Van Wilder, V., Moshelion, M., and Chaumont, F. (2004). Interactions between plasma membrane aquaporins modulate their water channel activity. *Plant Cell* 16, 215–228. doi: 10.1105/tpc.017194
- Finn, R. D., Clements, J., Arndt, W., Miller, B. L., Wheeler, T. J., Schreiber, F., et al. (2015). HMMER web server: 2015 update. *Nucleic Acids Res.* 43, 30–38. doi: 10.1093/nar/gkv397
- Frick, A., Järvinen, M., and Törnroth-Horsefield, S. (2013). Structural basis for pH gating of plant aquaporins. *FEBS Lett.* 587, 989–993. doi: 10.1016/j.febslet.2013.02.038
- Glasziou, K. T., and Gayler, K. R. (1972). Storage of sugars in stalks of sugar cane. *Bot. Rev.* 36, 471–488. doi: 10.1007/BF02859248
- Grigoriev, I. V., Nordberg, H., Shabalov, I., Aerts, A., Cantor, M., Goodstein, D., et al. (2011). The genome portal of the department of energy joint genome institute. *Nucleic Acids Res.* 42, D26–D31.
- Grof, C. P. L., Byrt, C. S., and Patrick, J. W. (2013). "Phloem transport of resources," in *Sugarcane: Physiology, Biochemistry, and Functional Biology*, eds P. Moore and F. Botha (Chichester: John Wiley & Sons Ltd), 267–305.
- Grof, C. P. L., and Campbell, J. A. (2001). Sugarcane sucrose metabolism: scope for molecular manipulation. *Aust. J. Plant Physiol.* 28, 1–12.
- Hachez, C., Heinen, R. B., Draye, X., and Chaumont, F. (2008). The expression pattern of plasma membrane aquaporins in maize leaf highlights their role in hydraulic regulation. *Plant Mol. Biol.* 68, 337–353. doi: 10.1007/s11103-008-9373-x
- Hanaoka, H., Uraguchi, S., Takano, J., Tanaka, M., and Fujiwara, T. (2014). OsNIP3;1, a rice boric acid channel, regulates boron distribution and is essential for growth under boron-deficient conditions. *Plant J.* 78, 890–902. doi: 10.1111/tpj.12511
- Hawker, J. S. (1985). "Sucrose," in *Biochemistry of Storage Carbohydrates in Green Plants*, eds P. Dey and R. Dixon (New York, NY: Academic Press), 1–51.
- Herbers, K., and Sonnewald, U. (1998). Molecular determinants of sink strength. *Curr. Opin. Plant Biol.* 1, 207–216. doi: 10.1016/S1369-5266(98)80106-4
- Ho, L. C. (1988). Metabolism and compartmentation of imported sugars in sink organs in relation to sink strength. *Ann. Rev. Plant Physiol.* 39, 355–378. doi: 10.1146/annurev.pp.39.060188.002035
- Hoffmann-Thoma, G., Hinkel, K., Nicolay, P., and Willenbrink, J. (1996). Sucrose accumulation in sweet sorghum stem internodes in relation to growth. *Physiologia* 97, 277–284. doi: 10.1034/j.1399-3054.1996.970210.x
- Hove, R. M., Ziemann, M., and Bhave, M. (2015). Identification and expression analysis of the barley (*Hordeum vulgare* L.) aquaporin gene family. *PLoS ONE* 10:e0128025. doi: 10.1371/journal.pone.0128025
- Hsiao, T. C., and Acevedo, E. (1974). Plant responses to water deficits, water-use efficiency, and drought resistance. *Agric. Meteorol.* 14, 59–84. doi: 10.1016/0002-1571(74)90011-9
- Ibraheem, O., Botha, C. E. J., and Bradley, G. (2010). In silico analysis of cis-acting regulatory elements in 5' regulatory regions of sucrose transporter gene families in rice (*Oryza sativa* Japonica) and *Arabidopsis thaliana*. *Comput. Biol. Chem.* 34, 268–283. doi: 10.1016/j.combiolchem.2010.09.003
- Javot, H., Lauvergeat, V., Santoni, V., Martin-Laurent, F., Güclü, J., Vinh, J., et al. (2003). Role of a single aquaporin isoform in root water uptake. *Plant Cell* 15, 509–522. doi: 10.1105/tpc.008888
- Johanson, U., and Gustavsson, S. (2002). A new subfamily of major intrinsic proteins in plants. *Mol. Biol. Evol.* 19, 456–461. doi: 10.1093/oxfordjournals.molbev.a004101

- Johanson, U., Karlsson, M., Johansson, I., Gustavsson, S., Sjö, S., Fraysse, L., et al. (2001). The complete set of genes encoding Major Intrinsic Proteins in *Arabidopsis* provides a framework for a new nomenclature for Major Intrinsic Proteins in plants. *Plant Physiol.* 126, 1358–1369. doi: 10.1104/pp.126.4.1358
- Johansson, I., Karlsson, M., Shukla, V. K., Chrispeels, M. J., Larsson, C., and Kjellbom, P. (1998). Water transport activity of the plasma membrane aquaporin PM28A is regulated by phosphorylation. *Plant Cell* 10, 451–459. doi: 10.1105/tpc.10.3.451
- Kaldenhoff, R., and Fischer, M. (2006). Functional aquaporin diversity in plants. *Biochim. Biophys. Acta-Biomembr.* 1758, 1134–1141. doi: 10.1016/j.bbamem.2006.03.012
- Kamiya, T., Tanaka, M., Mitani, N., Ma, J. F., Maeshima, M., and Fujiwara, T. (2009). NIP1; 1, an aquaporin homolog, determines the arsenite sensitivity of *Arabidopsis thaliana*. *J. Biol. Chem.* 284, 2114–2120. doi: 10.1074/jbc.M806881200
- Karnovsky, A., Weymouth, T., Hull, T., Tarcea, V. G., Scardoni, G., Laudanna, C., et al. (2012). MetScape 2 bioinformatics tool for the analysis and visualization of metabolomics and gene expression data. *Bioinforma. Orig. Pap.* 28, 373–380.
- Keegstra, K. (2010). Plant cell walls. *Plant Physiol.* 154, 483–486. doi: 10.1104/pp.110.161240
- Klie, M., and Debener, T. (2011). Identification of superior reference genes for data normalisation of expression studies via quantitative PCR in hybrid roses (*Rosa hybrida*). *BMC Res. Notes* 4:518.
- Krogh, A., Larsson, B., von Heijne, G., and Sonnhammer, E. L. (2001). Predicting transmembrane protein topology with a hidden markov model: application to complete genomes. *J. Mol. Biol.* 305, 567–580. doi: 10.1006/jmbi.2000.4315
- Lang, A. (1990). Xylem, phloem and transpiration flows in developing Apple fruits. *J. Exp. Bot.* 41, 645–651. doi: 10.1093/jxb/41.6.645
- Lang, A., and Thorpe, M. R. (1989). Xylem, phloem and transpiration flows in a grape: application of a technique for measuring the volume of attached fruits to high resolution using archimedes'. *Principle. J. Exp. Bot.* 40, 1069–1078. doi: 10.1093/jxb/40.10.1069
- Leitao, L., Prista, C., Moura, T. F., Loureiro-Dias, M. C., and Soveral, G. (2012). Grapevine aquaporins: gating of a tonoplast intrinsic protein (TIP2;1) by cytosolic pH. *PLoS ONE* 7:e33219. doi: 10.1371/journal.pone.0033219
- Lescot, M., D'hais, P., Thijss, G., Marchal, K., Moreau, Y., Van De Peer, Y., et al. (2002). PlantCARE, a database of plant cis-acting regulatory elements and a portal to tools for in silico analysis of promoter sequences. *Nucleic Acids Res.* 30, 325–327. doi: 10.1093/nar/30.1.325
- Li, P., and Brutnell, T. P. (2011). *Setaria viridis* and *Setaria italica*, model genetic systems for the Panicoide grasses. *J. Exp. Bot.* 62, 3031–3037. doi: 10.1093/jxb/err096
- Li, R. Y., Ago, Y., Liu, W. J., Mitani, N., Feldmann, J., McGrath, S. P., et al. (2009). The rice aquaporin Ls1 mediates uptake of methylated arsenic species. *Plant Physiol.* 150, 2071–2080. doi: 10.1104/pp.109.140350
- Liu, D., Tu, L., Wang, L., Li, Y., Zhu, L., and Zhang, X. (2008). Characterization and expression of plasma and tonoplast membrane aquaporins in elongating cotton fibers. *Plant Cell Rep.* 27, 1385–1394. doi: 10.1007/s00299-008-0545-6
- Liu, Q. P., and Zhu, Z. J. (2010). Functional divergence of the NIP III subgroup proteins involved altered selective constraints and positive selection. *BMC Plant Biol.* 10:256. doi: 10.1186/1471-2229-10-256
- Luu, D. T., and Maurel, C. (2005). Aquaporins in a challenging environment: molecular gears for adjusting plant water status. *Plant Cell Environ.* 28, 85–96. doi: 10.1111/j.1365-3040.2004.01295.x
- Ma, J. F., Mitani, N., Nagao, S., Konishi, S., Tamai, K., Iwashita, T., et al. (2004). Characterization of the silicon uptake system and molecular mapping of the silicon transporter gene in rice. *Plant Physiol.* 136, 3284–3289. doi: 10.1104/pp.104.047365
- Ma, J. F., Tamai, K., Yamaji, N., Mitani, N., Konishi, S., Katsuhara, M., et al. (2006). A silicon transporter in rice. *Nature* 440, 688–691. doi: 10.1038/nature04590
- Ma, J. F., and Yamaji, N. (2008). Functions and transport of silicon in plants. *Cell. Mol. Life Sci.* 65, 3049–3057. doi: 10.1007/s00018-008-7580-x
- Ma, J. F., Yamaji, N., Mitani, N., Xu, X.-Y., Su, Y.-H., McGrath, S. P., et al. (2008). Transporters of arsenite in rice and their role in arsenic accumulation in rice grain. *Proc. Natl. Acad. Sci. U.S.A.* 105, 9931–9935. doi: 10.1073/pnas.0802361105
- Malz, S., and Sauter, M. (1999). Expression of two PIP genes in rapidly growing internodes of rice is not primarily controlled by meristem activity or cell expansion. *Plant Mol. Biol.* 40, 985–995. doi: 10.1023/A:1006265528015
- Martin, A. P., Palmer, W. M., Brown, C., Abel, C., Lunn, J. E., Furbank, R. T., et al. (2016). A developing *Setaria viridis* internode: an experimental system for the study of biomass generation in a C4 model species. *Biotechnol. Biofuels* 9, 1–12. doi: 10.1186/s13068-016-0457-6
- Maurel, C. (1997). Aquaporins and water permeability of plant membranes. *Annu. Rev. Plant Physiol. Plant Mol. Biol.* 48, 399–429. doi: 10.1146/annurev.arplant.48.1.399
- Maurel, C., Javot, H., Lauvergeat, V., Gerbeau, P., Tournaire, C., Santoni, V., et al. (2002). Molecular physiology of aquaporins in plants. *Int. Rev. Cytol.* 215, 105–148. doi: 10.1016/S0074-7696(02)15007-8
- Maurel, C., Verdoucq, L., Luu, D.-T. T., and Santoni, V. (2008). Plant aquaporins: membrane channels with multiple integrated functions. *Annu. Rev. Plant Biol.* 59, 595–624. doi: 10.1146/annurev.arplant.59.032607.092734
- McCormick, A. J., Watt, D. A., and Cramer, M. D. (2009). Supply and demand: sink regulation of sugar accumulation in sugarcane. *J. Exp. Bot.* 60, 357–364. doi: 10.1093/jxb/ern210
- Milne, R. J., Byrt, C. S., Patrick, J. W., and Grof, C. P. L. (2013). Are sucrose transporter expression profiles linked with patterns of biomass partitioning in Sorghum phenotypes? *Front. Plant Sci.* 4:223. doi: 10.3389/fpls.2013.00223
- Milne, R. J., Offler, C. E., Patrick, J. W., and Grof, C. P. L. (2015). Cellular pathways of source leaf phloem loading and phloem unloading in developing stems of Sorghum bicolor in relation to stem sucrose storage. *Funct. Plant Biol.* 42, 957–970. doi: 10.1071/FP15133
- Mitani, N. (2005). Uptake system of silicon in different plant species. *J. Exp. Bot.* 56, 1255–1261. doi: 10.1093/jxb/eri121
- Mizuno, H., Kasuga, S., and Kawahigashi, H. (2016). The sorghum SWEET gene family: stem sucrose accumulation as revealed through transcriptome profiling. *Biotechnol. Biofuels* 9, 1–12. doi: 10.1186/s13068-016-0546-6
- Moore, P. H. (1995). Temporal and spatial regulation of sucrose accumulation in the sugarcane stem. *Aust. J. Plant Physiol.* 22, 661–679. doi: 10.1071/PP9950661
- Moore, P. H., and Botha, F. C. (2013). *Sugarcane: Physiology, Biochemistry and Functional Biology*. Hoboken, NJ: John Wiley & Sons.
- Moore, P. H., and Cosgrove, D. J. (1991). Developmental changes in cell and tissue water relations parameters in storage parenchyma of sugarcane. *Plant Physiol.* 96, 794–801. doi: 10.1104/pp.96.3.794
- Mosa, K. A., Kumar, K., Chhikara, S., Mcdermott, J., Liu, Z. J., Musante, C., et al. (2012). Members of rice plasma membrane intrinsic proteins subfamily are involved in arsenite permeability and tolerance in plants. *Transgenic Res.* 21, 1265–1277. doi: 10.1007/s11248-012-9600-8
- Papini-Terzi, F. F. S., Rocha, F. R. F., Vencio, R. R. Z., Felix, J. J. M., Branco, D. S., Waclawovsky, A. J. A., et al. (2009). Sugarcane genes associated with sucrose content. *BMC Genomics* 10:120. doi: 10.1186/1471-2164-10-120
- Patrick, J. W. (1997). Phloem unloading: Sieve element unloading and post-sieve element transport. *Annu. Rev. Plant Physiol. Plant Mol. Biol.* 48, 191–222. doi: 10.1146/annurev.arplant.48.1.191
- Patrick, J. W., Botha, F. C., and Birch, R. G. (2013). Metabolic engineering of sugars and simple sugar derivatives in plants. *Plant Biotechnol. J.* 11, 142–156. doi: 10.1111/pbi.12002
- Péret, B., Li, G., Zhao, J., Band, L. R., Voß, U., Postaire, O., et al. (2012). Auxin regulates aquaporin function to facilitate lateral root emergence. *Nat. Cell Biol.* 14, 991–998. doi: 10.1038/ncb2573
- Pfeiffer, T. W., Bitzer, M. J., Toy, J. J., and Pedersen, J. F. (2010). Heterosis in sweet sorghum and selection of a new sweet sorghum hybrid for use in syrup production in appalachia. *Crop Sci.* 50, 1788–1794. doi: 10.2135/cropsci2009.09.0475
- Rae, A. L., Grof, C. P. L., and Casu, R. E. (2005). Sucrose accumulation in the sugarcane stem: pathways and control points for transport and compartmentation. *Field Crop. Res.* 92, 159–168. doi: 10.1016/j.fcr.2005.01.027
- Rae, A. L., Jackson, M. A., Nguyen, C. H., and Bonnett, G. D. (2009). Functional specialization of vacuoles in sugarcane leaf and stem. *Trop. Plant Biol.* 2, 13–22. doi: 10.1007/s12042-008-9019-9
- Reddy, P. S., Rao, T. S. R. B., Sharma, K. K., and Vadez, V. (2015). Genome-wide identification and characterization of the aquaporin gene family in *Sorghum bicolor* (L.). *Plant Gene* 1, 18–28. doi: 10.1016/j.jplgene.2014.12.002

- Reinders, A., Sivitz, A. B., Starker, C. G., Gantt, J. S., and Ward, J. M. (2008). Functional analysis of LjSUT4, a vacuolar sucrose transporter from *Lotus japonicus*. *Plant Mol. Biol.* 68, 289–299. doi: 10.1007/s11103-008-9370-0
- Rohwer, J. M., and Botha, F. C. (2001). Analysis of sucrose accumulation in the sugar cane culm on the basis of in vitro kinetic data. *Biochem. J.* 358, 437–445. doi: 10.1042/bj3580437
- Sakurai, J., Ishikawa, F., Yamaguchi, T., Uemura, M., and Maeshima, M. (2005). Identification of 33 rice aquaporin genes and analysis of their expression and function. *Plant Cell Physiol.* 46, 1568–1577. doi: 10.1093/pcp/pci172
- Schmalstig, J. G., and Cosgrove, D. J. (1990). Coupling of solute transport and cell expansion in pea stems. *Plant Physiol.* 94, 1625–1633. doi: 10.1104/pp.94.4.1625
- Schuermans, J. A. M., van Dongen, J. T., Rutjens, B. P. W., Boonman, A., Pieterse, C. M. J., and Borstlap, A. C. (2003). Members of the aquaporin family in the developing pea seed coat include representatives of the PIP, TP and NIP subfamilies. *Plant Mol. Biol.* 53, 655–667. doi: 10.1023/B:PLAN.0000019070.60954.77
- Siefritz, F., Biela, A., Eckert, M., Otto, B., Uehlein, N., and Kaldenhoff, R. (2001). The tobacco plasma membrane aquaporin NtAQP1. *J. Exp. Bot.* 52, 1953–1957. doi: 10.1093/jexbot/52.363.1953
- Slewinski, T. L. (2011). Diverse functional roles of monosaccharide transporters and their homologs in vascular plants: a physiological perspective. *Mol. Plant* 4, 641–662. doi: 10.1093/mp/sss051
- Slewinski, T. L. (2012). Non-structural carbohydrate partitioning in grass stems: a target to increase yield stability, stress tolerance, and biofuel production. *J. Exp. Bot.* 63, 4647–4670. doi: 10.1093/jxb/ers124
- Somerville, C., Youngs, H., Taylor, C., Davis, S. C., and Long, S. P. (2010). Feedstocks for lignocellulosic biofuels. *Science* 329, 790–792. doi: 10.1126/science.1189268
- Spyropoulos, I. C., Liakopoulos, T. D., Bagos, P. G., and Hamodrakas, S. J. (2004). TMRPres2D: High quality visual representation of transmembrane protein models. *Bioinformatics* 20, 3258–3260. doi: 10.1093/bioinformatics/bth358
- Takano, J., Wada, M., Ludewig, U., Schaaf, G., Von Wirén, N., and Fujiwara, T. (2006). The *Arabidopsis* major intrinsic protein NIP5;1 is essential for efficient boron uptake and plant development under boron limitation. *Plant Cell* 18, 1498–1509. doi: 10.1105/tpc.106.041640
- Tarpley, L., Vietor, D. M., Tarpley, L., Vietor, D., Miller, F., Guimarães, C., et al. (2007). Compartmentation of sucrose during radial transfer in mature sorghum culm. *BMC Plant Biol.* 7:33. doi: 10.1186/1471-2229-7-33
- Törnroth-Horsefield, S., Wang, Y., Hedfalk, K., Johanson, U., Karlsson, M., Tajkhorshid, E., et al. (2006). Structural mechanism of plant aquaporin gating. *Nature* 439, 688–694. doi: 10.1038/nature04316
- Tournaire-Roux, C., Sutka, M., Javot, H. H., Gout, E. E., Gerbeau, P., Luu, D.-T. T., et al. (2002). Cytosolic pH regulates root water transport during anoxic stress through gating of aquaporins. *Nature* 425, 187–194.
- Turgeon, R. (2010). The puzzle of phloem pressure. *Plant Physiol.* 154, 578–581. doi: 10.1104/pp.110.161679
- Uehlein, N., Lovisolo, C., Siefritz, F., and Kaldenhoff, R. (2003). The tobacco aquaporin NtAQP1 is a membrane CO₂ pore with physiological functions. *Nature* 425, 734–737. doi: 10.1038/nature02027
- Viola, R., Roberts, A. G., Haupt, S., Gazzani, S., Hancock, R. D., Marmiroli, N., et al. (2001). Tuberization in potato involves a switch from apoplastic to symplastic phloem unloading. *Plant Cell* 13, 385–398. doi: 10.1105/tpc.13.2.385
- Vogel, J. (2008). Unique aspects of the grass cell wall. *Curr. Opin. Plant Biol.* 11, 301–307. doi: 10.1016/j.pbi.2008.03.002
- Waclawovsky, A. J., Sato, P. M., Lembke, C. G., Moore, P. H., and Souza, G. M. (2010). Sugarcane for bioenergy production: an assessment of yield and regulation of sucrose content. *Plant Biotechnol. J.* 8, 263–276. doi: 10.1111/j.1467-7652.2009.00491.x
- Walsh, K. B., Sky, R. C., and Brown, S. M. (2005). The anatomy of the pathway of sucrose unloading within the sugarcane stalk. *Funct. Plant Biol.* 32, 367–374. doi: 10.1071/FP04102
- Wei, W. X., Alexandersson, E., Golldack, D., Miller, A. J., Kjellborn, P. O., and Fricke, W. (2007). HvPIP1;6, a barley (*Hordeum vulgare* L.) plasma membrane water channel particularly expressed in growing compared with non-growing leaf tissues. *Plant Cell Physiol.* 48, 1132–1147. doi: 10.1093/pcp/pcm083
- Welbaum, G. E., and Meinzer, F. C. (1990). Compartmentation of solutes and water in developing sugarcane stalk tissue. *Plant Physiol.* 93, 1147–1153. doi: 10.1104/pp.93.3.1147
- Welbaum, G. E., Meinzer, F. C., Grayson, R. L., and Thornham, K. T. (1992). Evidence for the consequences of a barrier to solute diffusion between the apoplast and vascular bundles in sugarcane stalk tissue. *Funct. Plant Biol.* 19, 611–623.
- Werner, D., Gerlitz, N., and Stadler, R. (2011). A dual switch in phloem unloading during ovule development in *Arabidopsis*. *Protoplasma* 248, 225–235. doi: 10.1007/s00709-010-0223-8
- Wingenter, K., Schulz, A., Wormit, A., Wic, S., Trentmann, O., Hoermiller, I. I., et al. (2010). Increased activity of the vacuolar monosaccharide transporter TMT1 alters cellular sugar partitioning, sugar signaling, and seed yield in *Arabidopsis*. *Plant Physiol.* 154, 665–677. doi: 10.1104/pp.110.162040
- Wood, R., Patrick, J. W., and Offler, C. E. (1994). The cellular pathway of short-distance transfer of photosynthates and potassium in the elongating stem of *Phaseolus vulgaris* L. Stem anatomy, solute transport and pool sizes. *Ann. Bot.* 73, 151–160. doi: 10.1006/anbo.1994.1018
- Yonekura-Sakakibara, K., and Saito, K. (2013). Transcriptome coexpression analysis using ATTED-II for integrated transcriptomic/metabolomic analysis. *Methods Mol. Biol.* 1011, 317–326. doi: 10.1007/978-1-62703-414-2_25
- Zelazny, E., Borst, J. W., Muylaert, M., Batoko, H., Hemminga, M. A., and Chaumont, F. (2007). FRET imaging in living maize cells reveals that plasma membrane aquaporins interact to regulate their subcellular localization. *Proc. Natl. Acad. Sci. U.S.A.* 104, 12359–12364. doi: 10.1073/pnas.0701180104
- Zhang, W.-H., Zhou, Y., Dibley, K. E., Tyerman, S. D., Furbank, R. T., Patrick, J. W., et al. (2007). Nutrient loading of developing seeds. *Funct. Plant Biol.* 34, 314–331. doi: 10.1071/FP06271
- Zhao, X. Q., Mitani, N., Yamaji, N., Shen, R. F., and Ma, J. F. (2010). Involvement of silicon influx transporter OsNIP2;1 in selenite uptake in rice. *Plant Physiol.* 153, 1871–1877. doi: 10.1104/pp.110.157867

Conflict of Interest Statement: The authors declare that the research was conducted in the absence of any commercial or financial relationships that could be construed as a potential conflict of interest.

Copyright © 2016 McGaughey, Osborn, Chen, Pegler, Tyerman, Furbank, Byrt and Grof. This is an open-access article distributed under the terms of the Creative Commons Attribution License (CC BY). The use, distribution or reproduction in other forums is permitted, provided the original author(s) or licensor are credited and that the original publication in this journal is cited, in accordance with accepted academic practice. No use, distribution or reproduction is permitted which does not comply with these terms.

Advantages of publishing in Frontiers



OPEN ACCESS

Articles are free to read,
for greatest visibility



COLLABORATIVE PEER-REVIEW

Designed to be rigorous
– yet also collaborative,
fair and constructive



FAST PUBLICATION

Average 85 days from
submission to publication
(across all journals)



COPYRIGHT TO AUTHORS

No limit to article
distribution and re-use



TRANSPARENT

Editors and reviewers
acknowledged by name
on published articles



SUPPORT

By our Swiss-based
editorial team



IMPACT METRICS

Advanced metrics
track your article's impact



GLOBAL SPREAD

5'100'000+ monthly
article views
and downloads



LOOP RESEARCH NETWORK

Our network
increases readership
for your article

Frontiers

EPFL Innovation Park, Building I • 1015 Lausanne • Switzerland
Tel +41 21 510 17 00 • Fax +41 21 510 17 01 • info@frontiersin.org
www.frontiersin.org

Find us on

